Variable geometry turbocharging: Optimisation and control.

Roberts, E. W.

Award date:
1984

Awarding institution:
University of Bath

VARIABLE GEOMETRY TURBOCHARGING; OPTIMISATION AND CONTROL

submitted by:

E.W. ROBERTS for the Degree of Ph.D.

of the University of Bath

1984

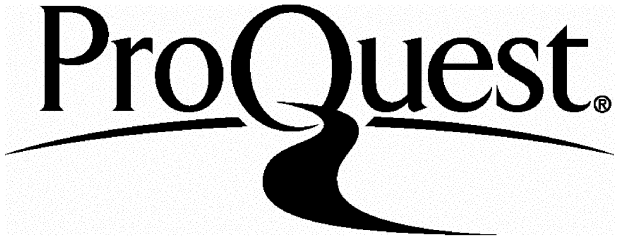

SUMMARY

The future European trends for truck diesels include improvements to acceleration performance, economy and higher torque over a wider speed range (where maximum speeds are being reduced). A variable geometry turbocharger together with electronic control can combine the conflicting requirements of flexibility and economy in one engine.

This thesis investigates the complete testing of a HOLSET turbocharger equipped with a variable area turbine (based on volute exit area and ring sleeve design) applied to an automotive type TL11 engine rated at 190 kW @ 2100 rev/min. Control was effected by a programmable digital controller and was extended to include variable injection timing and electronic governing functions. An optimal type control strategy was implemented.

A description is included of the test facility and the features adopted such that the electronic control system could be developed effectively. An account on the control implementation is given together with details on the design and development of the control parameters. Different control algorithms both steady state and transiently were assessed and resulted in a torque back-up of 46% at 59% of rated speed compared with 21% at 62% of rated speed for the base. Significant improvements to part load efficiency were achieved e.g. .225 kg/kWh island increased by 25%. Boost scheduling controlled ring sleeve position and resulted in enhanced engine acceleration.

The limitation to this work included mechanical, breathing and efficiency parameters. These were investigated theoretically. The practical and theoretical work indicated that with appropriate developments an SFC characteristic with better than .200 kg/kWh is readily attainable. Appropriate conclusions were drawn together with suggestions for further work.

ACKNOWLEDGEMENTS

I would like to gratefully acknowledge the help given by the following:

Professor Frank Wallace for his supervision and guidance. Brian Walsham, The SERC and HOLSET ENGINEERING respectively for initiating the move and making the sponsorship possible.

The participating partners of the HOLSET ENGINEERING Co. Ltd., LEYLAND VEHICLES, DEPARTMENT OF INDUSTRY and DOWTY FUEL SYSTEMS for their excellent technical and material support, and to the many others who contributed indirectly.

Mr. Dave Howard for his assistance on the control side, Mr. Ian Marsh and Mr. Peter Prest who designed and fitted the extensive instrumentation used.

Mr. Anthony Elly and Mr. Keith Britten for building the rig and remaining genial even in times of adversity and also to Mr. Ken Pepler (machine shop) who discharged his responsibilities so satisfactorily.

My thanks are also due to Mrs. Hazel Ford and Mrs. Janet Thomas for typing this manuscript competently.

I wish to express my special gratitude to my parents for their support and guidance throughout.

CONTENTS

(The above data is too bulky to be bound within this thesis but may be viewed at the School of Engineering, University of Bath).

1. INTRODUCTION

1.1. History & Review of the Diesel Engine

Automotive diesel engines first came into general use in the early 1930's. Dr. Rudolf Diesel had invented the compression ignition engine some 30 years previously but its application had been limited to large marine and industrial power plants.

The first automotive diesel power units were exhibited by the pioneer engine builders, MAN and Daimler-Benz in the period 1924-25. However it was not until the economic pressures of high fuel taxation in the early 1930's that considerable effort was put into automotive diesel development by practically all the makers of buses and lorries throughout Europe. By 1939 the petrol engine had been entirely displaced from large buses and heavy trucks.

There are, however, drawbacks with the diesel engine. In the first instance it is more expensive to build than a petrol engine. This is because it has to withstand higher loadings due to its higher compression ratios (typically 16:1 versus 9:1) and demands a higher standard of manufacture. It is heavier for a given power or less powerful for a given size, the latter mainly because it runs at a lower maximum crankshaft speed and higher air fuel ratios. General performance is rougher and more noisy than that of its petrol counterpart, these adverse effects being the more noticeable at low and idling speeds.

Reliability and starting from cold are good as the engine is unaffected by humidity, dew or condensation and longevity is very much better.

In general terms the diesel engine has a 30-40% advantage in fuel consumption over an equivalent petrol engine. This is due to the way power is regulated in a petrol engine which is achieved by throttling. This increases the pumping losses and hence specific fuel consumption (SFC) resulting in poor part load efficiency when compared with the diesel

engine (Fig. 1.1) although lean burn engines partly overcome this problem.

Power regulation in a diesel engine is achieved by reducing the fuel supply. Diesel engines are capable of running on very weak mixtures; this is because fuel is injected directly into the cylinder. Consequently the fuel system is divorced from it's unrestricted air induction system. A govenor is however required to regulate the injected fuel system to prevent the engine from stalling or overspeeding.

The advantages of a diesel engine include:

(i) a reduced fire risk (for vehicle and storage)

(ii) no evaporation problems

(iii) improved exhaust gas quality

(iv) good torque at low speed

and

(v) an ability to accept shock loads without stalling.

Other automotive applications where the diesel engine has found great favour include:

(i) tractors

(ii) delivery trucks

(iii) off-road vehicles

(iv) taxi cabs

for the reasons outlined above.

1.2. Automotive Requirements (1, 18)

Over the past 25 years power outputs from truck engines have increased dramatically to cope with increased load-carrying capacity, higher speeds and legislation of minimum brake horsepower per ton. This is

to effect lower journey times and more efficient operation. Space and weight is a limiting criterion and any means by which small engines can be made to produce more power is a distinct advantage.

Additionally an engine producing constant power (rising torque with decreasing speed) throughout a wide engine speed range is the ideal source of power for a road vehicle (Fig. 1.2).

It reduces the number of gearbox ratios and the number of gearchanges necessary (Fig. 1.3). Other benefits include improved transient response, lower fuel consumption and lower noise levels. The requirement for rising torque with decreasing speed in automotive engines is the subject of this thesis.

Whilst a constant power diesel engine is impracticable in practice a degree of 'torque back up' is highly desirable. Torque back up is a comparison between torque at rated speed and the maximum available and is defined as:

$$\frac{\tau \text{ max} - \tau \text{ rated}}{\tau \text{ rated}}$$

The speed at which this occurs is also important, as the lower the speed the greater the flexibility during operation. It is defined as:

$$\text{SPEED ELASTICITY (\% of rated speed)} = \frac{\text{rev/min at peak torque}}{\text{rev/min at maximum power}}$$

It is difficult to achieve a high level of torque back up without some loss of maximum power. Considerable effort has been directed at this problem and some interesting and ingenious solutions have been proposed.

1.3. Factors Affecting the Limiting Performance of a 4-Stroke Diesel Engine

The two main factors affecting limiting performance in a diesel engine are peak cylinder pressure and utilization of air respectively.

1.3.1. Peak cylinder pressure will be limited by the strength of the cylinder head gasket and bearings which is in turn a function of weight and cost.

Air utilization and hence power can be increased by:

1. enlarging cylinder displacement
2. raising engine speed
3. increasing charge density before induction

1.3.2. Enlarging cylinder displacement

In a modern commercial vehicle space is at a premium. For this reason increasing cylinder displacement or adding cylinders is normally precluded.

1.3.3. Increasing engine speed

The power output of an engine can be raised by increasing the crankshaft speed with due regard to inertia, piston velocity, lubrication, fuel injection equipment, combustion and volumetric efficiency. In practice it is found that the maximum indicated mean effective pressure (imep) varies considerably with speed.

In practice naturally aspirated engines are smoke limited to

approximately 7 bar bmep and will be a function of volumetric efficiency. This is usually a flat characteristic over the useful speed range. Torque back up of the order of 20% can only be achieved at the expense of rated power which is not an effective solution.

The modern trend in automotive engines is to reduce rated speed. Fuel consumption is reduced because of limited top speed and lower engine friction. Engine frictional losses increase as the square of engine speed, but only linearly when power or engine capacity is increased. Other benefits of reducing maximum engine speed include lower component stresses and noise.

1.3.4. Increasing charge density

Other things being equal, the total power developed in an engine cylinder depends upon the mass of the charge induced which is limited by the existing ambient pressure and temperature of the air. Resonance effects of the inlet and exhaust tracts can be used to achieve a certain amount of pressure charging at selected speeds.

A much greater increase in charge density can be obtained by compressing the charge before induction with some type of supercharger. Supercharging is defined as "the increasing of the mass of air in the combustion chamber over that induced by normal atmospheric pressure, ram effect and dynamic effects by any means whatsoever".

A Roots or other positive displacement blower or a centrifugal compressor may be used for this purpose. The supercharger may be gear driven from the crankshaft. Alternatively power may be derived from a turbine driven by the exhaust gases the device then being known as a turbocharger.

Supercharging can increase the nett power output considerably. Brake thermal efficiency, however, remains substantially the same.

This method of increasing power output has been successfully applied to automotive diesel engines. A review of supercharging follows.

1.4. Supercharging

1.4.1. Mechanical supercharger

The engine driven compressor was one of the earliest attempts at pressure charging. The pressure ratios have been limited to approximately 1.5:1 with a low adiabatic efficiency. They also generated a high pitch whine.

The major drawback with mechanical superchargers is that delivery is not load dependent, resulting in high specific fuel consumption (SFC) at light loads. Further developments have been effectively curtailed by the development of turbocharging.

1.4.2. Exhaust driven supercharger (Fig. 1.4(i))

In turbocharging use is made of a turbine for converting thermal and potential energy in the exhaust into mechanical energy. The turbine drives via a shaft a centrifugal compressor which compresses the combustion air and transfers it to the cylinder. The pressure energy is partially returned to the engine but the thermal energy is that which would have been wasted.* The exhaust gas turbocharger is free-running i.e. its shaft is not mechanically connected to the crankshaft of the engine. The unit is responsive to both engine load and speed changes. Load sensitivity is an advantage since it means that boost will only be provided when the engine requires it. Excessive speed sensitivity is not a desirable feature particularly in the automotive application as the engine has to operate over a very wide speed range, whereas turbochargers only work satisfactorily within a fairly narrow speed band.

*A T-S diagram of the process is shown in Fig.1.17 and discussed in 1.8.

1.4.3. Turbocharger description

The turbine stage can be of two types, an axial flow machine where the flow is wholly or mainly parallel to the axis of rotation or a radial inflow device. In the radial machine the gas enters via a volute and flows directly onto the wheel or through a fixed nozzle onto the impeller (Fig. 1.4(ii)) in the plane of rotation and exhausts in an axial direction. Fig. 1.4(iii) illustrates the radial turbine's characteristic and non-dimensional swallowing capacity.

On large stationary and marine engines axial flow machines are used exclusively since they are more efficient. Radial inflow machines are used principally in applications under 1000 kW where the wheel is not too large to cast in one piece. The radial turbine operates more efficiently with large pressure ratios and small mass flows than its axial counterpart.

(i) Centrifugal Compressor

The compressor consists of an impeller, diffuser and housing. The impeller rotates at high speed and imparts angular momentum to the fluid. The diffuser slows the air down and causes it to increase in pressure and temperature. A further pressure rise may occur in the housing. The operating range is limited due to low efficiency (60%) and surge, a region of instability and represents a limit to good torque back-up. The flow range will usually be about 2:1. This means that the maximum useful flow rate at 2:1 pressure ratio will be twice the flow at the surge limit to give a broad and efficient flow range.

The centrifugal compressor characteristic is shown in Fig. 1.4(iv) together with the engine operating condition for constant power output.

(ii) Lubrication system

The turbine shaft is supported by plain bearings mounted inboard and lubricated by the engine oil system. Their advantages include robustness and long life. The oil supply assists in cooling the bearings particularly on the turbine end.

1.4.4. Constant pressure and pulse turbocharging

There are two major and distinct methods of turbocharging a diesel engine termed 'constant pressure' and 'pulse' operation respectively. The original method patented by Dr. Buchi in 1906 (27) was the constant pressure system and refers to the method of conveying the exhaust gas energy to the turbine. A constant pressure is attained by using a single large manifold which dampens out the pulsations exhausting into a single entry turbine. This system gives very good full load full speed performance but at the expense of poor part load and acceleration characteristics.

The pulse system attempts to utilize the high kinetic energy of the gases leaving the exhaust valve by improving the transmission of energy from the cylinder to the turbine. This is done by grouping certain cylinders whose exhaust processes are suitably separated in time. Three cylinder grouping respond best and it follows that more than one turbine entry is required. This 'pulse' system imparts good part load and acceleration characteristics and is widely used throughout Europe.

1.4.5. Pulse convertors (37)

When cylinder groupings of two or four are fed into a turbine entry, large unsteady flow and pulse interference effects occur in a 720^{o} cycle. A pulse convertor attempts to prevent the effect of a pressure wave from one cylinder interfering with the exhaust process of another whilst at the same time minimising flow unsteadiness at turbine entry and maximising the available energy. This is achieved in practice by using appropriately sized nozzles (0.65 - 0.8 area ratios) at the junctions of the manifolds (Fig. 1.5).

1.4.6. Aftercooling

Turbocharging increases the charge density by increasing inlet mani-

fold pressure. However, it is impossible to compress air without raising its temperature (Fig. 1.6). The object of pressure charging is to increase the density of the air; any temperature rise partly offsets this gain. If an aftercooler is added between the turbocharger and the engine the charge density can be increased substantially which makes it possible to effect considerable improvements in performance and appreciable reduction in the thermal loading due to turbocharging. This represents a very cost effective method of increasing power output. The term intercooling is often applied.

1.4.7. Advantages of turbocharging

The advantages of turbocharging can be summarised as:

(a) A large increase in torque and power for an engine of given swept volume.

(b) Reduction in SFC due to improvement in mechanical efficiency coupled with certain thermodynamic effects.

(c) Reduction in engine length for a given power output.

(d) Reduction in cost per installed horsepower.

(e) Reduction in installation weight for a given power output.

(f) Reduction in maintenance cost of engine for a given power output.

(g) Reduction of percentage heat to coolant and reduced cooling requirements.

(h) Reduction in engine noise level.

(i) Improved exhaust gas quality.

(j) Less derating with reduced barometric pressure.

1.4.8. Disadvantages of turbocharging

(a) Transient response.

The main disadvantages of turbocharging is poor transient response and certain associated problems. These are described in the next section.

1.5. Transient Response

The main disadvantage of turbocharging lies in the emission of black smoke when accelerating or starting. Engine acceleration is important in the automotive application. At low loads and speeds very little boost is developed and under a sudden heavy fuel demand the engine is behaving instantaneously as an overfuelled naturally aspirated engine with a consequent 'puff' of black smoke, though the engine acceleration is rapid.

A partial solution to this can be provided by fitting boost controlled fuel pumps or other devices which depress maximum fuel until a pre-determined boost level is reached. This boost control however causes the engine and turbocharger to accelerate more slowly.

The turbo-lag as it is known is due to the finite time it takes for the pressure to build up in the manifolds and the turbine torque required to overcome its own inertia when accelerating. It follows that turbocharger response becomes worse with increased ratings.

1.6. Matching the Single Stage Turbocharger to the 4-Stroke Automotive Engine (13)

The automotive engine with its requirement for good torque back-up is not ideally suited to the single stage turbocharger. This is because the engine has a much broader efficient range of operation than the turbocharger, thus a compromise has to be made in matching.

For constant engine power a 'horizontal'line (Fig. 1.4(iv)) is required on the compressor map at say 2:1 pressure ratio. Consequently the turbine stage needs at least the same expansion ratio to give the appropriate power balance. The flow characteristic of a turbine is similar to that of a fixed area nozzle Fig. 1.4(iii) rather than that of the impeller and is thus completely inappropriate.

At present a compromise solution to this narrow speed band is found by rating the engine to an acceptable smoke level at low speeds accepting the fact that maximum torque will occur at a higher speed (Fig. 1.7) than would be obtained on a naturally aspirated engine and keeping the boost at full speed to a level which will maintain acceptable cylinder pressures. Currently typical values would be 15-20% torque back-up at 60-65% of rated speed.

The work reported in this thesis concerns itself primarily with improving the torque speed characteristic of a single stage turbocharged engine and minimising SFC.

Some interesting techniques have been adopted to overcome the limitations outlined above. These include the 'high torque formula' (LEYLAND), MAXIDYNE (MACK) and Maxi-torque (BERLIET) which are conventional single stage turbocharged engines with high torque back up; typically 25-50%. This is achieved by artificially depressing top end power (that is tailoring fuel delivery) with some consequent disadvantage in bulk and power to weight requirements (Fig. 1.8).

1.6.1. Wastegating

Small indirect injection automotive diesel engines with a comparatively large speed range (> 3000 rev/min) effect a good match by using a wastegated turbine stage. This means that some exhaust gas is by-passed around the turbine at high engine speed. Control is normally accomplished by boost pressure sensing. There is an SFC penalty due to the higher exhaust back pressure. Applications in Europe have been confined to light vans and motor cars. (Fig. 1.9). A review follows of the systems developed to improve the torque speed characteristic of the four-stroke diesel engine.

1.7. High Torque Back-up Systems

1.7.1. Two stage fixed geometry turbocharging (Fig. 1.10), (11, 42)

Higher specific power over a wide speed range can be accomplished by connecting two fixed geometry turbochargers in series. This overcomes the problems of narrowing compressor flow range and low overall turbocharger efficiency at high pressure ratios. It allows for a smaller high pressure turbocharger which imparts a good low speed torque characteristic. A considerable increase in airflow and hence rating in excess of 24 bar bmep can be achieved. Transient response is also enhanced. The drawback of the system is the added complexity and space considerations for the ducting and coolers. To date only CUMMINS in America have released such an automotive engine commercially (though in small quantities) beginning in 1981. It is rated at 14 bar bmep @ 2100 rev/min and 17 bar at 1400 rev/min with a pressure ratio of 3:1.

1.7.2. Compounding

There is no mechanical connection between the turbocharger and the engine which when properly matched is self governing i.e. no nett power is extracted from the turbocharger shaft. There are attractions in a system in which the turbocharger shaft and engine crankshaft are linked together thereby allowing any surplus power developed by the turbine over the compressor to be fed back to the output shaft and improving overall efficiency. Such a scheme is known as a compound scheme, that is one in which the output power is delivered by both reciprocating and rotating expanders.

If the engine and the associated components are connected through epicyclic gearing then it is termed a differential compound scheme. Wallace (8) has proposed such a scheme using a variable geometry turbine which gives a continuously rising torque characteristic with

decreasing speed together with good efficiencies (Fig.1.11).

Cummins have published a paper (38) on a turbocompound scheme (Fig.1.12) installed in a vehicle which gave encouraging results. The scheme basically comprises a low pressure turbine geared to the output shaft. The high pressure stage is a conventional (but efficient) single stage. This arrangement allows a tighter h.p. turbine stage to be used which results in a good engine torque speed characteristic with improved transient performance.

The principal problem with all compound schemes lies with the differing rotational speeds of turbine and engine which implies a high gear ratio. The reliability and efficiency of such gear drives are problematical and this has effectively precluded their general use to date.

1.7.3. Hyperbar system (39, 40)

The Hyperbar scheme overcomes the problem of limited operating range of the turbomachinery when compared to the engine by use of a controlled by-pass such that regardless of engine load and speed the operating point remains within the compressor map (Fig. 1.13). In order that a power balance between turbine and compressor be maintained at low engine speeds an auxiliary combustion chamber is required necessitating a control scheme. The auxiliary system is also used to start the low compression ratio engine. High ratings (21 bar bmep) are possible but at the expense of part load efficiency due to the auxiliary combustion chamber. A limited commercial operation on the French Railways is the only application to date, although the scheme was intended primarily for military applications.

1.7.4. Comprex system (24, 41)

An alternative method to achieve desirable automotive type torque

speed characteristics is by a pressure wave machine (patented in 1910). It is not a flow machine and uses a specially designed engine driven cell wheel (Fig. 1.14). By suitable dimensioning and timing the wheel transmits waves directly from exhaust to inlet. It absorbs very little power, transient response is very good torque back-up is considerably enhanced, smoke and emissions are better but SFC is normally worse at rated conditions.

The disadvantages include cost and sensitivity to manifold restrictions, also different trims are more difficult to accommodate. Only one tractor manufacturer VALMET of Finland has adopted the system commercially. The system is being developed by BBC of Switzerland.

1.7.5. CSER Resonant intake system (Fig. 1.15)

This system which has no moving parts and involves relatively small cost can improve low speed torque considerably (7.14) on a turbo-charged engine. This is achieved by use of a resonant intake system tuned to improve volumetric efficiency at low engine speed. The manifolding is arranged such that a positive pressure wave arrives at the point of inlet valve closure thereby enhancing cylinder filling. The system utilizes a compact resonant volume and pipes. It lends itself ideally to three and six cylinder engines on the four stroke cycle but has also been adapted for use on V8 engines (22). It follows that at high engine speeds the volumetric efficiency is somewhat worse. MAN were the first engine manufacturer to introduce this system on their production six-cylinder engines in 1982.

1.7.6. Variable geometry VG) turbocharging (3, 4, 9, 19)

Fundamentally the swallowing capacity of the fixed turbine stage even if 100% efficient limits the torque back-up available. Ideally the energy availability at turbine inlet needs to be increased i.e. a smaller turbine housing or swallowing capacity. The wastegated

turbine stage with its small housing gives good results but with an efficiency penalty. A variable area radial inflow turbine giving a range of swallowing capacities would enable it to maintain an adequate pressure drop and hence power for driving the compressor even with a reduced mass flow at low engine speed. This solution provides good torque back-up, improved transient response and a wider speed range.

The smallest swallowing capacity is used to obtain maximum low speed engine torque whilst the fully open condition allows rated power to be obtained without excessive back pressure. A control scheme is required to reduce the swallowing capacity with decreasing engine speed and increasing load utilizing possibly a pneumatic system based on speed and load. Alternatively a microprocessor based electronic controller could give optimum matching.

It is this scheme for overcoming the limitations of fixed geometry turbocharging discussed previously which forms the basis of the present project. Particular emphasis has been placed on control and optimisation of the variable area radial inflow turbine relative to the engine.

Fig.1.16a and b gives a general characterisation of the steady state torque and transient response attainable with the different charging systems discussed above.

The following section examines how variable geometry might be applied to a single stage radial inflow turbine. The mechanism by which thermal and potential energy are transformed into mechanical energy in the radial flow turbine is discussed.

1.8. Variable Geometry Schemes

In a centripetal turbine energy is transferred from the fluid to the rotor in passing from a large radius to a smaller radius. The product of moment of absolute momentum at entry to the rotor imparted by the volute must be greater than at the rotor exit (Fig. 1.17)

[i.e. UC_ϕ where U = rotor peripheral velocity

C_ϕ = tangential component of absolute flow velocity

defines the moment of momentum]

Therefore to achieve maximum efficiency a large UC_ϕ term at inlet with a zero term at outlet is required. For a given efficiency turbine power depends on flow rate and isentropic head which is in turn a function of temperature and expansion ratio.

In a VG scheme an attempt is made to increase the tangential component of velocity at rotor entry whilst decreasing the volute exit angle with respect to the tangential direction (increasing turbine torque). It is intended to increase the momentum term and expansion ratio with the smaller area; mass flow will remain sensibly constant because the engine behaves as a positive displacement machine.

If the process takes place efficiently, turbine torque rises faster than the reduction of swallowing capacity.

This increase in turbine torque can be accomplished by reducing one of the flow path areas in the turbine[1], the wheel exit area[2], volute exit, (throat) area[3], or tongue area, (Fig. 1.18).

Controlling wheel exit area is difficult without throttling - a process of zero efficiency. Two stage and power turbine schemes achieve the same end by different means (see Section 1.71 and 1.72).

The radial turbine is particularly well suited for the incorporation of variable geometry schemes in the throat area since simple and easy to manufacture geometries result.

VG based on throat area (Fig 1.19b) can be achieved by pivoted nozzle vanes where nozzle angle as well as throat area are varied simultaneously. The location of the pivot point is significant since it determines the location of the throat in respect of rotor inlet. The pivot point should be located as close as possible to the rotor inlet in order to avoid excessive losses at small nozzle angles. Large leakage is possible with this design and the mechanism involved is quite complex and could be expensive.

An alternative approach is that of mating plates or ring sleeves (Fig. 1.19a) whereby the throat area is decreased from the design value. Its advantages include simplicity and low leakage. The disadvantage however is a reduced control range and an excessive step in axial width between nozzle exit and rotor inlet at off design operation. This causes a sudden expansion of the flow after the nozzle throat which adversely affects turbine efficiency. This effect becomes progressively worse with decreasing nozzle area.

Another concept is to vary the degree of admission, this can be effected in different ways, e.g. a segmented stepwise change of nozzle area with all 'open' nozzles neighbouring or alternating with 'closed' nozzles can be chosen.

Flaxington and Szczupak (21) in their paper reviewed methods of varying tongue area for VG schemes. These are illustrated in Fig. 1.20. This method is ideally suited for nozzless turbines. Care must be taken to avoid throttling and asymetric flow in designs such as I and II.

The performance of the different systems as reported by Balje (12) are contained in Fig. 1.21.

1.8.1. Review of variable geometry work at Bath

Many researchers at Bath and elsewhere have directed their efforts at simulating and quantifying the benefits of VG turbocharging. These include Ghadiri-Zareh (2) who tested a series of differently sized volutes on turbocharged Perkins 6.354 and Leyland 500 engines. (Varying Tongue Area) Fig. 1.23 shows these results. They indicate that considerable benefits accrue with a small mass flow turbine in the mid-range in terms of smoke emission, torque and specific fuel consumption (SFC).

Ziarati (20) working with a Perkins T6.354 diesel engine used ring sleeve spacers to restrict the nozzled volute throat area and found that engine performance was enhanced down to 56% axial restriction.

Baghery (10) used a continuously variable device based on the volute throat utilised a 'zip fastener' design - again tested on a Perkins 6.354. The 'zip fastener' design consists of two nozzle rings each with half the number of original blades and each blade half the length of the original blades. The half ring moves across into the spaces between the opposing fixed vanes restricting the volute inlet area to a maximum of 50% of its original value. The design which is based on a HOLSET H1 unit gives a mass flow turn down ratio of 46% (Fig.1.24) which is strongly non-linear being most efficient in the restricted position. Turbine efficiencies with zero restriction are somewhat worse than the base and result in a higher SFC particularly on the limiting torque curve (LTC). Tests were conducted in both steady state and transient modes. Torque back-up was considerably improved from 34 to 56% at 54 and 46% of rated speed respectively (fully open and restricted respectively). The maximum power however was derated to compensate for a mismatch between turbocharger and engine.

Transient tests were not conclusive due to the absence of smoke readings, however the enchanced air fuel ratios imply less transient smoke. Limitations to this work included cylinder pressure and compressor surge. The author advocated a variable fuel injection timing device and a more comprehensive control scheme than a simple boost

schedule to benefit part load SFC and emissions possibly based on a digital electronic closed loop and scheduling system.

1.8.2. Other VG schemes

Watson presented a paper (22) - Fig. 1.22 proposing a scheme using the conventional meridionally divided vaneless turbine housing and altering the A/R ratio (varying tongue area) by inserting a sliding section and moving the tongue to a different location. This has the effect ov moving the critical section to a point with a different cross-sectional area and achieving a full 360^{o} matching scroll. A 120^{o} arc was selected for the first prototype system which it was calculated gave a 40% reduction in area. Whilst the system was not optimised he succeeded in reducing peak torque speed from 71 to 61% of rated speed and increasing peak torque from 14 to 33%. Unfortunately the device was strongly non-linear giving zero or maximum turn down.

Berenyi et al at Teledyne Continental (5) applied a swivelling nozzle scheme to both compressor and turbine on a very high output diesel engine. Peak torque was found to occur at 65% (previously 92%) of rated speed. Torque back-up was increased to 16% from 3%. Transient performance was also enhanced.

Cummins (Chapple et al - 6) proposed a scheme based on a moveable wall within the volute which they claimed gave good results.

Aerodyne Dallas have released a VG turbocharger suitable for passenger cars and small commercial vehicles using variable area turbine nozzles in a single entry turbine case. The control scheduling of the nozzle is left to the engine manufacturer. Improved transient performance and better part-load efficiency are claimed.

1.9. Electronic Engine Controls

Over the past fifteen years there has been increasing emphasis on improving the diesel engine in terms of:-

1. legislation on emissions
2. improved fuel consumption
3. more power and torque back-up
4. tighter conformity of production units
5. more peripheral devices

These requirements are very dependent on application and country. e.g. emissions in the USA, fuel consumption and driveability in Europe.

To meet increasingly stringent specifications a number of 'add-on' hydro mechanical solutions have been evolved. These include:-

1. boost control
2. temperature and boost control advance
3. temperature control of idling speed
4. emission control valves,

each of these applications requiring a major development exercise.

At the same time analogue and digital electronic components were reducing in cost and increasing in capability and reliability. The use of electronic engine controls allows much greater flexibility in scheduling and control. The benefits resulting from electronic control can be summarised as:

1. an improvement in fuel consumption
2. lower emission levels
3. better driveability
4. better governing/speed control
5. better starting in terms of noise and smoke
6. reduction in application time

In addition peripheral features such as cruise control, trip computer, instrumentation displays and diagnostics can easily be implemented.

Full authority digital control systems are advantageous where the control requirements are very complex and also where there is a need for programmability.

1.10 Current Programme of Work

The work described herein is primarily experimental and is a logical extension of Baghery's (10) work applied to a larger (4") frame size HOLSET designed turbocharger. The work consisted of the following:

1. a new test bed was constructed
2. an electronically closed loop control system was implemented with digitally stored characteristics. An optimised transient strategy was also determined
3. the limitations imposed by mechanical constraints during testing were investigated theoretically.

1.10.1. Construction of a new test bed

In order that the benefits accuring from a digital engine management system can be quantified accurately when compared with the mechanically optimised base engine, a new test bed was constructed. The specifications can be found in the relevant SOCIETY OF AUTOMOTIVE ENGINEERS (SAE) standards (45-53). The test bed is fully described in Chapter 2.

1.10.2. Electronic engine control

The object of this work was to control and optimise the variable geometry turbocharger as fitted to a Leyland TL11 automotive diesel engine. The engine displaces 11ℓ and produces a maximum power of 190 kW at 2100 rev/min. This represents the premium segment of the automotive market.

The variable geometry prototypes all based on the volute exit area were designed and developed by the HOLSET ENGINEERING CO.LTD.

Control was facilitated by a digital controller based on the closed loop and stored characteristics. To enhance the variable geometry capability and allow greater flexibility a variable fuel injection timing device and an electronic governor were designed and built at

the University. The associated interfaces and actuators for the three parameters were evolved specifically for this project. The development of the control system is fully described in Chapter 3.

The test programme consisted of the following:

1. steady state testing of the standard engine
2. transient testing of the standard engine
3. steady state testing of the three variable geometry prototypes
4. steady state testing of the final dynamically variable prototype turbocharger
5. transient testing of the dynamically variable prototype turbocharger.

1. Steady State Tests

The standard engine was rigorously tested to evaluate a datum performance for steady state conditions. A number of variable geometry prototypes were then assessed on the limiting torque curve (LTC) for various restrictions. The final prototype was fully tested and the parameters controlled such as to optimise engine SFC over the whole torque speed range. Fuelling was increased to take advantage of the variable geometry turbocharger with due regard to smoke, turbine inlet temperature and cylinder pressure. Maximum power remained the same at 190 kW.

The likely benefits accruing from an optimised configuration were assessed by running a 'back to back' test with the base build on a Route and Simulated Vehicle Program (RSVP). These results together with all the steady state tests are reported in Chapter 4.

2. Control System

The positions of the control parameters corresponding to optimum engine conditions were noted and formed arrays which were stored digitally within the controller. In operation the arrays formed a closed loop 'look up table' as a function of engine speed and load such that the

engine always operated at its maximum efficiency.

3. Transient Work

The transient tests were of the constant speed fuel step type where load was applied by a hydrostatic dynamometer. Engine response was assessed by load acceptance and smoke emission. The standard engine was first tested to determine a datum performance. The different VG configurations were then tested. Finally a control strategy investigation was conducted with the final build (Mk II b) unit.
These tests are fully described in Chapter 5.

1.10.3. Theoretical investigation

A theoretical model was developed to predict engine performance based on the quasi-steady filling and emptying method. This was used to predict engine performance when constaints imposed by mechanical limitations were reached. The parameters investigated included better turbomachinery and turn down efficiencies, improved engine breathing and the effects of lowering compression ratios.

Full details of these predictions can be found in Chapter 6.

Finally Chapter 7 presents the conclusions from this work together with suggestions for further work.

LIST OF FIGURES

LIST OF FIGURES Cont/d:-

NOTE :

At 25% load, petrol consumption is nearly double and at 75% load it is still more than half as much again.

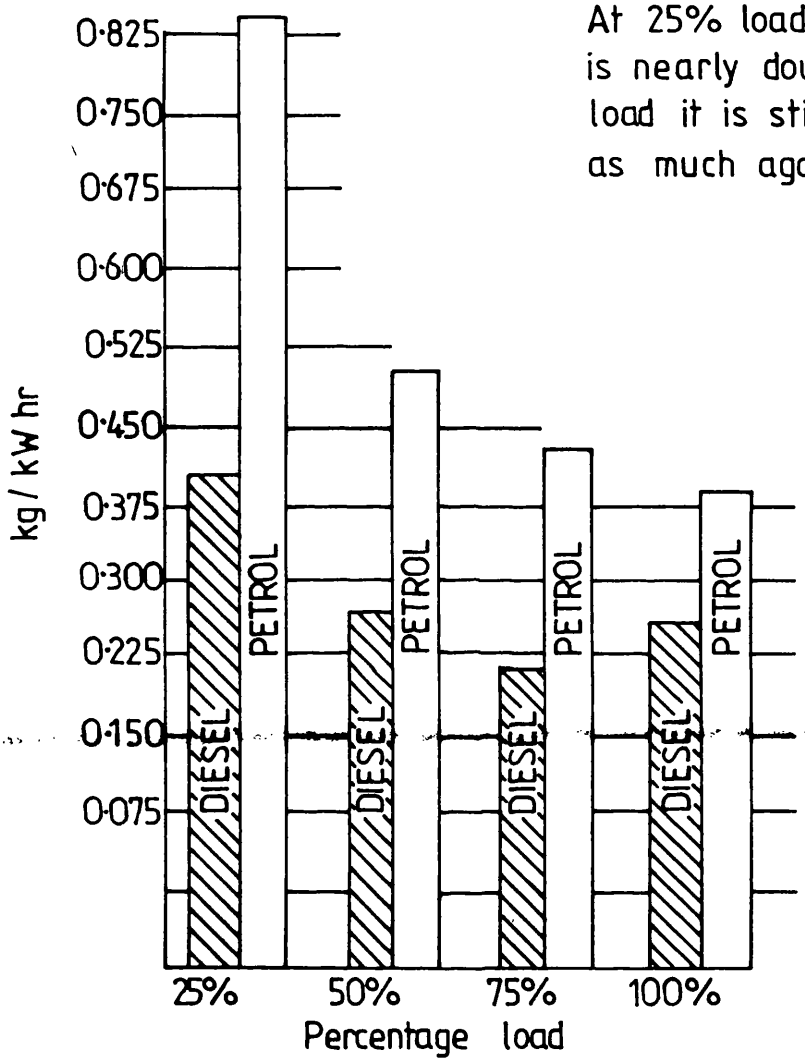

FIG.1.1 COMPARISON BETWEEN PETROL AND DIESEL 8L ENGINES FUEL CONSUMPTION

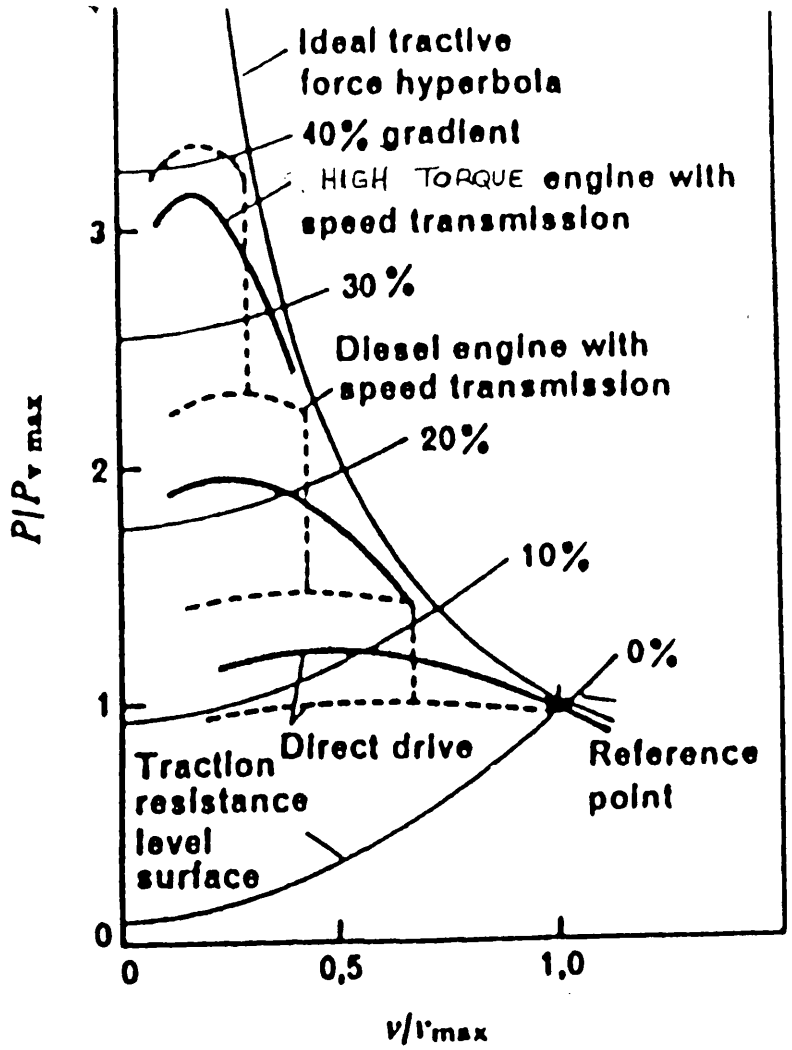

Performance map ~ CONSTANT OUTPUT ENGINE CHARACTERISTIC fig 1.2

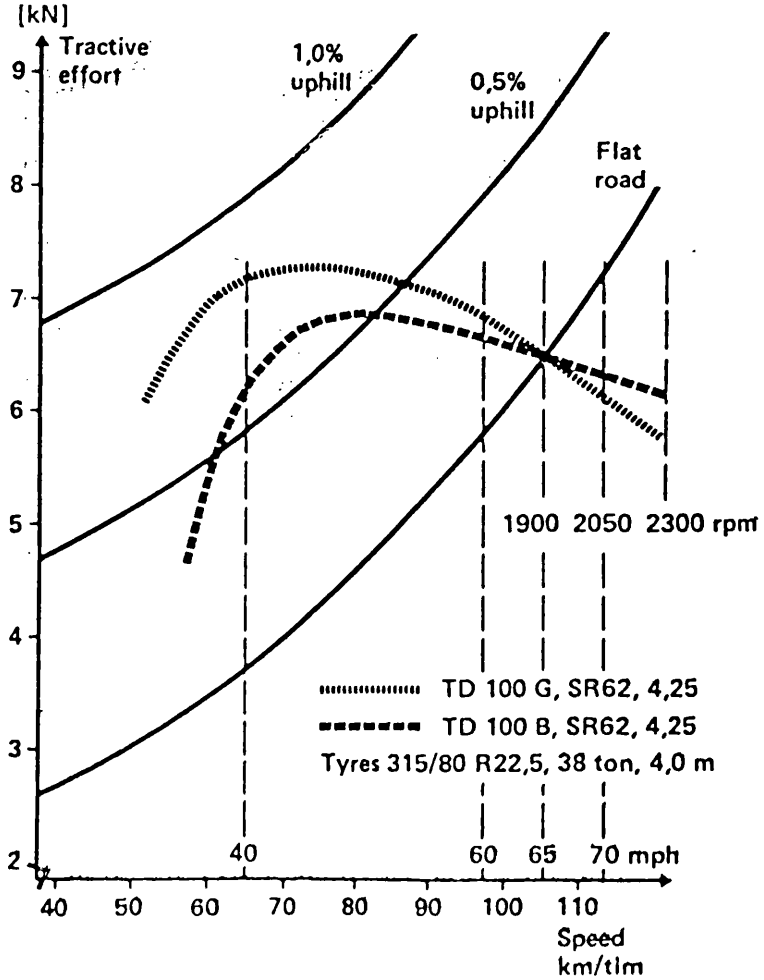

COMPARISON OF TORQUE RISE WITH HILL CLIMBING ABILITY. fig 1.3

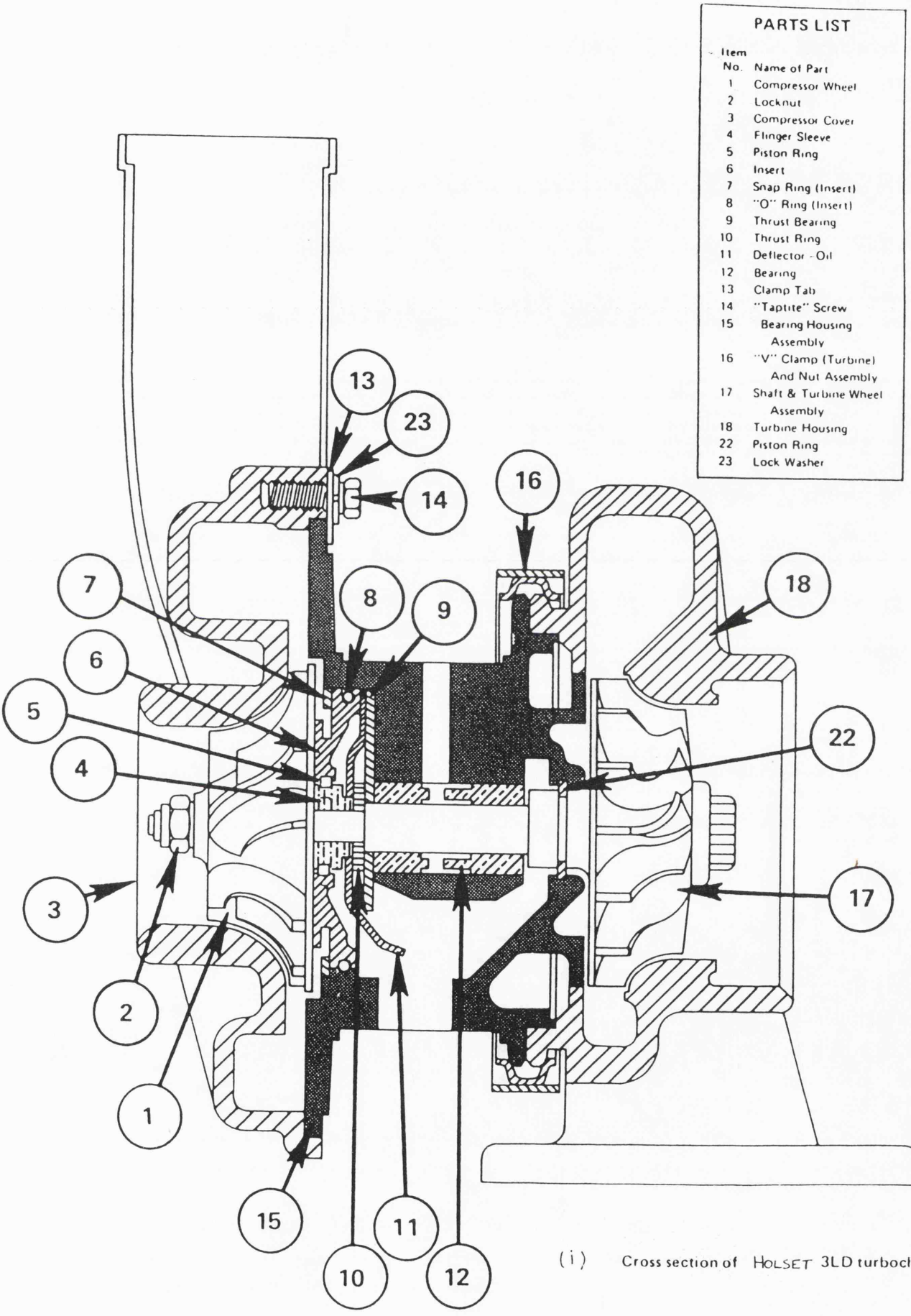

(i) Cross section of HOLSET 3LD turbocharge

TURBOCHARGER FORM AND CHARACTERISTIC - fig 1.4

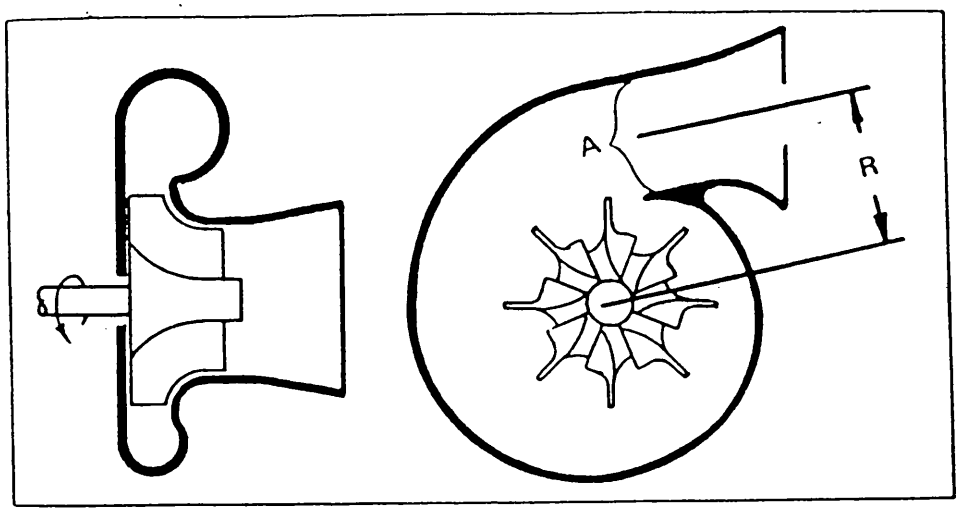

(a)

VANELESS TURBINE HOUSING

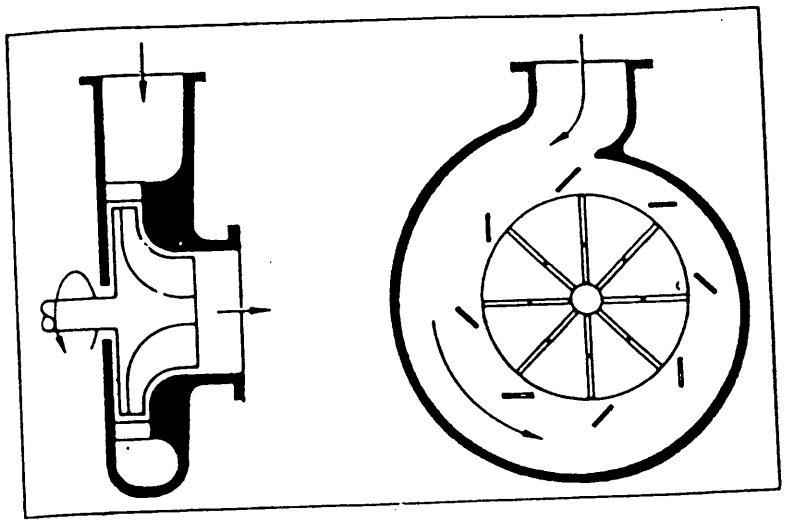

(b)

VANED TURBINE HOUSING

(ii) COMARISON OF VANED AND VANELESS RADIAL TURBINE

fig 1.4 CONTD

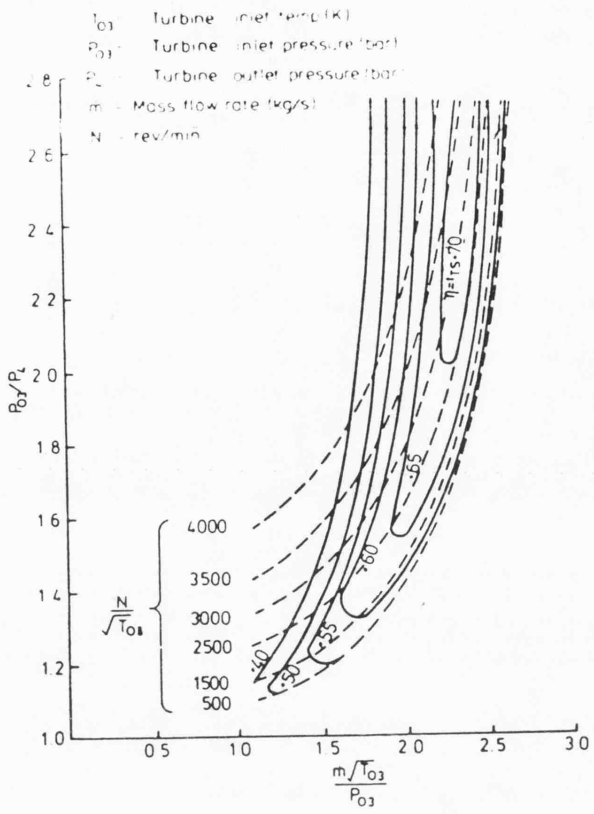

Radial flow turbine characteristic (ref 13)

(a)

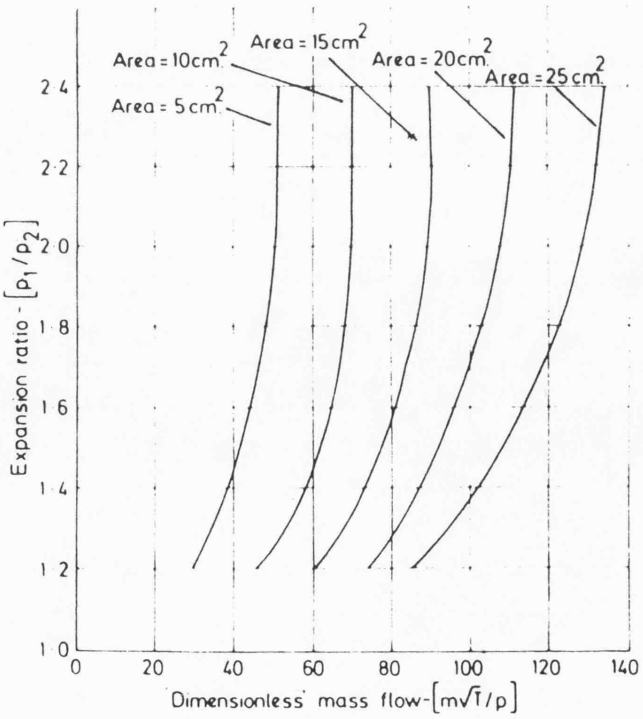

Swallowing capacity of different turbine housings suitable for 125 kW 5.5l truck engine

(b)

RADIAL INFLOW TURBINE CHARACTERISTIC (iii)

fig 1.4 CONTD

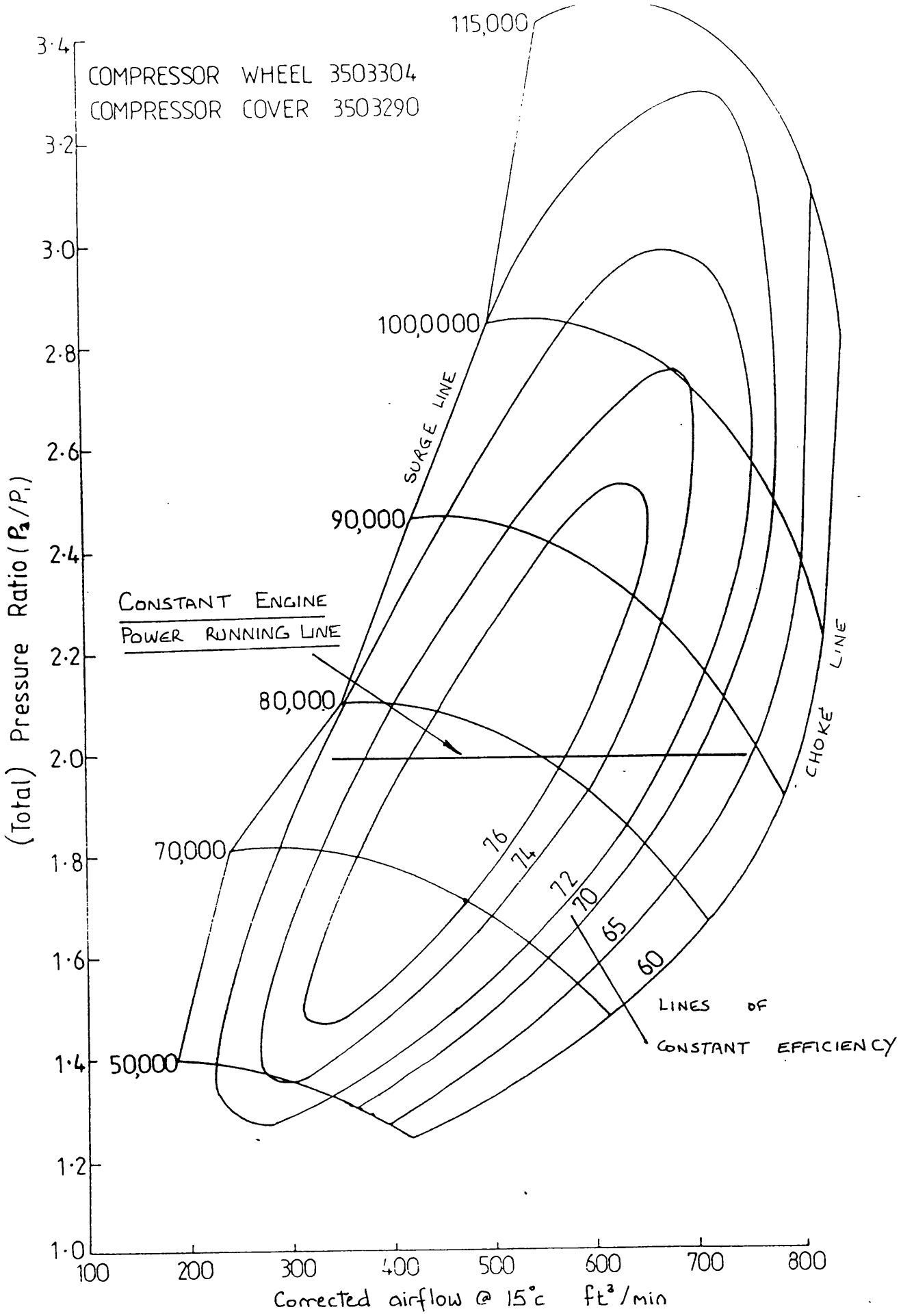

CENTRIFUGAL COMPRESSOR CHARACTERISTIC

fig 1.4 CONTD

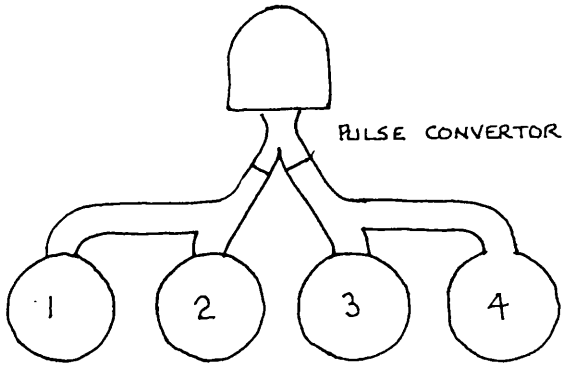

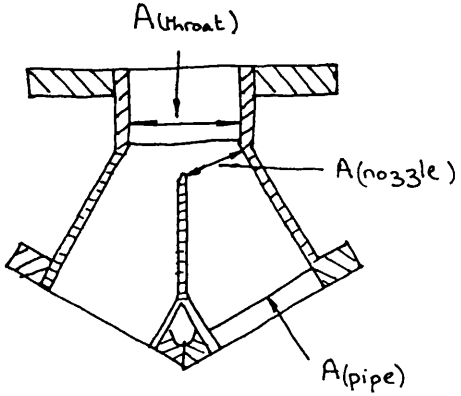

Area ratio (nozzle) = A_N / A_P (0.65 - 0.80)

Area ratio (throat) = $A_{TH} / 2A_P$ (0.5 - 1.0)

fig 1.5 EXHAUST MANIFOLD ARRANGEMENT (FOUR CYLINDER ENGINE) AND PULSE CONVERTOR DETAILS

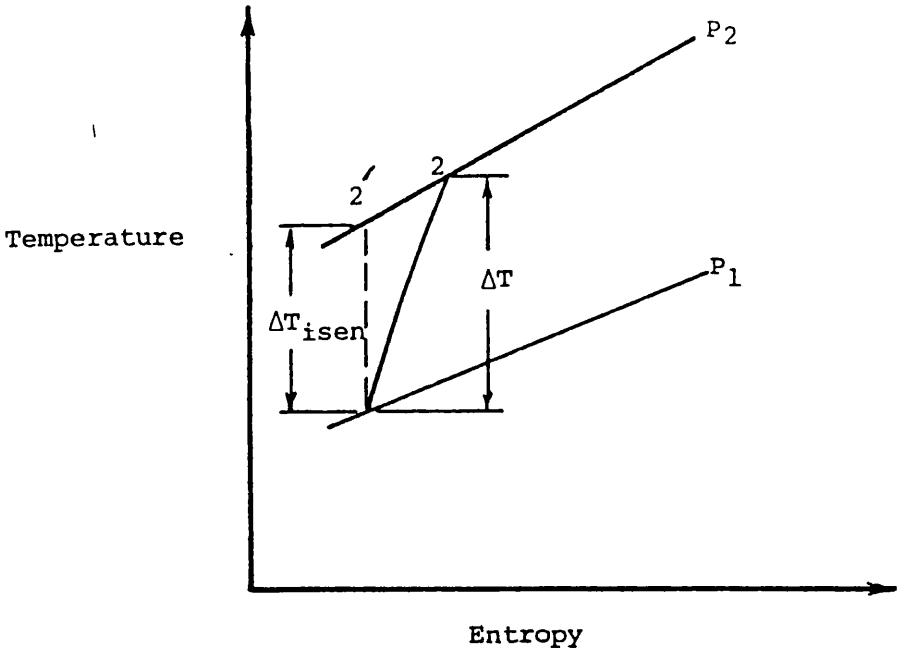

(a) Temperature - entropy diagram for compression

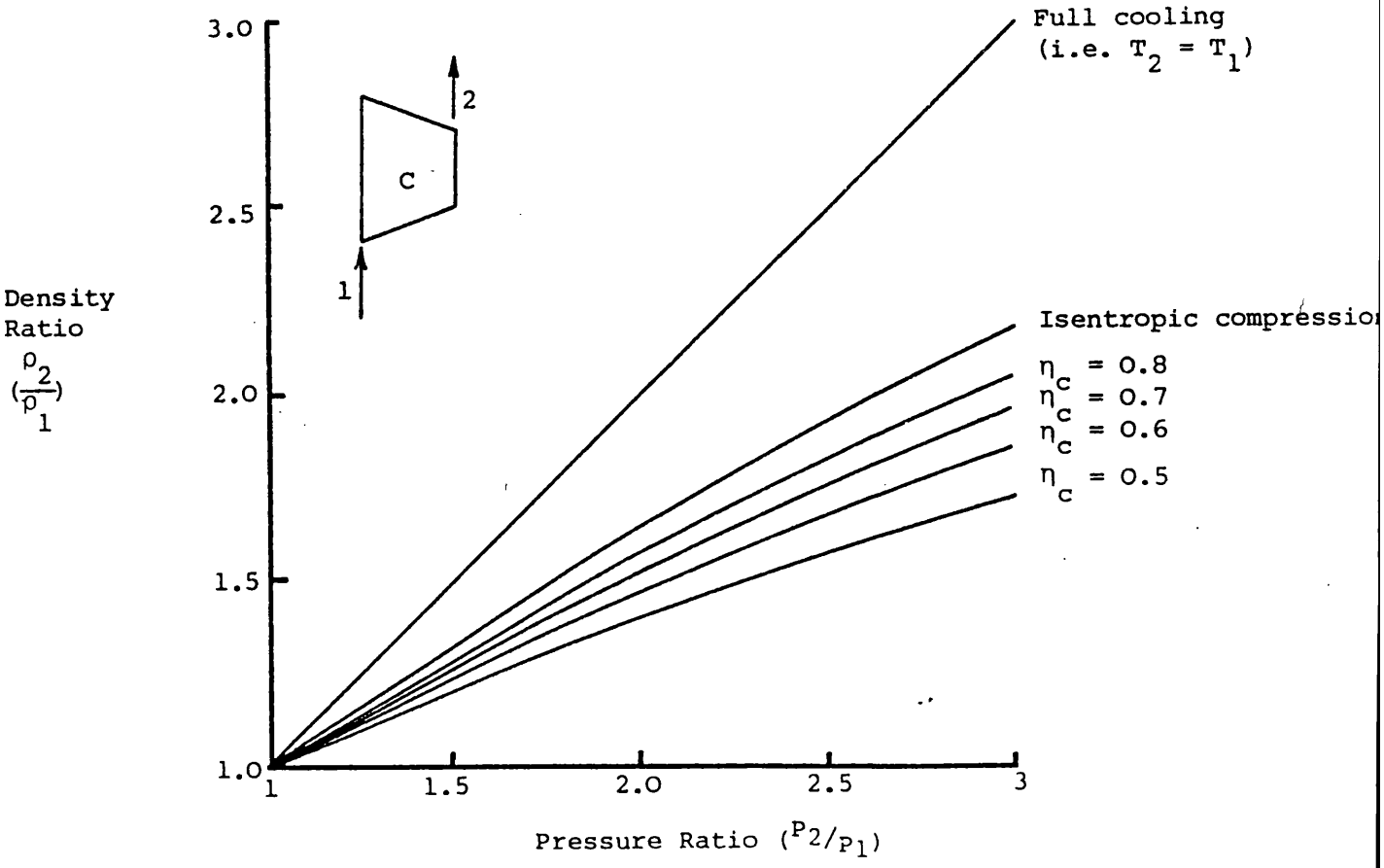

(b) Effect of compressor efficiency on air density in the inlet manifold

ADVANTAGE OF AFTERCOOLING fig 1.6

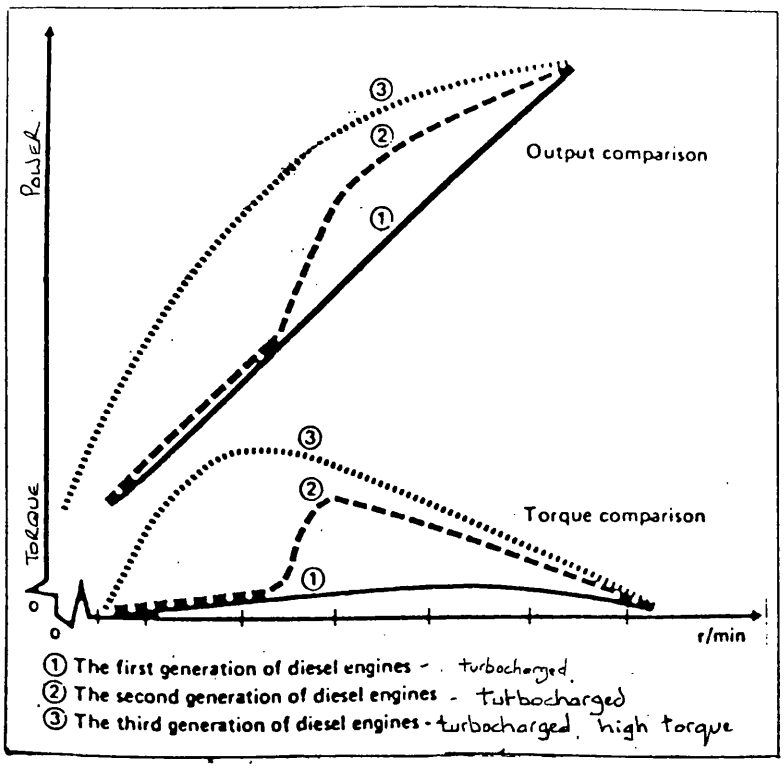

fig 1.7 MATCHING THE TURBOCHARGED ENGINE

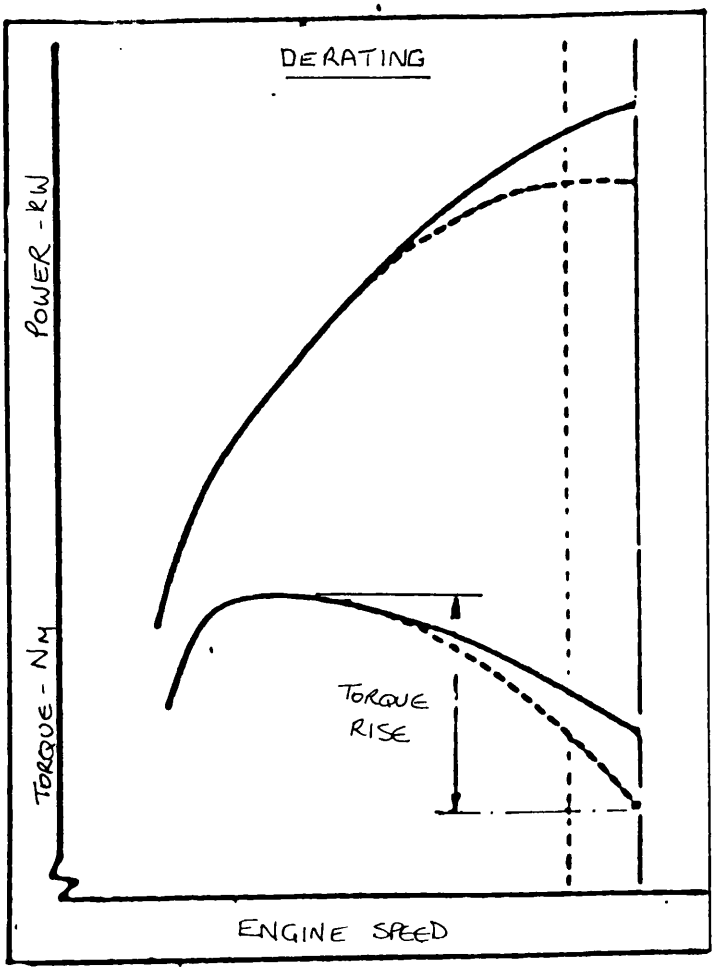

HIGH TORQUE FORMULA ENGINES fig 1.8

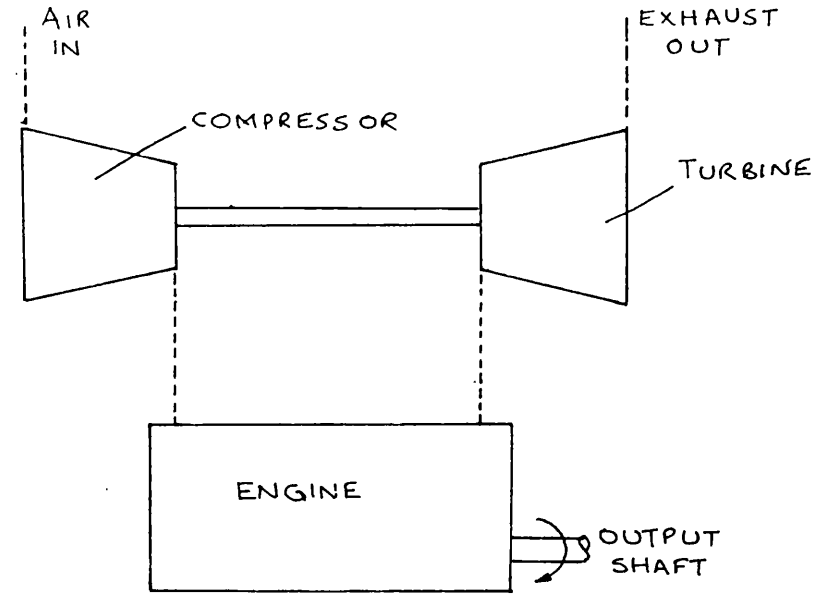

(a) SINGLE STAGE TURBOCHARGED ENGINE

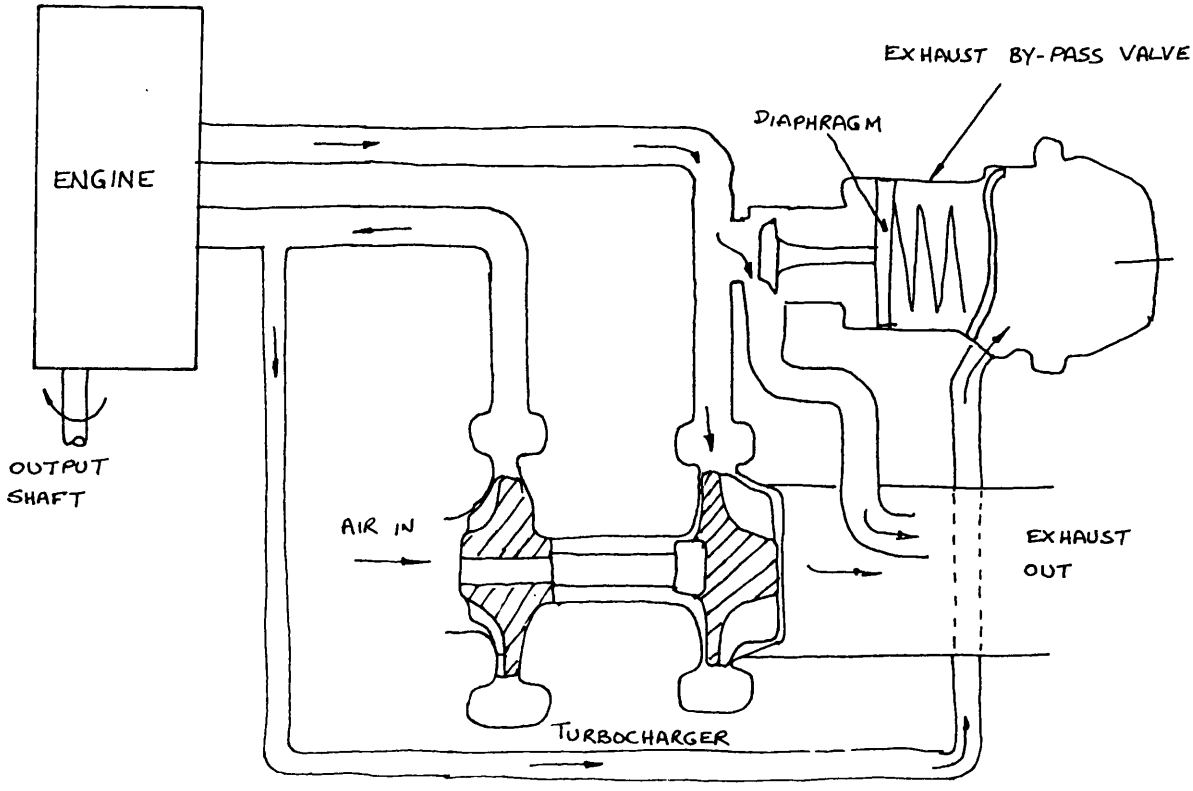

(b) SINGLE STAGE TURBOCHARGED ENGINE - WASTEGATED

fig 1.9 SCHEMATIC SINGLE STAGE TURBOCHARGED ENGINE

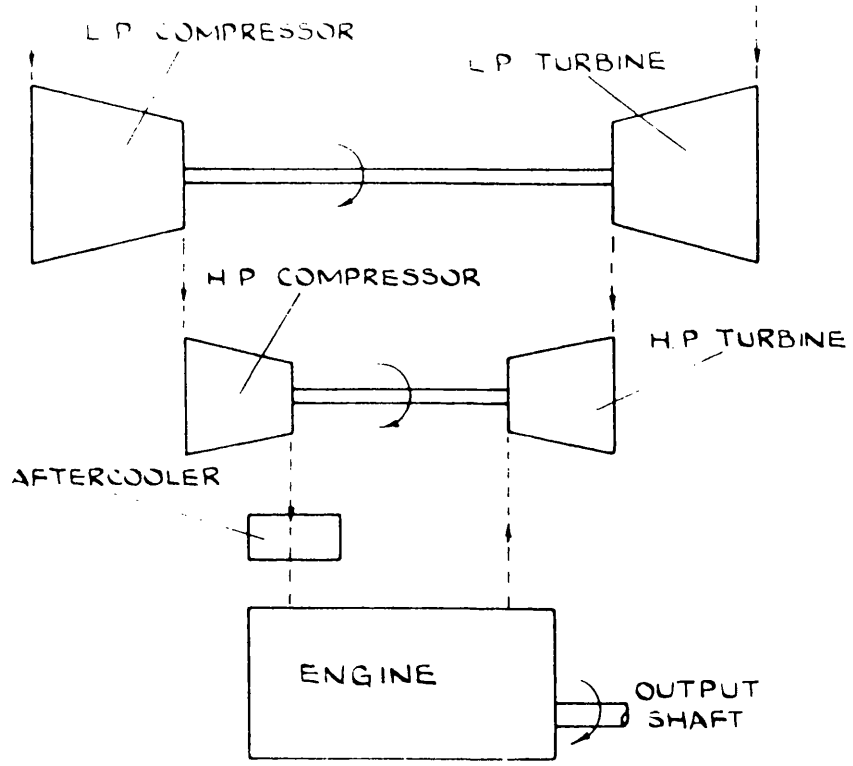

FIG. 1.10 TWO STAGE TURBOCHARGED ENGINE

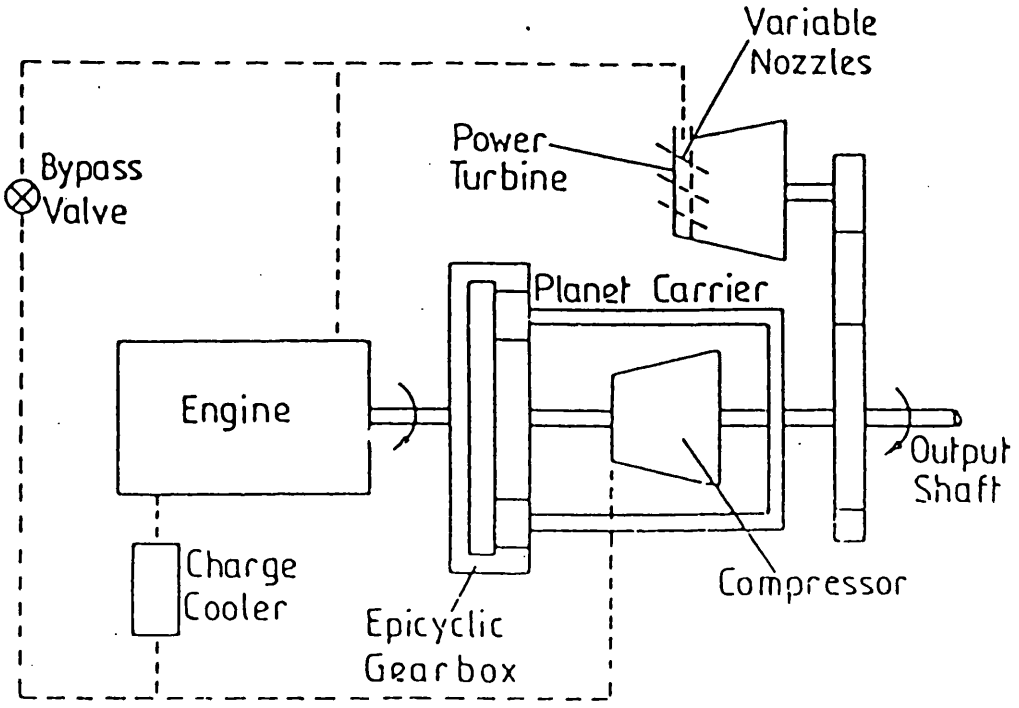

Fig 1.11 DIFFERENTIAL COMPOUND ENGINE

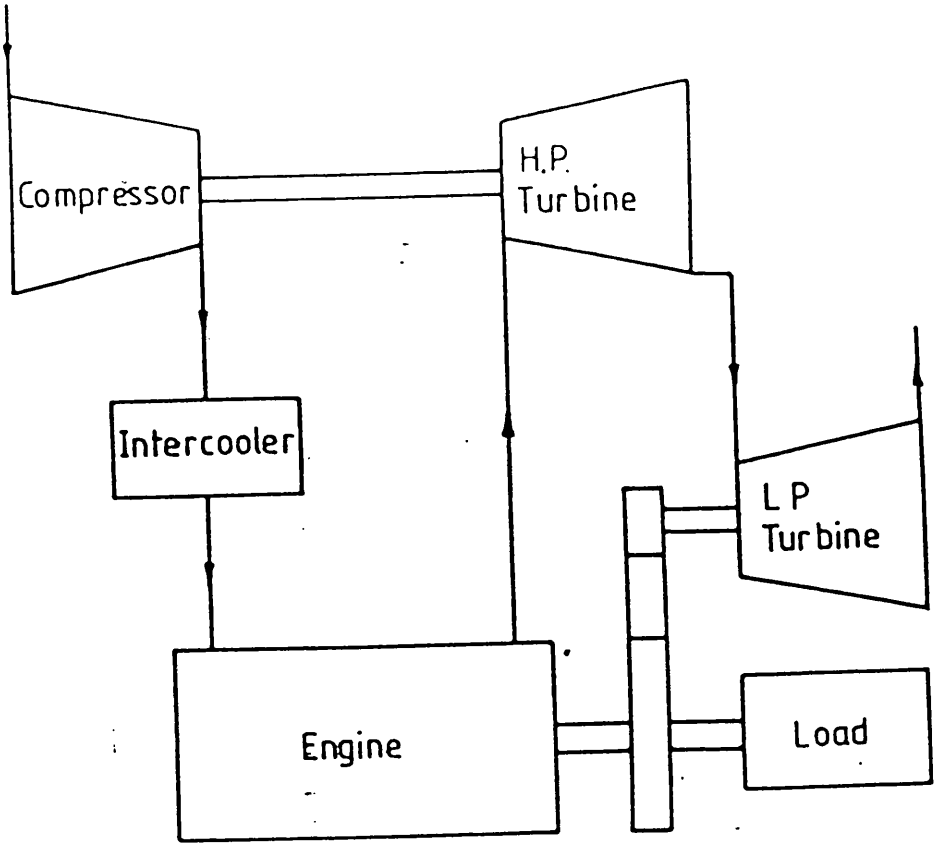

FIG. 1.12 CUMMINS COMPOUND ENGINE SCHEME

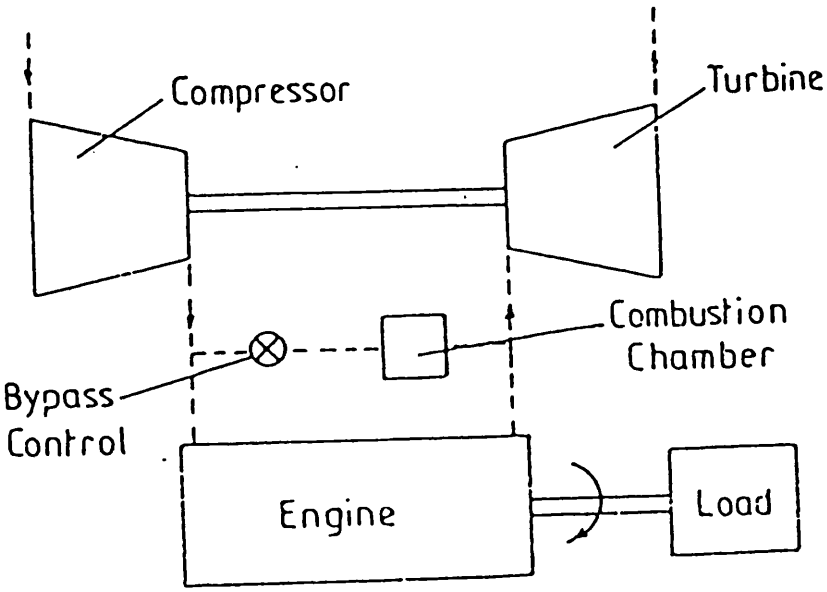

Fig. 1.13 The Hyperbar, A System With Secondary Combustion Chamber.

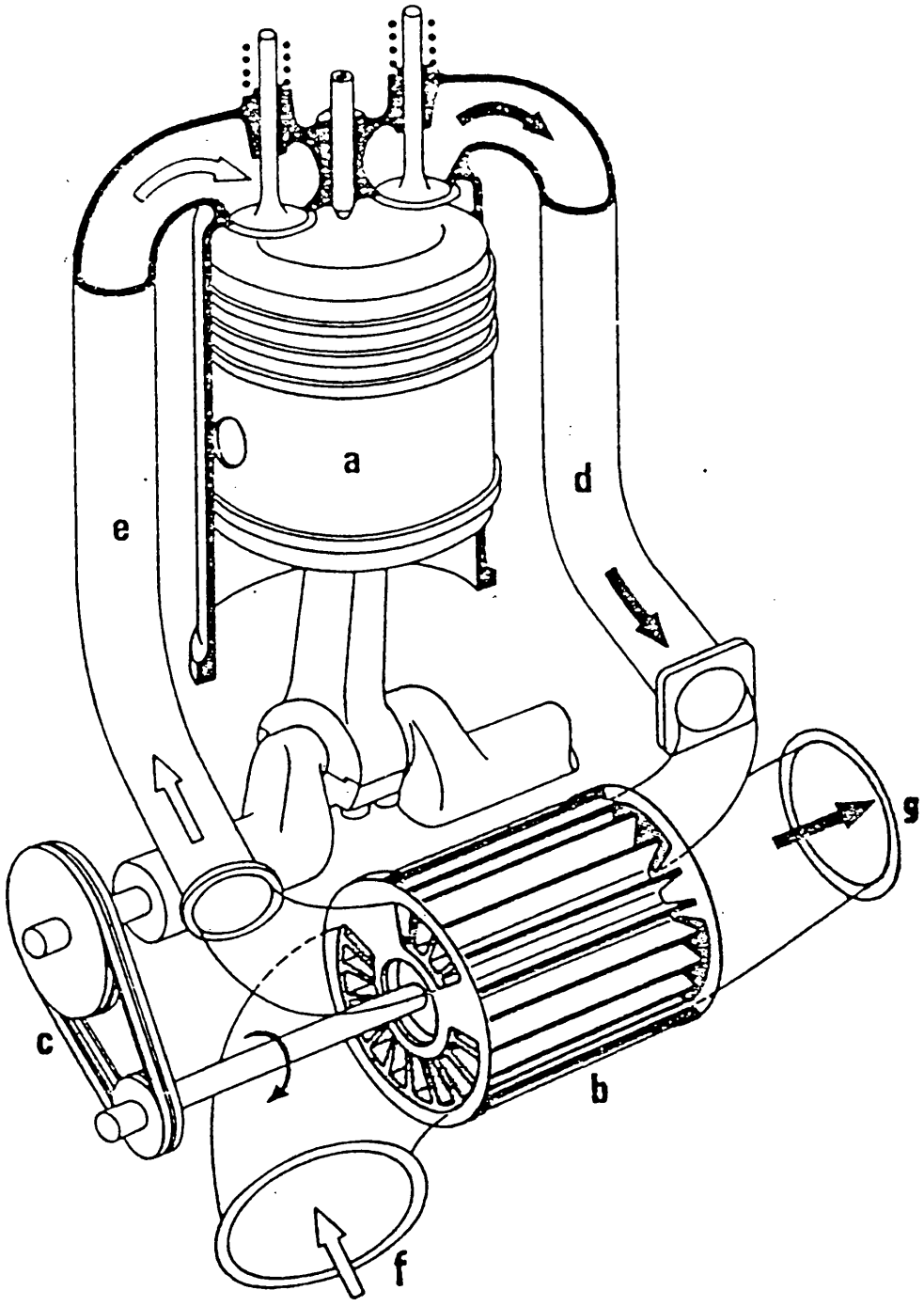

COMPREX: Pressure -wave Machine

as a super-charger

a: Engine
b: Cell-wheel
c: Belt drive
d: High-pressure gas
e: High-pressure air
f: Low-pressure air
g: Low-pressure gas

FIG. 1.14 COMPREX SYSTEM

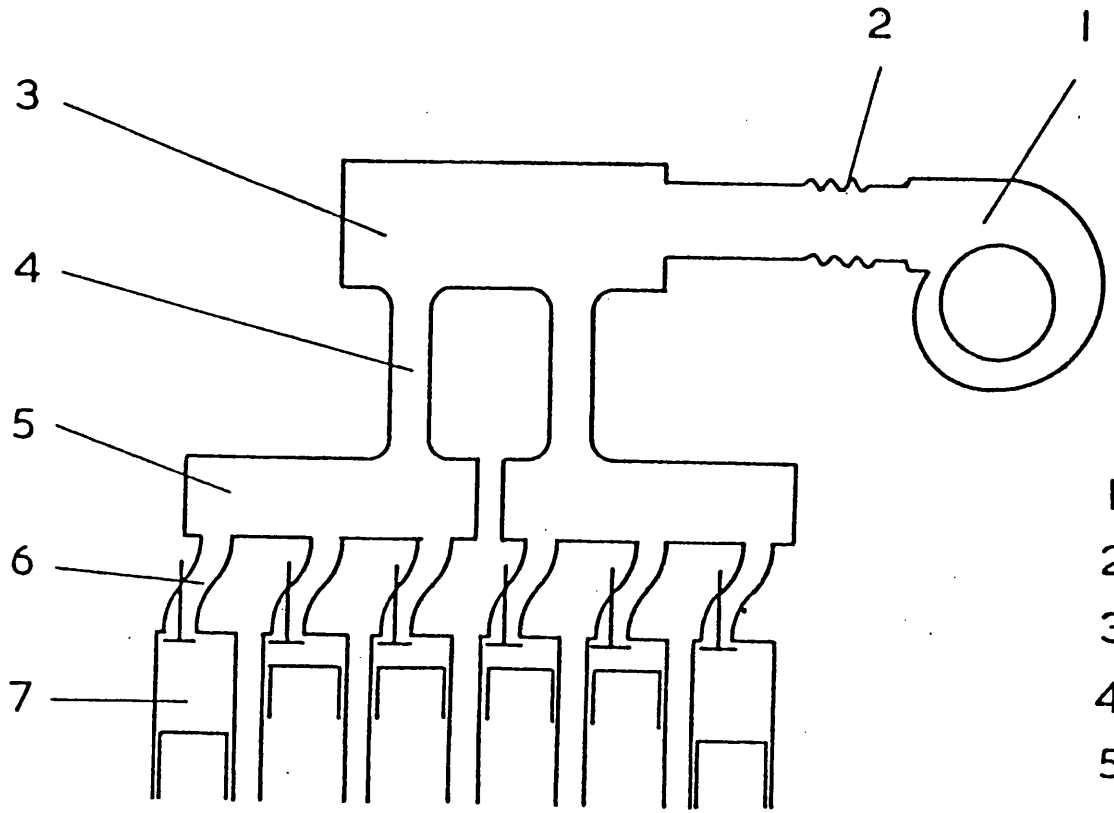

1. Turbocharger
2. Connecting pipe
3. Damping volume
4. Resonance pipe
5. Resonance pipe
6. Inlet duct
7. Cylinder

fig 1.15 CSER RESONANT SYSTEM

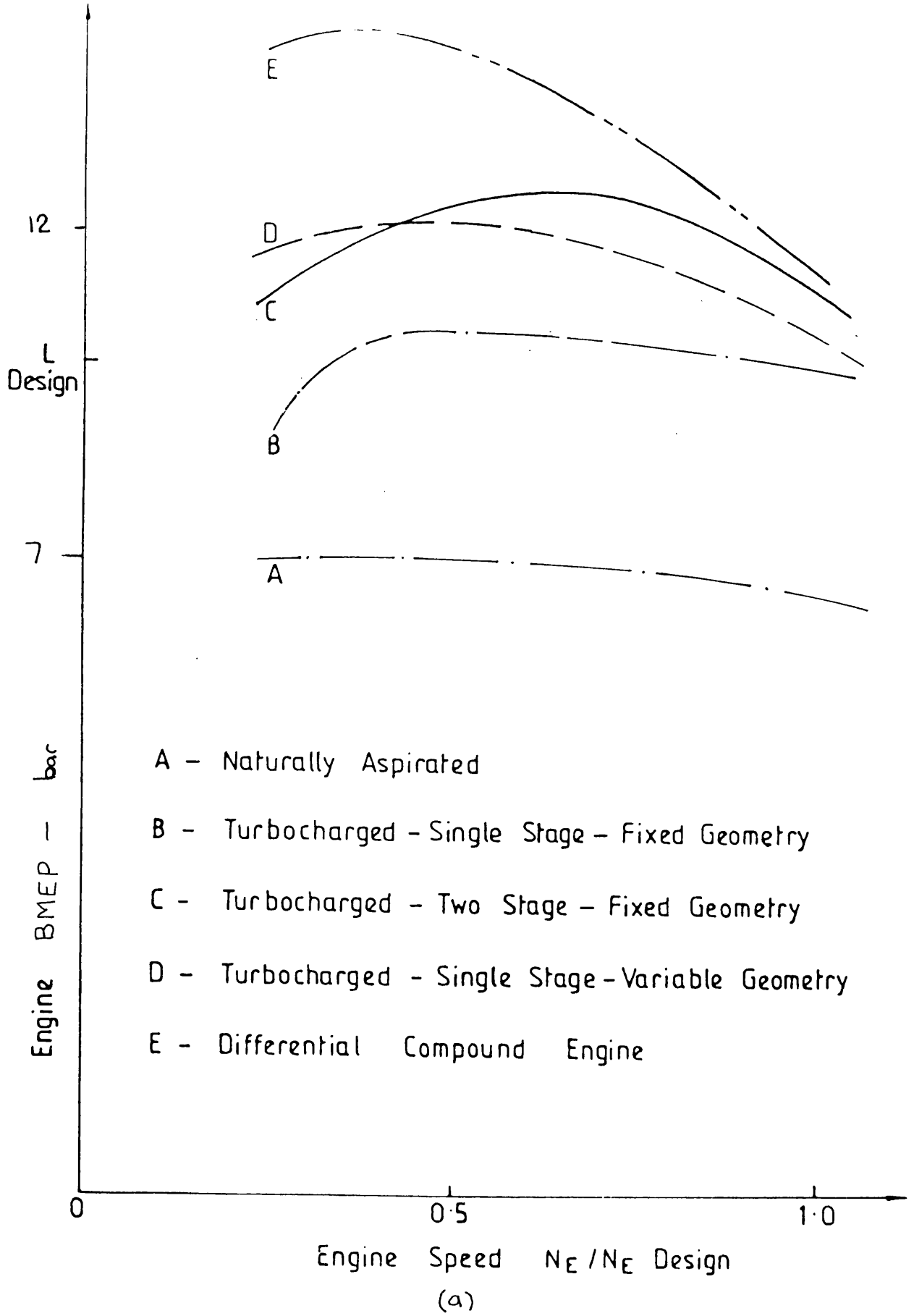

FIG. 1 16 STEADY STATE TORQUE AND ACCELERATION CHARACTERISTICS OF DIFFERENT PRESSURE CHARGING SYSTEMS

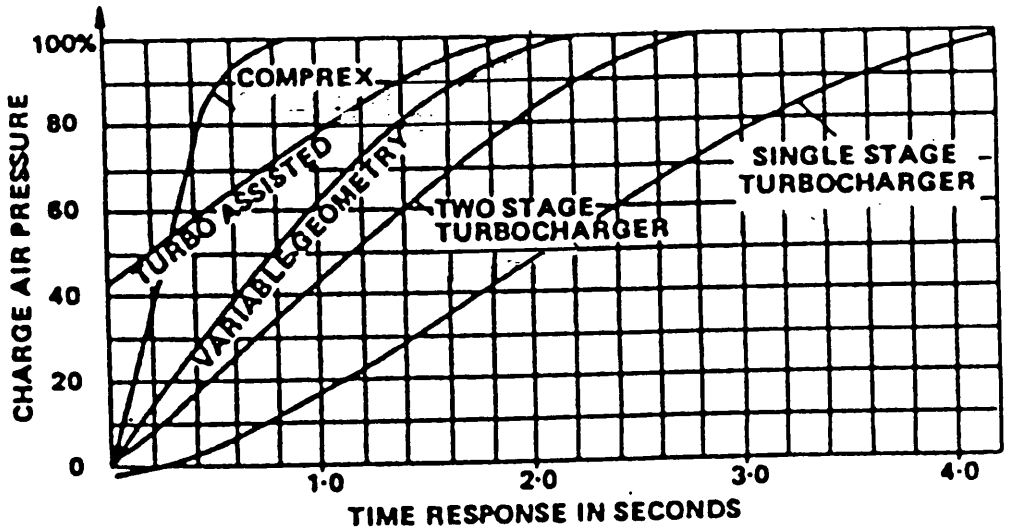

Charge air response. Time characteristic of several rapid boost schemes for various degrees of turbocharging.

(b)

fig 1.16 CONTD

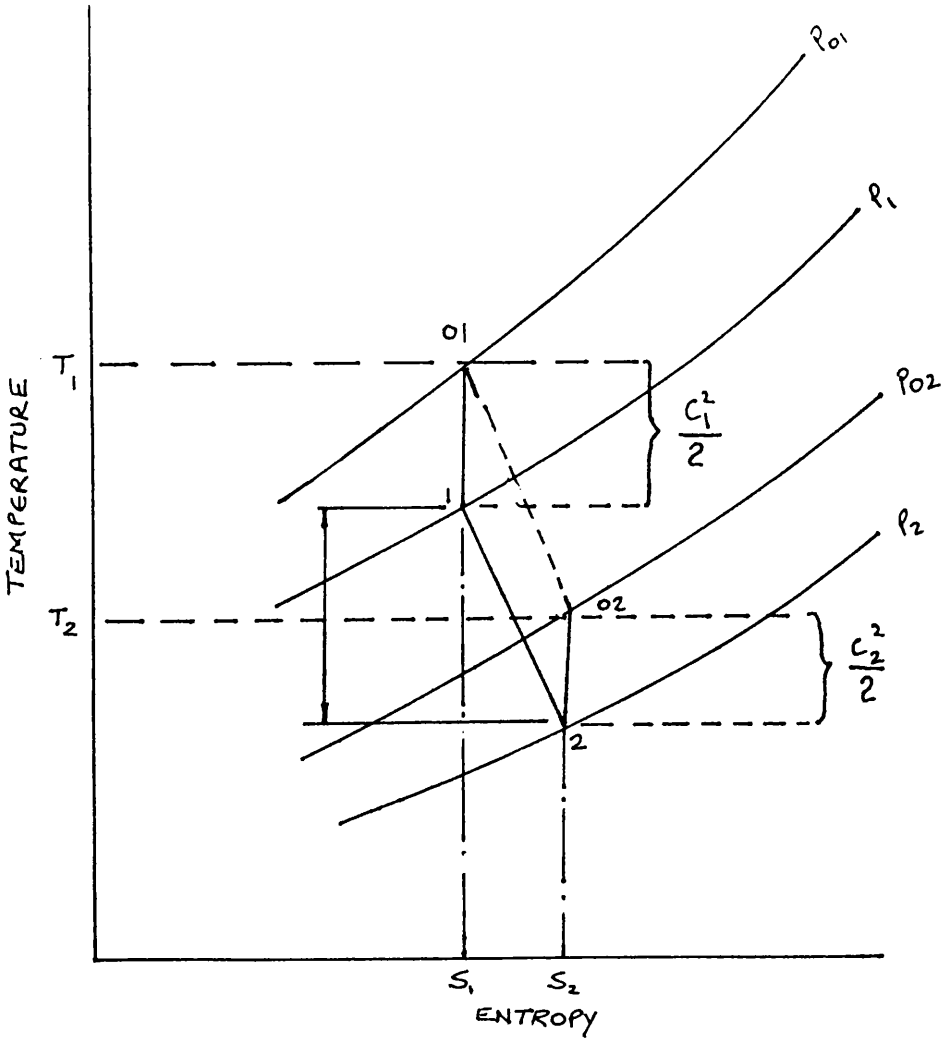

TEMPERATURE - ENTROPY DIAGRAM FOR A RADIAL TURBINE ROTOR

(a)

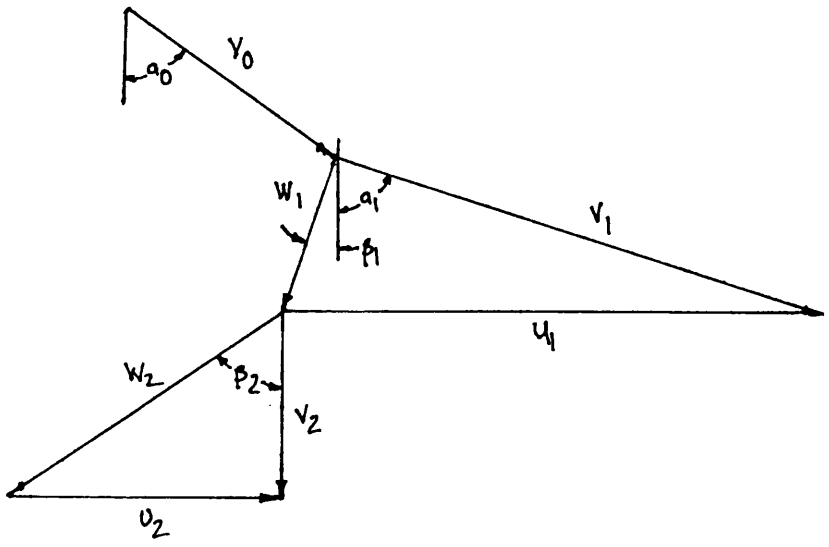

VELOCITY DIAGRAM

(b)

T-S AND VELOCITY DIAGRAM FOR I.F.R TURBINE fig 1.17

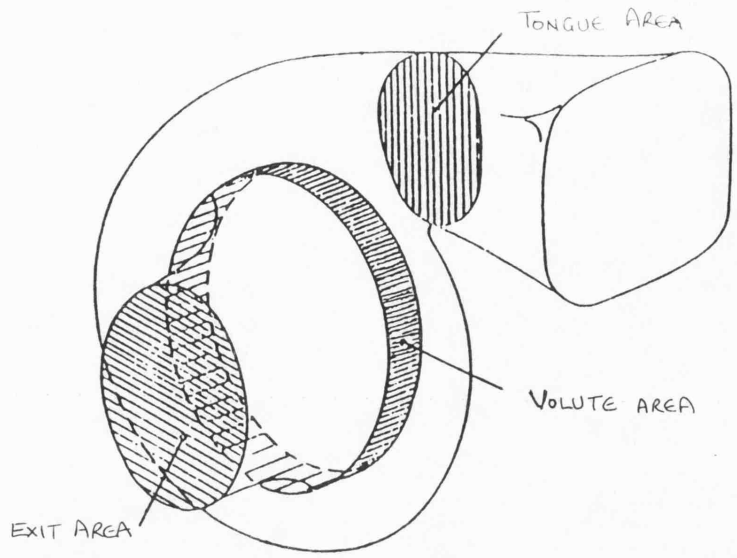

Fig 1.18 Potential control areas in the turbine flow path

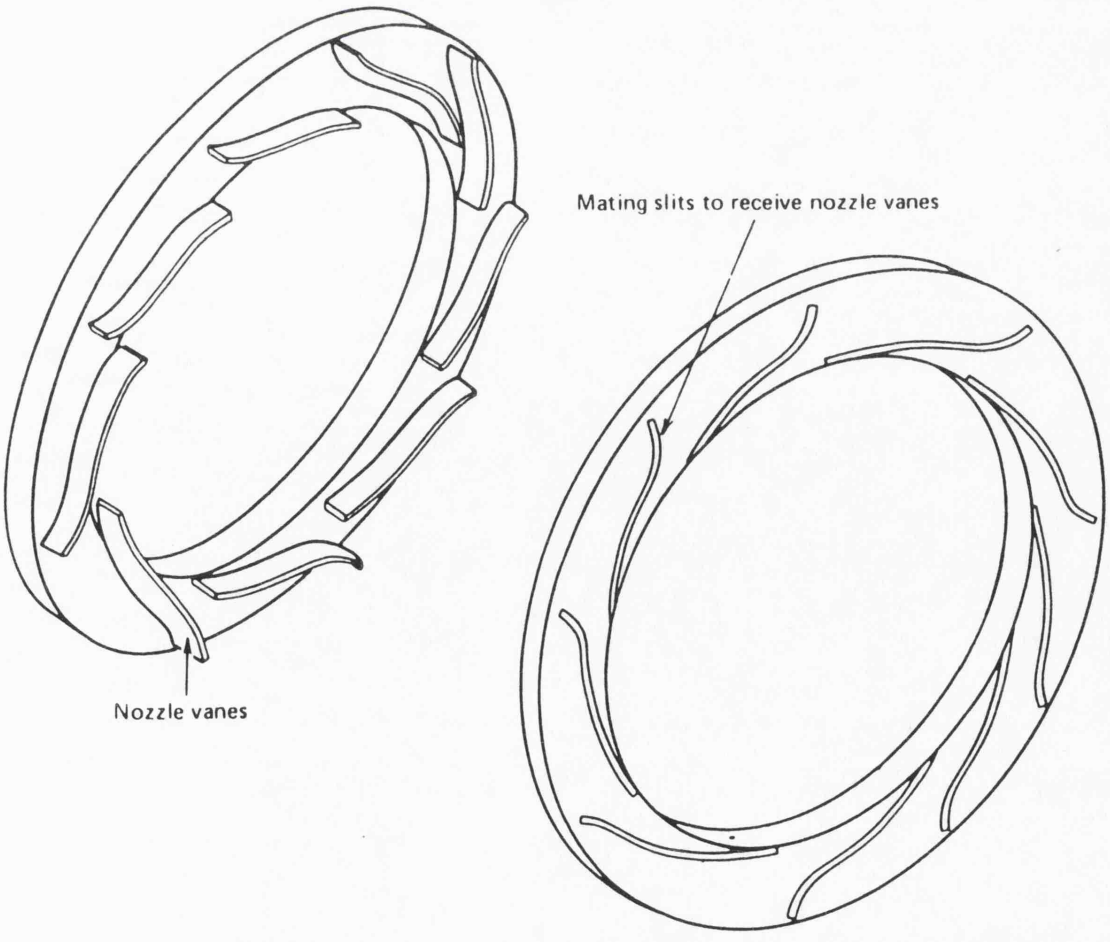

(a) Variable nozzle "mating plate" schematic. (ref 12)

fig 1.19 VG SCHEMES BASED ON VOLUTE AREA

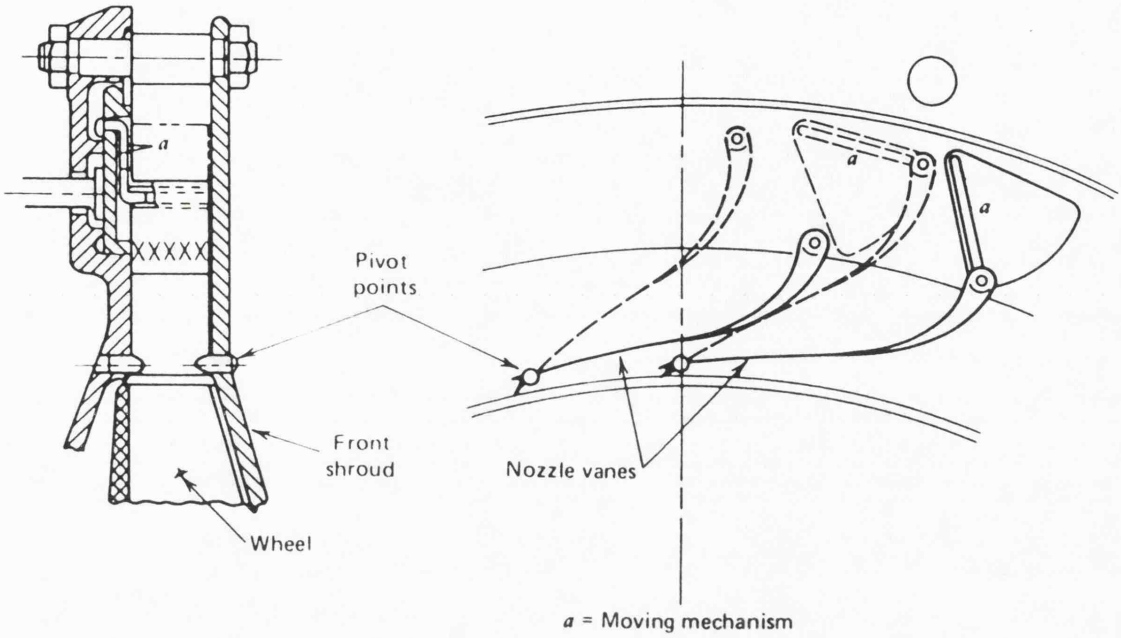

(a)

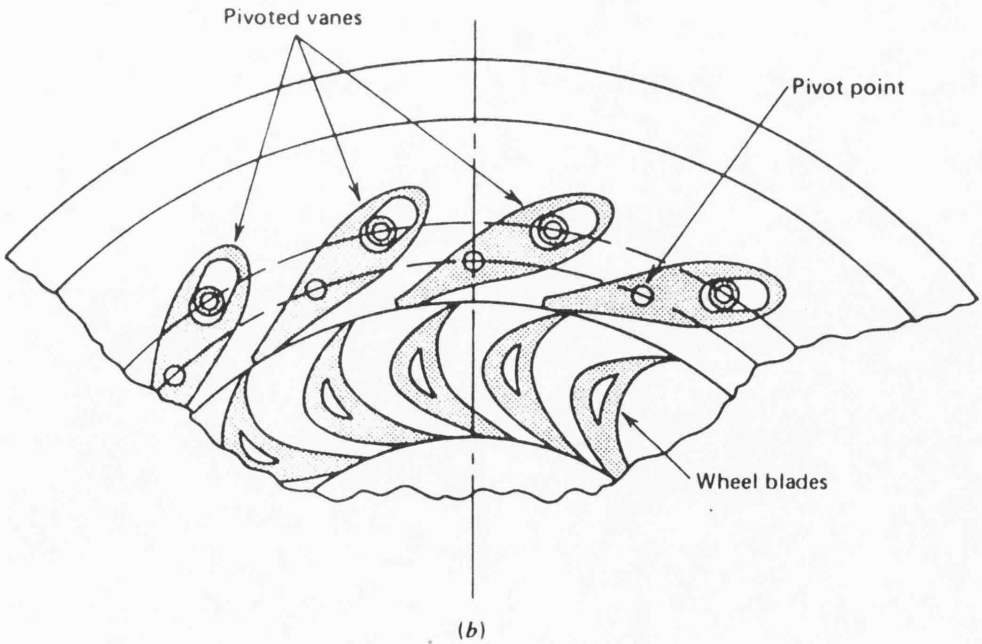

(b)

(b) Schematics of variable nozzles with pivoted vanes (ref.12)

(b)

fig 1.19 CONTD

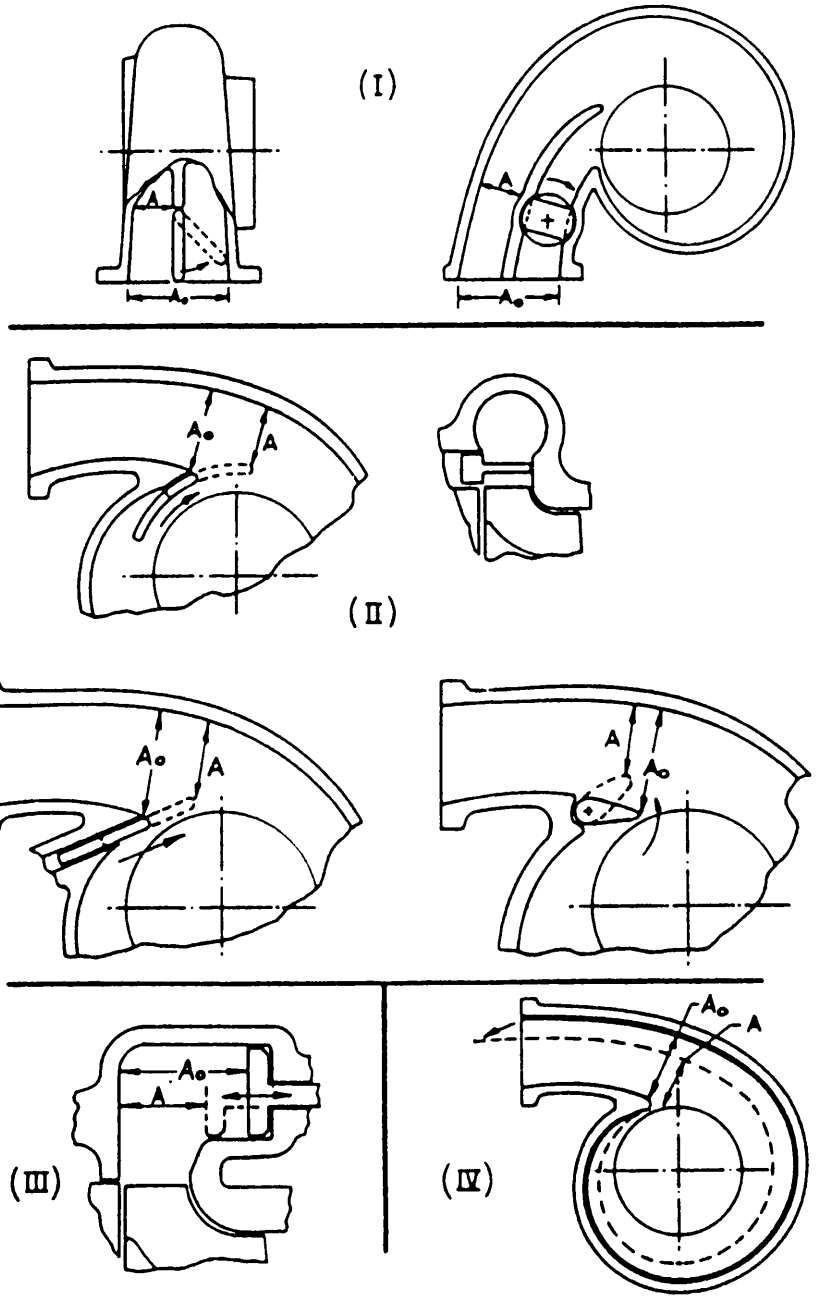

Fig 1.20 Schematics showing control on the tongue area (ref 21)

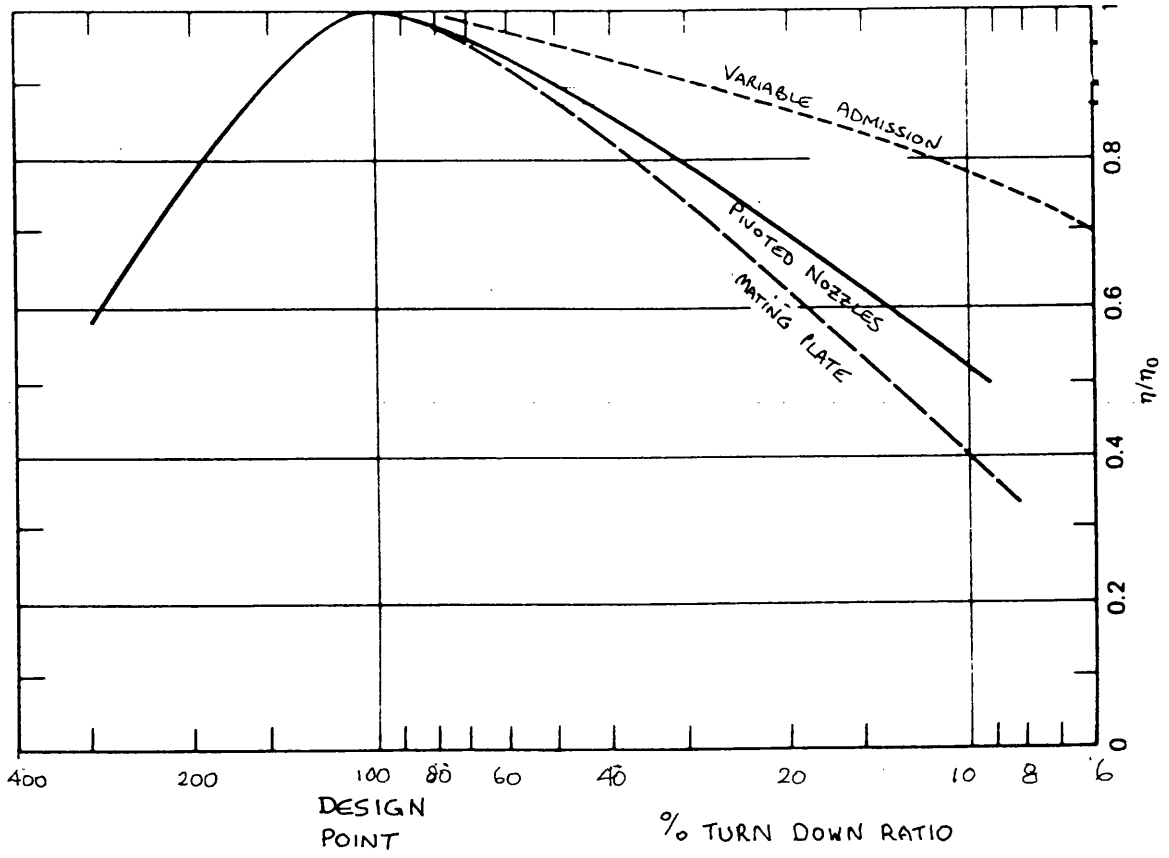

fig 1.21 VARIABLE NOZZLE EFFECTS IN RADIAL TURBINE

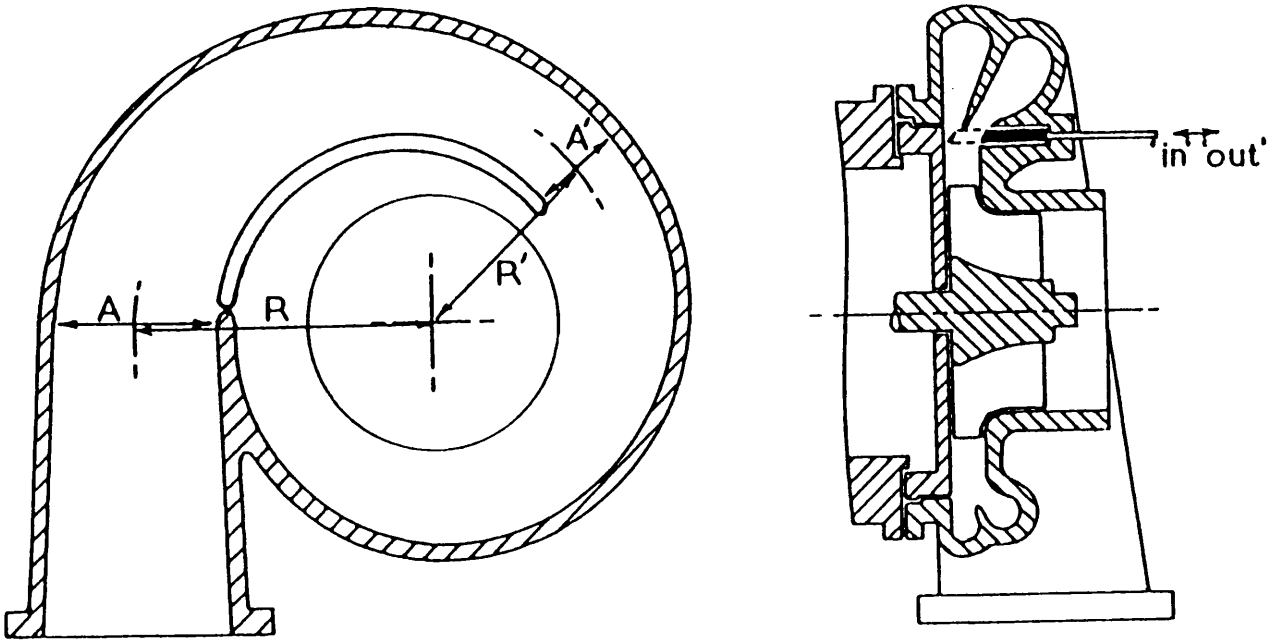

Fig 1.22 Variable geometry turbocharger schematic (ref 22)

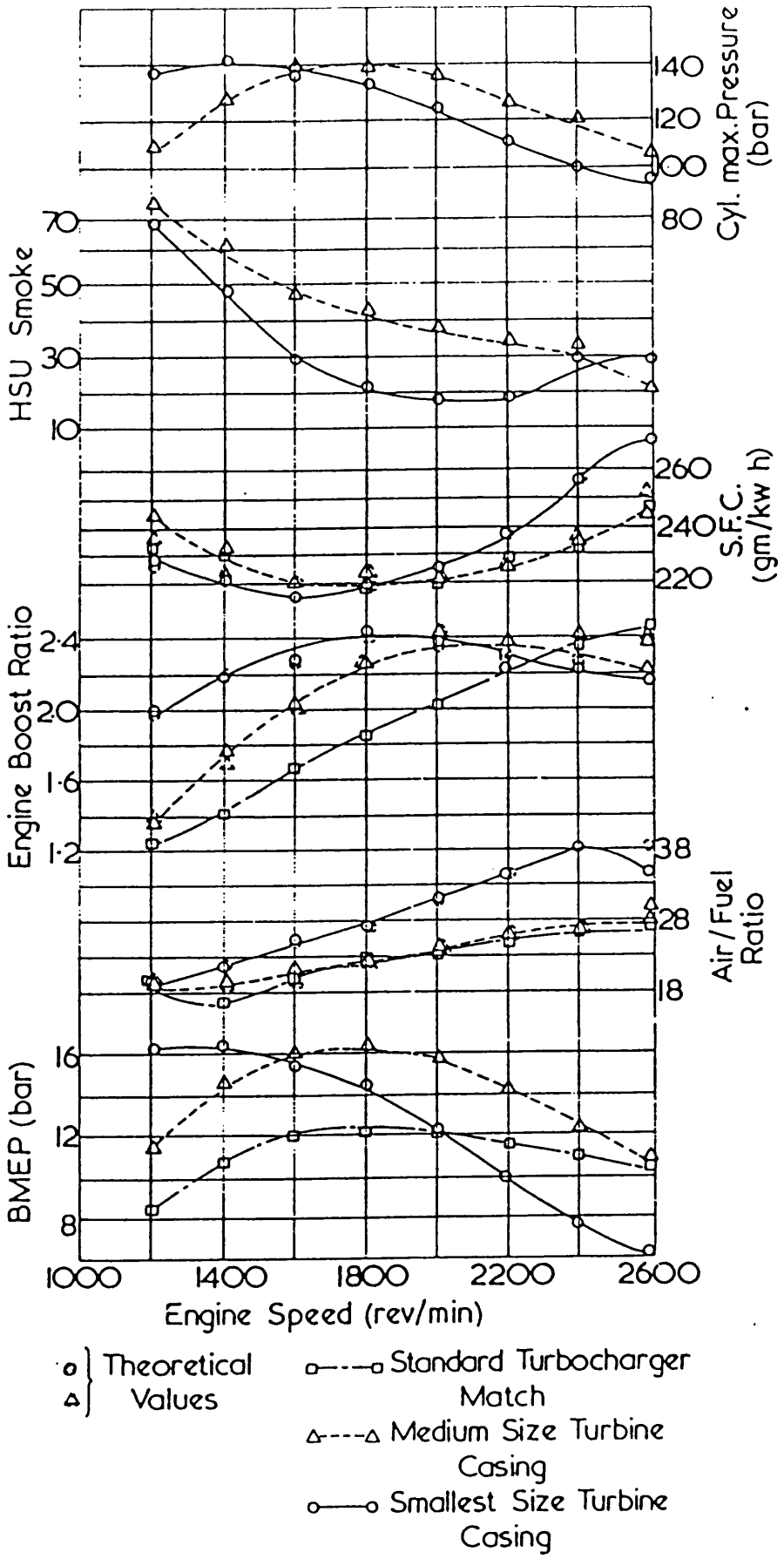

Fig.1.23 **Performance of Leyland 520 Engine Using Three Different Turbine Casings.**

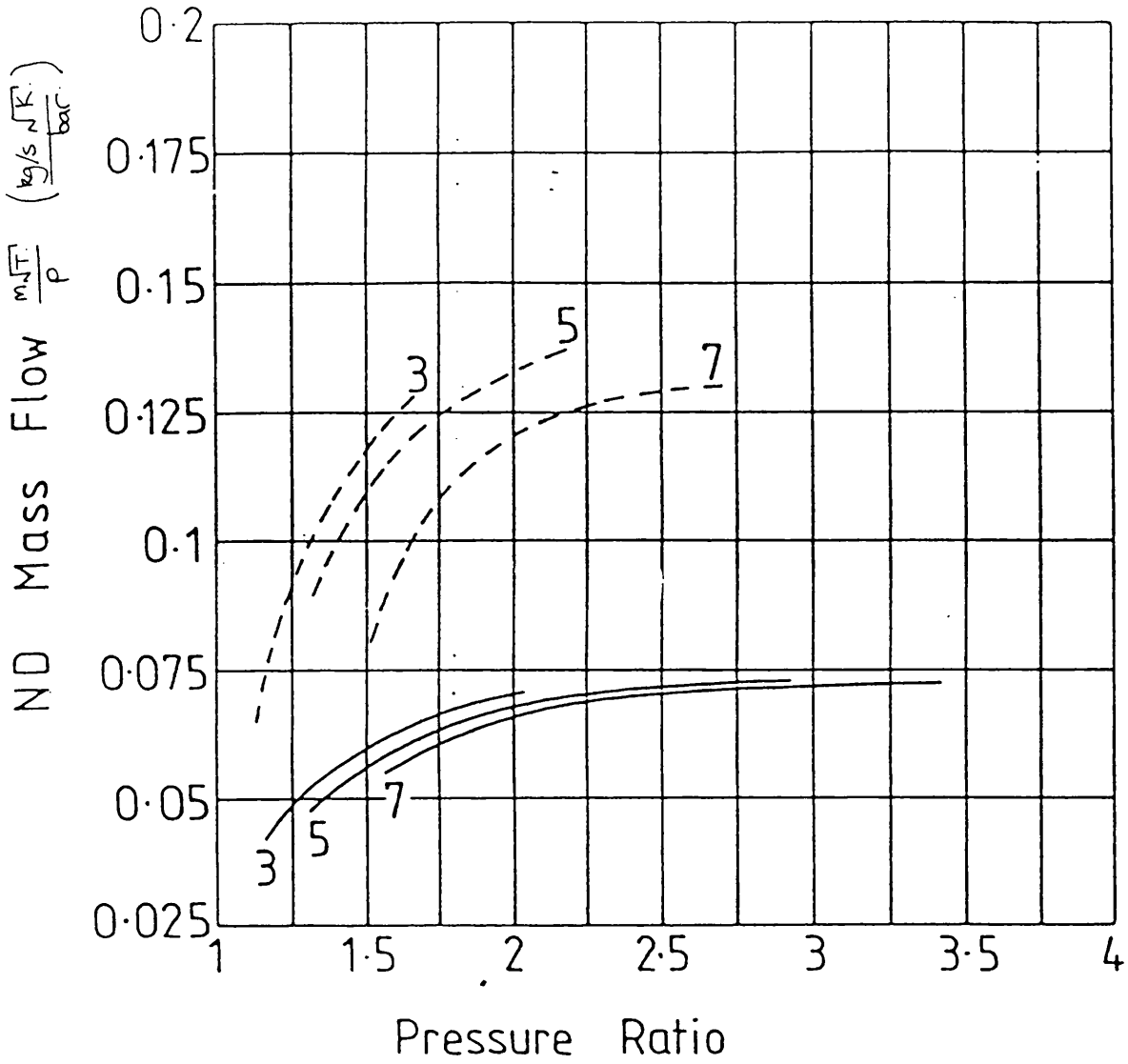

FIG 1.24 ND TURBINE MASS FLOW v PRESSURE RATIO
0% and 50% RESTRICTION

2. DESCRIPTION OF TEST FACILITY

2.1. Introduction

A significant proportion of the project was involved with the construction of a new test facility. This chapter describes in some detail how the test bed was built. The British Standards Institution and Society of Automotive Engineers (SAE) produce detailed specifications for engine testing (45-53). These were adhered to in every case. The control scheme adopted for this work was a microprocessor based closed loop system with digitally stored characteristics. The stored characteristics correspond to the optimum settings for the control parameters determined during engine tests. It is therefore very important to evaluate accurately and repeatably engine performance in all the configurations tested.

The SAE standards referred to above necessitated new features and attention to parameters which hitherto had not been standard practice within the School. These included temperature control of engine inlet air, fuel and coolant and careful attention to fuel supply. A full account of the instrumentation used is given and a note is included on the special precautions necessary when testing an engine with a variable area turbocharger, electronic governor and a variable injection timing device.

Finally the method developed for data acquisition both steady state and transiently are described. The chapter begins with a description of the engine used for the experimental work.

2.2. Major Components

2.2.1. Engine (Fig. 2.1)

The engine on which the tests were carried out was the LEYLAND TL11/11a diesel engine of 11 litres displacement. It is an automotive in-line,

turbocharged, non-charge cooled direct injection six cylinder diesel engine with a specification and rating as follows:-

Engine Designation

Leyland TL11/11 Four Stroke Turbocharged Diesel Engine
11 litres displacement 9.7 bar bmep

Rating: 190 kW @ 2100 rev/min
1017 Nm @ 1300 rev/min

Number of cylinders:	6	Cylinder bore:	127.08 mm
Firing order:	153624	Stroke:	146.05 mm
Direct injection engine		Compression ratio:	15.75:1
Static injection timing:	22^{o} BTDC	Con Rod length:	266.7 mm
(Variable timing device fitted)			

Valve Timing

				No.1
134^{o}	374^{o}	350^{o}	590^{o}	A.T.D.C.F.
EVO	EVC	IVO	IVC	

Valve Geometry

	Inlet	Exhaust
Head diameter	55 mm	46.5 mm
Seat angle	30^{o}	30^{o}
Seat width	3.6 mm	2.8 mm
Number per cylinder	1	1
Diagram of Valve Lift	See Fig.6.4	

Inlet & Exhaust Manifold

Inlet manifold volume	4.88 L	
Exhaust manifold layout		
	Front	Rear
Internal volume	1.38 ℓ	1.2 ℓ
Internal surface	817 cm^2	681 cm^2

No Intercooler Fitted

Turbocharger Type/Standard

Turbocharger Designation	Holset H2B
Type/Specification of Turbo	H2B 8081C L25A3

Single stage, nozzless twin entry unit

Turbine Data

Nozzle outlet diameter (mm)	79
Tip Rotor Diameter at entry (mm)	81
Outer diameter at exit (mm)	72
Inner (Hub) diameter at exit (mm)	26
Volute throat area on each entry (cm^2)	12.5
Blade angle at rotor entry (deg)	90
Blade pitch at exit	0.133
Rotor entry blade thickness (mm)	1
Width just upstream of rotor entry (mm)	14
Blade thickness at rotor exit outside (mm)	1
Blade thickness at rotor exit inside (mm)	4.5
Volute inlet equivalent diameter of each entry (mm)	46
No. of blades	10

Fuel Injection Equipment

Fuel injection pump	CAV in line jerk pump
Type	P5476 with boost control
Static timing	22^{o} BTDC

Auxiliaries

Automotive compressor removed

Engine Block

For each cylinder and piston	
Surface area of cylinder head (cm^2)	97.95
Exposed to bore (cm^2)	
Surface area of piston crown (cm^2)	184.44
Surface area of cylinder bore from top of block to first	
Piston ring at TDC (cm^2)	107.01
Surface area of combustion chamber (cm^2)	547.12

Accurate and repeatable engine testing requires careful attention to the following:

1. Loading
2. Fuel supply
3. Air inlet system
4. Cooling arrangement.

It follows that if these are carefully regulated then all other measured parameters can be relied upon. The method of applying load to the engine is considered first.

2.2.2. Dynamometer (Fig. 2.2 and 2.3)

2.2.2.1. Description

A new dynamometer based on a proprietory hydrostatic pump was constructed for the project, it was designed and made at the University. The engine was connected to the loading system by means of two Bibby half gear couplings and an in-line torque transducer. The engine and dynamometer

were mounted directly on a skid frame which was isolated from the floor by anti-vibration mountings. Load was applied by a hydrostatic pump mounted in a hinged cradle supported by a load cell (Fig. 2.4). The cradle was carefully aligned to within 0.1×10^{-3} m of the axis of the engine to minimise misalignment. The energy absorbed by the pump was rejected as heat to a cooling pond by a SERCK tubular heat exchanger.

The method of mounting the dynamometer was highly innovative and was a development due to Professor Bowns of the Fluid Power Group, School of Engineering, University of Bath. By mounting the pump in a cradle and using two inexpensive self-aligning bearings in an oil filled reservoir and supporting the other end by a load cell with rose bearings considerable savings in cost can be made. The unit is suitable for motoring or loading though for the tests reported only loading was available. Early results showed that vibrations transmitted through the skid frame are amplified. This results in poor signal to noise ratio and filtering reduces response to an unacceptable level; development is continuing. For all the tests reported, torque readings were based on the conventional in-line torque transducer.

The hydrostatic pump is a LUCAS HD2-3000 unit. This is an axial piston and swash plate design. The inherent advantages of this type of loading system are its compactness, robustness and a rising torque with decreasing speed characteristic. In addition due to its low inertia and high response it is well suited for transient testing e.g. a fuel step at constant speed. The pump requires an oil supply at 14 bar to lubricate the slipper pads. This was supplied by an externally driven gear pump. The circuit is as shown in Fig.2.5.

The engine could be loaded in three modes; these were:

1. constant torque
2. constant speed
3. windage i.e. torque α (speed)^2

The constant torque mode was used to determine the engine characteristics

at part load. The feedback signal was derived from the in-line torque transducer.

The constant speed control was used principally for transient work. The speed signal was derived from an engine driven encoder.

Windage control sets a position of the valve which results in a torque which is proportional to the square of the pump speed and is controlled in open loop mode. Limiting torque curves are normally tested in this mode.

The dynamometer was able to effect tight control in all modes of operation although some difficulties were experienced with transient operation. These are discussed below.

2.2.2.2. Operation

Pump pressure (engine load) is controlled by a two stage ABEX DENISON electro-hydraulic valve (Fig. 2.6). In the first stage a solenoid operated proportional pressure control valve (Type SEO3) using a flapper is used to control remotely a larger R4VO6 relief valve. The control valve regulates the orifice area proportional to the current passing through the solenoid Dynamometer torque therefore is approximately proportional to solenoid current. The maximum relief pressure is set by an external handwheel which preloads a spring. Fig. 2.7 shows the torque speed envelope for the dynamometer.

Constant torque and constant speed modes are regulated by using proportional, integral and derivative controllers (PID) or three term controllers (Fig. 2.11). Torque or speed set point is selected by means of potentiometers and is compared by the controller with the instantaneous value of the primary sensing element. If there is any difference between the two signals the controller sends an electrical output signal to the SEO3 solenoid valve to bring the variable value to set point valve, thus eliminating any deviation.

Proportional control, as the name implies, provides a graduated control of a process variable which on its own can give rise to oscillating behaviour and a velocity lag which is proportional to damping ratio. Integral control is added to reduce offset (viscous friction) and is achieved by integrating the error signal. This increases the order of the governing equation and may make the system unstable. The advantage of integral control is that much more accurate control is possible. Derivative control is achieved by combining velocity feedforward with feedback and has a stabilizing effect on the system since it decreases the order of the differential equation by one. It makes the system more lively since it senses rates of change of input. Feedforward was initially derived from the governor set point.

2.2.2.3. Transient operation

The transient response of the engine was assessed by selecting the constant speed mode and applying a fuel step to the engine. It was found in practice that engine speed excursions occured and there were problems with repeatability. This was associated with:

1. dynamometer oil temperature
2. the feed forward mechanism
3. the pump itself.

Oil temperature altered the stability of the dynamometer, therefore testing was always conducted with an oil temperature (metal) of 36^{o}C. The feed forward signal based on governor set point proved very unsatisfactory, as it was operator dependent, rate and duration of movement both affecting the overall results. The feed forward signal was eventually taken from the rack itself which together with a new pump gave very satisfactory results.

2.2.3. Fuel system (Fig. 2.8)

Several significant modifications were made to the fuel supply system. Fuel consumption repeatability was a difficulty experienced by previous researchers at the University, e.g. Aldis (24) and Baghery (10). This was associated with the difference in height of the diesel fuel tank when compared with the measuring equipment which affected part filling in the fuel injection pump.

The pump is a volumetric device sensitive to variations in pressure and temperature. The 'head' difference resulted in a significant change in performance when changing from the tank to the measuring mode. A pressure reducing valve was positioned at the same height as the measuring equipment to eliminate the discrepancy referred to above. As a consequence performance was unaffected by switching between tank and beaker.

The spill return was plumbed directly into the feed line downstream from the weigh gear as this simplifies the arrangement of pipes. To avoid temperature and pulsation effects the fuel inlet was passed through two damping chambers which also contained cooling elements. The fuel temperature was controlled manually to 37.5 ± 5^{o} C. (Previously there had been no temperature control). A mercury manometer was installed in the line after the fuel filter; this gave an early warning of fuel injection problems such as air entrapment.

The specific gravity of the fuel was measured and recorded periodically. To calculate specific fuel consumption (SFC) an average of three readings was taken for the time to consume 0.2 kg of fuel.

Repeatability was greatly enhanced with the above features to an extent where resolution to one hundredths of a second was usefully possible.

2.2.4. Air inlet system

A major innovation was to include a facility to control the air inlet temperature to a predetermined value. This was facilitated by passing the inlet air through a heat exchanger connected to engine jacket water. A three term controller type 407 with variable P.I.D. control made by Control & Readout Ltd., with a valve drive output was used together with a platinum resistance thermometer to sense and control air temperature. Testing was normally conducted with the air heated to 25 ± 1° C.

A 6 m long .125 m diameter pipe was required to direct the heated air through a variable restrictor to the engine (Fig. 2.9). To avoid standing wave effects at the nozzle a 50 litre drum with a baffle plate at inlet was constructed. A honeycomb section which straightened the flow was included and positioned 0.4 m in front of the nozzle.

Unfortunately due to space constraints the drum had to be positioned some 1 m and three right angle bends away from the compressor inlet. (This gives a classic swirl generating case).

The inlet section was 0.0625 m diameter and of smooth section. There will, however, be an implied error in compressor efficiency due to pressure losses in this ducting. Nevertheless, since the inlet tract is the same for each turbocharger configuration, the results are self consistent.

2.2.5. Water system (Fig. 2.10)

Cooling water was originally drawn directly from a purpose built pond and pumped around the test cells and through the engines. This was considered unsatisfactory as a single failure could evacuate the entire system with potentially disastrous results. A closed loop system was therefore constructed for the centre cell communicating with the common system through a liquid/liquid heat exchanger. A six gallon header tank kept the engine water jacket full. This was

in turn fed directly by a ballcock arrangement from the pond.

To effect tighter control over coolant temperature a Landis & Gyr three term controller type RWF 61.10 was used to good effect together with a nickel resistor thermometer and proportional electro-hydraulic motor (0 - 10 v). Coolant temperature was controlled to $89 \pm 1^{\circ}$ C.

2.3. Instrumentation (Fig. 2.13)

2.3.1. Gaseous and liquid temperatures

All temperatures were measured by using two chrome-alumel type thermocouples for each station. The thermocouples were wired to a multi-terminal selector switch with the output leads wired to a digital voltmeter. This device has built in cold junction compensation.

For greater accuracy all thermocouples excepting those upstream of the turbine were shrouded in pockets (Fig. 2.14). The thermocouple readings measuring the temperature rise across the compressor and water outlet temperature were displayed digitally to one significant place of decimals for greater accuracy.

The thermocouples used in the exhaust manifold were 1.5 mm diameter sheathed in stainless steel. The low frequency response of these units gives a 'mean' temperature which is time averaged rather than mass flow averaged which is that desired. This affects the calculated turbine efficiency.

2.3.2. Pressure measurement (Fig. 2.15)

Water and mercury manometers were used as appropriate to measure static pressure. The readings were a mean of three equispaced holes on one cross section. The pressure tappings were carefully made according to 'a compressor routine test code' (N.A. Dimmock (26)).

The comments above pertaining to frequency response of thermocouples and the calculation of turbine efficiency are equally applicable to pressure measurements in the exhaust manifold.

Compressor outlet and pre-turbine pressures were additionally measured by electrical transducers for transient and control purposes.

The two transducers were of the same type viz. strain gauge force rod and diaphragm, Type P700 manufactured by Schaevitz. The bridge formed by the gauges is compared with a bridge regulated voltage supply, the output is then amplified using standard signal conditioning circuits in the form of plug in cards. The basic electronic measuring system is illustrated in Fig. 2.12. A calibration of 0-2 bar vented gauge corresponded to 0-10 v. The output was then interfaced with the analogue to digital (A/D) convertors for the purpose of control or transient data acquisition. The output could be displayed on a digital voltmeter by means of a multi-terminal selector switch. The transducers were positioned as close as possible to the manifolds and required cooling.

2.3.3. Air consumption

An Airflow Development inclined airflow manometer with a range of 0-250 mm water gauge (WG) was used to evaluate air mass consumption. Two nozzles of 0.056 m and 0.075 m diameter designed to BS 1042 were manufactured to cover the flow range required. A low differential pressure (0-250 mm WG) capacitative type transducer manufactured by Furness (FC040) was used to give an electronic output. This was found to operate very satisfactorily.

2.3.4. Fuel consumption

A conventional mass balance system combined with a digital electronic timer and tachometer was used to determine fuel flow rate and engine speed. A Hall effect switch turned the timer on and off. In addition a Brooks Micro-oval II positive displacement flowmeter was used for instantaneous volume flow readings. The display was analogue in $m^3/s \times 10^{-6}$.

2.3.5. Torque Measurement

Two types of transducer were fitted to the experimental rig:

(i) a tyco type JP1000 load cell

(ii) an inline device

All results were taken with the latter device. This discussion is therefore restricted to this type.

The original transducer was manufactured by British Hovercraft and was based on a necked and strain gauged shaft. The electrical output was transmitted through brushes and slip rings and then displayed by a digital voltmeter calibrated in Nm (0-1500 Nm ≡ 0-10 v).

The unit generally operated satisfactorily; however, problems were experienced at speeds greater than 2000 rev/min when the brushes bounced intermittently. After several attempts to cure this problem had failed the unit was replaced very late in the programme by a similar Vibrometer unit which proved satisfactory.

The in-line Vibrometer torque transducer is based on the amplitude modulation method, which consists of modifying the amplitude of a voltage with the torsion. This unit has a non-contact transmission system for bridge excitation and torque signal pick-off; thus the measurement is not affected by slip ring problems (Fig. 2.16). The basic principle of a rotary transmission system is shown and consists of two transformers with a rotating and stationary part.

2.3.6. Speed

The engine and turbocharger speed signals were derived by simple inductive type sensors and displayed by means of Orbit digital counters. The dynamometer speed signal for closed loop transient operation was derived from an engine driven optical encoder.

(i) Engine speed was generated from a sensor mounted on the flywheel starter ring which has 159 teeth. For engine overspeed protection another inductive sensor is mounted on a 120 teeth wheel located immediately behind the flywheel.

(ii) Turbocharger speed was measured by an inductive sensor mounted in the shroud of the compressor casing. Pulses were generated with the passage of blades; a buffer amplifier with a gain of 10 was required before conditioning. The waveforms are then converted to a stream of fast edged pulses by a trigger circuit before being fed into the Orbit counter.

For an analogue output engine and turbocharger speed required a frequency to voltage (f/v) convertor. The fast edged pulses were converted to rectangle waveform. An integrator then provided a mean voltage proportional to area.

(iii) The dynamometerspeed signal was measured by a HOHNER AUTOMATION 3000 series encoder. The encoder works on the Moiré fringe principle, 720 square waves are generated per revolution. The unit was lined up and mounted on a substantial steel bracket on the front of the engine. It was driven through two Simplatroll zero backlash couplings separated by a 0.075 m shaft. It proved extremely difficult to drive the encoder reliably. The couplings would operate for approximately 50 hours before failing through fatigue.

2.3.7. Smoke measurement

The author noted that smoke measurements had presented a number of difficulties to previous researchers at Bath. Aldis (24) had commented on the existing transient smokemeters as being very unsatisfactory.

Smoke measurement was accomplished by:

1. BOSCH SPOT SMOKEMETER - (STEADY STATE).
2. A full flow Opacimeter device - (steady state and transient proved excellent.

(i) Bosch Spot Smokemeter (Fig. 2.17)

A spring-operated sampling pump pulls a fixed volume (1/3 L) of exhaust gas from the exhaust stream through a controlled density paper filter disc causing it to darken in relation to the exhaust gas soot content. A separate battery powered photoelectric device measures the light reflected from the darkened filter. Readout is by a milliammeter calibrated in O - lO deg. of darkening. Fig. 2.17 shows the operating principle of the photoelectric evaluation system. Calibration is accomplished with a calibrated perforated grid which corresponds to a 5.O BOSCH reading. Before samples are taken the sampling tube should be purged with compressed air. An average of three readings is then taken.

(ii) Full Flow Smoke Opacimeter (Fig. 2.18)

The transient smokemeter manufactured at the University is similar in construction to the BERKLEY CELESCO (25). Measurement is accomplished by passing light pulses through the engine exhaust stream and detecting the loss in light transmission due to smoke with a photo-electric detector. The relative light energy loss is translated into both an opacity and a smoke density signal which is displayed digitally.

The unit requires a clean compressed air supply to blow over the lenses and prevent smoke deposition. A dedicated clean water supply at $30^{o}C$ is also necessary to stabilize temperatures.

In service the device has proved itself very successful. A plot of BOSCH versus opacity readings (Fig. 2.19) over a period of time gave sufficient confidence to use the opacimeter for all steady state work recording values directly in BOSCH units. Repeatibility and reliability have proved excellent.

2.3.8. Crank angle degree marker and trigger

The crank angle degree marker generated 3^{o}, 30^{o} and TDC (relative to cylinder 6). The output from the 120 teeth wheel was conditioned with suitable electronics to generate the above with a variable delay. A separate top dead centre (TDC) marker was mounted on the flywheel. The position of the TDC marker was accurately determined by filling the cylinder with oil and rotating the engine until the highest point was determined. This was checked by comparing the output of cylinder 6 motoring with the TDC position.

A Hall effect switch mounted on the fuel pump drive generated a signal to trigger the oscilloscope.

2.3.9. Needle lift

An instrumented American Bosch type AKN 88m/-78-4855 fuel injector fitted in cylinder 6 with ADB-140M-221-7 nozzle assembly was used to measure dynamic timing and duration of injection. The system operates on the inductive principle. A Bently Nevada proximitor detector was used to process the signal which was then displayed on an oscilloscope.

Problems were experienced with fuel leaking through the cable outlet in the injector body.

2.3.10. Fuel line pressure

An AVL type 41DP500K strain gauged diaphragm transducer was used to measure fuel line pressure. It was mounted as close as possible to the injector on cylinder 6. Care must be taken to introduce the minimum dead volume so that injection characteristics do not change. A bridge amplifier then processed the signal which was displayed on a four channel oscilloscope.

2.3.11. Barometer

Barometric pressure was recorded by means of a Druck DPI 201 digital pressure indicator with a range of 1.2 bar absolute. Pressure was sensed by means of a strain gauged diaphragm and appropriate circuitory.

2.3.12. Vapour pressure

Vapour pressure was measured by using a sling wet and dry bulb Hygrometer and determining the relative humidity directly from a chart. The saturated vapour pressure corresponding to prevailing ambient conditions was fed into the reduction program and vapour pressure calculated by multiplying by the relative humidity.

2.3.13. Cylinder pressure

A KISTLER 6121 piezo-electric transducer was used to measure cylinder pressure. The 6121 transducer is a non-water cooled unit and relies on engine jacket water for cooling. It is therefore very important to keep the engine coolant full and below the boiling point at all times.

The installation is very neat, the transducer is flush with the flame

face and can be withdrawn for cleaning and calibrating without removing the rocker cover (Fig. 2.20). The transducer has the advantage of excellent frequency response (up to 100 Kc), very wide and linear operating conditions and the ability to fit into a small space.

A Vibrometer charge amplifier type TA/3/c was used to process the signal which could be displayed on the oscilloscope or a digital peak voltage detecting meter. Calibration of the transducer was achieved with a purpose built rig using high pressure nitrogen. In operation drift was minimal and repeatability was good.

2.3.14. Fuel rack position

A Sangamo linear variable differential transducer type AC/15 was mounted on the rack at the front of the pump. It was directly interchangeable between the two fuel pumps which were used during the project. Linearity was measured at 0.3% and hysteresis was minimal.

2.3.15. Safety parameters

In addition to the above oil pressure, oil temperature and water temperature were recorded to indicate whether steady state conditions had been reached.

2.4. Failure Detection (Fig. 2.22)

The safety of the test facility was assured by a number of conditional interlocks and failure detection devices which either give warnings or automatically shut down the test rig in the event of failure or improper operation. Critical parameters were monitored by duplicated sensors.

The engine could not be started until the following conditions had been satisfied:

1. compressed air supply on
2. air shut off valve activated
3. external water pressure present
4. smokemeter water on

In the event of any safety parameter failing, i.e:-

1. loss of engine oil pressure
2. loss of water pressure
3. high water temperature
4. high oil temperature
5. loss of air pressure
6. loss of smokemeter water

The engine would itself shutdown.

To cater for the failure requirements of the three control parameters the following features were included:- In the event of the engine overspeeding an absolute air shut off valve was located in the inlet passage activated by an adjustable overspeed trip (< 2500 rev/min). The speed signal was derived from an independent 120 teeth wheel.

Protection from under and over boosting was afforded by adjustable set points on the boost pressure and turbine inlet temperature transducers respectively which shut the engine down when activated.

To complement the above, pull wires running down both sides of the test cell were installed such that shut down could be effected from

within the cell.

In addition two 3.5 kg carbon dioxide extinguishers were connected to the inlet tract of the engine effecting an independent means of shut down from the test console.

2.5. Data Acquisition

2.5.1. General

Data acquisition for steady state and transient tests were evolved specifically for this project. A coherent and rational system was developed to handle the extensive test programme. The methods adopted are described.

2.5.2. Steady state

All steady state results were logged manually in a test book (Fig. 2.23).

A list of those parameters measured and derived are included in Fig. 2.23,24. The raw data was reduced on a PET micro-computer. The data was then plotted manually on standardised graphs. A comparison of test results using a light box is then very straightforward. A flow chart for the reduction program is included in Fig. 2.26. A program listing can be found in Appendix 1.

2.5.3. Transient data acquisition (Fig. 2.27)

The engine was fully instrumented for transient testing. The parameters measured are given in Fig. 2.27. Each transducer after suitable conditioning has an analogue output of 0-10 v corresponding to an appropriate physical range.

The Digital PDP8E mini-computer was used to acquire data. This was located in another laboratory and connected by co-axial cable land lines and analogue to digital convertors. A flow chart for the Fortran program is included in Fig. 2.28. Transient data was recorded over 3 s with a sampling rate of 0.1 s. The program being capable of sampling at 2 ms per channel.

2.5.3.1. Procedure for recording data

A teletype printer was located in the laboratory where the program was started and the appropriate conversion factors and graph scales entered, including the number of channels, sample rates etc. Finally pressing the return key started the program. At the same instant the engine transient was initiated. Data was read directly into memory until acquisition was complete, then converted to engineering units and stored on disc. After the transient was completed it was possible to plot the parameters referred to above to assess whether the transit was acceptable.

If acceptable the program was re-run in data-presentation mode and the results printed. Graphs were then plotted by hand.

2.5.4. Electronic data acquisition

The outputs of cylinder pressure, needle lift and fuel line pressure to a base of crank angle were recorded using a TEKTRONIX Type 3A74 four channel oscilloscope and polaroid land camera (Fig. 2.29).

2.6. Experimental Procedure

The engine was first warmed up until oil bulk temperature and water jacket temperature achieve steady state values. This takes approximately 45 minutes at medium load. The desired torque and speed are then selected. Fuel, air inlet and water temperatures are then set within the appropriate limits. All parameters are then logged. This 'top line' is then run through the reduction program. If the results appear satisfactory the test continues. Approximately 10 to 15 minutes are allowed for steady state conditions to be achieved between readings.

Finally before shutting down, the engine is allowed to idle for five minutes or until the turbine inlet temperature falls below 200^{o} C.

2.7. Calibration

All transducers were calibrated periodically as appropriate. A calibration graph for each component is included, i.e:

torque transducer
cylinder pressure
inlet manifold pressure
exhaust manifold pressure
air flow
fuel rack position
ring sleeve position (VG).

LIST OF FIGURES

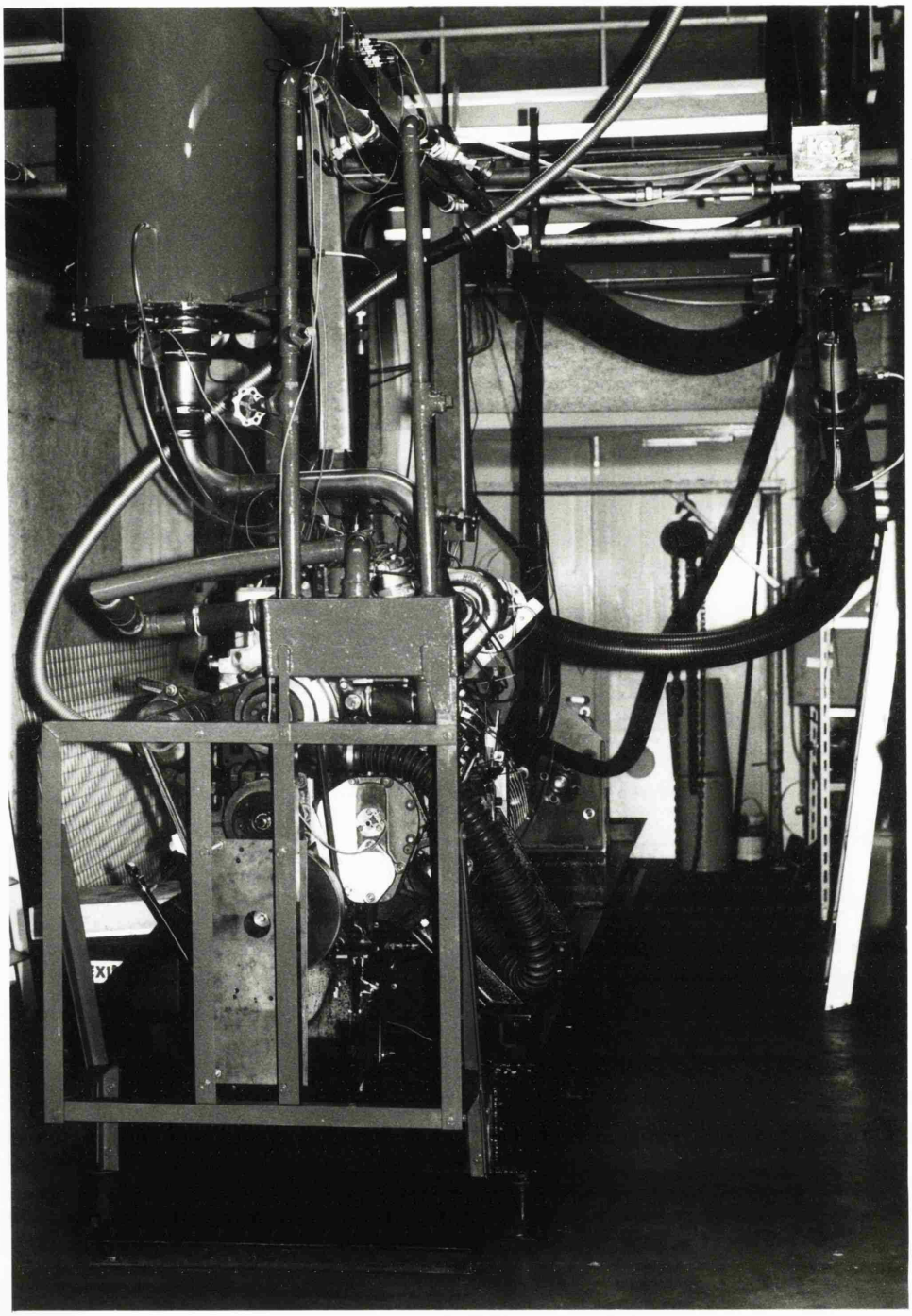

fig 2.1 TEST CELL

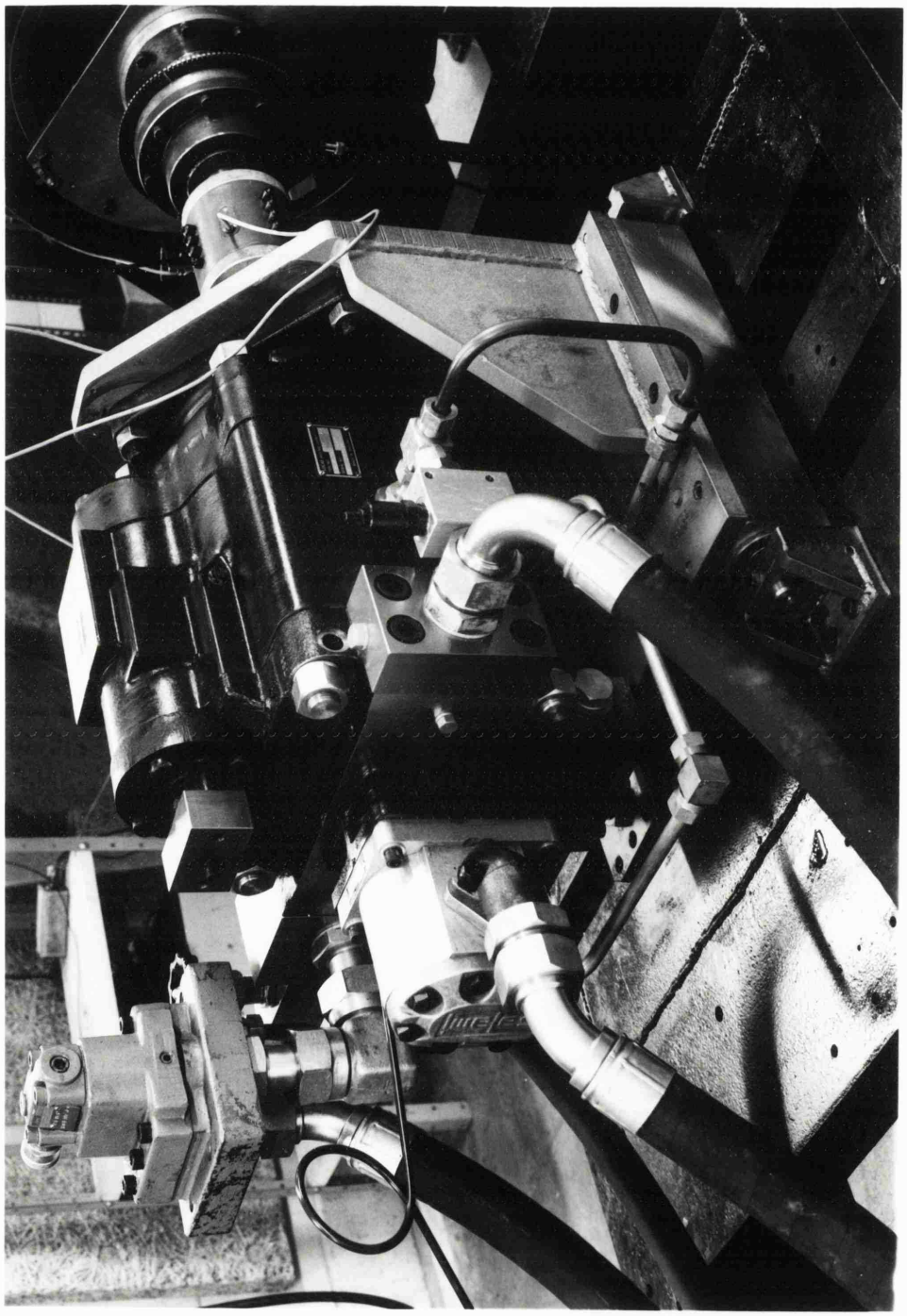

fig 2.2 DYNAMOMETER

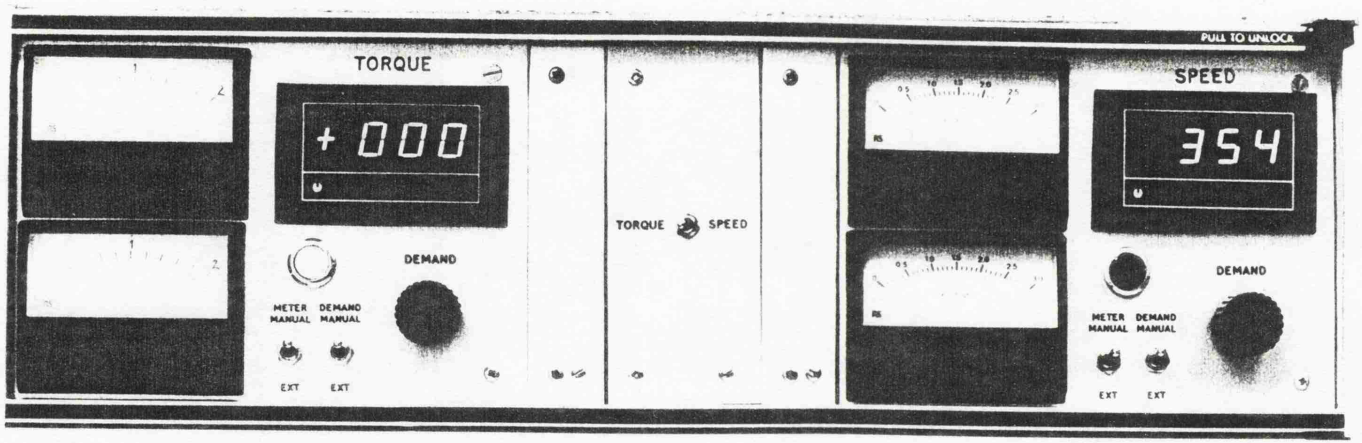

Fig 2.3 DYNAMOMETER CONTROLS

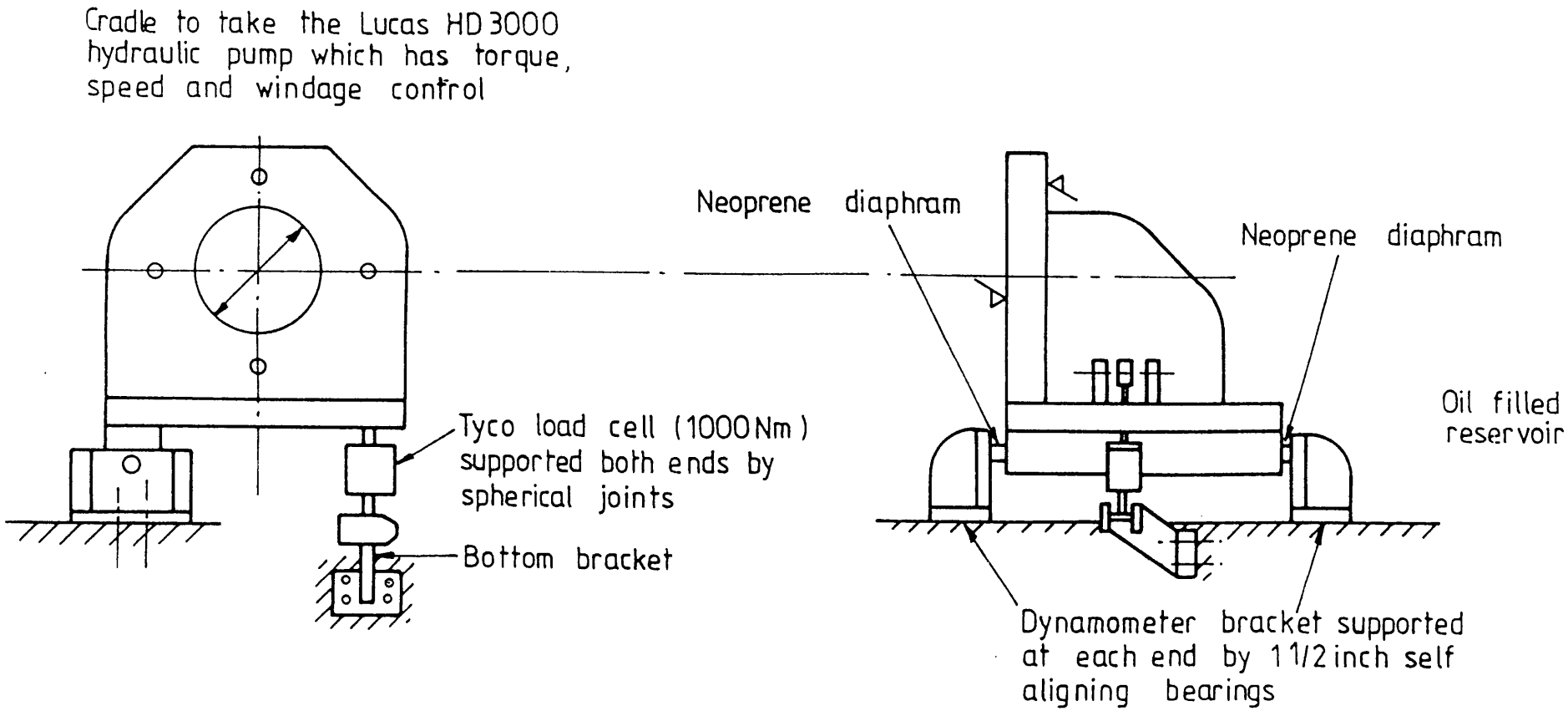

FIG 2.4 DYNAMOMETER FIXING ARRANGEMENTS (LOW INERTIA HIGH RESPONSE TYPE)

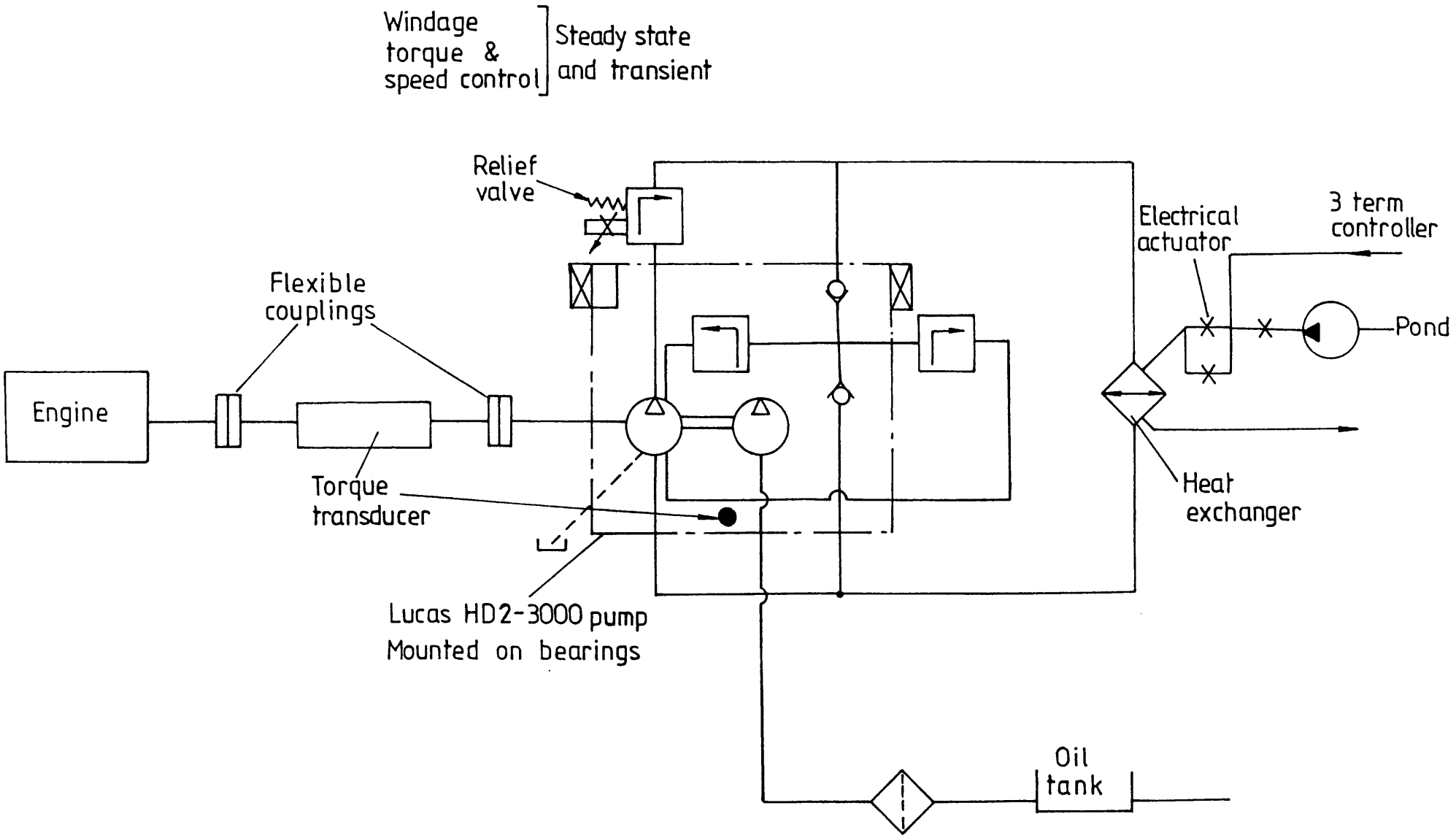

FIG. 2.5 ENGINE LOADING SYSTEM

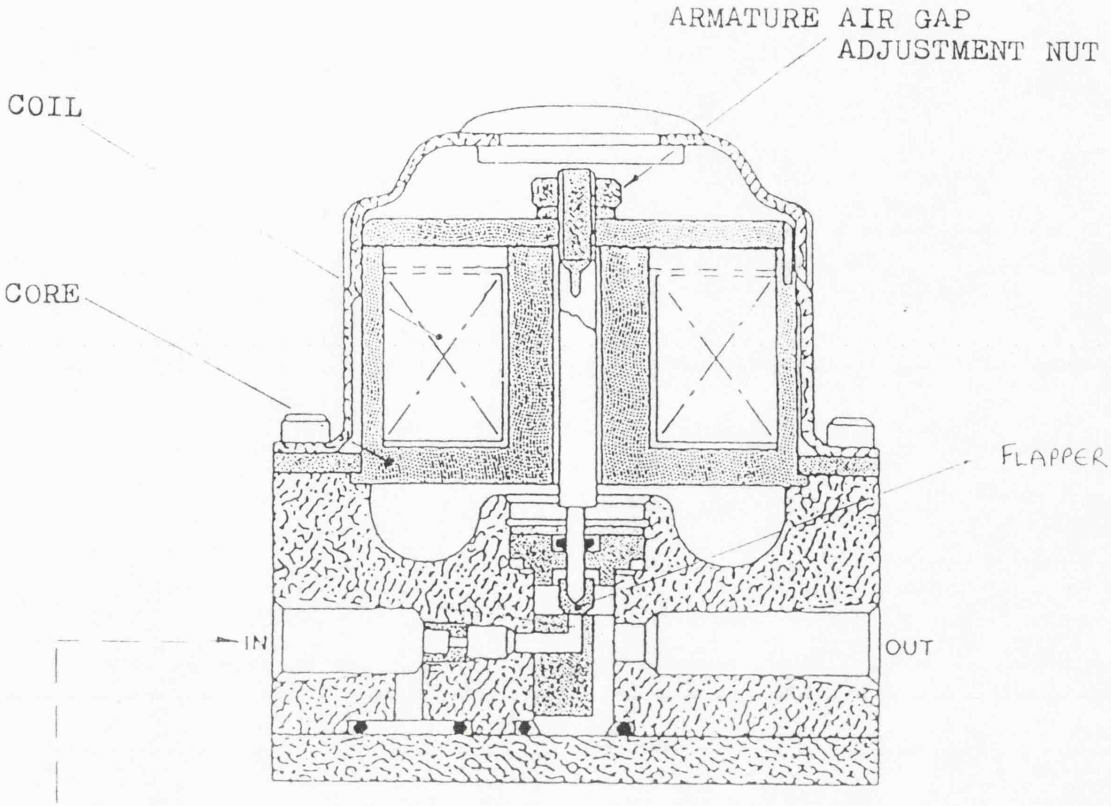

PILOT STAGE (ABEX DENISON SE03)

EXTERNAL
CONNECTION
LINE

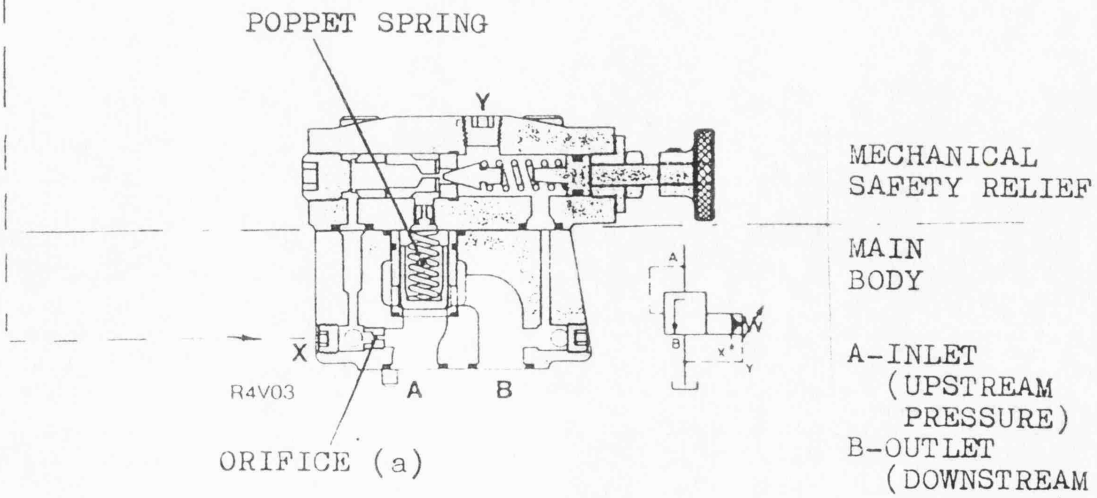

MAINSTAGE (ABEX DENISON)
(R4V10 SIMILAR DESIGN)

FIGURE 2.6 PRESSURE CONTROL VALVE ASSEMBLY
(TWO STAGE)

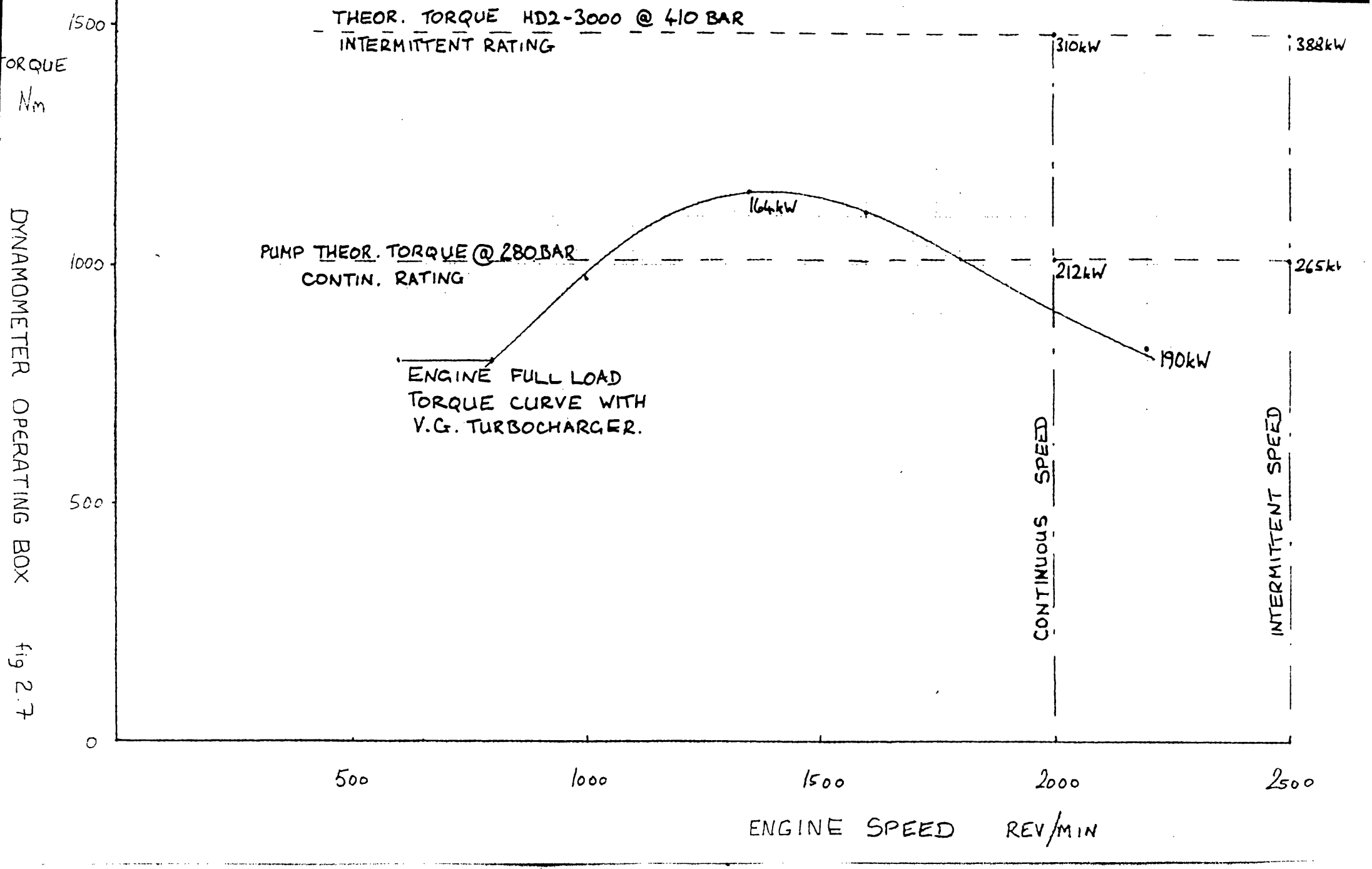

DYNAMOMETER OPERATING BOX fig 2.7

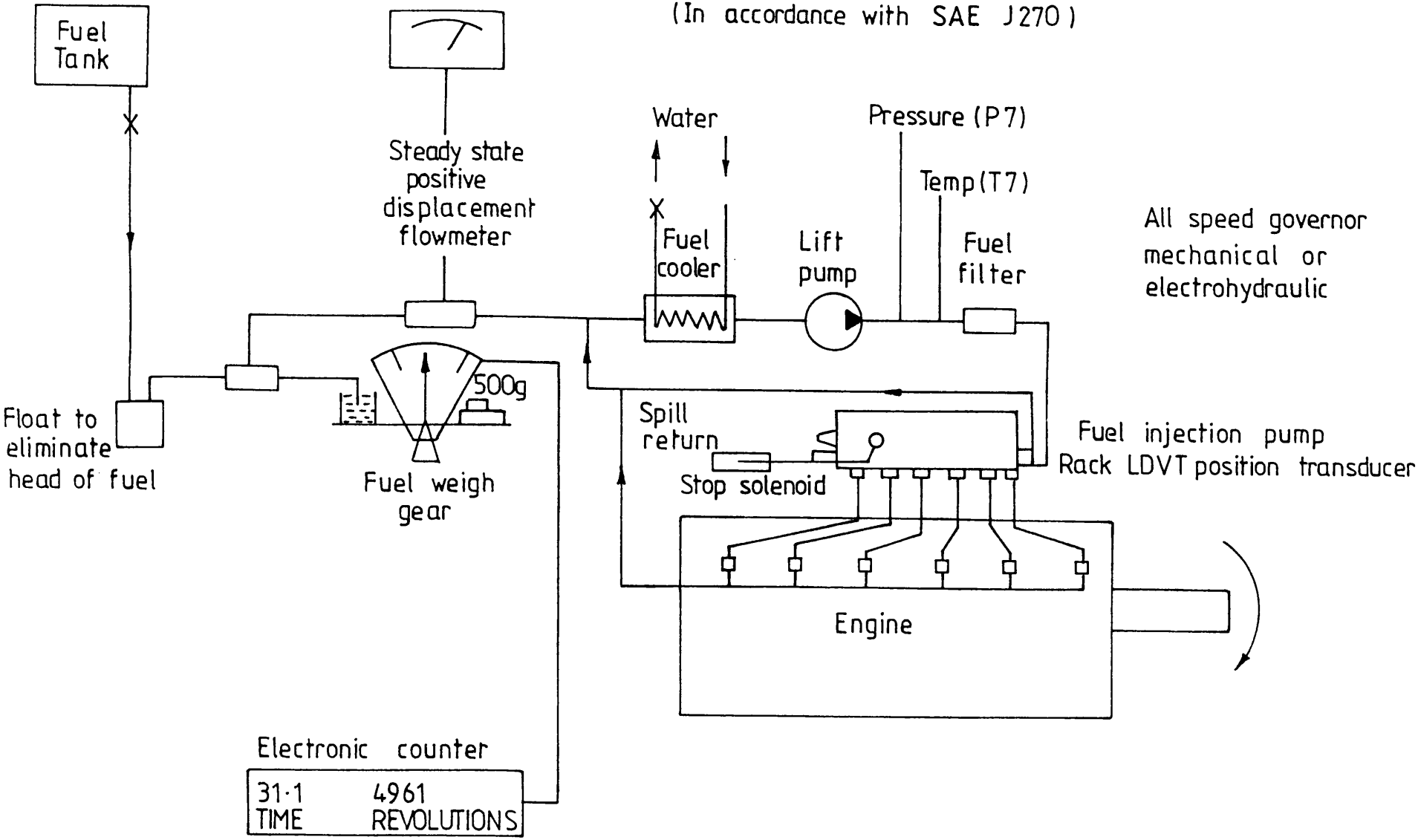

FIG. 2.8 FUEL SUPPLY ARRANGEMENTS

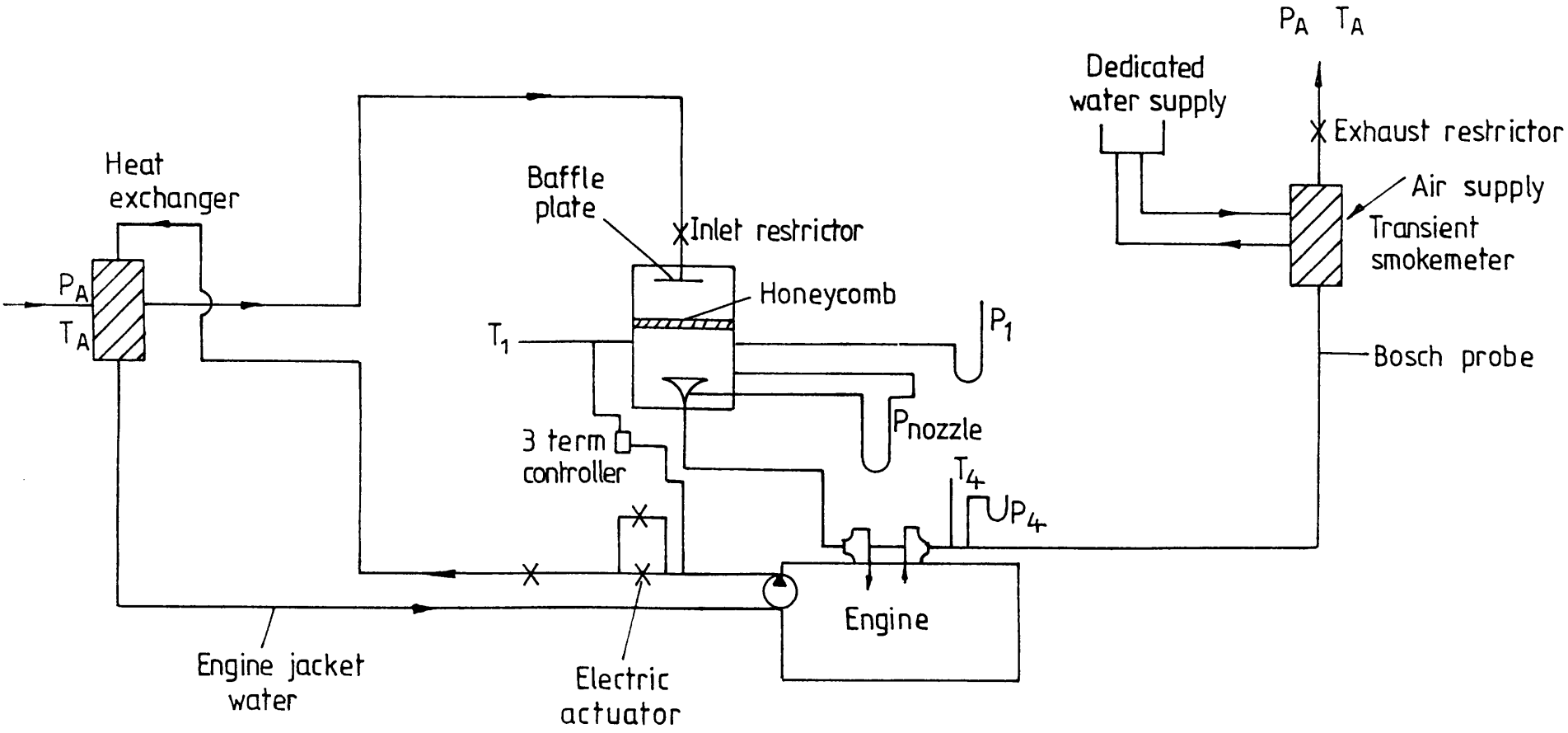

FIG. 2.9 ENGINE INLET AND EXHAUST ARRANGEMENT

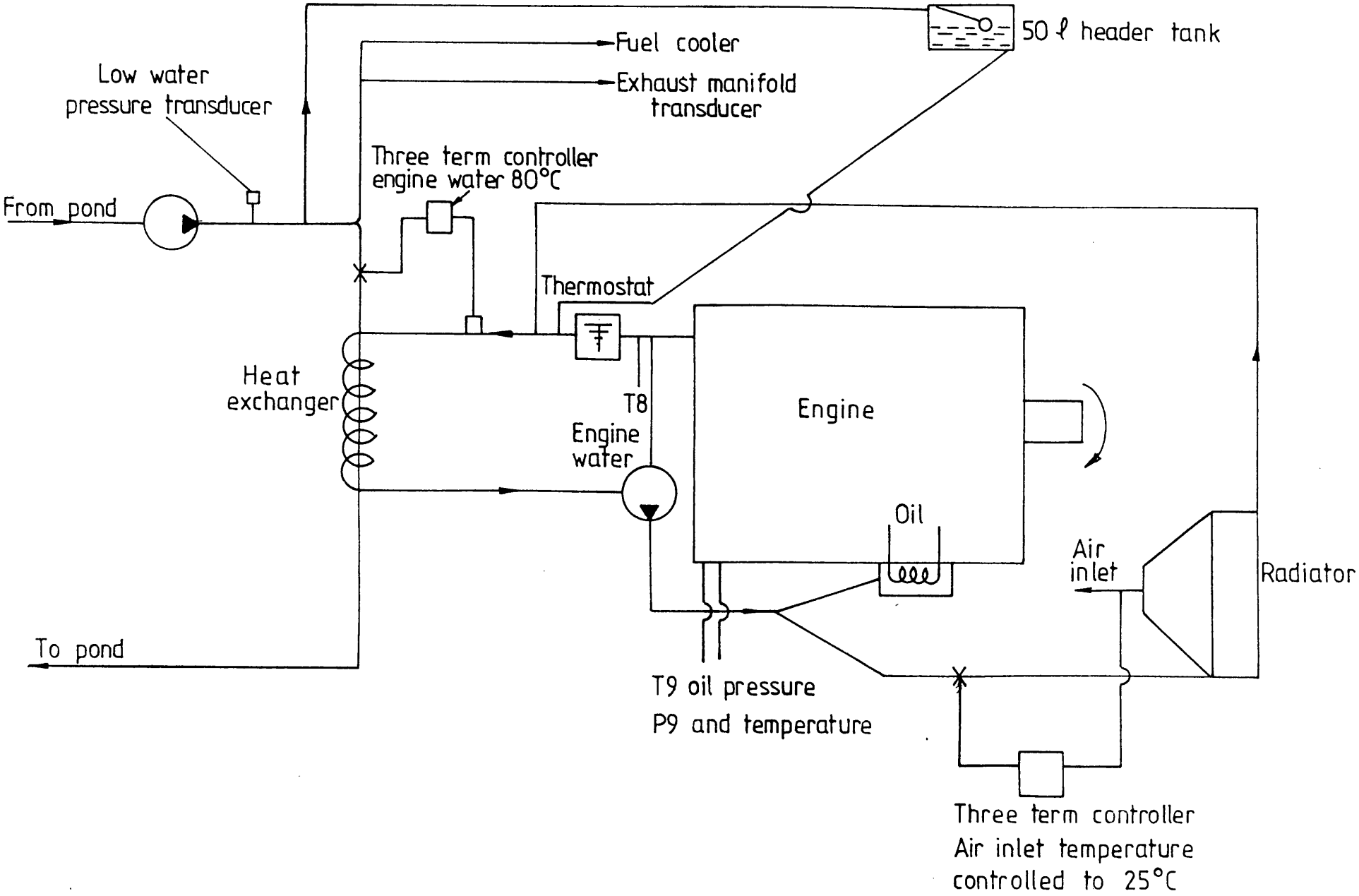

FIG 2.10 WATER SERVICES

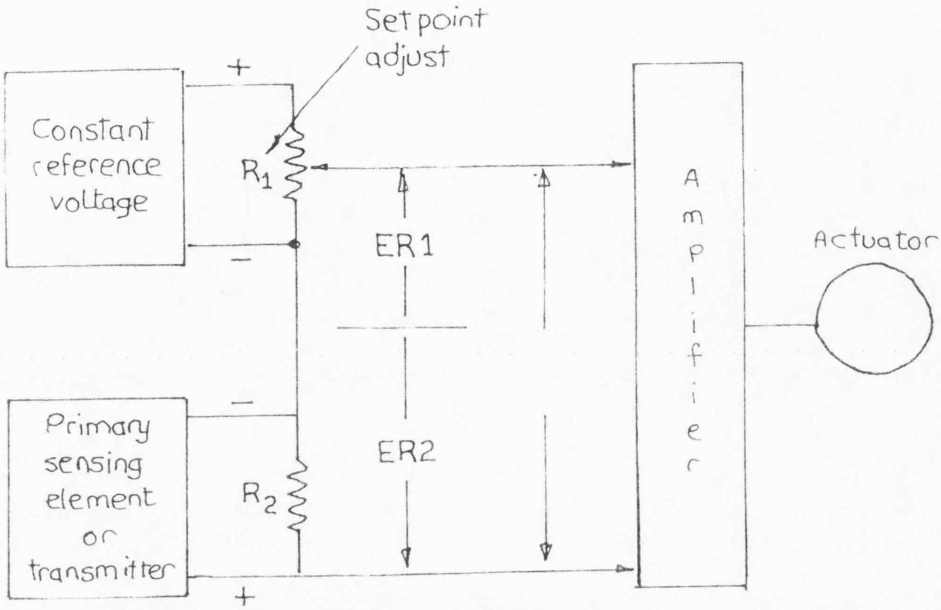

fig 2.11 Basic principle of electrical controller

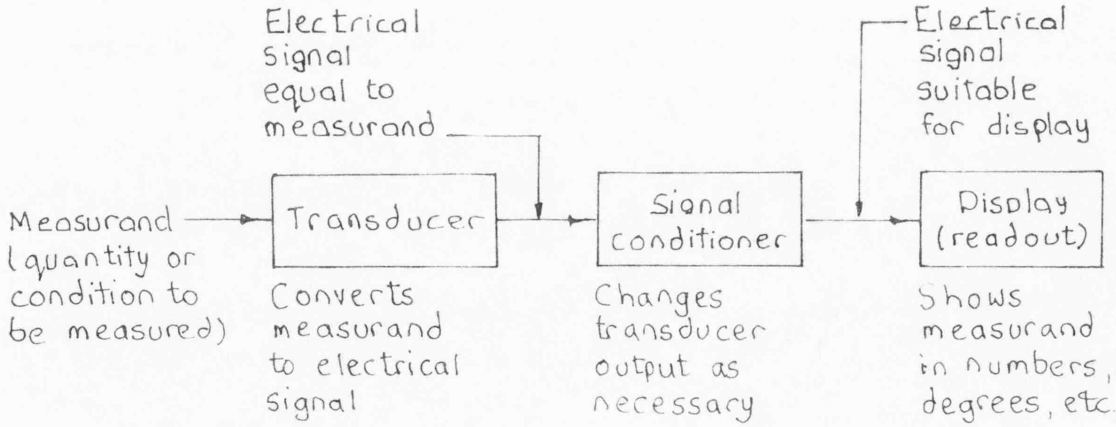

fig 2.12 Basic electronic measuring system

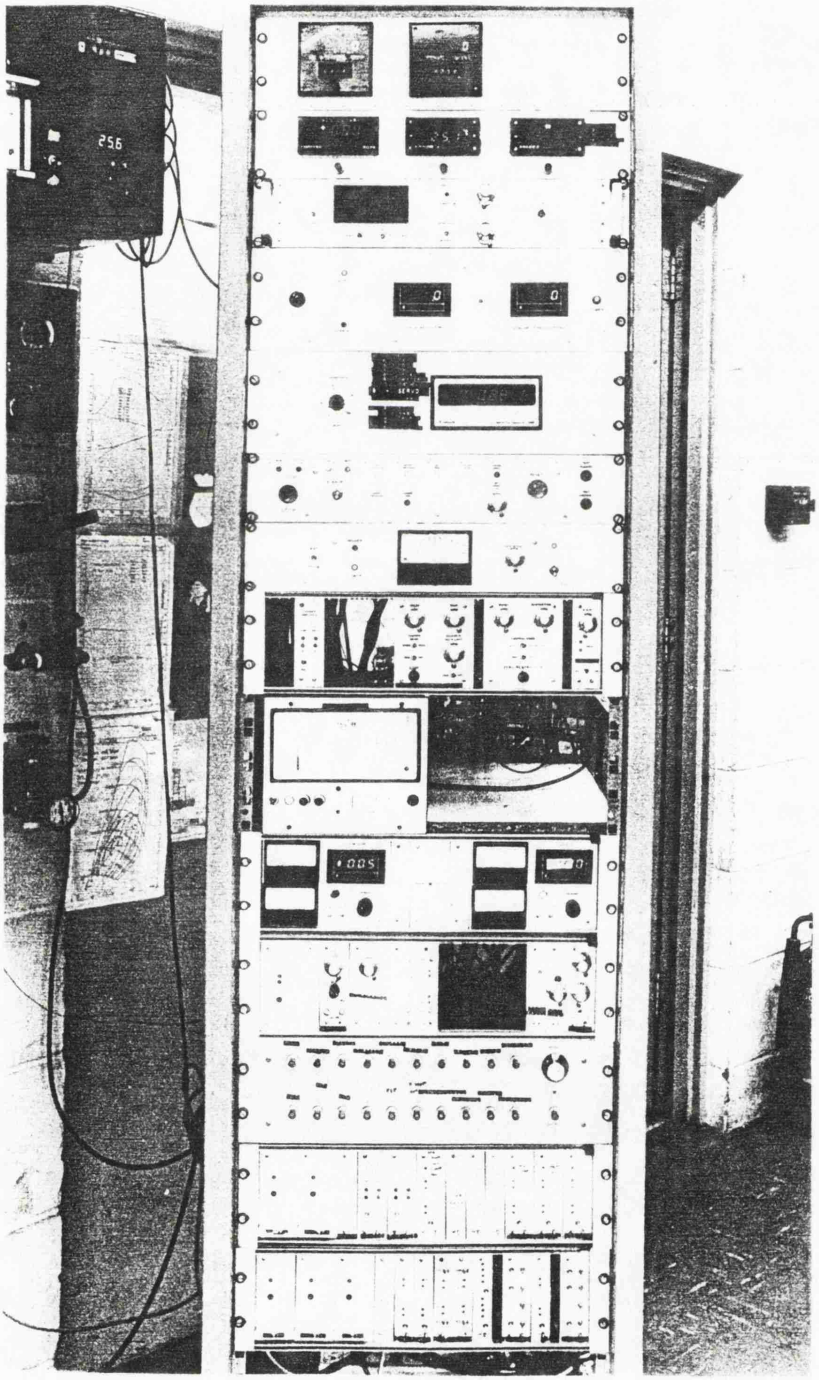

fig 2.13 General Instrumentation

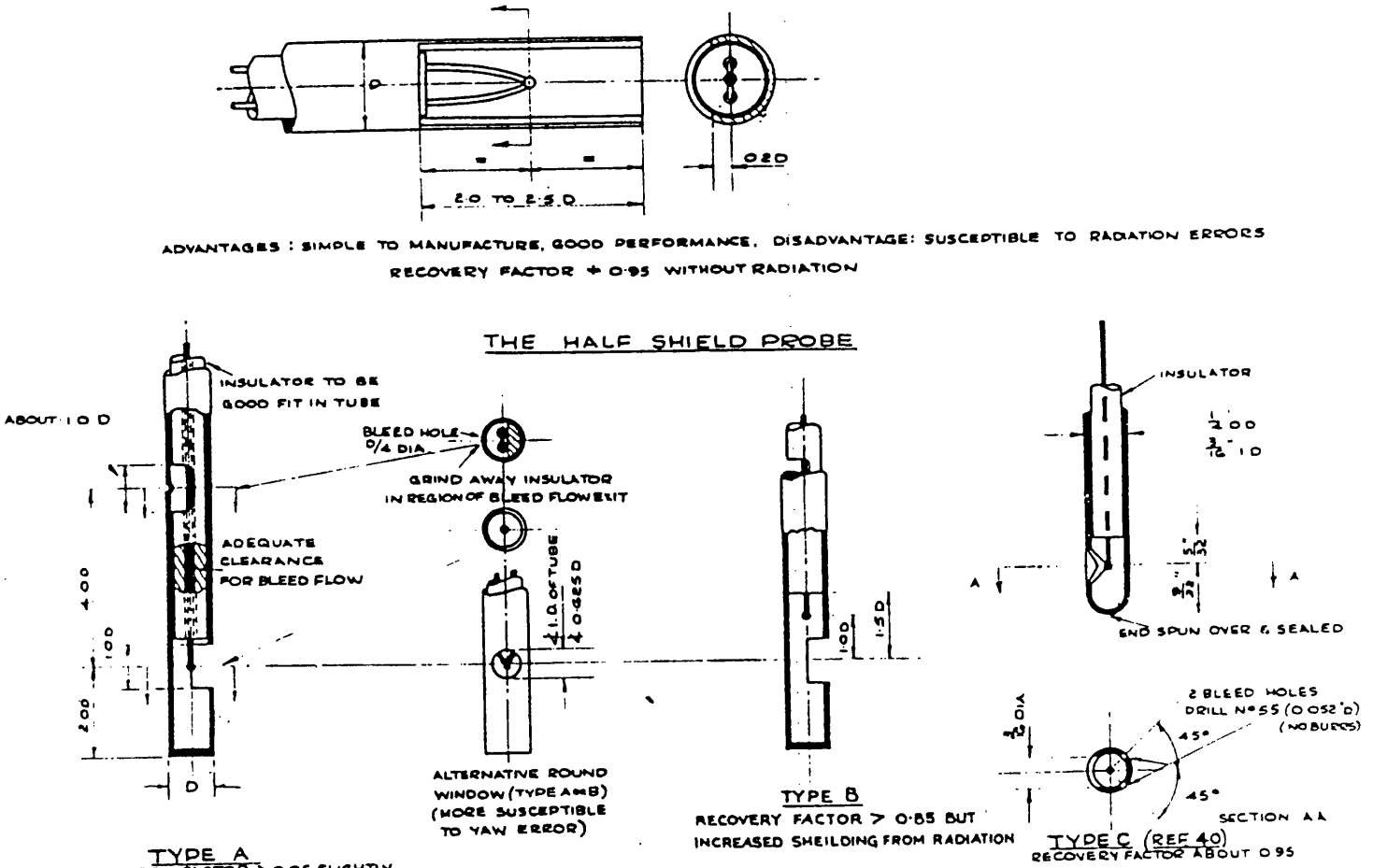

Thermocouple probes. (ref 26)

fig 2.14 THERMOCOUPLE PROBES

fig 2.15 STATIC PRESSURE TAPPING DETAILS

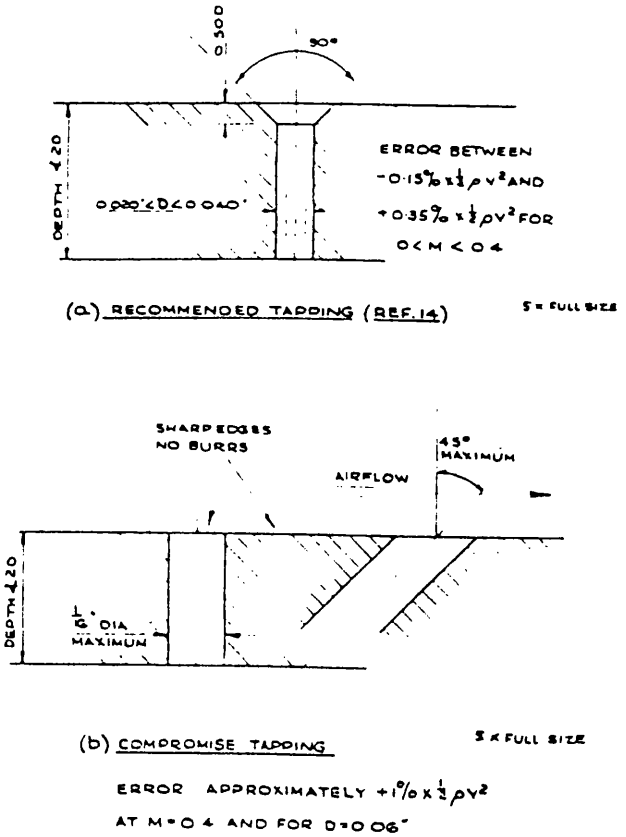

Static-pressure wall tappings. (ref 26)

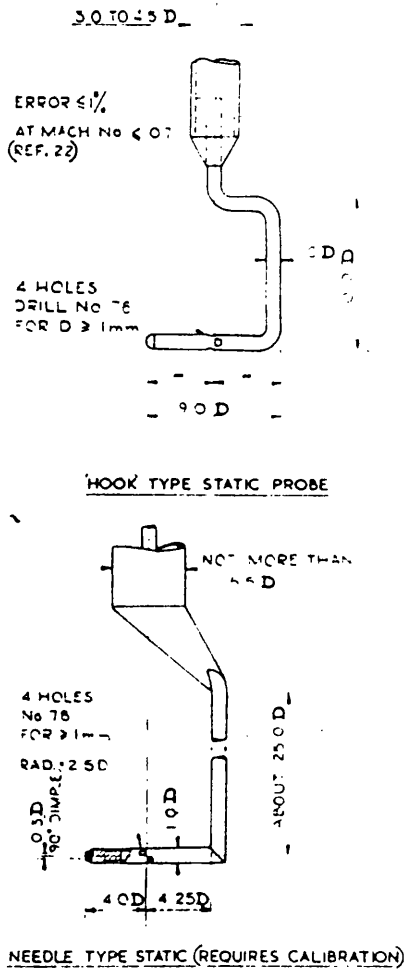

Static-pressure probes.
(Dimensions in arbitrary units - millimetres are suitable.)

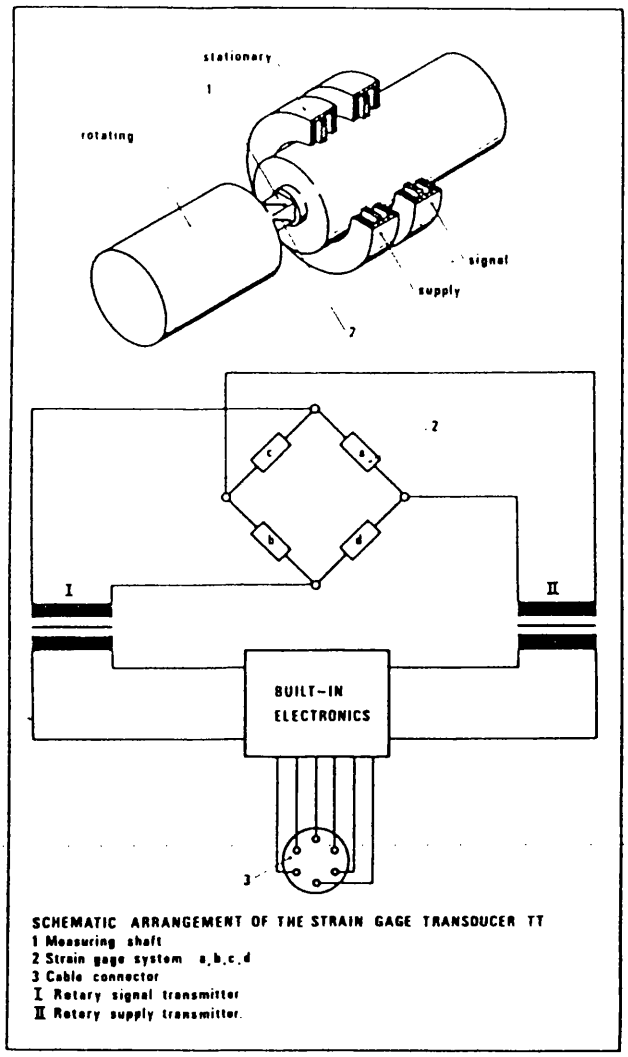

SCHEMATIC ARRANGEMENT OF THE STRAIN GAGE TRANSDUCER TT
1 Measuring shaft
2 Strain gage system a,b,c,d
3 Cable connector
I Rotary signal transmitter
II Rotary supply transmitter.

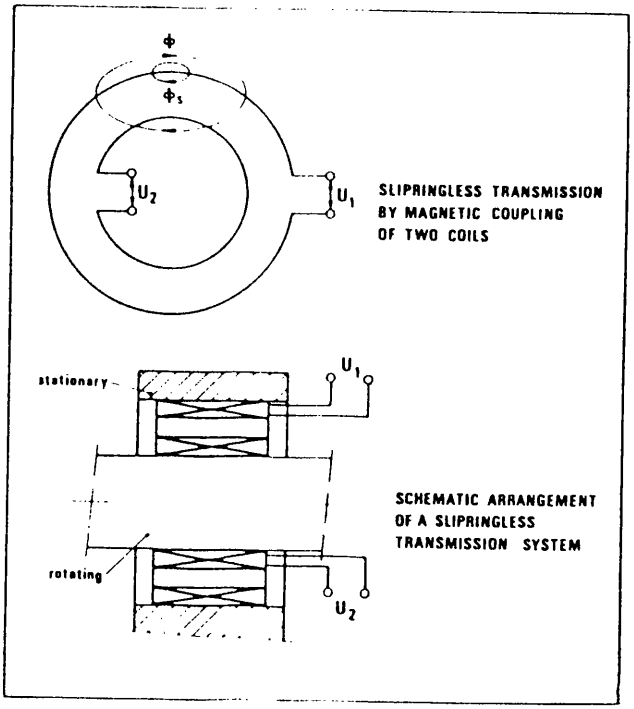

SLIPRINGLESS TRANSMISSION BY MAGNETIC COUPLING OF TWO COILS

SCHEMATIC ARRANGEMENT OF A SLIPRINGLESS TRANSMISSION SYSTEM

Fig 2.16 VIBROMETER TORQUE TRANSDUCER

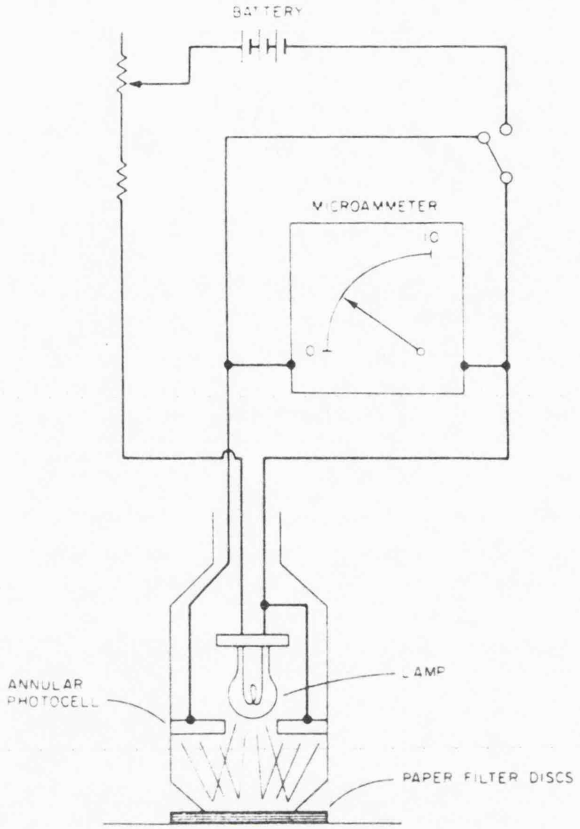

PHOTOELECTRIC EVALUATION UNIT OF BOSCH "SPOT" SMOKEMETER

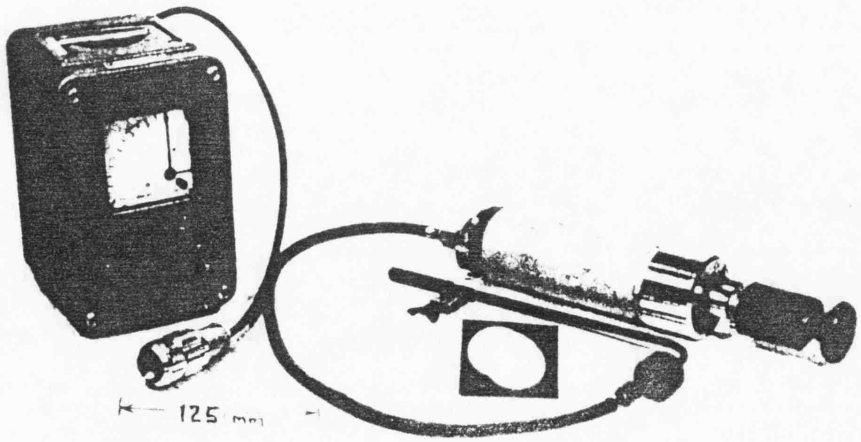

fig 2.17 BOSCH SMOKEMETER

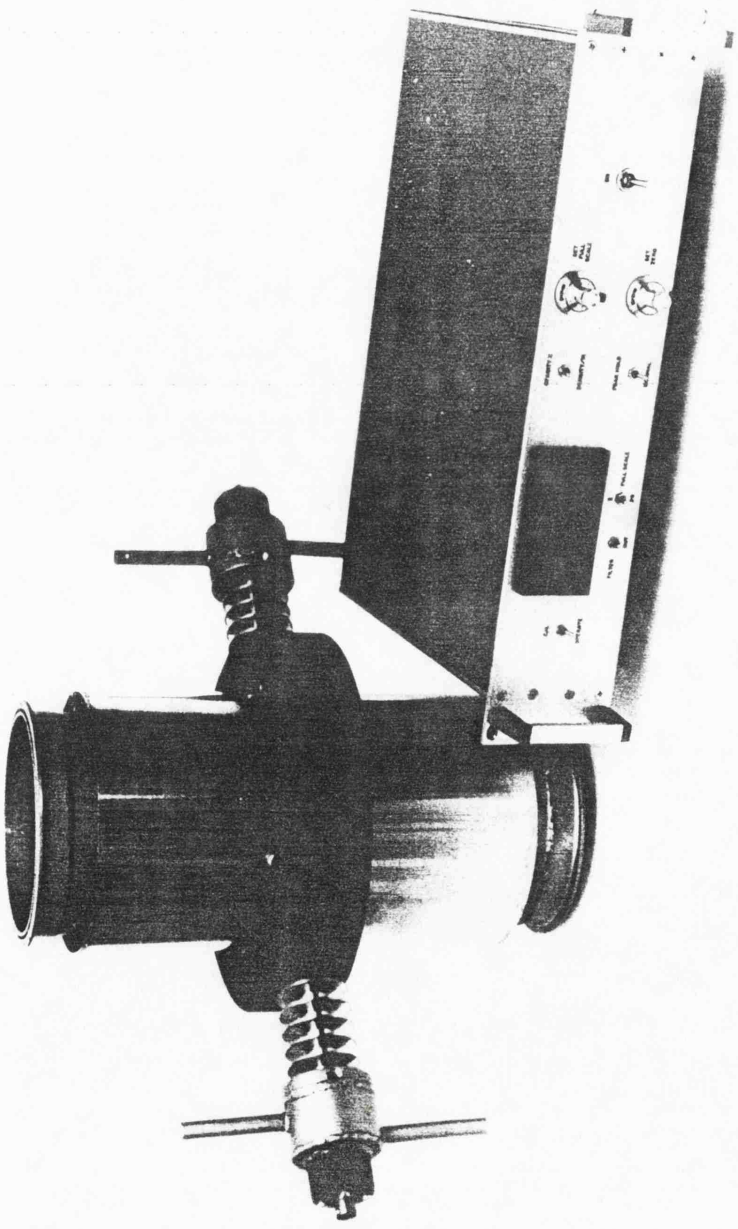

fig 2.18 FULL FLOW SMOKE OPACIMETER

Engine LEYLAND TL11 ENGINE—11.1L DISPLACEMENT Drawn By E W Roberts.

Title Calibration from engine results of Bosch vs OPACIMETER.

Test No.	Timing	Amb'nt °C	Barometer mm Hg.

Holset / Leyland / Dowty / DoI Contract

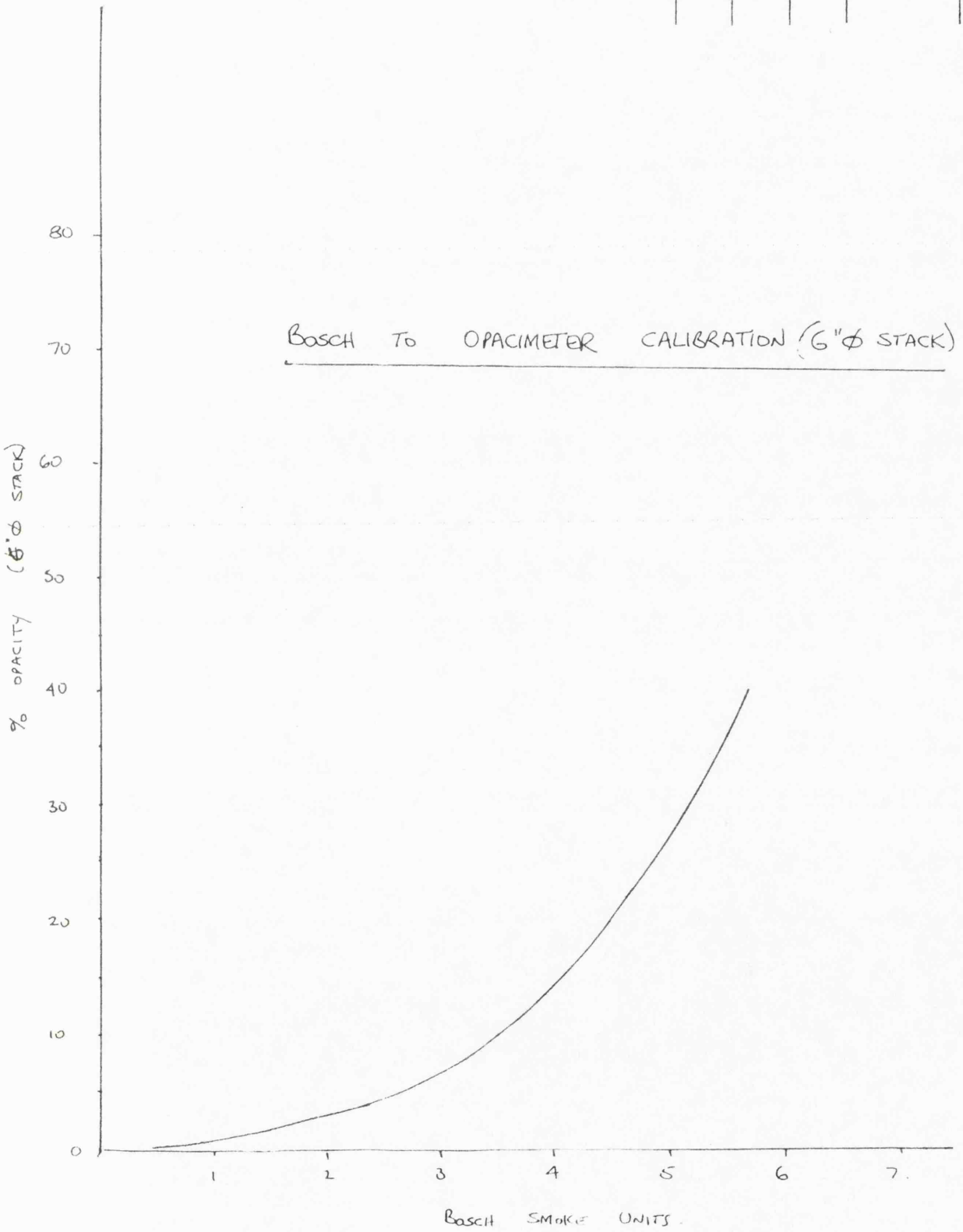

fig 2.19

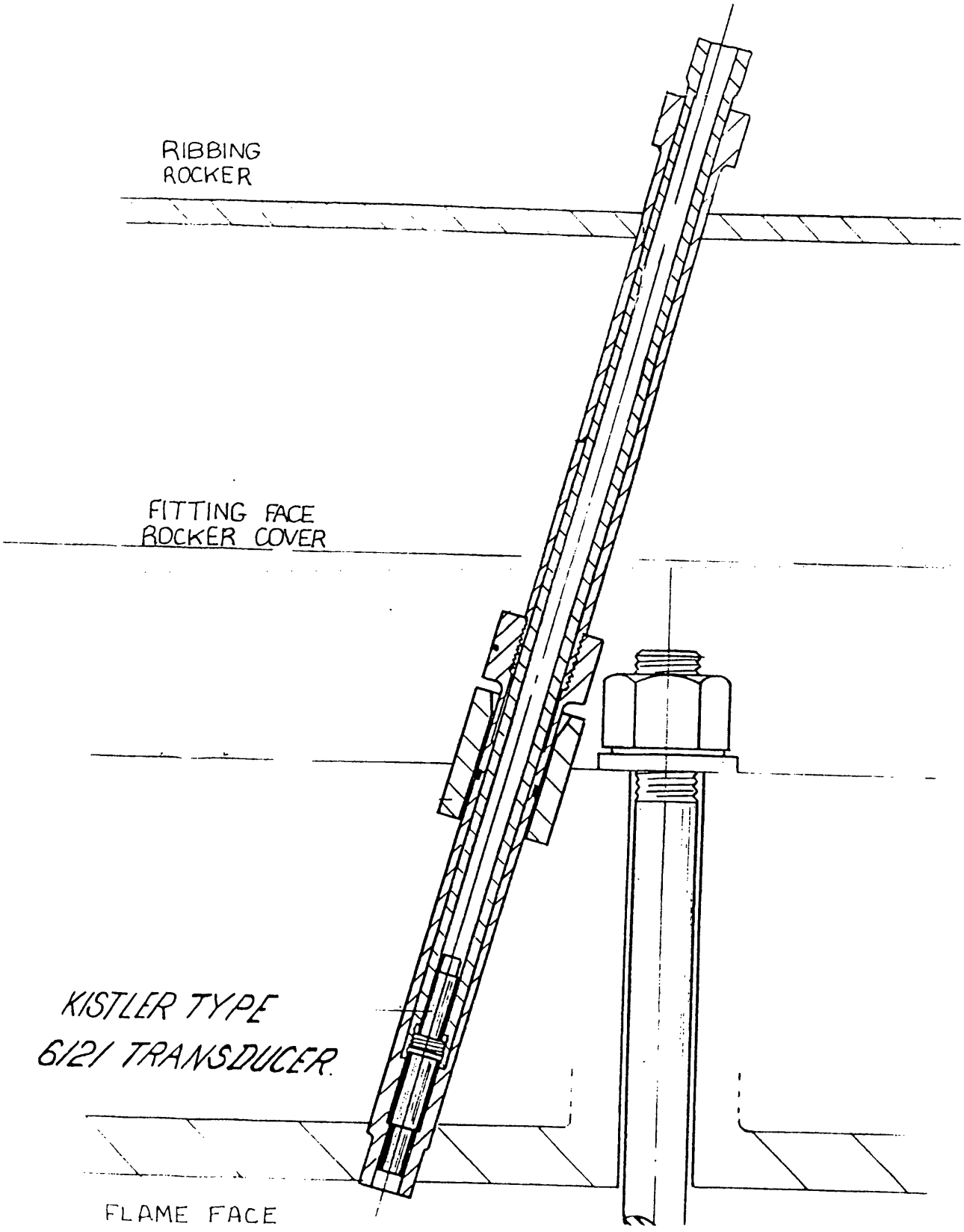

fig 2 20 INSTALLATION OF CYLINDER PRESSURE TRANSDER

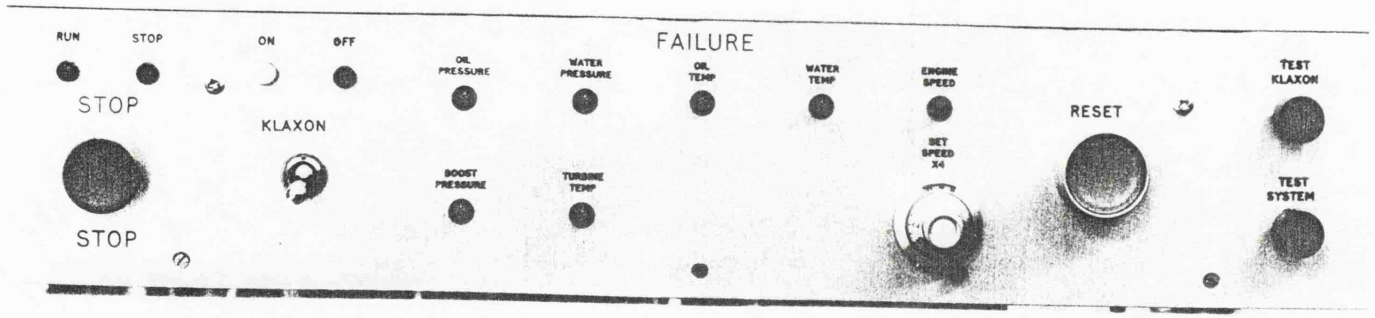

fig 2.21 FAILURE PANEL

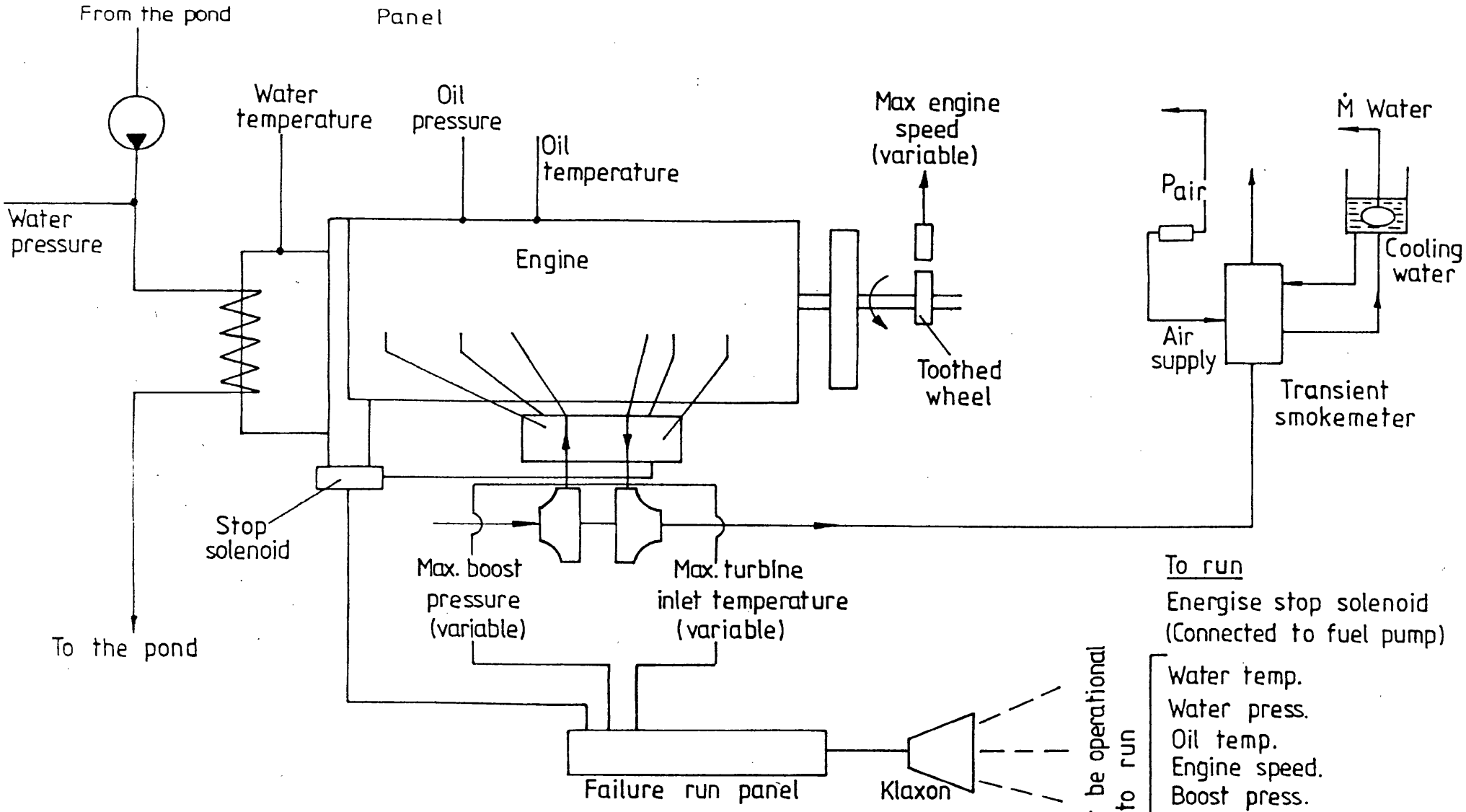

FIG. 2.22 FAILURE PANEL

Engine Type & No. LEYLAND TL11 ENGINE - 7962756 | Object of Test TIMING SWING INVESTIGATION | Page Serial No. 146

Bed No. 2 | Ambient Temp. 22°C | Engine Displacement 11·10 litres | Date 6th AUGUST 1982

Engine Rating Nett 190 kW at 2100 rev/min | Turbocharger Build H2B5085C L25A3 | Barometer Reading 988 mbar

Time	Engine rev/min	Torque Nm	Engine kW	Fuel Consumption secs	kg/hr	kg/kW hr	Turbo Speed	Vap Press	Air Inlet	Air Nozzle	Boost Press	Boost Temp	Exhaust Before Turbo	Exhaust After Turbo	Fuel °C	Fuel mmHg	Eng Water °C In	Eng Water °C Out	Engine Oil °C	Engine Oil psi	Smoke Bosch	Smoke Celesco	Electronic Instrumentation Dyn. Tim. BTDC deg	Cyl. Press. bar	Line Press. bar	VG Pos mm		
11.30	1350	1350	·4	47.8	1033		70800	·82	103/25.0	2.6	501/100.9		369/716	359/692	36/649	45	300	72	85.8	92	45	3.2	1.4	①	4.66	-	@	10.43	437.2
	1350	1020	·4	45.4	1045		69700	·80	98/26.3	2.5	481/100.5		356/715	346/690	36/651	24/47	300	72	86.1	95	44	2.8	6.4	③	5.12	-	⑥	10.45	
	1350	1029	·4	48.9	1052		69280	·79	95/27.0	2.4	468/99.4		345/712	337/684	35/646	25/47	300	72	86.2	96	44	2.6	5.4	④	5.39	—	ⓒ	10.45	
	1350	1023	·4	49.6	1077		68200	·78	95/27.2	2.45	459/97.3		342/707	332/678	34/641	22/45	300	73	86.2	96	44	2.5	4.0	⑤	5.8	-	ⓓ	10.49	
	1350	1025	·4				68350	·72	93/27.3	2.39	461/99.1		341/710	332/690	35		420												
	1350	1019	·4	48.1	1046		68500		92/27.3	2.40	458/99.5		339/710	332/657	34/644	26/49	290	73	87.0	97	44	2.2	3.7	⑥	6.13	-	ⓔ	10.45	
	1350	995	·4	48.7	1047		68800		94/27.6	2.40	461/100.3		342/718	339/658	34/649	27/49	280	74	86.7	97	44	2.1	3.0	⑦	6.151	-	ⓕ	10.44	
12.56	EASE OFF. - STOP																											438.2
	9th AUGUST 1982. FUEL TANK TOPPED UP. BATTERIES CHARGED. ETC. (NEL TOPPED UP. TEST 51																											
11.20		W 42M					998 mbar .21°C																					
	800	2000	2				48420		24/24.3	0.68	217	65.5	146	146	19			84.7				26.2	⑤	5.36	-		10.44	
			SLOT DOWN - FUEL DELIVERY PROBLEMS																									
	800	871	·2	40.5	535		47400	0.74	25/25.2	0.64	213/63.2		144/666	144/633	19/625	22/40	190°	64	84.3	87	35	4.16	15	⑦	5.68		ⓐ	10.49	
	800	882	·2	40.6	545		47700	·74	25/27.0	0.66	219/66.8		145/675	144/646	18/635	22/43	170°	65	84.4	90	35	4.38	20	⑥	5.50		ⓑ	10.50	
	800	900	·2	40.6	550		47900	·64	25/27.4	0.68	216/67.8		147/683	147/653	18/640	24/44	170°	66	84.5	91	35	4.66	25	⑤	5.29		ⓒ	10.48	
	800	896	·2	43.7	586		47300	·70	25/28.0	0.64	214/68.0		145/683	145/650	18/635	23/45	170°	66	84.4	91	35	5.10	30	④	5.02		ⓓ	10.60	
	850	900	·2	46.0	598		47400	·64	25/28.0	0.64	215/68.5		144/682	144/652	18/635	23/45	100°	65	84.4	91	35	5.3	33	③	4.7		ⓔ	10.60	
	850	902	·2	47.9	636		48000	·64	25/28.5	0.64	215/68.9		146/687	146/652	18/635	24/46	150°	66	84.3	90	35	5.4	36	②	4.4		f	10.61	
13.16	EASE OFF. BLEED FUEL SYSTEM.																											
	800	400	·2	96.5	1293		—	·60	21/25.0	0.54	50/35.4		66/361	69/320	7/323	24/42	255°	60	78.8	81	34	0.9	1.0	①	3.44		ⓐ	7.50	
	800	400	·2	97.6	1304		—	·60	21/25.0	0.54	49/36.0		66/357	69/320	7/320	21/42	215°	60	78.9	81	34	0.83	1.1	②	3.70		ⓑ	7.52	
	800	400	·2	95.2	1270		—	·66	19/24.9	0.54	49/36.1		66/361	69/332	7/326	23/42	210°	60	79.4	81	34	1.3	2.0	④	4.10		ⓒ	7.50	BLACK
	800	400	·2	93.1	1245		—	·66	20/25.2	0.54	49/36.9		67/370	69/339	7/334	23/42	200	59	80.1	82	34	1.3	3.4	⑤	4.21		ⓓ	7.50	SMOKE
	800	400	·2	91.3	1226		—	·70	21/25.4	0.54	49/37.5		69/377	71/345	7/342	22/41	190	59	80.7	83	34	1.56	3.0	⑥	4.12		ⓔ	7.75	
	800	400	·2	89.1	1197		—	·70	20/25.5	0.54	53/38.2		72/384	74/357	7/343	23/43	180	60	81.1	83	34	2.2	5.0	⑦	4.17		f	7.81	
15.10	EASE OFF																TESTS											
15.20	STOP																						STORAGE SCOPE OUT					442.2

Total Running Time :- 448 (181.22)

Tested by CC

Injection Timing STANDARD 22° BTDC 'NOMINAL' VT(SH.)

Pressure Charger Make & Serial No.

Fuel Injection Pipes 24 ins. LONG - 6 x 2 mm dia.

Fuel Pump Make & Serial No. CAV MAJORMEC PS476 (ANEROID CONTROL)

Compressor Serial No. NOT FITTED

Injectors Make & Type AMERICAN BOSCH SET TO 235 ATS

CONTRACT :-

HOLSET/LEYLAND/DOWTY/DEPT. OF INDUSTRY/UNIVERSITY OF BATH

Remarks :- NO CRANK ANGLE MARKERS. RACK OSCILLATING. UNDULL INVESTIGATING.

UNIVERSITY OF BATH

SCHOOL OF ENGINEERING

fig 2.23 TEST BOOK

DATA INPUTS

GENERAL ENGINE PARAMETERS

N - NO OF REVS
Y - TIME TAKEN (SECS)
Q - TORQUE (LBF FT)
N1- TURBO SPEED (REV/MIN)
S1- SMOKE BOSCH (DIVISIONS)
D2- SMOKE CELESCO (%)
D - DYNAMIC TIMING (DEGREES BIDC)
DO- DURATION OF INJECTION (DEGREES)
O - RELATIVE HUMIDITY (RATIO)
X - V.G. POSITION (%RESTRICTION)
M - MASS WEIGHT USED IN WEIGH GEAR (KG)
M7- FUEL FLOW (M13/S) * 1E-6

TEMPERATURES

TO - FUEL BEAKER TEMP. (DEG C)
T1 - AIR INLET TEMP (DEG C)
T2 - BOOST TEMP. (DEG C)
T3 - PRETURBINE TEMP FOR ENTRY (1) (DEG C)
T4 - STACK TEMP. (DEG C)
T5 - WATER INLET TEMP (DEG C)
T6 - WATER OUTLET TEMP (DEG C)
T7 - FUEL TEMP (DEG C)
T8 - PRETURBINE TEMP. FOR ENTRY (2) (DEG C)
T9 - OIL TEMP (DEG C)

PRESSURES

P0 - CYLINDER PRESSURE (DIVISIONS
P1 - INLET DEPRESSION (MM H20) (G)
P2 - BOOST PRESSURE (MMHG)(G)
P3 - PRETURBINE PRESSURE FOR ENTRY (1) (MMHG) (G)
P4 - STACK PRESSURE (MMHG)(G)
P5 - AIR NOZZLE PRESSURE (INCH H20) (G)
P6 - FUEL LINE PRESSURE (DIVISIONS)
P7 - FUEL PRESSURE (MMHG)(G)
P8 - PRETURBINE PRESSURE FOR ENTRY (2) (MMHG)(G)
P9 - OIL PRESSURE (LB/SQ IN)

fig 2.24 INPUT PARAMETERS

VARIABLE OUTPUTS

T - AVERAGE PRETURBINE TEMP DEG C
TO - FUEL BEAKER TEMP DEG C
T1 - AIR INLET TEMP DEG C
T2 - BOOST TEMP DEG C
T3 - PRETURBINE TEMP DEG C
T4 - STACK TEMP DEG C
T5 - WATER TEMP IN DEG C
T6 - WATER TEMP OUT DEG C
T7 - FUEL TEMP DEG C
T8 - PRETURBINE TEMP DEG C
T9 - OIL TEMP DEG C

P0 - CYLINDER PRESS BAR (G)
P1 - AIR INLET PRESS KPA (G)
P2 - BOOST PRESS TOTAL KPA (G)
P3 - AVERAGE PRETURBINE PRESS KPA (G)
P4 - STACK PRESSKPA (G)
P6 - FUEL LINE PRESS BAR (G)
P7 - FUEL PRESS KPA (G)
P8 - B.M.E.P. (BAR)
P9 - OIL PRESS KPA (G)

N - ENGINE SPEED REV/MIN
Q - TORQUE NM
P - POWER KW
N1 - CORRECTED TURBO SPEED
F1 - S.F.C. KG/KWHR
F2 - FUELLING MG/SHOT/CYCLE
M6 - EXHAUST TURBINE FLOW (IN12*K10.5/MIN)
M4 - N.D. TURBINE MASS FLOW KG/S*SQRT (K)/BAR
M1 - FUEL MASS FLOW KG/S*1E-3
M7 - FUEL VOLUME FLOW (M13/S)*E-6
M2 - AIR FLOW (KG/S)E-3)
R1 - AIR FUEL RATIO
R2 - PRESS RATIO
R3 - EXPANSION RATIO
X - V.G. POSITION (%)
N2 - N.D. TURBO SPEED (REV/SEC/K10.5)
E0 - VOLUMETRIC EFFY (%)
E1 - THERMAL EFF (%)
E2 - COMPRESSOR EFF (%)
E3 - OVERALL EFF (%)
E4 - TURBINE EFF (%)
F3 - FUEL INJECTED/CYCLE (MM13/CYCLE)
R4 - SPOUTING VELOCITY/C. RATIO
S1 - SMOKE BOSCH
D1 - DENSITY RATIO
D0 - DURATION OF INJECTION (DEG)
S2 - SMOKE CELESCO
D - DYNAMIC TIMING DEG
V1 - AIR FLOW CUBIC FT/MIN
V0 - CORRECTED VOL FLOW M13/SEC
V - VAPOUR PRESS KPA(ABS)

fig 2.25 OUTPUT PARAMETERS

DATA

REDUCTION PROGRAM

FLOW CHART

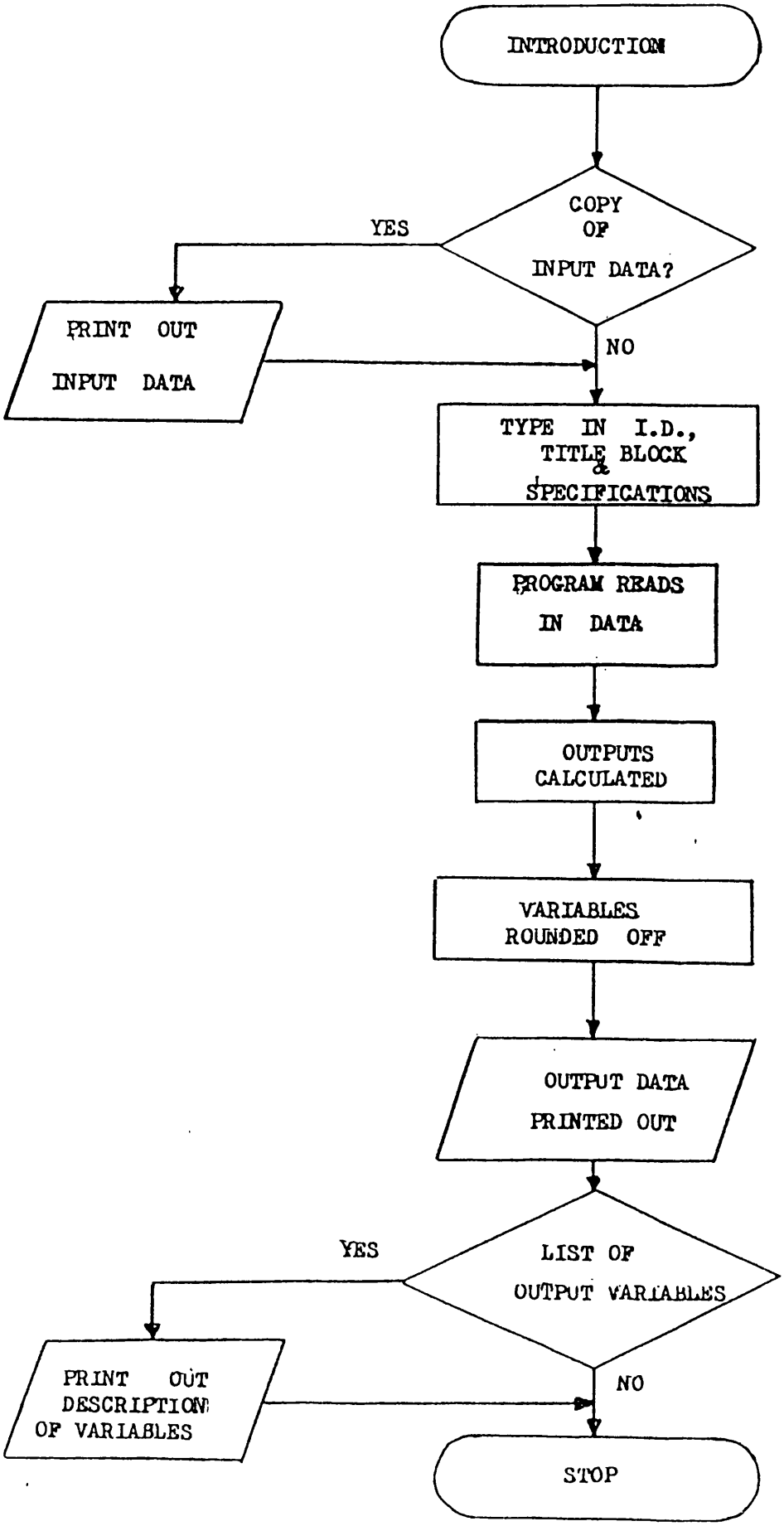

fig 2.26 Flow Chart Steady State Program

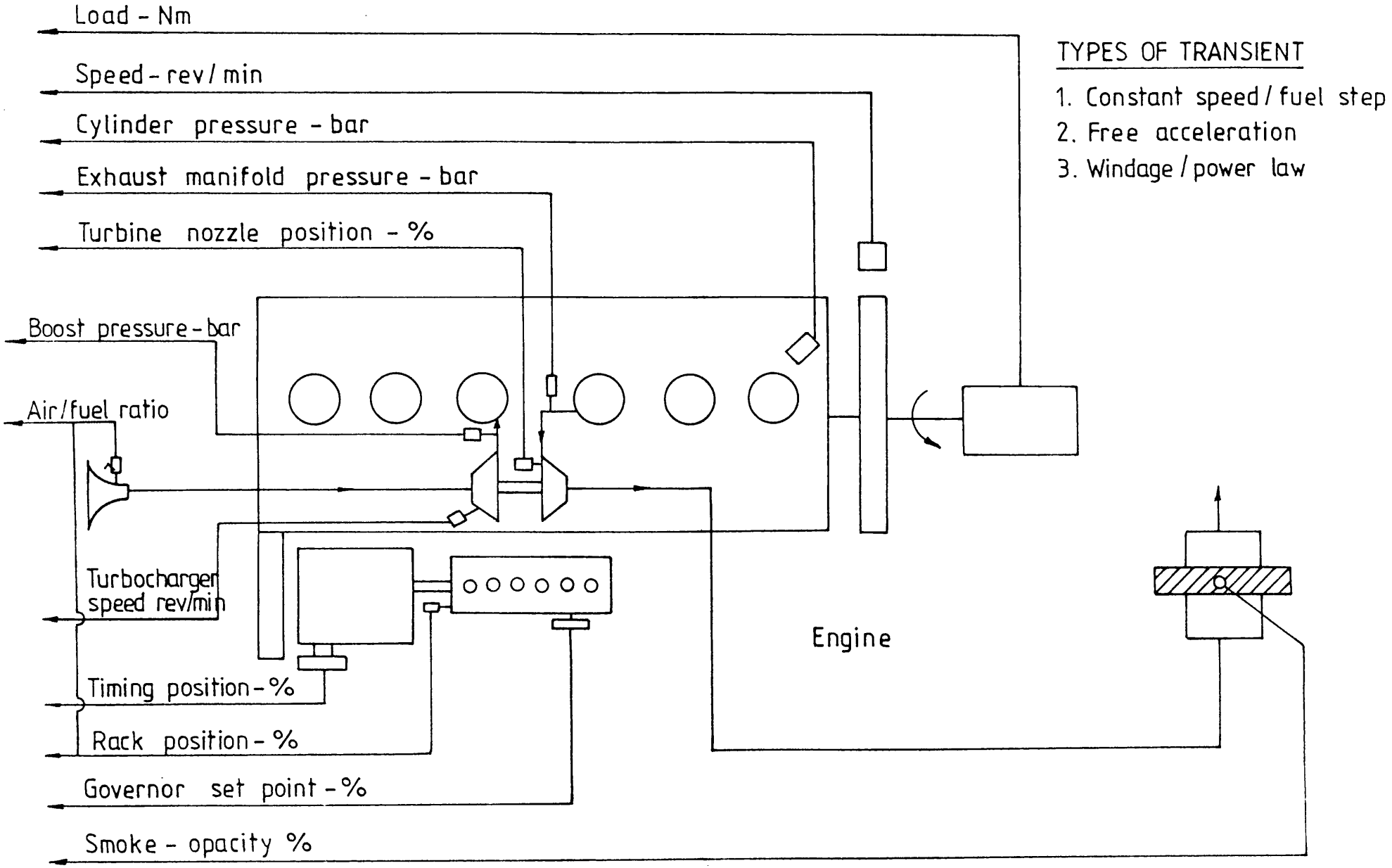

FIG 2.27 ENGINE TRANSIENT OUTPUT SIGNALS

Processed and outputted to a basis of time by the PDP8L

FIG. 2.2'B FLOW - CHART FOR DATA - AQUISITION PROGRAM

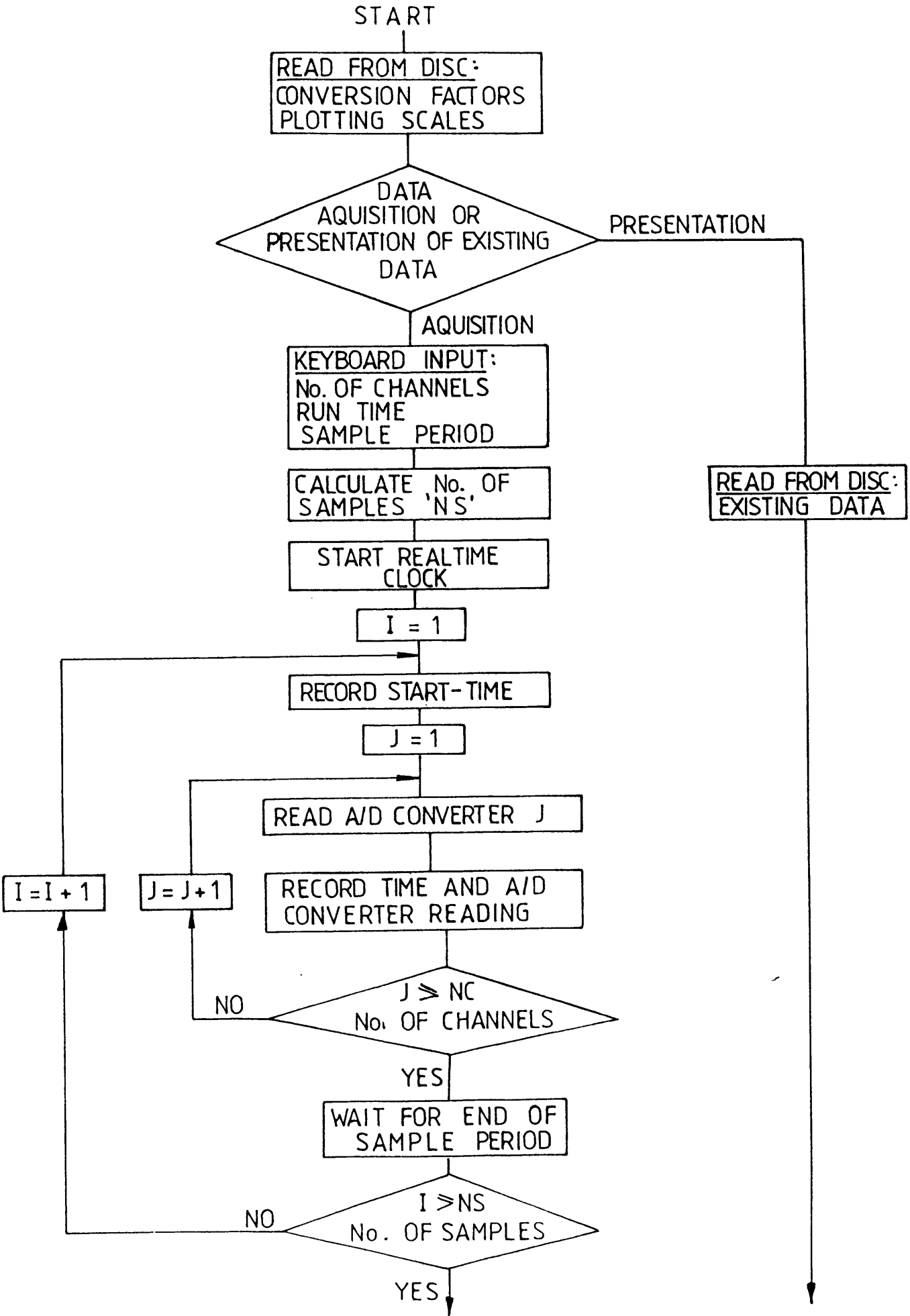

FIG. 2.28 FLOW-CHART FOR DATA-AQUISITION PROGRAM

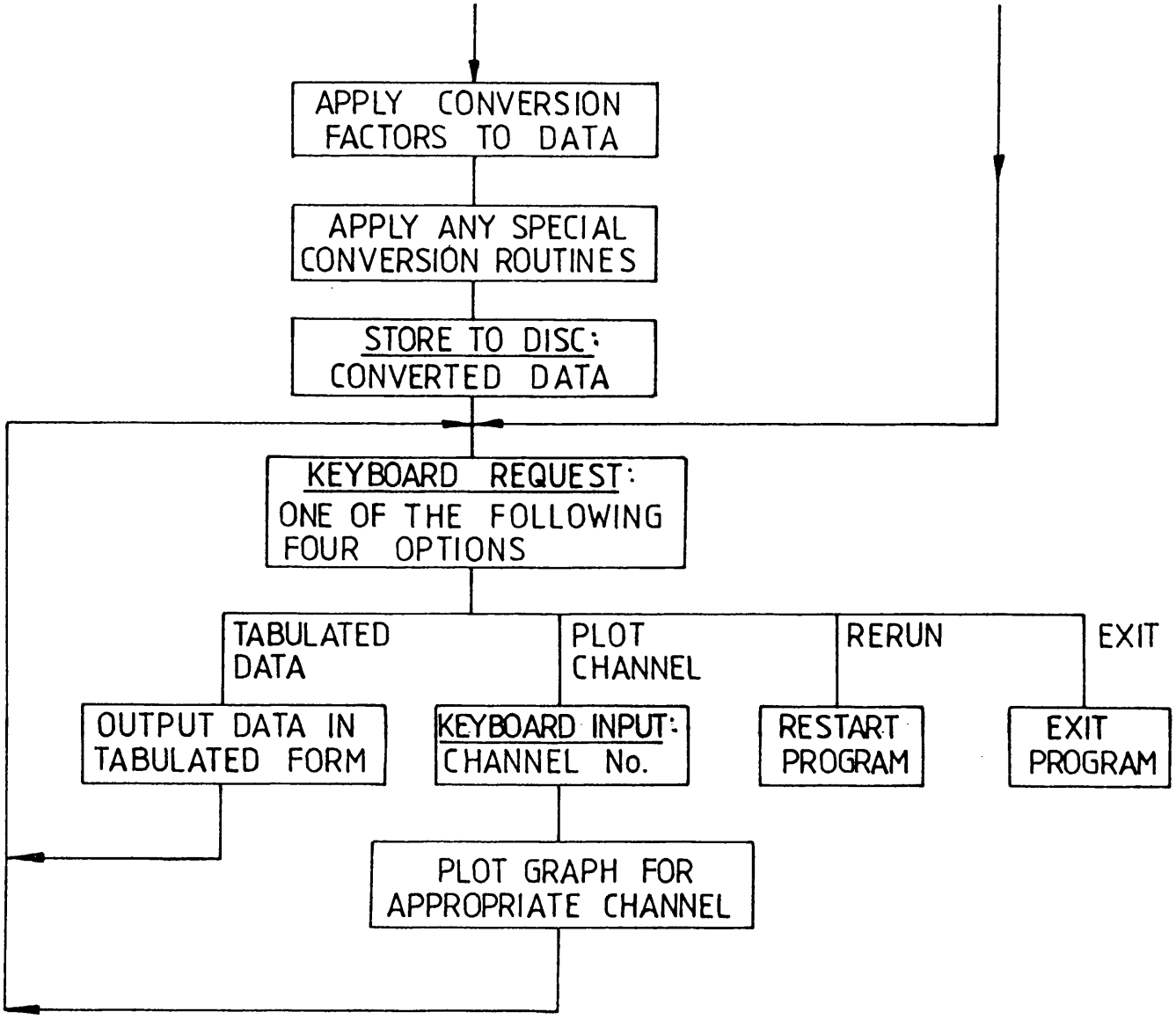

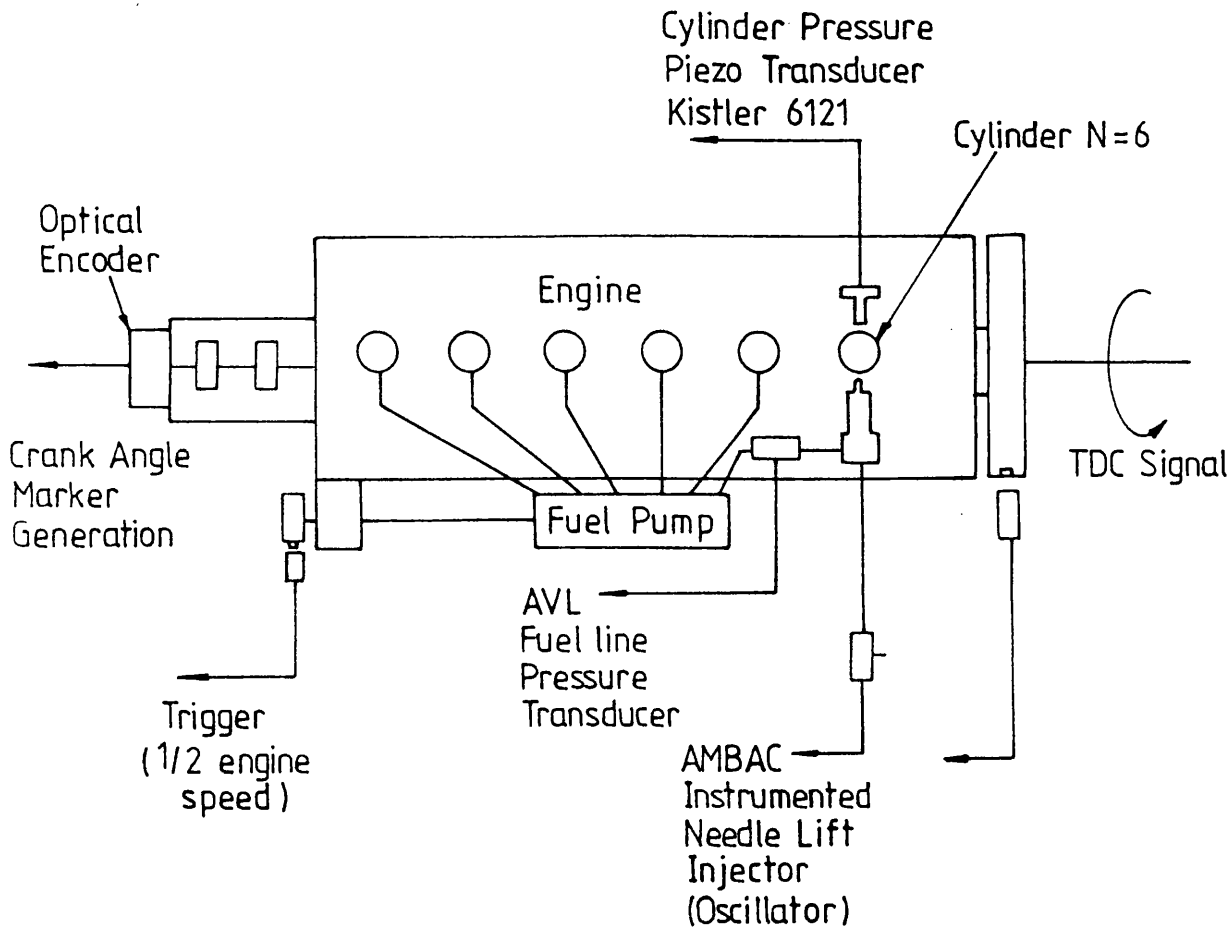

1. Cylinder Pressure
2. Needle Lift
3. Fuel Line Pressure
4. To a Base of Crank Angle 5°, 30° and TDC

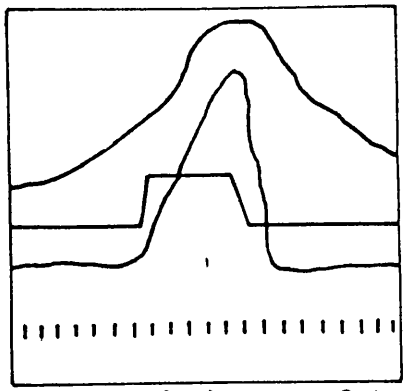

Typical Oscilloscope Output

FIG. 2.29 ELECTRONIC INSTRUMENTATION

Engine LEYLAND TL11 ENGINE — 11.1L DISPLACEMENT Drawn By. E.W. Roberts.

Title CALIBRATION CHECK ON VIBROMETER ... TORQUE TRANSDUCER.

Test No.	Timing	Amb'nt °C	Barometer Ins. Hg.

Holset / Leyland / Dowty / DoI Contract

APPLIED TORQUE.	MEASURED TORQUE.
183 Nm	160 Nm
488	480
795	782
1084	1080
1373	1369

Found to be SATISFACTORY.

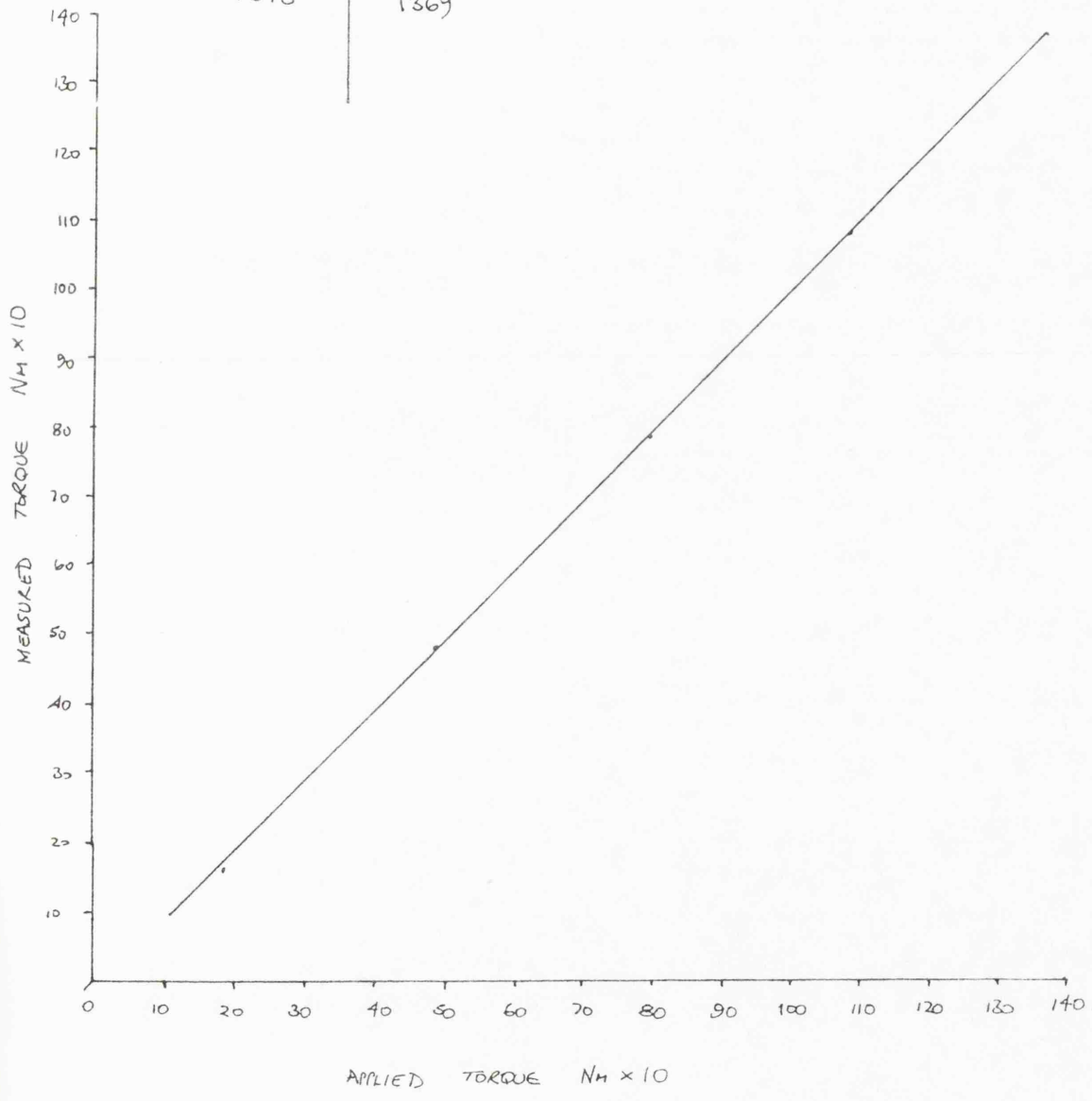

Fig 2.30 (c)

Engine LEYLAND TL11 ENGINE — 11.1L DISPLACEMENT Drawn By. E W Roberts

Title KISTLER TYPE 6121 PIEZO CYLINDER PRESSURE TRANSDUCER.

Test No.	Timing	Amb'nt °C	Barometer Ins. Hg.
—	—	—	—

Holset / Leyland / Dowty / DoI Contract

CALIBRATION CURVE

CONFIRM. 24/1/83.

Pressure (bar)	Volts
10	·366
20	·8695
30	1·383
40	1·913
50	2·435
60	2·952
70	3·462
80	3·967
90	4·476
100	5·018
110	5·558
120	6·087
130	6·601
140	7·104

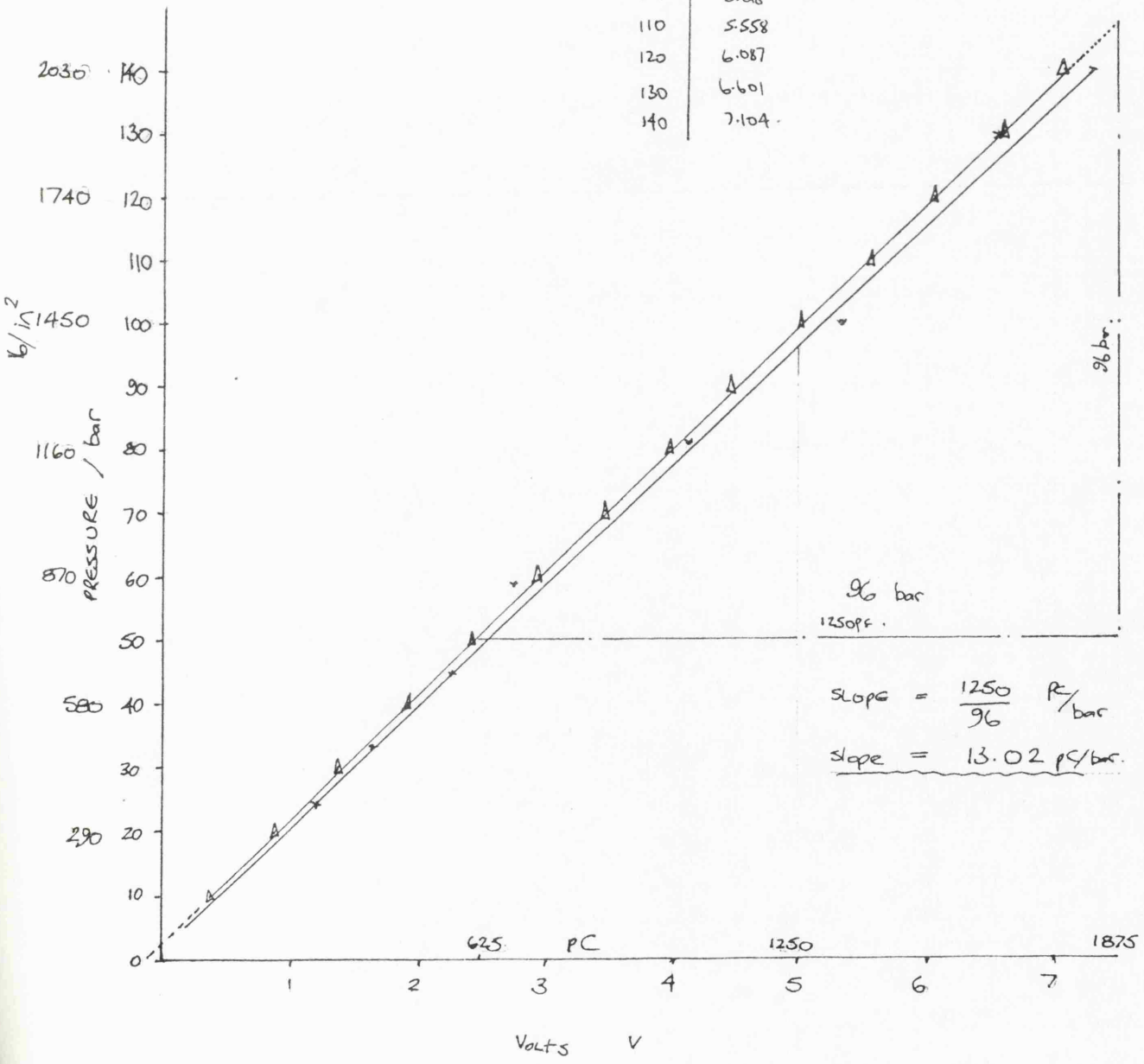

Slope = $\frac{1250}{96}$ pC/bar

Slope = 13.02 pC/bar.

fig 2.30 (ii)

Engine LEYLAND TL11 ENGINE—11.1L DISPLACEMENT Drawn By E.W ROBERTS.

Title SCHAEVITZ CALIBRATION GRAPH · INLET & EXHAUST.

Holset / Leyland / Dowty / DoI Contract

Test No.	Timing	Amb'nt °C	Barometer mm Hg.
–	–	–	–

Note.! THESE ARE NEW TRANSDUCERS & REPLACE THOSE PREVIOUSLY USED WHICH ARE NOW U/S. EHR.

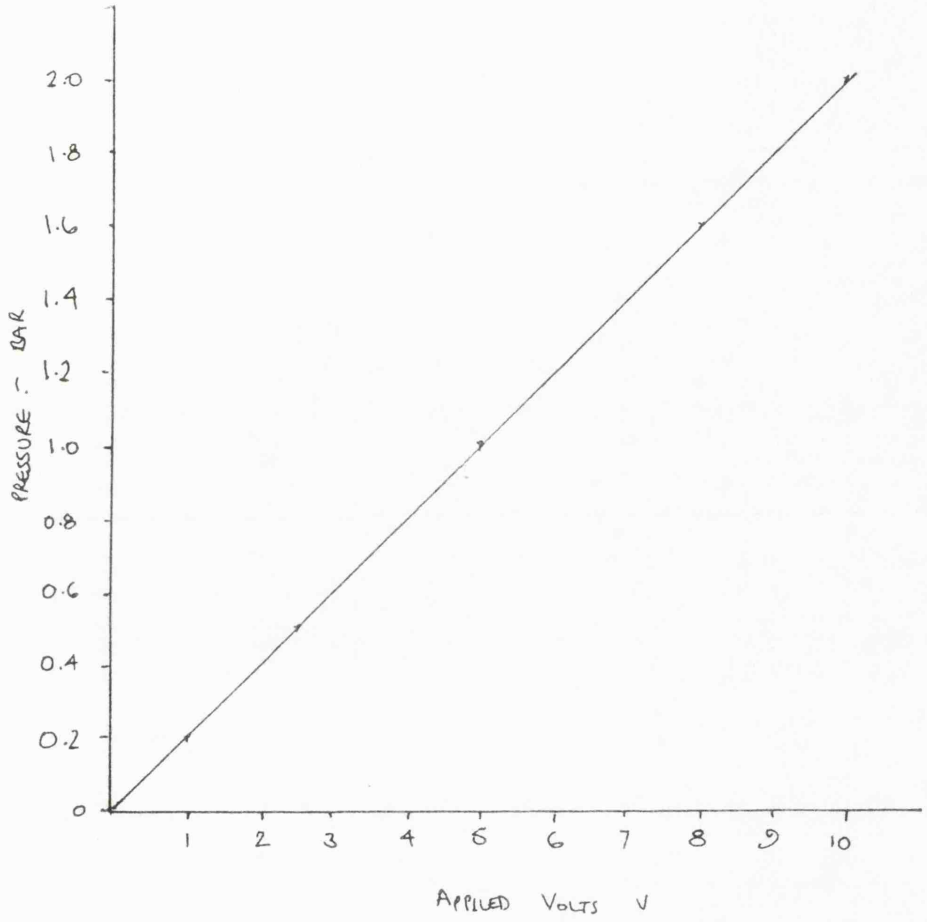

CALIBRATION CURVE FOR INLET & EXHAUST PRESSURE TRANSDUCERS (0 35b, VG)

2 bar = 10v.

fig 2.30 (iii)

Engine LEYLAND TL11 ENGINE—11.1L DISPLACEMENT Drawn By. E.D ROBERTS.

Title CALIBRATION OF FURNESS AIRFLOW TRANSDUCER.

Test No.	Timing	Amb'nt °C	Barometer Ins. Hg.	
/	/	/	/	/

Holset / Leyland / Dowty / Dol Contract

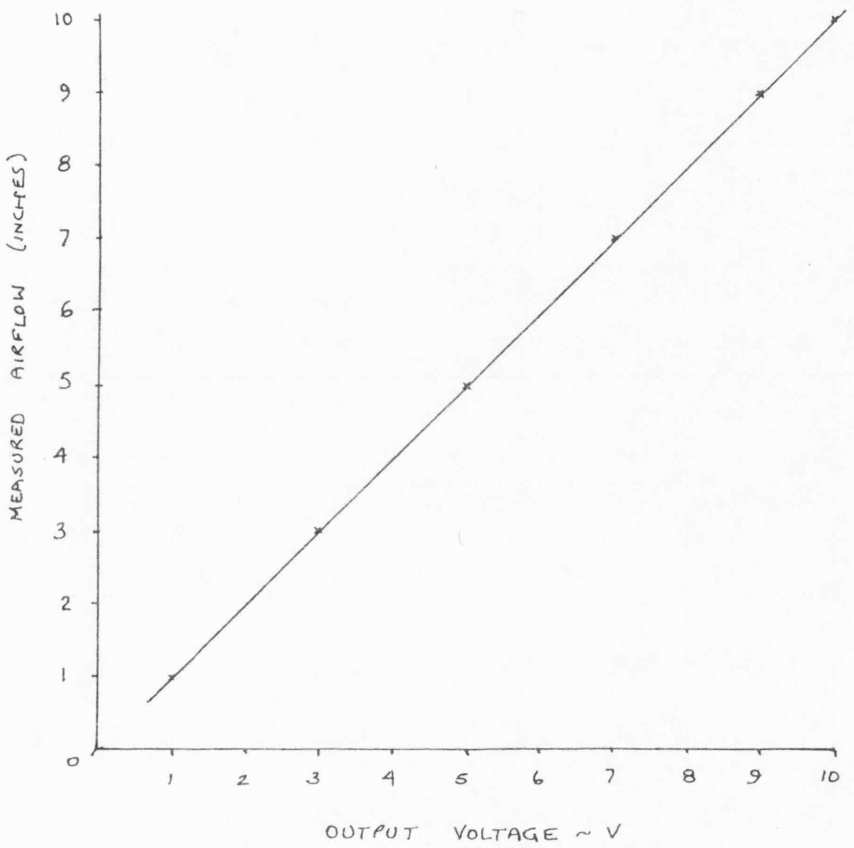

fig 2.30 (iv)

Engine LEYLAND TL11 ENGINE—11.1L DISPLACEMENT Drawn By E.W. Roberts.

Title CALIBRATION OF MAJORMEC PUMP UNDER ELECTRONIC CONTROL (SANGAMO AE 15)

Holset / Leyland / Dowty / DoI Contract

Test No.	Timing	Amb'nt °C	Barometer mm Hg.
—	—	—	—

NOTE! MAX RACK SETTING SHOULD BE APPROXIMATELY 6 VOLTS MAXIMUM.

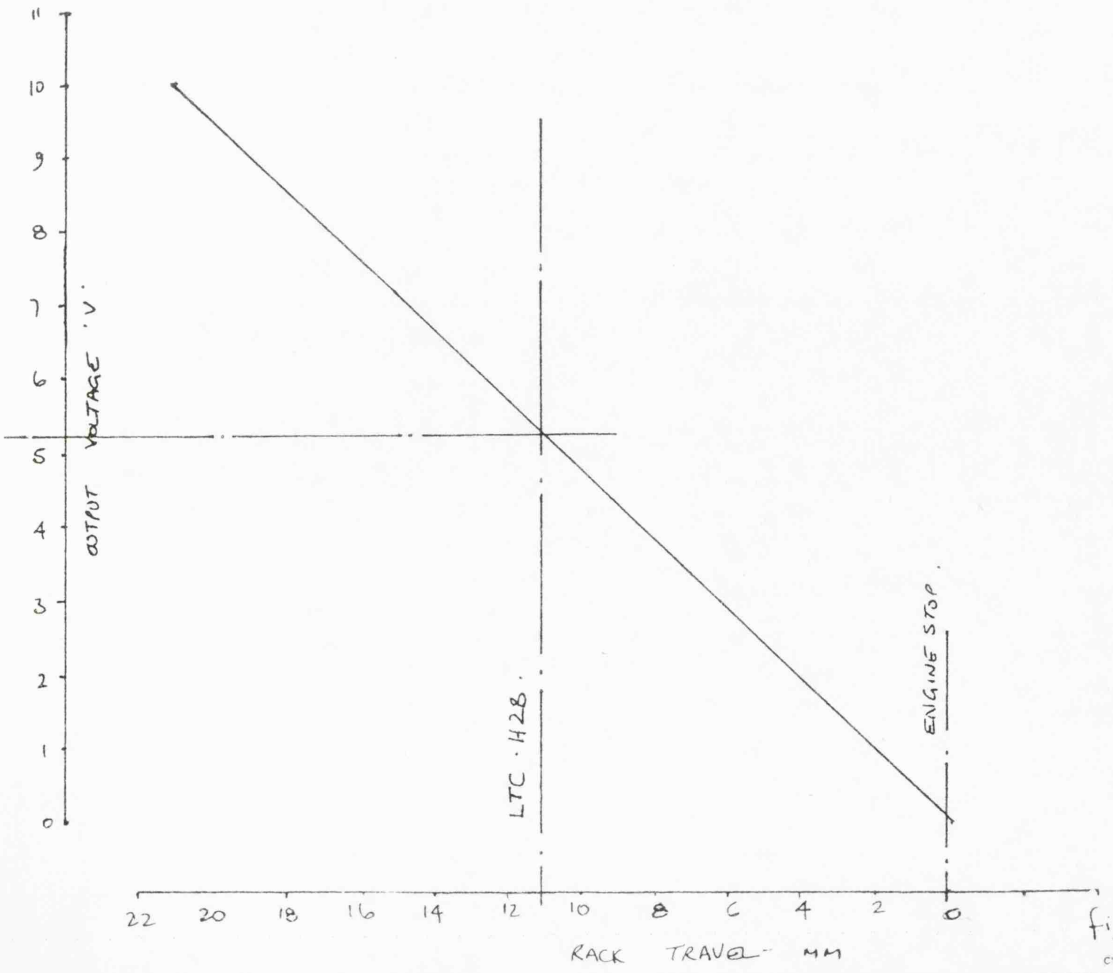

fig 2.30 (v)

Engine LEYLAND TL11 ENGINE—11.1L DISPLACEMENT Drawn By. E W ROBERTS

Title CALIBRATION OF RING SLEEVE POSITION (SCHAEVITZ TYPE 201) PNEUMATIC

Test No.	Timing	Amb'nt °C	Barometer Ins. Hg.
—	—	—	—

Holset / Leyland / Dowty / DoI Contract

PNEUMATIC ACTUATION

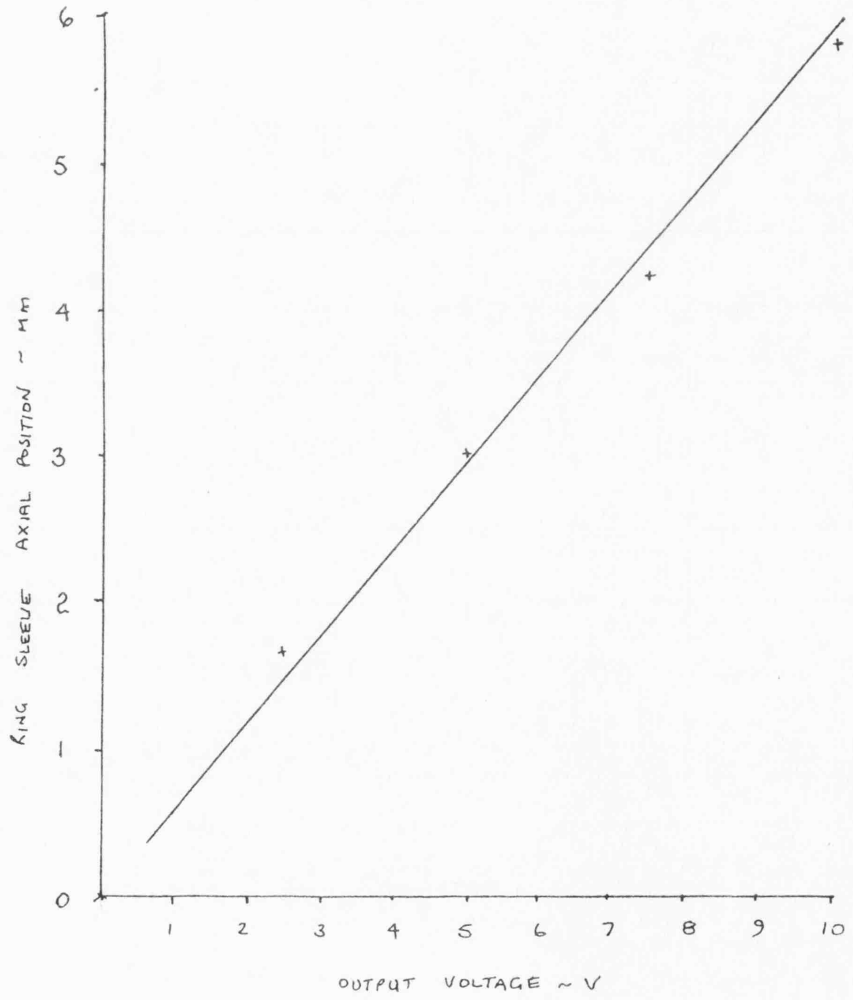

fig 2.30 (Vi)

3. DEVELOPMENT OF CONTROL SYSTEM

3.1. Introduction (62, 64)

It was stated in Chapter 1 that a turbocharged automotive diesel engine had the capability for limited torque back up and speed range due to the tendency of the radial inflow turbine towards increased swallowing capacity with decreased rotational speed; as a consequence matching is a compromise. Compressors with wide efficient flow ranges at moderate boost are available and as a result surge is not considered to be a problem with moderately rated engines.

A solution to this matching problem is a turbocharger with a variable geometry turbine stage. This is a turbine which has a characteristic of a small turbine housing at low speed and a larger housing at high speed. A mass flow turn down ratio of the order of 2:1 would allow 'torque back up' of approximately 50% at 50% of rated speed which is the design aim. It would also improve transient response. This thesis investigates complete engine turbocharger testing with a purpose built Holset turbocharger, equipped with a variable geometry turbine nozzle ring, applied to a Leyland TL11 diesel engine. A variable geometry scheme must include a control system. This could be based on boost pressure acting through a pneumatic controller or through hydraulics. To benefit part load SFC and emissions a more comprehensive control scheme is required. The growth of digital electronics and the development of the microprocessor has made it possible to realise much greater flexibility in scheduling and control.

This chapter describes the development of a microprocessor control system which allows for the optimisation and control of a variable area turbocharger applied to the TL11 engine. The microprocessor based electronic control is aiming to attain much more precise engine control than is possibly with mechanical or analogue electronic systems.

A microprocessor control system is made up of three control blocks; Fig. 3.1.

1. the transducers which monitor the operating conditions.
2. the central processing unit or controller which acts on their information in accordance with a stored program.
3. the actuators, which execute the commands of the control unit.

In the case of a high torque back up engine the additional torque developed must be reflected in a higher cylinder pressure for a given compression ratio. Retarding injection timing allows control of this parameter though usually at the expense of SFC. To extend the variable geometry capability and take advantage of the flexibility of the microprocessor control system a variable injection timing device was included in the control scheme. To develop the VG concept effectively, greater flexibility and a suitable interface to the microprocessor were required for the governing function. An electronically governed fuel pump was therefore also included.

The large range of functions of the microprocessor enables the control parameters to be ideally adapted to all the operating modes of the engine. This would be virtually impossible with conventional procedures for manual adjustment on the test bed and in the vehicle owing to the large number of variations.

The control strategy adopted was that of the closed loop and digitally stored characteristic (that is not self optimising). Compared with other solutions the closed loop control with digitally stored characteristic makes possible the following:

(a) to shape the full load characteristic independent of temperature

(b) to attain the ideal emissions/fuel consumption compromise

(c) to shape the torque curve for smooth acceleration

(d) by monitoring the air flow and storing the desired characteristic it is possible to operate the engine

at lower smoke levels during acceleration and at high altitudes

(e) to select the best start of injection value for any operating condition from a programmed map

(f) to compensate for wear

(g) to have the possibility of extending the electronic diesel engine control system to other systems e.g.

(i) exhaust brake
(ii) transmission
(iii) isochronous governor
(iv) diagnostics
(v) monitoring
(vi) display
(vii) cruise control

An optimal control system depends on engine test information determined previously.

The positions of the control parameters corresponding to optimum engine conditions were noted and formed arrays which were stored digitally within the microprocessor. In operation the arrays formed a closed loop look up table as a function of engine speed and load. To control the variable area turbocharger a boost control schedule was adopted to allow for any parametric or structural changes in the system. Fig. 3.2/3 is a block and schematic diagram of the engine control system.

In this chapter the control implementation for the variable area inflow radial turbine and the associated control parameters of timing and fuelling are described. It also includes an account of the design and development of the control parameters themselves.

3.2. Microprocessor Controller (65)

3.2.1. General

The major disadvantage of microprocessor based control systems for development programs is that the writing of control programs requires specialist knowledge usually beyond the scope of the control engineer.

A minicomputer allows the control program to be developed in a 'high level' language which minimises the need for specialist programming whilst maintaining speed of operation.

The high level language instructions allow the use of arithmetic operators, maximum and minimum functions, integration, differentiation, program loops, jumps and non-linearities implemented by 'look-up tables'.

The choice of controller was restricted to the following:

1. The Commodore PET Microcomputer - 8 bit machine
2. DEC PDP8E (connected by land lines) mini-computer - 12 bit machine
3. DEC PDP-11/34 (connected by land lines) mini-computer - 16 bit machine
4. the DEC LSI 11/23 mini-computer - 16 bit machine

The School has standardised on the above machines. The best controller for the project was considered to be the LSI 11-23 and a unit was purchased.

3.2.2. Description (Fig. 3.4)

The DEC LSI 11/23 is a 16 bit microcomputer in the PDP 11/LSI 11 range of computers. DEC has many years operating experience with this range of machines and supplies compressive, proven software. The LSI 11 operates on 16 bit words and can address 64 K bytes directly or 256 K bytes with memory management. The system used for this project consists of:-

1. The LSI 11/23 processor with the memory management option and floating point arithmetic hardware.
2. 160 bytes of RAM.
3. VT103 Video Terminal.
4. Dual RX02 Floppy Disc Drive.
5. Serial Printer.
6. Analogue to digital convertors board (A/D) (8 differential analogue inputs).
7. Digital to analogue convertors board (D/A) (4 analogue outputs).

The software used on the system is the RT-11 operating system with two high-level languages available (Fortran and Basic) and one low level language (MACRO-11 assembly language). The RT-11 operating system is a single user system giving comprehensive file handling capabilities and efficient user program development and execution.

3.2.3. Operation

In the control system described, signals from the transducers are converted to corresponding numerical quantities that are fed to the controller. Physical quantities (pressure, position etc) are converted to an electrical signal by the transducers. Input and output signal conditioning circuits are required to convert input signals to suit the controller circuitory (0-10 v) and to amplify the outputs to a suitable level (0-10 v) for the actuators. The electrical signals are converted to numerical quantities in a form suitable for the microcomputer by analogue to digital convertors (A/D). The interface modules consist of analogue inputs multiplexed into a 12 bit A/D and a D/A whose output is demultiplexed to several analogue outputs. Because of its high speed the controller is able to calculate the effect of every change in the inter relationship among the variables and quickly produce output signals which adjust the set point of each parameter to produce the most efficient operation. The controller then compares the input signals from the transducers with the readjusted set points and

sends appropriate signals to the various actuators via digital to analogue (D/A) convertors.

3.3. Actuators & Control

Three actuation systems were considered based on:
1. pneumatics, 2. electrics and 3. hydraulics.

Execution times better than 0.1 s were required (so as not to interfere with engine transients) necessitating the use of servo-mechanisms.

The components of a servo are subjected to severe loading due to the constant changes in commands; additionally a diesel engine represents a very hostile environment in which to mount transducers and actuators. This is because they are subjected to:

1. vibration, 2. high temperature, 3. an atmosphere of lube and fuel oil.

The merits of the three different actuating media are next discussed with regard to their suitability for a diesel engine control system.

3.3.1. Pneumatic Actuation (Ref. 61)

Pneumatic actuation is employed in wastegated applications, boost pressure being used as the controlling variable. The advantages include:
(1) simplicity, (2) cheapness, (3) reliability, (4) cleanliness,
(5) no fire risk, (6) can exhaust to atmosphere.

The disadvantages could be summarised as:

1. extreme accuracy is difficult
2. speed of response is poor (compressible flow)
3. interfacing to the microprocessor could be difficult

The poor speed of response makes pneumatics an unsuitable medium for transient work. Nevertheless the VG turbocharger as originally used was designed for pneumatic control, its use in that form being limited to steady state tests. The required control pressure was provided by an external compressor and applied to the actuators.

3.3.2. Electric actuation (63)

Electric actuation is achieved by d.c. motor or stepper motor.
A stepper motor is a rotary device which is made to move in discrete steps, e.g. 1.8^{o} when excited from a switched d.c. supply. A high maximum torque to inertia ratio is required for good control. The rotary output torque of these motors is converted to linear force by using a lead screw or rack and pinion. Bearings and structures must be of high accuracy and extremely stiff. The advantages of electric actuation include:-

Stepper Motor	D.C. Motor
1. readily available power supply	✓
2. good accuracy	✓
3. not expensive	✓
4. no risk of fire	✓
5. robustness	
6. can be stalled without risk	
7. open loop control	
8. holding torque	

Disadvantages include bulk and they are affected by vibration and resonance.

Electrical actuation is used in many applications. However, its use for diesel engine control was ultimately not considered suitable in view of the bulk and sensitivity to vibration of such systems.

3.3.3. Hydraulic actuation (Ref. 23, 60)

Hydraulic systems at high pressure produce very large forces. Such forces can be used to provide power for rapid acceleration and accurate positioning. Other advantages include:-

1. The working fluid carries away heat generated allowing smaller and lighter components.

2. The hydraulic fluid also acts as a lubricant and makes possible long component life.
3. There is no phenomenon in hydraulic components comparable to the saturation and losses in magnetic materials of electrical machines. The torque developed by an electric motor is proportional to current and is limited by magnetic saturation. The torque developed by hydraulic actuators is proportional to pressure difference. The actuators therefore develop relatively large torques for comparatively small devices.
4. Hydraulic actuators have the highest speed of response; fast starts, stops and speed reversals are possible. Torque to inertia ratios are large with resulting high acceleration capability. Thus higher loop gains and bandwidths are possible with hydraulic actuators in servo loops.
5. Hydraulic actuators can run stalled without damage.
6. Hydraulic actuators have higher stiffness, that is, inverse of slope of speed-torque curves, compared to other drive devices since leakages are low.

The disadvantages include:

1. a hydraulic power supply is required.
2. components have tight tolerances and are consequently expensive
3. there is a fire and explosion hazard
4. filtering is required.

On balance, having carefully considered the three systems outlined above electrohydraulic actuation was chosen as offering the most favourable system for diesel engine control, not least because of the availability of much of the required electrohydraulic equipment and of the necessary expertise within the School of Engineering.

3.3.3.1. Electrohydraulic valves (Fig. 3.5)

The interface between the hydraulic circuit and the electrical signal is provided by electro-hydraulic valves. These were originally made for the aerospace industry to satisfy their needs for a fast response servo control system and became available in the late 1940's. They are capable of performance superior to that of any other type of servo. Fig. 3.6.

Two stage servo valves were used for all three control parameters so that electrical input is low. In these valves a force motor positions a flapper in the first stage whilst the second stage is a closed centre four way sliding spool valve. The hydraulic pre-amplifier substantially multiplies the force output of the force motor to a level sufficient to overcome considerable flow forces, stiction forces and forces resulting from acceleration or vibration.

The force motor is a simple permanent magnet device which produces forces proportional to input current. Since displacement rather than force is required, a spring is used to provide the reaction force. The ability of these valves to regulate precisely the flow of hydraulic fluid accurately means that they can be used to control with accuracy the movement of a piston or a motor. The proportionality between input signal and actuator velocity lends itself readily to the formation of closed loop control systems. The error position of the servo loop consists of feedback transducers which measure the quantity being controlled and electronic amplifiers furnish a signal to the servo valve to close the loop.

1. Operation

The input signal induces a magnetic charge in the armature and causes a deflection of the armature and the flapper. The assembly pivots and increases the size of one nozzle orifice and decreases the size of the other. This action creates a pressure differential and causes the spool to move. It continues until feedback torque equals input signal torque. The flapper with its forces in equilibrium is thus restored to its null possition between the nozzles.

2. Servo Valve - Selection

To size a servo valve knowledge of the actuator area given by:

$$A = \frac{Fs}{Ps}$$ is required. A = area^2 - m^2

Fs = Force stalled - N

Ps = supply pressure - N/m^2

In this application forces were minimal and not a prerequisite but rather speed of response. The smallest actuators available from within the School or commercially were chosen. The absence of a significant load means that the servo valve load flow approximated to the no-load flow given by:

$$QnL = QL \sqrt{\frac{Ps}{Ps-PL}}$$ where Ps = 140 bar

The servo valve flow capacity is rated at 70 bar pressure drop and is increased 10% for margin. The rated flow is given by:

$$Q_R = 1.1 \times QNL \times \sqrt{\frac{70}{Ps}}$$

It is important not to oversize servo valve flow capacity as this will needlessly reduce system accuracy.

In each case slew rates better than 0.1 s were required. Due to the low load, highest performance in terms of frequency response and stability was readily obtainable. The rated flow was then compared with those valves available from within the School and an appropriate unit chosen for each control parameter. A summary of the type and form of actuator used in the project is given in Fig. 3.7. These are discussed more fully under the appropriate control parameter headings.

The choice of electro-hydraulic actuation necessitated transducers to close the loop. The selection of appropriate transducers is considered in the following passage.

3.4. Transducers

3.4.1. General

Transducers were required to monitor position as a feedback signal in the closed loop control systems of timing, rack and nozzle position. Transducers were also required to monitor engine speed and pressure in the inlet manifold to facilitate boost control. A note on the difficulties associated with measuring engine torque is included.

3.4.2. Selection of transducers

The following factors were considered when making the choice of transducer:-

1. sensitivity, accuracy and resolution
2. life and cost
3. frequency response
4. temperature, atmosphere, vibration and shock considerations
5. mechanical considerations

A transducer can be one of three basic types - resistor, inductor or capacitor. A review of those types applicable to this work are considered.

(i) Resistive Transducers (Fig. 3.8)

In a resistive transducer the measureand is converted into a change of resistance.

Conductive Plastic Potentiometer

This type of displacement transducer is made up of sub-micron conductive particles in thermosettling resin matrix. The track is smooth chemically inert, hard wearing with a low noise output. Good mechanical and environmental performance with virtually infinite resolution are possible.

(ii) Strain Gauged Pressure Transducer

Strain gauges are transducers designed to detect small fractional changes

in dimensions which occur when a body is stressed. Fig. 3.8 illustrates the principle of the diaphragm transducers whose relatively small displacement lie within the span of strain gauges. These gauges are unbonded, that is the wires are stretched directly between insulating supports mounted on a flexible spring strip. Four gauges are usually employed to form all four arms of the active bridge.

(iii) Inductive Transducer (Fig. 3.9)

The simple linear inductive transducer has two inductive coils wound on a hollow former. An iron core can be moved within the former and represents the motion being monitored. Its advantages include non-contacting, and infinite resolution. However, it needs rather a large core and generally has poor linearity.

(iv) Linear Differential Variable Transformer (LVDT) (Fig. 3.8 & 9)

The LDVT is an inductive transformer with three windings, an energising coil and two secondary detecting coils. In the central null position the voltage induced in each secondary will be the same. Displacement of the core will cause a greater voltage to be induced in one of the secondaries and hence an output.

Its advantages are:-

1. infinite resolution
2. frictionless movement
3. a low mass core
4. a long mechanical life
5. operation at high temperature in hostile environments is possible.

(v) Capacitive Transducers (Fig. 3.8)

In a capacitive transducer the measureand is converted into a change of capacitance. The change of capacitance is effected by a change in area but the necessary plate area often renders them bulky.

Having considered the foregoing the most appropriate transducers for each parameter were selected as follows:-

(a) Engine Speed

Engine speed was generated by means of an inductive transducer mounted on the flywheel starter ring. Its advantages include:

1. simplicity
2. cheapness
3. no mechanical contact
   and
4. long mechanical life

(b) Boost Pressure Transducer

Two existing resistive element type pressure transducer (described in Section 2.2.1) were used to measure boost for the following reasons:

1. availability
2. resolution
3. cost
   and
4. frequency response

(c) Position Transducer

LDVT's were the position transducers used in every case. Their inherent advantages in terms of temperature, linearity, availability and cost made them the most appropriate choice.

(d) Torque Measurement

Torque which is a measure of the ability of an engine to do work and engine speed are essential operating parameters for any engine management system. Whilst engine speed is easily measured the same is not true of torque. There is a limited selection of commercially available sensors and actuators and unfortunately these do not include torque (57). Engine torque measurement in a vehicle is difficult as ideally it should be measured at the output end of the crankshaft (58). Magnetic based torque sensors currently being developed are not suitable for simple add

on installations on most production power trains. It will have to be built into new engine and transmission design. Applications are likely from sometime in the late 1980's. In the absence of direct measurement of torque a surrogate variable was used, that is, rack position using logic based on a system model. (Fig. 3.10).

A summary of the type and specification of all transducers used in the project is given in Fig. 3.11. These are discussed more fully under 'control parameters'.

The next section describes the method of controlling the variable geometry turbocharger and the associated control parameters and includes a description of the design.

3.5. Description of Control Parameters

3.5.1. Variable geometry turbocharger

Two distinct and separate VG units were assessed, designated Mk I and Mk II respectively. The units were designed and built by the HOLSET ENGINEERING CO. LTD.

3.5.1.1. Mk I VG unit

(a) General Description

The Mk I unit was based on a production nozzled twin flow unit (Fig.3.12) where the turbine stage is divided circumferentially at 180°. A twin flow was chosen (Fig. 3.14) for its good transient response and pulse operation which increases turbine energy in the mid-range. A twin flow design of turbine also allows for the possibility of fitting an adjustable nozzle in the volute exit area whereas an axially divided configuration (twin entry) presents more difficulties. A sliding ring sleeve was used to achieve a progressive reduction in effective turbine inlet area (Fig. 3.13). This device was not dynamically remotely variable but could be altered in fixed discrete steps of 0, 10, 30 and 50% area restriction. For an effective VG design the reduction in area must give good flow guidance with the minimum efficiency penalty. The design aim was to achieve a 50% turn down ratio in non-dimensional mass flow with a corresponding area turn down. The Mk I VG turbocharger was fully tested but gave disappointing results due to excessive leakage behind the nozzle. (These results are presented and discussed in Chapter 4). For the above reasons the Mk I unit was abandoned in favour of the Mk II turbocharger.

3.5.1.2. Mk II VG unit (Figure 3.16)

(a) General Description

The Mk IIa unit was a single entry nozzled device again with a sliding ring sleeve in the volute exit area with a restrictor of pressed steel.

It was based on a HOLSET H2C production unit but with the turbine stage designed specifically for VG operation. A single entry unit lacks the characteristic 'bulge' of pulse operation in the mid-speed range and therefore some turn down will be required to achieve an equivalent swallowing capacity at peak torque. In its favour however an efficient unit will have better SFC at rated conditions due to lower friction losses. Transient response will be better than its fixed geometry counterpart due to its variable geometry capability.

The performance of the Mk IIa unit was assessed on the limiting torque curve by testing in the fully open and restricted positions. The results indicated that significant modifications were required to achieve an efficient turn down ratio. These modifications included a piston ring on the heat shield annulus and a different arrangement of fixing the nozzle ring. This allowed a more substantial restrictor to be fitted improving the traversing characteristic. Fig. 3.17 is a photograph of the hardware. Careful attention was required when building the unit as leaks and over-tightening could lead to difficulties. Several problem areas with regard to leakage were noted and sealing was assisted by careful application of jointing compound.

Final matching necessitated a larger swallowing capacity turbine which was effected by a larger inducer turbine wheel and housing. (Fig. 3.15). A smaller diameter inducer compressor wheel and cover were fitted to increase surge margin. (Originally H2C8640 now H2C8625). The unit was designated the Mk IIb and is the subject of this thesis.

(b) Actuation & Control

The ring sleeve was controlled initially by pneumatic power and for the later tests by hydraulics.

(i) Pneumatic Operation

Pneumatics powered the fully dynamically variable ring sleeve with control from the test console. Good position control was attainable

with minimum dither. The nozzle position was, however, sensitive to pre-turbine pressure. A fixed input pressure gave variable restriction dependent on engine speed and load; a position feedback signal was therefore essential. A Schaevitz miniature high temperature (200° C) type 201-01 LDVT transducer sensed the ring sleeve position but control was open loop.

The pneumatic actuators were derived from wastegated applications. They consisted of a neoprene diaphragm of 0.00196 m^2 area with an appropriate spring (Fig. 3.18). The unit was biased to the fully restricted position. Two actuators operated on the ring sleeve and were positioned either side of the bearing housing within the existing turbocharger silhouette (Fig. 3.16).

Modifications

The pneumatic actuators at minimum travel and supply pressure allowed hot exhaust gases to flow over the diaphragms. Problems were then experienced with overheating of the neoprene diaphragm and 'Sindanyo' insulating washers. A non-return valve and better washer material (Kinel 5505) together with a maximum turbine inlet temperature (TIT) of 700° C alleviated these problems. It was noted, however, that the non-return valve induced some undesirable modulation in the actuator. The unit ran for a total of 97 hours and 34 minutes.

Closed loop operation of the pneumatic actuators for transient investigation was difficult due to the designed leakage path into the turbine housing, causing excessive offset for any electro-pneumatic device. A closed loop control system based on hydraulics was considered the 'best' solution. Limited space in the region around the bearing housing, high temperatures and problems of synchronisation with two actuators made the design task very difficult.

(ii) Electro-Hydraulic Operation

A system was designed using a single actuator mounted on the compressor housing and connected to the nozzle ring by a balanced pivot (Fig.3.19).

Compressed air was used to form a dynamic seal between the turbine housing and atmosphere. This design overcomes to a large extent those difficulties outlined above.

Unfortunately, using conventional hydraulic mineral oil very near to hot surfaces presents an extreme fire and explosion hazzard. (The hydraulic power supply was connected to a common 250 gallon tank). The hydraulic requirements for flow and pressure were determined (see Appendix 3), leading to the purchase of a dedicated BOSCH servo pack together with an accumulator and water glycol working fluid (Fig. 3.20). An anti-rupture valve was also installed. This prevents large loss of fluid in the event of sudden failure. The supply pressure was set to 140 bar.

The hydraulic actuation system was designed to achieve full restriction i.e. 100% restriction - 12 mm to cater for exhaust braking and allow for further development.

(a) Sensors & Control

A balanced pivot connected the double acting actuator with a balanced area of 129×10^{-6} m^2 to the ring sleeve. It was made without piston seals so as to allow leakage flow for cooling. The LDVT position transducer was mounted directly behind the actuator on the compressor housing. The transducer was a Schaevitz high temperature ($\lesssim 200^{o}$ C) type 301/01 with a large bore to core clearance and a maximum travel of 0.010 m. Linearily was better than 0.5%.

The electro-hydraulic valve was a Bendix type 312/686 and was mounted remotely on a rail alongside the engine. The valve had a rated flow of 0.84 L/min and allowed a ring sleeve slew rate of 0.015 s. Boost pressure was sensed by a water cooled Schaevitz P700 resistive element pressure transducer (0-2 bar vented gauge) mounted on the inlet manifold.

The control electronics were mounted remotely in the test console. Nozzle position or constant boost (within the limitations of the

turbocharger) could be selected as desired by ten turn potentiometers alternatively the demand could be by an external voltage input. Nozzle position was effected by a simple proportional control. Boost control was facilitated by matching a boost demand signal against a boost feedback signal and the error signal used to drive the servo valve using a P + I algorithm. The control algorithm is shown in Fig. 3.21 and a schematic representation in Fig. 3.22. The boost controller is essentially as described in Section 2.2.2.

(b) Modifications

A resonance condition was noted around 900 rev/min. This manifested itself in the fatigue of the turbocharger back plate. An integral back plate and heat shield solved this problem.

A problem was also experienced with the mechanism partially seizing at high temperatures. This was traced to the differential expansion of the ring sleeve compared with the back plate. Increasing the respective clearances alleviated this problem. No further difficulties were noted.

The final steady state tests and all transient work included this closed loop control. The electro hydraulic unit ran for 83 hours and the VG unit for a total of 180 hours (at the time of writing) and operated very satisfactorily.

3.5.2. Variable fuel injection timing

3.5.2.1. Introduction

It was stated earlier that a variable injection timing device was considered desirable because it would allow closer control over combustion performance since the higher peak torque possible with a variable geometry turbocharger would be reflected directly in higher cylinder pressures. Retarding injection allows control of the

maximum cylinder pressure but at the expense of fuel consumption. Ideally therefore at high torque levels start of injection would be retarded as appropriate and optimised at all other conditions, this strategy being easily facilitated with micro processor control. Injection timing also affects emissions and noise output. A brief review of the mechanism by which fuel injection takes place and its implication for combustion efficiency is appropriate at this stage.

3.5.2.2. Fuel injection equipment considerations

The fuel injection pump fitted to the Leyland TL11 engine is a LUCAS/CAV Majormec type P5476 with boost control (Fig. 3.23). The unit is a six element (barrel and plunger assembly) in-line jerk pump with helix control (22 mm linear movement). The plunger stroke is 10 mm and the plunger diameter is 11 mm. The pump is used in conjunction with American BOSCH inwardly opening valve fuel spray nozzles. The TL11 engine has a controlled turbulence (based on inlet passage) open chamber type combustion system. Great care will have been taken in matching the fuel injection equipment to the engine in terms of timing and duration of injection for optimum specific fuel consumption (SFC) and will be a compromise.

Duration of injection is a function of many parameters including nozzle opening pressure, tubing bore, and length, cam profile and trapped fuel volume, but essentially is very difficult to alter dynamically.

A characteristic of the jerk pump is that start of injection always takes place at the same point with a variable end of injection. Injection timing is a function of injection lag, ignition lag, engine speed and the combustion characteristics of the engine. In the case of the TL11 a fixed timing was selected for the higher speed range. For automotive engines operating over a wide speed range variable injection timing is preferable. Timing should be advanced at high speeds so that injection will not be delayed nor combustion be incomplete. It should be retarded at low speeds for improved starting,

slower idling and to lessen combustion knock. It is also desirable for the beginning of injection to be advanced with increase of load at constant speed such that end of injection is always at the same point.

Realising the benefits of variable injection timing, many automotive diesel engine manufacturers e.g. Mack, Caterpillar, Gardner, Hino have equipped their engines with timing advance couplings attached to the drive end of the pump. In most cases the timing lever and governor lever are interconnected to obtain semi automatic variation in timing with engine speed. These devices are normally based on helical splines of opposite lead, timing is varied by axially shifting the sleeve. The helix angle is usually small (6 - 7^{o}) giving maximum timing swing of 24^{o} crank angle. For a wider range of timing variations planetary gear timing devices have been built (AVL, type VA100300). Automatic timing devices have been developed based on flyweights and hydraulics e.g. Robert Bosch and Mack.

Cummins found it necessary to adopt variable timing with their pressure/time (PT) system on the recently introduced two stage high output engine to alleviate light load hydrocarbons, acceleration smoke, idle roughness and unacceptable cold smoke levels.

3.5.2.3. Variable timing design

When the design of the VT unit was being considered no suitable remote controlled units were commercially available. Therefore it was decided to design and manufacture a unit at the University, occupying the space normally taken by the air compressor (Fig. 3.24). On the basis of cost, time and availability timing gears and an actuating lever for a GARDNER 6XLB were purchased and a unit developed around these components (Fig. 3.25).

The GARDNER system involves moving a splined collar axially relative to the fuel pump driving gear within the gear case, the unit being

supported between the gear case and the fuel pump. The modifications required to adapt the unit to the TL11 engine included modifying the bearing housing on the gear case end, machining straight splines on the GARDNER collar and manufacturing a suitable adaptor (Fig. 3.26). Self aligning bearings were used on the timing gear end and plain bearings at the other, thrust being taken by washers on the adaptor. Special emphasis was directed at minimising gear back-lash and making the drive strong enough to withstand injection pump and actuation force. Pressure lubrication was adopted to minimise wear and actuating forces. This oil drains back to the sump through holes in the gear case. The timing gears were contained within a case with an identical sihlouette to the automotive compressor. (Fig. 3.27).

3.5.2.4. Actuators and control

Actuation in the GARDNER unit was by a linkage to the governor and hence speed demand. For the TL11 a hydraulic Clippard Minimatic heavy duty double acting cushioned actuator with 0.022 m bore and a cut down stroke of 0.038 m was used to power the device. It was mounted at one end by a rod clevis assembly and at the other end by a clevis mounting bracket. A spring biased the unit to the retarded position. The feedback signal was provided by a Penny & Giles dc/dc 60^{o} rotary variable differential transformer (rvdt). Linearity is better than ± 0.5% with infinite resolution. The transducer was mounted directly on the actuating lever shaft.

The electro-hydraulic valve was a Moog model 76-338 giving a maximum flow rate of 4 L/min allowing a slew rate of 0.1 s. Dead band about null was 2%, rated current was 8 mA with a coil resistance of 1000 Ω. To alleviate any temperature effects the Moog valve was mounted on a rail parallel to the engine. The valve was protected by a Pall 3 Micron filter.

The analogue electronic controls were mounted remotely in the test

console. Simple proportional control was achieved by a ten turn potentiometer (or computer input) which gave a timing swing related to the flywheel of 23^{o} crank angle. In the event of failure the unit failed in the fully retarded position. Fig. 3.22 is a schematic of the VT device. The control algorithm is shown in Fig. 3.21.

3.5.2.5. Modifications

The unit has run a total of 251 hours at the time of writing. The most significant problems experienced were associated with the actuator mounting bracket. It was very soon realised that the pressed steel clevis mounting bracket was not strong enough. This was replaced by a more substantial bracket. The arm supporting the actuator repeatedly came loose, welding this bracket in situ solved the problem.

The unit proved a very reliable and useful development tool.

3.5.3. Fuel injection pump

3.5.3.1. Introduction

The existing CAV Majormec pump was fitted with an all-speed hydro-mechanical governor with boost control. Governor weights provide a speed sensitive signal which is then amplified by the servo-assembly. This uses the power generated by the oil pressure of the engine lubrication system to control engine fuel supply, the governor being capable of responding to quite minor changes of engine speed.

Majority opinion is that the most favourable application of electronic diesel governing could be achieved by retaining a mechanical injection pump with its proven high pressure precision and timely quantity control for the individual cylinder and by replacing the mechanical governor with an electronic one.

When compared to the conventional mechanical system described electronic control permits easier matching and greater flexibility and the combining of the control system with the other control circuits described. The flexibility of closed loop control satisfies far more easily idle speed, a shaped torque curve, easier starting and transient strategies.

Unfortunately no suitable electronically governed fuel pumps were commercially available for the TL11 engine. Therefore a unit was designed and manufactured at the University around the Majormec fuel pump using hydraulics, a servo valve and an analogue controller as the governor.

3.5.3.2. Description

The following facilities were available with the electronic governor:

(i) all-speed governing
(ii) direct rack position control
(iii) remotely variable maximum rack stop.

The elctronic control was facilitated by removing the CS governor internals and fixing an end plate to which was attached an integral actuator and electro-hydraulic valve. A shaft drive was bought out of the rear to allow a speed signal or tachogenerator to be fitted to allow for future developments. Fig.3.28 shows the arrangement.

3.5.3.3. Actuators & control

The all-steel hydraulic actuator had a bore of 0.011 m and a stroke of 0.022 m. The actuating force even under conditions of cold oil are minimal. Rack position was measured by a Sangamo type AC/15 LDVT transducer. It has a linear range of 0.03 m with a linearity of ± 0.3%. The transducer was mounted at the front of the pump.

This feature allowed the same transducer to be fitted to the original Majormec pump with CS governor. The Dowty electro-hydraulic valve has a rated flow of 2 L/min and was protected by a Pall 3 micron filter. The speed feedback signal for all-speed governing was derived from an inductive transducer mounting on the flywheel housing in close proximity to the flywheel teeth (159). Droop was set to 10% the same as the CS governor.

The electronics were mounted remotely in the test console. The analogue control is implemented with suitable OP-AMP circuitory and provides facilities for adjusting feedback loop gains (droop). Three ten-turn potentiometers controlled constant speed demand, fuel rack and maximum rack position respectively. For constant speed operation a speed demand signal is matched against the speed feedback signal and the error signal used to drive the servo-valve by P + I control. Direct rack operation was facilitated by a simple proportional control. The general control principles are described in Section 2.2.2. The control algorithm is shown in Fig. 3.21 and a schematic representation in 3.22. A stop button returned the rack to the no-fuel position by grounding the power to the servo-valve. The rack being biased to no fuel.

Precautions were required to protect the engine from accidental overspeed. This was provided by means of an absolute shut off valve mounted in the air inlet to the engine. This necessitated the use of manometers traps for airflow and inlet depression manometers. Threshold over speed was regulated by means of a ten turn potentiometer on the failure panel. An inductive transducer mounted above a dedicated 120 teeth wheel generated the speed signal for the over-speed protection.

3.5.3.4. Modifications

The unit proved very reliable in service. However it was noted that at 1300 rev/min a pronounced rocking of the pump occurred. A stabilizer

bar was added between the rear of the pump and engine frame, no further problems were noted.

At the end of the project 182 hours had been satisfactorily completed by the fuel pump.

3.6. Overview

A literature search revealed the following engine control systems applicable to this work.

3.6.1.

Isuzu a Japanese engine manufacturer announced in the first quarter of 1983 an electronic control for the turbine wastegate. The turbocharger was a IHI type RHB52 (50 mm diameter turbine). A stepping motor was used together with a Knock system (adaptive control) to allow higher boost during acceleration and to provide optimum boost to suit the engine's needs irrespective of ambient conditions.

3.6.2.

At the end of 1981 HINO of Japan brought out a very similar variable timing system to that described above for a turbocharged engine of similar capacity. Power to drive the actuator was derived from a second stage hydraulic pump based on engine oil and a crude electro-hydraulic. Performance was reported to be much better but was not substantiated.

3.6.3.

A paper was published in 1982 (16) outlining the American BOSCH approach to electronically controlled fuel pumps for the future. An in-line pump designated the model 200 with 0.010 m plungers and 0.011 m which has a similar capacity to the Majormec was announced. It contained an integral timing device based on an axially moving sleeve and helical splines within the fuel pump body. Timing was varied by stepper motor hydraulic spool valve and an actuator powered by engine oil. The rack was controlled by stepper motor. The

electronics were mounted on the pump and used fuel cooling. A transducer mounted in the inlet manifold sensed boost and shaped the fuel delivery characteristic including transient operation.

LIST OF FIGURES

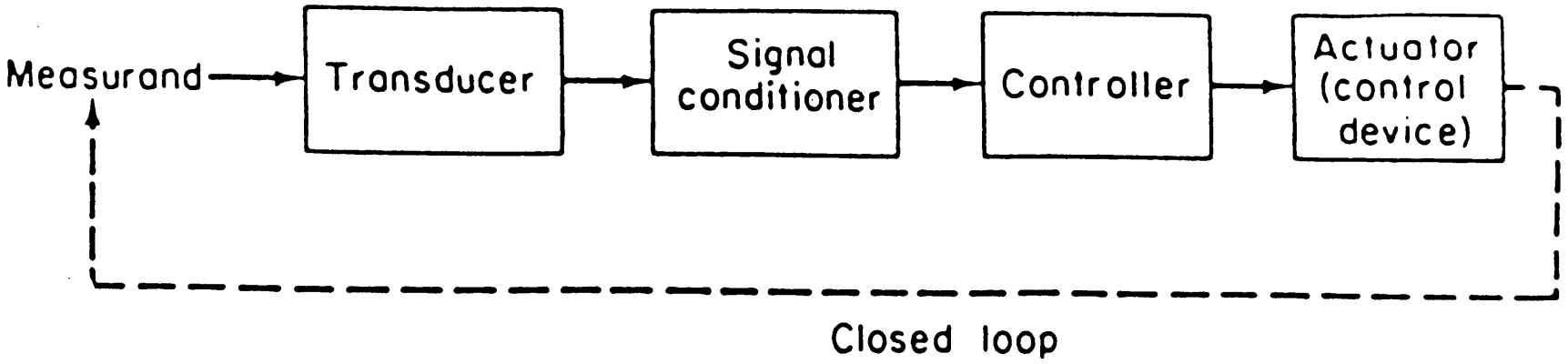

Figure 3.1 **Basic electronic control system.**

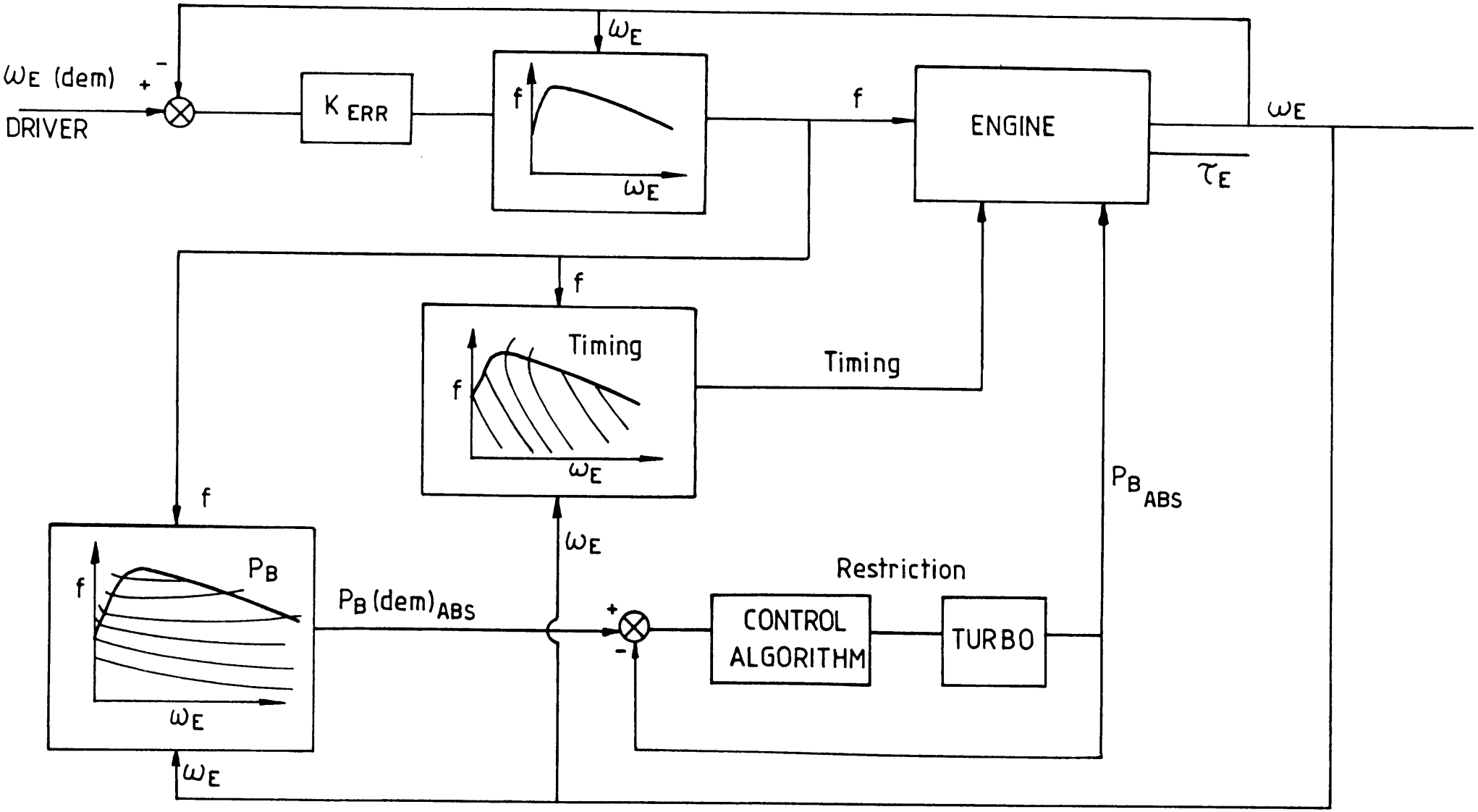

FIG. 3.2 BLOCK DIAGRAM OF CONTROL SYSTEM

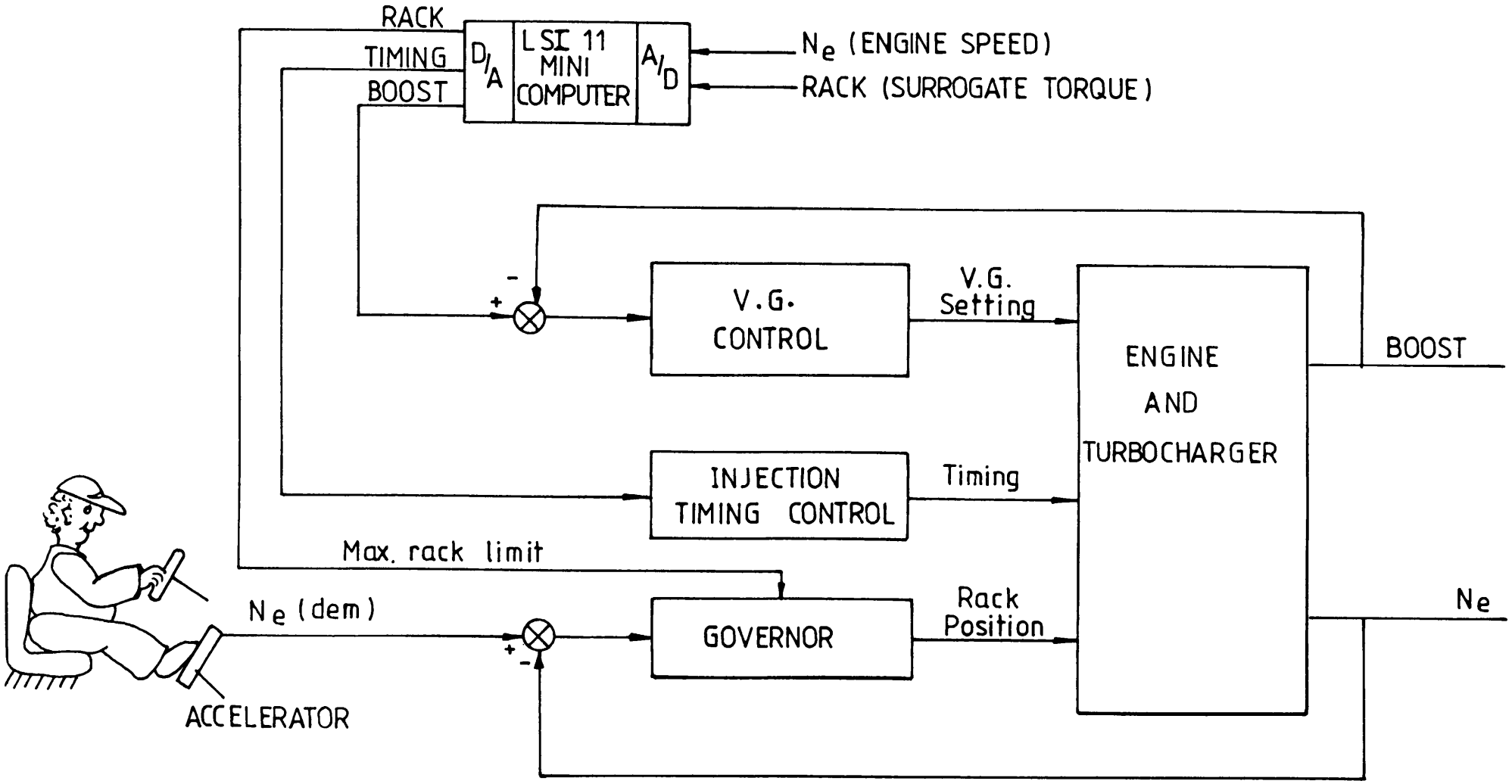

FIG. 3.3 SCHEMATIC OF COMPUTER CONTROL

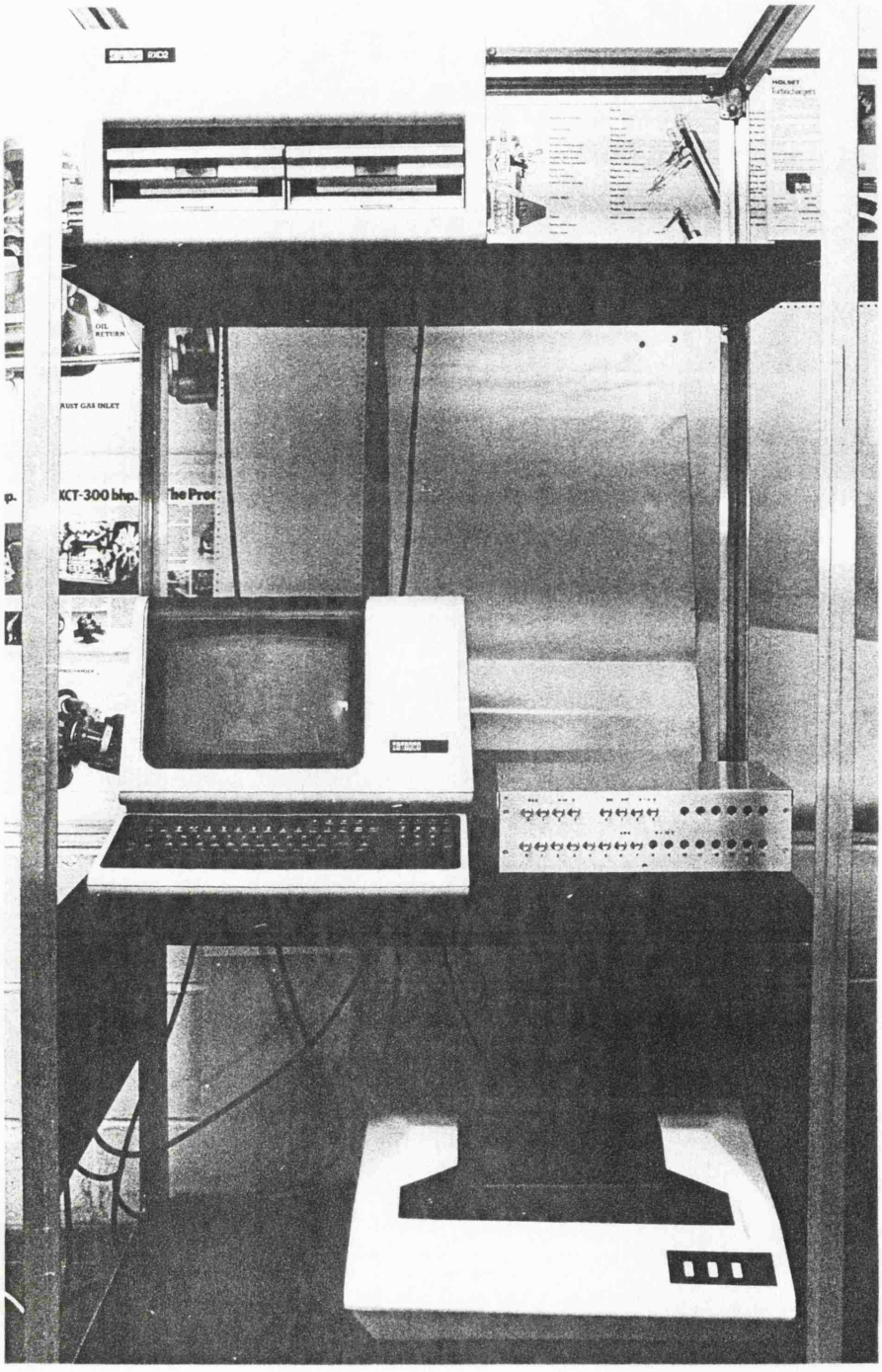

fig 3.4 LSI 11/23 MICRO-COMPUTER

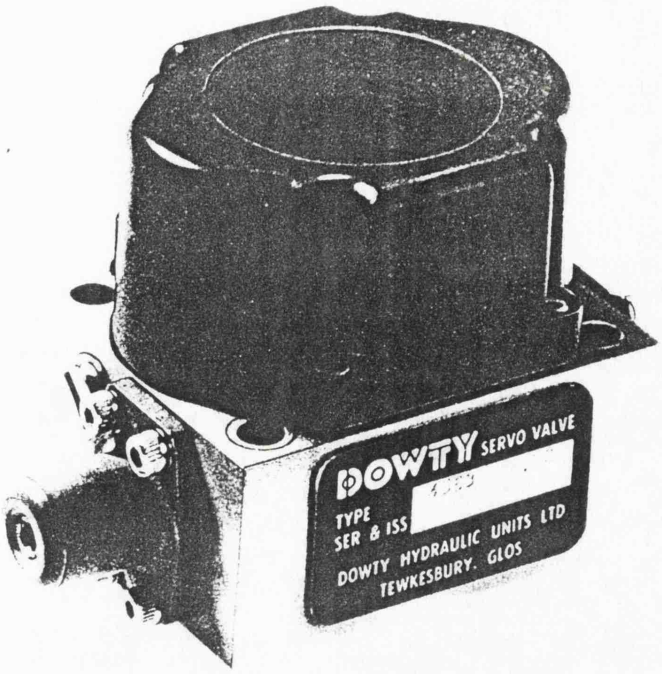

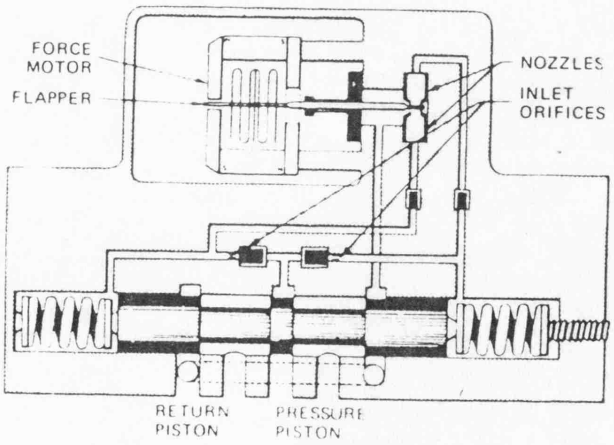

fig 3.5 ELECTRO - HYDRAULIC VALVE

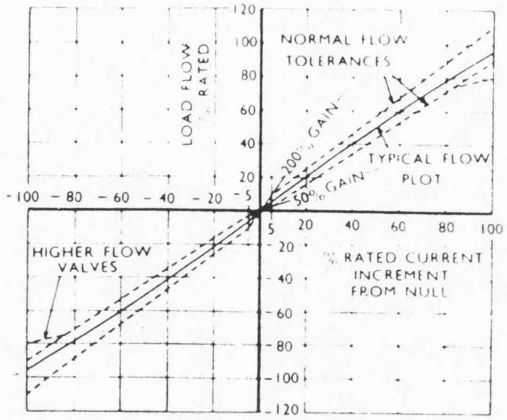

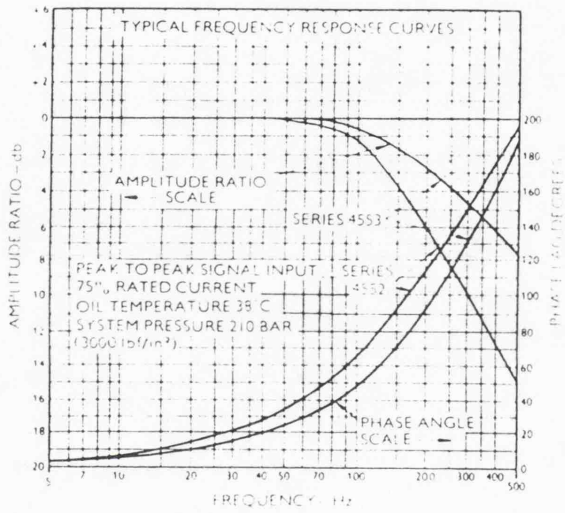

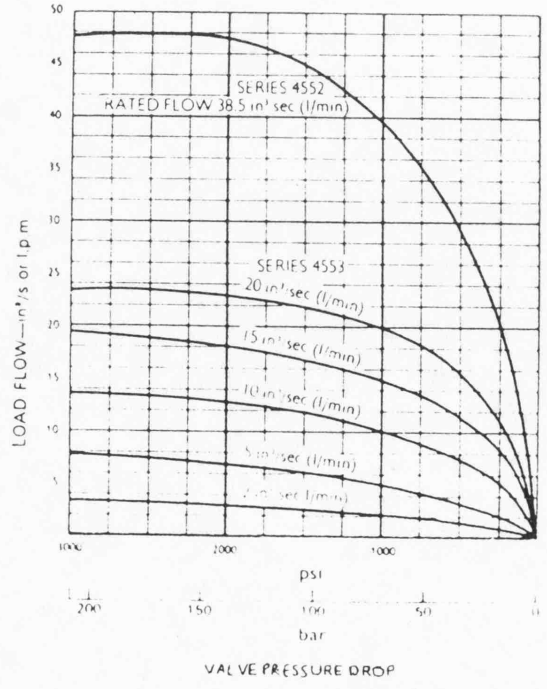

fig 3.6 PERFORMANCE CHARACTERISTICS OF ELECTRO-HYDRAULIC SERVO VALVE

PARAMETER	ACTUATOR	MOUNTING	*INTERFACE VALVE	CONTROL	MEDIUM
INJECTION PUMP	UNIVERSITY INTEGRAL WITH ELECTRO-HYDRAULIC VALVE (.011 ϕ × .022	DIRECT FUEL PUMP RACK	BENDIX 312/68b	CLOSED LOOP DIRECT RACK or SPEED CONTROL	REMOTE SERVO PACK SUPPLYING WATER GLYCOL @ 105 bar - RATED FLOW 1.5L/min + 1L ACCUMULATOR
INJECTION TIMING	CLIPPARD MINIMATIC (.022 ϕ × .038)	DIRECT ACTUATING LEVER	MOOG 76-338	CLOSED LOOP TIMING POSITION	AS ABOVE
VG TURBO-CHARGER	PNEUMATIC-HOLSET ENGINEERING (OPEN LOOP) (× 2) UNIVERSITY (.0215 ϕ × .006)	DIRECT RING SLEEVE INDIRECT BALANCED PIVOT	NONE DOWTY 4552	OPEN LOOP RING SLEEVE POSITION CLOSED LOOP RING SLEEVE POSITION or BOOST CONTROL	REMOTE AIR COMPRESSOR @ 4 bar REMOTE SERVO PACK AS ABOVE

*ALL ELECTRONICS REMOTE FROM ENGINE

FIG. 3.7. SUMMARY OF ACTUATION & CONTROL

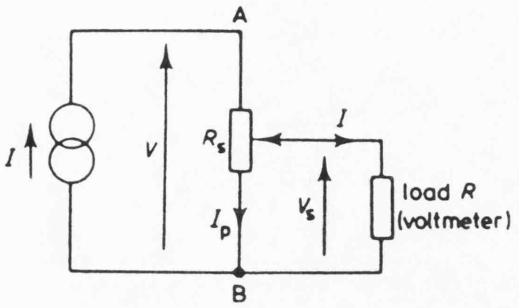

RESISTIVE DISPLACEMENT TRANSDUCER

(a)

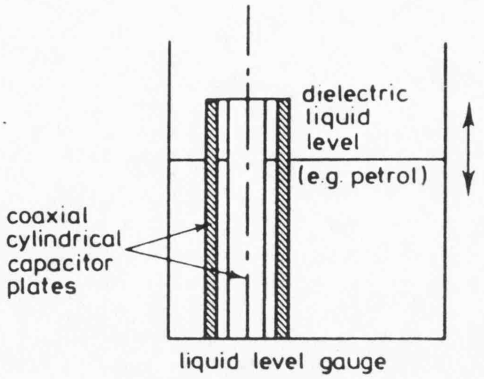

CAPACITIVE DISPLACEMENT TRANSDUCER

(b)

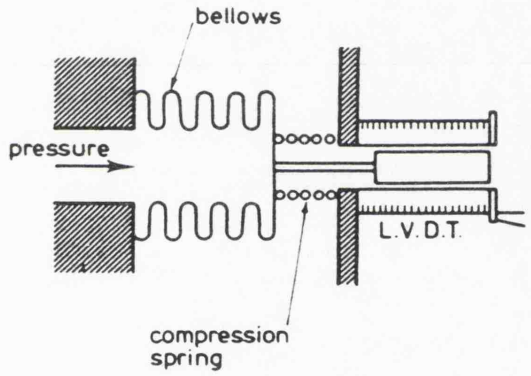

LDVT PRESSURE TRANSDUCER

(c)

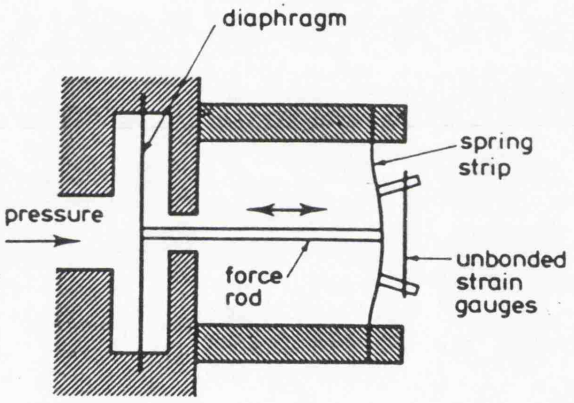

STRAIN GAUGED / DIAPHRAGM TYPE PRESSURE TRANSDUCER.

(d)

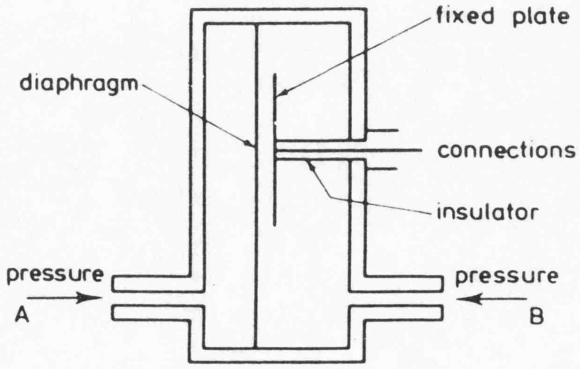

CAPACITIVE PRESSURE TRANSDUCER.

(e)

Fig 3.8 DIFFERENT TYPES OF TRANSDUCER.

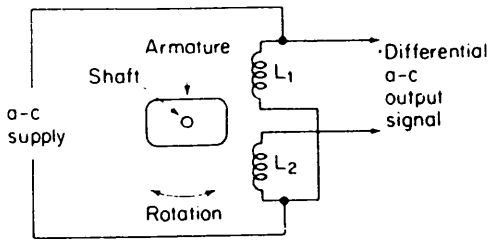

Variable-reluctance transducer.

(a)

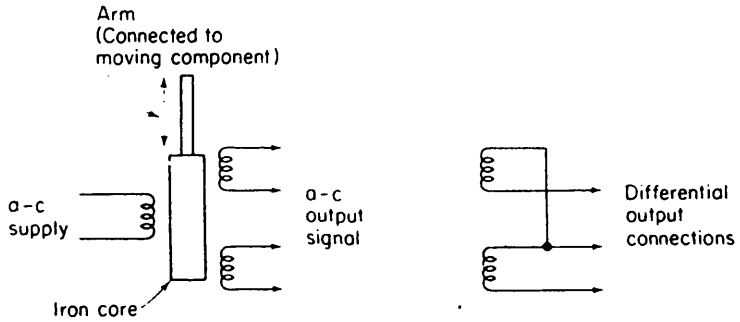

Linear variable differential transformer (LVDT).

(b)

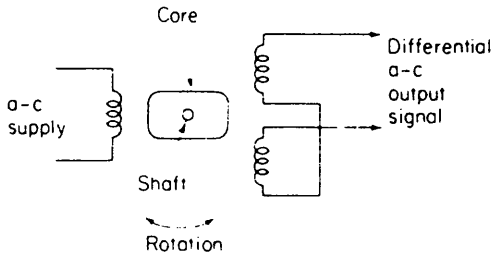

Rotary variable differential transformer (RVDT).

(c)

fig 3.9 LDVT AND RDVT TRANSDUCERS

Engine: LEYLAND TL11 ENGINE — 11.1L DISPLACEMENT Drawn By S.W. Robell.

Title CALIBRATION OF MOTORTECH PUMP PS334/A UNDER ELECTRONIC CONTROL.

Power Curve Rating — 190 kW at 2100 rev/min

Holset / Leyland / Dowty / DoI Contract

Test No.	Timing	Amb'nt °C	Barometer mm Hg.
80	VARIABLE	22.	

RACK POSITION IS IN MM.

Note! VARIABLE TIMING DEVICE FITTED.

MAP CONSTRUCTED FROM 93 POINTS.

RACK VERSUS TORQUE CHARACTERISTIC.

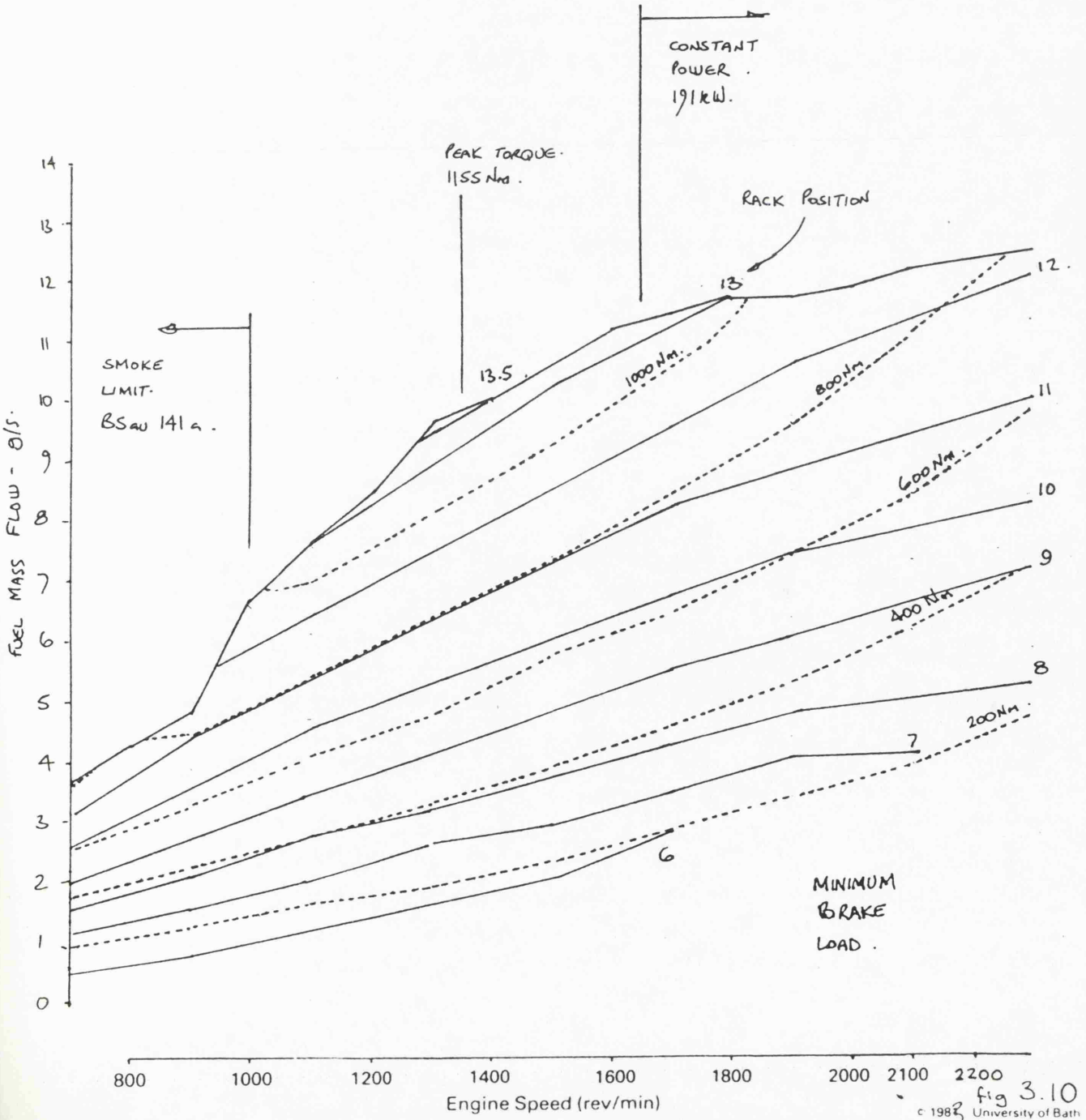

fig 3.10

PARAMETER	TYPE OF TRANSDUCER	MAKE & SPECIFICATION	MOUNTING
ENGINE SPEED	INDUCTIVE (frequency)	ORBIT	DIRECT (Flywheel)
ENGINE TORQUE	LDVT (Position)	SANGAMO AC/15	INDIRECT (Fuel Pump Rack
INJECTION PUMP	AS ABOVE	AS ABOVE	DIRECT (Fuel Pump Rack)
INJECTION TIMING	RDVT (Position)	PENNY & GILES DC/DC 60°	DIRECT (Actuating Lever)
VG TURBOCHARGER	LDVT (Position)	(PNEUMATIC) SCHAEVITZ 201/01 SCHAEVITZ 301/01	DIRECT (Built into Actuator) INDIRECT (Via Balanced Pivot)
BOOST PRESSURE	RESISTIVE ELEMENT (Pressure)	SCHAEVITZ P700	INDIRECT (Via Inlet Manifold Pressure)

FIG. 3.11. SUMMARY OF TRANSDUCER TYPE & SPECIFICATION

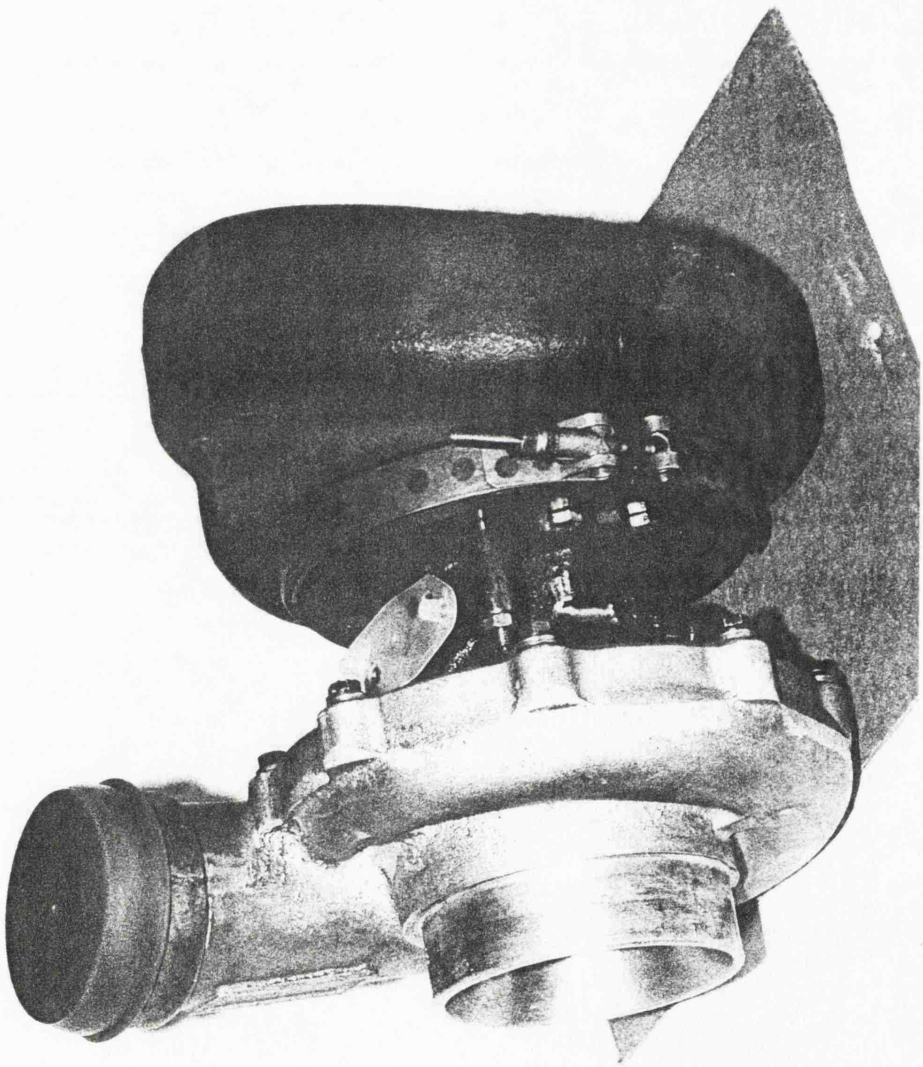

fig 3.12 MK I VG TURBOCHARGER (TWIN FLOW)

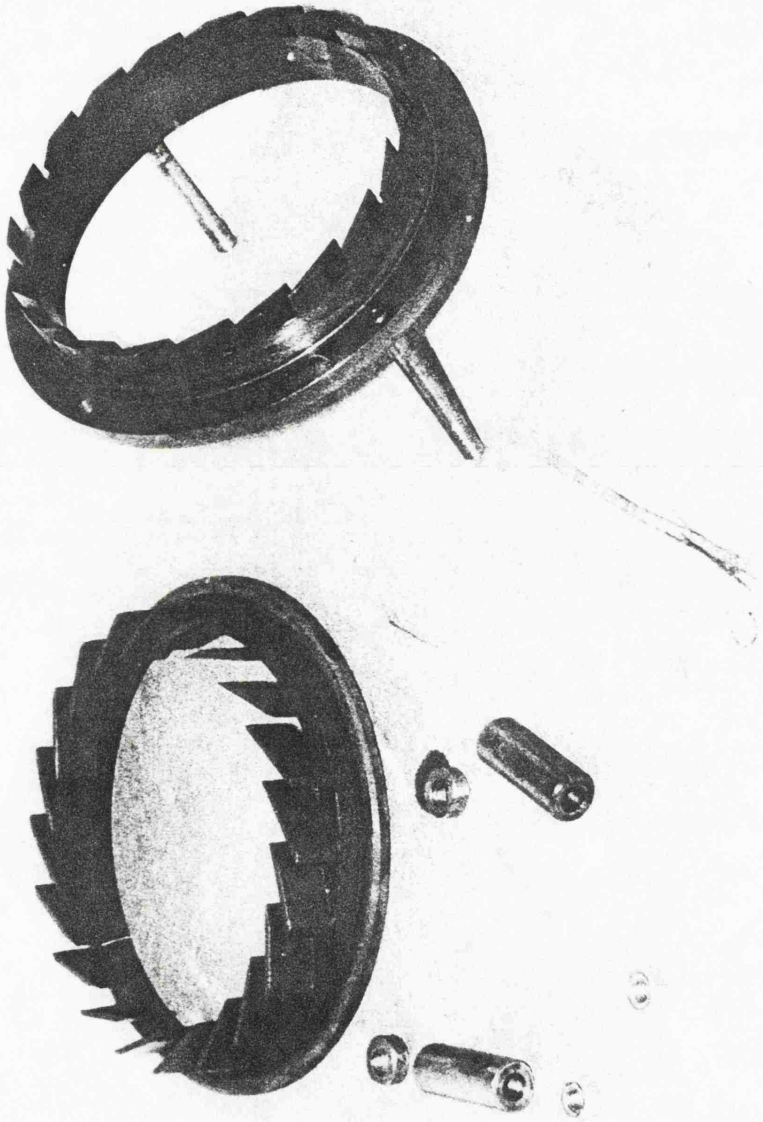

fig 3.13 MK I VG NOZZLE RING

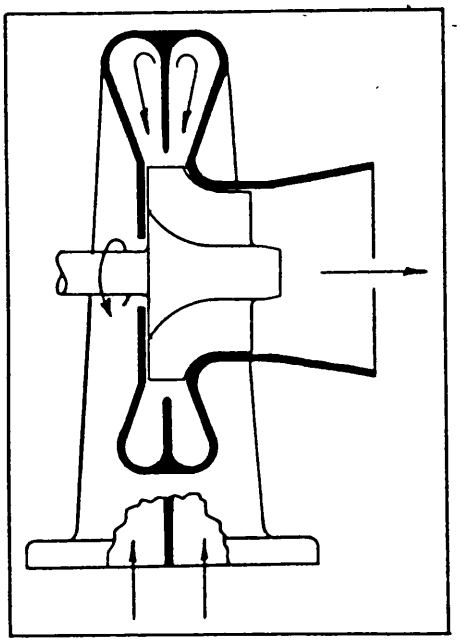

AXIALLY - DIVIDED TURBINE
(TWIN ENTRY HOUSING)
(a)

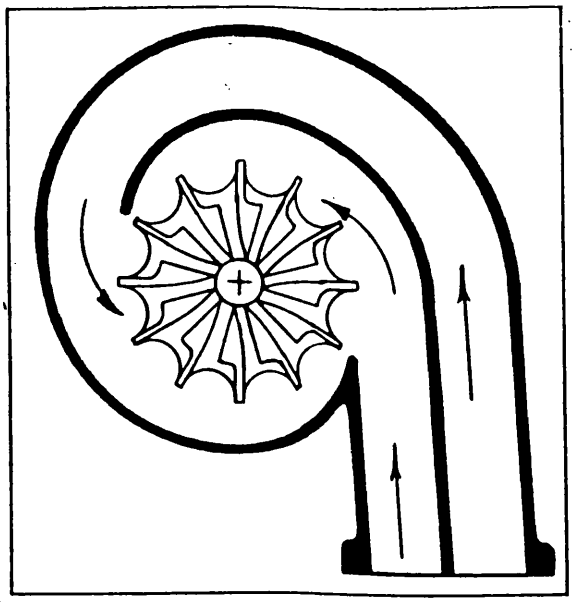

180° DIVIDED TURBINE HOUSING
(TWIN FLOW HOUSING)
(b).

fig 3.14 - TYPES OF TURBINE HOUSING

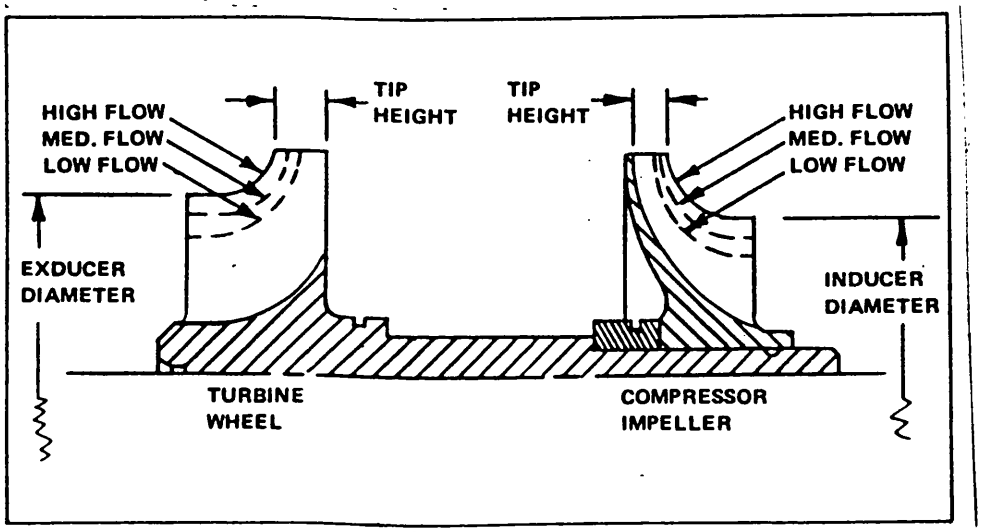

fig 3.15 CONTOUR RELATIONSHIP FOR DIFFERENT FLOWS

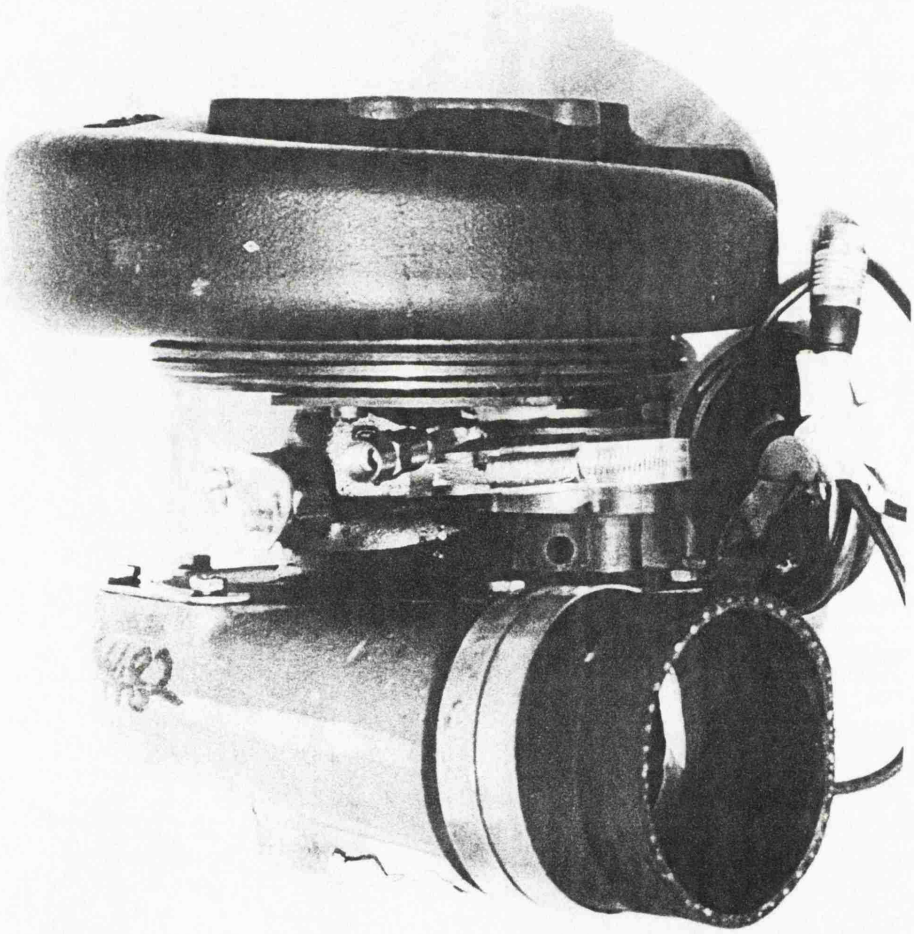

fig 3.16 MK II VG TURBOCHARGER

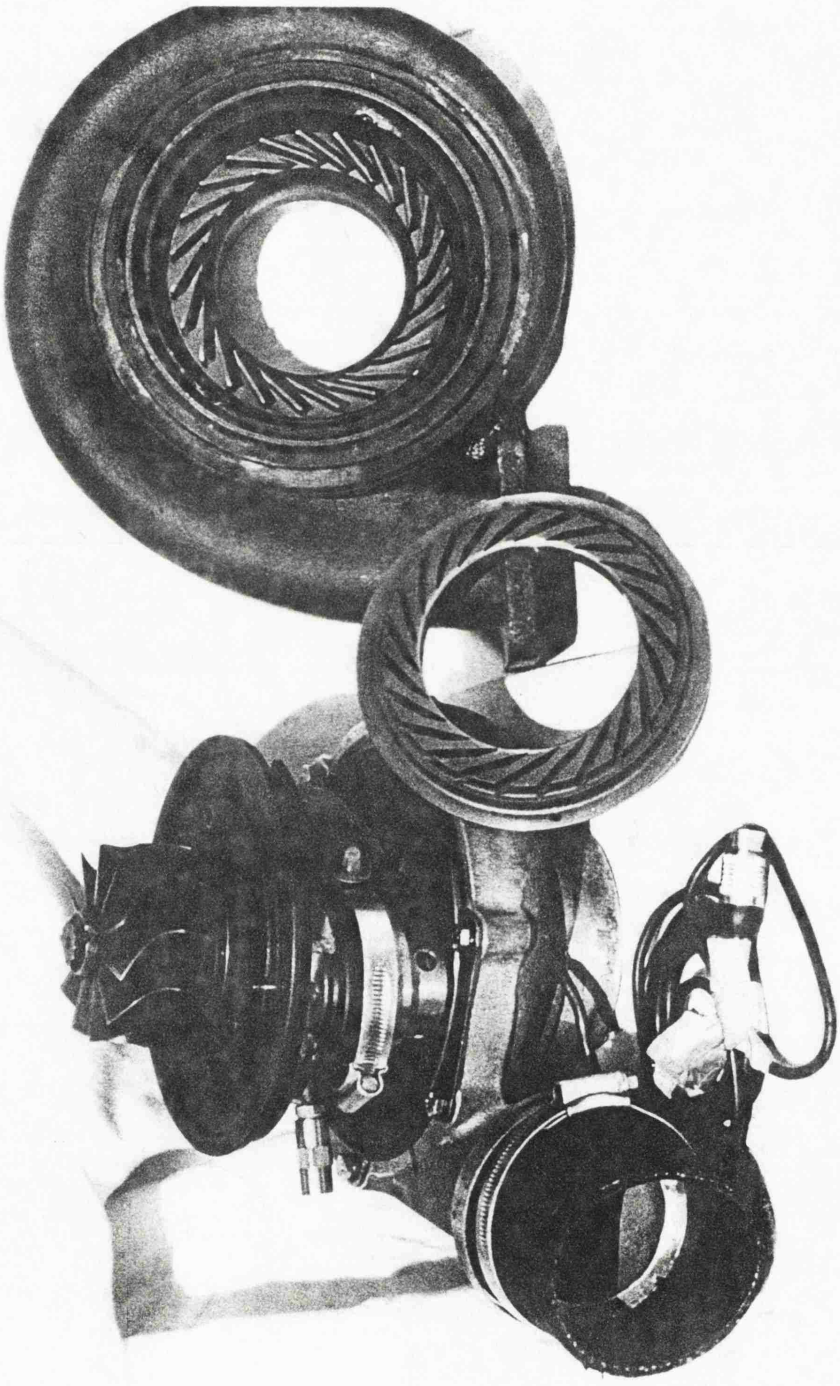

fig 3.17 MK II VG INTERNAL COMPONENTS

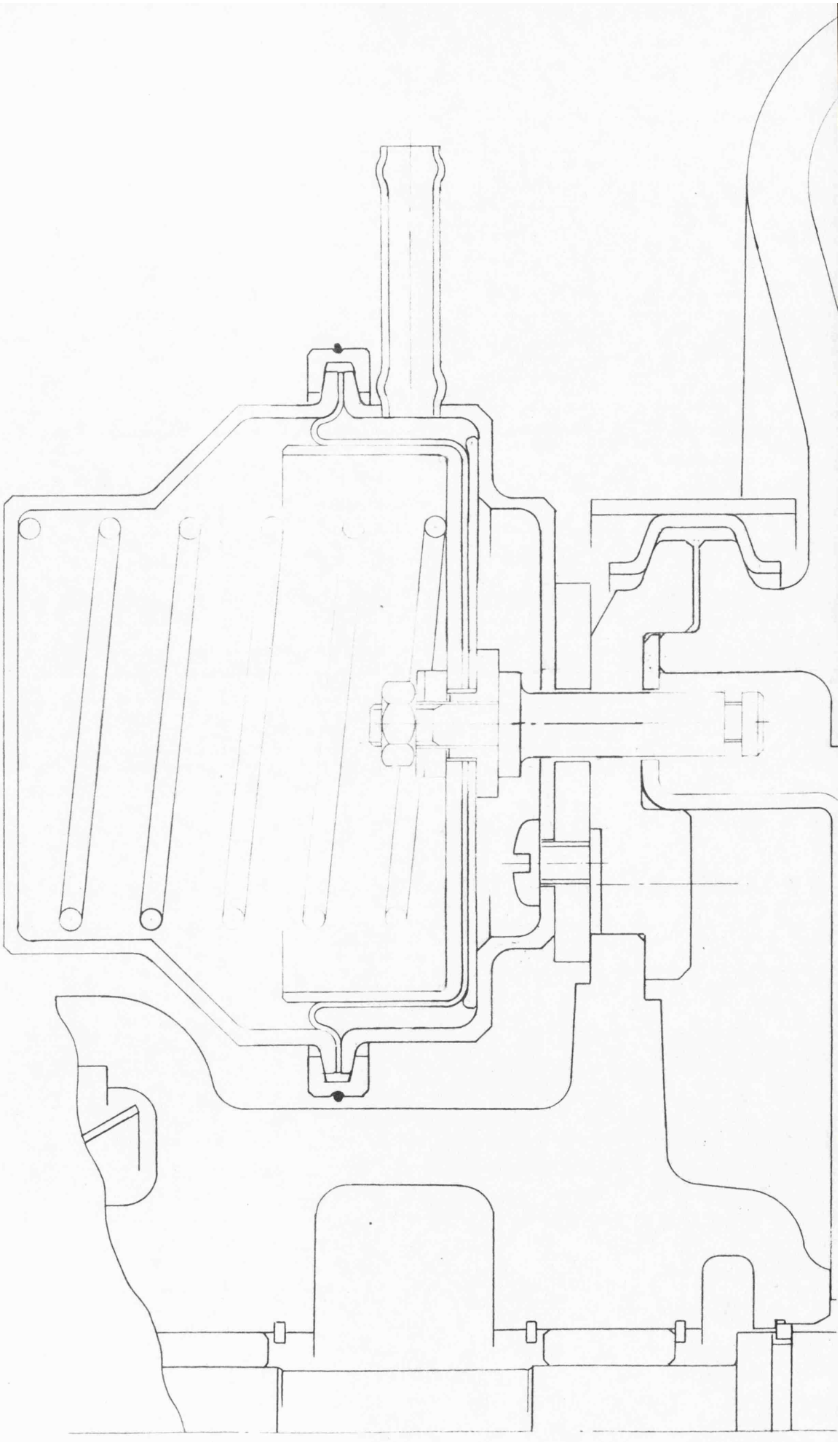

fig 3.18 MKII VG PNEUMATIC ACTUATOR

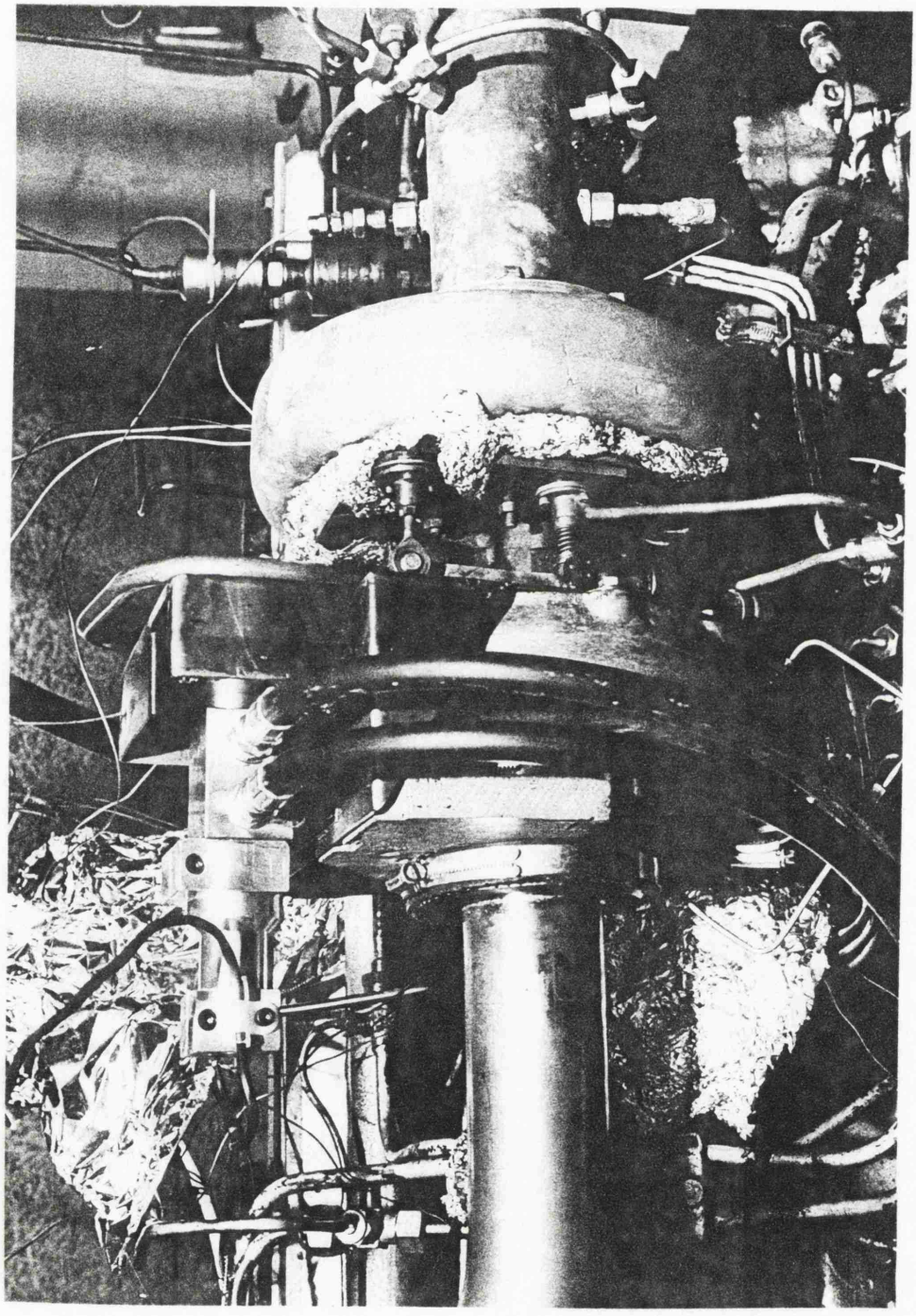

ELECTRONICALLY CONTROLLED

Fig 3.19 MKII VG TURBOCHARGER 'in-situ'

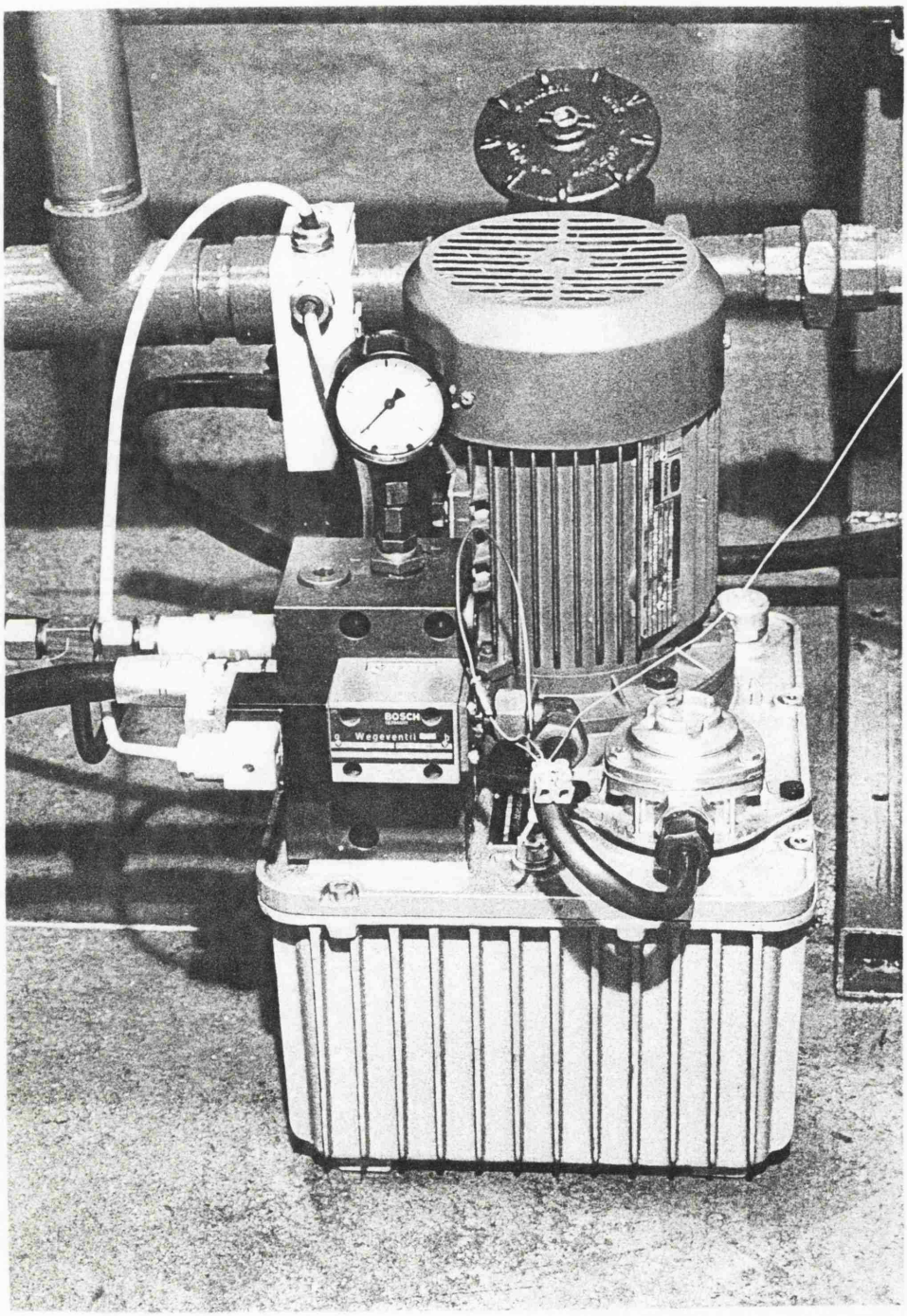

Fig 3.20 HYDRAULIC SERVO PACK

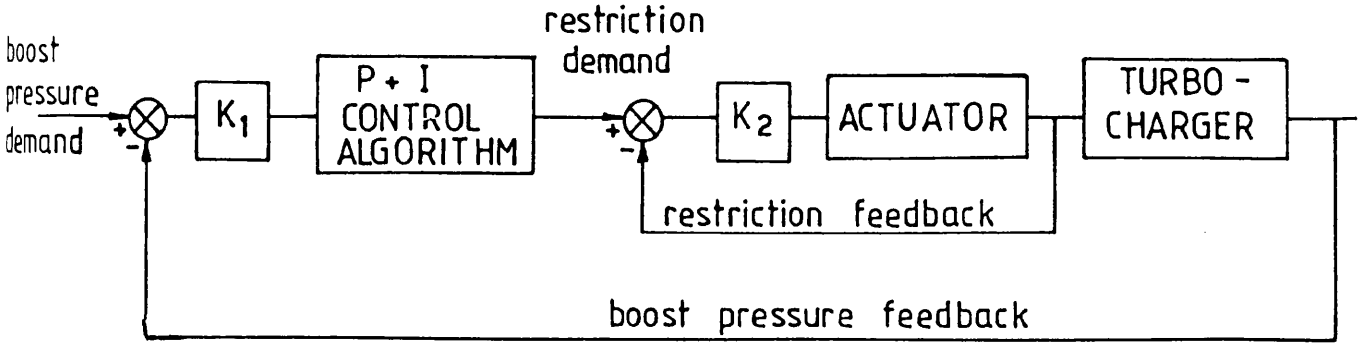

(a) TURBINE RESTRICTION CONTROL

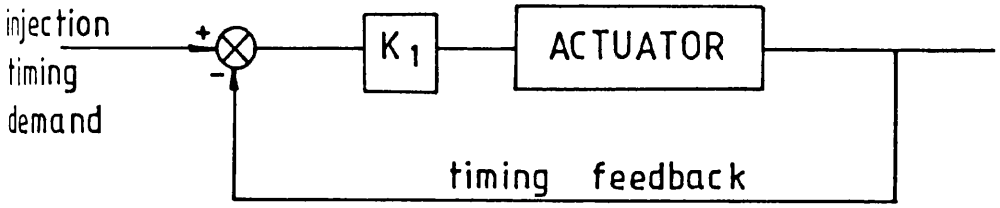

(b) INJECTION TIMING CONTROL

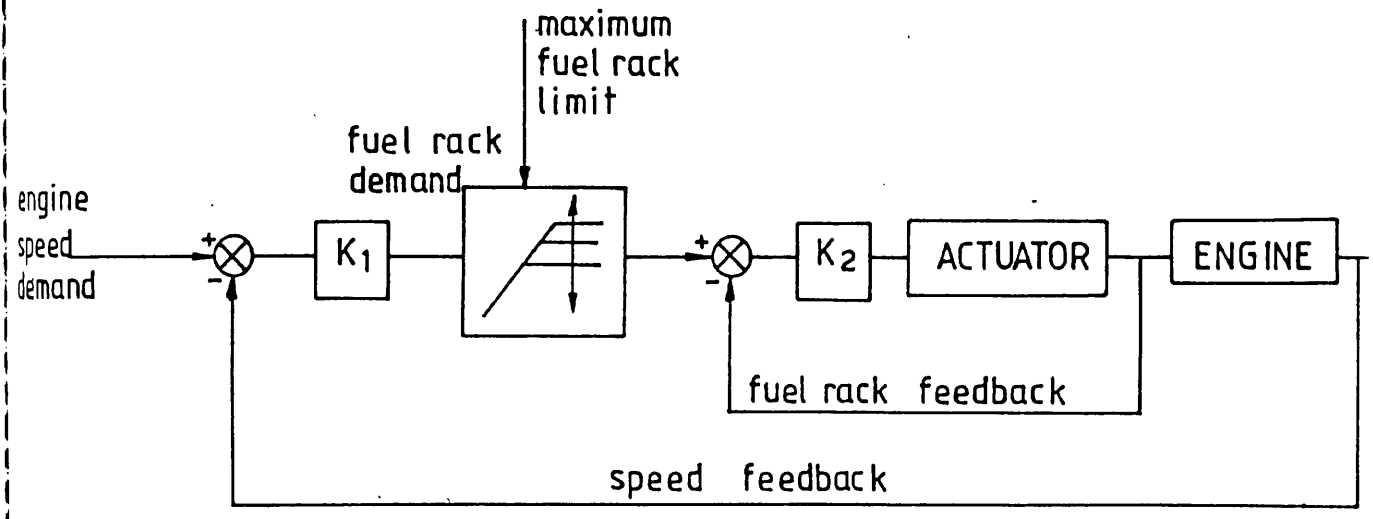

(c) FUEL PUMP CONTROL

NOTE: All demands can be either by manual adjustment (potentiometer setting) or by external voltage inputs (computer generated if required)

FIG 3.21 CONTROL LOOPS

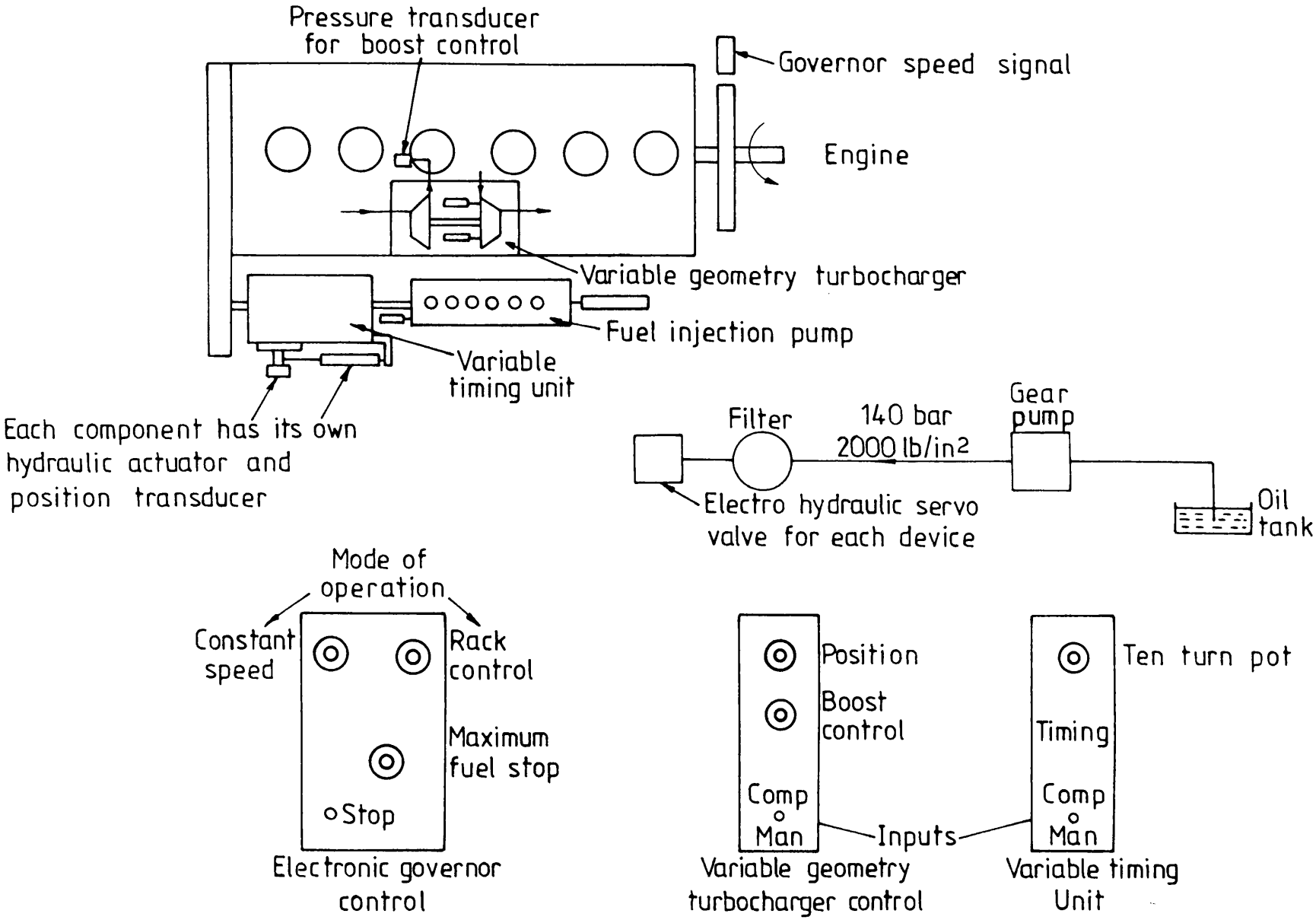

FIG 3.22 CONTROL PARAMETERS (ELECTRO-HYDRAULIC DEVICES)

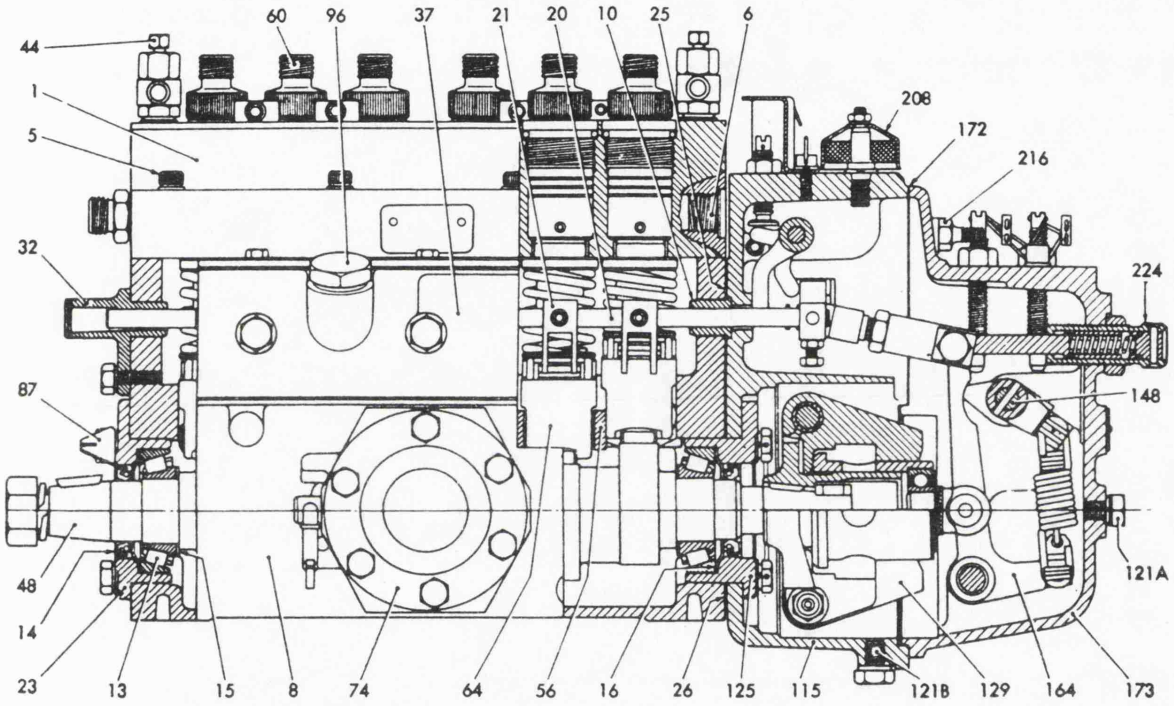

1	Pump Body	25	Jointing Ring	115	Governor Housing
5	Pump Body Screw	26	Jointing	121A	Governor Oil Level Plug
6	Gallery Plug	32	Control Rod Cover	121B	Governor Oil Drain Plug
8	Cambox	37	Inspection Cover	125	Bearing Housing
10	Control Rod Bush	44	Air Vent Valve	129	Governor Flyweight
13	Taper Roller Bearing	48	Camshaft	148	Speed Control Shaft
14	Oil Seal	56	Tappet Locating T-Piece	164	Crank Lever
15	Shims	60	Delivery Valve Holder	172	Jointing
16	Washer	64	Tappet	173	Governor Cover
20	Control Rod	74	Feed Pump	208	Breather Cap
21	Control Fork	87	Timing Indicator	216	Pillar Stud
23	Bearing Housing	96	Filler Plug	224	Damper Screw

fig 3.23 **SECTIONAL VIEW OF TYPICAL PUMP**

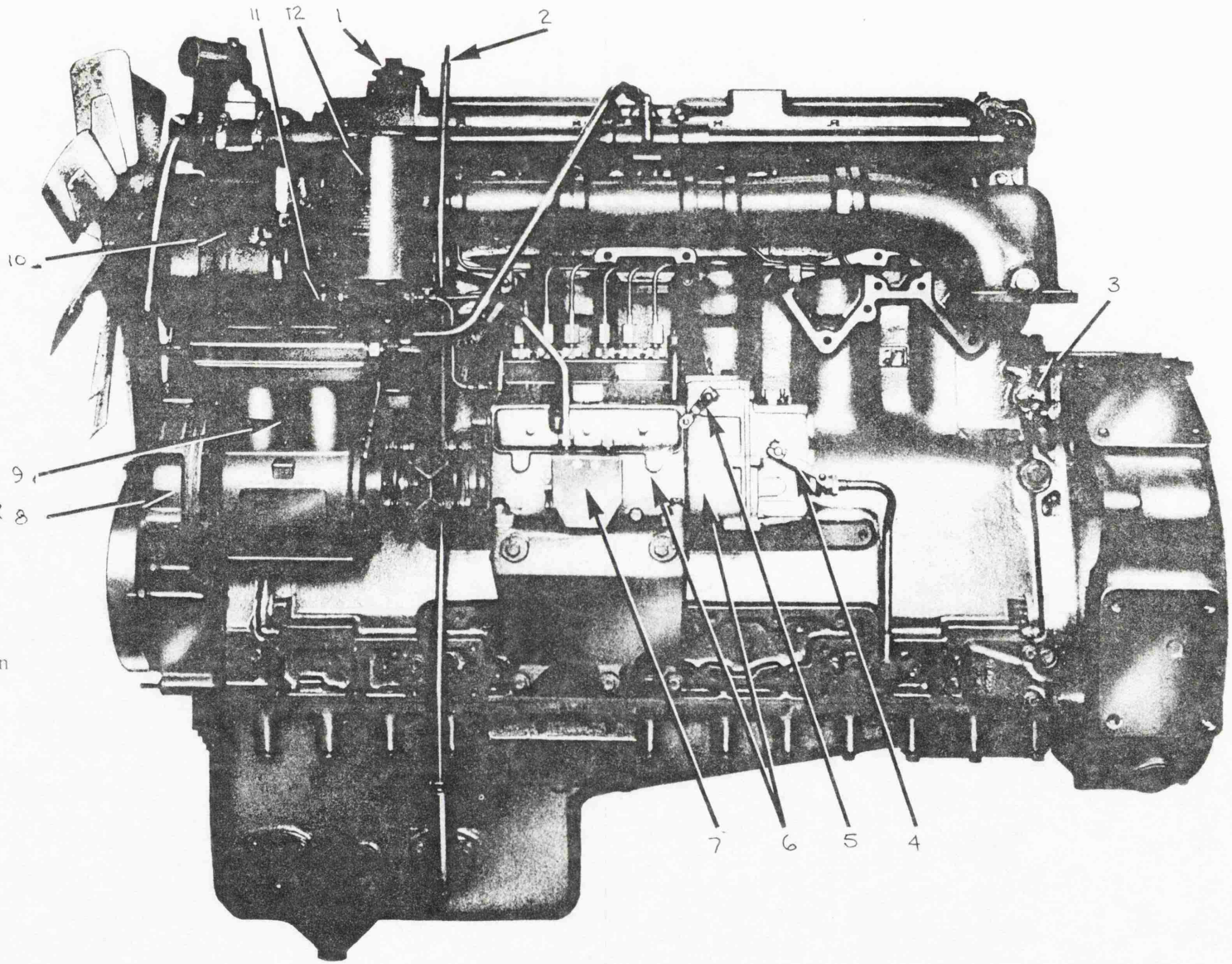

L.H. view of engine * 9 *
SHOWING COMPRESSOR 8

1. Oil filler cap
2. Dipstick
3. Coolant drain tap
4. Speed control lever
5. Stop lever and excess fuel button
6. Injection pump and governor
7. Feed pump and priming lever
8. Wheelcase
* 9. Air compressor *
10. Alternator
11. Fuel pressure relief valve
12. Fuel filter

fig 3.24

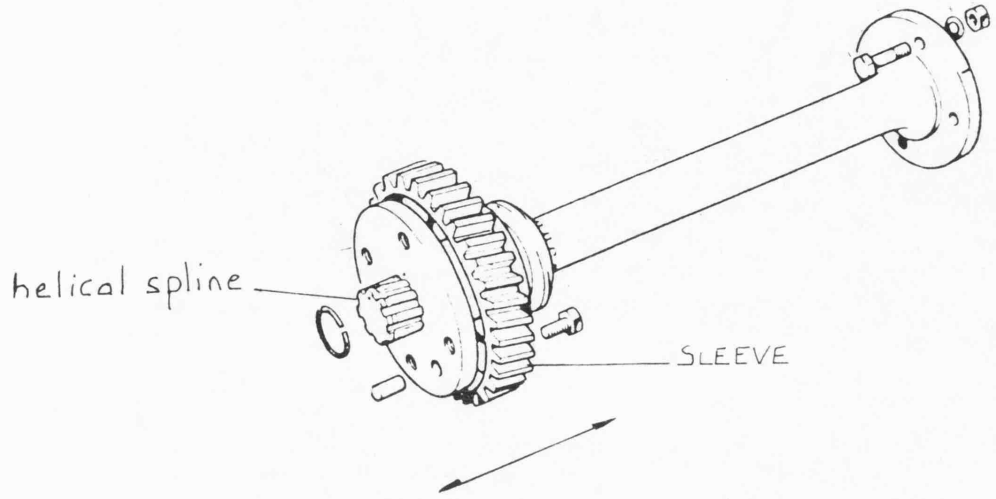

(a) TIMING GEARS

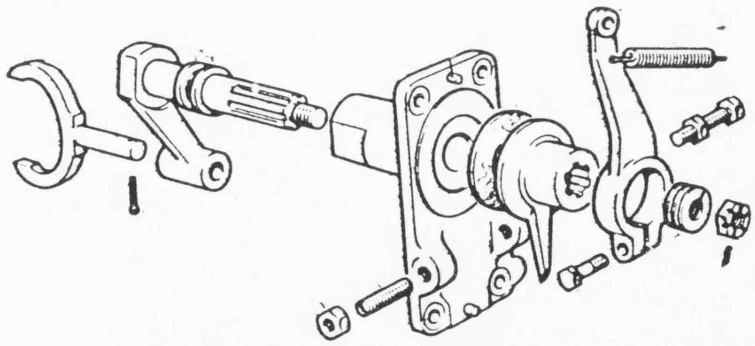

(b) ACTUATING LEVER

fig 3.25 VARIABLE TIMING PARTS

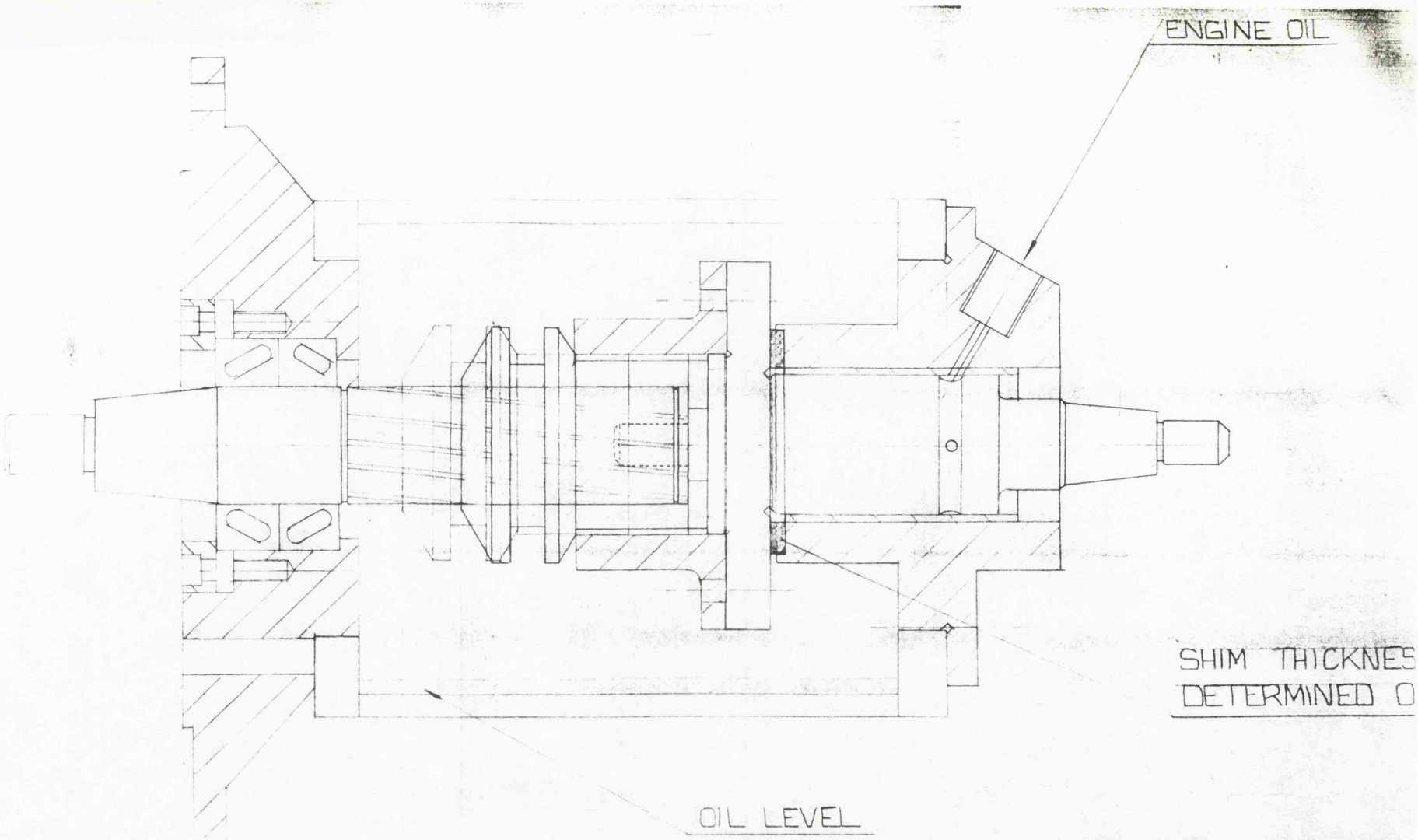

fig 3.26 Cross Section of Variable Timing Unit

ITEM No.	DRAWING No.	DESCRIPTION	No.

UNIVERSITY OF BA

SCHOOL OF ENGINEERING

TOLERANCES	DRAWN	CHECKED
	E W Roberts	
SCALE 1:1	DATE 22/7/82	APPROVED

TITLE
VARIABLE TIMING UNI
LEYLAND TL11

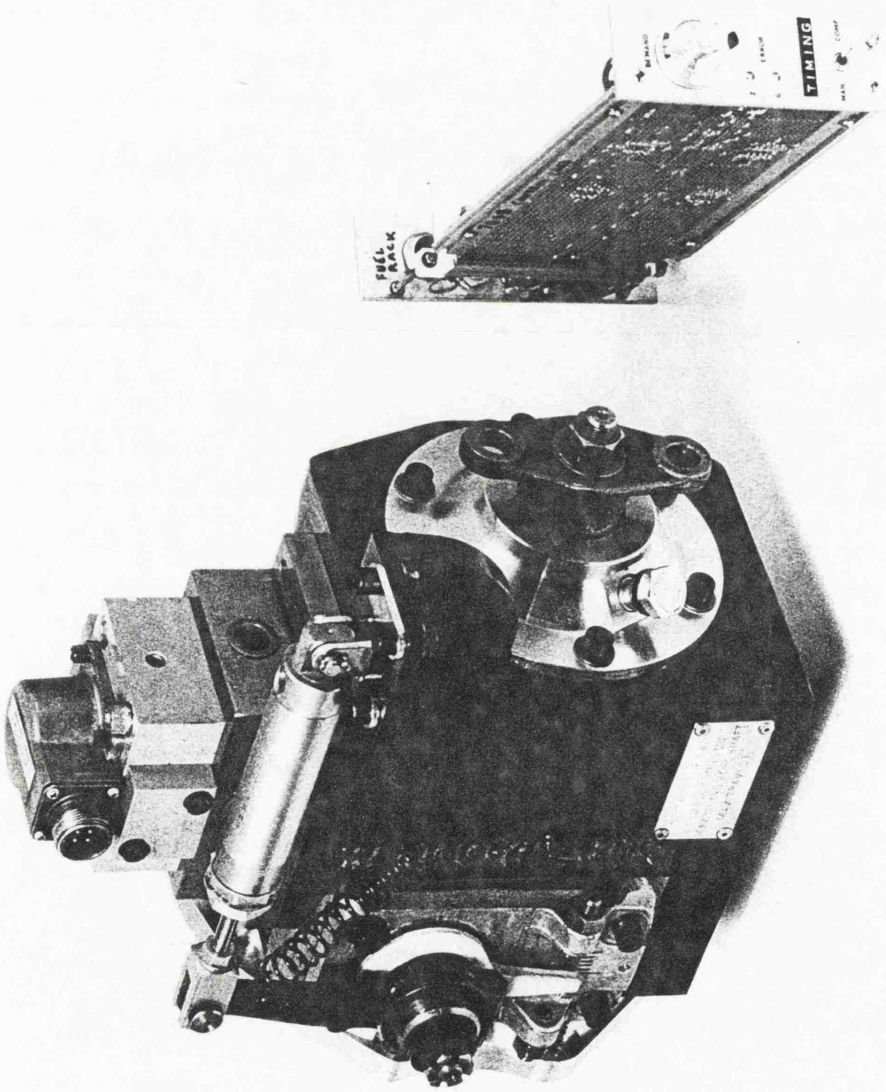

fig 3.27 VARIABLE TIMING UNIT

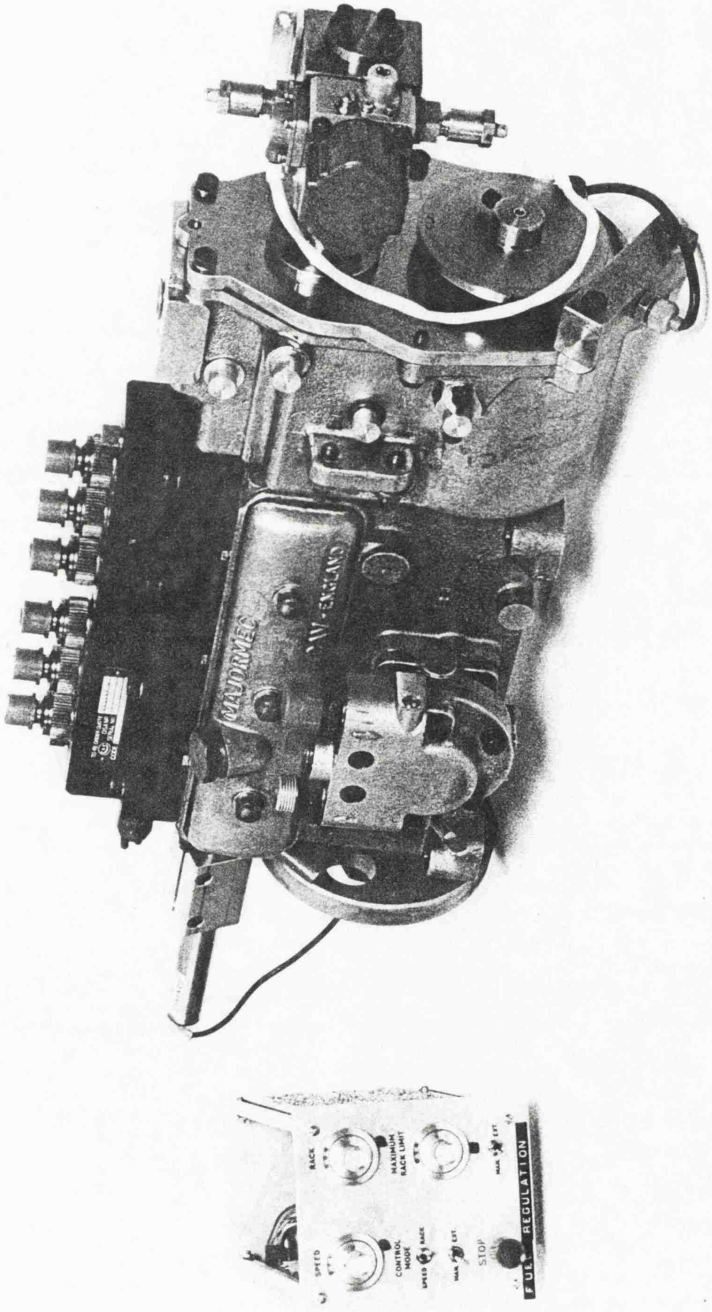

fig 328 ELECTRONICALLY GOVERNED FUEL PUMP

4. STEADY STATE RESULTS

4.1 Introduction

In Chapter 3 the control implementation was described. This chapter presents the comprehensive steady state results for the different control algorithms tested with the MKII(b) variable area turbocharger. It also includes the test results for the earlier VG prototypes (discussed in section 3). The mapping exercises included all the control parameters i.e. turbocharger area, injection timing and fuelling. However, before attempting the full optimisation, the performance of the final VG turbocharger was characterised by a limited parametric study at selected speeds and loads. Similarly the effects of varying injection timing were also characterised by performing a similar parametric study.

Two algorithms were assessed (i) an optimal type solution and (ii) a simplified schedule. The object of the optimisation tests was to determine the optimum settings for boost (turbine restriction) and injection timing for the TL11 engine under steady state operating conditions for the whole load speed range and to determine also the shape of the ideal full load fuelling schedule. These settings for the control parameters were stored as arrays (maps) in the micro-processor.

Secondly, a simplified boost and timing schedule was tested to assess the implied SFC and torque penalty using equations to generate the demands.

The results thus determined were assessed by a road and simulated vehicle program. This quantified the benefits of any improvements which a vehicle would be expected to give in terms of reduced journey times and enhanced fuel consumption (miles per gallon-mpg) over selected routes.

A list of tests corresponding to the various configurations tested throughout the project are included in fig. 4.0. As an aid to clarity

and ease of presentation the supporting data of reduced results, part load results, electronic and RSVP results corresponding to the list of fig. 4.0 are included in appendices.

Finally, the results presented include a full characterisation of the base engine such that comparisons with the VG configurations could be drawn. A presentation of these results follows.

4.2 Calibration Tests with the Standard Turbocharger

This section deals with the assessment of the performance of the base LEYLAND TL11 engine fitted with the standard HOLSET H2B twin entry turbocharger designated the H2B8081c L25 A3. Basically the turbocharger consists of a radial inflow nozzleless compressor and impeller of 81 mm diameter, a bearing housing and a twin entry nozzleless turbine casing with an effective inlet area of 25 cm^2.

4.2.1 Test procedure

From the base tests up to and including the MKII(b) VG turbocharger tests the engine was fitted with fixed injection timing (22° BTDC static). After test 19 the boost control device was overridden for the duration. This was to avoid hunting and as an aid to repeatibility. For each configuration tested power was set to 190 kW @ 2100 rev/min with the following parameter settings :

1) exhaust back pressure 78 mm (3") Hg
2) inlet depression pressure 355 mm (14") WG
3) fuel gallery temperature 37½°C ± 5
4) air inlet temperature 25°C ± 1
5) water jacket temperature 88°C ± 2

4.2.2 Results Format

The format adopted for presenting the engine results is as follows :-

a) a compressor map with engine operating line superimposed.
b) an engine determined turbine swallowing graph.

c) peak cylinder pressure (p_{max}) ∿ bar
brake mean effective pressure ∿ bar
smoke ∿ Bosch
fuel delivery ∿ mg/shot
power ∿ kW

LTC PARAMETERS

d) exhaust temperature (T1T) ∿ °C
air mass flow ∿ kg/s
turbocharger speed ∿ rev/min
compressor and turbine pressure ∿ bar

LOAD-SPEED MAP ISO-CONSUMPTION LOOPS

Other parameters plotted as necessary included :

1) volumetric efficiency - %
2) compressor efficiency
3) overall air fuel ratio
4) VG turn down schedule
5) timing schedule

4.2.3 Presentation of Results

On arrival the engine was tested on the limiting torque curve (LTC) in standard form and performance compared with the manufacturers' results for that engine. Engine performance in each case was very similar (fig. 4.1).

(i) LTC PERFORMANCE

The engine with the H2B turbocharger was rigorously tested so as to establish a datum performance, Fig. 4.2 shows the compressor map with the engine running line and lines of constant engine speed superimposed. The bulge of the LTC at peak torque is characteristic of twin entry pulse operation and imparts a good torque back-up to the engine. Below 1100 rev/min the torque falls rapidly as the boost control becomes operative. The compressor is well matched to the engine, giving good efficiencies whilst maintaining an adequate surge margin. Torque back-up on the TL11 engine was found to be 21% at 62% of rated speed. (1057 Nm @ 1300 rev/min). The useful power range was therefore

restricted to 800 rev/min i.e. from 2100 to 1300 rev/min. The torque back-up attained was higher than the LEYLAND designed value of 17% (1017 Nm @ 1300 rev/min) and is attributed to the higher back pressure necessitating a higher fuelling level to attain rated power. Throughout the project power was selected rather than fuelling. Fig. 4.3 shows the non-linear nature of the turbine swallowing capacity (based on manometer mean values of pressure and mean temperature). It can be seen from fig. 4.4 that specific fuel consumption (SFC) is a minimum of .210 kg/kWh at 1300 rev/min (peak torque) design point and rises on either side. This is due in part to the turbomachinery efficiency which is reflected as positive pumping work (fig. 4.5) and also injection timing and speed effects. Smoke free operation is limited to 20:1 air fuel ratio at peak torque; air fuel ratio rises to 26:1 at 2100 rev/min. Below peak torque smoke emission* rises rapidly due to reduced turbine power and volumetric efficiency. Above peak torque turbine inlet temperature (TIT) and peak cylinder pressure (p_{max}) become limiting factors. For this engine on the LTC with a 15.75:1 compression ratio, turbine inlet temperatures (TIT) are typically 650°C with cylinder pressures (p_{max}) of 115 bar. Fig. 4.6 is a graph of dynamic timing; this shows that injection takes place at 12½°BTDC at 2100 rev/min advancing with reduced speed to 18°BTDC at 800 rev/min. Injection period varies between 22° crank angle at rated conditions to 12° at 800 rev/min. Fuel line pressure has a maximum value of 600 bar at rated speed. Peak cylinder pressure has a flat characteristic of approximately 115 bar over the useful power range. The results presented in fig. 4.6 are supported by oscilloscope photographs contained in appendix 5, section 1, sheets 1 to 6 corresponding to conditions within cylinder 6 (on the LTC) for speeds between 2100 and 800 rev/min.

(ii) PART LOAD PERFORMANCE

Fig. 4.7 shows the iso-consumption loops for the whole load speed regime. Below approximately 50% torque the lines become much closer

*generally a Bosch smoke number of 3.5 is not noticed by casual observers while a Bosch smoke number of 2.5 is considered to be nearly invisible.

together and increase rapidly in value. This is because parasitic and frictional effects predominate SFC improves below the LTC especially near peak torque (matched point) due to better combustion and turbomachinery efficiency. It should also be noted that the SFC contours rise rapidly at the right hand side as speed effects become dominant (i.e. friction and speed^2). Ideally the SFC islands should be large with a low value.

Fig. 4.8 is the iso-consumption loop for the naturally aspirated version of the TL11 engine and is included for comparison. This shows that SFC islands are larger but of higher value. Torque back up is 17½% at 40% of rated speed (fig. 4.9). The useful speed range is 1200 rev/min (i.e. 2000-800 rev/min). However, rated power is only 134 kW and peak torque is 300 Nm (30%) less than its turbocharged counterpart. It is also apparent that SFC on the LTC is very much flatter (though of higher value) than when turbocharged. From inspection of figures 4.7 and 4.8, it should be appreciated that a different driving technique is required for a turbocharged automotive vehicle when compared with a naturally aspirated type.

Ideally the characteristics associated with a high torque back up engine should be :

1) a wide speed range i.e. 1100 rev/min.
2) a 'flat' low value SFC characteristic .200 kg/kWh on the LTC.
3) large SFC islands.

whilst operating within the mechanical, thermal and legal limits of the engine i.e. cylinder pressure, turbine inlet temperature and smoke (fig. 4.10).

4.3 Characterisation Tests with the V.G. Turbochargers

Three separate and distinct V.G. configured turbochargers were tested corresponding to the MKI, MKII(a) and MKII(b) units respectively. A description of the design and development is given in section 3.5.1. The MKI unit is considered first of all.

4.3.1 MkI V.G. Turbocharger (Twin Flow) Results

The performance of the MKI twin flow V.G. turbocharger was fully determined by testing on the LTC and at constant brake mean effective pressures (bmep) of 2,4,6 and 8 bar (corresponding to torque levels of 130,260,390 and 520 Nm) and nominal percentage restrictions of the turbine, with the sliding ring sleeve in a series of fixed discrete position of 0,10,30 and 50%. The speed range covered was from 800 to 2100 rev/min in steps of 200 rev/min. The turbocharger was designated the H2C 8640.27Ø.

The performance of the V.G. configured engine was evaluated by inspection of the power curve with standard fuelling with the turbine stage either fully open or fully restricted. In the fully restricted case the power curve was begun at the lowest speed and progressively increased until choking of the turbine stage occurred. It follows therefore that with an efficient turn down ratio of about 50%, the effective power curve will be restricted to approximately 1200 rev/min. and below.

It is a pre-condition for the successful application of V.G. turbo-charging that engine SFC on the LTC with the turbine stage fully open be comparable with the base performance. This is because in automotive applications vehicles are expected to operate at high speed and load conditions, e.g. motorways, for a disproportionately long time.

(i) LIMITING TORQUE CURVE RESULTS.

To enable a valid comparison to be made between the base H2B unit and the V.G. MkI unit, it was important to ensure that the inlet manifold pressure at rated conditions was similar in each case, i.e. that the engine turbocharger match was the same. When initially tested the MKI turbine had too small a swallowing capacity with consequent overboosting at the rated condition. The turbine inlet area was increased by

machining the trailing edge of the nozzle blades from 6.1 to 6.8 mm thus increasing the effective turbine inlet (throat) area. Very satisfactory performance was obtained with the nozzle set to zero restriction, SFC comparing favourably with the base, the characteristic bulge of twin-flow pulse operation being apparent (fig. 4.11).

The unit was then re-tested with an effective turbine inlet 50% of the original value. This was effected by fitting spacing shims. The fuelling was the same for both tests.

The result was disappointing as an engine speed of 2000 rev/min. was obtainable on the LTC. This showed that the actual turn down ratio was considerably less than 50%, Fig. 4.11. The compressor map shows the engine running in the fully open and restricted cases. At peak torque there was an increase in turbocharger speed of only 4000 rev/min. Graph 4.12 shows that the turbine non-dimensional swallowing capacity ($m \sqrt{T/P}$) decreased only 16% for a 50% area turn down, consequently engine performance was little affected. As expected only small benefits in SFC, smoke and T1T below peak torque were noted at the expense of cylinder pressure which rose typically by 6 bar (Figs. 4.13 and 4.14).

(ii) PART LOAD PERFORMANCE

The iso-consumption loops for the unrestricted case were comparable with the base (fig. 4.15). The islands were typical of a nozzled unit which characteristically have a narrow but more efficient operating range. For the fully restricted case the SFC islands are worse particularly as expected at high speeds (fig. 4.16). Part load performance graphs are included in appendix 4, section 2, sheet 1 to 4. However, only 0 and 50% restrictions are presented as the differences for 20 and 30% are very small.

The small turn down in non-dimensional mass flow of the turbine can be explained by leakage behind and around the restrictor in the volute exit area. The exhaust gas thus enters the wheel in an unregulated manner. This destroys the flow guidance which adversely affects efficiency. In view of the disappointing results it was decided to curtail development of the twin flow MKI unit and develop a completely

new purpose built and designed VG turbocharger. This was based on a single entry design, again with a variable inlet throat area and with the object of achieving a much better turn down ratio (2:1) with good efficiencies. This design was designated the MKII(a) unit.

4.3.2 MKII(a) VG Turbocharger results

The MKII(a) unit was assessed on the LTC as before with fixed discrete restrictions corresponding to 0, 30 and 50% respectively. The MKII(a) unit had the manufacturer's number H2C8625N Z31U3 and consisted of a single entry nozzled turbine stage with a moving ring sleeve in the volute exit area. A smaller inducer compressor housing and impeller were fitted to allow a greater surge margin. The turbocharger match of rated power was similar to the base.

(i) LTC RESULTS

The compressor map (fig. 4.17) shows that the characteristic bulge of pulse operation is no longer apparent. In the fully restricted case 1600 rev/min was possible before the turbine stage became choked suggesting a higher turn down ratio. At 1300 rev/min there is a rise in turbocharger speed of 12000 rev/min to 75000 which is equivalent to a .24 gain in pressure ratio, and corresponds to a 30% turn down ratio (fig. 4.18). This graph compares the swallowing capacities of the base and unrestricted cases together with 30 and 50% restriction. Note the characteristic rapid onset of choking with the nozzled unit at expansion ratios greater than 1.6. Inspection of this graph suggests that this is mildly non-linear i.e. the initial movement has little effect and also that this configuration had a tighter turbine stage (fully open) to effect the same boost level implying a less efficient turbine stage.

The test with the turbine throat area unrestricted was compared with the base (fig. 4.19/20). Unlike the MKI unit there is a pronounced degradation in performance - typically 2% worse SFC, between 2100 and 1200 rev/min. Smoke was comparable between 1800 and 1200 rev/min., thereafter being up to ½ Bosch worse. This was because airflow was reduced by 4.6% across the whole speed range, and this in turn, was

reflected in a higher TIT (+ 25%). Therefore to achieve base performance some turn down is required before up-fuelling is possible. This highlights the disadvantage of a single entry unit.

Figs. 4.21/4.22 show the effect of applying increasing restriction. It can be seen that this has the beneficial effect of increasing boost and hence air mass flow. This reduces smoke by 1.2 Bosch at 1300 rev/min to 1.2 whilst SFC decreases by 1.4% to .211 kg/kWh. TIT, however, drops by only 15°C. This is because pre-turbine pressure increases disproprtionally when compared with boost, implying an efficiency penalty and reducing beneficial scavenging.

These results confirmed the potential benefits of VG turbocharging. However, a 30% turn down ratio was considered unsatisfactory. The comparatively low value was again attributed to leakage behind and around the restrictor. Further development of the VG mechanism produced a unit designated the MKII(b).

4.3.3 MKII(b) TURBOCHARGER RESULTS

The effort had been directed principally at minimising the internal leakage paths. This unit was the first to have a fully remotely dynamically variable VG capability. Actuation was by two pneumatic actuators mounted either side of the bearing housing. Power was supplied by an external compressor. A transducer in the actuator gave the axial position of the ring sleeve, the system being under open loop control.

The performance of the unit was assessed as before. As with the MKI unit it was found necessary to increase the swallowing capacity of the turbine to produce an inlet manifold pressure with the comparable base at rated power. This was facilitated by fitting a larger exducer turbine housing and wheel.

The unit was assessed with restrictions of 0,25,40 and 50% on the LTC. To minimise the number of graphs and aid clarity the 'best' results from the restriction tests have been merged and then compared directly with the base results. This means effectively operation with 50% restriction between 700 and 1300, with 40% between 1300 and 1700 rev/min and fully open thereafter to 2100 rev/min.

(i) LTC PERFORMANCE

Fig. 4.23 shows the compressor map with the operating lines for the various restrictions tested. Note again the 'flat' characteristic usually associated with a single-entry turbine. Further inspection of the compressor map reveals that at 1300 rev/min the turbocharger speed is increased from 59700 to 77000 rev/min (with a 50% restriction) corresponding to a substantial pressure ratio rise of 0.52. This is equivalent to an increase in overall air fuel ratio of 3.4 (from 18.6 to 22.1).

The engine determined swallowing capacity curves (fig. 4.24) show that a 35% turn down ratio was achieved for a 50% axial restriction, turn down being approximately linear with 0, 25, 40 and 50% axial restriction.

The following two figures (4.25 and 4.26) present the test results for the VG configured cases and are compared with base performance. From these figures it can be seen that in the unrestricted case (1700-2100 rev/min) the base imparts a larger pressure differential across the cylinders implying a better turbine efficiency. This is reflected in a higher SFC of 3.5% for the VG, TIT is some 50°C higher whilst smoke is 0.3 Bosch better.

In the range 1300-1700 rev/min with a restriction of 40% the SFC is comparable. Turbocharger speed increases 5000 rev/min over base and results in a small increase in air mass flow, smoke emission is consistently 0.4 Bosch better. Cylinder pressure is higher due to the enhanced boost, TIT, however, remains up to 50° higher.

Below 1300 rev/min the maximum 50% restriction is applied, this shows SFC to be marginally better than base. Smoke is considerably improved as the VG becomes effective. Turbocharger speed rises by 8000 rev/min, whilst airflow remains substantially the same but TIT reduces by 20°C below base.

It was disappointing to note that the improved density ratio 1.38 to 1.6 (base 1.39) at 1500 rev/min was not reflected in a very much higher air mass flow.

Fig. 4.27 considers those parameters which primarily influence engine breathing, i.e. compressor efficiency, turbocharger speed, density ratio, volumetric efficiency and air mass flow. From inspection of this graph it appears that the discrepancy can be attributed to greater air throughput during valve overlap of the base build, i.e. the difference between trapped air fuel ratio (TAFR) and overall air fuel ratio (OAFR), which is a function of pressure differential. This would explain why smoke is reduced when TIT remains the same. Unfortunately scavenge ratio can only be inferred not measured, this underlines the importance of an efficient turbine stage.

4.4 Control Parameter Investigation

The results with the MKII(b) unit were considered sufficiently encouraging to proceed further and to attempt a full dynamic optimisation with respect to injection timing and boost (turbine restriction), the object being to maximise the available torque with regard to experimental, thermal and mechanical limits (fig. 4.10), and to determine the best SFC and minimum smoke over the whole load/speed regime. Rated power was to remain the same at 190 kW @ 2100 rev/min.

First, however, it was necessary to evaluate and characterise the effects of timing and restriction on the full and part load performance of the TL11 engine. To this end two series of tests were performed :

1) a boost investigation
2) an injection timing investigation

The investigations were concentrated at 1800, 1300 and 800 rev/min. Fuelling was adjusted such that the engine produced standard LTC torque, 700°C TIT or 4 Bosch smoke as appropriate. A further test was performed at 50% of LTC to investigate part load operation.

4.4.1 Boost Investigation

These results are presented to a base of restriction. A limited number of oscilloscope photographs corresponding to conditions within cylinder 6 under different levels of boost were taken and are presented in appendix 5, section 2, sheet 1 of 3.

(i) 1800 rev/min LIMITING TORQUE CURVE, Fig. 4.28

A maximum restriction of 25% was applied at 1800 rev/min to avoid exceeding the cylinder pressure limit. Within this range it can be seen that SFC is nominally flat (max. difference 0.4%) and compares favourably with the base (.215 kg/kWh). Cylinder pressure rises by 3 bar to 120 bar over this range. Turbocharger speed increases with the higher turbine power by 3000 rev/min to 80000 rev/min. TIT is essentially the same and smoke negligible.

From the foregoing it can be seen that the engine reacts most favourably

to a fully open turbine stage.

(ii) 1800 rev/min - 50% of LIMITING TORQUE, Fig. 4.29

A 35% restriction was applied at 450 Nm. This results in a 2.7% SFC penalty. In the fully open position SFC is 2% worse than for the base build. Turbocharger speed rises by 1000 rev/min to 66000 rev/min and consequently p_{max} rises by 18 bar to 88 bar, TIT, however, remained constant. There was no smoke emission.

At this high speed there is sufficient mass flow at all loads to facilitate good combustion. Applying restriction does not therefore benefit the engine.

(iii) 1300 rev/min LIMITING TORQUE CURVE, Fig. 4.30

As expected, in this case the engine responds very favourably to increasing turbine restriction (0 to 50%). SFC reduces by 2.3% to .211 kg/kWh in the fully restricted case which is 0.9% better than the base value. Fuelling was adjusted to give 700°C TIT in the worst case (0%). At this condition smoke emission is 2.5 Bosch together with a peak cylinder pressure of 101 bar. Increasing turbine restriction is accompanied by an increase in turbocharger speed of 15,400 rev/min to 71000 rev/min while cylinder pressure rises by 12 bar to 113 bar. Smoke emission decreases by 1.5 Bosch to 1 and TIT reduces by 50°C to 650°C.

(iv) 1300 rev/min - 50% of LIMITING TORQUE, Fig. 4.31

Applying restriction at 450 Nm effects a 1.2% SFC penalty. Turbocharger speed rises by 10000 rev/min to 48ooo. However TIT reduces by only 7°C probably due to the engine operating in crossover. Smoke is negligible at this condition, p_{max} however rises by 12 bar to 86 bar.

At 1300 rev/min (peak torque) the engine responds favourably to the increased air mass flow significantly affecting smoke, TIT and SFC. At 50% torque there is no requirement for increased air and therefore an SFC penalty results with greater turn down.

(v) 800 rev/min LIMITING TORQUE CURVE, Fig. 4.32

At this speed the fuelling was adjusted such as to give a smoke level of 4 Bosch in the best case. The turbine power at this speed is very low due to the low massflow and expansion ratio available. Therefore applying even 50% restriction has only a small effect; nonetheless a 4.3% improvement in SFC was recorded (to .228 kg/kWh). This compares favourably with the base (+1.3%). The other parameters responded as follows:-

TIT remained constant at 650°C

P_{max} rose by 5 bar to 106 bar

turbocharger speed increased by 7000 rev/min

smoke improved by 0.7 to 4 Bosch.

(vi) 8000 rev/min - 50% of LIMITING TORQUE, Fig. 4.33

The engine at 400 Nm is essentially naturally aspirated. SFC at zero restriction again compares favourably with the base (1.8% better). Increasing restriction results in a 1.4% increase in SFC to .225 kg/kWh. TIT is constant at 360°C, whilst p_{max} rises by only 3 bar to 79 bar. Smoke emission improves by 0.6 to 1.0 Bosch.

The results confirm the engine requirements for increasing restriction with decreasing speed (< 1700 rev/min) and increasing load (> 700 Nm). Excessive restriction results in a high cylinder pressure and an SFC penalty due to increased pumping work. The study also shows that when correctly matched the VG configuration has an SFC comparable with the base engine. Fuel consumption at part load is not critically affected by restriction, being typically 2% worse. This study gives a very useful insight into the engine turbocharger interaction and proved very useful in the mapping exercise described later in this chapter (section 4.5.1).

4.4.2 Timing Investigation

A timing investigation was performed at the same speeds but with the standard H2B turbocharger fitted. Injection timing was varied over approximately 14° crank angle and six points were taken. The results are presented on a speed basis as timing is essentially a speed function. (Ignition delay). A limited number of oscilloscope photographs

corresponding to conditions within cylinder 6 with different injection timings were taken and are presented in appendix 5, section 3, sheets 1 to 11.

The noise results are considered at the end of this section.

(i) 1800 rev/min LIMITING TORQUE CURVE, Fig. 4.34.

From inspection of fig. 4.34, it can be seen that advancing timing from 7 to 18°BTDC has the beneficial effect of decreasing SFC by 6% to .211 kg/kWh whilst torque increases by 70 Nm to 990 Nm. Over this range p_{max} rises from 92 to 127 bar whilst turbocharger speed decreases by 2000 rev/min to 82000 rev/min with the lower temperature (25°C) and pressure. Smoke emission reduces by 1.1 Bosch to zero.

(ii) 1800 rev/min - 50% LIMITING TORQUE, Fig. 4.35.

At 50% load the torque was held constant and fuelling allowed to find its own level. The results indicate that timing is less critical and benefits from retarding when compared with the optimum LTC value. The same characteristics as above for p_{max}, smoke and turbocharger speed were recorded.

(iii) 1300 rev/min LTC, Fig. 4.36

Inspection of this figure suggests that optimum timing is close to the standard timing. However, compared with fig. 4.34, it can be seen that SFC rises steeply with increasing advance (0.7% per °CA). Cylinder pressure rises with increasing advance from 102 to 124 bar whilst smoke decreases from 1.8 to 1.2 Bosch. For constant fuelling torque peaks at 1000 Nm reducing to 945 Nm.

(iv) 1300 rev/min - 50% of LTC, Fig. 4.37.

At the condition this injection timing is clearly too advanced and SFC is continuing to show improvement with maximum retard. It is interesting to note that with excessive advance smoke emission begins to rise again from 0.2 to 0.6 Bosch, other characteristics being as above.

(v) 800 rev/min LTC, Fig. 4.38

The comments applied to 1300 rev/min above are equally applicable at 800 rev/min, i.e. the engine is on the limits of advance. With increasing advance (from 10 to 21° BTDC) cylinder pressure rises by 16 bar to 96 bar, whilst smoke decreases from 3.9 Bosch to 3.2. TIT is nominally flat whilst torque decreases by 45 Nm to 730 Nm. SFC rises from .215 to .229 Kg/kWh over the range.

(vi) 800 rev/min - 50% of LTC, Fig. 4.39

At 50% of limiting torque the same trends as those on the LTC are apparent, that is reducing SFC with retard to 13.5° BTDC. It is interesting to note, however, that smoke improves by 1.2 Bosch to 0.5 with increasing retard. The reason for this is not clearly understood.

From the foregoing it can be appreciated that the static injection timing of 22° BTDC is a compromise between peak torque and rated speed. This would indicate that optimising injection timing would be expected to yield SFC gains at high speeds (> 1800 rev/min) and low speeds (< 1500). The tests confirm that injection timing should be advanced with increasing speed for a given fuelling level or torque. This is because ignition delay is essentially a function of time rather than crank angle. For constant speed operation end of injection should be held constant. Thus as load (duration of injection) increases start of injection should be advanced.

These tests included an assessment of noise emissions and these suggest on the LTC that noise increases with increasing advance. This is readily apparent at 50% torque. In addition, at idle speeds, subjectively, noise was noticeably reduced. In all probability it will be the legal requirement for the control of emissions and noise which will force engine manufacturers to consider electronic control of injection timing.

4.5 Control Algorithm Investigation

Two control algorithms were assessed, viz:-

i) an optimal type solution
ii) a simplified schedule

An optimal solution is one where the performance of the engine is fully determined on a test bed and the results stored digitally in arrays within the microprocessor.

A simplified schedule was based on the results of the above tests and characterised by means of equations, essentially ignoring non-linearities. The optimal solution is considered first.

4.5.1 Optimisation and mapping

The object of the steady state tests was to determine the optimum settings for boost (turbine restriction) and injection timing for minimum SFC under steady operating conditions and also the full load (LTC) fuelling schedule consistent with the engine's mechanical, smoke and thermal limits (fig. 4.10). For all the tests reported the fuel pump was controlled electronically.

i) OPTIMISATION

Optimising for best SFC was a dynamic process. During testing it was ascertained very quickly tht the interaction between timing and VG setting was small making optimisation effectively a two stage iterative process;

i.e.	fix VG setting - vary timing	Optimise by measuring SFC
	fix 'best' timing - vary VG setting	" " " "
OPTIMISED SETTINGS	fix 'best VG setting - vary timing	) Small differences
	fix 'best' timing - vary VG setting	)

For the above process the engine was run in the all-speed governing mode whilst the dynamometer was set to constant torque demand, such that enhanced engine efficiency was reflected in an increase in speed and a reduction in fuel rack position, i.e. running down the droop line. Other

parameters (apart from fuel consumption) which were found to be important included the cylinder pressure trace, (to select an approximate timing), smoke emission and pressure differential across the engine.

On the LTC the limits imposed by cylinder pressure, turbine inlet temperature and smoke became the limiting criteria. In the absence of established SFC values a comparison was drawn with the base H2B configured engine.

The load-speed map was determined by testing in 200 rev/min increments between 700 and 2300 rev/min from minimum brake load to LTC in 100 Nm increments.

The results are divided into the following parts :

1) limiting torque curve performance figs. 4.40-4.45
2) load-speed maps, figs. 4.46-4.55
3) part load results, Appendix 4 - Section 3 - Sheet 1 to 18.
4) electronic instrumentation, Appendix 5 - Section 4 - Sheet 1 to 5.

ii) LIMITING TORQUE CURVE, Fig. 4.40

It should be noted that the boost pressure at rated power is somewhat less than base and that described in Section 4.3.3. This larger swallowing capacity is attributed to increased movement of the ring sleeve in the volute exit area due to modified pistons. This had the effect of reducing SFC at high speed and load.

From inspection of the compressor maps (figs. 4.40/4.41), it can be seen that the map width is adequate for the enhanced operating range of the engine. The turbine stage is 50% restricted up to 1400 rev/min and then progressively opened up to its maximum value at 1800 rev/min and above. Fig. 4.41 compares the LTC running line with that of the base. A rising pressure ratio characteristic is required from 1800 rev/min to 1300 rev/min to cater for up-fuelling and a lower turbine efficiency. It becomes immediately apparent, however, that a boost control schedule based on springs and diaphragms is completely in appropriate. Fig. 4.42 shows the engine determined swallowing capacity curves; turn down ratio was found to be 38% at 1.7 expansion ratio.

Figs. 4.43 and 44 compare the optimised torque curves with the base H2B curves. This shows that SFC on the LTC is comparable (< 2%); however, torque has been increased by 10% without adversely affecting smoke emission. A constant power output of 191 kW was maintained down to 1700 rev/min. Both the TIT and p_{max} limits are held over the range 2300 - 1000 rev/min highlighting the advantage of tight electronic control. Turbocharger speed has been held below 90,000 rev/min but above 80,000 rev/min from 2300 to 1300 rev/min, air mass flow reflecting this trend. Fig. 4.45 shows that air fuel ratio on the LTC is maintained between 25.5 and 20 to 1.

One unfortunate characteristic highlighted was that of compressor efficiency which (around peak torque) decreases with increasing torque as the engine running line passes through the high efficiency island. It was found difficult to decrease the peak torque speed due to a combination of larger turbine housing, conservative p_{max}.and breathing. Both the compressor efficiency characteristic and valve timing favour high speed operation; thus the rated speed was increased to 2300 rev/min to investigate the effects on SFC and demonstrate that the VG turbocharger operates efficiently over a wider speed range.

Nevertheless a maximum torque of 1155 Nm was recorded. This represents a torque back up of 46% at 59% of rated speed and compares favourably with 21% at 62% of rated speed for the base. The useful speed range has thus increased by 17½%.

iii) LOAD SPEED MAPS - Figs. 4.46 - 4.55

A plot of SFC reveals that part load performance has been substantially improved. The 0.225 kg/kWh island is 25% bigger; & that for 0.240 kg/kWh is 30% bigger. (Fig. 4.46 shows the base H2B iso-consumption loops and is included for comparison). These improvements are primarily attributed to timing and are concentrated below peak torque to the left of the map. Thus the characteristic onion rings become more speed dependent. The SFC map also contains a 10 mode-weighted cycle showing the most used areas of the operating box. Fig. 4.48 attempts to quantify the SFC benefits accruing to the optimised case; this clearly shows the benefits of de-speeding.

The following figure (4.49) is a plot of boost pressure. This shows that within the control range of the turbine the engine responds most favourably to constant boost pressure for a given load i.e. constant air fuel ratio. The control range of the turbine is small when compared with the operating range of the engine such that volumetric and turbomachinery efficiencies effects are small.

Fig. 4.50 is a schedule of turbine restriction and shows as expected the requirement of increasing restriction with decreasing speed and increasing load. The results clearly show that a greater turn down ratio (perhaps as much as 4:1) is required to reduce peak torque speed below 1300 rev/min. They also suggest that the engine could usefully use a larger turbine housing giving, for example, 22:1 air fuel ratio at rated conditions.

Fig. 4.51 shows the smoke plot indicating remarkably low levels. It is only below 1000 rev/min that smoke emission necessitates de-fuelling. Substantial injection advance was applied below 1000 rev/min to reduce smoke and increase torque (at the expense of SFC).

Fig. 4.52 is the timing schedule, this confirms that timing (with a jerk pump) is sensitive to both speed and load and follows the pattern anticipated in section 4.4.2. As the limits of p_{m-x} are approached around peak torque increasing retard is applied to regulate cylinder pressure (at the expense of SFC). A 19° crank angle timing swing was utilised. Below peak torque the timing is substantially retarded and it is this area which has yielded the largest SFC gains. However, even with timing controls it is clear that the p_{max} limit of 127.5 bar is too conservative and greater gains can only be achieved with pressures of the order of 140 bar (2030 lb/in^2).

The following two figures, (4.53 and 4.54) are contour maps of boost and timing respectively.

Fig. 4.55 presents the graph of dynamic timing and duration of injection for the optimised configuration and is compared with the base. The fuel injection equipment (fie) and combustion system worked very satisfactorily at the higher ratings. It is apparent that the optimised

case has a more advanced timing across the whole speed range. This is associated with optimum timing being determined by the end of injection. Lengthening of the injection period (no evidence of secondary injection) by up-fuelling necessitates advancing the timing for optimum SFC with consequent increased cylinder pressure. There were no fuel line pressure results for the optimised case. The results presented are supported by oscilloscope photographs corresponding to conditions within cylinder 6 on the LTC in 200 rev/min increments between 700 and 2300 rev/min in appendix 5, section 4, sheets 1 to 5.

Appendix 4 contains the part load results and includes plots of important engine parameters to a base of bmep at constant speed.

On completion of the optimisation tests the engine build was changed to the base configuration and a power curve performed to validate the above work. The results are presented in fig. 4.56 and are considered satisfactory.

4.5.2 Simplified Schedule

In the proceeding section the results for the full manual optimisation were presented. For a production application these would be stored as arrays and interpolated continuously. An alternative but less flexible approach is to make a close approximation to those characteristics determined by linearising and generating demands by means of equations. This section examines the implied penalty in improved torque and part load fuel consumption of a simplified boost and timing schedule based on this approach.

Figs. 4.52 and 4.57 show the original and linearised timing maps. The simplified timing map lacks the advance below peak torque which is not critically important. However, the omission of retard at and around peak torque is a serious limitation.

Fig. 4.58 shows the simplified boost pressure schedule. This is based on a plot of boost pressure against rack within the control range of the turbine stage which is limited to a narrow engine speed range (fig. 4.41).

A straight line fit of the higher point was used because it is at the higher boost pressures that the match becomes critical. Over the limited control range of the turbocharger (compared with the engine) this is a valid assumption as changes of volumetric and turbomachinery efficiencies are small.

For this series of tests a computer control system based on inputs of speed and rack position was commissioned. The commissioning presented no problems other than an oscillating rack position at high torque which in turn led the computer to demand an oscillating boost pressure. This instability was only present with all-speed governing, not with direct rack operation (two-speed).

The electro-hydraulic actuation system described in section 3.5.1 was implemented for this series of tests. The results indicated that performance was little affected by this change. Efficiencies remained substantially the same whilst some loss of turn down was noted in the fully open position - in all probability due to slight fouling of the ring sleeve retaining mechanism.

The results are divided into the following parts :

1) limiting torque curve performance, figs. 4.59 - 4.62
2) load-speed maps, figs. 4.63 - 4.64
3) part load results - Appendix 4 section 4 - sheet 1 to 8.

SIMPLIFIED SCHEDULE LTC RESULTS.

The compressor map, fig. 4.59, compares the running lines for the optimised and simplified cases respectively. It can be seen that a lower pressure ratio exists at peak torque and rather more at rated power, inferring a torque deficit and SFC penalty respectively.

The turbine swallowing capacity curve was identical in the fully restricted case. However, fully open performance was slightly worse (fig. 4.60).

Fig. 4.61 compares the two LTC performances.

It is immediately apparent that the simplified schedule appears to offer significant SFC advantage (+4%) over the whole speed range without suffering a torque deficit. Whilst there were small differences to engine restrictions and the ring sleeve was always more open the results are difficult to interpret. A check on instrument calibration revealed that both the torque and cylinder pressure transducers were reading low. It would appear that the removal of the torque transducer for a dynamometer investigation had affected the calibration. Unfortunately no back to back tests with the base were initiated.

TORQUE SPEED MAPS (Figs. 4.63 - 64).

The iso-consumption map confirms the foregoing in that substantial improvements even at very light loads have apparently occurred. Comparison with fig.4.47 reveals that the characteristic shape is the same. However, the values are considered to be slightly suspect. Fig. 4.64, the iso-boost map with lines of constant restriction confirms the engine requirement for constant air fuel ratio at a given torque level. Restriction is applied from 1800 rev/min and below to the maximum of 50% at 1300 rev/min. The results clearly indicate that substantially more turn down could be usefully employed. Peak torque speed was once again at 1300 rev/min. The part load supporting results are contained in Appendix 4, section 4, sheet 1 to 8.

4.6 Assessment using the Road Simulation (RSVP) Program

4.6.1 General

To assess the likely benefits in a vehicle due to improvements in both torque-back-up and part load efficiency the results were analysed using the LEYLAND ROUTE AND SIMULATED VEHICLE PROGRAM (RSVP). This program based on research work at Bath University simulates various routes by including data on gradients, speed limits and bends etc. to a base of time. It includes models of the vehicle for rolling resistance, drag, transmission efficiences and gear changes. The input data are the number of gears, wheels, axle ratio, vehicle weight, upshift and downshift speeds, moments of inertia etc. Fig. 4.65 is a typical data echo. The program also requires an engine iso-consumption map which is reduced to WILLENS LINES and digitised (fig. 4.66). The program works out route distance, elapsed time and fuel consumed (fig. 4.67) from which it calculates average speed and fuel consumption, the total number of gear shifts and engine revolutions and also the gross earning factor (GEF) - a weighted factor as a function of speed and fuel consumption.

The two routes assessed for this work were the 'West Yorkshire' run, a 23 mile hilly cross country route, and a 90 mile high speed motorway route. The results for both the base and optimised VG configurations were analysed. It should be noted that the program does not take account of any enhanced transient performance.

Table 4.68 compares the output with the following engine/gearbox builds; (the supporting evidence is included in Appendix 6)

1) BASE TL11 rated at 2100 rev/min 10 speed gearbox
2) BASE TL11 rated at 2300 rev/min 5 speed gearbox
3) VG TL11 rated at 2100 rev/min 10 speed gearbox
4) VG TL11 rated at 2300 rev/min 5 speed gearbox
5) Intercooled TL11 rated at 2000 rev/min 10 speed gearbox (Leyland Results).

Inspection of this table reveals that for the 2100 rev/min case (1 + 3) on the motorway run the differences were :

MPG + 1%

MPH + 2.1%

GEF + 3.2%

and gear changes reduced from 46 to 33 in favour of the VG unit. For the W. Yorkshire run the corresponding figures were :

MPG - 0.48%

MPH + 4.5%

GEF + 4.1%

and the number of gear changes was reduced by 10 to 64. The same trends are apparent with the enhanced speed range together with the 5 speed gearbox. Comparing next the performances of the two VG configured engines (2 + 4) it can be seen that for the motorway case the results were :

MPG - 2.9%

MPH -

GEF - 3.0%

The number of gear changes is reduced by 9 to 24.

On the W. Yorkshire route the corresponding figures are :

MPG + 0.8%

MPH -

GEF + 0.2%

However, the number of gear changes has reduced by almost one half to 33.

A comparison is included of the intercooled (air to air) 224kW(300 bhp) TL11 tested at Leyland. The test conditions are not identical and favour the Leyland engine; these are reflected in the better figures, e.g.

	MOTORWAY	W. YORKSHIRE
MPG	1.4%	4.7%
MPH	1.4%	0.7%
GEF	2.9%	5.4%

The number of gear changes was almost identical with the VG for both the motorway and W. Yorkshire routes.

The results clearly show that :-

1) the vehicle (when fully laden) operates for most of its time in that region on the LTC between peak torque and rated speed.

2) torque-back-up rather than rated power is the solution to reduced gear change.

The operating range for improved part load SFC recorded in the optimisation tests does not coincide wholly with that used on the road. To utilize this area it would be necessary to reduce peak control speed, to say 1050 rev/min. This problem has already been discussed. To effect a lower SFC on the LTC at higher speeds a larger more efficient turbine is required. However, this affects the absolute level of turn down possible. This implies therefore a much greater turn down than 40% is required. To achieve realistic torque-back-up values considerably higher cylinder pressures must be reliably possibly i.e. 140 bar.

The program clearly demonstrates that enhanced torque-back-up reduces the number of gear changes. However, it would be more appropriate to use higher back axle ratio and expect a better fuel consumption at the expense of gear change. No attempt was made to examine the effects on light load operation. The program reaffirms that SFC on the LTC is crucial to good vehicle fuel consumption.

LIST OF FIGURES

LIST OF FIGURES cont'd

LIST OF FIGURES cont'd

HRS. to DATE.	TEST NO.	LOG SHEET NO.	DATE OF TEST	DESCRIPTION OF TEST	COMMENTS
0	10	100	17/9/81	Power Curve	Base H2B 8081c L25A3
	11	104	28/9/81	Power Curve	Accepted Base Performance
	12	105	29/9/81	Loops : 2100	
	13	105	29/9/81	Loops : 1900	
	14	106	1/10/81	Loops : 1700	
	15	107	1/10/81	Loops : 1500	
	16	106	1/10/81	Loops : 1300	
	17	107	2/10/81	Loops : 1100	No smoke readings
	18	107	2/10/81	Loops : 900	
	19	107	2/10/81	Loops : 700	
	20	110	30/10/81	Electronic Instrumentation	CVL press reading suspect These results presented with 104.
	21	114	18/11/81	Const. Torque 2 bar	Prototype VG H2C 8640.240
	22	114	18/11/81	Const. Torque 4 bar	Fully open
	23	114(a)	25/11/81	Const. Torque 6 bar	
	24	114	25/11/81	Const. Torque 8 bar	
	25	116	2/12/81	Const. Torque 2 bar	VG 10% closed
	26	116	2/12/81	Const. Torque 4 bar	
	27	117	2/12/81	Const. Torque 6 bar	
	28	117	2/12/81	Const. Torque 8 bar	
	29	118	2/12/81	Power Curve	
	30	121	9/12/81	Const. Torque 2 bar	VG 30% closed
	31	121	9/12/81	Const. Torque 4 bar	
	32	122	9/12/81	Const. Torque 6 bar	
	33	122	9/12/81	Const. Torque 8 bar	
	34	124	16/12/81	Const.Torque 2 bar)	VG 50% closed
	35	124	16/12/81	Const. Torque 4 bar))	These include cyl. press
	36	125	16/12/81	Const. Torque 6 bar)	readings
	37	125	16/12/81	Const. Torque 8 bar))	
	38	129	17/2/82	Power Curve	Fully open H2C 8640.270
	39	130	17/2/82	Power Curve	50% restriction H2C 8640.270
90	40	135	7/4/83	Power Curve	Base H2B 8081C L25A3
	41	137	18/5/82	Power Curve	MK.II VG H2C8625.Z3IU3 (open)

FIG. 4.0 - LIST OF ENGINE TESTS

HRS. to DATE.	TEST NO.	LOG SHEET NO.	DATE OF TEST	DESCRIPTION OF TEST	COMMENTS
	42	138	9/6/82	Power Curve	MKII VG 50% closed
	43	138	9/6/82	Power Curve	MKII VG 30% closed
164 VT Unit fitted	44	143	2/8/82	Power Curve	Base H2B8081C L25A3. Electronic Instrumentation
	1000	143	2/8/82	Minimum load condition	3 points
	45	144	4/8/82	Loops	Base : 1300 rev/min
	46	144	4/8/82	Loops	Base : 1500
	47	144	4/8/82	Loops	Base : 1800
	47(a)	144	5/8/82	Loops	Base : 2100 (2 points)
	48	145	5/8/82	Loops	Base : 1100
	49	145	5/8/82	Loops	Base : 800
	50	145	5/8/82	Constant Torque (50% of LTC)	Timing Investigation @ 1300 rev/min
	51	146	6/8/82	Limiting Torque	Timing Investigation @ 1300 rev/min
	52	146	9/8/82	Limiting Torque	Timing Investigation @ 800 rev/min
	53	146	9/8/82	Constant Torque	Timing Investigation @ 800 rev/min
	54	147	9/8/82	Limiting Torque	Timing Investigation @ 1800 rev/min
	55	147	9/8/82	Constant Torque	Timing Investigation @ 1800 rev/min
205 (41)	56	158	13/8/82	Photographs to Match	Tests 50 - 55
205 VG MKIIb	57	203	11/10/82	Power Curve	H2C 8625 Z31U3
	58	203	11/10/82	Power Curve	Under pneumatic control - 50%
	59	203	11/10/82	Power Curve	25% restriction
	60	204	13/10/82	Power Curve	40% restriction
	61	204	13/10/82	LTC/1300	Vary VG
	62	204	17/10/82	Loops	Vary VG
	63	205	19/10/82	LTC/800	Vary VG
	64	205	21/10/82	Loops	Vary VG
	65	205	21/10/82	LTC/1800	Vary VG
	66	206	22/10/82	Loops	Vary VG
231.22	67	208	26/11/82	LTC	50% restriction
New Pump fitted	68	209	6/12/82	LTC	0% " (airflow suspect)
Electric governed pump	69	209	6/12/82	LTC	50% " "

FIG. 4.0 - LIST OF ENGINE TESTS(cont'd)

HRS. to DATE.	TEST NO.	LOG SHEET NO.	DATE OF TEST	DESCRIPTION OF TEST	COMMENTS
	70	210	7/12/82	LTC	50% tongue
	71	210	7/12/82	LTC	0% tongue
	72	211	20/12/82	LTC	50% attempt optimisation
254.02	72(A)	211	20/12/82	LTC	50% " "
	73	212	31/1/83	1300 - Loops	Optimising
	74	212	31/1/83	1500 - Loops	Mapping
	75	213	4/2/83	1700 - Loops	H2C 8625 Z31U3 (MkIIb)
	76	214	8/2/83	1900 - Loops	Pneumatically actuated
	77	214	8/2/83	2100 - Loops	VT. unit fitted
	78	215	8/2/83	2300 - Loops	Electronically governed
	79	215	8/2/83	1100 - Loops	
	80	216	15/2/83	900 - Loops	
	81	216	15/2/83	700 - Loops	
313	82	217	16/2/83	Power Curve	
	* Dynamometer Failure				
	83	219	7/4/83	Power curve	Base H2B 8081C L25A3 (with boost control)
	84	220	12/4/83	1300 - Loops	Timing and noise
	85	220	12/4/83	800 - Loops	investigation
	86	220	12/4/83	1300 - Loops	
	87	222	12/4/83	800 - Loops	
	88	222	12/4/83	1800 - Loops	
	89	222	12/4/83	1800 - Loops	
335					
Electronically controlled turbocharger	90	231	2/9/83	1300 - Loops	Simplified Schedule
	91	231	2/9/83	1500 - Loops	under computer
	92	232	6/9/83	1700 - Loops	control
	93	232	7/9/83	1900 - Loops	
	94	233	8/9/83	2100 - Loops	
	95	233	13/9/83	1100 - Loops	
	96	234	13/9.83	900 - Loops	
	97	234	14/9/83	700 - Loops	
	98	235/8	15/9/83	Power curve	

FIG. 4.0 - LIST OF ENGINE TESTS (cont'd)

Engine LEYLAND TL11—7962756 Project No. E.W ROBERTS.

Title COMPARISON BETWEEN LEYLAND AND BATH TEST RESULTS FOR BASE H2B ENGINE.

Power Curve

Test No.	Timing	Amb'nt °C	Barometer Ins. Hg.
11. LEYLAND	22	22	735.3

BATH BASE H2B

LEYLAND RESULTS. H2B

} BOTH RESULTS. FROM THE SAME ENGINE.

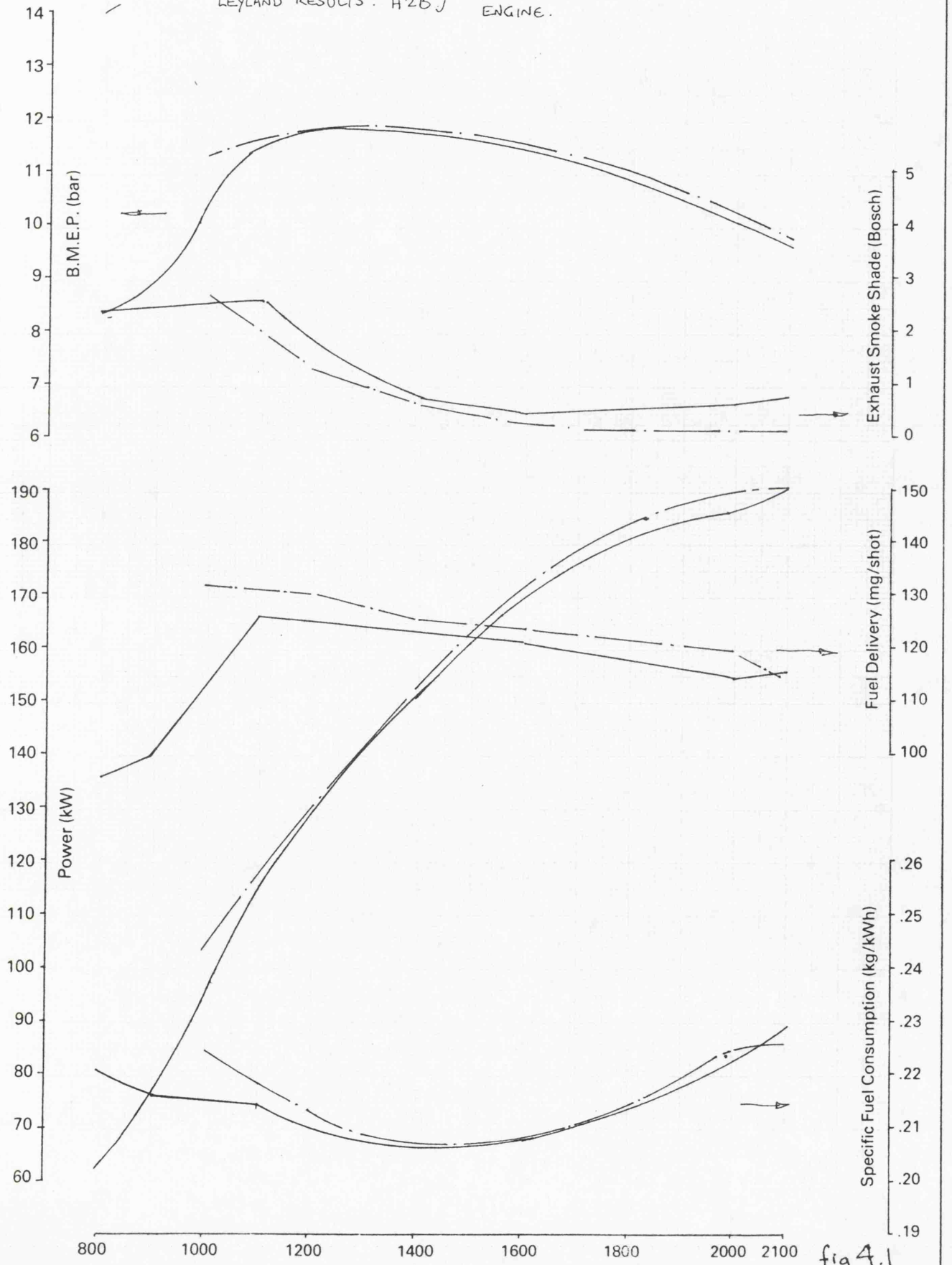

fig 4.1

COMPRESSOR PERFORMANCE

HUDDERSFIELD

DATE	29/9/81

MODEL	H2B-8081C LEYLAND TL11 190kW @ 2100rev/min	REF. NO.	T 895 11

Turbo 11 - 19
cover no 3500525
wheel no 61821

BASE ~ BOOST CONTROL

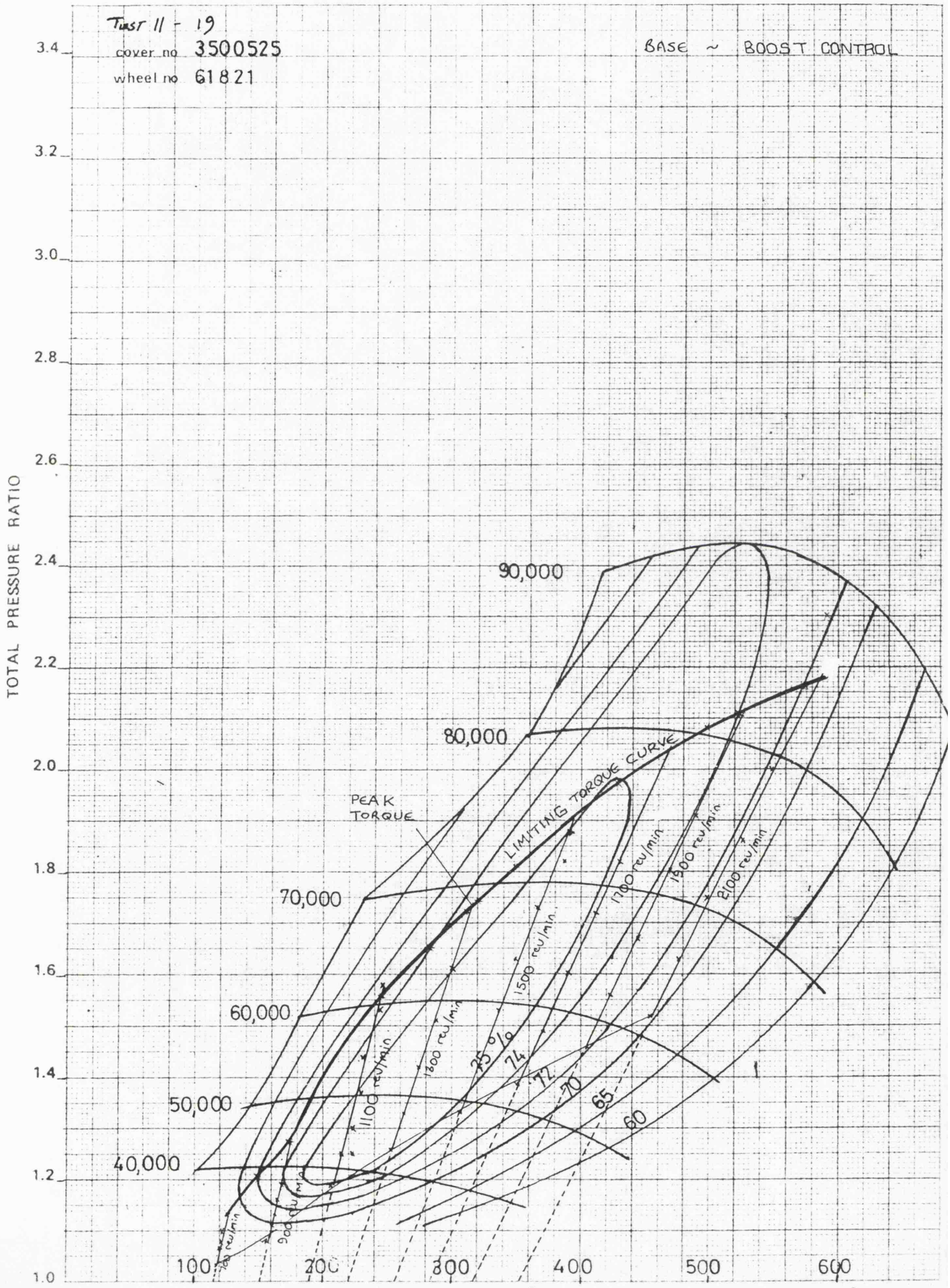

fig 4.2 ER/

Engine LEYLAND TL11 ENGINE—11.1L DISPLACEMENT Drawn By... E.N. ROBERTS

Title... BASE TWIN ENTRY TURBINE SWALLOWING CAPACITY... H2B 8081C L25A3

Holset / Leyland / Dowty / Dol Contract

Test No.	Timing	Amb'nt °C	Barometer Ins. Hg.
11	22	-	-

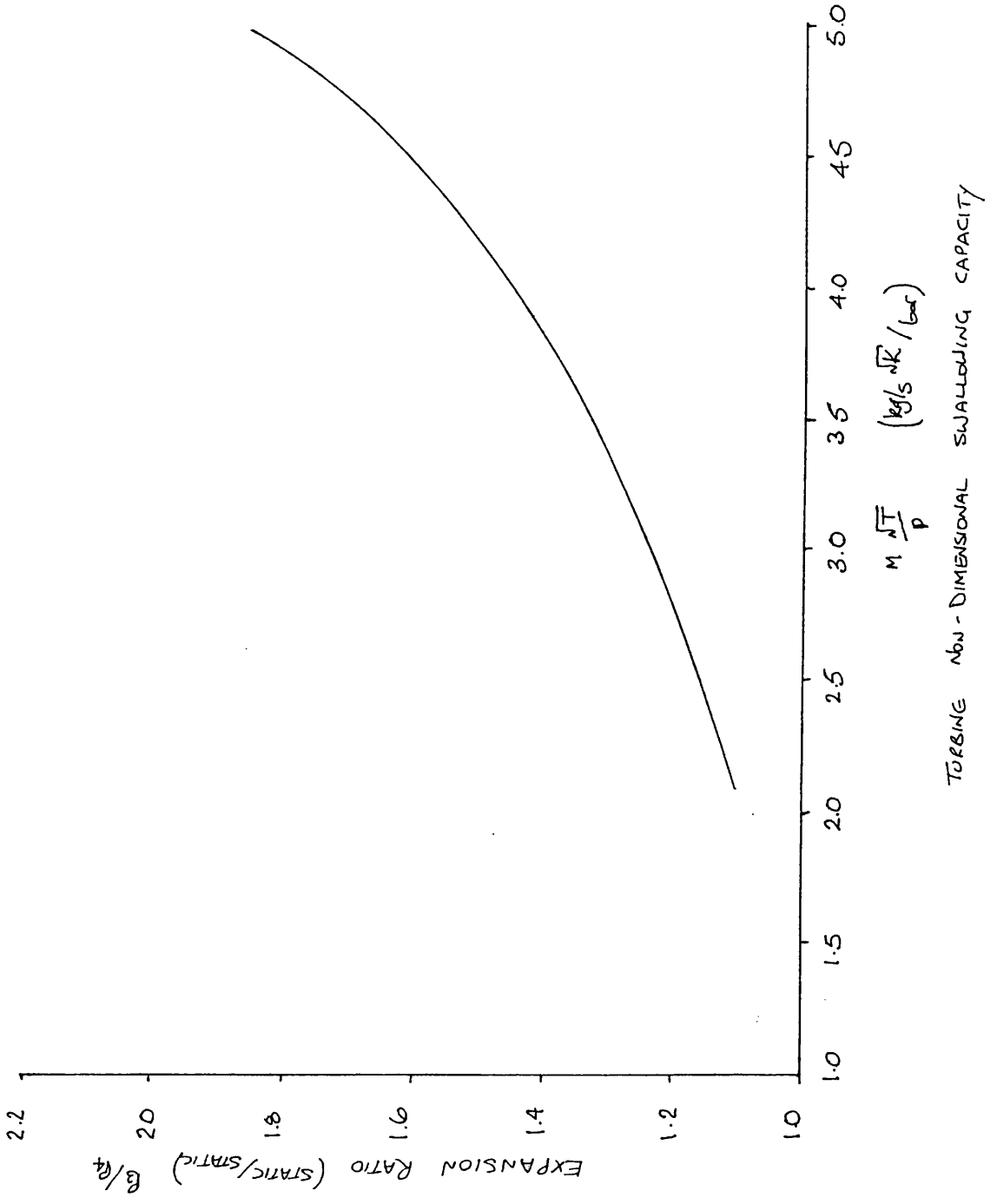

fig 4.3

Engine LEYLAND TL11—7962756 Project No. EWR

Title BASE LINE TEST H2B8081C L25 A3 NO BOOST CONTROL

Power Curve

Test No.	Timing	Amb'nt °C	Barometer Ins. Hg.
40	22	18	763.1

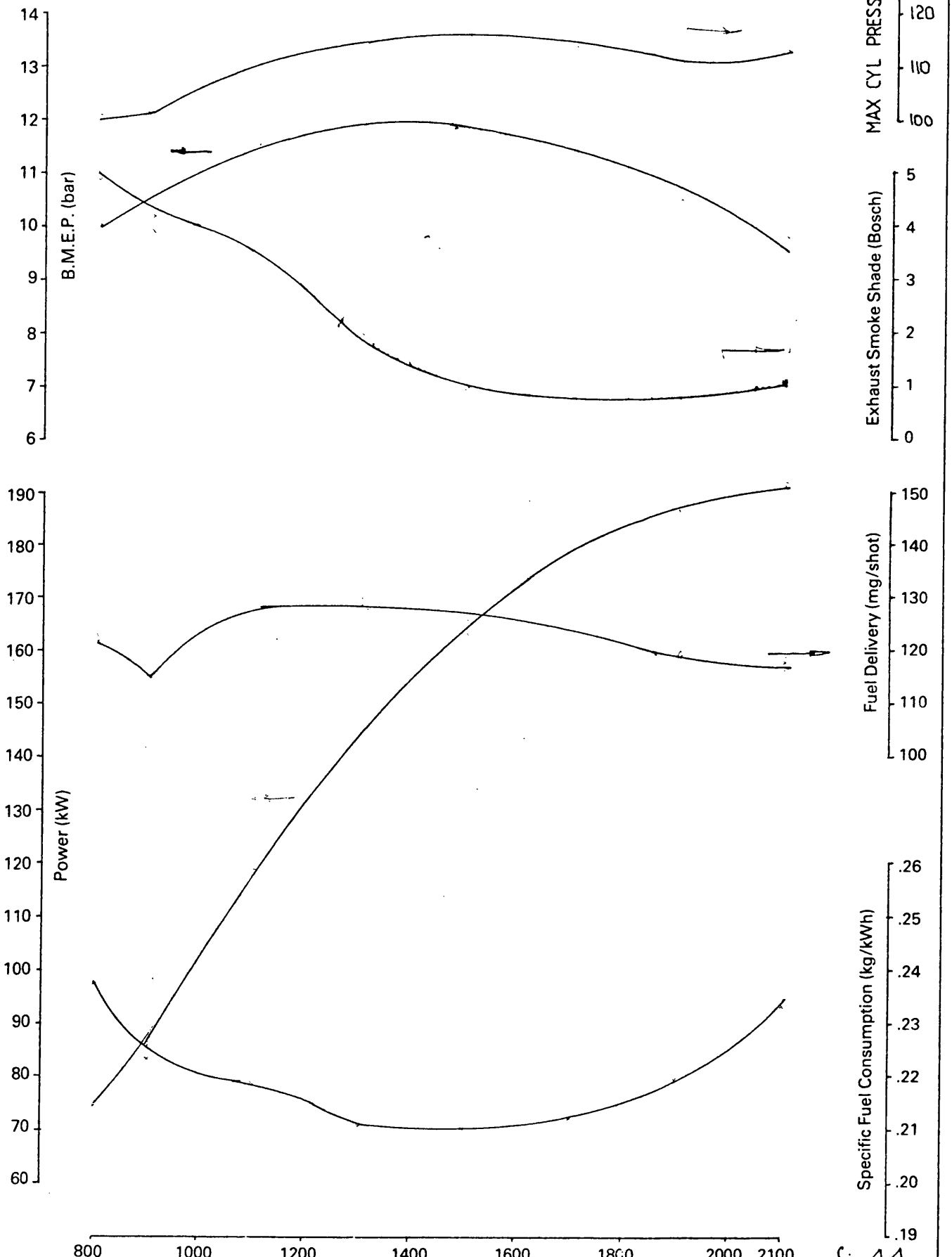

fig 4.4

Engine LEYLAND TL11—7962756 Project No. EWR

Title BASE LINE TEST H2B8081C L25A3 NO BOOST CONTROL

Power Curve

Test No.	Timing	Amb'nt °C	Barometer Ins. Hg.
40	22	18	763.1

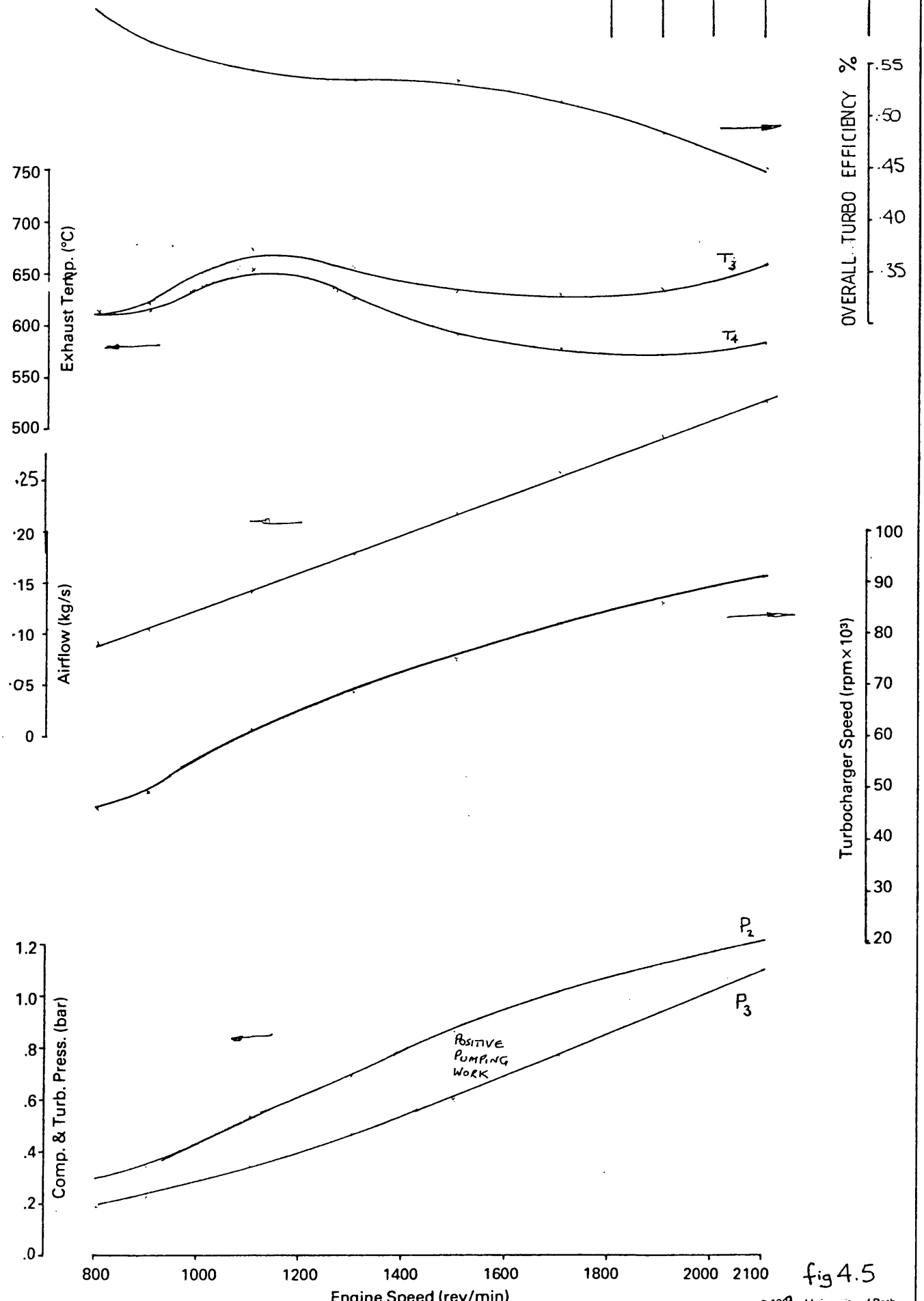

fig 4.5

Date ..... Graph .....

Engine LEYLAND TL11 ENGINE—7962756—CELL 2 Drawn By Ed Roberts

Title FUEL INJECTION EQUIPMENT CHARACTERISTIC FOR BASE H2B CONFIGURATION ON THE LTC

Power Curve Rating—190 kW at 2100 rev/min

Electronic Instrumentation

Holset / Leyland / Dowty / DoI Contract

Test No.	Timing	Amb'nt °C	Barometer mm Hg.
44	22	–	–

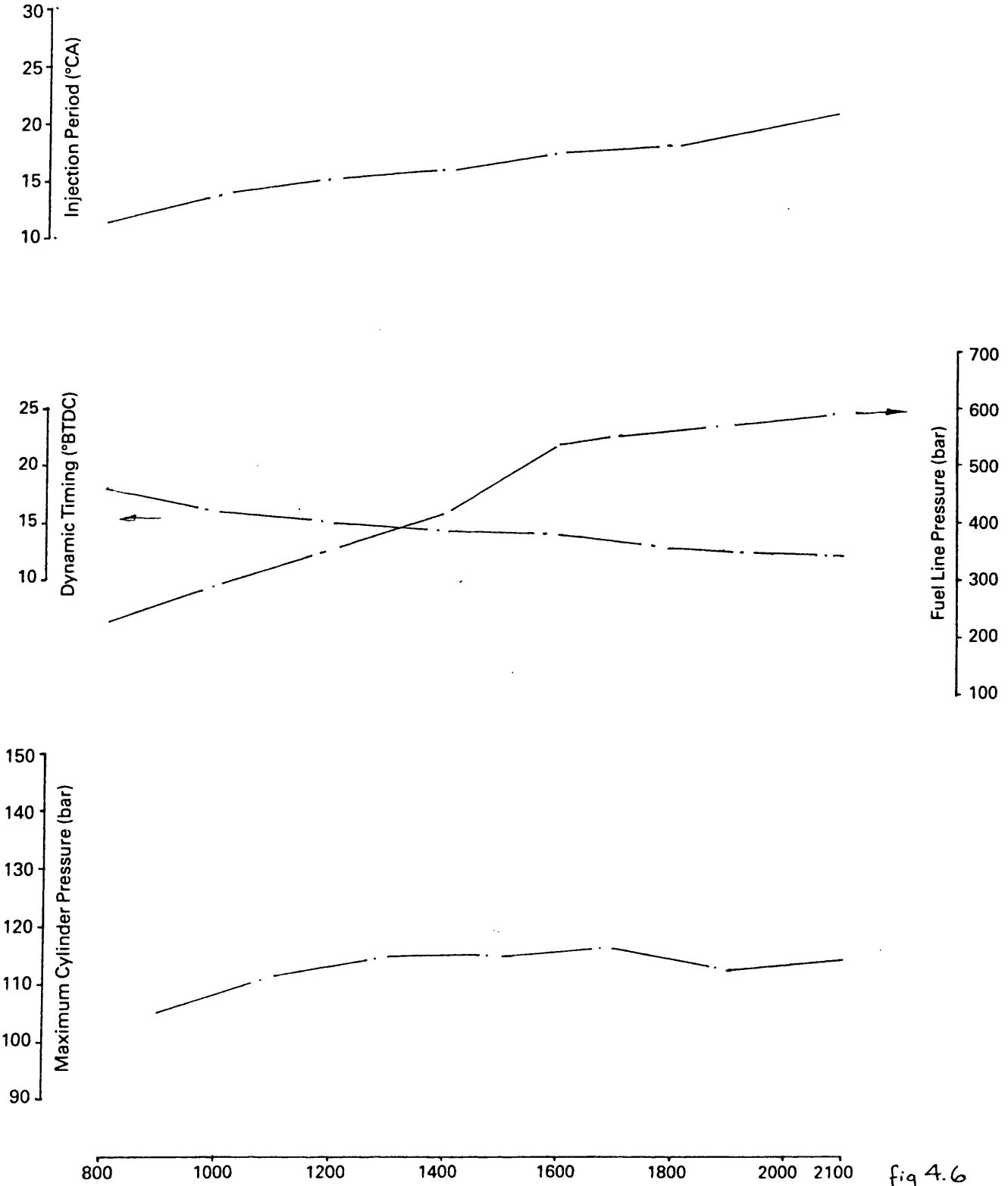

fig 4.6

Date ... Graph ...

Engine LEYLAND TL11 ENGINE—11.1L DISPLACEMENT Drawn By. E W Roberts.

Title ISO - CONSUMPTION CURVES H2B 808IC L25A3 - BASE PERFORMANCE

Test No.	Timing	Amb'nt °C	Barometer Ins. Hg.
45 49	22	-	—

Holset / Leyland / Dowty / DoI Contract

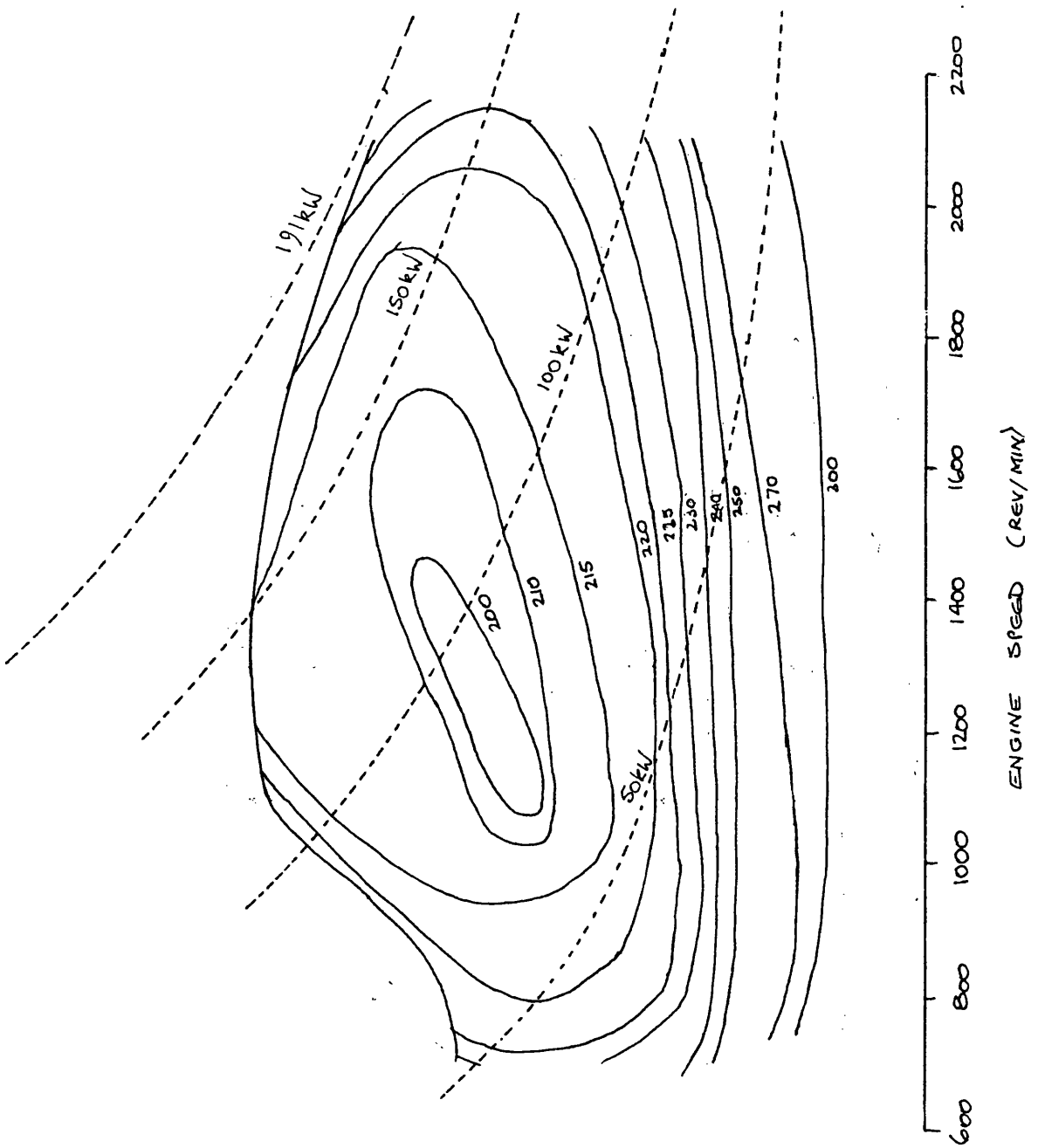

fig 4.7

Engine LEYLAND 'L11 ENGINE—11.1L DISPLACEMENT

Drawn By. E W Roberts

Title 160 - CONSUMPTION CURVES - L11 NATURALLY ASPIRATED.

Test No.	Timing	Amb'nt °C	Barometer Ins. Hg.
LEYLAND	16	25	30.12

Holset / Leyland / Dowty / DoI Contract

134.2 kW @ 2000 rev/min. 730 Nm @ 800 rev/min

180 bhp. @ 2000 rev/min.

17.5% TORQUE BACK UP @ 40% OF RATED SPEED.

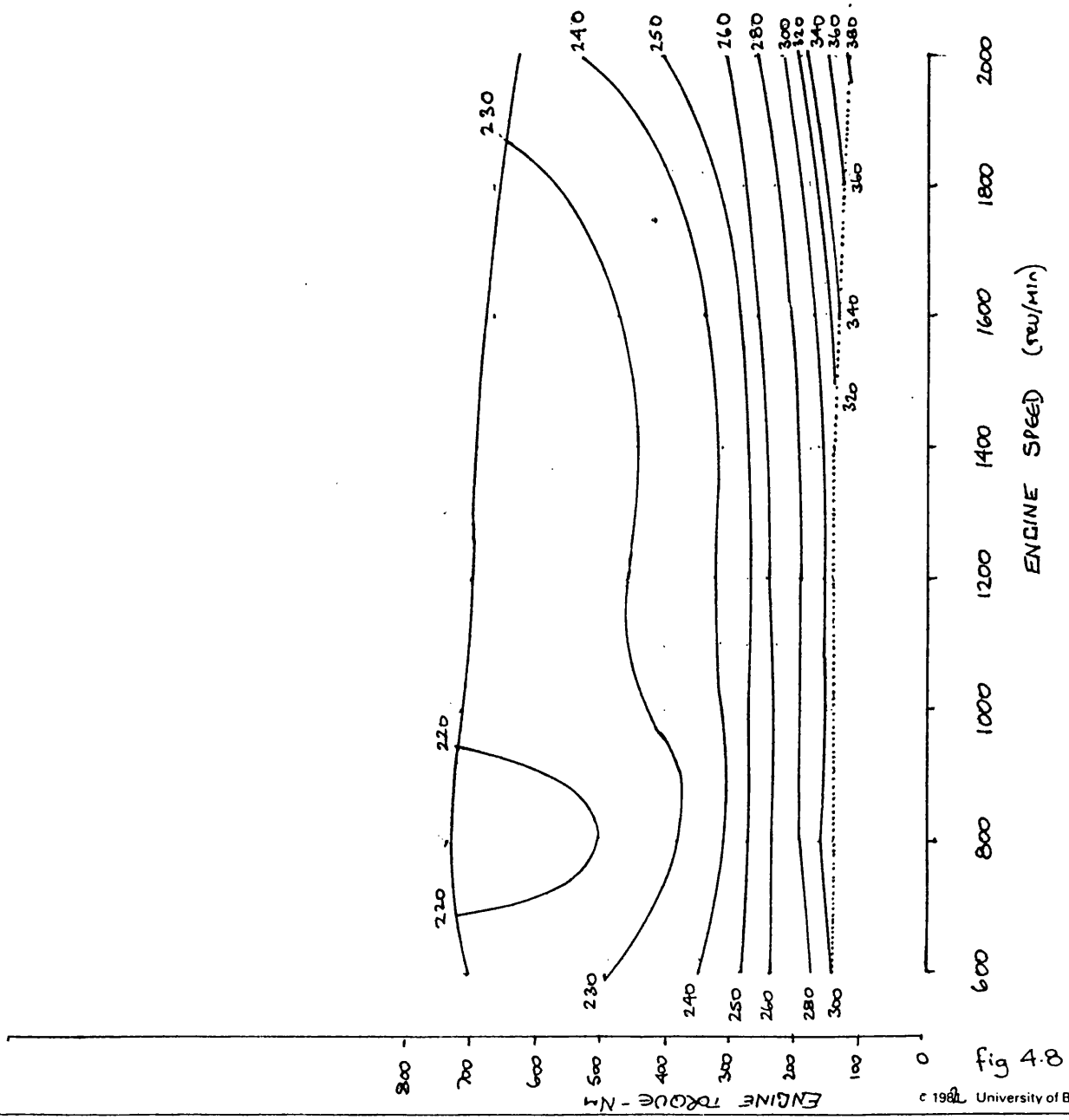

fig 4.8

Engine LEYLAND L11 Project No. E W ROBERTS.

Title LEYLAND L11 · NATURALLY ASPIRATED · (LEYLAND SUPPLIED DATA)

Power Curve

Test No.	Timing	Amb'nt °C	Barometer Ins. Hg.
LEYLAND	16	25	765.0

134.2 kW @ 2000 rev/min ~ 730 Nm @ 800 rev/min
180 bhp @ 2000 rev/min

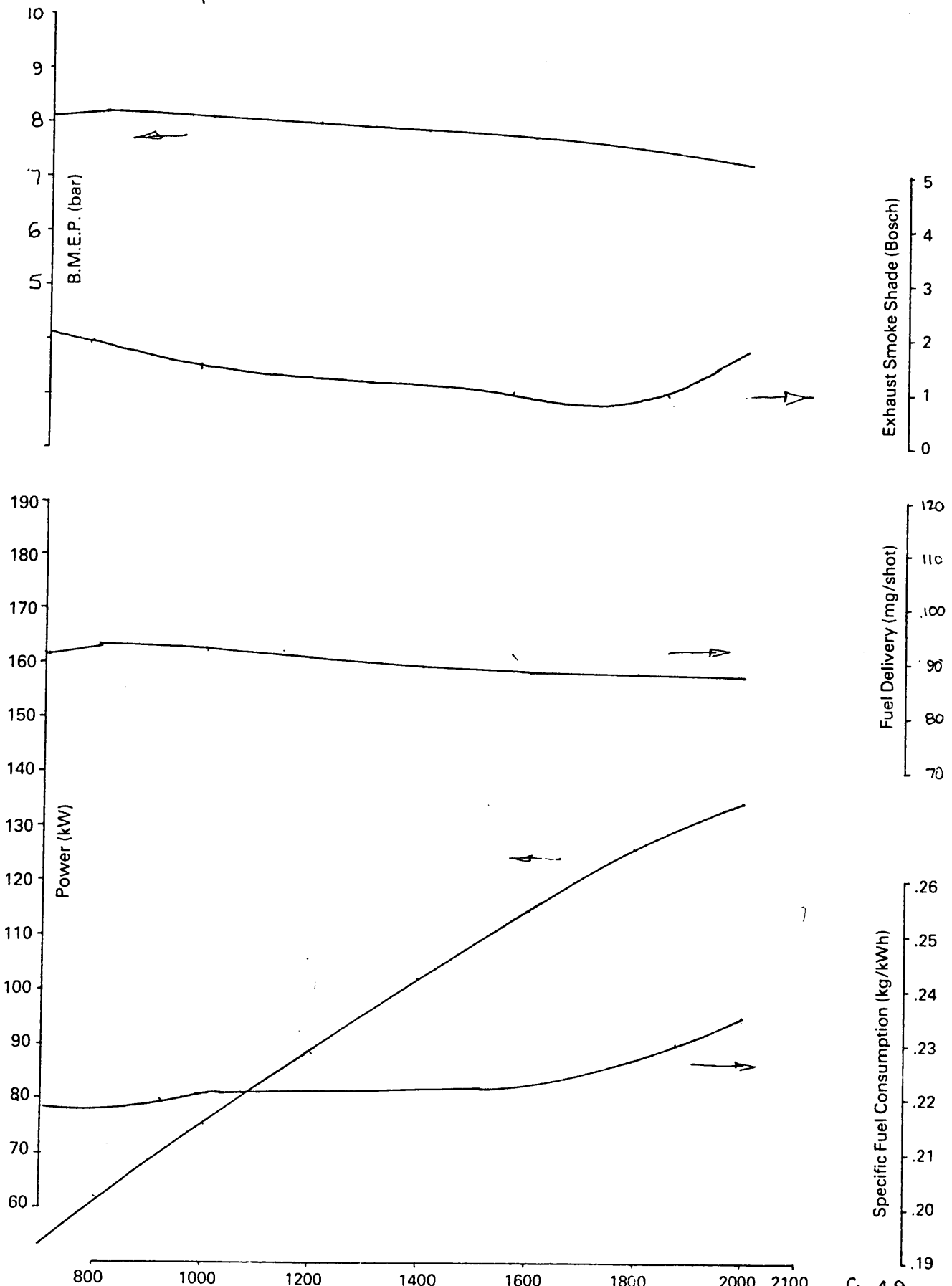

fig 4.9

Engine LEYLAND TL11 ENGINE—11.1L DISPLACEMENT

Drawn By. E W ROBERTS

Title LIMITING ENGINE PARAMETERS

Holset / Leyland / Dowty / Dol Contract

Test No.	Timing	Amb'nt °C	Barometer Ins. Hg.
LEYLAND	—	25°C	—

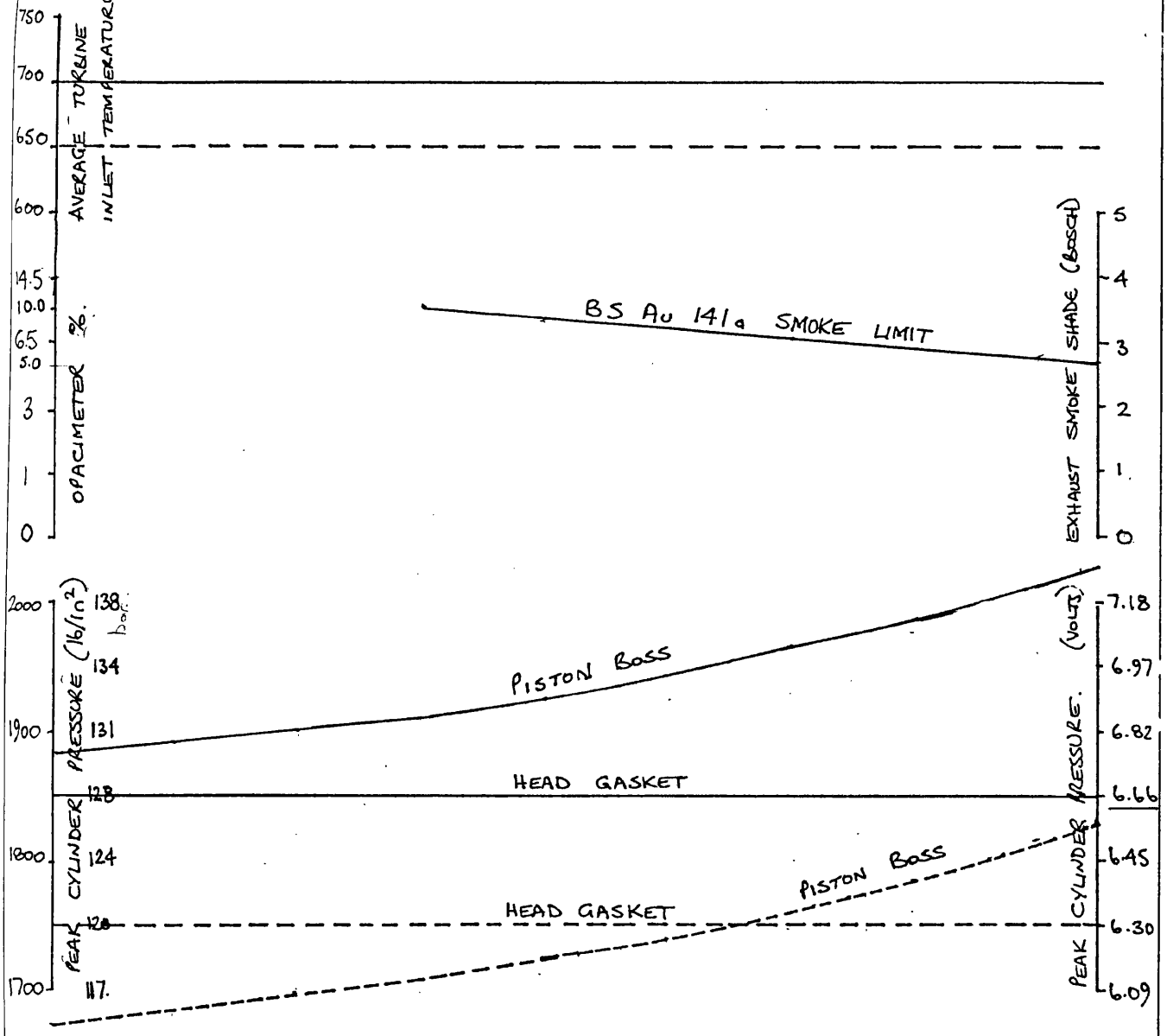

COMMERCIAL . LIMITS.

EXPERIMENTAL LIMITS.

$$SFC = \frac{M \times 572.96 \times 10^3}{n \times T} \quad \frac{kg}{kW\,h}.$$

M = Mass of fuel
n = number of revs
T = Torque in Nm.

Note! If M = 0.5 constant = 286.48.
M = 0.2. constant = 114.59

400 600 800 1000 1200 1400 1600 1800 2000

ENGINE SPEED (rev/min).

fig 4.10

LEYLAND TL11 . LIMITING TORQUE CURVE - CONSTANT FUELLING . 190 KW @ 2100 rpm

HOLSET ENGINEERING CO. LTD.
HUDDERSFIELD

COMPRESSOR PERFORMANCE

DATE	11-6-80
REF. No.	T1166

MODEL	H2C-864ON .270 MKI VG (TWIN FLOW)

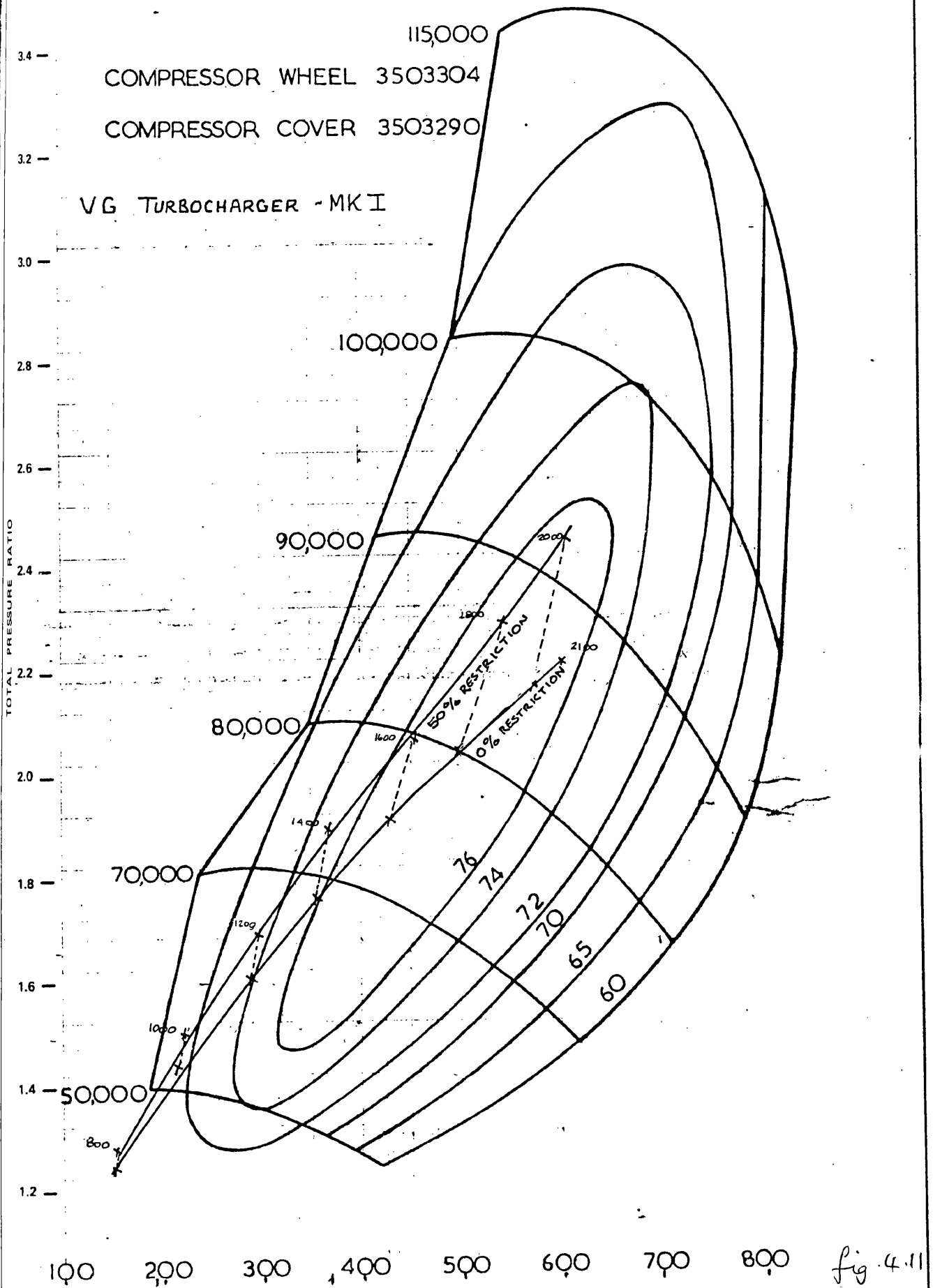

fig. 4.11

Engine LEYLAND TL11 ENGINE—11.1L DISPLACEMENT

Title SWALLOWING CAPACITIES FOR H2B L2593 & H2C .270" (FIXED VG) MKI VG TWIN FLOW

Date ..... Graph ..... p.n.

Drawn By. E.o Roberts

Holset / Leyland / Dowty / DoI Contract

Test No.	Timing	Amb'nt °C	Barometer Ins. Hg.
38	22	–	—
39			
11			

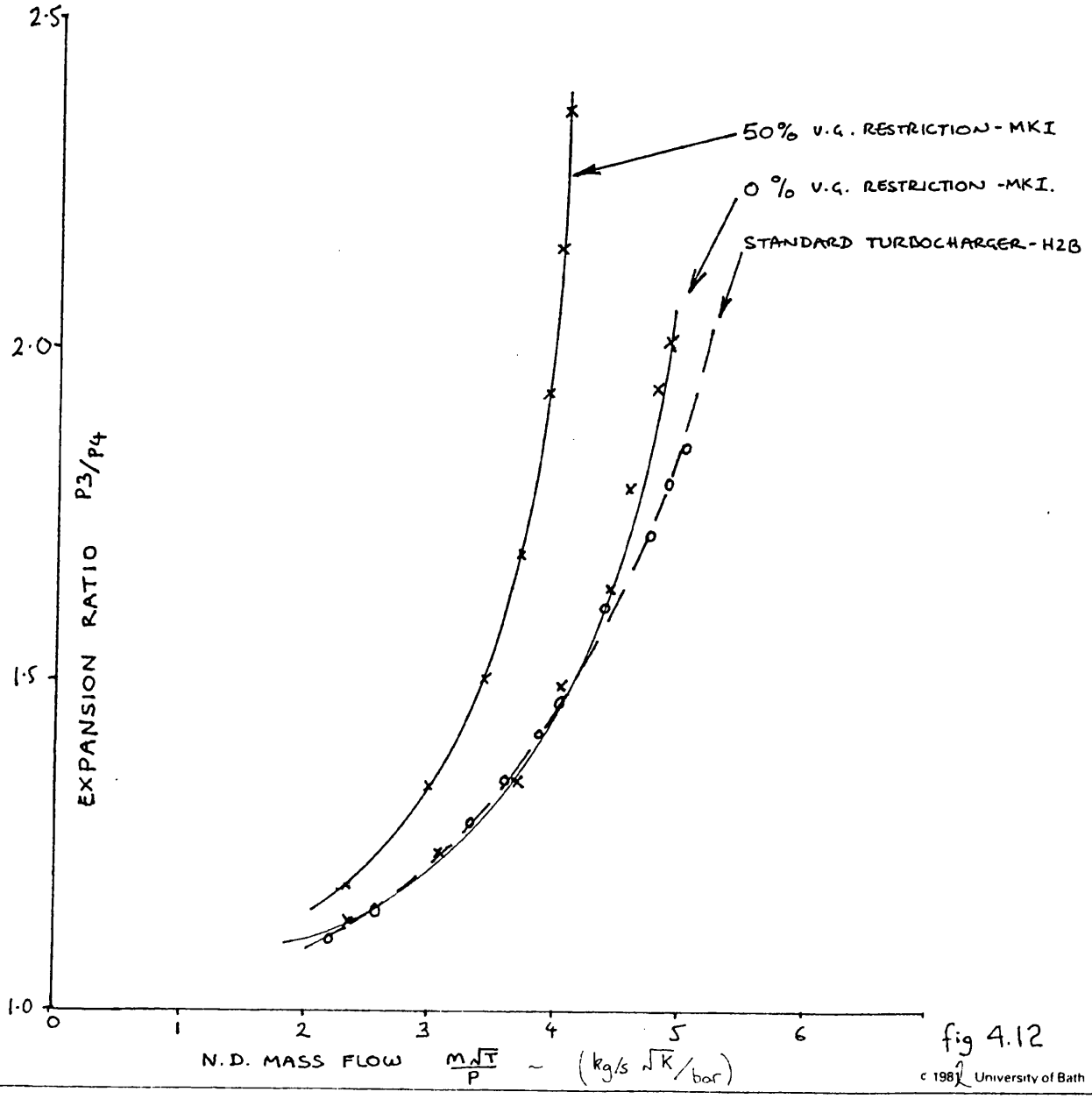

fig 4.12

Engine LEYLAND TL11—7962756 Project No.

Title H2C 8690-270 FIXED VG TURBOCHARGER - MKI TWIN FLOW (FIXED DISCRETE SETTINGS)

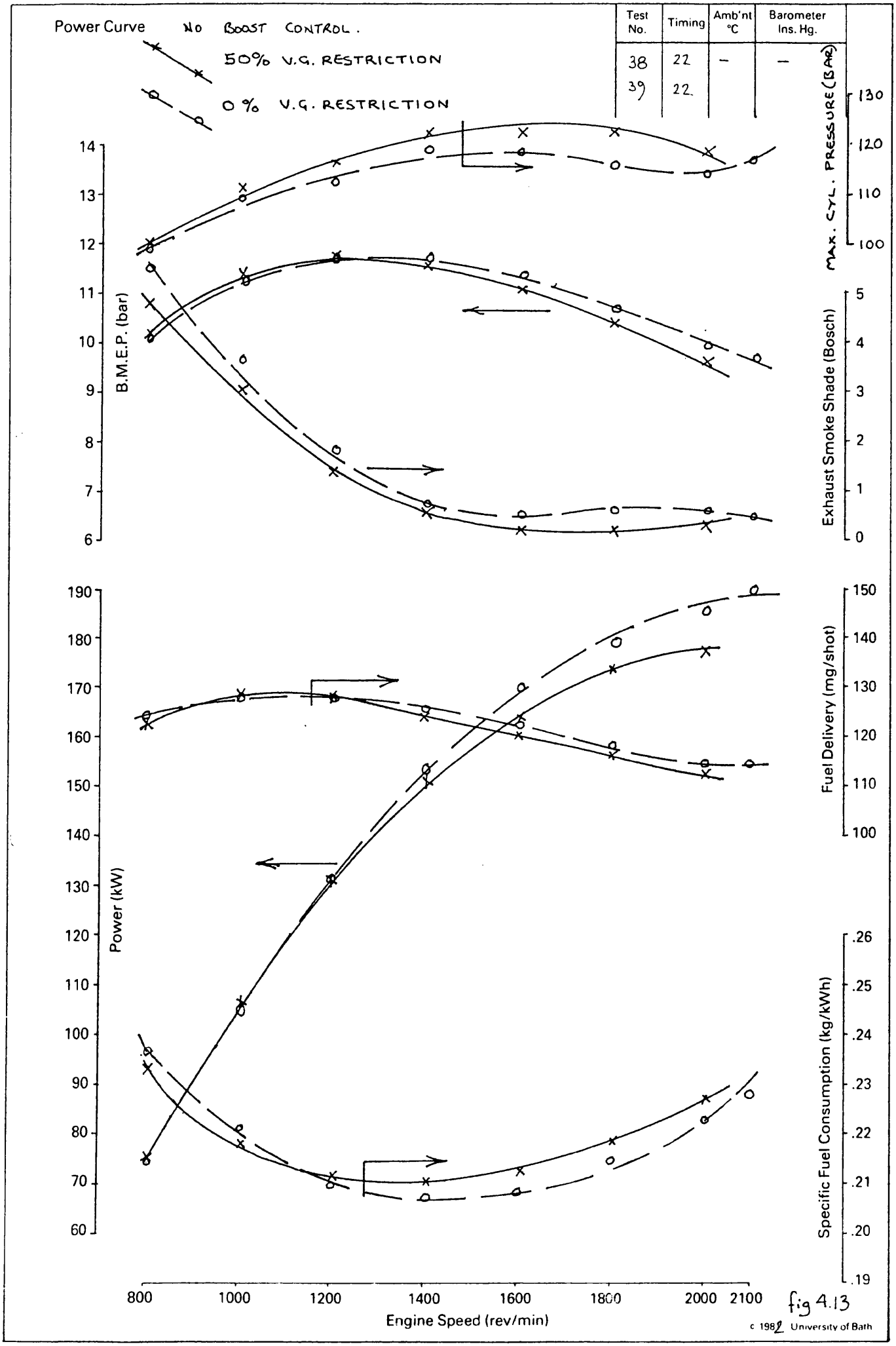

fig 4.13

Date ..16/2/82.. Graph ..9..

Engine LEYLAND TL11—7962756 Project No. .....

Title H2C 8640 .210" FIXED VG TURBOCHARGER - MK I TWIN FLOW (FIXED DISCRETE SETT...

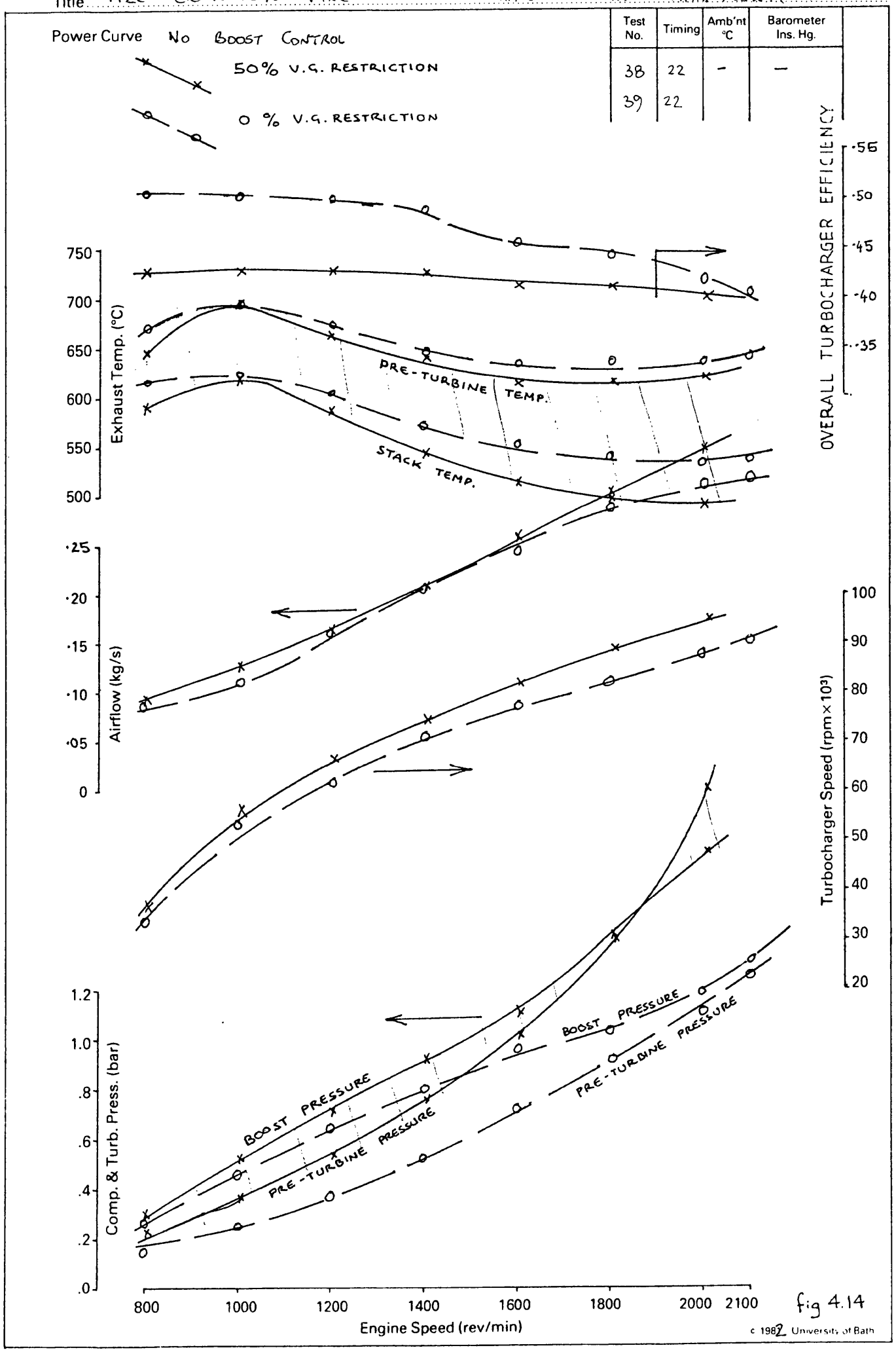

fig 4.14

Engine LEYLAND TL11 ENGINE—11.1L DISPLACEMENT Drawn By. EWR

Title 150 - CONSUMPTION CURVES H2C 8640N / 270 : FULLY OPEN : - MK I VG TWIN FLOW

Test No.	Timing	Amb'nt °C	Barometer Ins. Hg.
21-24	22	20	—

Holset / Leyland / Dowty / Dol Contract

LINES OF CONSTANT POWER.

LINES OF CONSTANT SMOKE.

No BOOST CONTROL

190 kW @ 2100 rev/min.

ALL UNITS gm/kW h.

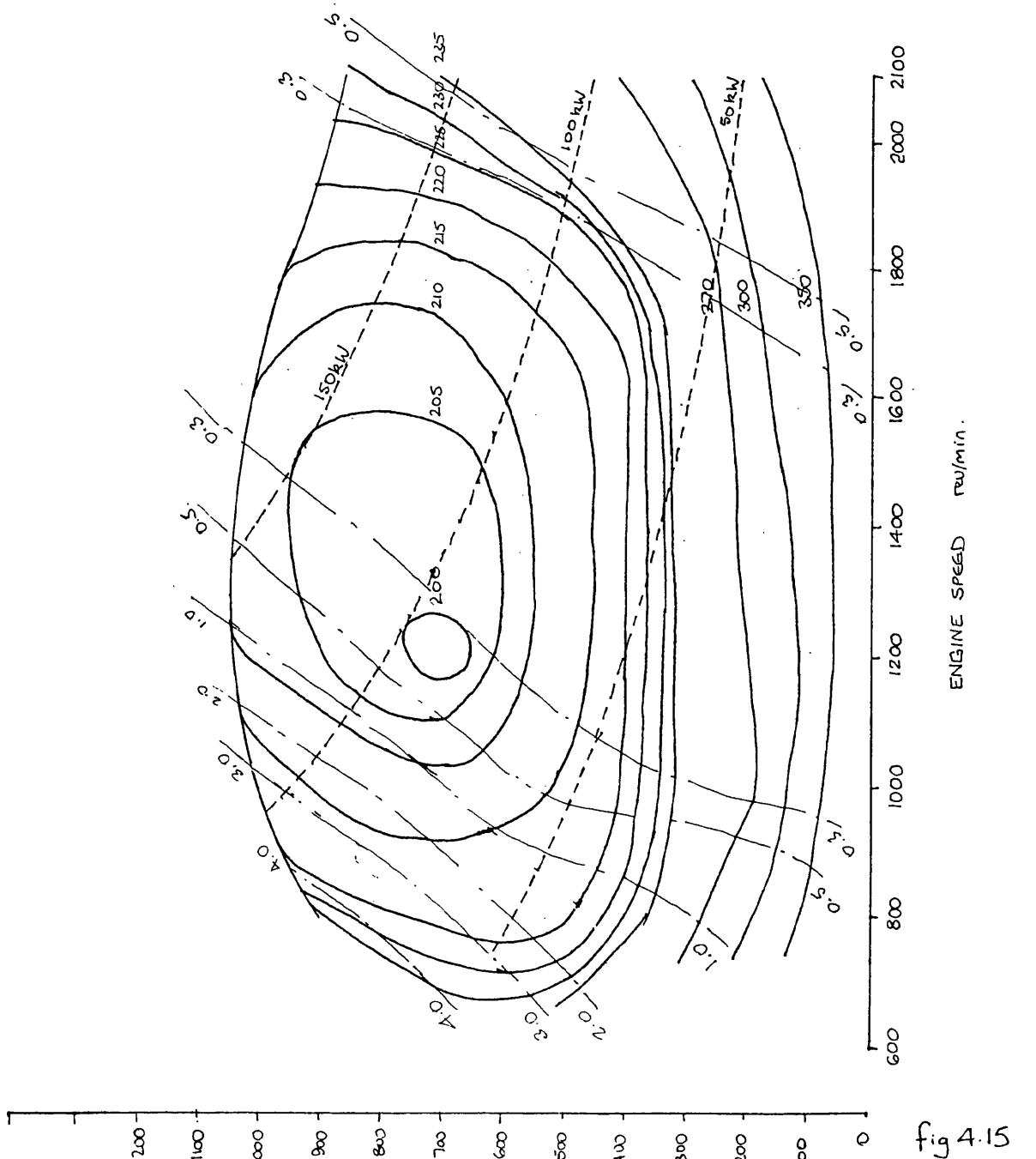

fig 4.15

Engine LEYLAND TL11 ENGINE—11.1L DISPLACEMENT

Date [illegible] Graph 07/3/ + 09

Drawn By. EWR

Title ISO - CONSUMPTION CURVES H2C 8640N / 270 FULLY CLOSED 50% - MK I VG TWIN FLOW

Test No.	Timing	Amb'nt °C	Barometer Ins. Hg.
34 37	22	20	~

Holset / Leyland / Dowty / Dol Contract

LINES OF CONSTANT POWER.

LINES OF CONSTANT SMOKE.

NOTE.! No BOOST CONTROL
190 kW @ 2100 rev/min.
UNITS gm/kWh

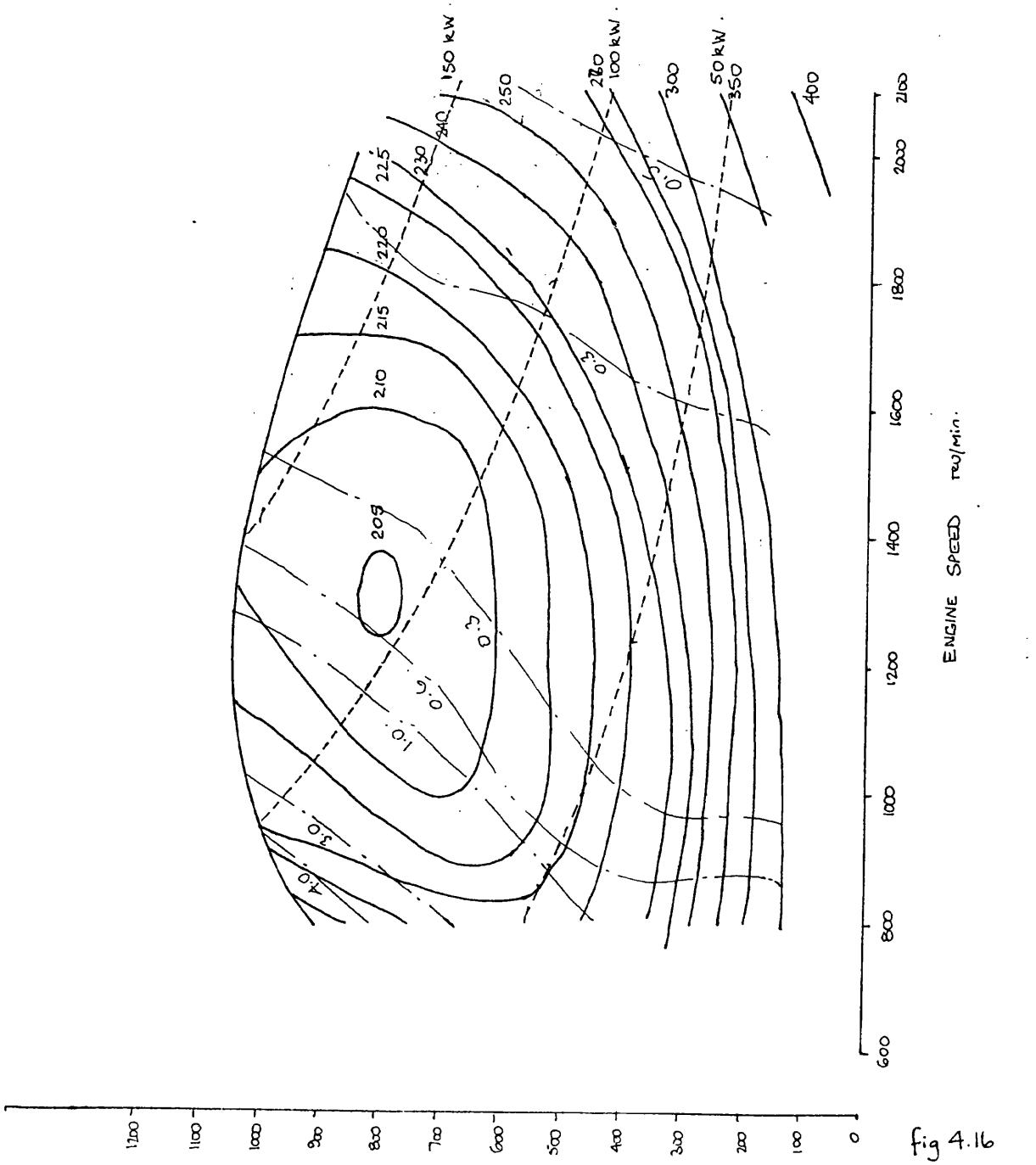

fig 4.16

COMPRESSOR PERFORMANCE

HOLSET ENGINEERING CO. LTD.
HUDDERSFIELD

MODEL	H2C — 8625N Z3103 - MKII(a)

DATE	12-6-80
REF. No.	T1168

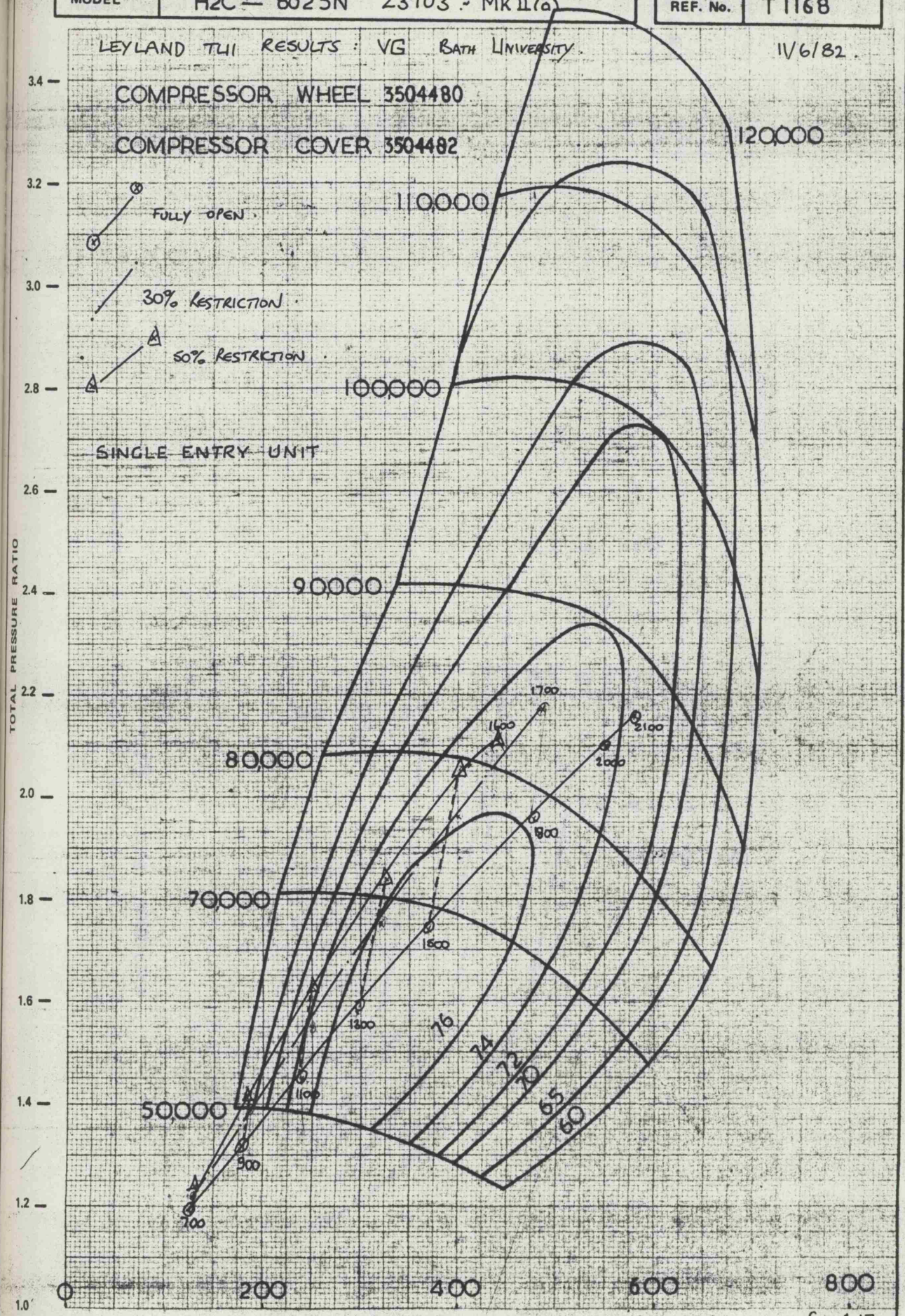

fig 4.17

Date ... Graph ...

Engine LEYLAND TL11 ENGINE—11.1L DISPLACEMENT Drawn By. E W ROBERTS

Title TURBINE SWALLOWING CAPACITIES : (ENGINE) - TURBOCHARGER TYPE :- H2C 8625N Z310

Holset / Leyland / Dowty / DoI Contract

Test No.	Timing	Amb'nt °C	Barometer Ins. Hg.
41	22	–	–
38			
39			
40			

MK II (a) VG (SINGLE ENTRY) 30% TURN DOWN RATIO.

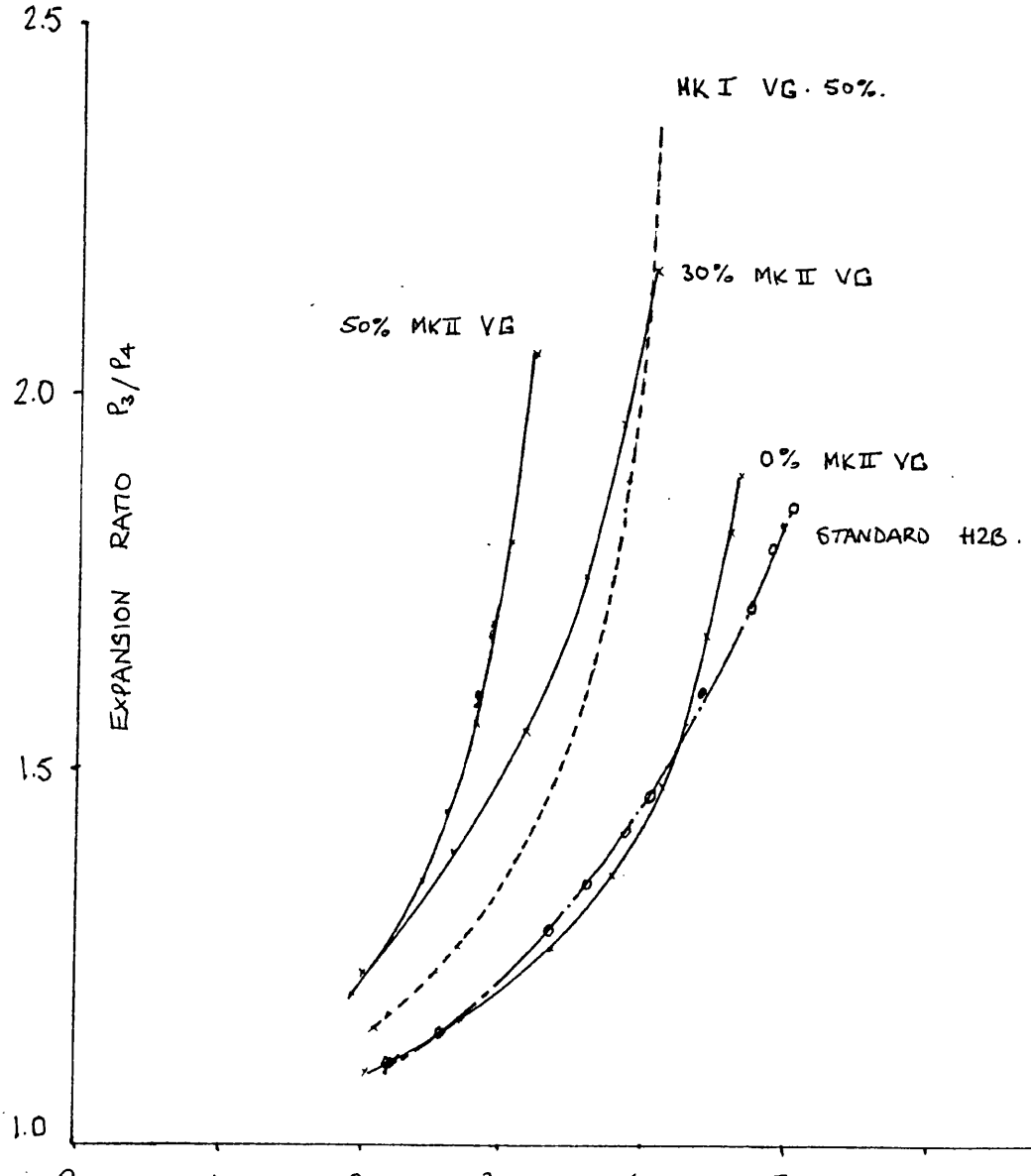

fig 4.18

Engine LEYLAND TL11—7962756 Project No. Eurobus

Title H2C 8625N / Z31U3 FULLY OPEN & H2B 8081C L25A3 base

Power Curve No BOOST CONTROL

Test No.	Timing	Amb'nt °C	Barometer Ins. Hg.
41	22	–	–
40			

H26 8081C L25 A3 - BASE

H2C 8625N Z31U3 - FULLY OPEN (MKIIa)

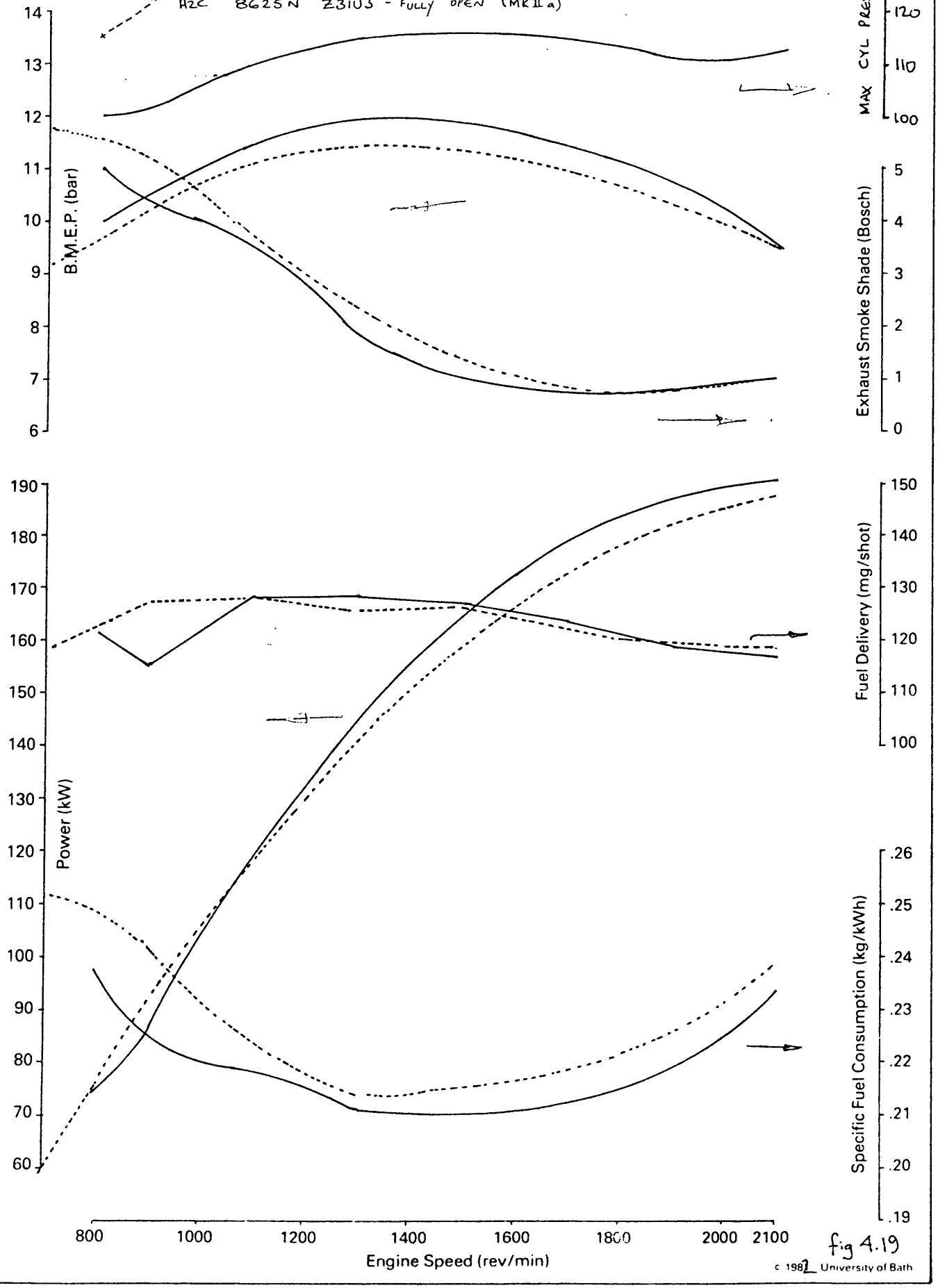

fig 4.19

Date ... JUNE 1982 Graph .....

Engine LEYLAND TL11—7962756 Project No. EW 6077

Title A COMPARISON OF THE BASE UNIT WITH THE MKII(a) VG FULLY OPEN (SINGLE ENTRY)

Power Curve No BOOST CONTROL

Test No.	Timing	Amb'nt °C	Barometer Ins. Hg.
40 41	22	–	–

H2B 8081C L25 A3 - base

H2C 8625N Z3103 - FULLY OPEN (MKIIa)

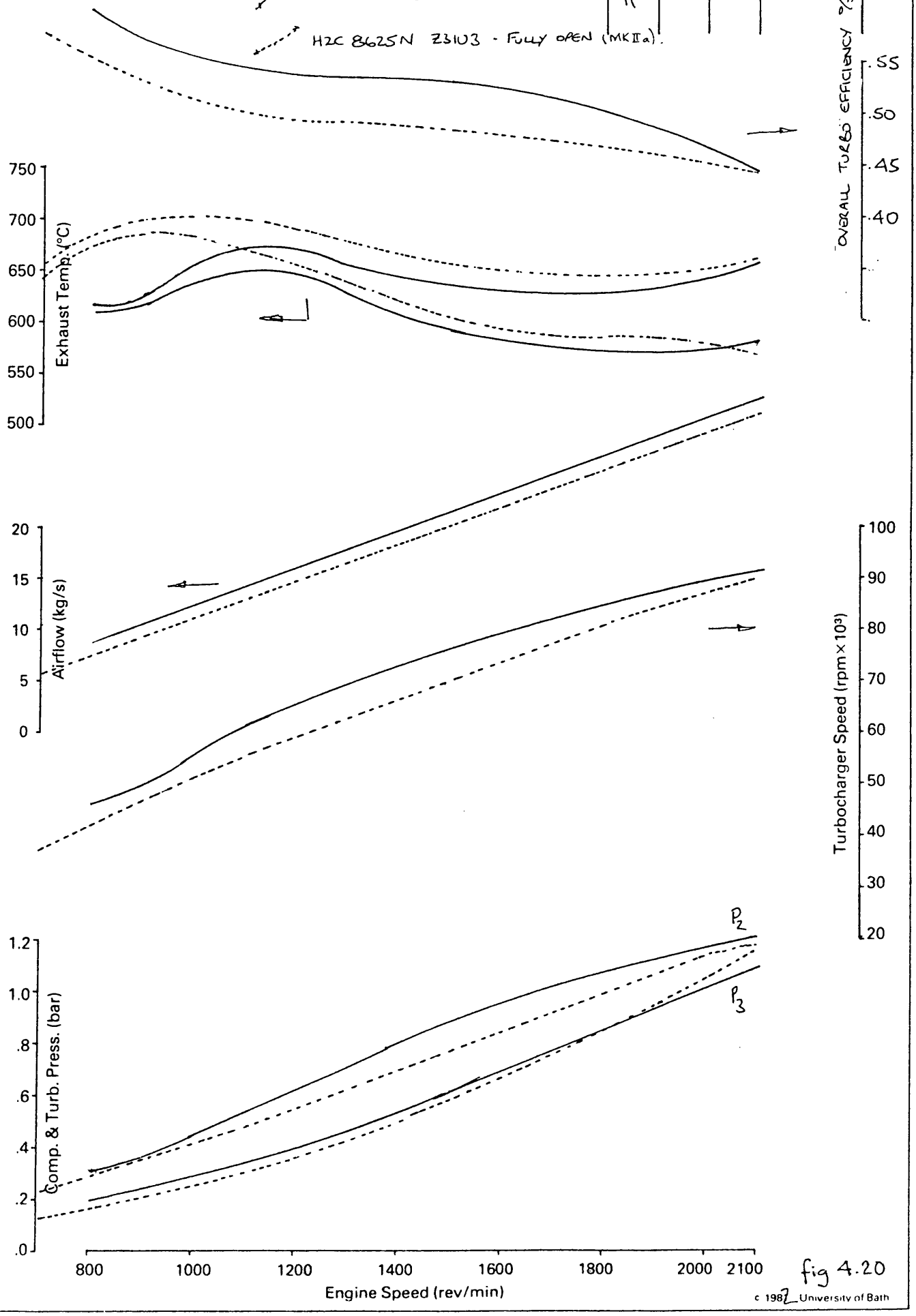

fig 4.20

Engine LEYLAND TL11—7962756 Project No. E W ROBERTS

Title H2C 8625N / Z3103 MK II(a) SINGLE ENTRY (FIXED DISCRETE RESTRICTIONS)

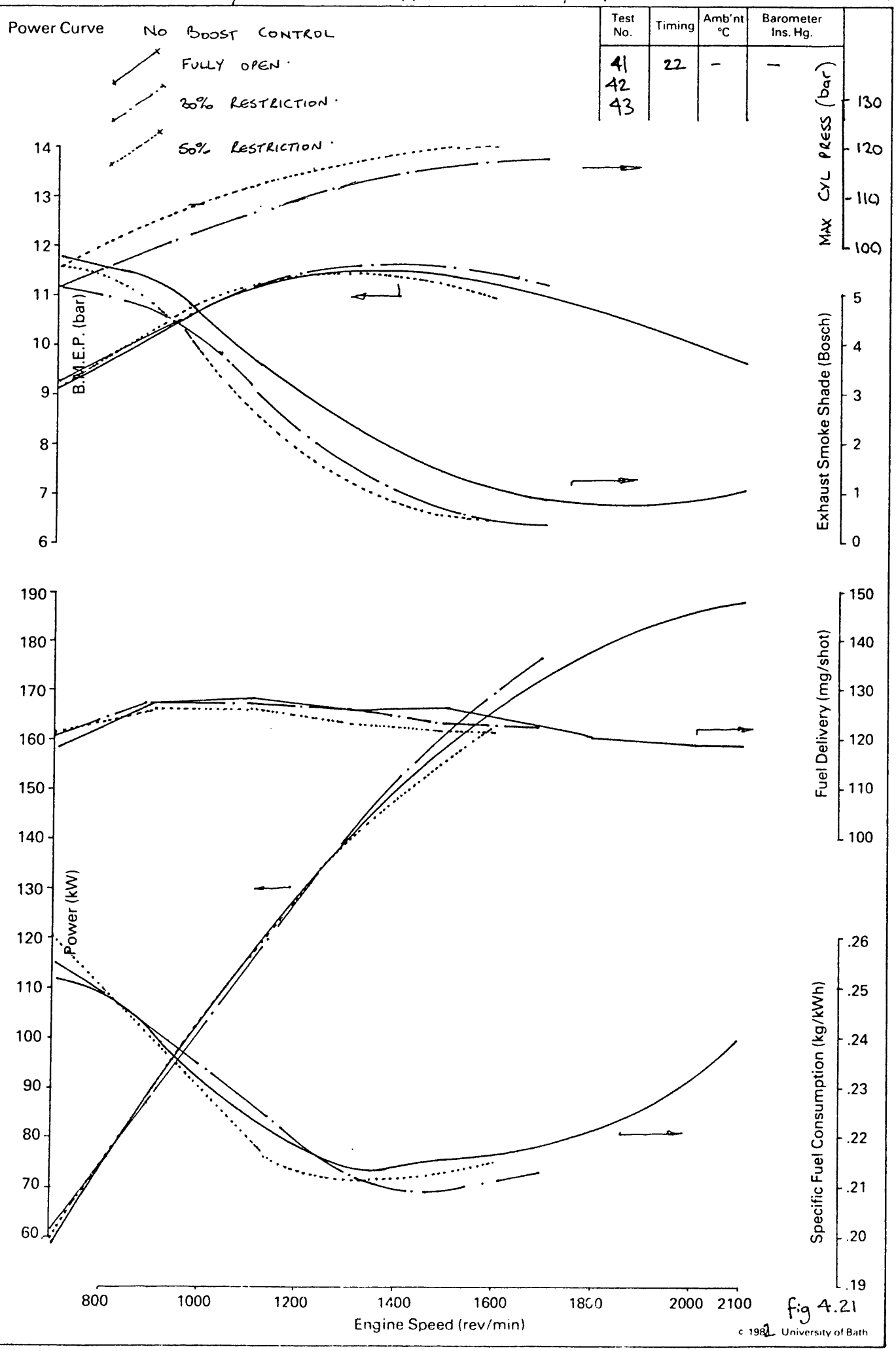

fig 4.21

Engine LEYLAND TL11—7962756 Date ..../..../82 Graph ....
S.H. Loft
Title H2C 8625 N / Z3103 MK II (a) SINGLE ENTRY (FIXED DISCRETE RESTRICTIONS)

Power Curve No BOOST CONTROL

Test No.	Timing	Amb'nt °C	Barometer Ins. Hg.
41	22	–	–
42			
43			

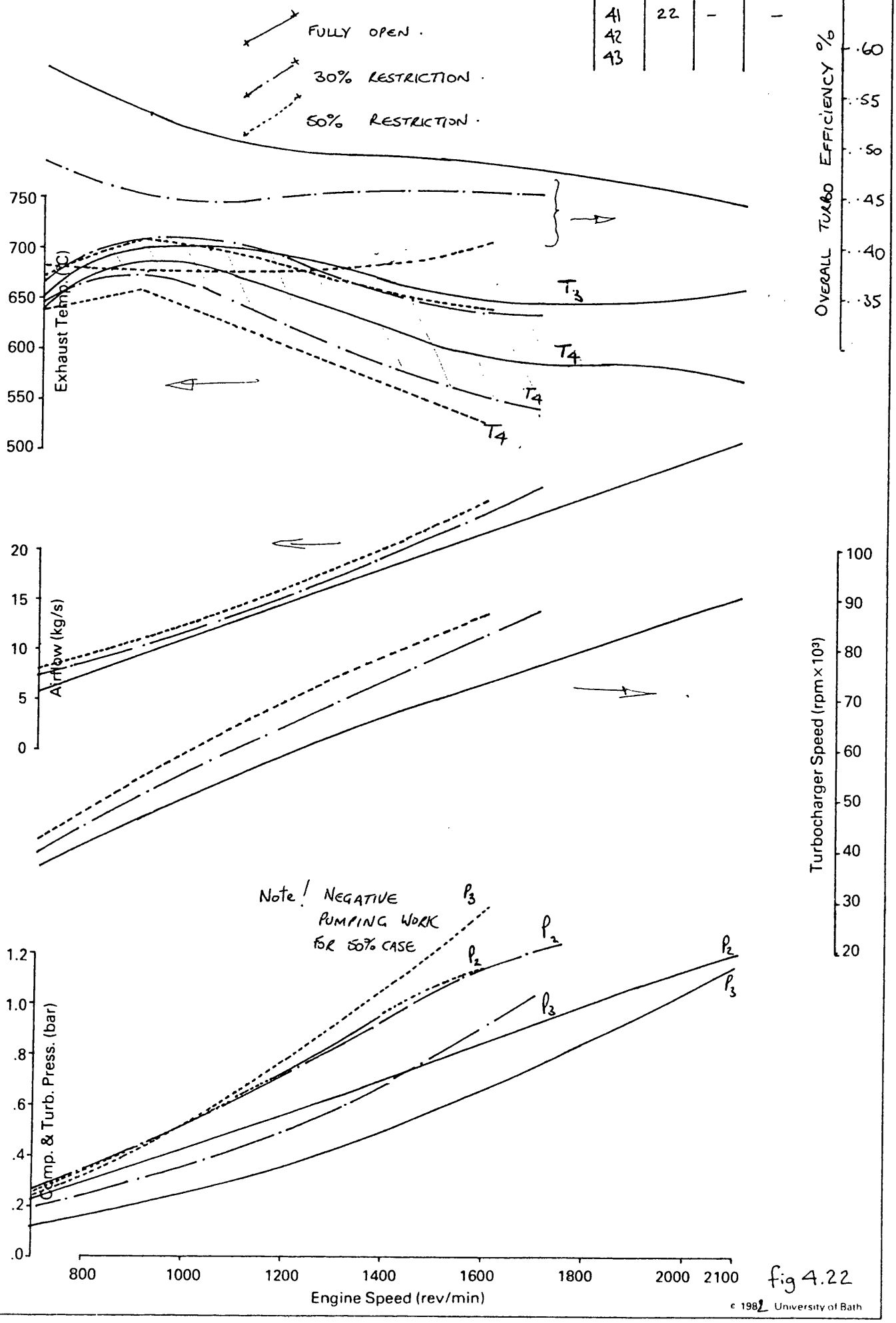

fig 4.22

COMPRESSOR PERFORMANCE

HOLSET ENGINEERING CO. LTD.
HUDDERSFIELD

MODEL	H2C — 8625N - Z31U3. (MKII b)

DATE	12-6-80
REF. No.	T1168

TESTS 57-60.

COMPRESSOR WHEEL 3504480

COMPRESSOR COVER 3504482

LEYLAND TL11/11 RATING: 190kW @ 2100rev/min.

POWER CURVES WITH VARYING

TURBINE RESTRICTION (SINGLE ENTRY)

(PNEUMATIC OPERATION)

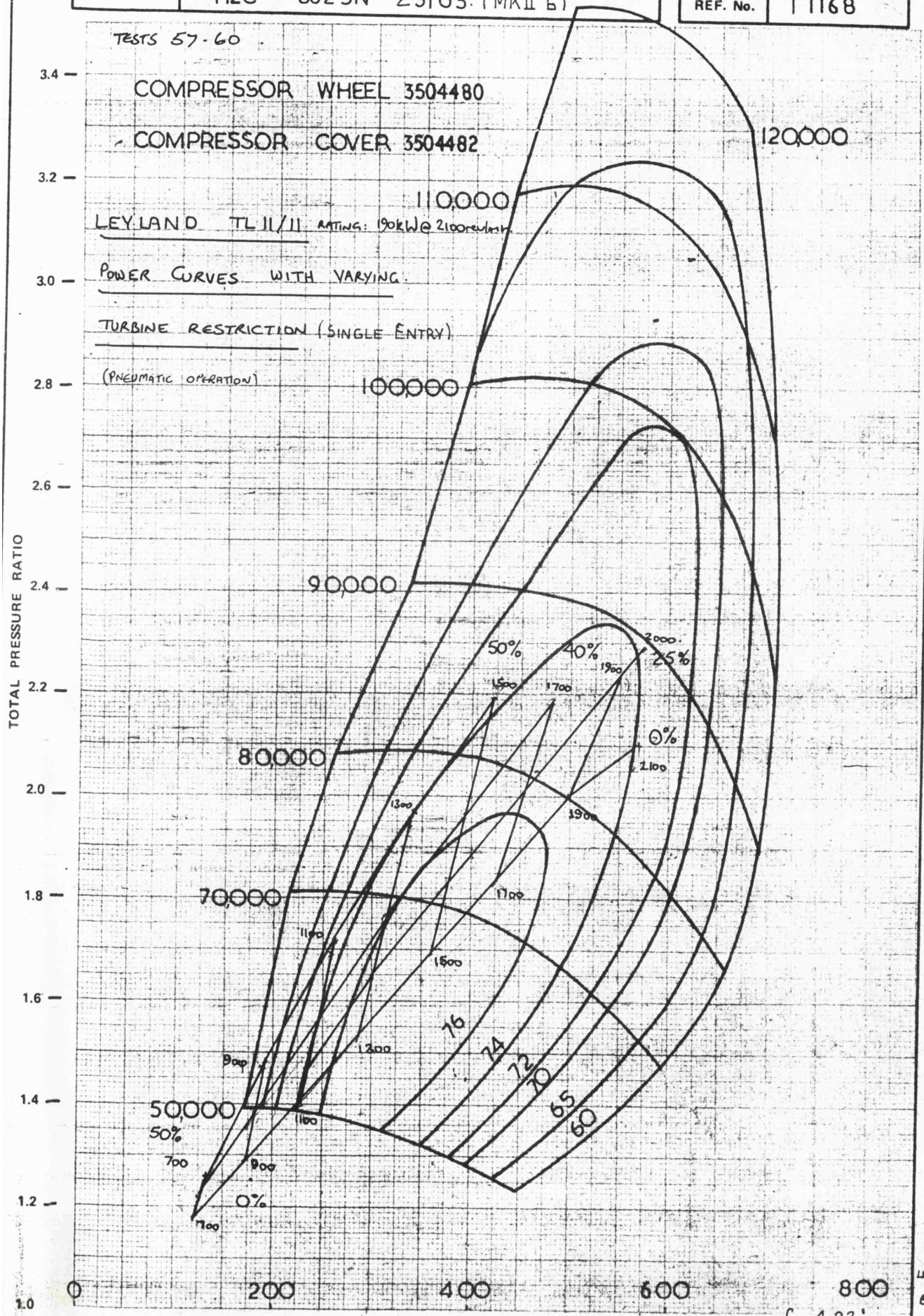

fig 4.23

Engine LEYLAND TL11 ENGINE—11.1L DISPLACEMENT

Drawn By. E W ROBERTS.

Title ENGINE 'TURBINE SWALLOWING' CAPACITY CURVES. - VG. TURBOCHARGER. SINGLE ENTRY.

H2C 8625N · Z3103 · PNEUMATIC OPERATION · MK II b

Holset / Leyland / Dowty / Dol Contract

Test No.	Timing	Amb'nt °C	Barometer Ins. Hg.
57-60	22°	~	~

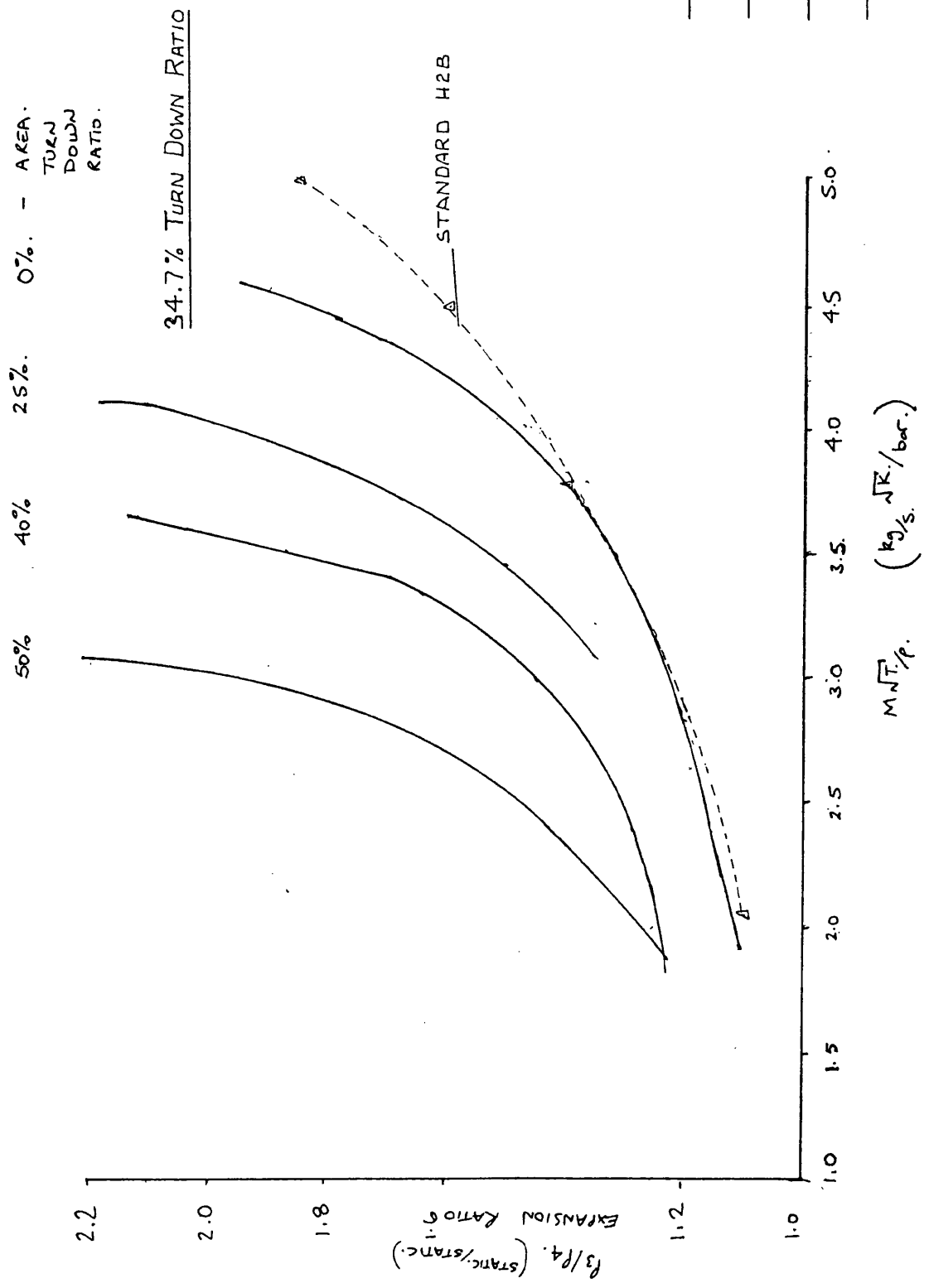

fig 4.24

Engine LEYLAND TL11—7962756 Project No. E W ROBERTS.

Title COMPARISON BETWEEN BASE & VG TURBO WITH VARIOUS RESTRICTIONS : PNEUMATIC OPERATION

Power Curve — 190 kW @ 2100 rev/min. / No boost CONTROL : MK II (b)

Test No.	Timing	Amb'nt °C	Barometer Ins. Hg.
40 57-60	22°	—	—

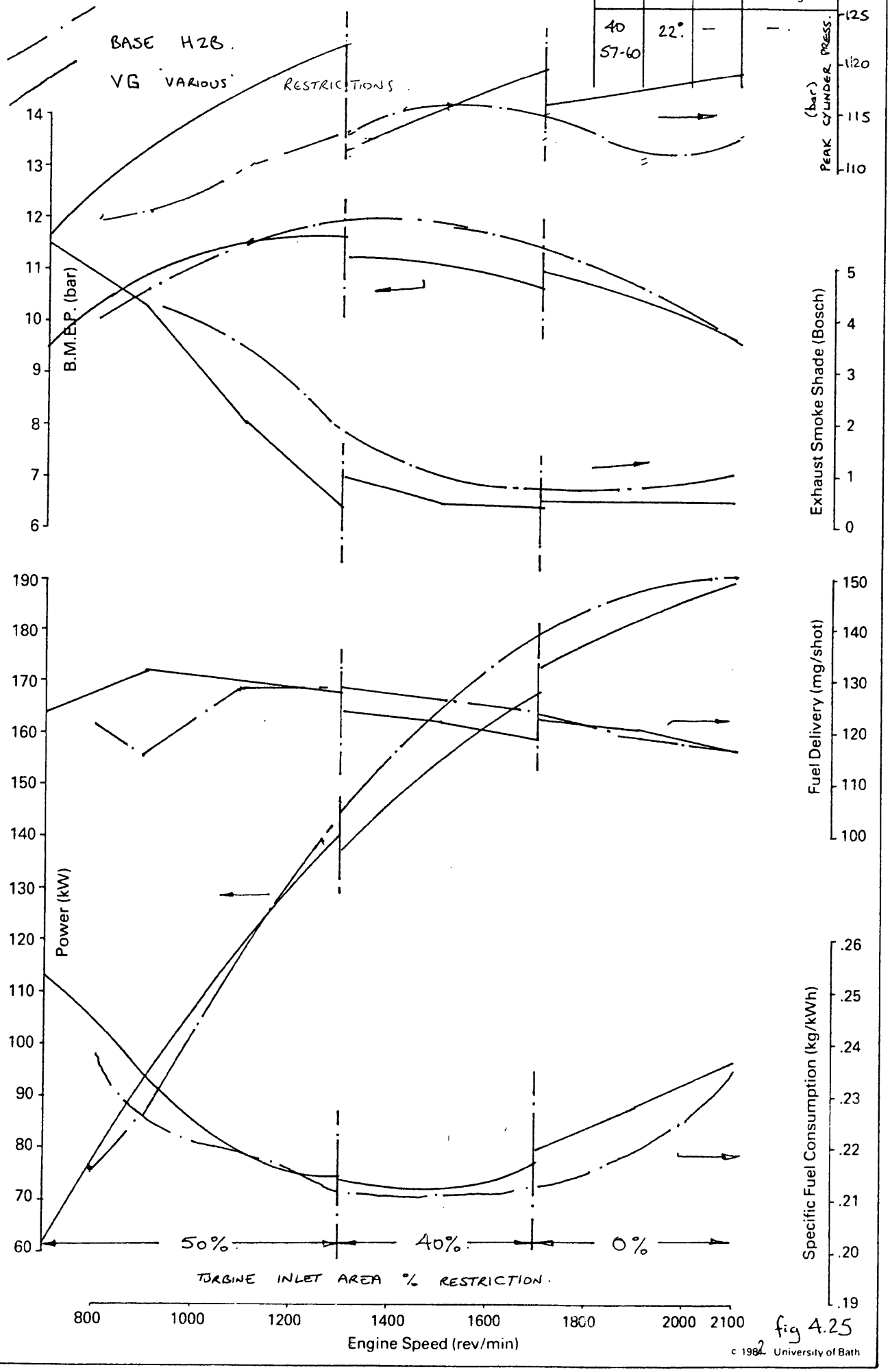

fig 4.25

Date ..... Graph .....

Engine LEYLAND TL11—7962756 Project No. E W Roberts

Title COMPARISON BETWEEN BASE & VG TURBO WITH VARIOUS RESTRICTIONS. MK II b H2C8625 Z3103

Power Curve – 190kW @ 2100 rev/min / No boost control.

Test No.	Timing	Amb'nt °C	Barometer Ins. Hg.
40 57.60	22°	25	~

Base H26.

VG . VARIOUS . RESTRICTIONS (PNEUMATIC OPERATION)

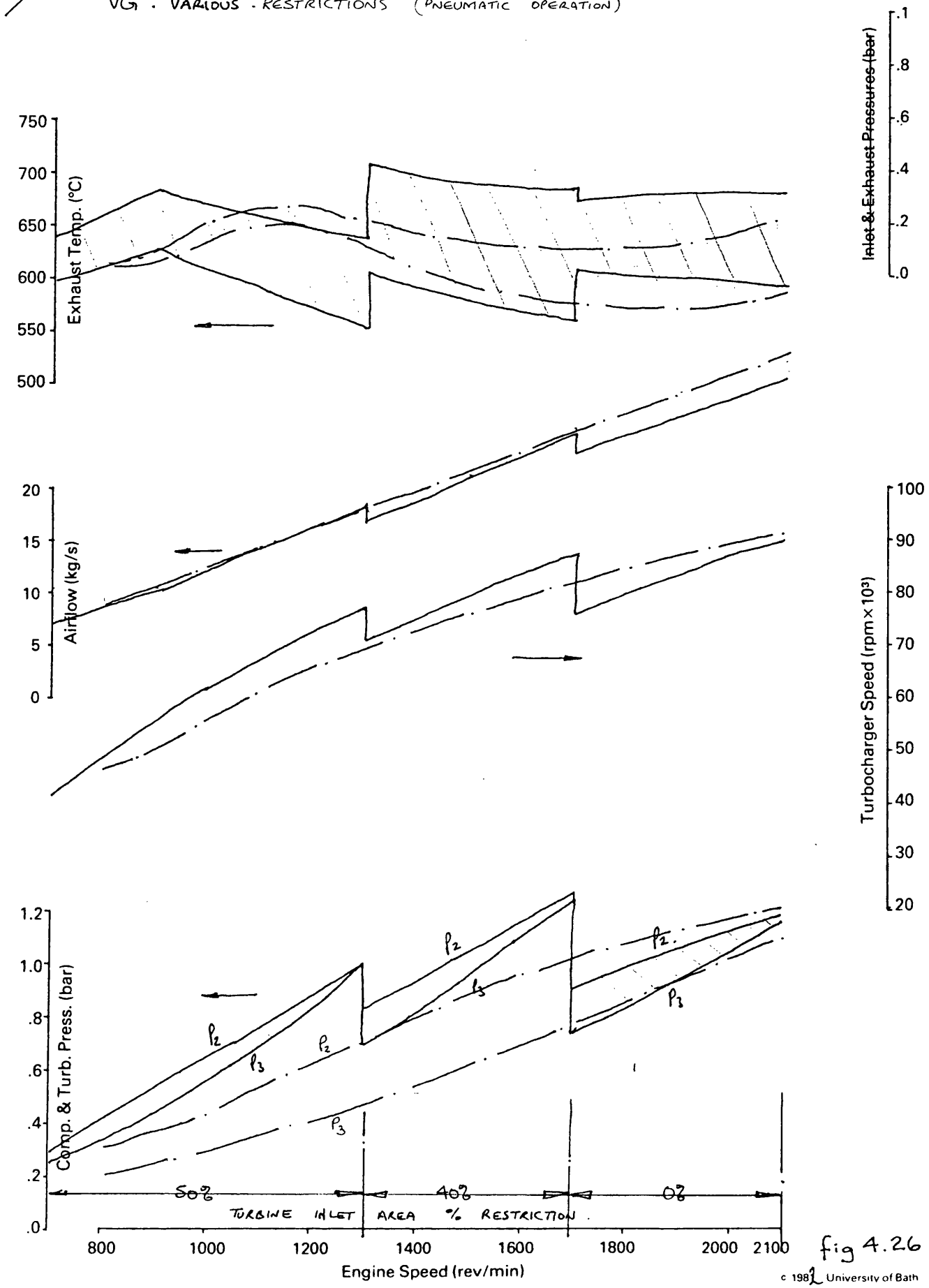

fig 4.26

Date ..... Graph .....

Engine LEYLAND TL11 ENGINE—11.1L DISPLACEMENT Drawn By E W Roberts.

Title COMPARISON OF BASE & VG FULLY OPEN & CLOSED FOR ENGINE BREATHING.

Power Curve Rating—190 kW at 2100 rev/min

Holset / Leyland / Dowty / DoI Contract

Test No.	Timing	Amb'nt °C	Barometer mm Hg.
40 57 58.	22°	25.	

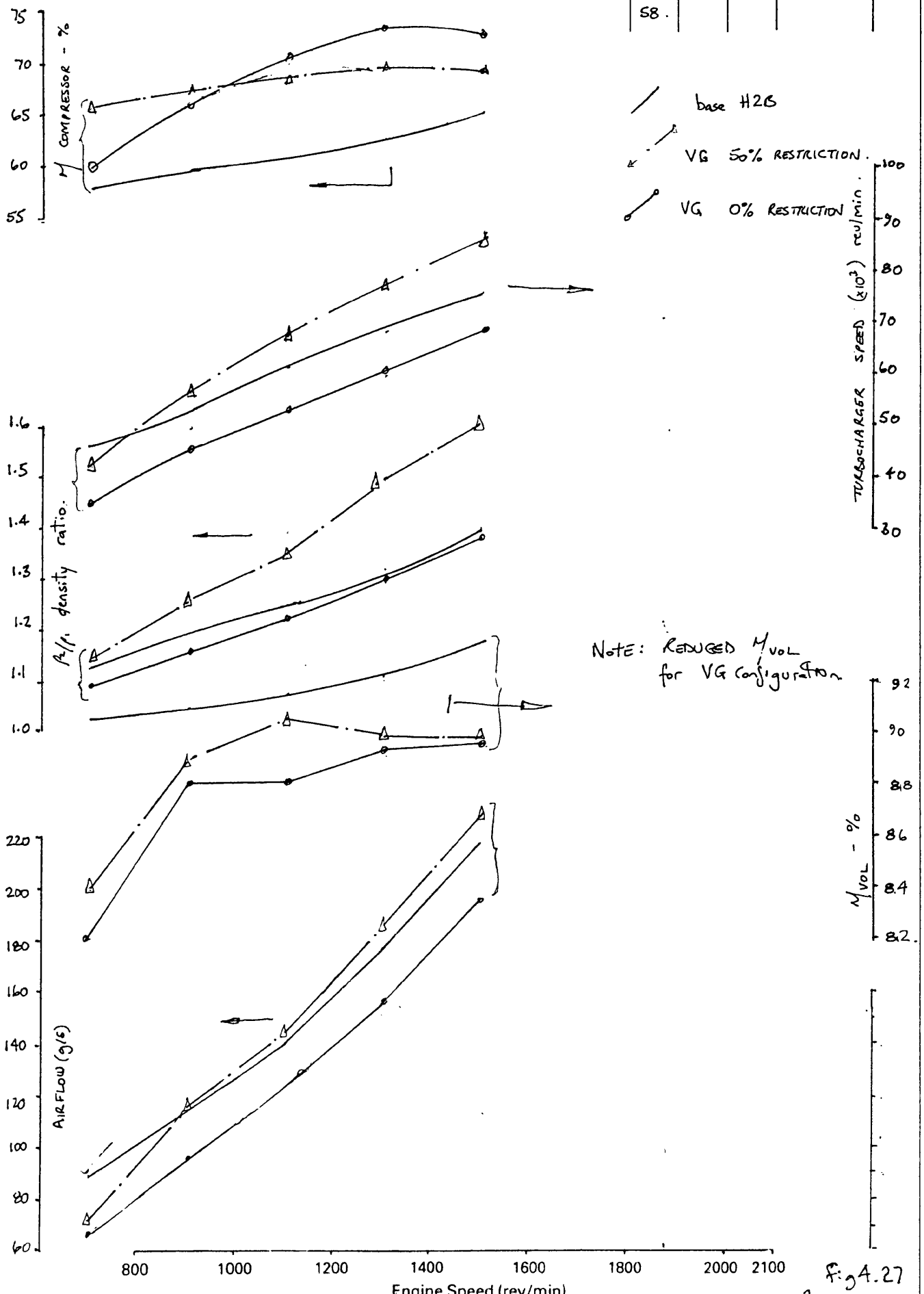

Note: Reduced η_{VOL} for VG configuration

Fig 4.27

Engine LEYLAND TL11 ENGINE—11.1 DISPLACEMENT - MkII(b) Drawn By E W Roberts

Title VG INVESTIGATION : H2C 8625N : Z3103 : VARYING RESTRICTIONS Rating—190 kW at 2100 rev/min

Constant Speed Curve at 1800 rev/min LTC

Holset / Leyland / Dowty / DoI Contract

Test No.	Timing	Amb'nt °C	Barometer Ins. Hg.
65	22	25	738.14

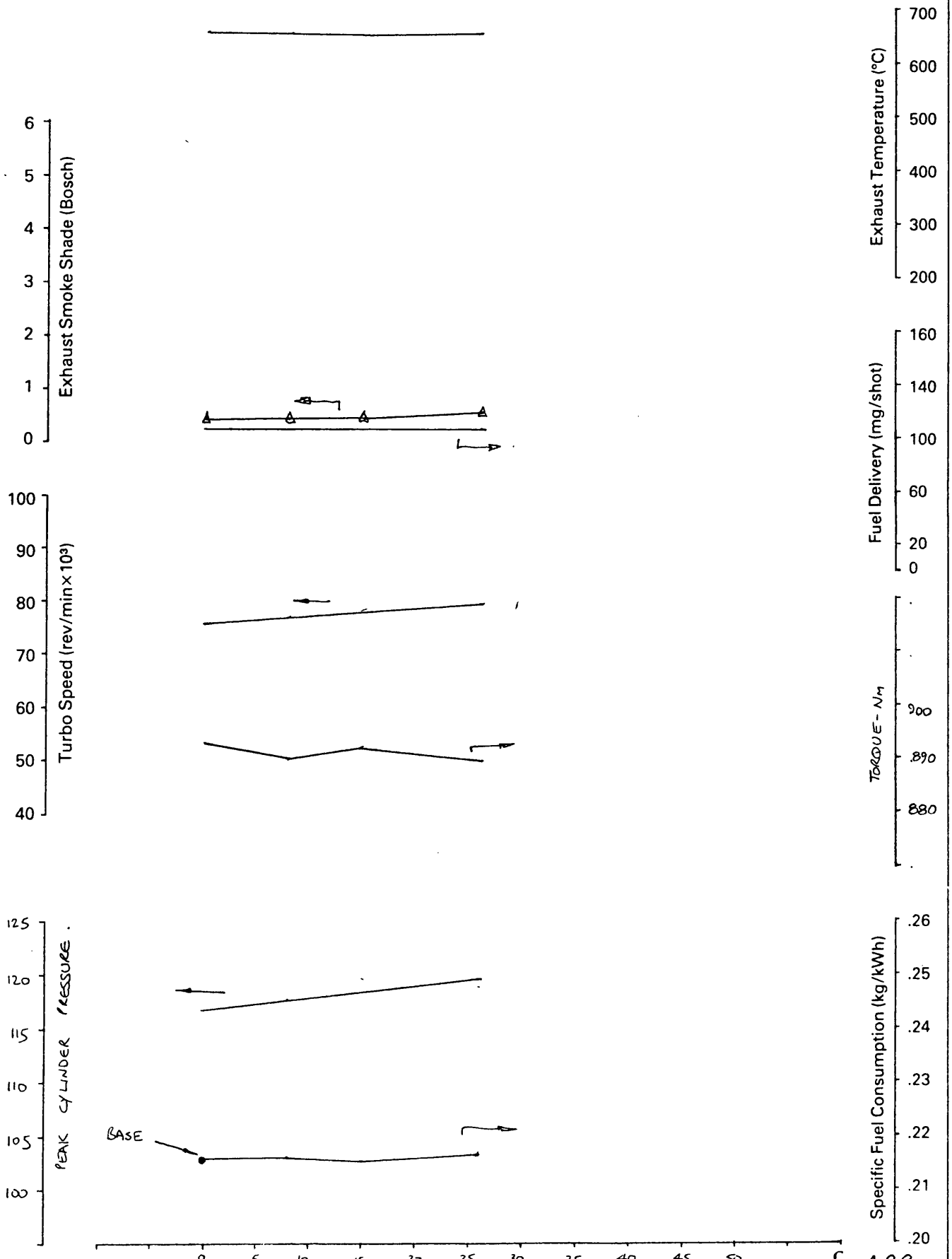

fig 4.28

Engine LEYLAND TL11 ENGINE—11.1 DISPLACEMENT MKII 6 Drawn By E W Roberts

Title VG INVESTIGATION : H2C 8625N 23103 : VARYING RESTRICTIONS . Rating—190 kW at 2100 rev/min

Constant Speed Curve at 1800 rev/min 50% LT.

Holset / Leyland / Dowty / DoI Contract

Test No.	Timing	Amb'nt °C	Barometer Ins. Hg.
66	22	24	732.14.

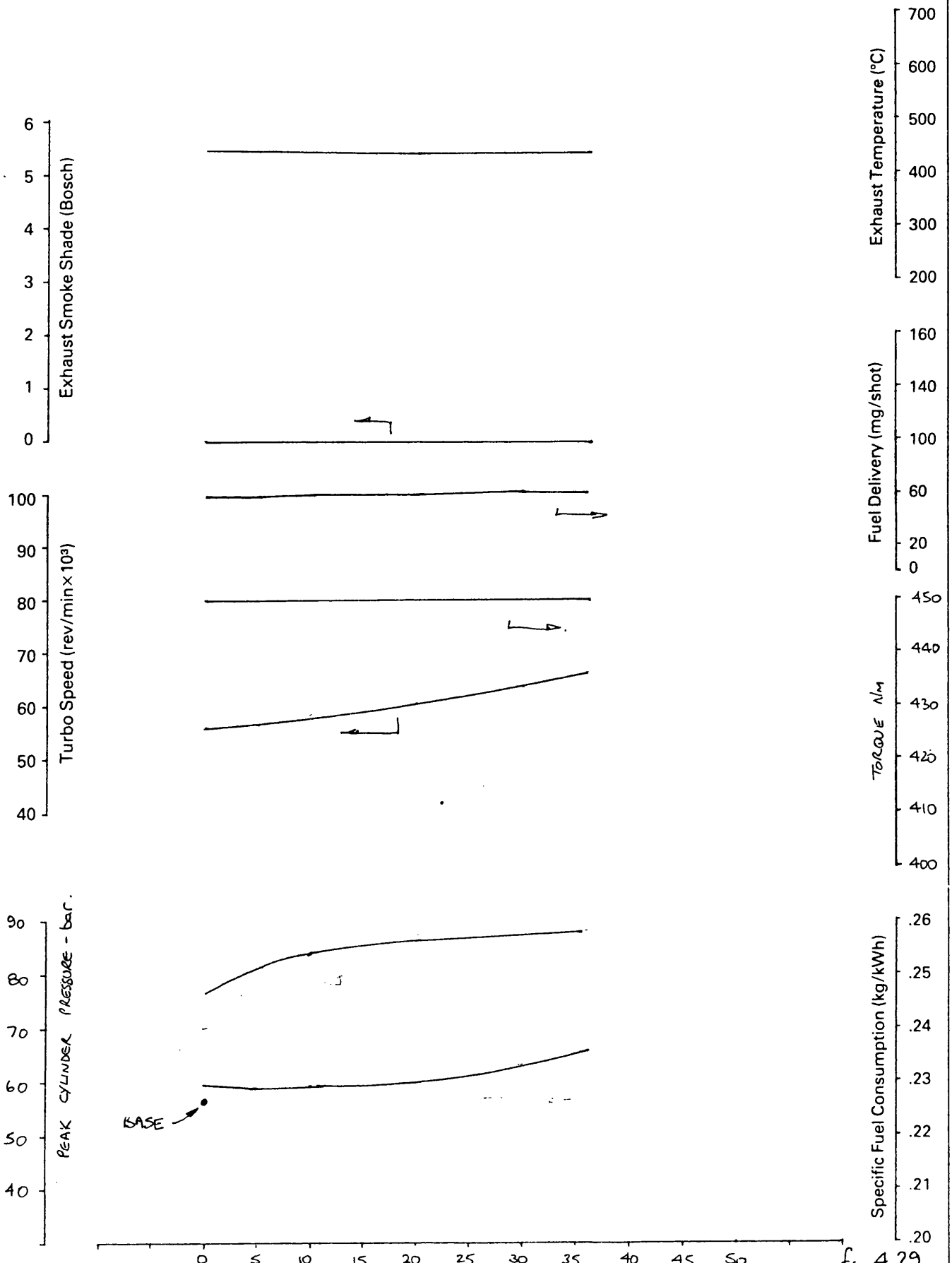

fig 4.29

Date 12/10/84. Graph 61.

Engine LEYLAND TL11 ENGINE—11.1 DISPLACEMENT MK II b Drawn By E W Roberts.

Title VG INVESTIGATION : H2C 8625N 7310 3 VARYING RESTRICTIONS . Rating—190 kW at 2100 rev/min

Constant Speed Curve at 1300 rev/min LIMITING TORQUE CURVE

Holset / Leyland / Dowty / DoI Contract

Test No.	Timing	Amb'nt °C	Barometer Ins. Hg.
61	22	22	729.9

FUELLING SET TO GIVE 700°C IN WORST CASE

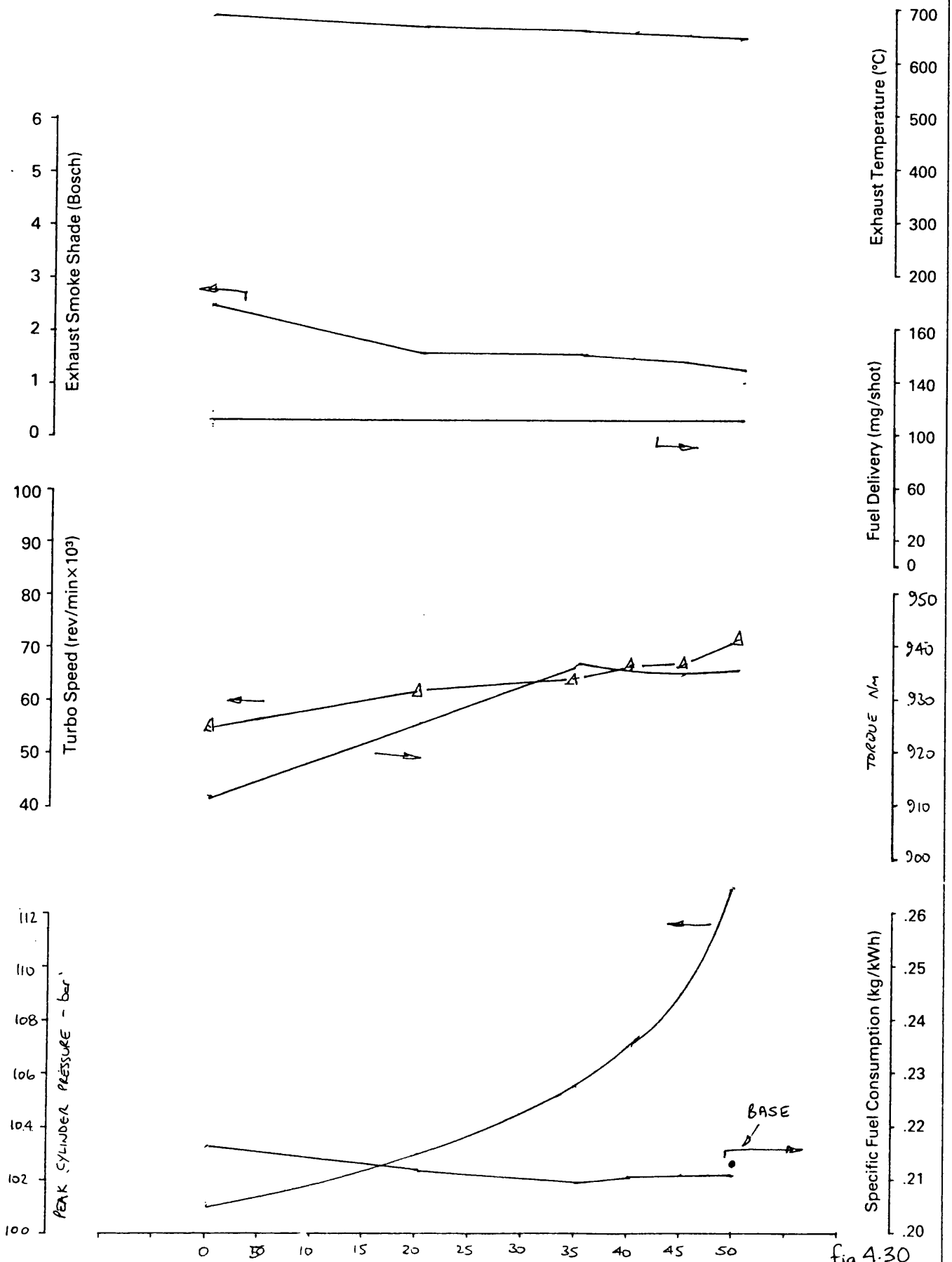

fig 4.30

Engine LEYLAND TL11 ENGINE—11.1 DISPLACEMENT MKII (6) Drawn By E W Roberts.

Title VG INVESTIGATION : H2C 8625N Z3103 : VARYING RESTRICTIONS. Rating—190 kW at 2100 rev/min

Constant Speed Curve at 1300 rev/min 50% LT.

Holset / Leyland / Dowty / DoI Contract

Test No.	Timing	Amb'nt °C	Barometer Ins. Hg.
62	22	22	729.9

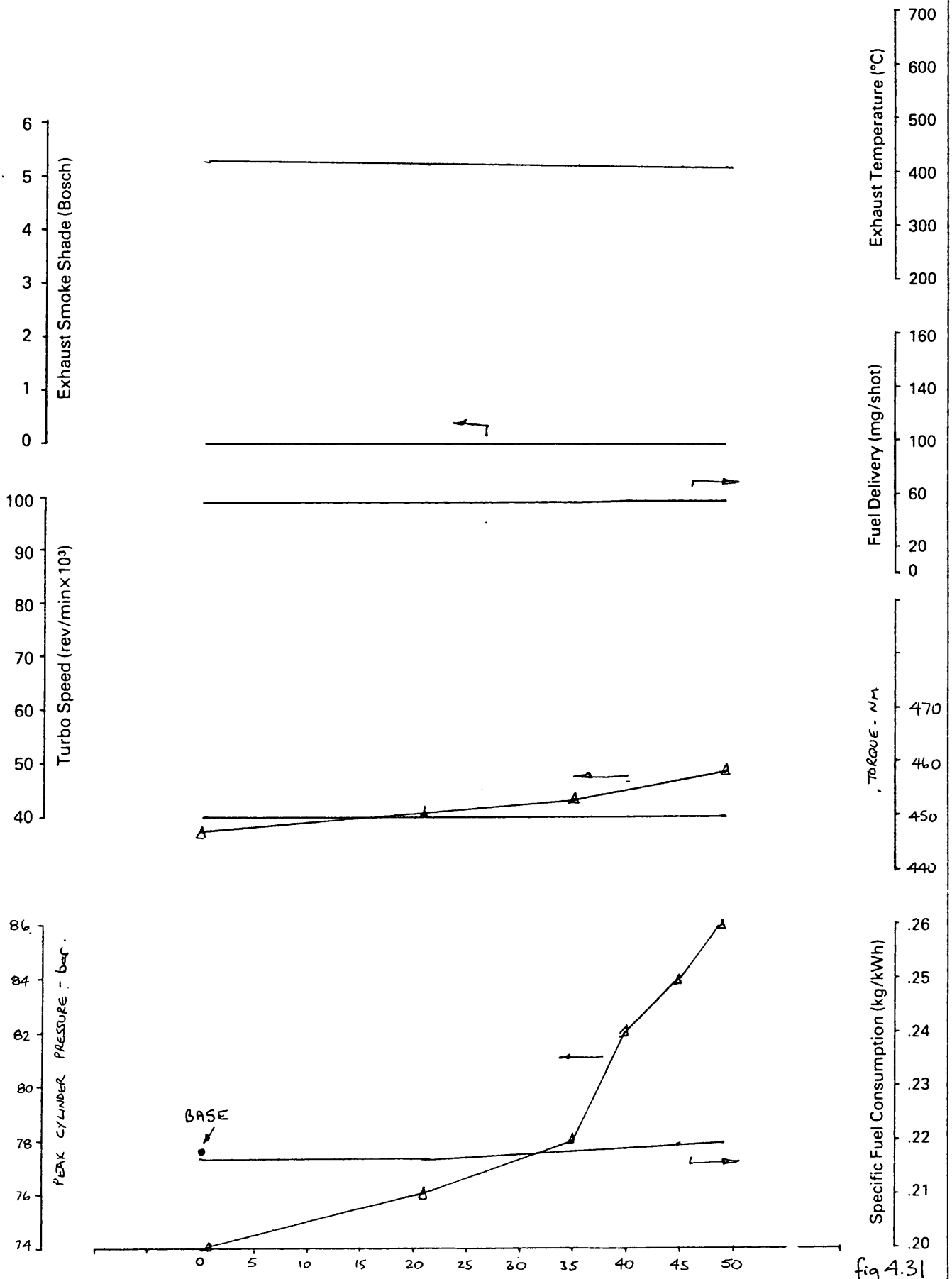

fig 4.31

Engine LEYLAND TL11 ENGINE—11.1 DISPLACEMENT MKII(L) Drawn By E W Roberts

Title VG INVESTIGATION : H2C 862S N Z3103 : VARYING RESTRICTIONS Rating—190 kW at 2100 rev/min

Constant Speed Curve at 800 rev/min

Holset / Leyland / Dowty / DoI Contract

Test No.	Timing	Amb'nt °C	Barometer Ins. Hg.
63	22	22	742.65

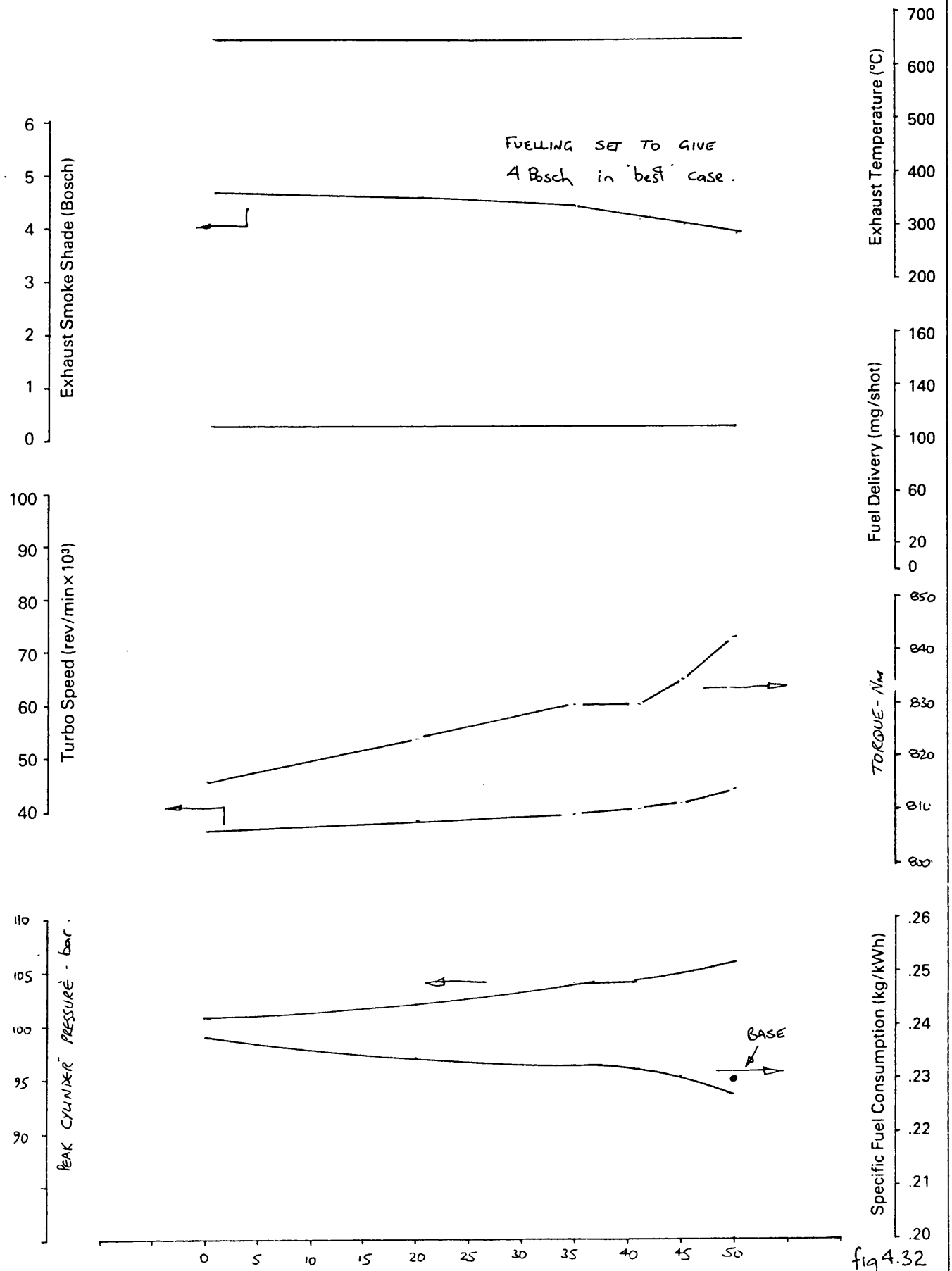

fig 4.32

Engine LEYLAND TL11 ENGINE—11.1 DISPLACEMENT MKII 6 Drawn By E W Roberts.

Title VG INVESTIGATION : H2C 8G2SN Z3103 VARYING RESTRICTIONS. Rating—190 kW at 2100 rev/min

Constant Speed Curve at 800 rev/min 50% LT.

Holset / Leyland / Dowty / Dol Contract

Test No.	Timing	Amb'nt °C	Barometer Ins. Hg.
64	22	25	738.14.

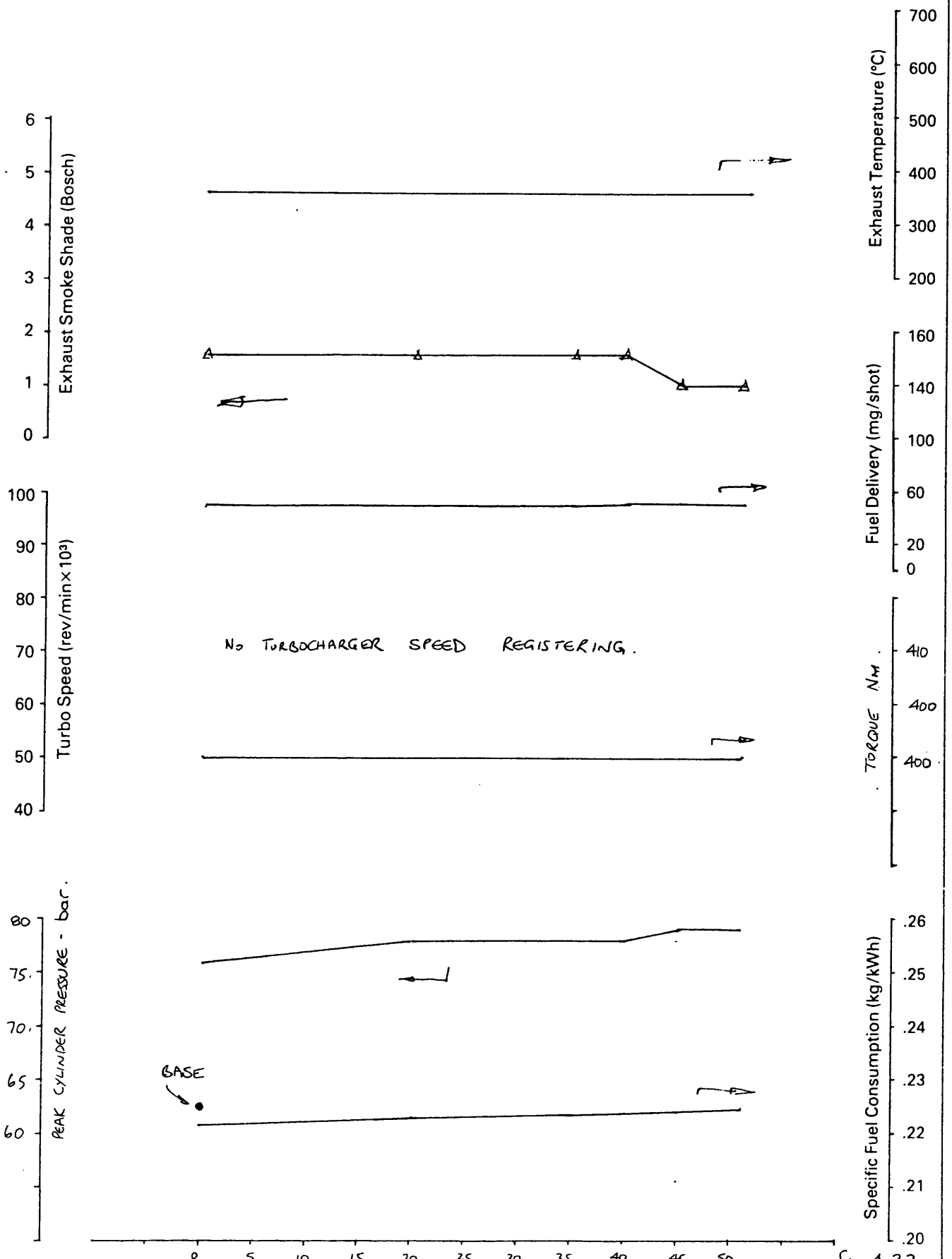

fig 4.33

Engine LEYLAND TL11 ENGINE—11.1 DISPLACEMENT

Drawn By S.E. ROUCHOTAS

Title ... Rating—190 kW at 2100 rev/min

Constant Speed Curve at 1300 rev/min

Holset / Leyland / Dowty / Dol Contract

Test No.	Timing	Amb'nt °C	Barometer Ins. Hg.
88			

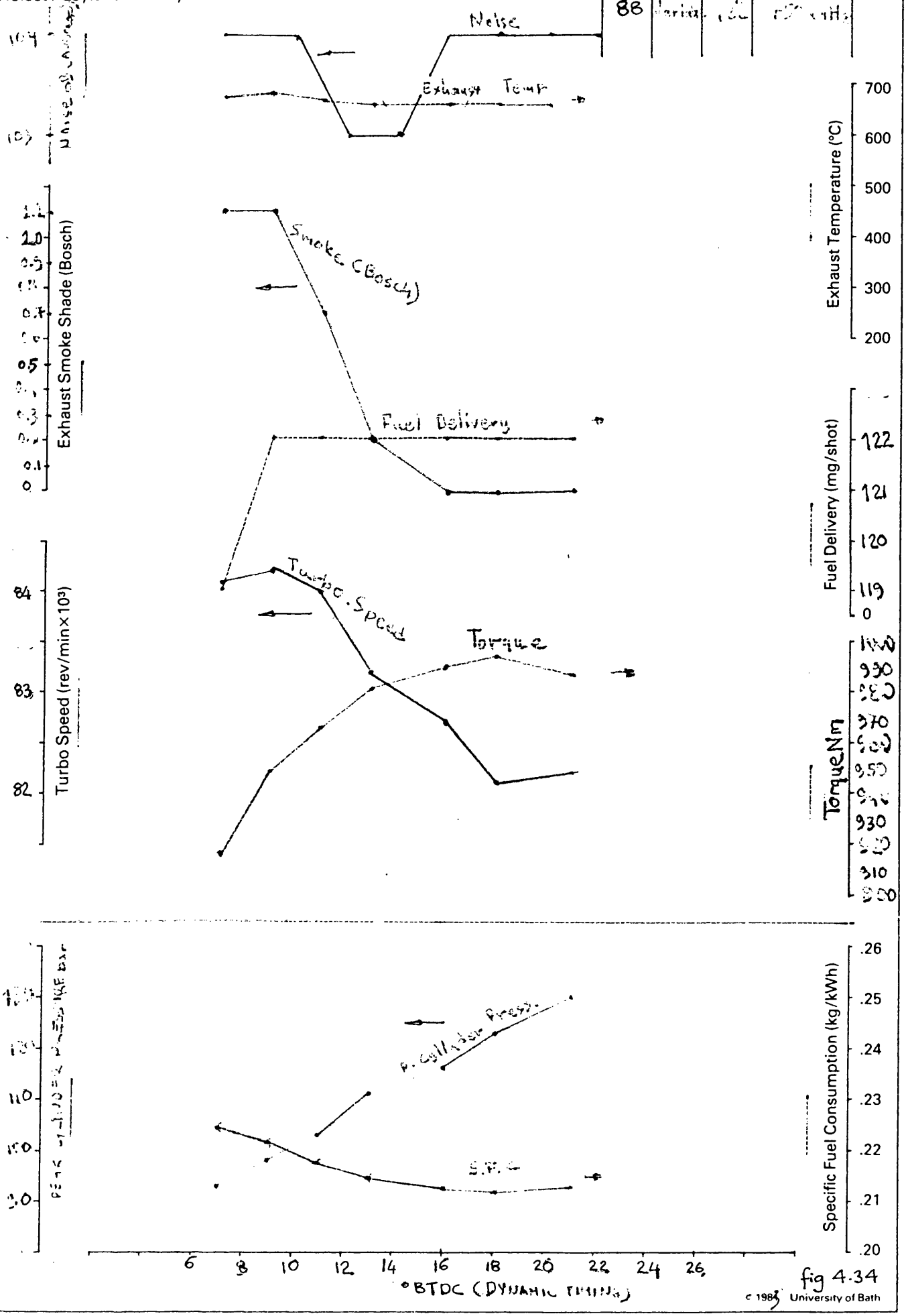

fig 4.34

Engine LEYLAND TL11 ENGINE—11.1 DISPLACEMENT

Drawn By S.E. ROUCHOTAS

Title TIMING SWING INVESTIGATION ~ H2B TURBOCHARGER

Rating—190 kW at 2100 rev/min

Constant Speed Curve at 1800 rev/min ~ 50% TORQUE

Holset / Leyland / Dowty / DoI Contract

Test No.	Timing	Amb'nt °C	Barometer Ins. Hg.
89	Variable	12°	30 ins Hg

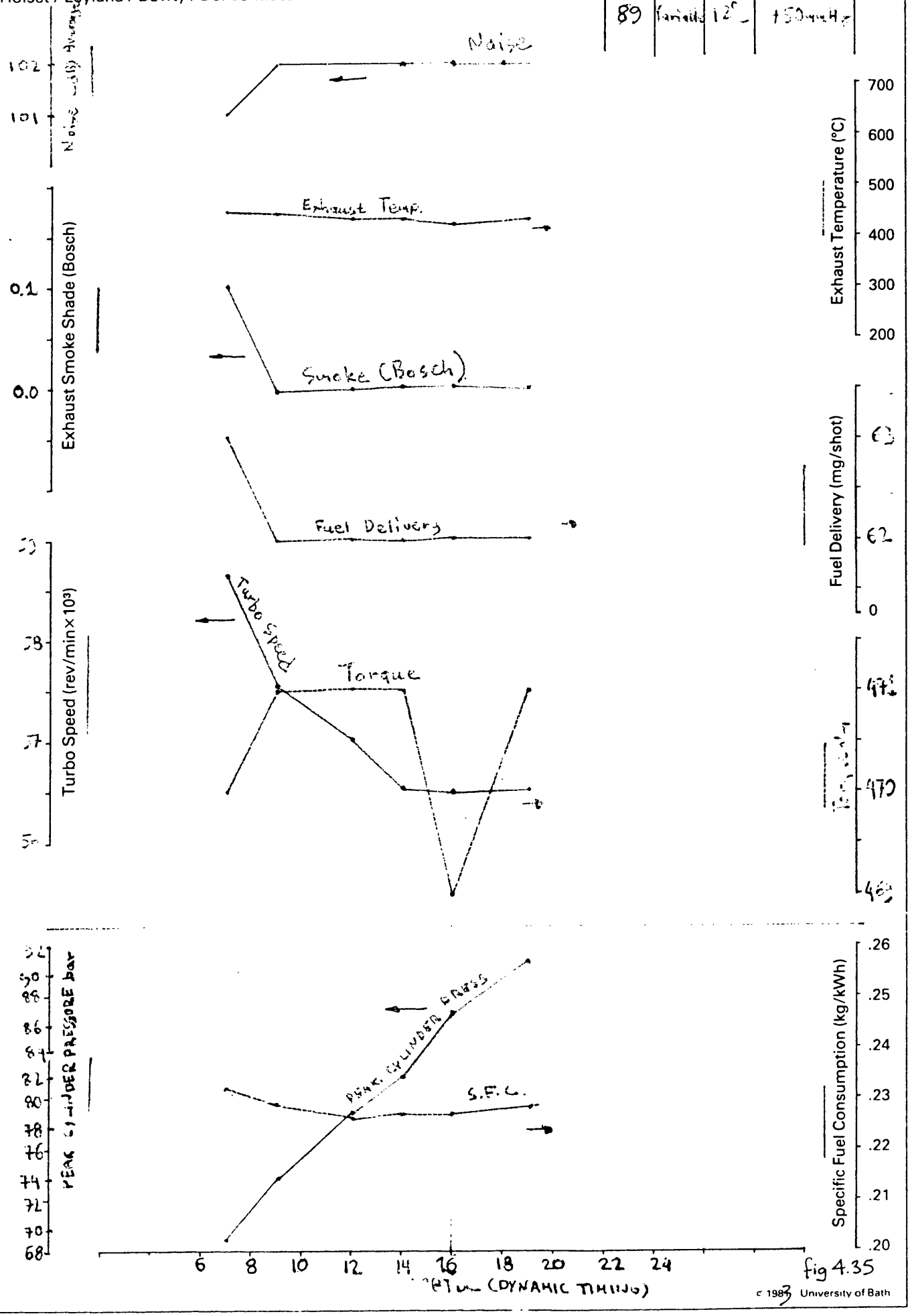

fig 4.35

Engine LEYLAND TL11 ENGINE—11.1 DISPLACEMENT

Drawn By S.E. ROUCHOTAS

Title TIMING SWING INVESTIGATION - H2B TURBOCHARGER

Rating—190 kW at 2100 rev/min

Constant Speed Curve at 1300 rev/min LTC

Holset / Leyland / Dowty / DoI Contract

Test No.	Timing	Amb'nt °C	Barometer Ins. Hg.
84	Variable	12°C	750mmHg

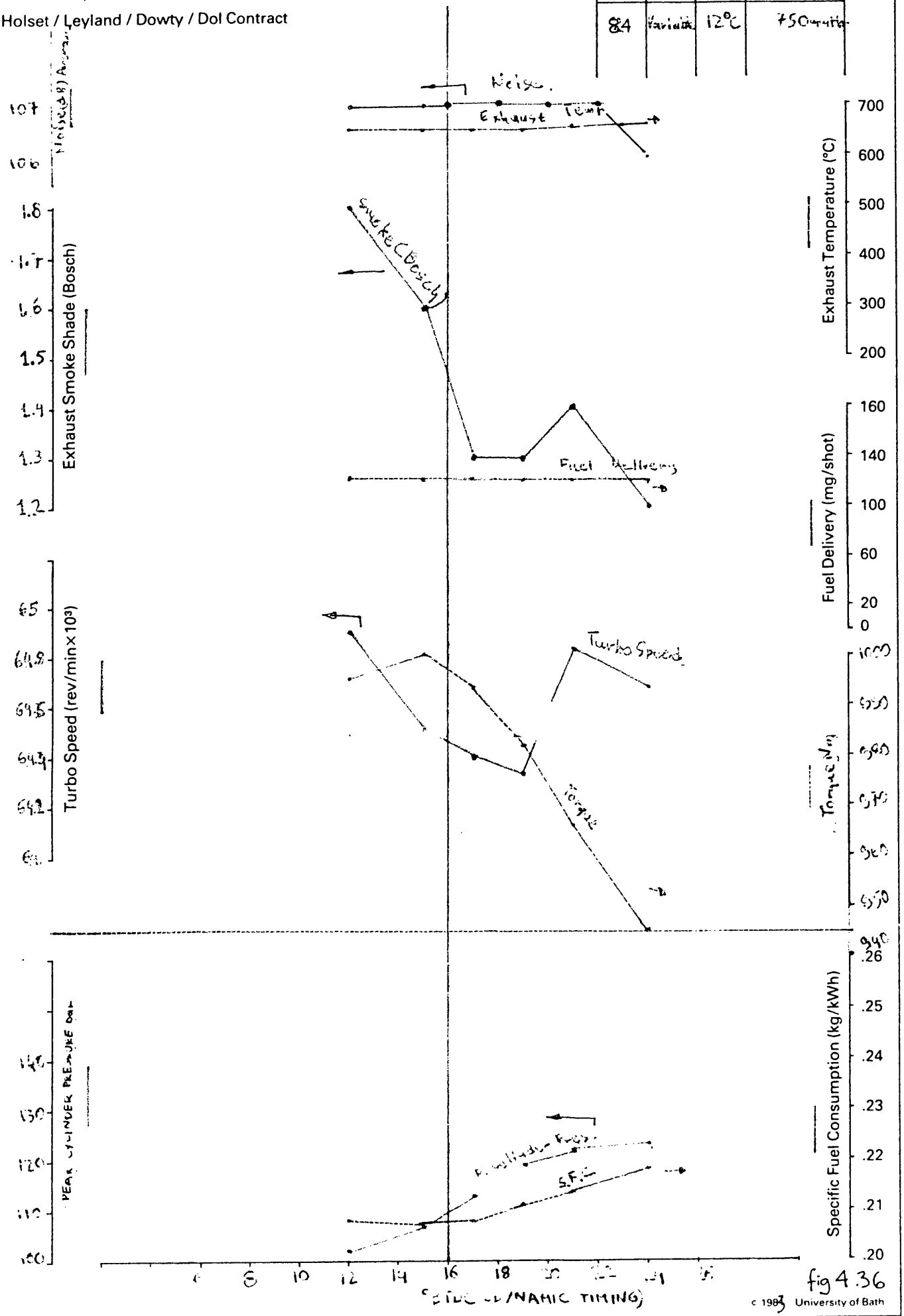

fig 4.36

Engine LEYLAND TL11 ENGINE—11.1 DISPLACEMENT Drawn By S.E. ROUCHOTAS

Title TIMING SWING INVESTIGATION - 50: H2B: TURBO: Rating—190 kW at 2100 rev/min

Constant Speed Curve at 1300 rev/min 50% TORQUE.

Holset / Leyland / Dowty / DoI Contract

Test No.	Timing	Amb'nt °C	Barometer Ins. Hg.
86	Variable	12°C	750 mm Hg

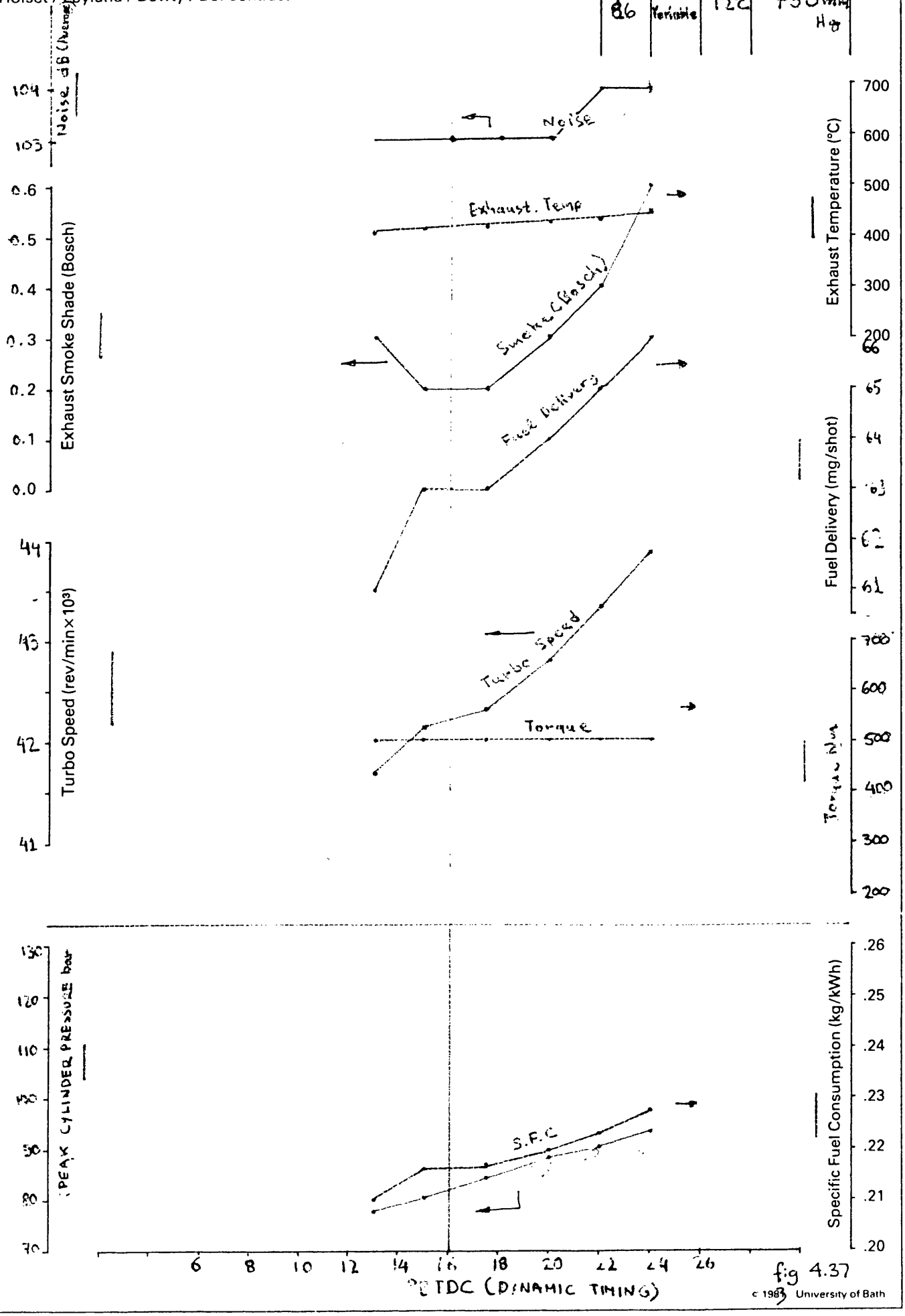

fig 4.37

Engine LEYLAND TL11 ENGINE—11.1 DISPLACEMENT

Drawn By P. E. KOUCHOTAS

Title TIMING SWING INVESTIGATION - H2B TURBOCHARGER

Rating—190 kW at 2100 rev/min

Constant Speed Curve at 800 rev/min LTC

Holset / Leyland / Dowty / DoI Contract

Test No.	Timing	Amb'nt °C	Barometer Ins. Hg.
85			

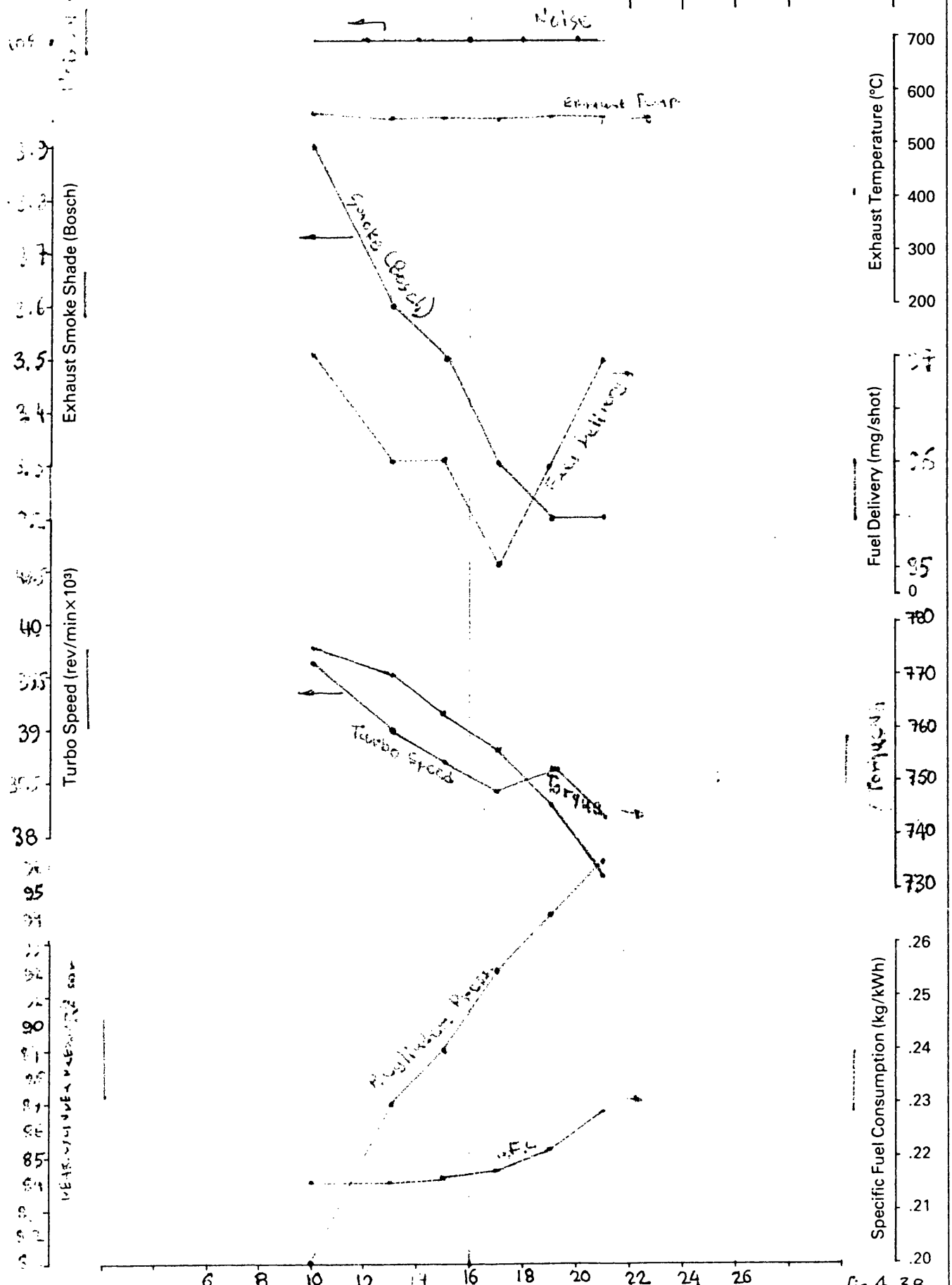

fig 4.38

Engine LEYLAND TL11 ENGINE—11.1 DISPLACEMENT

Drawn By S.E. ROUCHOTAS

Title TIMING SWING INVESTIGATION - S. H2B TURBOCHARGER

Rating—190 kW at 2100 rev/min

Constant Speed Curve at 800 rev/min 50% LTC

Holset / Leyland / Dowty / DoI Contract

Test No.	Timing	Amb'nt °C	Barometer Ins. Hg.
87	Variable	12°C	750mmHg

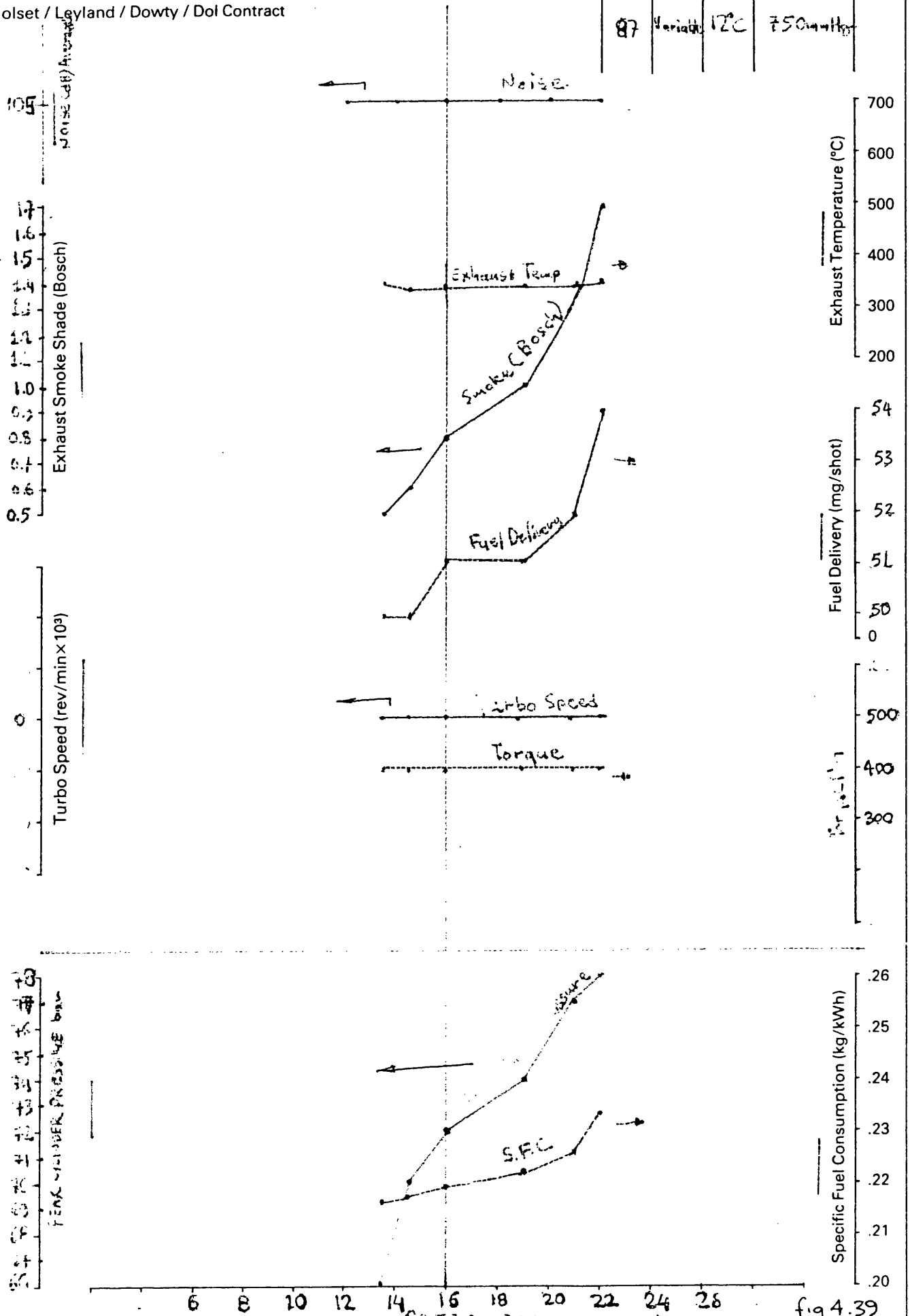

fig 4.39

COMPRESSOR PERFORMANCE

LEYLAND TL11/11 191 kW @ 2300
1155 Nm @ 1360 rev/min.
VARIABLE TURBINE RESTRICTION / TIMING / FUELLING.

HOLSET ENGINEERING CO. LTD.
HUDDERSFIELD

MODEL	H2C — 8625N Z31011 · MKII(b)

DATE	12-6-80
REF. No.	T1168

COMPRESSOR WHEEL 3504480

COMPRESSOR COVER 3504482

RESULTS FROM DYNAMIC OPTIMISATION

120,000
110,000
100,000
90,000
80,000
70,000
50,000

50% VG POSITION
0%
(BASE)
1350 rev/min
1100
1000
900
800
700
600
500
400
300
200
MINIMUM BRAKE LOAD.
76
72
70
65
60

TOTAL PRESSURE RATIO

3.4
3.2
3.0
2.8
2.6
2.4
2.2
2.0
1.8
1.6
1.4
1.2
1.0

0
200
400
600
800

AIRFLOW C.F.M. @ 15°

Fig 4.40

COMPRESSOR PERFORMANCE

HOLSET ENGINEERING CO. LTD.
HUDDERSFIELD

DATE	12-6-80
REF. No.	T 1168

MODEL	H2C — 8625N

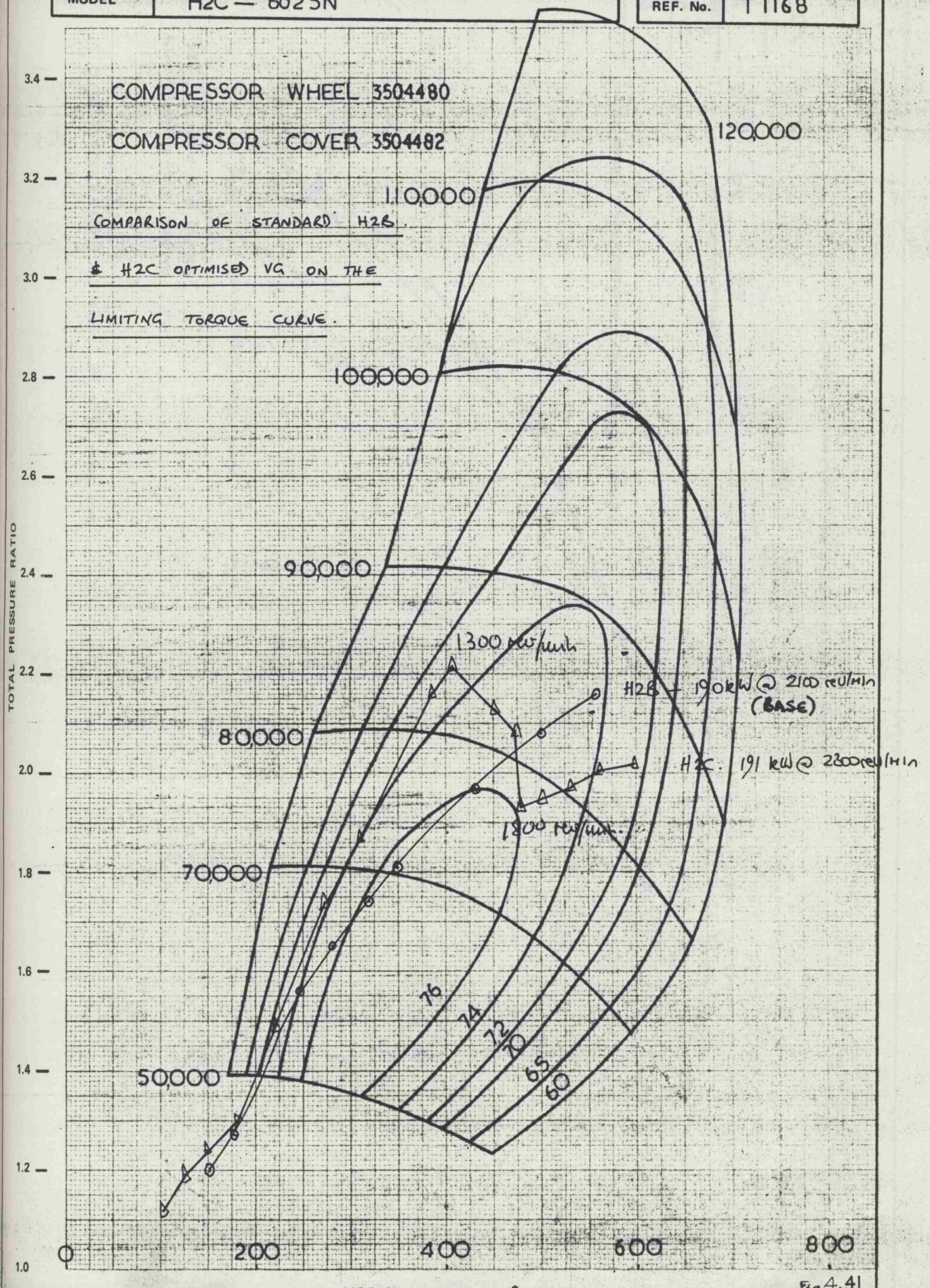

Fig 4.41

Date 19/2/83 Graph

Engine LEYLAND TL11 ENGINE—11.1L DISPLACEMENT Drawn By. E W Roberts

Title COMPARISON OF BASE H2B & OPTIMISED VG SWALLOWING CAPACITIES : (MK II (b))

Test No.	Timing	Amb'nt °C	Barometer Ins. Hg.
80	VARIABLE (22)	22	~

Holset / Leyland / Dowty / DoI Contract

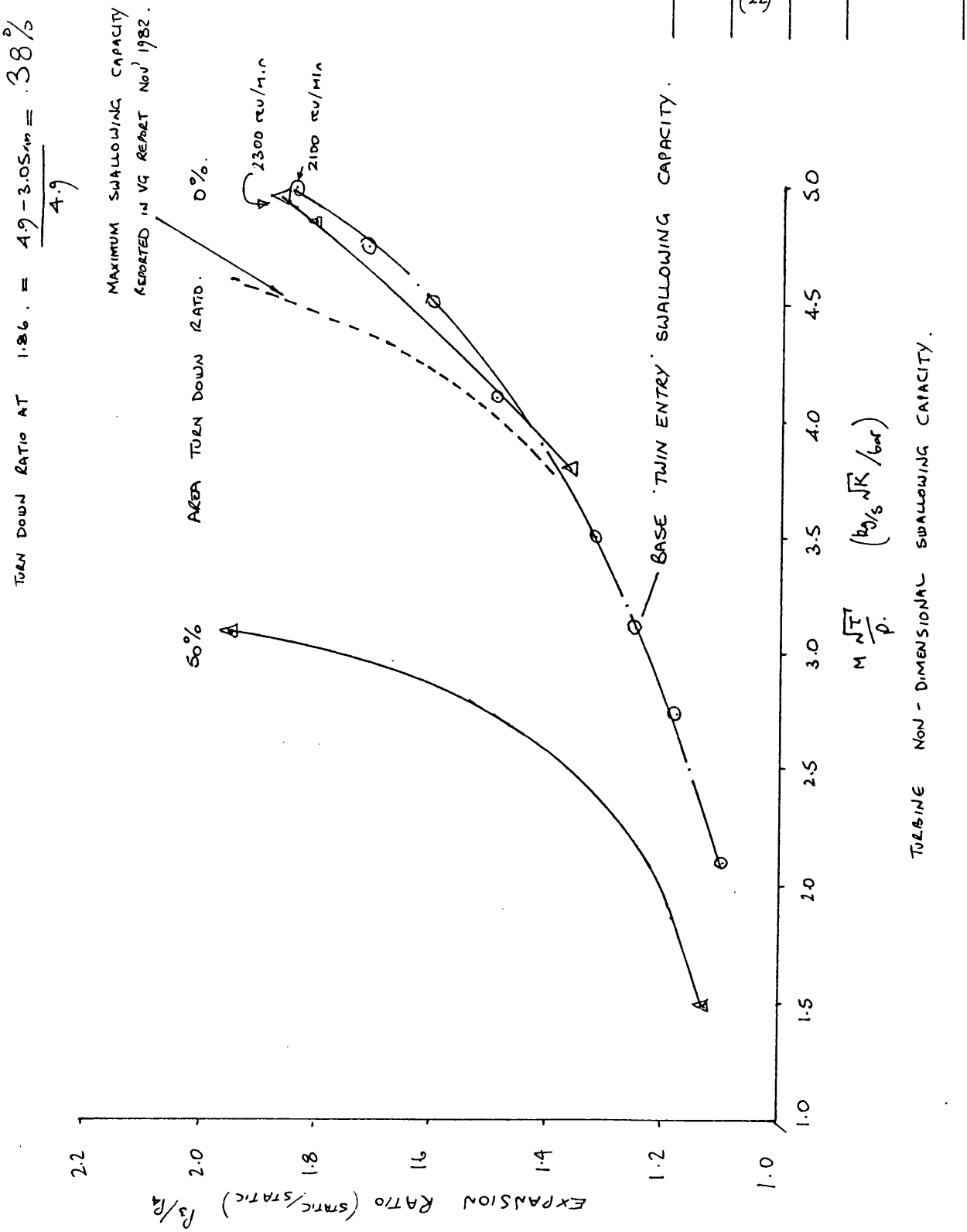

Fig 4.42

Engine LEYLAND TL11—7962756 Project No. E.W Roberts

Title COMPARISON OF BASE H2B. WITH OPTIMISED H2C PERFORMANCE (MK II 6)

Power Curve RATING: 191 kW. H2C BASE: 190 kW @ 2100 rev/min 1050 Nm @ 1300
191 kW @ 2300 rev/min 1150 Nm @ 1350

Test No.	Timing	Amb'nt °C	Barometer Ins. Hg.
82	VICASIS	22	763.

NOTE! BASE HAS NO BOOST CONTROL.

VG.
H2B. (BASE)

B.M.E.P. (bar)

Peak Cylinder Pressure. bar

Exhaust Smoke Shade (Bosch)

Power (kW)

Fuel Delivery (mg/shot)

Specific Fuel Consumption (kg/kWh)

Engine Speed (rev/min)

Fig 4.43 © 1983 University of Bath

Engine LEYLAND TL11—7962756 Project No. E.O. Roberts

Title COMPARISON OF BASE H2B WITH OPTIMISED H2C. (MK II b)

Power Curve BASE: 190 kW @ 2100 rev/min 1050 Nm @ 1300 rev/min.
H2C 191 kW @ 2300 rev/min. 1150 Nm @ 1350 rev/min.

Test No.	Timing	Amb'nt °C	Barometer Ins. Hg.
B2	VARIABLE (22)	22	753

Note! BASE HAS NO BOOST CONTROL.

H2C

H2B (BASE)

ADVANCE WITH DECREASING SPEED TO REDUCE SMOKE (AT EXPENSE OF SFC)

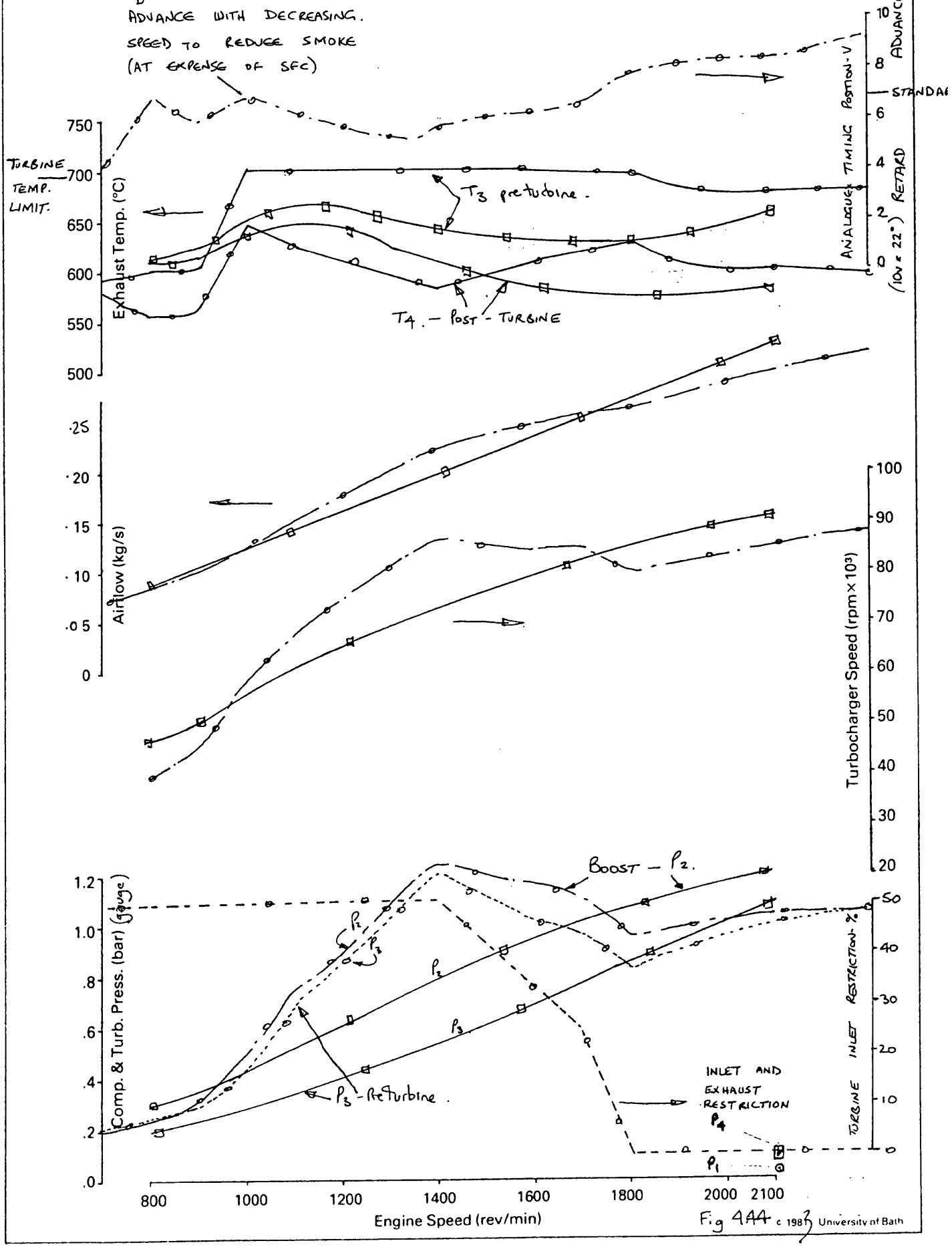

Fig 444 © 1987 University of Bath

Engine LEYLAND TL11 ENGINE—11.1L DISPLACEMENT

Drawn By E W Roberts

Title COMPARISON OF VOLUMETRIC & COMPRESSOR EFFICIENCY

Rating—190 kW at 2300 rev/min

OPTIMISED VG - MK II(b)

Holset / Leyland / Dowty / DoI Contract

Test No.	Timing	Amb'nt °C	Barometer Ins. Hg.
73 - 82	Variable	22	753

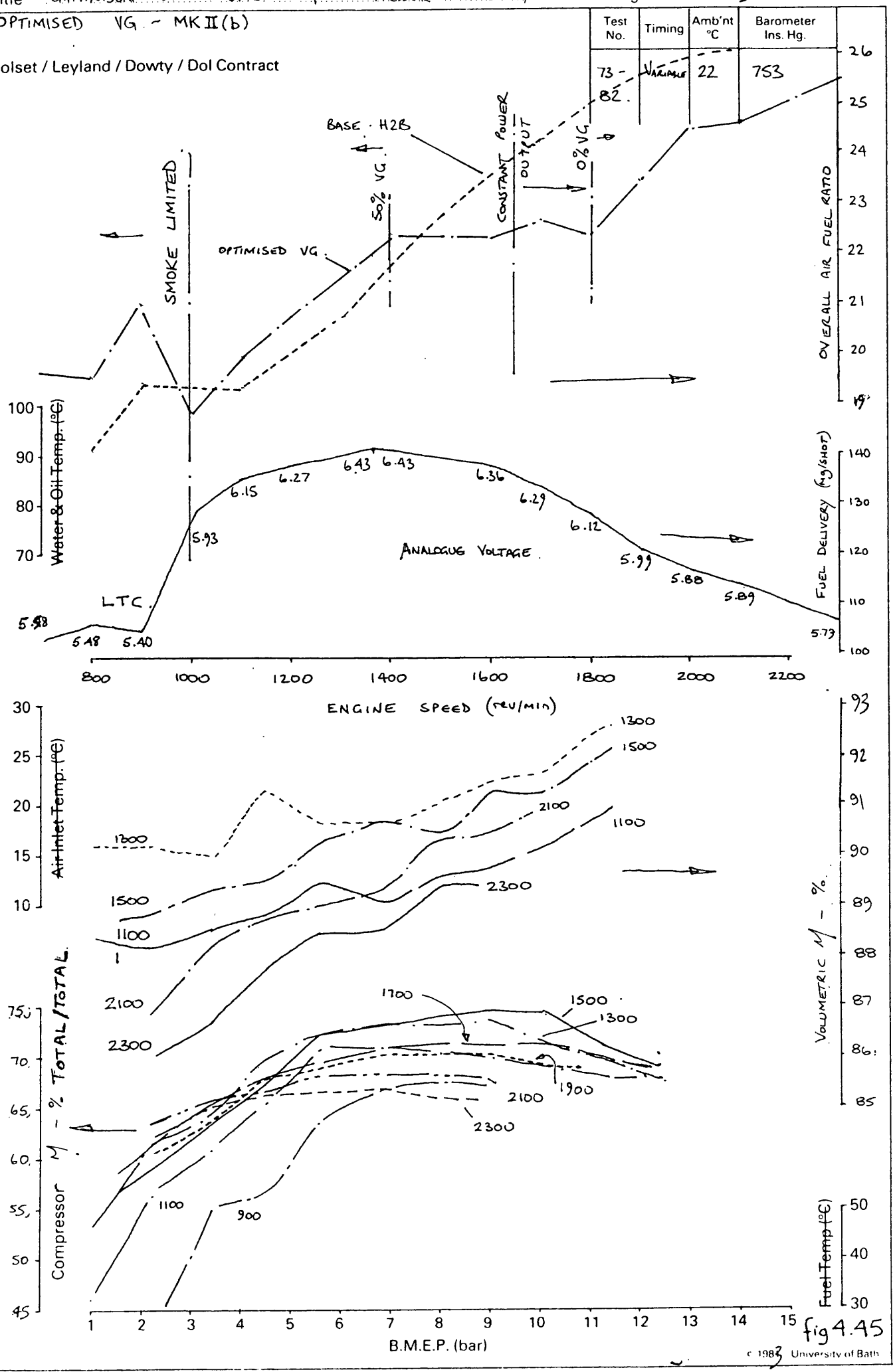

fig 4.45

Engine LEYLAND TL11 ENGINE—11.1L DISPLACEMENT Drawn By E W Roberts

Engine LEYLAND TL11 ENGINE—11.1L DISPLACEMENT Drawn By E W Roberts

Title ISO - CONSUMPTION CURVES H2B80B1C L25A3 - BASE PERFORMANCE

Test No.	Timing	Amb'nt °C	Barometer Ins. Hg.
	22		

Holset / Leyland / Dowty / DoI Contract

Holset / Leyland / Dowty / DoI Contract

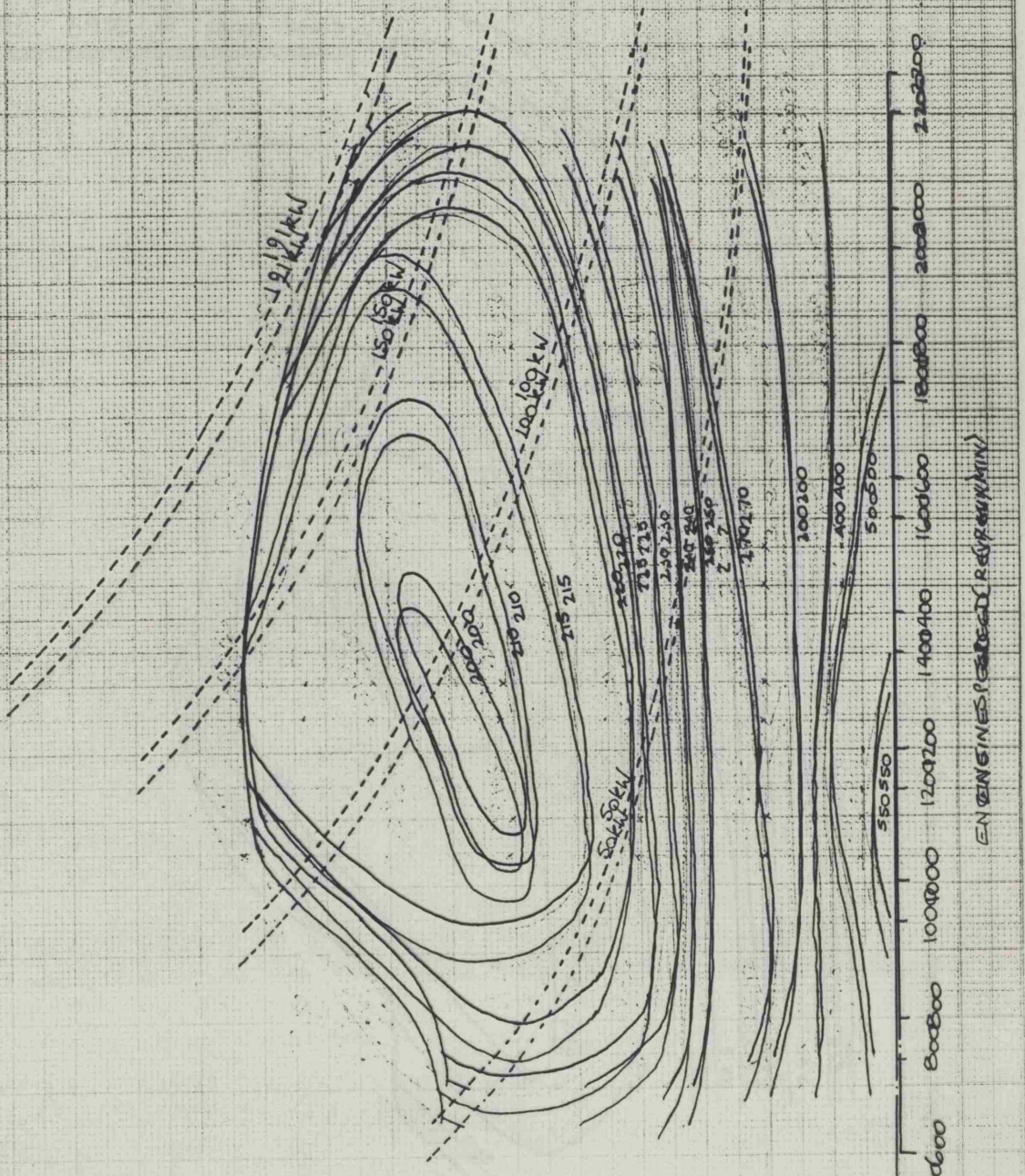

fig 4.46

Engine LEYLAND TL11 ENGINE—11.1L DISPLACEMENT Drawn By. C W Roberts.

Title ISO - CONSUMPTION CURVES H28 80 81C L25A3 - BASE PERFORMANCE

Test No.	Timing	Amb'nt °C	Barometer Ins. Hg.
	22		

Holset / Leyland / Dowty / DoI Contract

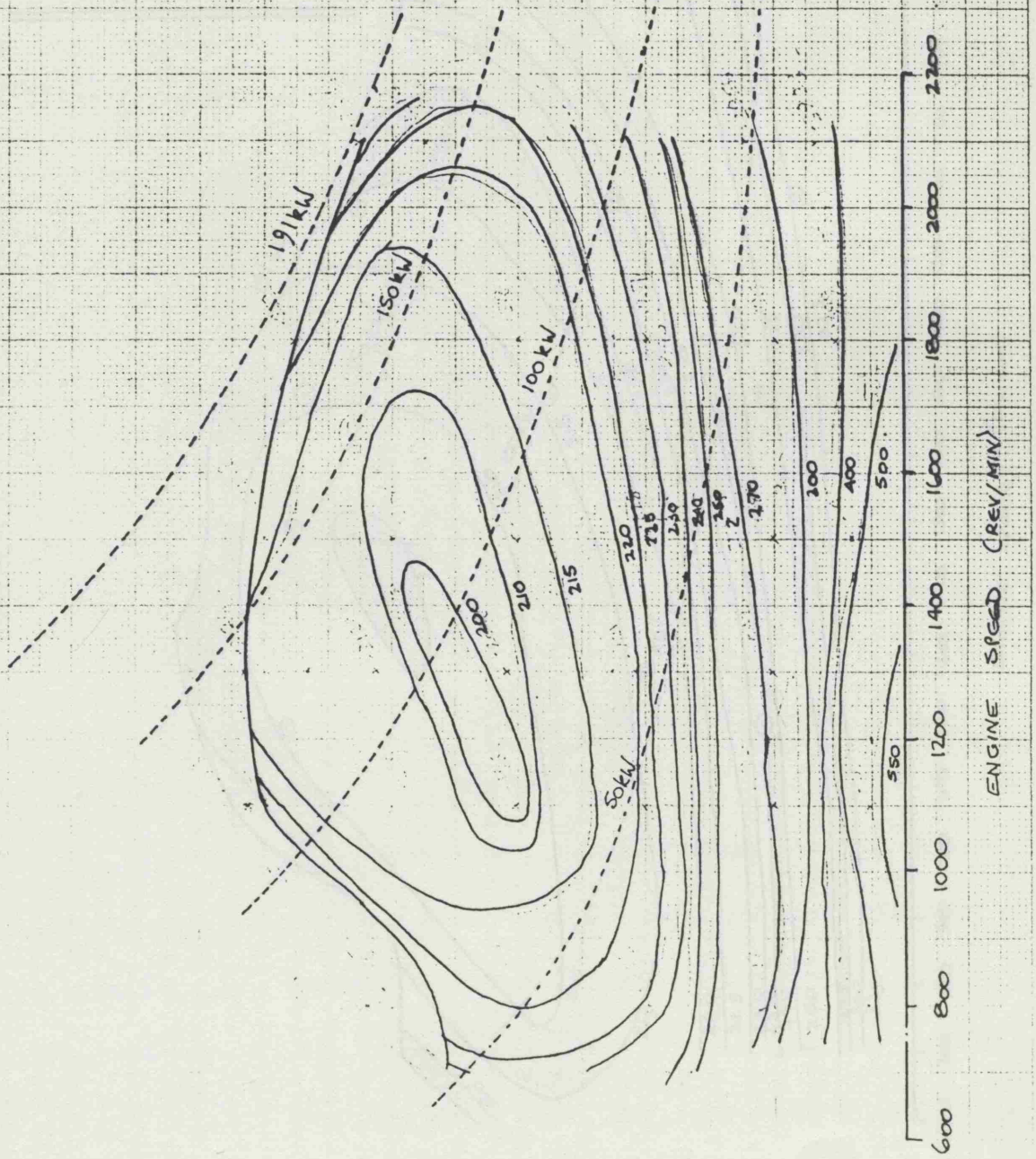

ENGINE TORQUE - Nm

1200 1100 1000 900 800 700 600 500 400 300 200 100 0

Fig 4.46

Engine LEYLAND TL11 ENGINE—11.1L DISPLACEMENT Drawn By. E W ROBERTS

Title ISO - CONSUMPTION CURVES - H2C 8625 Z31U11 - MK II (b)

STEADY STATE OPTIMISATION

Test No.	Timing	Amb'nt °C	Barometer Ins. Hg.
73 82	VARIABLE	25	—

Holset / Leyland / Dowty / DoI Contract

OPTIMISED WITH REGARD TO (TURBINE INLET AREA) BOOST & FUEL INJECTION TIMING.

191 kW @ 2300 rev/min.

1155 Nm @ 1360 rev/min.

46% TORQUE BACK UP.

@ 59% OF RATED SPEED.

CONTROL PARAMETERS

① INJECTION TIMING : DYNAMIC VARIABLE DEVICE.

② FUEL PUMP : CAV MAJORMEC P5534/A
ELECTRONIC GOVERNING.
DIRECT RACK OR ALL SPEED.
REMOTE VARIABLE FUEL STOP.

③ TURBOCHARGER : HOLSET H2C 8625 Z31U11.
WITH VARIABLE AREA TURBINE STAGE

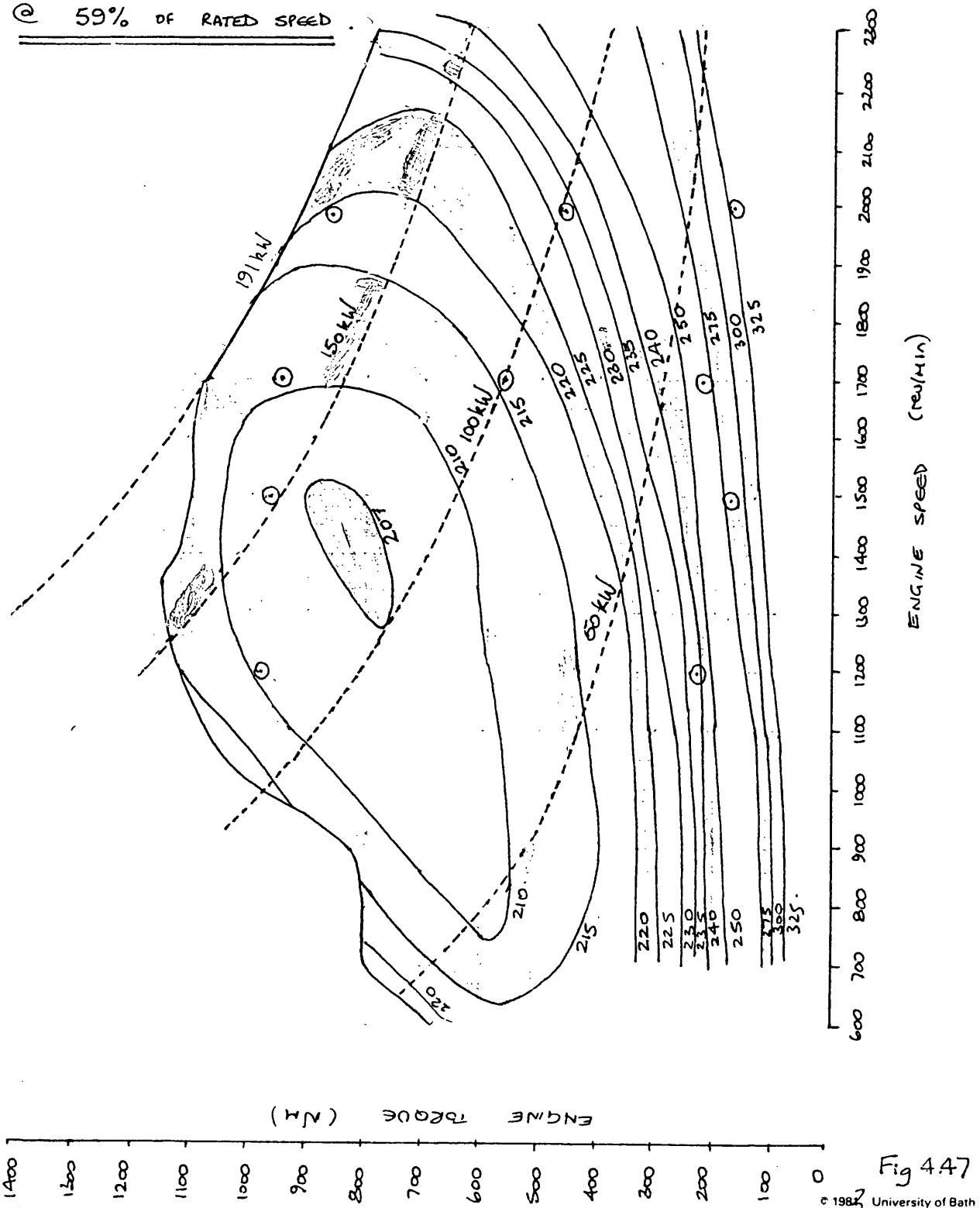

Fig 447

Date ..... Graph .....

Engine LEYLAND TL11 ENGINE—11.1L DISPLACEMENT Drawn By. E W ROBERTS

Title COMPARISON OF SFC FOR VARIOUS L11 CONFIGURATIONS

Test No.	Timing	Amb'nt °C	Barometer Ins. Hg.
~	~	~	~

Holset / Leyland / Dowty / DoI Contract

QUANTIFIED BENEFITS

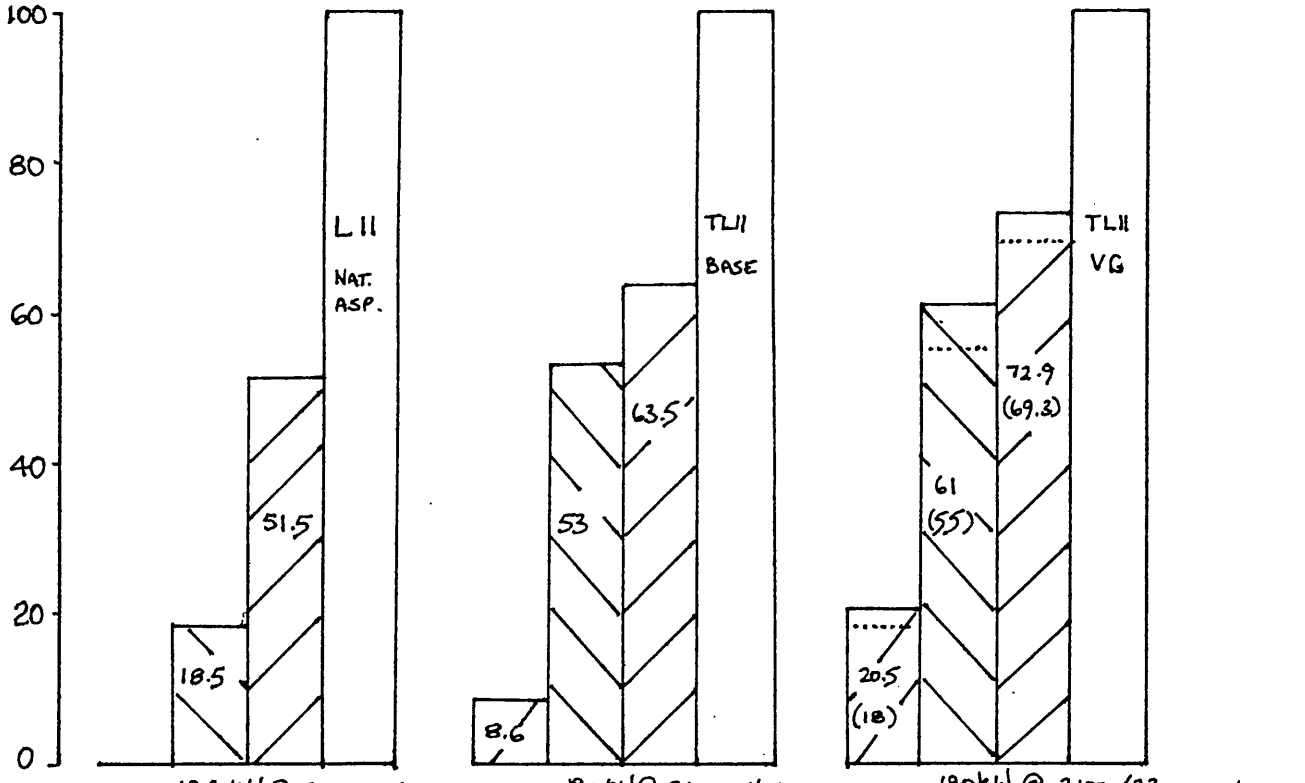

210 225 240

THE CROSS HATCHED BARS REPRESENT THE PERCENTAGE OF THE WHOLE USEABLE FUEL EFFICIENCY ENVELOPE AT BETTER THAN 210, 225 and 240 g/kWh SPECIFIC FUEL CONSUMPTION. THE FIGURES FOR THE VG CONFIGURATION SHOW THE BENEFIT OF HOLDING TO A 2100 rev/min limit.

fig 4.48

Engine LEYLAND TEST ENGINE — 11.1L DISPLACEMENT Drawn By. D. HOWARD

Title BOOST PRESSURE (KN/m^2 above 1 BAR) AS A FUNCTION OF SPEED & LOAD

STEADY-STATE OPTIMISATION

Test No.	Timing	Amb'nt °C	Barometer Ins. Hg.
73 - 82	VARIABLE	22	—

Holset / Leyland / Dowty / DoI Contract

191 KW @ 2300rpm 1155 Nm @ 1360rpm

46% TORQUE BACK UP @ 59% OF RATED SPEED

LINES OF CONSTANT INLET MANIFOLD PRESSURE

KN/m^2 above 1 BAR

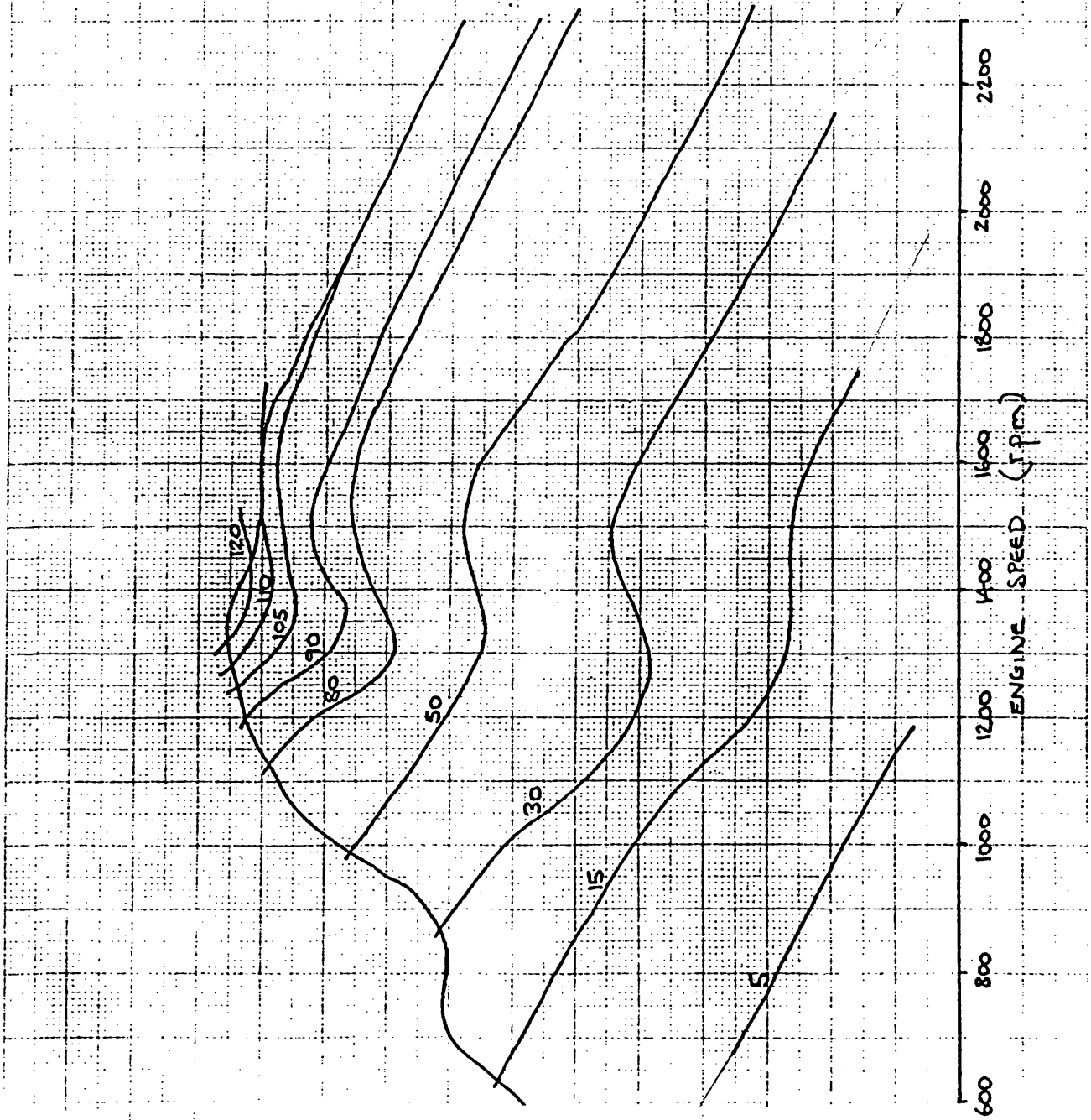

ENGINE TORQUE (Nm)

1200 1100 1000 900 800 700 600 500 400 300 200 100 0

fig 4.49

Engine LEYLAND TL11 ENGINE—11.1L DISPLACEMENT Drawn By. E W ROBERTS.

Title TURBINE INLET RESTRICTION (SMOOTHED) - % AS A FUNCTION OF SPEED & LOAD.

STEADY STATE OPTIMISATION.

Holset / Leyland / Dowty / Dol Contract

Test No.	Timing	Amb'nt °C	Barometer Ins. Hg.
73-82	Variable	25	~.

191 kW @ 2300 rev/min } 46% Torque - back-up @
1155 Nm @ 1350 rev/min } 59% of RATED SPEED.

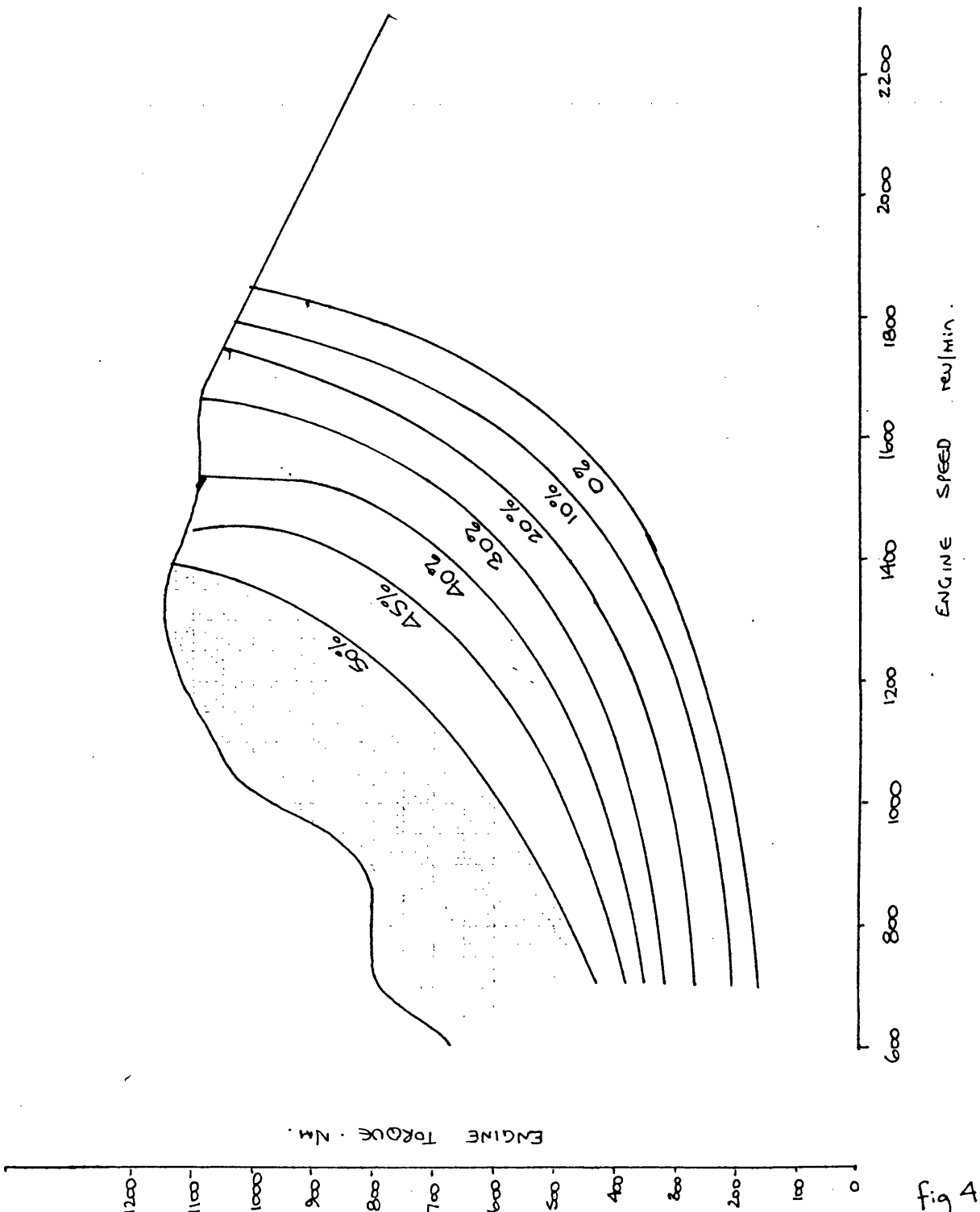

fig 4.50

Engine LEYLAND TL11 ENGINE—11.1L DISPLACEMENT

Drawn By. Eio Roberts

Title BOSCH SMOKE FOR THE OPTIMISED VG BUILD (MK II (b))

STEADY STATE OPTIMISATION

Holset / Leyland / Dowty / DoI Contract

Test No.	Timing	Amb'nt °C	Barometer Ins. Hg.
73-82	VARIABLE	22.	~

191 kW @ 2300 rev/min.

1155 Nm @ 1350 rev/min.

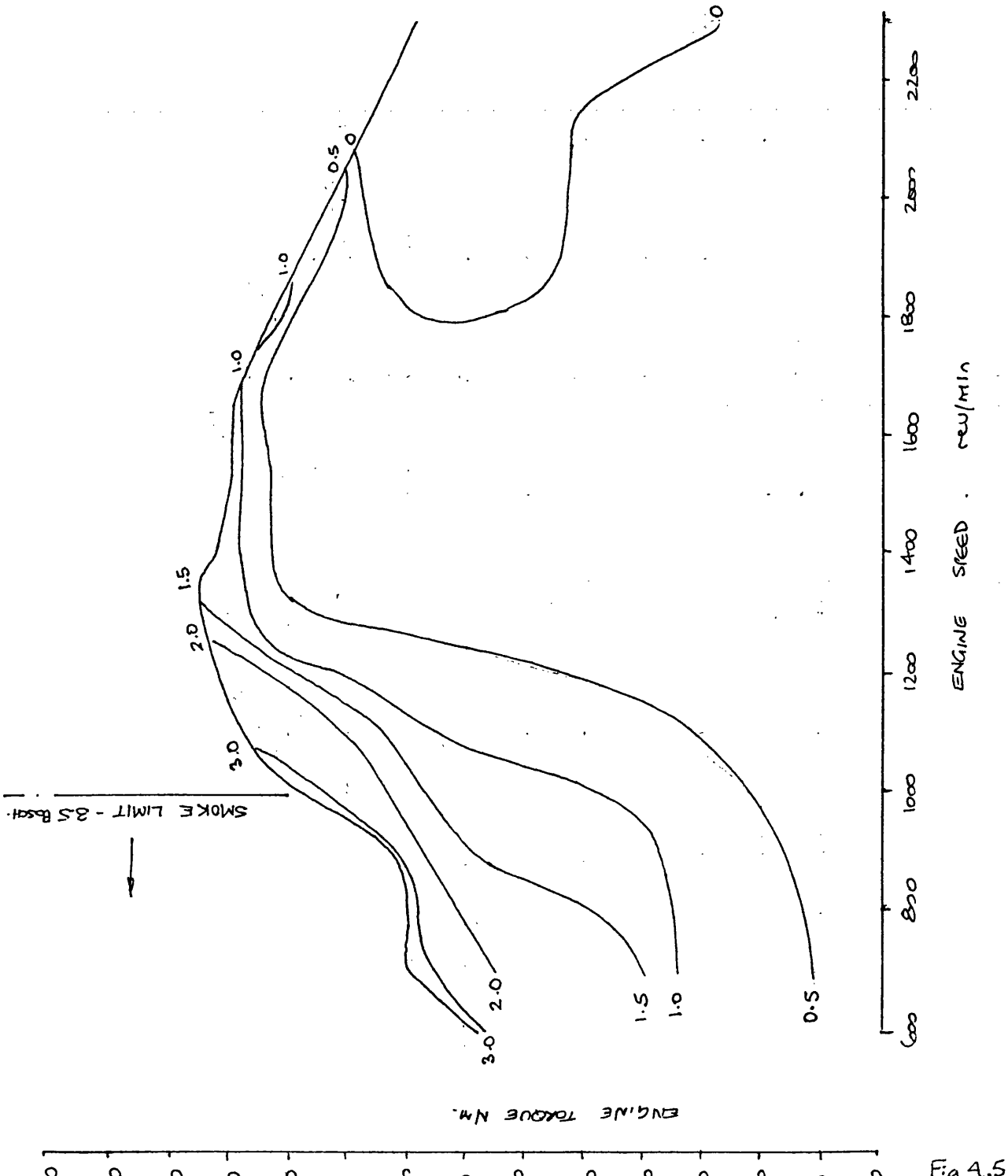

Fig 4.51

Engine LEYLAND TL11 ENGINE—11.1L DISPLACEMENT Drawn By. E.W.Roberts.

Title VARIABLE TIMING (STATIC) °BTDC or analogue voltage ( ) - as a function of speed & load.

STEADY STATE OPTIMISATION.

Holset / Leyland / Dowty / DoI Contract

Test No.	Timing	Amb'nt °C	Barometer Ins. Hg.
73-82	VARIABLE	25°C	

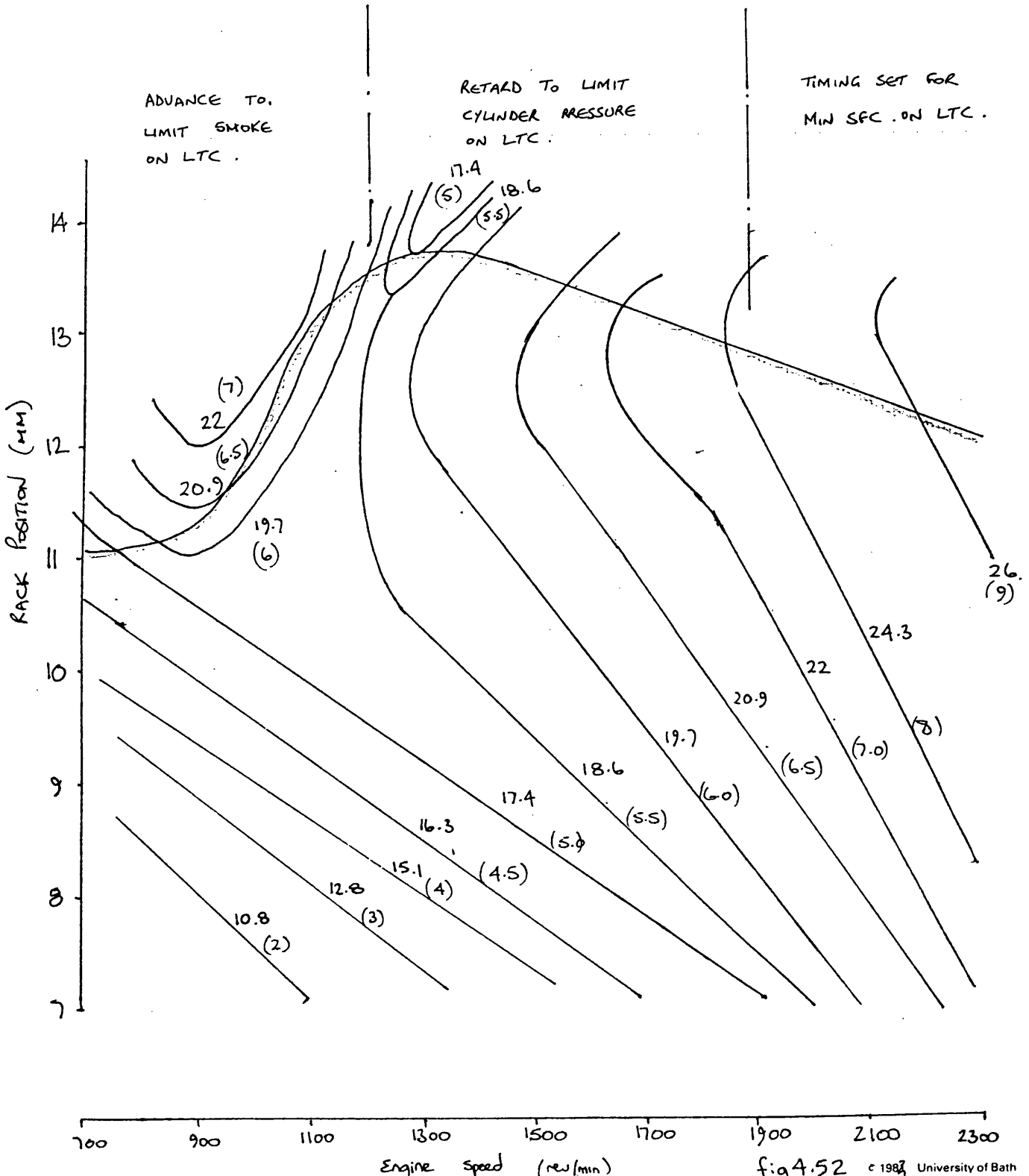

fig 4.52

Date..... Graph.....

Engine LEYLAND TL11 ENGINE—11.1L DISPLACEMENT Drawn By. E W ROBERTS

Title 3-D OPTIMISATION SURFACE OF VARIATION OF ENGINE BOOST PRESSURE

Holset / Leyland / Dowty / DoI Contract

Test No.	Timing	Amb'nt °C	Barometer Ins. Hg.
73 – 82	VARIABLE	25	—

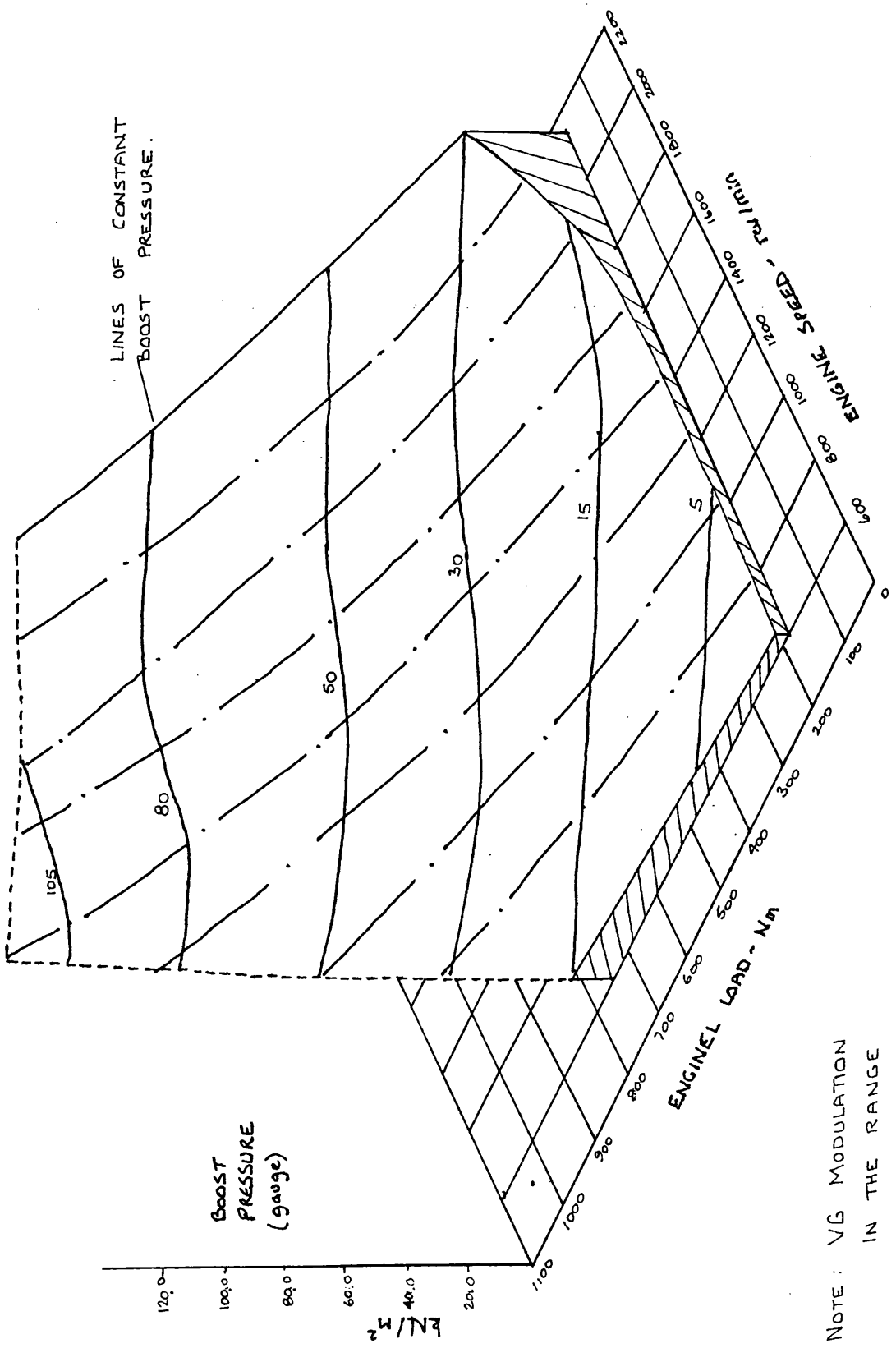

NOTE: VG MODULATION IN THE RANGE 1200 - 1600 rev/min

fig 4.53

Date..... Graph.....

Engine LEYLAND TL11 ENGINE—11.1L DISPLACEMENT Drawn By.... E.W. ROBERTS

Title.... 3-D ..... OPTIMISATION ..... SURFACE ..... OF ..... VARIATION ..... OF ..... INJECTION ..... TIMING .....

Test No.	Timing	Amb'nt °C	Barometer Ins. Hg.
73 – 82	VARIABLE	25	--

Holset / Leyland / Dowty / DoI Contract

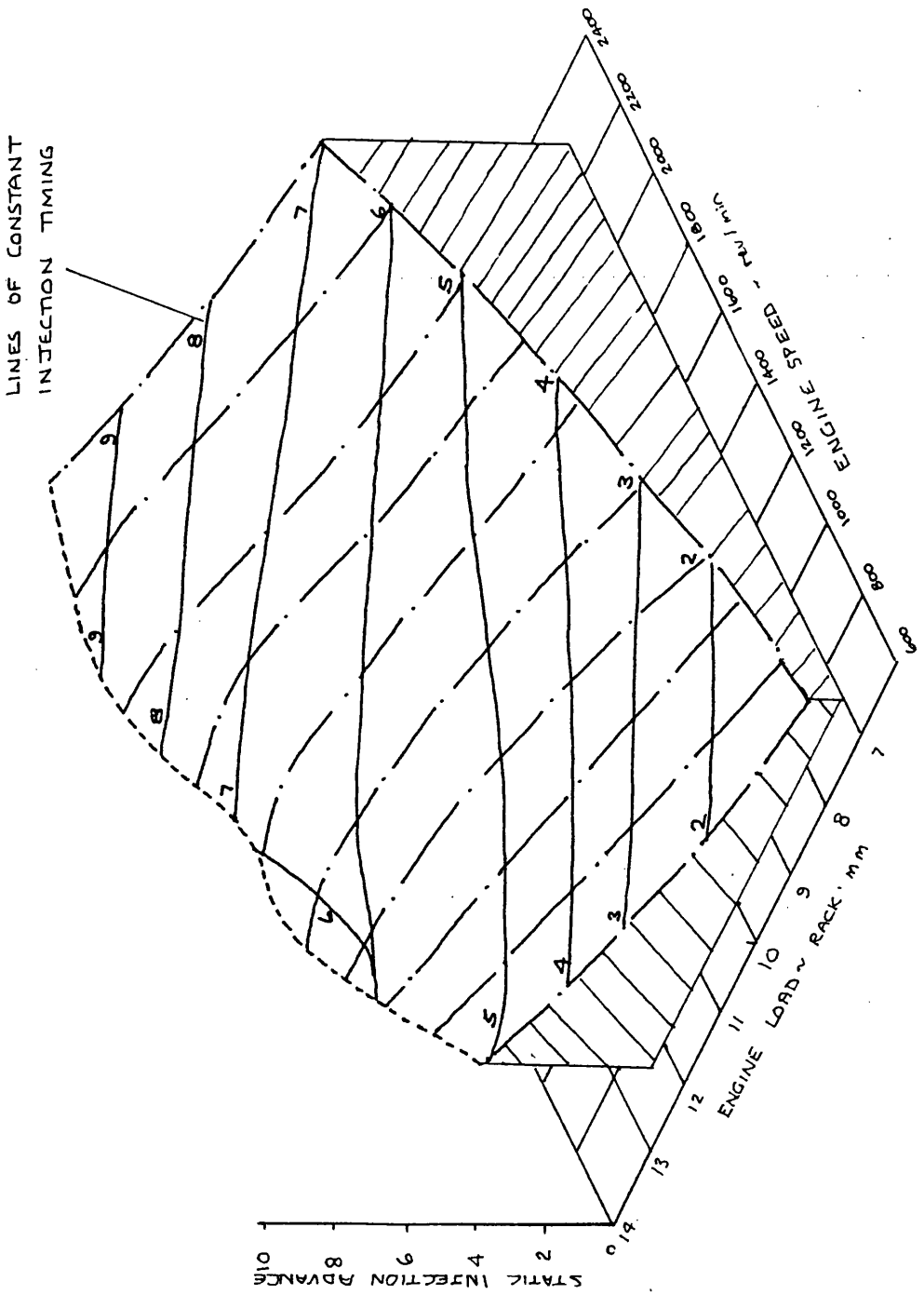

fig 4.54

Date ..... Graph .....

Engine LEYLAND TL11 ENGINE—7962756—CELL 2 Drawn By E.W. ROBERTS

Title COMPARISON OF BASE H2B WITH OPTIMISED VG (MK II 14)

Power Curve Rating—190 kW at 2100 rev/min

Electronic Instrumentation RESULTS

Holset / Leyland / Dowty / DoI Contract

Test No.	Timing	Amb'nt °C	Barometer mm Hg.
–	VARIABLE	25	~

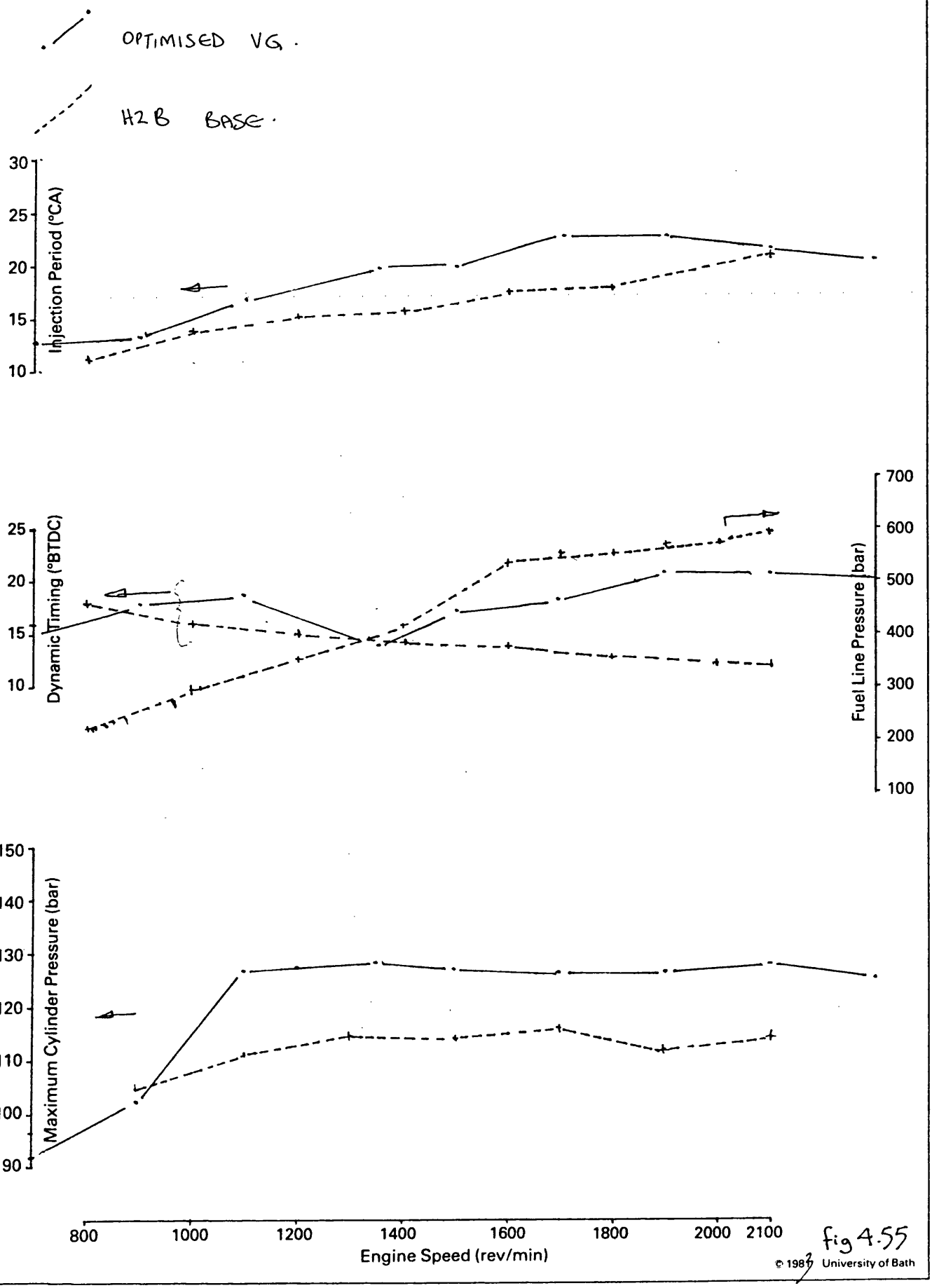

fig 4.55

Engine LEYLAND TL11—7962756 Project No. E.D. ROBERTS

Title BASE LTC. H28.80BIC L25A3. VIBROMETER. T/TRANSDUCER

Power Curve

Test No.	Timing	Amb'nt °C	Barometer Ins. Hg.
83	22.	20	730.5.

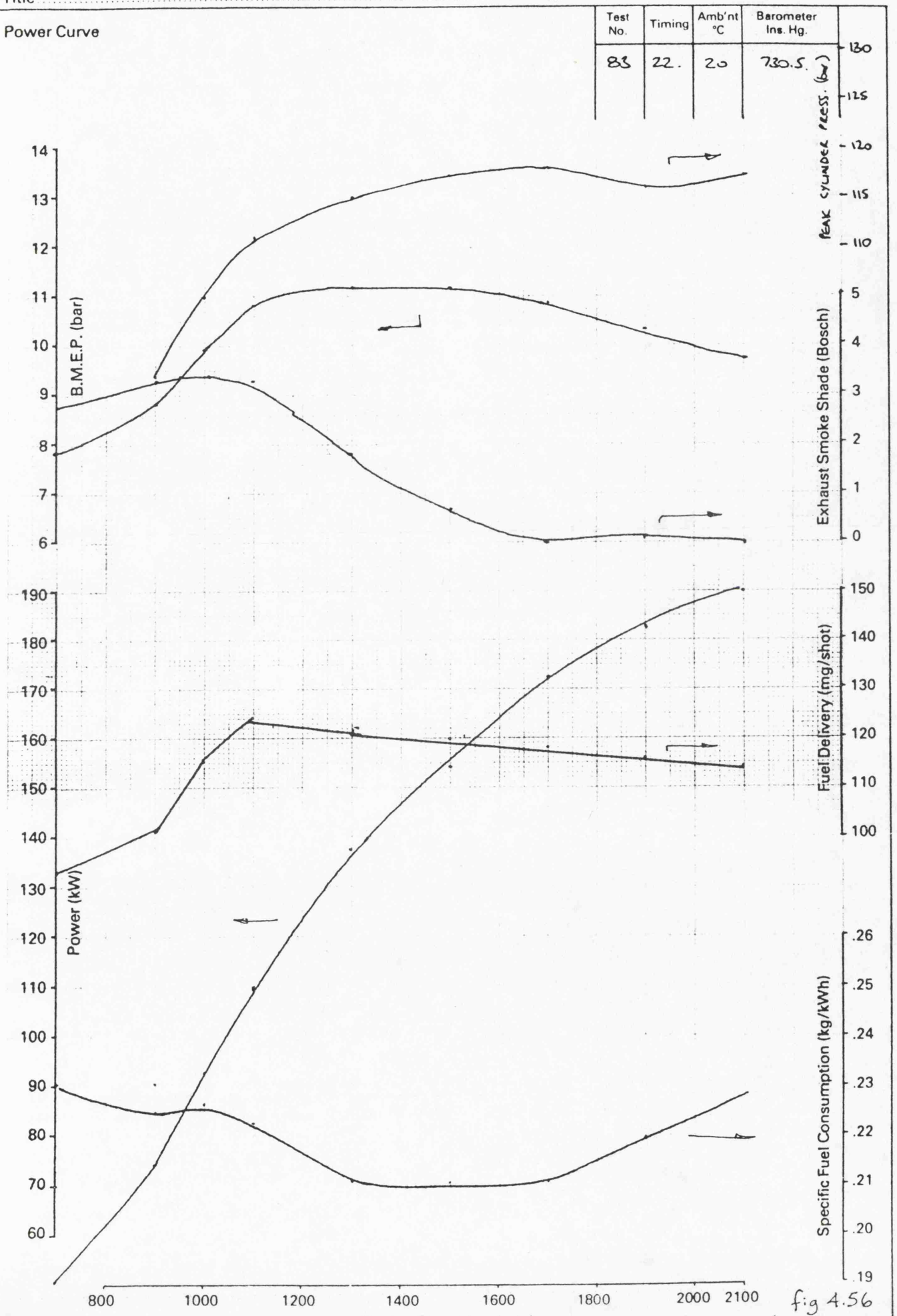

fig 4.56

Engine LEYLAND TL11 ENGINE—11.1L DISPLACEMENT Drawn By.....E.W.ROBERTS.....

Title.....SIMPLIFIED TIMING SCHEDULE.....

Test No.	Timing	Amb'nt °C	Barometer Ins. Hg.
~	~	~	~

Holset / Leyland / Dowty / DoI Contract

TIMING ~ ANALOGUE VOLTAGE · V.

0-10 v ≈ 22° @ flywheel

EQUATION: TIMING = 1/250 (rev/min − 500) + 1/3.125 (rack − 5)

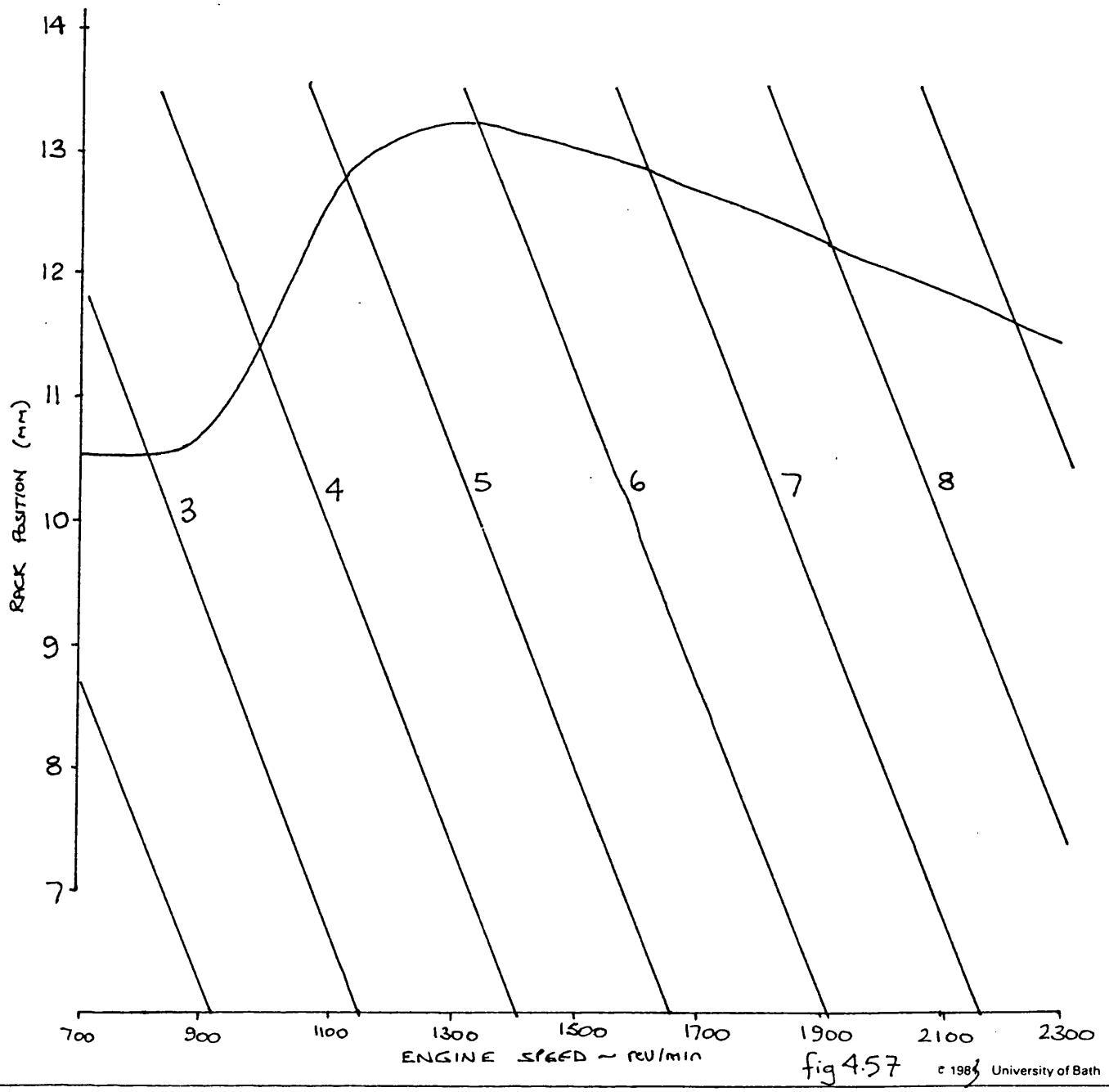

fig 4.57

Date 11.01.85 Graph

Engine LEYLAND TL11 ENGINE—11.1L DISPLACEMENT Drawn By. Ed Roberts

Title SIMPLIFIED BOOST SCHEDULE .

Test No.	Timing	Amb'nt °C	Barometer Ins. Hg.
~	~	~	~

Holset / Leyland / Dowty / DoI Contract

BOOST PRESSURE RELATIVE TO 750 mm hg (abs)

BOOST VERSUS RACK CHARACTERISTIC @ 1400 rev/min.

STRAIGHT LINE FIT GIVEN BY : BOOST = 205 (rack − 9.4)

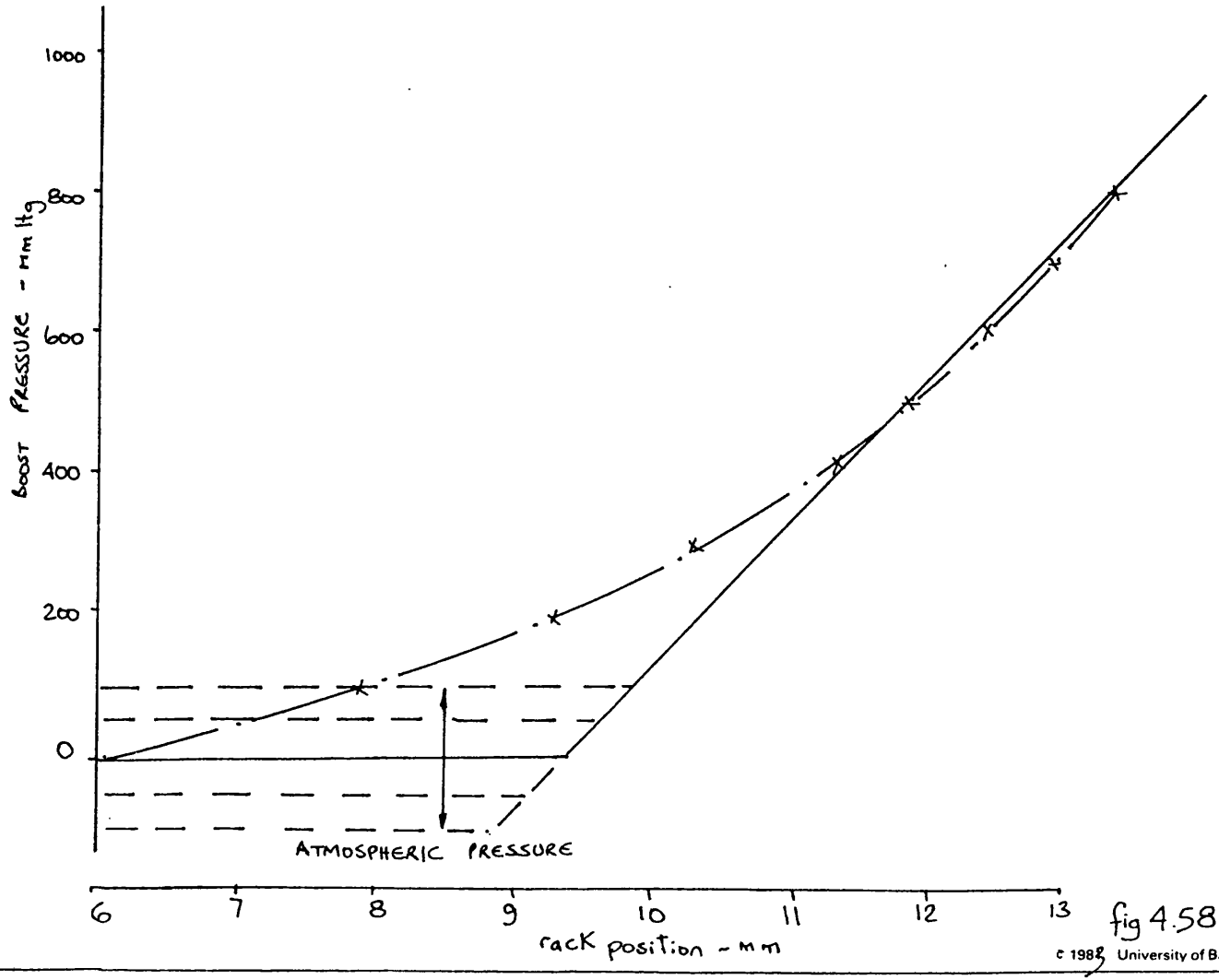

fig 4.58

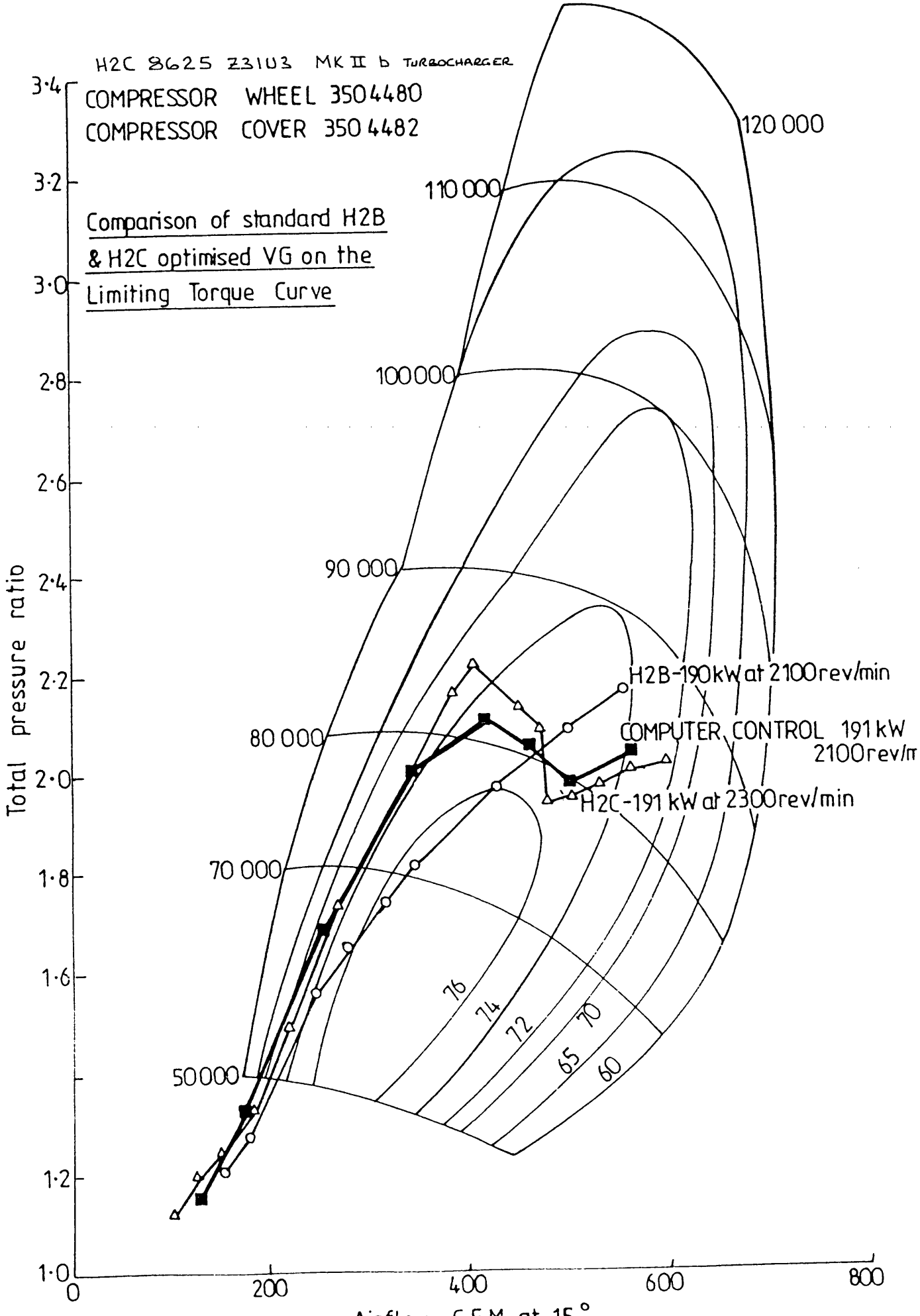
H2C 8625 Z3103 MK II b TURBOCHARGER
COMPRESSOR WHEEL 3504480
COMPRESSOR COVER 3504482
Comparison of standard H2B & H2C optimised VG on the Limiting Torque Curve
120 000
110 000
100 000
90 000
80 000
70 000
50 000
76
74
72
70
65
60
H2B-190kW at 2100rev/min
COMPUTER CONTROL 191 kW 2100rev/m
H2C-191 kW at 2300rev/min
Total pressure ratio
3·4
3·2
3·0
2·8
2·6
2·4
2·2
2·0
1·8
1·6
1·2
1·0
0
200
400
600
800
Airflow CFM at 15°

FIG. 4.59

Engine LEYLAND TL11 ENGINE—11.1L DISPLACEMENT Drawn By DH.

Title SWALLOWING CAPACITY UNDER ELECTRO-HYDRAULIC ACTUATION

H2C 8625N 73103 · ELECTRONIC OPERATION MKII b

Holset / Leyland / Dowty / DoI Contract

Test No.	Timing	Amb'nt °C	Barometer Ins. Hg.
98	~VARIABLE	25~	~

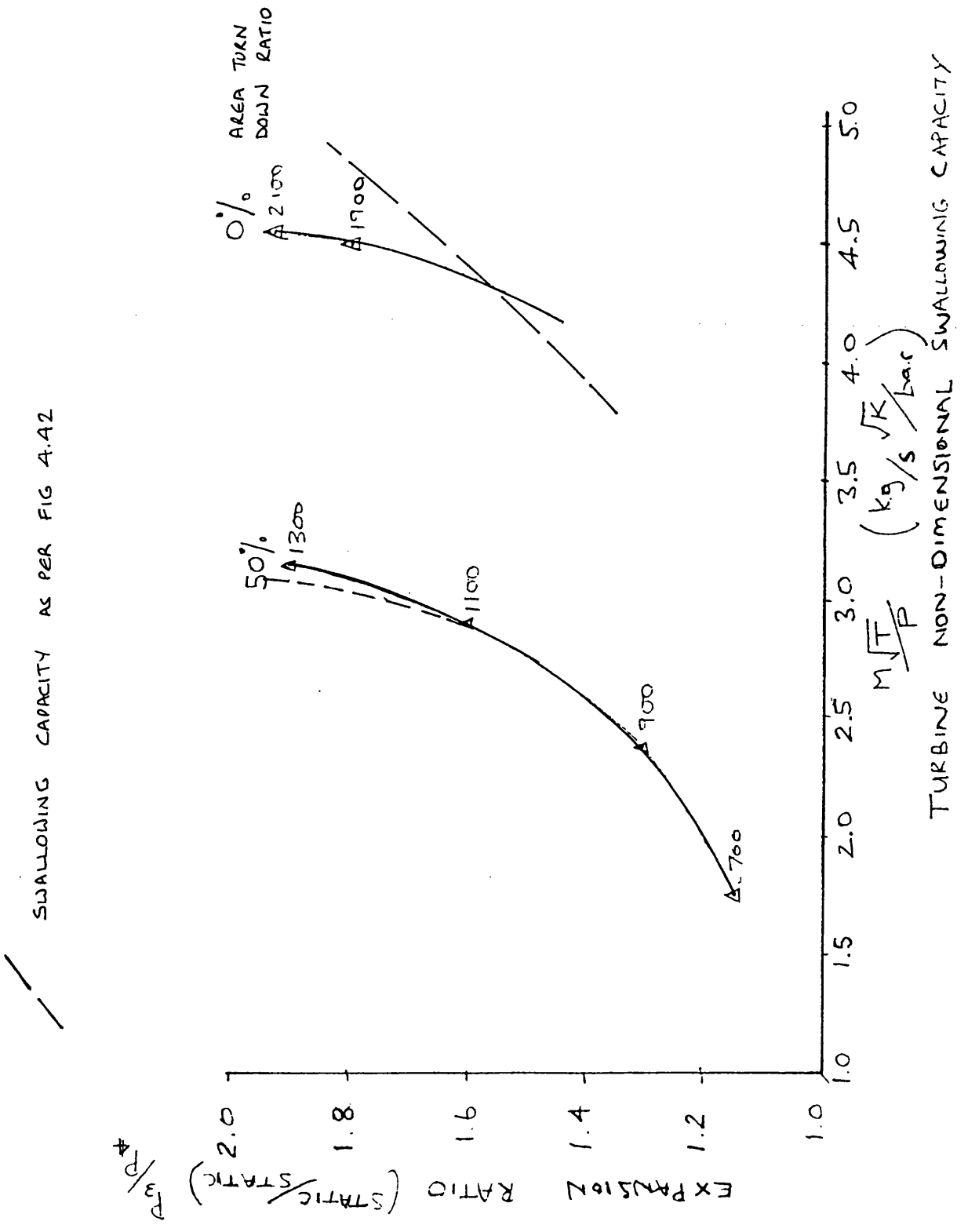

fig 4.60

Engine LEYLAND TL11—7962756 Project No. E.D. ROBERTS

Title COMPARISON OF OPTIMISED SCHEDULE WITH SIMPLIFIED ALGORITHM

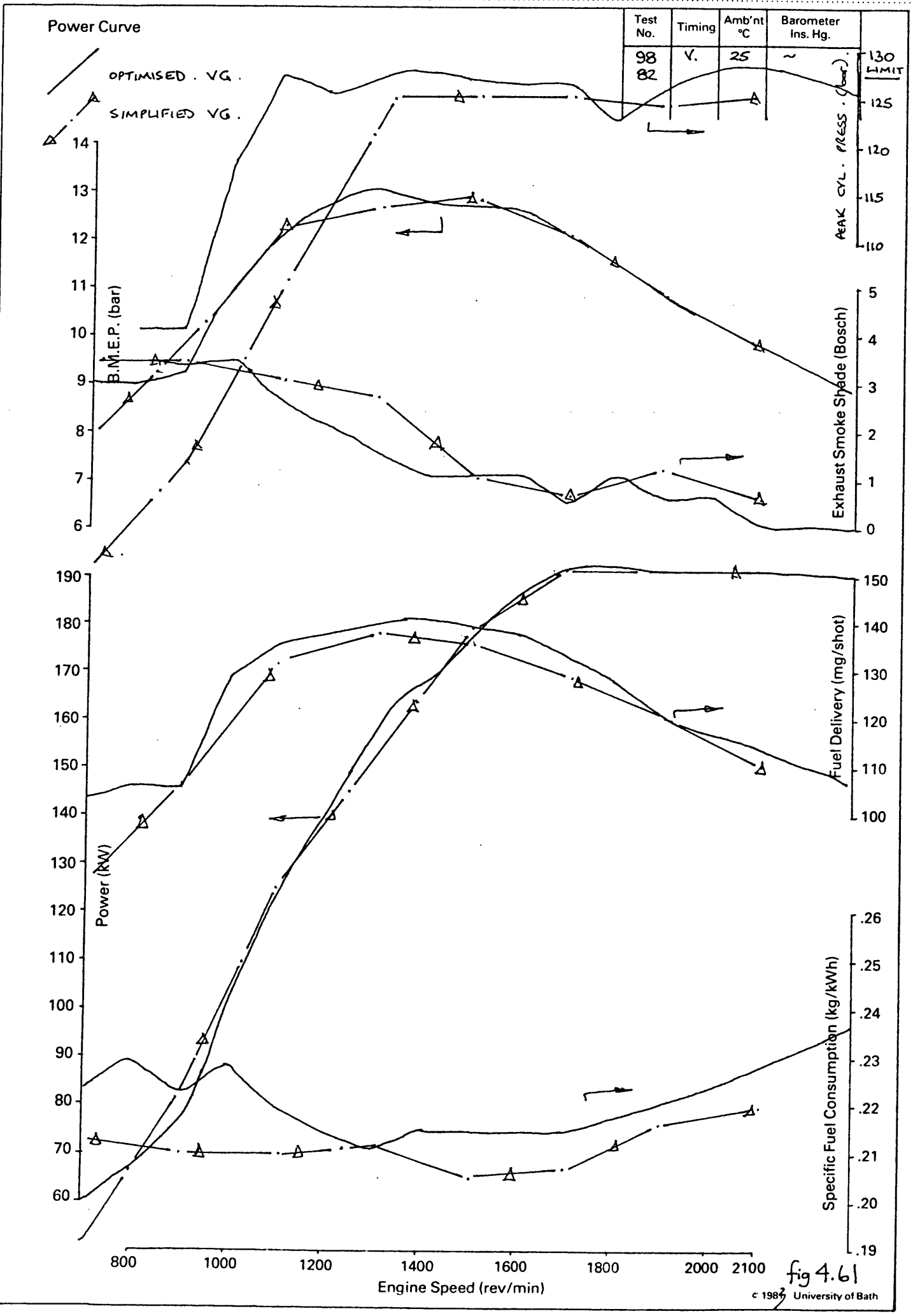

fig 4.61

Engine LEYLAND TL11—7962756 Project No. E.D. ROBERTS

Title COMPARISON OF OPTIMISED SCHEDULE WITH SIMPLIFIED ALGORITHM

Power Curve

Test No.	Timing	Amb'nt °C	Barometer Ins. Hg.
98 82	V	25	–

OPTIMISED VG

SIMPLIFIED VG (COMPOTER CONTROL)

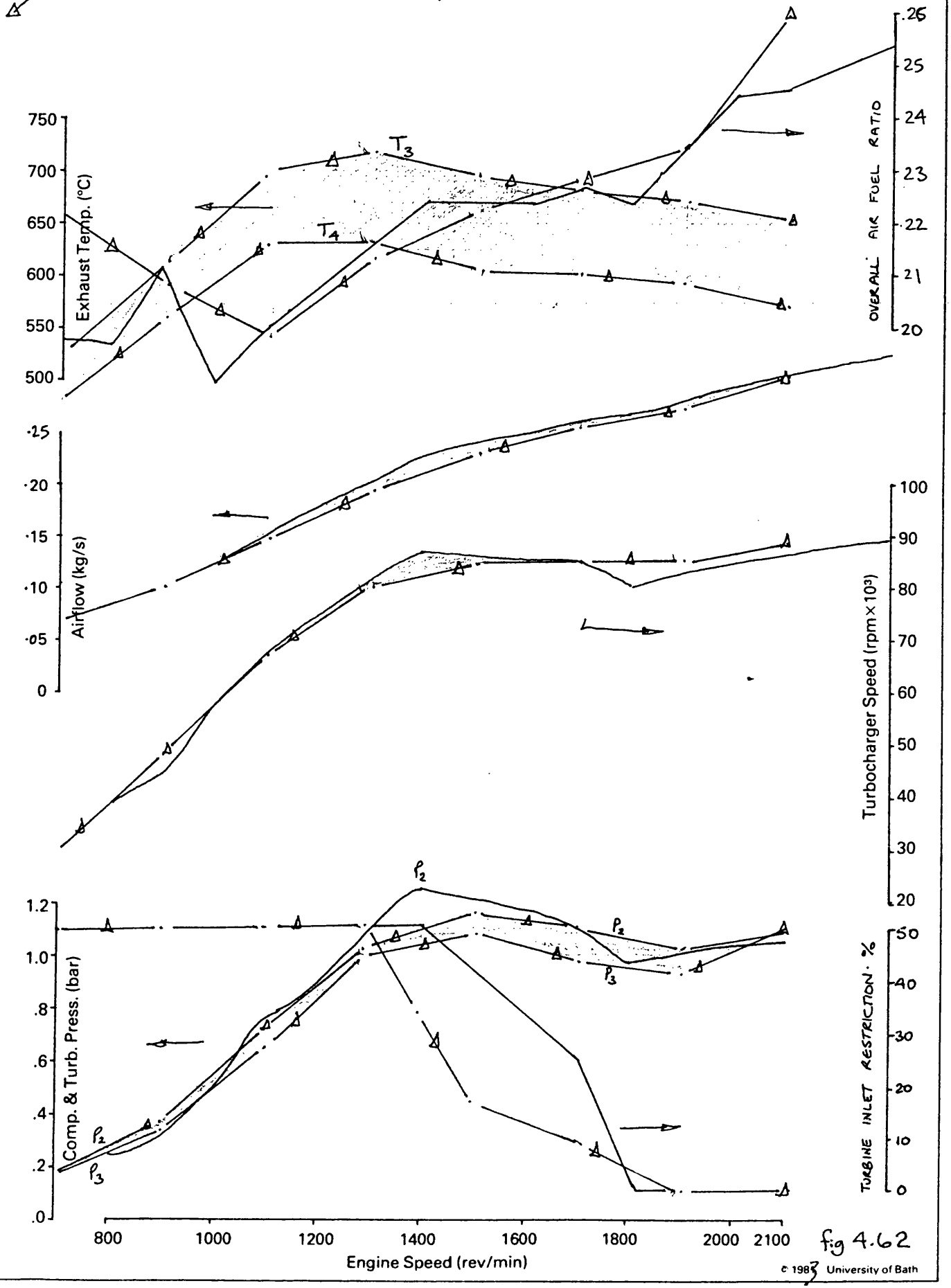

fig 4.62

ISO - CONSUMPTION CURVES UNDER COMPUTER CONTROL

S.F.C. — g / kW. hr. ~ SIMPLIFIED ALGORITHM.

Test No.	Timing	Amb'nt °C	Barometer Ins. Hg
90 98	V.	25	~

HOLSET H2C 8625N 231U3 TURBOCHARGER · MKII(b)

UNDER ELECTRONIC CONTROL.

191 kW @ 2100 rev/min

1100 Nm @ 1300 rev/min

27% TORQUE BACK UP

@ 62% OF RATED SPEED

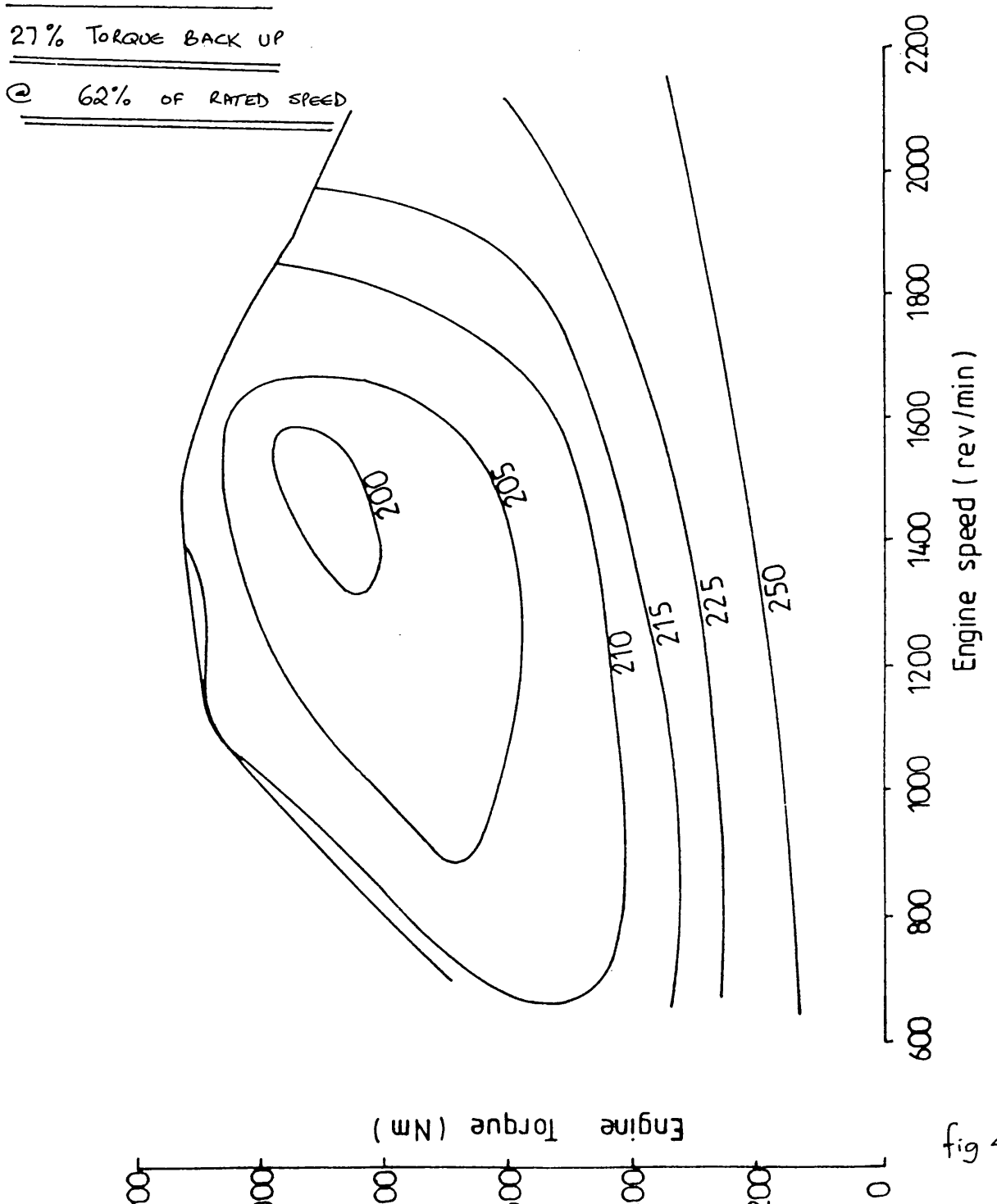

fig 4.63

Engine LEYLAND TL11 ENGINE—11.1L DISPLACEMENT Drawn By UTL

Title 150 – BOOST CURVES UNDER COMPUTER CONTROL

Holset / Leyland / Dowty / DoI Contract

Test No.	Timing	Amb'nt °C	Barometer Ins. Hg.
90-98	VARIABLE	25	~

STATIC BOOST OVER 750 mmHG ABS.

LINES OF CONSTANT INLET MANIFOLD PRESSURE WITH

LINES OF CONSTANT RESTRICTION SUPERIMPOSED.

ELECTRONICALLY CONTROLLED TURBOCHARGER · MK II (6)

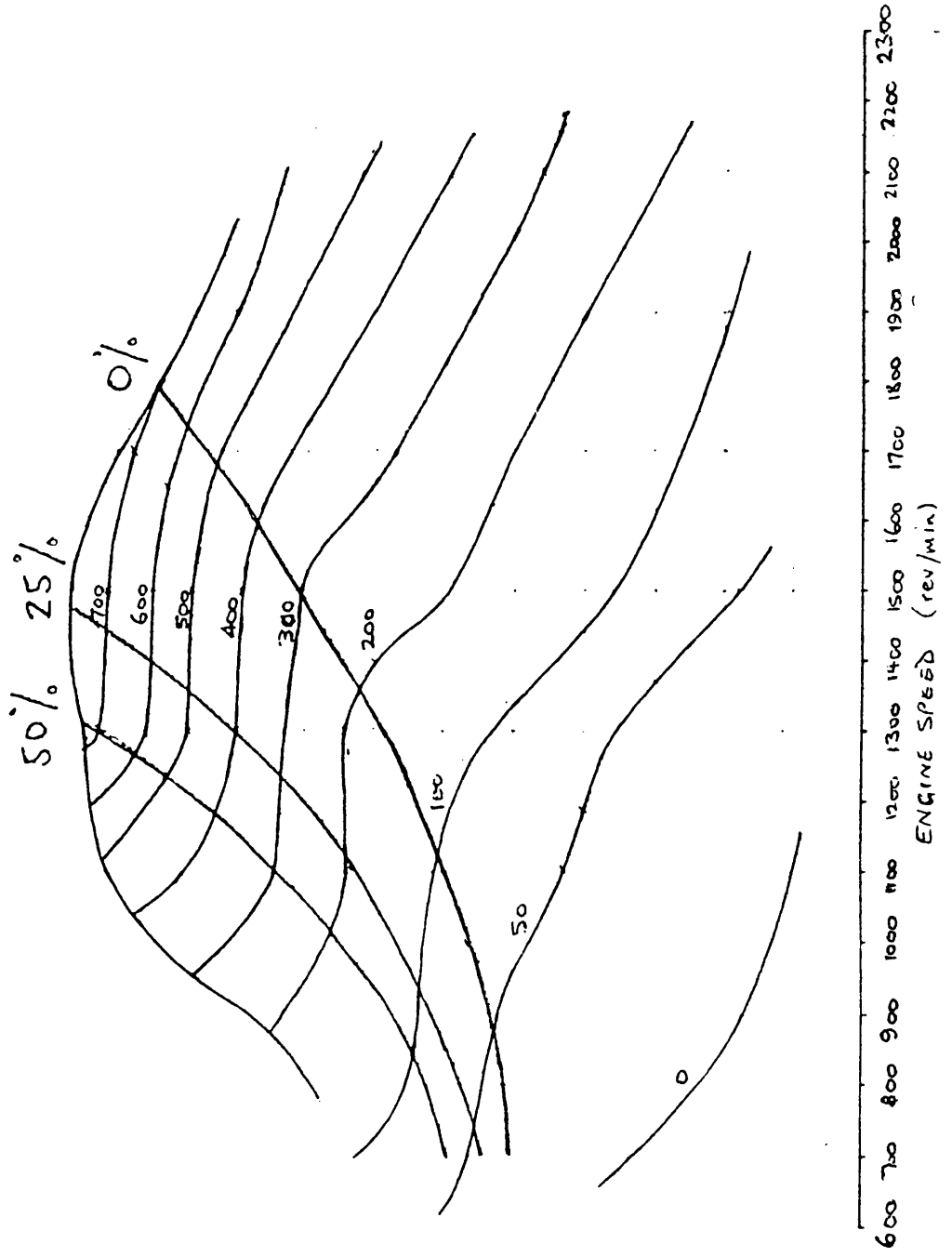

fig 4.64

****
ROUTE AND SIMULATED VEHICLE PROGRAM
****

VEHICLE TYPE - %% T45 ROADTRAIN %%

GROSS VEHICLE WEIGHT	-	32.00	(TONS)
EFFECTIVE FRONTAL AREA	-	67.30	(FT**2)
WHEEL REVS/MILE	-	504.00	
NO. OF WHEELS	-	14	
NO. OF DRUMS	-	8	
DRAG COEFFICIENT	-	0.67	

ENGINE TYPE - TL11 BATH

RATED POWER	-	255.1	BHP	AT	2300. RPM
MAX. TORQUE	-	833.3	LBF-FT	AT	1400. RPM
MAX. SET SPEED	-	2530.	(RPM)		
MIN. SET SPEED	-	500.	(RPM)		
GOV. RUN-OUT SLOPE	-	0.335	(RPM/LBF-FT)		
MOMENT OF INERTIA	-	70.0	(LBM-FT**2)		

ENGINE SPEED	-	800.	1000.	1200.	1400.	1600.	1800.	2000.	2300.
MAX. TORQUE CURVE (LBF-FT)	-	590.0	722.7	826.0	833.3	811.2	752.2	671.1	552.6
FRICTION TORQUE (ENGINE)	-	58.1	56.0	69.2	80.6	92.8	106.9	152.9	179.0
FRICTION TORQUE (AUXILLIARIES)	-	0.0	0.0	0.0	0.0	0.0	0.0	0.0	0.0

GEARBOX TYPE - SST 5

NO. OF GEARS	-	5				
MAX. EFFICIENCY	-	0.96				
RATIOS	-	8.86	5.04	2.89	1.74	1.00

AXLE DATA -

RATIO	-	3.7
MAX. EFFICIENCY	-	0.96

ROUTE AND SIMULATED VEHICLE PROGRAM (RSVP) DATA ECHO ~ fig 4.65

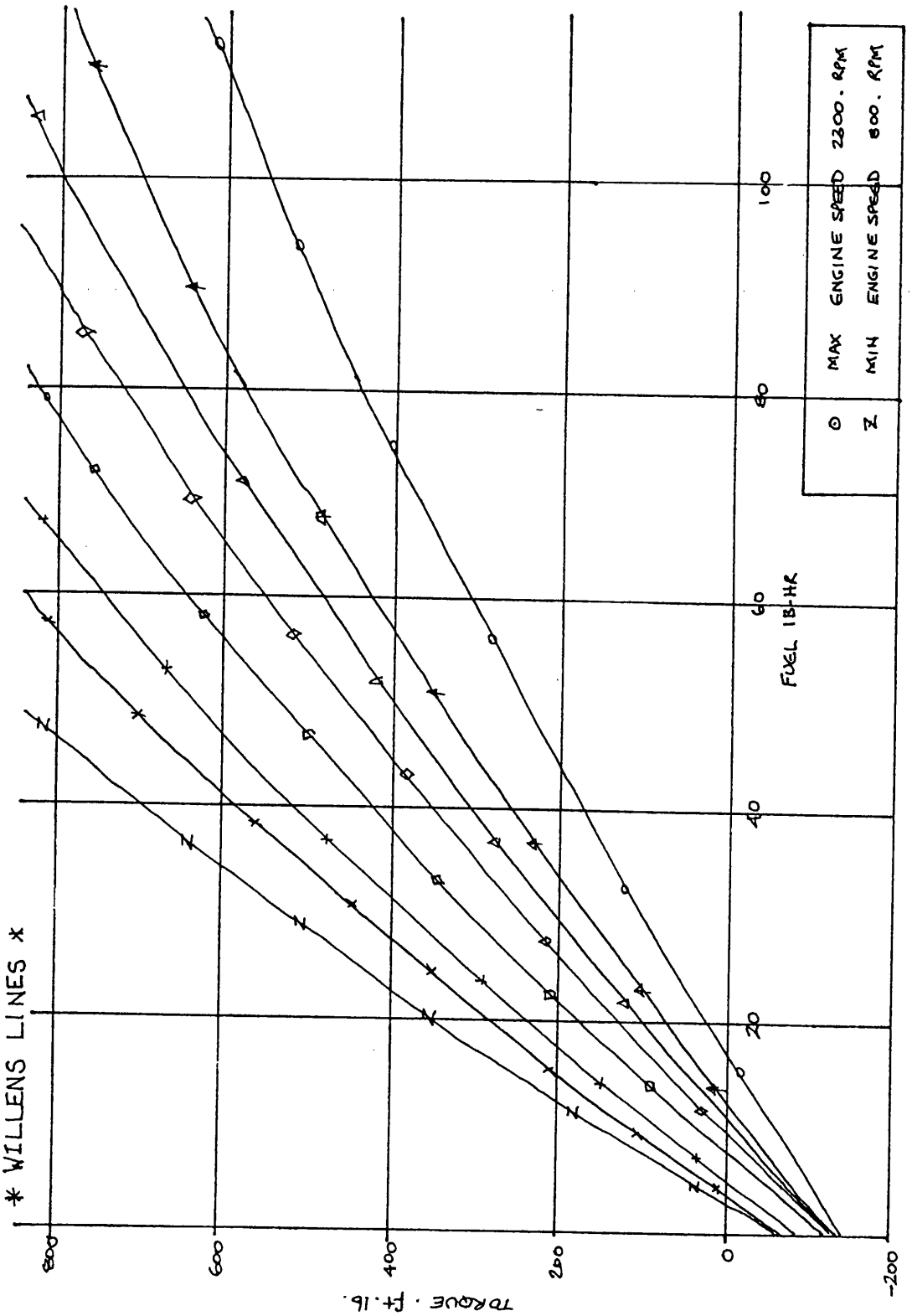

OPTIMISED VG

WILLENS LINES (RSVP) fig 4.66

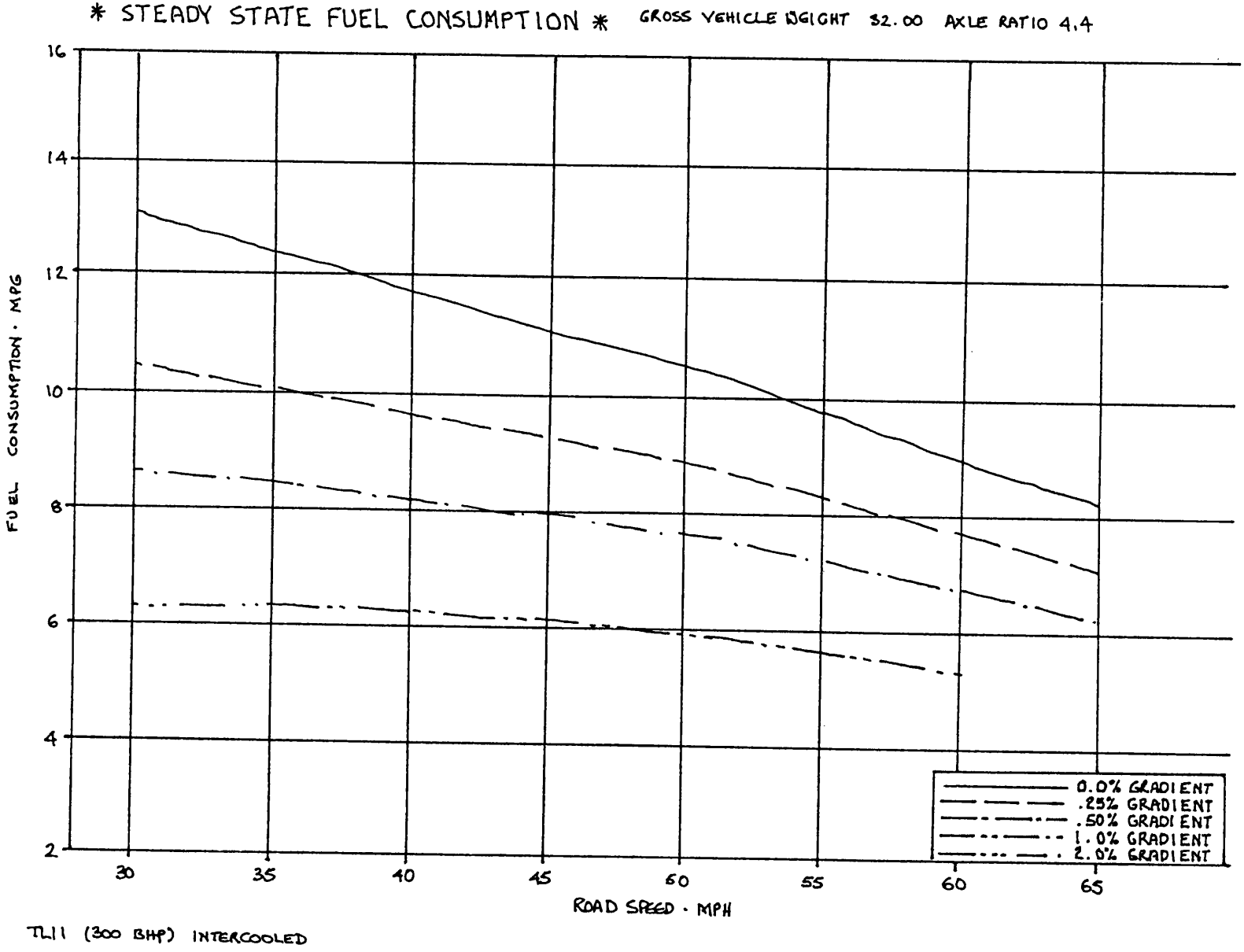

STEADY STATE FUEL CONSUMPTION - Fig 4.67

	(1) Bath TL11 with VG	(2) Bath TL11 with VG	(3) Bath TL11 original spec	(4) Bath TL11 original spec	(5) TL11 - 224 kW Intercooled
Max. Engine rev/min	2100	2300	2100	2300	2000
Gearbox speeds	10	5	10	5	10
Motorway Route - Leyland to Carlisle					
MPG	8.57	8.32	8.48	8.28	8.69
MPH	55.11	54.99	53.97	54.43	55.89
GEF	15 108	14 643	14 640	14 412	15 544
No. of Gear Changes			46	25	
Mixed Route Section of West Yorkshire					
MPG	6.27	6.32	6.30	6.23	6.57
MPH	38.55	38.15	36.87	37.23	38.82
GEF	7739	7721	7433	7419	8157
No. of Gear Changes	64	33	74	37	64

TABLE OF RESULTS - FIG. 4.68

5. EXPERIMENTAL PROGRAMME - TRANSIENT TESTS

5.1. Introduction

In Chapter 4 the steady state performance of the engine was assessed by testing different control strategies to determine the best SFC and torque back up. In a vehicle application transient performance is equally important. This chapter therefore assesses the implications of the different control strategies on the engine's transient behaviour in terms of load acceptance and smoke emission. The results of this analysis will influence the overall control strategy adopted. The tighter turbine housing and variable timing capability of the VG engine imply enhanced vehicle transients and reduced smoke emission.

The tests reported herein are of the unit transient type, that is the dynamometer is run in constant speed demand mode and the engine subjected to a fuel step. This represents a severe test which cannot be reproduced in a vehicle. It places a heavy demand on the dynamometer and some difficulties were encountered which were essentially overcome in the control algorithm investigation with the Mk IIb unit. These are discussed in Section 2.2.2. The tests however clearly show the response of the turbocharger and any benefits can be readily seen.

The data was recorded by a high speed DEC digital data acquisition system connected by land lines, the program being run for 3 s reading data in 0.1 s intervals. The parameters recorded (as appropriate) were:

1. engine speed - rev/min
2. turbocharger speed - rev/min
3. load - Nm
4. inlet and exhaust manifold pressures - bar (static gauge)
5. smoke - % opacity
6. cylinder pressure - bar
7. airflow - kg/s
8. ring sleeve position - %
9. rack position - non-dimensional

10. timing position - analogue voltage
11. governor set point (gsp) - %

This chapter contains the following results:

1. A characterisation of the base build Fig. 5.1 - 5.3.
2. A timing investigation with the standard turbocharger, Fig. 5.4 - 5.15.
3. Fixed restriction results for the Mk I VG (twin flow), Fig. 5.16 - 5.20.
4. A control algorithm investigation with the Mk IIb unit, Fig. 5.21 - 5.36.

The boost control device on the fuel pump was disconnected for all the tests reported. Three speeds were selected for 1 to 3 above to assess the overall performance levels. Tests were conducted with the fuelling adjusted in each case to give 190 kW @ 2100 rev/min together with the standard injection timing (22^{o} BTDC static). For 4 above the engine was configured with an electronic governor and electron hydraulic ring sleeve actuation allowing different control algorithms to be assessed. Four speeds were chosen to characterise the engine response; fuelling and timing were based on values determined during manual steady state optimisation tests. (Section 4.5).

5.2. Base Results

(a) 2100 rev/min, Fig. 5.1

The first figure shows the result for 2100 rev/min. Upon the manual application of full speed demand (gsp) the rack moves to full fuel in less than 0.1 s, and whilst engine speed should nominally be constant it can be seen that an excursion of 100 rev/min over 3 s has occurred. Load rises from 200 to 900 Nm in 1 s whilst turbocharger speed accelerates from 50,000 to 88,000 rev/min in approximately the same time. The smoke trace peaks at 24% dropping to 2% in 0.8 s. The exhaust and inlet manifold pressure traces are in cross over until 1.5 s, being approximately the same thereafter. The values presented

are static (gauge) pressures. The air flow trace is also included. It is readily apparent that both load acceptance and smoke emission are satisfactory at rated speed due to the high speed of the turbocharger at the beginning of the transient ensuring adequate air for combustion.

(b) 1400 rev/min, Fig. 5.2

At 1400 rev/min (60% rated speed) the load acceptance is comparable but due to the turbine's square law torque characteristic and the increased fuelling level, smoke emission is considerably worse. 900 Nm is accepted in 0.25 s rising progressively thereafter to 1060 Nm in 1.75 s. Turbocharger speed rises from 2,000 to 65,000 rev/min in 2 s. Smoke emission peaks at 60% reducing linearly to 5% in 1.5 s. There is a large positive pressure differential between boost and exhaust aiding scavenging. The boost and air flow characteristic are similar to the turbocharger trace. The engine speed excursion was minimal.

(c) 800 rev/min, Fig. 5.3

The 800 rev/min transient exhibited a large speed excursion and excessive smoke (due to the absence of a boost control). The turbocharger is very slow to accelerate achieving 40,000 rev/min (0.35 bar boost) in 1.5 s. Smoke peaks at 75% opacity reducing to 30% in 2.75 s. A positive pressure differential exists across the engine throughout the transient. The 950 Nm load is achieved in 1 s. The air flow trace reflects the engine speed excursion.

These base runs clearly identify the lack of boost pressure (i.e. turbocharger acceleration) at low engine speeds early in the transient manifesting itself as smoke emission and slower load acceptance. The base twin entry unit, however, minimises smoke by maintaining a good positive pressure differential at the lower speeds.

5.3. Timing Investigation

The effects of timing changes on transient behaviour of the engine fitted with the standard turbocharger were investigated by testing three set timing conditions corresponding to:

1. advanced 26.4° BTDC Static
2. standard 22° BTDC Static
3. retarded 15.4° BTDC Static
4. retarded to advanced during the transient

Three speeds were investigated, they were 1800, 1300 and 800 rev/min respectively. To effect test 4 above the ten turn potentiometer input was switched to computer demand fractionally after the fuel step. The demand voltage was fed in by a DC voltage generator corresponding to the advanced timing set point. This was achieved manually.

(a) 1800 rev/min

Fig. 5.4 represents the 'advanced timing case at 1800 rev/min (26.4° BTDC). This graph shows that torque rises from 200 to 980 Nm over 35 with the application of a fuel step. The engine speed excursion is acceptably small over this period. Turbocharger speed rises from 42,000 to 80,000 rev/min. The total emission of smoke equalled 4 sq. units peaking at 25% opacity returning to 3% steady state.

Fig. 5.5, representing the standard timing case, shows a final torque of 980 Nm when the engine is subjected to an identical fuel step, turbocharger speed is the same as before and smoke emission is higher at 7.2 sq. units where the peak is now 30% opacity returning to 6% opacity steady state.

The retarded injection case (15.4° BTDC) for the same conditions, produces a lower torque of 920 Nm and a higher turbocharger speed of 82,000 rev/min reflecting the higher exhaust temperature. Smoke emission peaks at 35% opacity returning to 4% opacity steady state.

It was previously determined (Chapter 4) that ideally timing should be retarded at light load at constant speed. Fig. 5.7 shows results for

advancing the timing through the transient as load is taken up. Load acceptance is improved and a torque value of 980 Nm retained, turbocharger speed rises to 90,000 rev/min whilst smoke peaks at 39% opacity falling to 5% steady state, the total area being 6.5 sq. units. Timing is advanced in less than 0.1 s with the application of a fuel step. Cylinder pressure rises from 65 to 135 bar, the analysis, however, takes no account of rates of change of pressure. The transient response and smoke emission of the engine are very satisfactory in all cases due to the high speed of the turbocharger (+ 40,000 rev/min) at the beginning of the fuel step ensuring an adequate supply of air for combustion throughout the transient.

(b) 1300 rev/min, Fig. 5.8

At this condition, the engine speed excursion is somewhat worse making load acceptance difficult to ascertain accurately. The results, however, clearly show the deficit of air at the beginning of the transient. Engine torque rises from 200 to 1,000 Nm in 1.5 s and the turbocharger accelerates from a few thousand rev/min to 55,000 rev/min in the same period. Smoke peaks at 42% reducing to 4% steady state, the total area under the graph being 10 sq. units.

For the standard timing (Fig. 5.9) a steady state torque of 1,050 Nm is achieved with comparable turbocharger speeds, smoke peaking at 47% opacity, reducing to 7% steady state. This increase in attained torque from 1,000 to 1,050 Nm is in agreement with earlier findings which suggested that optimum timing at this speed is a little retarded relative to the standard value.

The retarded case (Fig. 5.10) achieves a 1,000 Nm torque but with considerably more smoke emission i.e. peak of 55%, steady state 10%.

The timing swing through the transient (Fig. 5.11) reveals a similar torque level and turbocharger speed. However, smoke peaks at 55% reducing to 5%. Cylinder pressure rises from 62 to 125 bar in 1.5 s.

(c) 800 rev/min

At 800 rev/min the engine speed excursions are somewhat worse. However the results are self consistent. For the advanced timing case (Fig. 5.12) a torque level of 880 Nm is achieved, there is negligible turbocharger speed and smoke emission is high; peaking at 65%, reducing to steady state 20%. The engine is overfuelled and clearly lacks a boost control device. Total area under the smoke trace is 26 sq. units.

Fig. 5.13 shows the results with the standard timing. The figures are 920 Nm, 85% opacity with a total area of 33 sq. units.

For the retarded case (Fig. 5.14) the corresponding figures are 920 Nm, 95% opacity and 44 sq. units.

Advancing the timing through the transient (Fig. 5.15) gives 880 Nm, 95% opacity with an area of 29 sq. units. Cylinder pressure rises from 63 bar to 110 bar in 0.4 s.

Whilst the engine is overfuelled in the above cases (due to the absence of a boost control), the effects of timing changes on smoke emission can be clearly seen. The tests indicate that it is feasible to alter injection timing at the same rate as rack.

The above results suggest that advancing timing relative to standard reduces both the steady state and transient emission of smoke at the expense of peak cylinder pressure. Taking advantage of the fast slew rate of the timing device allows the engine to benefit from part load retarded injection running, retaining an SFC advantage whilst minimising smoke emission during transients. It is possible to operate the engine at acceptable smoke levels during transients by monitoring the boost and storing the desired characteristic.

5.4. Fixed Restriction Results for the Mk I VG Turbocharger (Twin Flow Unit)

Tests were conducted with the unit either fully open or closed (fixed mechanical setting) at 900 and 1400 rev/min and fully open only at 2,100 rev/min. The fully open case at 2,100 rev/min is considered first of all.

(a) 2,100 rev/min (Fig. 5.16 cf. Fig. 5.1 for base build)
This test reveals an excessive engine speed excursion including overspeed which pulls the rack back from full fuel with consequent undesirable effects on load acceptance. Load acceptance would appear slower than in previous cases achieving 800 Nm in 1.5 s, turbocharger speed and smoke reflecting this trend. The manifold pressures are always in cross over suggesting a less efficient turbine stage.

(b) 1,400 rev/min (Fig. 5.17 & 5.18 cf. Fig. 5.2 for base build)
Fig. 5.17 presents the results for 1,400 rev/min with the turbine stage fully open. Clearly the load acceptance is somewhat worse than base; 1,000 Nm in 1 s; turbocharger acceleration can be seen to be slower, as well as boost and air flow. Nevertheless a good positive differential is maintained throughout the transient. The smoke peak is lower at 42% but the steady state value is somewhat worse at 7%. Engine speed excursion was also worse.

Comparing the above with Fig. 5.18 which is the fully restricted case, reveals that load acceptance has improved, 1,000 Nm being reached in 1.5 s. However, the turbocharger acceleration is comparable, boost pressure is higher. On the other hand the differential is worse; as a consequence smoke emission is correspondingly higher. Clearly transient performance has not been enhanced by a 50% restriction. (16% turn down).

(c) 900 rev/min (Figs. 5.19 & 5.20 cf. Fig. 5.3 for base build)
At 900 rev/min the same trends are apparent where load acceptance is marginally inferior with 50% axial restriction. Turbocharger

acceleration is markedly worse favouring the unrestricted case e.g. 40,000 rev/min in 1 s (0%) cf. 30,000 rev/min in 3 s (50%) whilst engine speed excursion are comparable.
Boost is similar in both cases but the differential is lower for the restricted case, smoke emission reflects the above. Quite clearly restricting the turbine inefficiently degrades transient performance.

The results show that the fully open VG performance is comparable with base and that peak smoke emission is substantially reduced with a twin flow device. However, the inefficient small turn down reverses the previously positive pressure differential, thus degrading engine transient performance overall. Development of the unit was curtailed in favour of the Mk II single entry device which was controlled by pneumatics and later by an electro-hydraulic actuating mechanism. The electro-hydraulic actuation allowed much greater flexibility in testing i.e. modulating the restrictor during transient, directly and indirectly.

As in the steady state results of Chapter 4 the Mk II(a) VG unit was assessed for its transient performance, the results for which are not presented due to the excessive engine speed exursions which occurred. The poor transient performance of the dynamometer is attributed to mechanical degradation of the hydraulic pump itself. Very shortly after these tests the pump failed completely. It was replaced by a reconditioned unit and the feed forward (derivative control element) was taken from rack position. This was very conveniently supplied from the electronically governed fuel pump which was fitted at this time. These changes resulted in much better and repeatable unit transients which are presented below for the Mk II(b) unit.

5.5. Control Algorithm Investigation with the Mk II(b) Unit

This section asseses the transient behaviour of the VG configured engine with different control algorithms. The elctro-hydraulically actuated ring sleeve operating with nozzle ring could complete full travel in less than 0.1 s.

Four speeds were investigated, viz. 1800, 1600, 1200 and 800 rev/min respectively. Four distinct tests were performed at each speed as appropriate, these were with:

1. the turbine stage fully open
2. maximum restriction consistent with speed and load
3. a restriction schedule i.e. turbine restriction (ring sleeve position) as a function of rack and engine speed (Fig. 5.21)
4. a closed loop boost control i.e. boost demanded as a function of rack position and engine speed, Fig. 5.22.

Functions 3 and 4 above were effected by switching from manual input (10 turn potentiometer) to computer demanded input, where a demand was fed in by a DC voltage generator corresponding to boost or restriction demand on the LTC. This was achieved manually.

Fig. 5.23 outlines the test configurations. Minimum load was set to 200 Nm in each case. The injection timing and maximum fuelling were set to the optimum values determined for the LTC performance under manual optimisation. Fig. 5.24 is a table presenting the results in a collated form.

(a) 1800 rev/min

At this speed the turbine is fully open under all loads. Therefore the assessment includes only the fully open and boost controlled cases respectively.

(i) Fully Open

The fully open case (Fig. 5.25) reveals that inlet manifold (boost) pressure achieves 80% of its steady state value in 1.25 s and has a

maximum value of 0.64 bar. Smoke emission was assessed by measuring the area under the trace and was found to be 13.2 sq. units peaking at 39% returning to 8% steady state. Peak cylinder pressure rises from 70 bar and peaks at 103 bar. The load rises from 200 Nm in 0.2 s to nominally 940 Nm and progressively thereafter to 1,000 Nm in 3 s. The engine speed exursion was minimal. The air mass flow characteristic is similar to that of the boost and turbocharger speed and rises from 183 to 245 g/s. Turbocharger speed acceleration was from 44,000 rev/min to 72,000 rev/min. The manifold pressures were always in crossover.

(ii) Turbine Under Boost Control (Fig. 5.26)
In this test a similar fuel step was applied; however, turbine restriction was applied by a closed loop proportional and integral (p + i) boost demand. From Fig. 5.26 it can be seen that initially the restrictor is fully open. As the rack moves to full fuel, a high boost pressure of 0.8 bar is demanded. Therefore the ring sleeve goes to its maximum value (for 0.4 s) thereafter progressively opening to 10% and eventually (9 s) to 0%. The system gain was adjusted to give optimum response at the speed. Boost pressure rises to 80% of its steady state value in only 0.7 s. Exhaust manifold pressure (P_3) rises to a peak of 1 bar before falling to 0.9 bar; reflecting the severe turbine restriction at the beginning of the transient. The area under the smoke trace is 9.5 sq. units, some 28% better than in the fully open case, due to the greater air availability earlier in the transient. The peak value is 35% returning to 6%.

Load rises in 0.2 s to 1020 Nm, engine speed excursion being minimal, cylinder pressure peaks at 124 bar. The air mass flow reaches a maximum of .262 kg/s. Turbocharger speed rises from 44000 to 79000 rev/min.

At 1800 rev/min the load acceptance, transient smoke and application of boost are all improved by using boost control. 80% of boost is achieved in a little over half the time of the fully open case. Transient smoke, however, does not improve in the same ratio due to

the large transient negative pressure differential. The exhaust manifold pressure never becomes excessive with large transient restriction.

(b) 1600 rev/min

At 1600 rev/min the optimisation tests showed that 34% restriction gave the best steady state performance. Therefore the VG configuration is within the control range of the turbine and the effects of modulating the turbine on the transient performance can be determined.

Thus all four tests are applicable.

(i) Fully Open Turbine, Fig. 5.27

The first test provides a datum performance with the unit fully open. This reveals that there is a large increase in transient and steady state smoke emission -24.8 sq. units (peak 56% - steady state 15%) reflecting the larger turbine housing and an inadequate air fuel ratio on the LTC. Boost pressure achieves 80% of its steady state value - 0.58 bar in 1.25 s. Turbocharger speed rises from 40,000 to 68,000 rev/min. Torque rises from 200 Nm to 1,050 Nm in 1.5 s. Peak cylinder pressure simultaneously rises from 54 to 100 bar.

(ii) 34% Restriction

Fig. 5.28 at 1,600 rev/min simulates a speed restriction schedule. A restriction of 34% is applied throughout the transient. The emission of smoke remains high at 20.4 sq. units and may be pessimistic when compared with test 302 below. Nevertheless torque acceptance is enhanced, 1,090 Nm being reached in 1.5 s. The boost pressure is considerably higher at 0.9 bar though turbocharger speeds are similar at 40,000 rev/min rising to 78,000 rev/min; 80% of boost pressure is achieved in 1.4 s.

This strategy results in a steady state part load SFC penalty.

(iii) Restriction Schedule, Fig. 5.29
Test 302 at 1600 rev/min is a test where the turbine stage is fully open at light load and closes to 34% restriction as a function of rack moving to full fuel. The results should be very similar to test 301 above; however, the smoke emission is significantly better at 12.5 sq. units and is attributed to the continued rise in turbocharger speed and boost after 1.5 s though the reasons for this are not clear. Load acceptances in both cases are, however, identical. The restrictor moves to its restricted position in less than 0.1 s. After 3 s boost pressure is 1.02 bar, 80% of which is achieved in 1.8 s. Turbocharger speed rises to 85,000 rev/min.

(iv) Boost Demand, Fig. 5.30
Test 303 is a boost demand. With the application of load the restrictor moves to the fully restricted position for 3.25 s before opening progressively to 34% in a further 2.25 s. Load acceptance is very similar to Case 3 above, though smoke emission is slightly better. Boost pressure, however, rises significantly faster achieving 1 bar in 2 s (compared with 3 s above). Nevertheless, P_3 rises faster to 1.3 bar. There is no 'peak' in the exhaust manifold trace.

At 1600 rev/min the effects of the four different strategies can be compared. The results clearly demonstrate that boost control significantly increases the rate of application of boost; however the engine is largely indifferent to the enhanced inlet manifold pressure due, it is thought, to the much larger negative pressure differential. The results suggest a speed determined restriction schedule would give almost identical results.

(c) 1200 rev/min
A dynamometer instability in a 50 rev/min speed band around 1300 rev/min militated against testing at this speed, therefore 1200 rev/min was chosen. A 50% restriction schedule is demanded on the LTC at this speed.

(i) Fully Open Case, Fig. 5.31
The fully open case reveals as expected a significant boost deficit, a maximum value of 0.28 bar being recorded, 80% of which is achieved in 1.7 s. Transient smoke is excessive at 47.2 sq. units (peak 75%). The load is accepted in 0.2 s to 880 Nm and to 1000 Nm thereafter in 2.5 s. Turbocharger speed rises from 28,000 to 48,000 rev/min.

(ii) 50% Restriction, Fig. 5.32
Test 201 assesses the same transient with a 50% turbine restriction. Boost pressure is a maximum at 0.58 bar, 80% of which is achieved in 1.75 s. Load acceptance is improved achieving 980 Nm in 0.2 s, rising progressively thereafter to 1080 Nm in a further 2.8 s. Smoke emission is considerably improved being a total of 26.3 sq. units (peak 57%). Turbocharger speed rises from 32,000 to 62,000 rev/min.

(iii) Restriction Schedule, Fig. 5.33
In this case the load acceptance and response is slightly worse in the first 2.5 s, response being identical thereafter. This is associated with the lower turbocharger speed at the beginning of the transient. Smoke emission is 33.7 sq. units (peak 72%). Turbocharger speed rises from 27,000 to 64,000 rev/min.

These results suggest that a speed determined restriction schedule gives significantly better transients in terms of smoke emisssion and boost pressure. This implies that a restricted turbine at low loads and speeds imparts significant advantages to transient performance.

(d) 800 rev/min, Fig. 5.34/35/36
Turbocharger response at this speed and load is largely unaffected by changes in control strategy due to the low fuelling and expansion levels. Turbocharger speed never rises above 30,000 rev/min. No appreciable differences to turbocharger and engine performance could be determined for the three strategies tested.

Summarizing, the results clearly show that increasing restriction enhances engine transient performance. The restrictor traverses the turbine in less than 0.1 s.

The closed loop boost control leads to significantly faster rise in boost pressure, though the negative pressure differential across the cylinders is somewhat worse. For all the tests with the Mk IIb unit the engine operated in crossover. Exhaust manifold pressure, however, never exceeds 1.5 bar(gauge)in the worst case.

A restriction schedule based on speed demand would appear to give the best results. The small energy advantage at the beginning of the transient appears significant.

LIST OF FIGURES

LIST OF FIGURES Cont/d:-

Engine LEYLAND TL11 ENGINE—11.1L DISPLACEMENT Drawn By. E.W. ROBERTS

Title BASE H2B 80BIC L25A3 TURBOCHARGER : CONSTANT SPEED TRANSIENT

Constant Speed Curve at 2100 rev/min

Holset / Leyland / Dowty / DoI Contract

Test No.	Timing	Amb'nt °C	Barometer Ins. Hg.
—	22	25	740.1

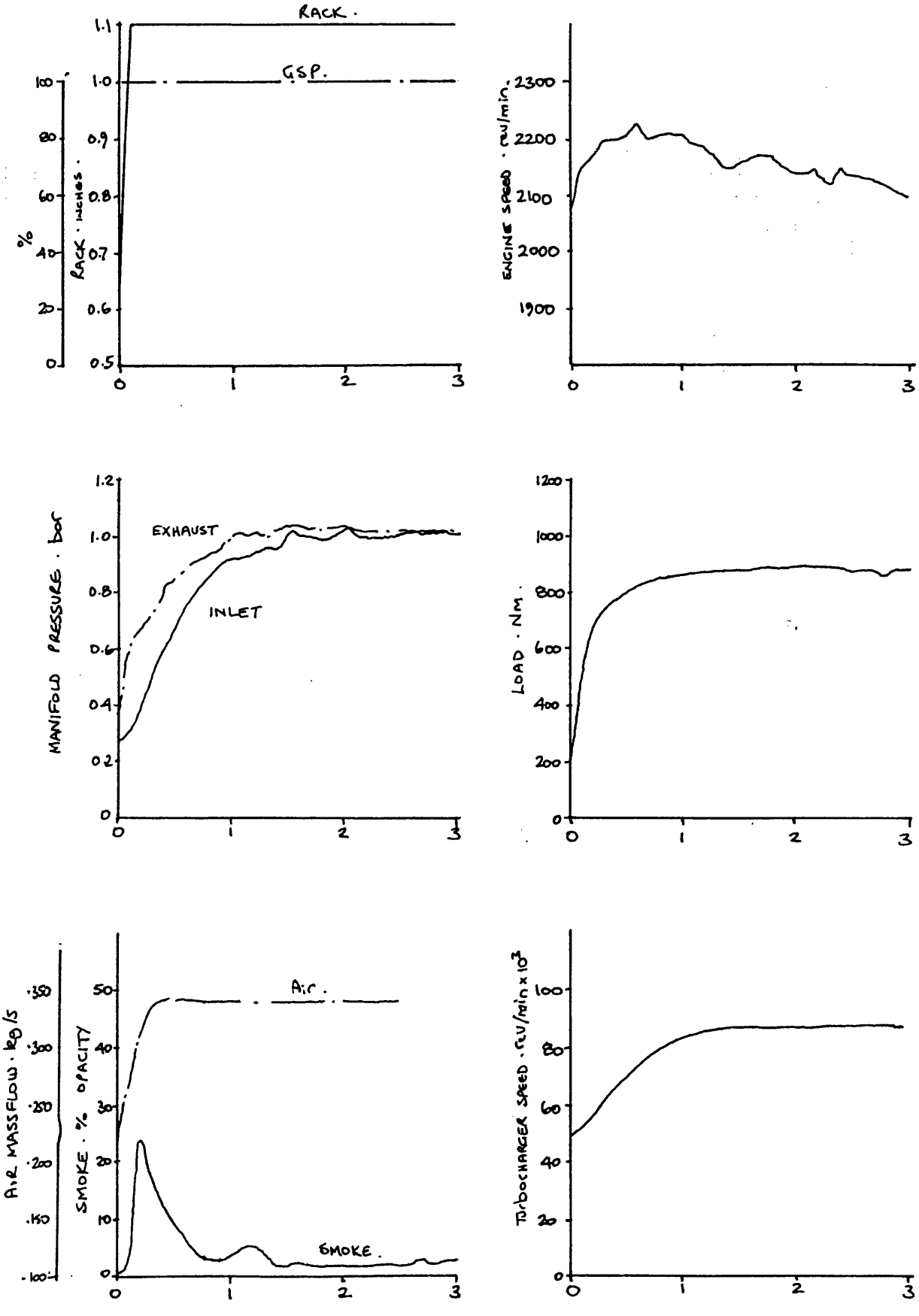

fig 5.1

Engine LEYLAND TL11 ENGINE—11.1L DISPLACEMENT Drawn By... Ed Roberts

Title BASE H2B 808IC L25 A3 · CONSTANT SPEED TRANSIENT

Constant Speed Curve at 1400 rev/min

Holset / Leyland / Dowty / DoI Contract

Test No.	Timing	Amb'nt °C	Barometer Ins. Hg.
-	22	25	740.1

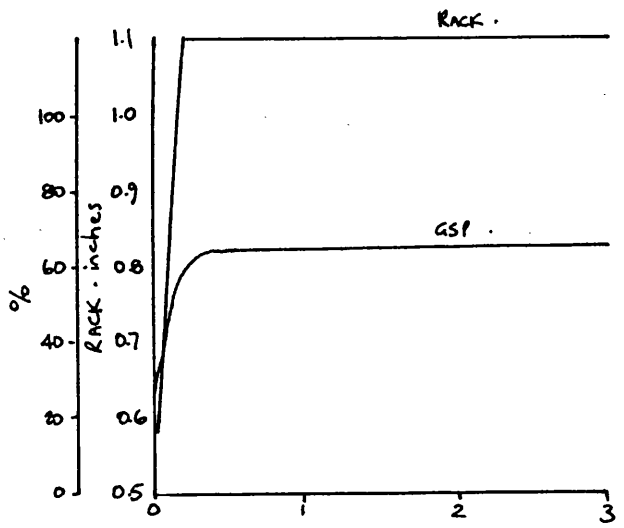

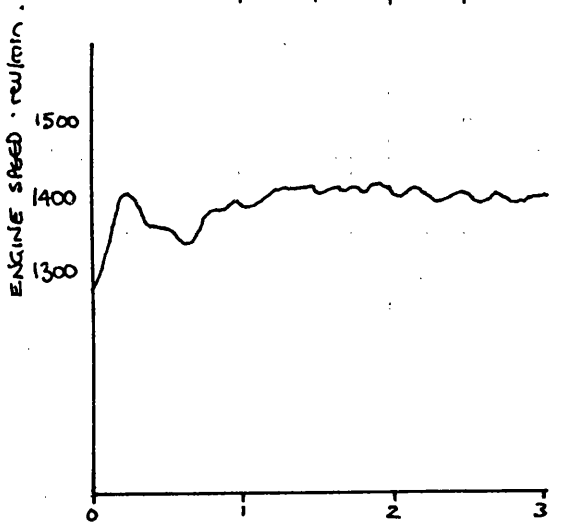

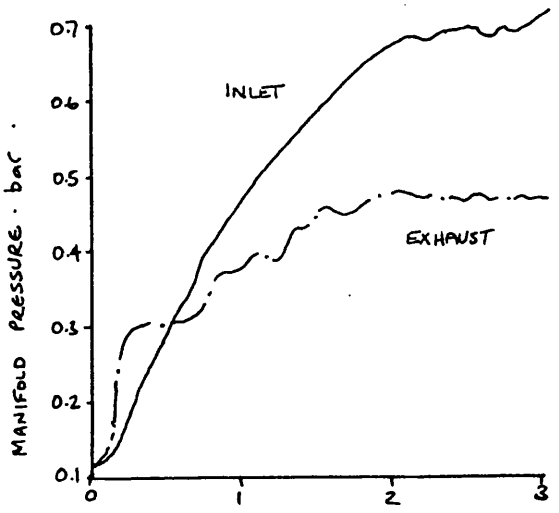

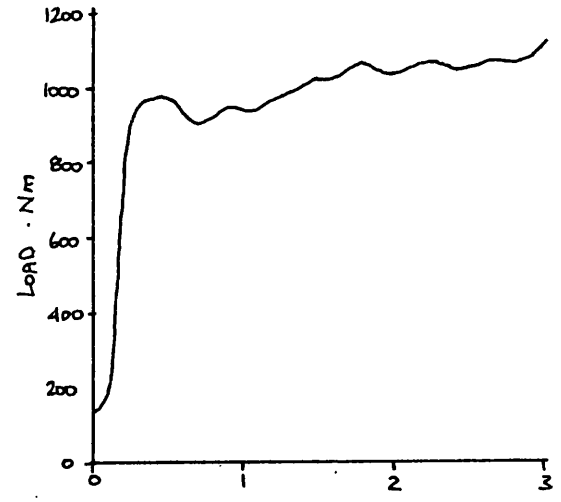

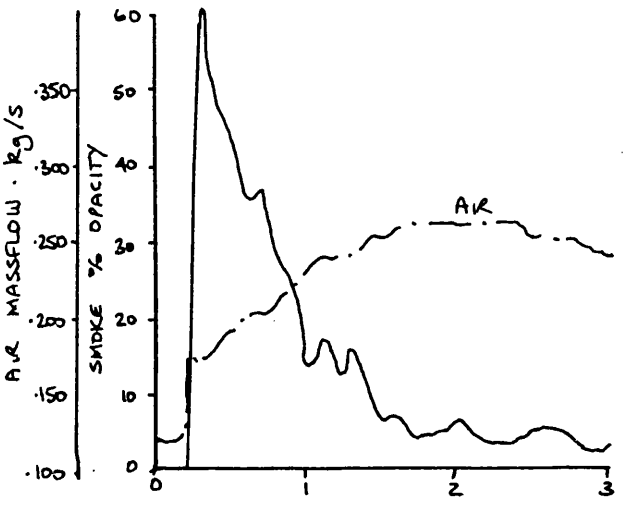

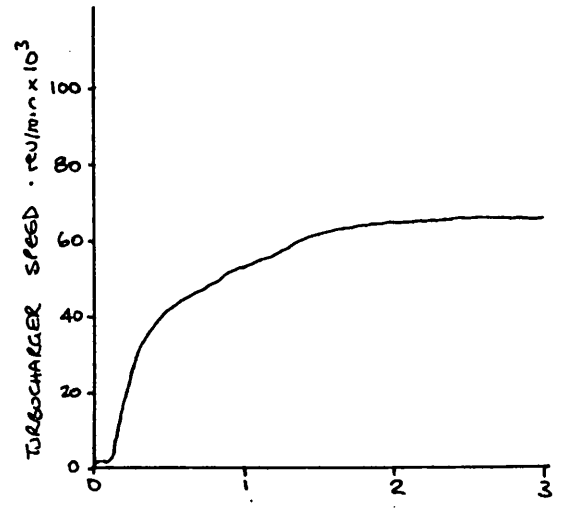

time ~ s

fig 5.2

Engine LEYLAND TL11 ENGINE—11.1L DISPLACEMENT Drawn By. E W ROBERTS

Title BASE H2B B0B1C L25 A3 - CONSTANT SPEED TRANSIENT

Constant Speed Curve at 800 rev/min

Holset / Leyland / Dowty / DoI Contract

Test No.	Timing	Amb'nt °C	Barometer Ins. Hg.
-	22	25	740.1

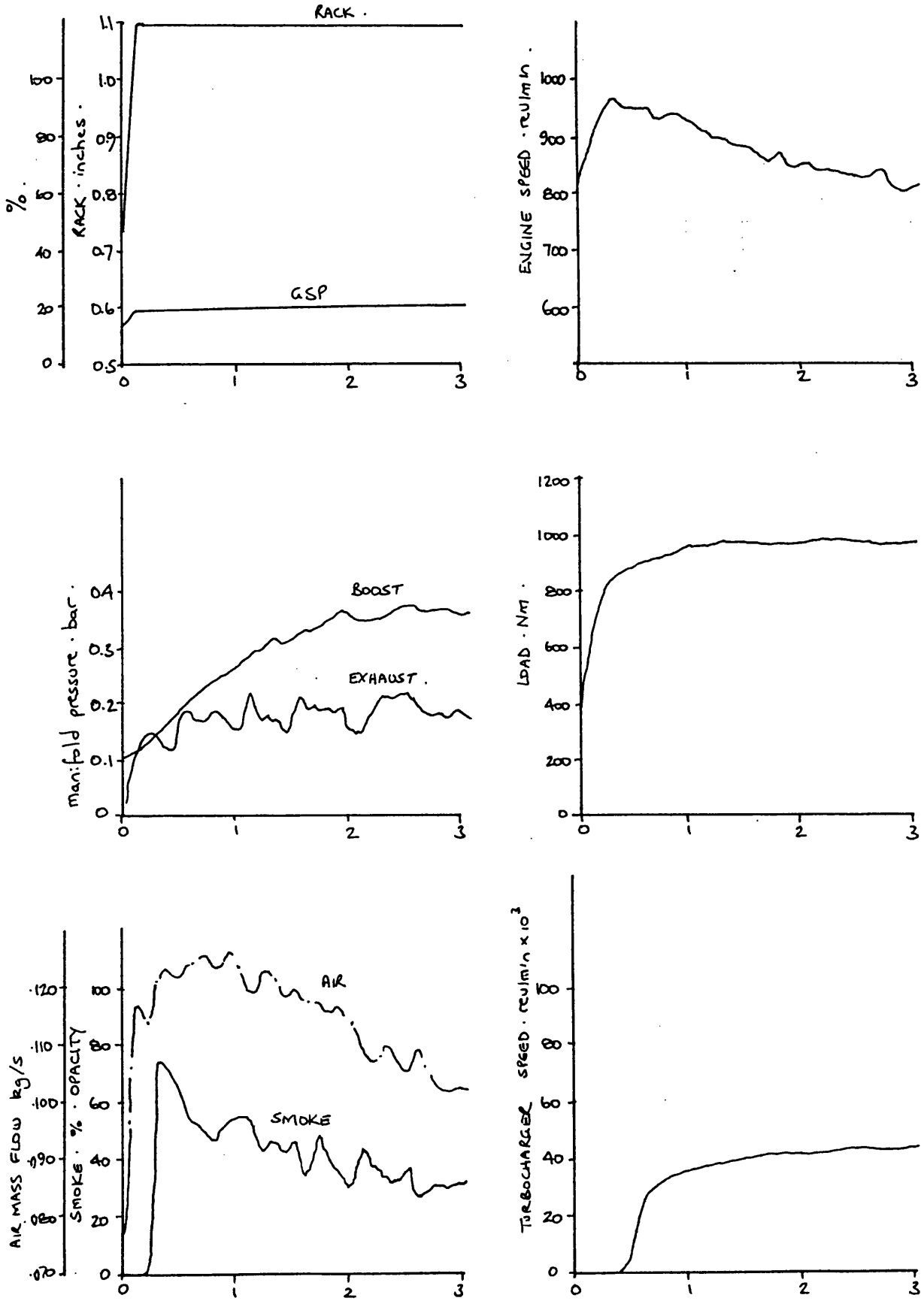

fig 5.3

Engine LEYLAND TL11 ENGINE—11.1L DISPLACEMENT Drawn By. E W Roberts

Title H2B 80BIC L25 TIMING INVESTIGATION

Constant Speed Curve at 1800 rev/min

Holset / Leyland / Dowty / DoI Contract

Test No.	Timing	Amb'nt °C	Barometer Ins. Hg.
	26.4	25	732

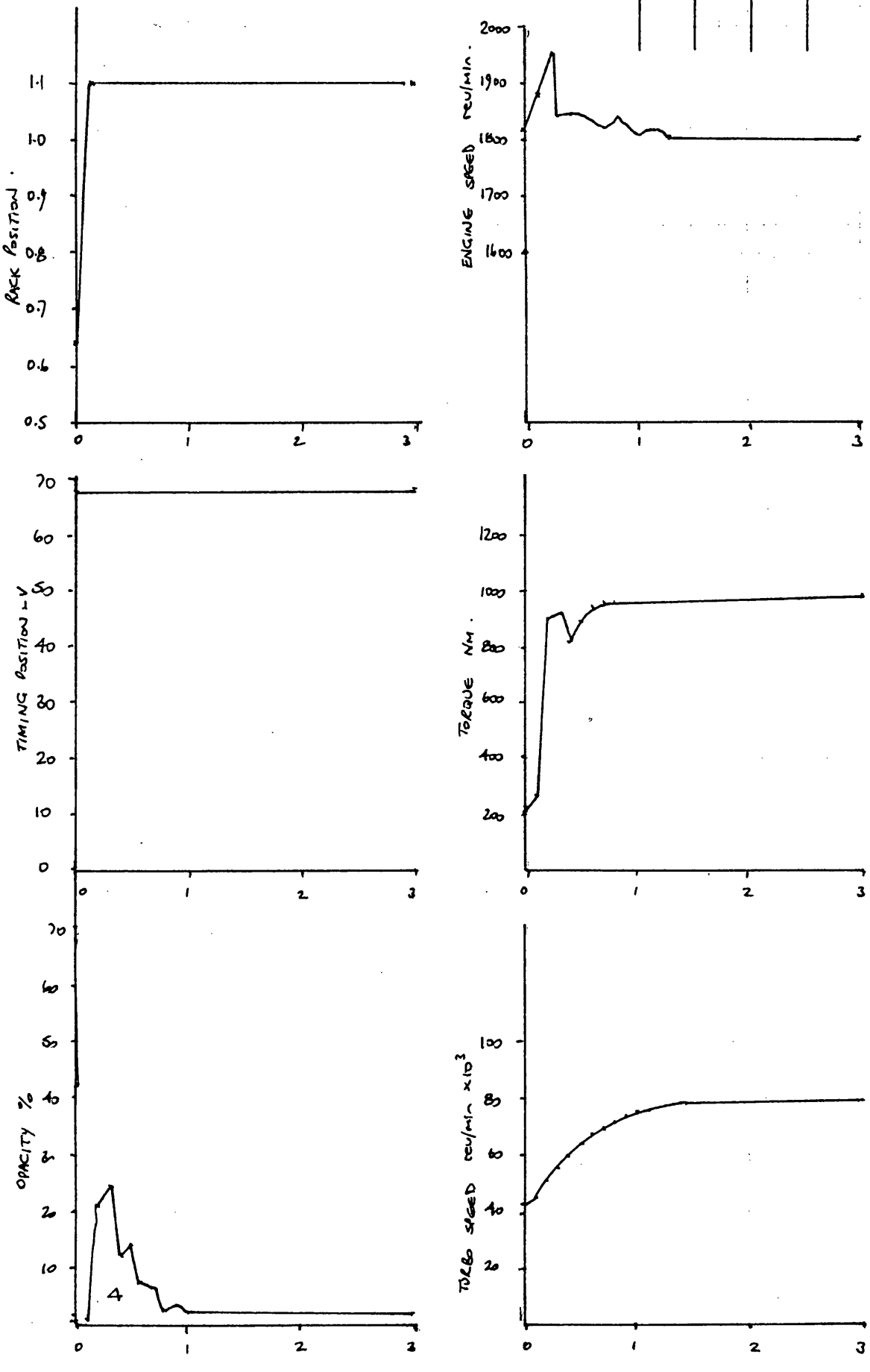

fig 5.4

Engine LEYLAND TL11 ENGINE— 11.1L DISPLACEMENT Drawn By. E W Roberts.

Title H2B 8081C L25A3 - TIMING INVESTIGATION

Constant Speed Curve at 1800 rev/min

Holset / Leyland / Dowty / DoI Contract

Test No.	Timing	Amb'nt °C	Barometer Ins. Hg.
-	22	25	731

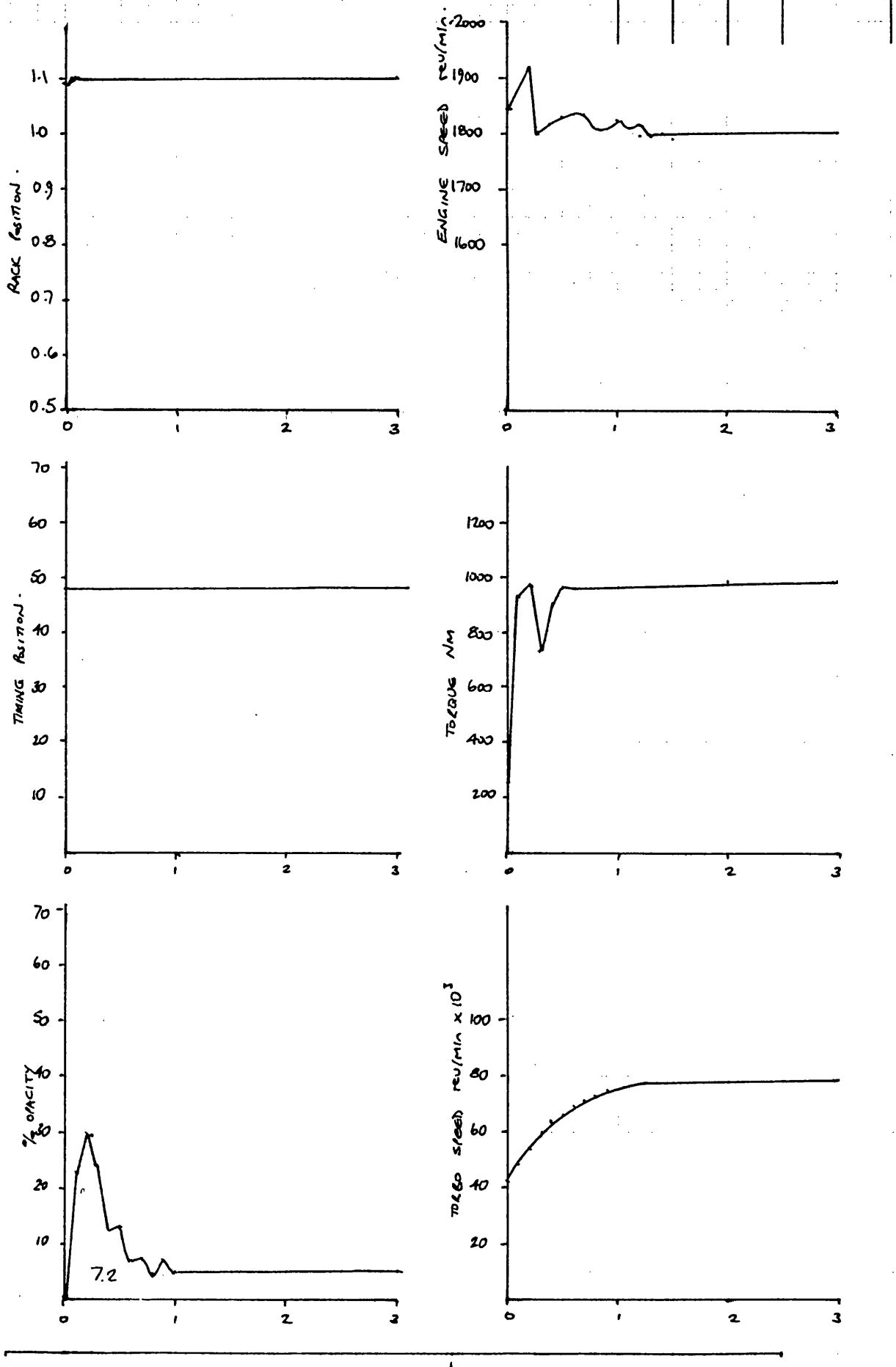

fig 5.5

Engine LEYLAND TL11 ENGINE—11.1L DISPLACEMENT Drawn By. E W Roberts.

Title H2B 80BIC L25A3 TIMING INVESTIGATION

Constant Speed Curve at 1800 rev/min

Holset / Leyland / Dowty / DoI Contract

Test No.	Timing	Amb'nt °C	Barometer Ins. Hg.
–	15.4	25	73

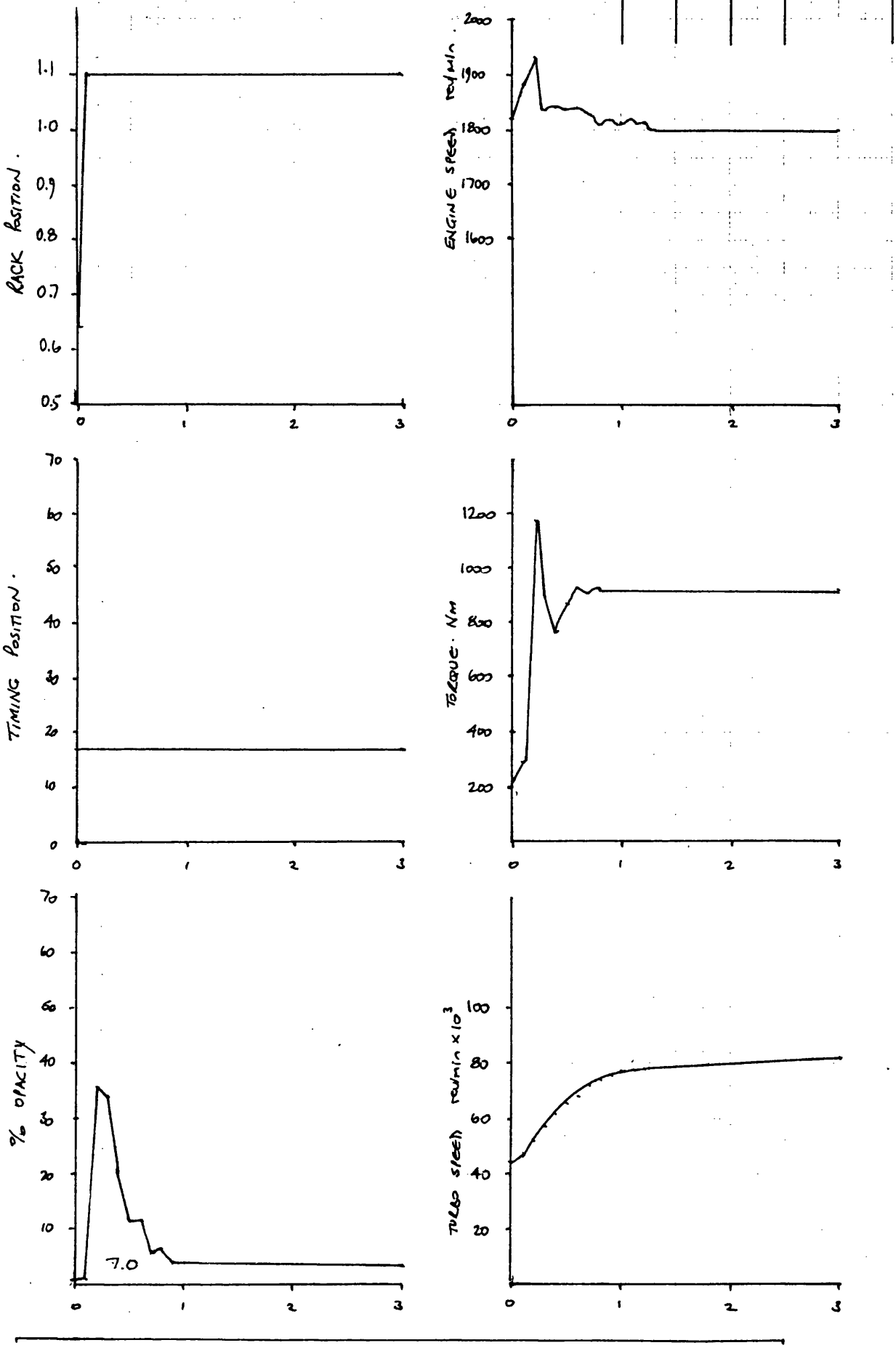

fig 5.6

Engine LEYLAND TL11 ENGINE—11.1L DISPLACEMENT Drawn By. E.W Roberts.

Title #2B 808IC L25 AB TIMING INVESTIGATION TRANSIENT TIMING SWING.

Constant Speed Curve at 1800 rev/min

Holset / Leyland / Dowty / DoI Contract

Test No.	Timing	Amb'nt °C	Barometer Ins. Hg.
—	15.4-26.4	25	781

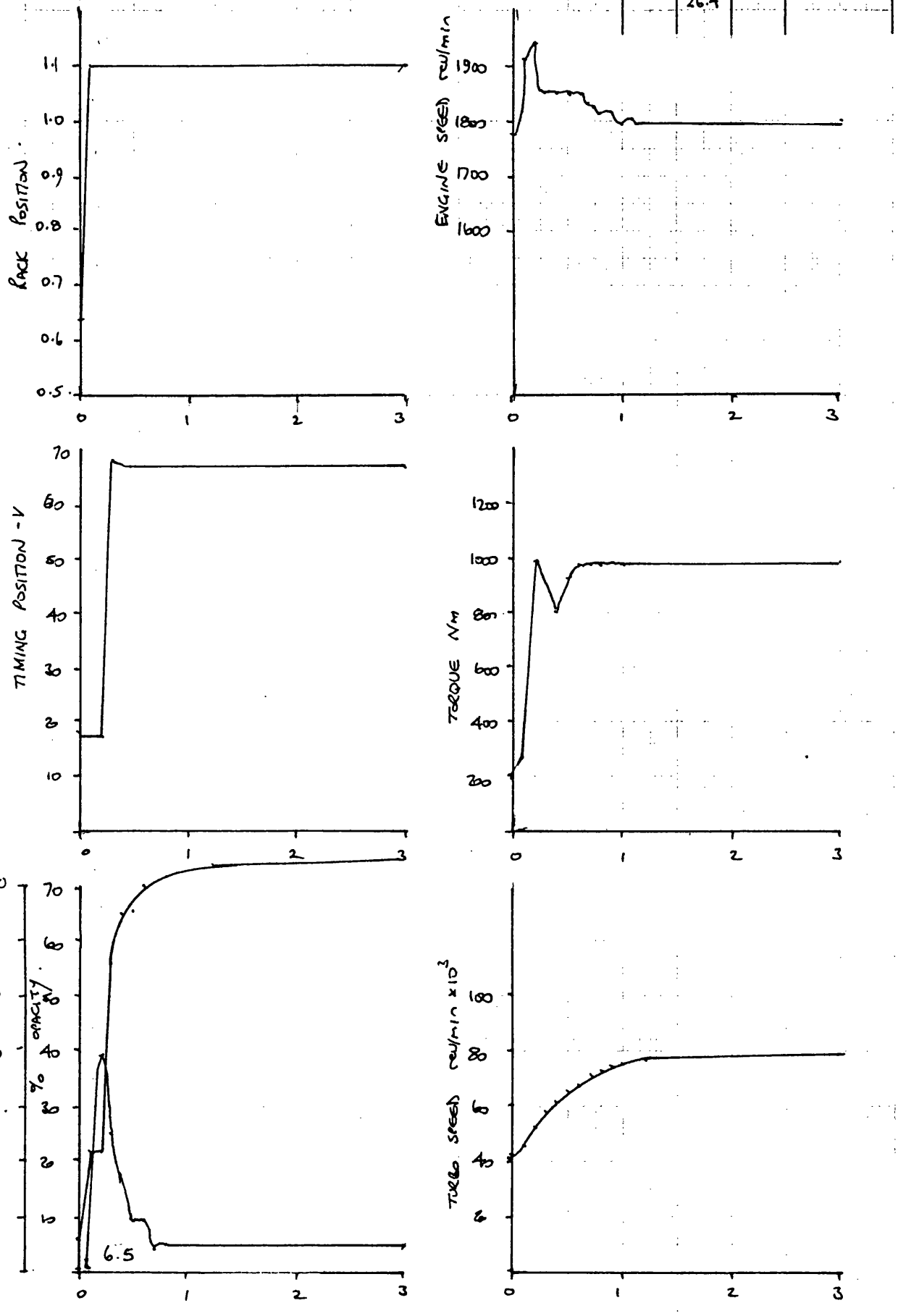

fig 5.7

Engine LEYLAND TL11 ENGINE—11.1L DISPLACEMENT Drawn By ELD Robertson.

Title H26.8081C L25A3 - TIMING INVESTIGATION

Constant Speed Curve at 1300 rev/min

Holset / Leyland / Dowty / Dol Contract

Test No.	Timing	Amb'nt °C	Barometer Ins. Hg.
-	26A	25	731

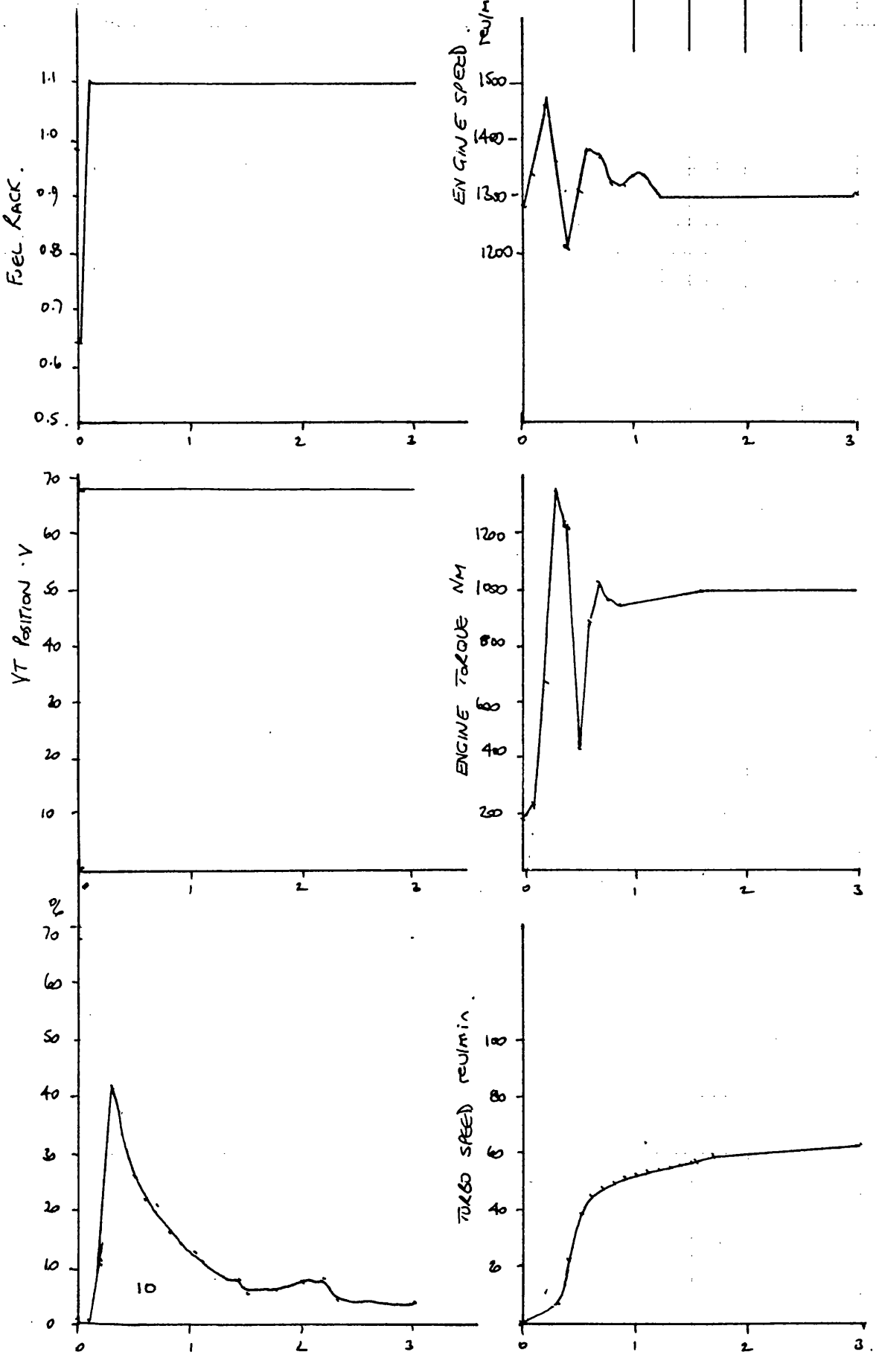

fig 5.8

Engine LEYLAND TL11 ENGINE—11.1L DISPLACEMENT Drawn By. EW ROBERTS.

Title H26 80BIC L25 A3 : BASE : TIMING INVESTIGATION

Constant Speed Curve at 1300 rev/min

Holset / Leyland / Dowty / DoI Contract

Test No.	Timing	Amb'nt °C	Barometer Ins. Hg.
~	22	25	731

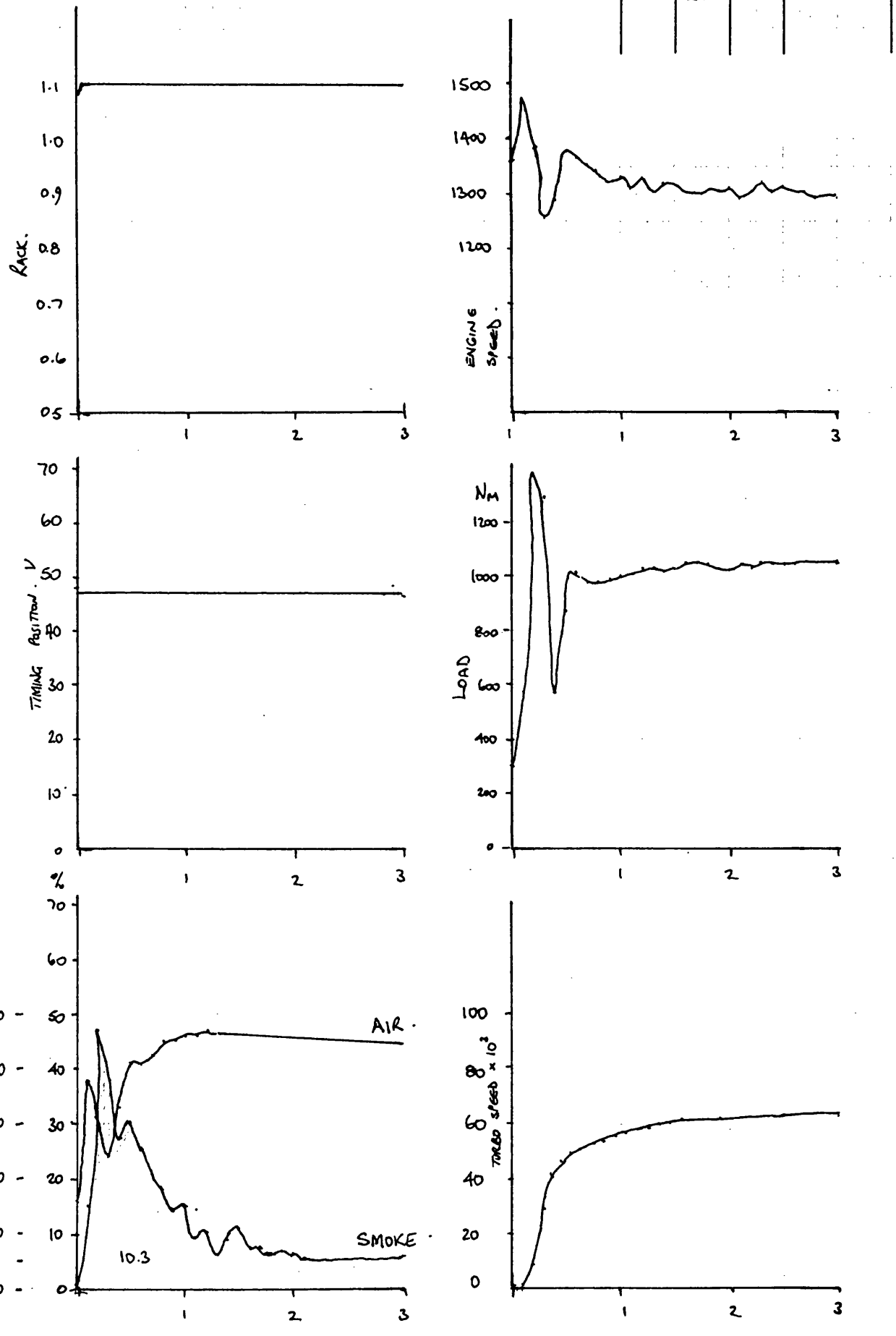

fig 5.9

Engine LEYLAND TL11 ENGINE—11.1L DISPLACEMENT Drawn By. EW Roberts.

Title H2B 8081C L25A3 TIMING INVESTIGATION

Constant Speed Curve at 1300 rev/min

Holset / Leyland / Dowty / DoI Contract

Test No.	Timing	Amb'nt °C	Barometer Ins. Hg.
—	15.4	25	731

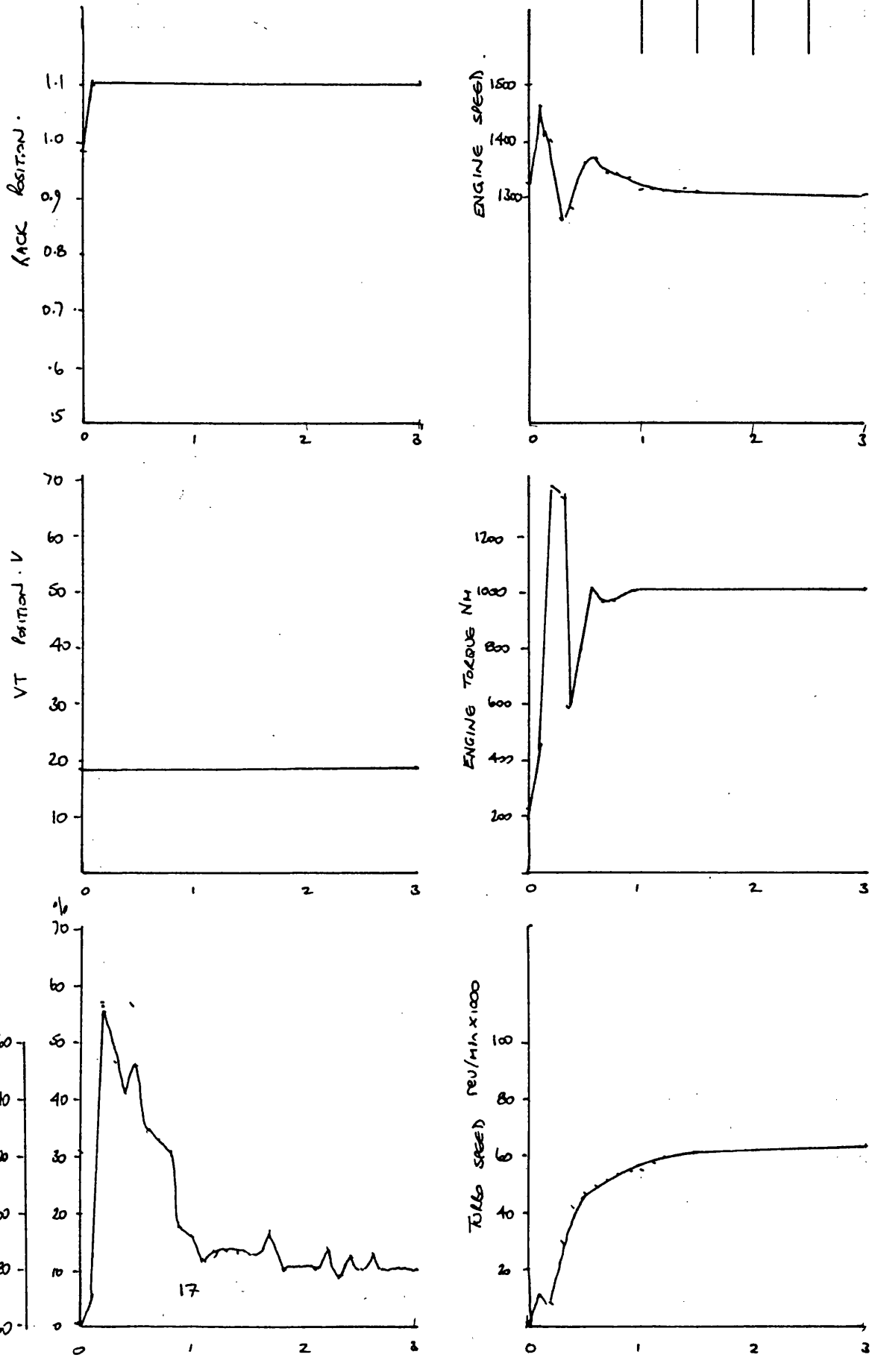

fig 5.10

Engine LEYLAND TL11 ENGINE- 11.1L DISPLACEMENT Drawn By. E.W Roberts

Title H2B 8081C L25A3 TIMING INVESTIGATION TRANSIENT TIMING SWINGS

Constant Speed Curve at 1300 rev/min

Holset / Leyland / Dowty / DoI Contract

Test No.	Timing	Amb'nt °C	Barometer Ins. Hg.
—	15.4-26.4	25	731

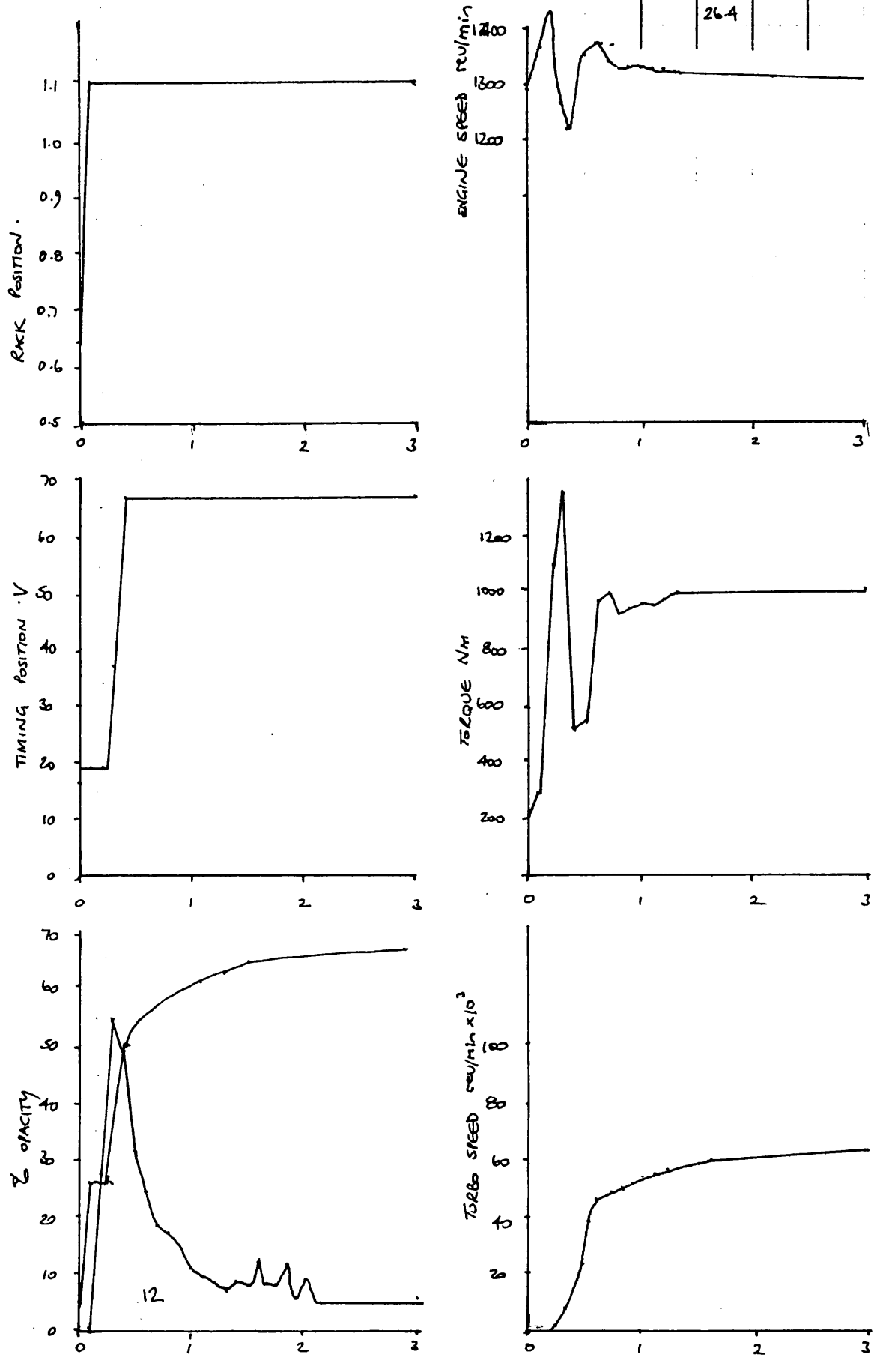

fig 5.11

Engine LEYLAND TL11 ENGINE—11.1L DISPLACEMENT Drawn By. EW Roberts.

Title H2B 808IC L25A3. TIMING INVESTIGATION

Constant Speed Curve at 800 . rev/min

Holset / Leyland / Dowty / DoI Contract

Test No.	Timing	Amb'nt °C	Barometer Ins. Hg.
–	26.4	25	731

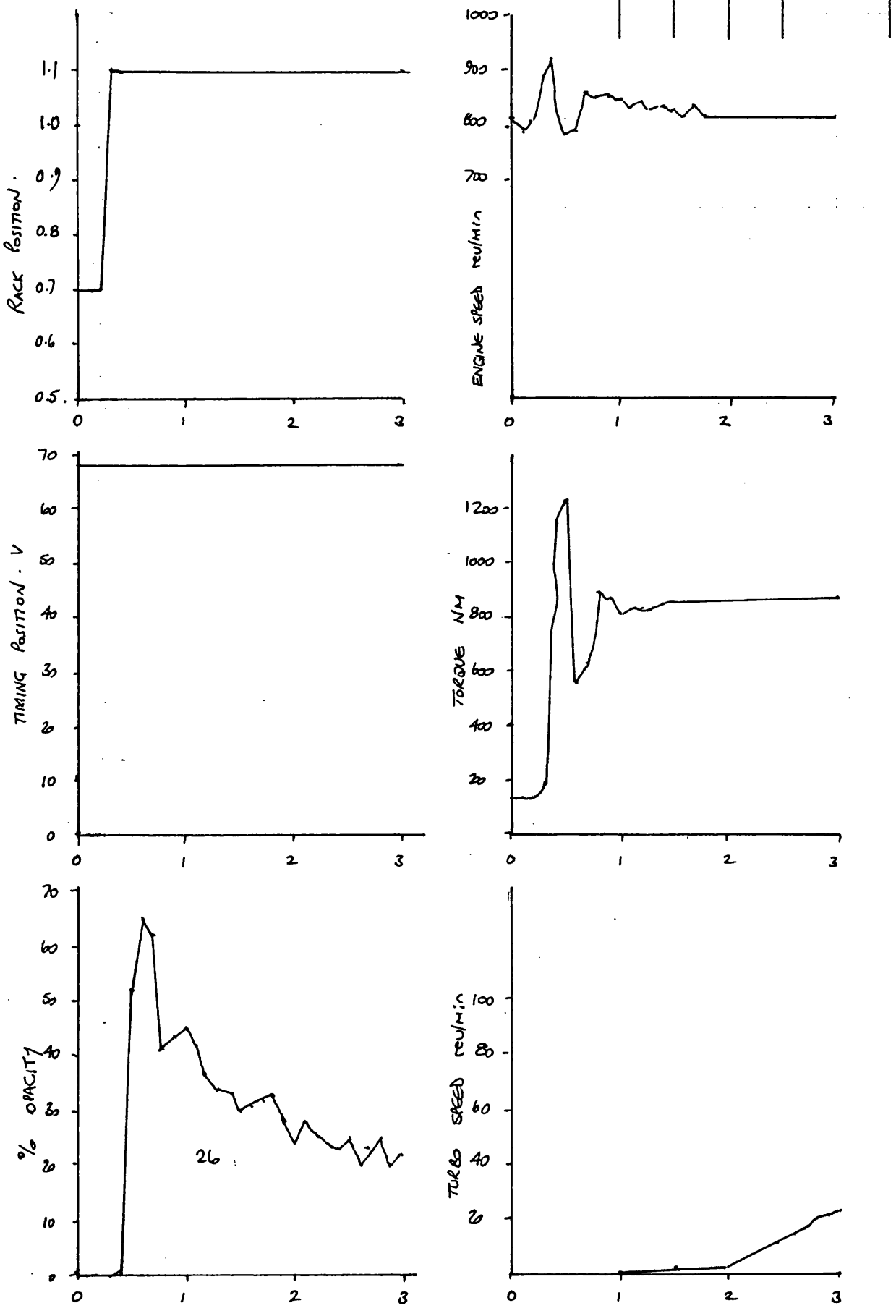

fig 5.12

Engine LEYLAND TL11 ENGINE—11.1L DISPLACEMENT Drawn By. EWRoberts

Title H2B 808IC L25 A3 'TIMING INVESTIGATION'

Constant Speed Curve at 800 rev/min

Holset / Leyland / Dowty / DoI Contract

Test No.	Timing	Amb'nt °C	Barometer Ins. Hg.
-	22	25	731

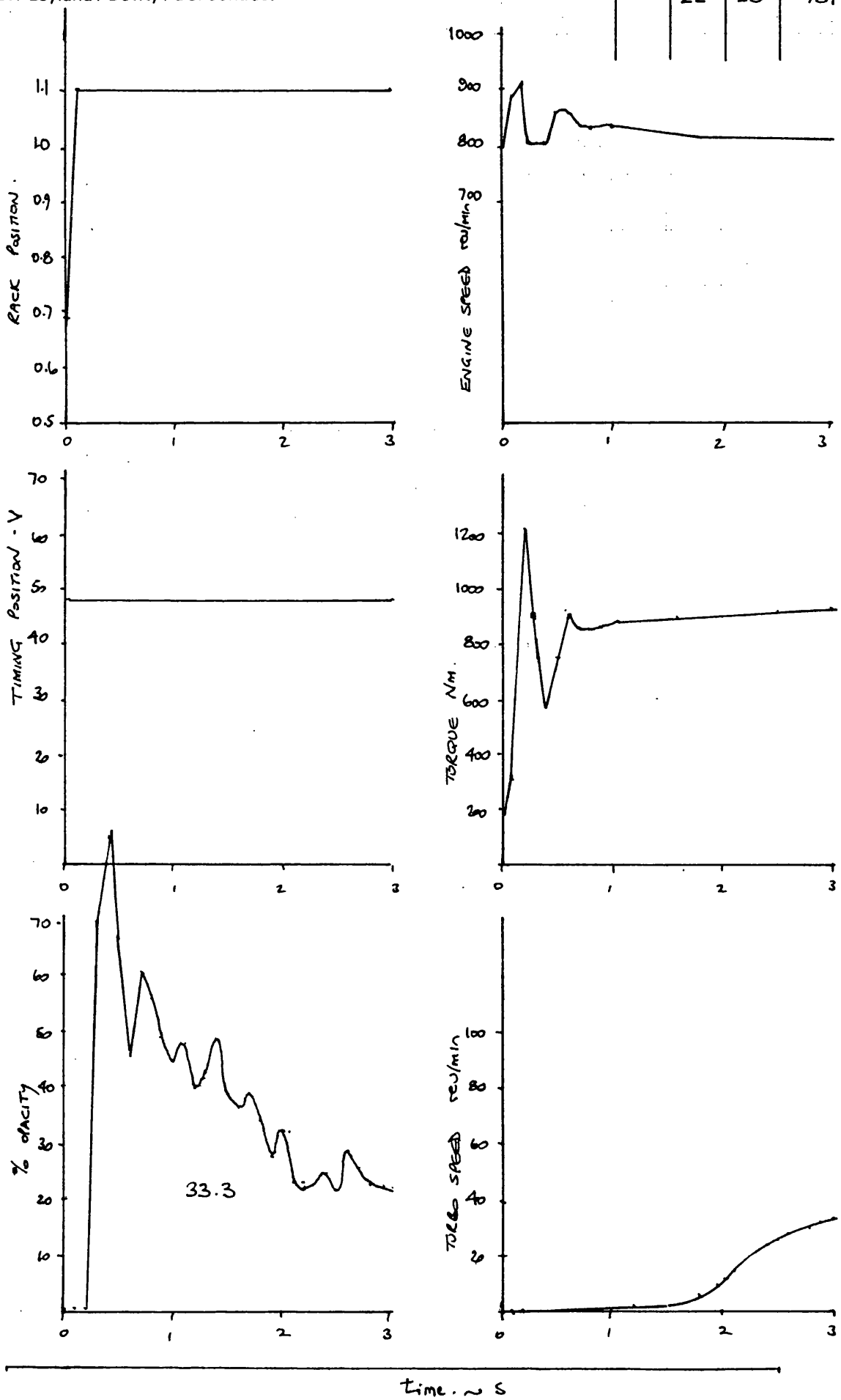

fig 5.13

Engine LEYLAND TL11 ENGINE—11.1L DISPLACEMENT Drawn By E.O Roberts

Title H2B 808IC L2SA3 TIMING INVESTIGATION

Constant Speed Curve at 800 rev/min

Holset / Leyland / Dowty / DoI Contract

Test No.	Timing	Amb'nt °C	Barometer Ins. Hg.
-	ISA	25	731

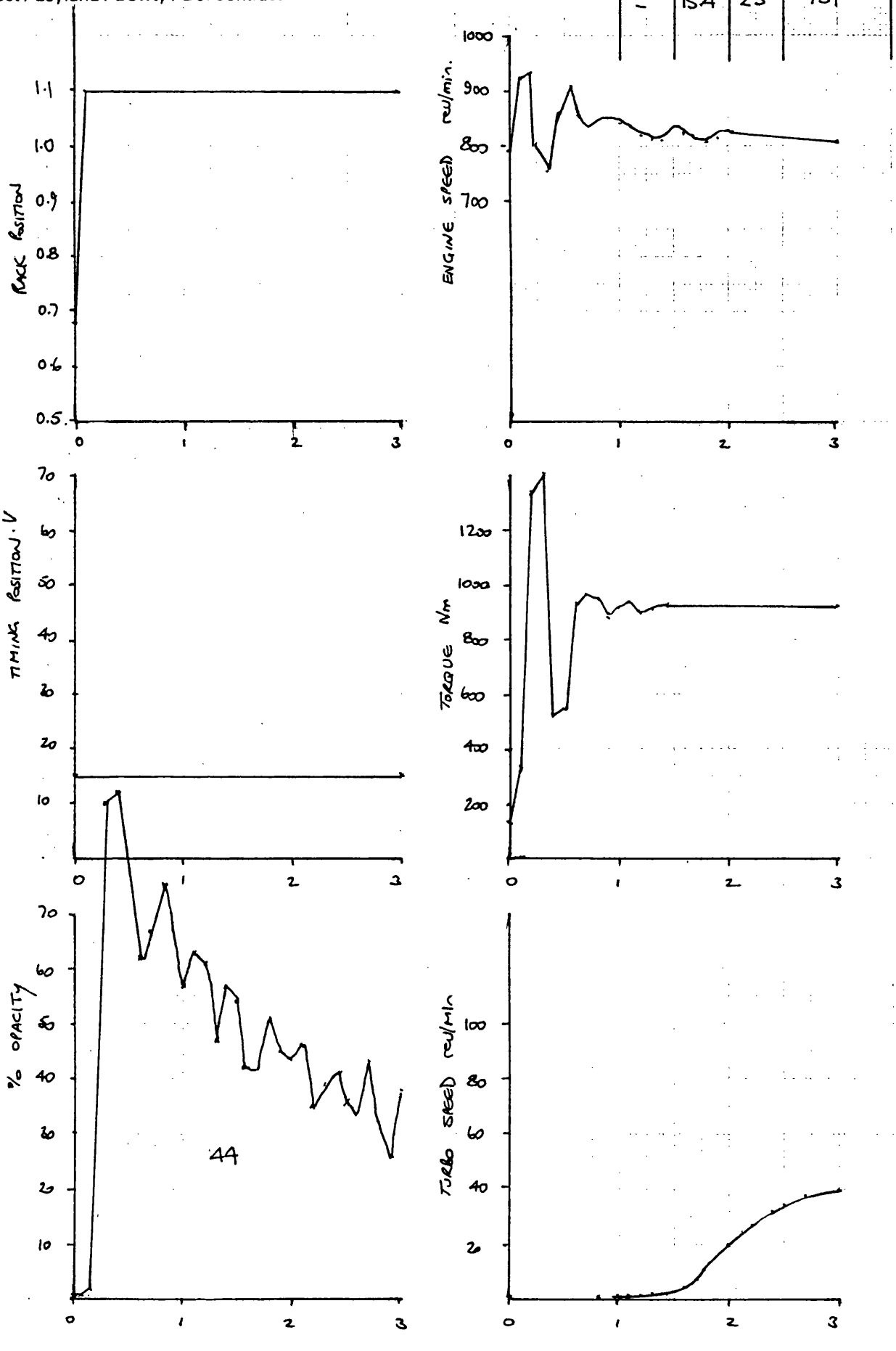

fig 5.14

Engine LEYLAND TL11 ENGINE—11.1L DISPLACEMENT Drawn By E W Roberts

Title H26 BOBIC L25A3 TIMING INVESTIGATION TRANSIENT TIMING SWING

Constant Speed Curve at 800 rev/min

Holset / Leyland / Dowty / DoI Contract

Test No.	Timing	Amb'nt °C	Barometer Ins. Hg.
–	15.4-26.4	25	731

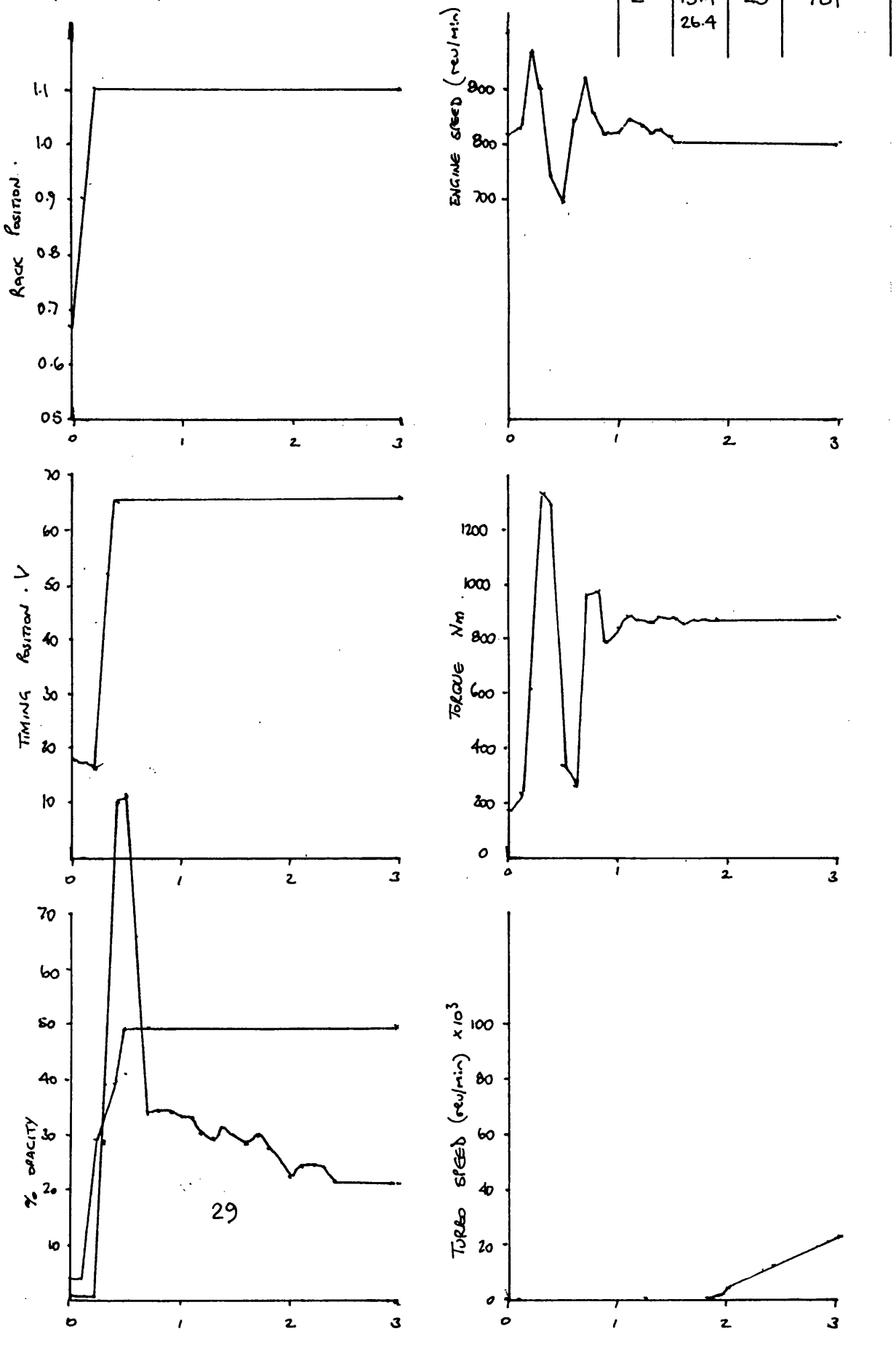

29

fig 5.15

Engine LEYLAND TL11 ENGINE—11.1L DISPLACEMENT Drawn By. E W ROBERTS

Title H2C 8640 · 270 · MK I · TWIN FLOW · FULLY OPEN · CONSTANT SPEED TRANSIENT

Constant Speed Curve at 2100 rev/min

Holset / Leyland / Dowty / DoI Contract

Test No.	Timing	Amb'nt °C	Barometer Ins. Hg.
–	22	25	751

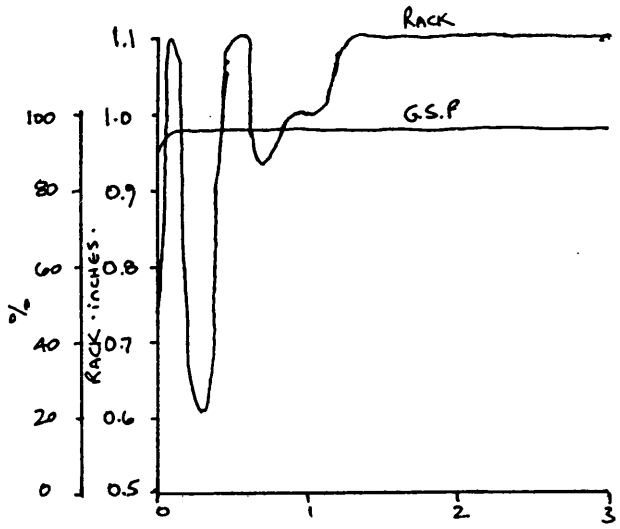

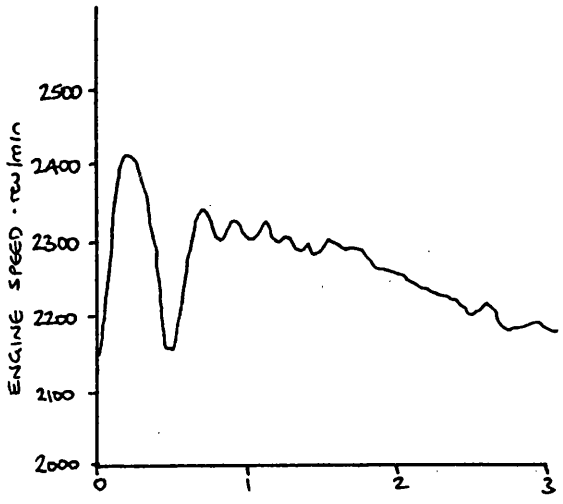

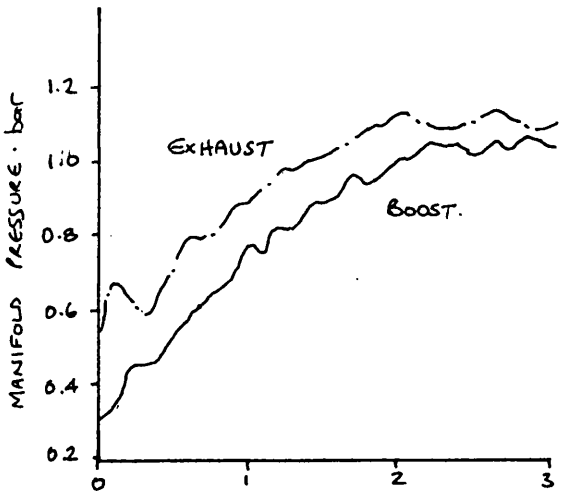

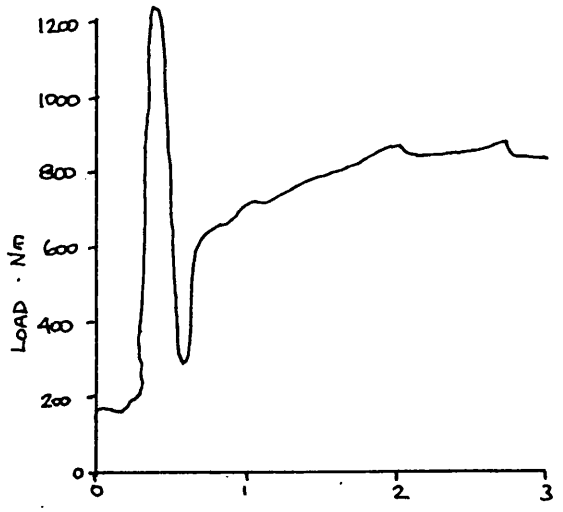

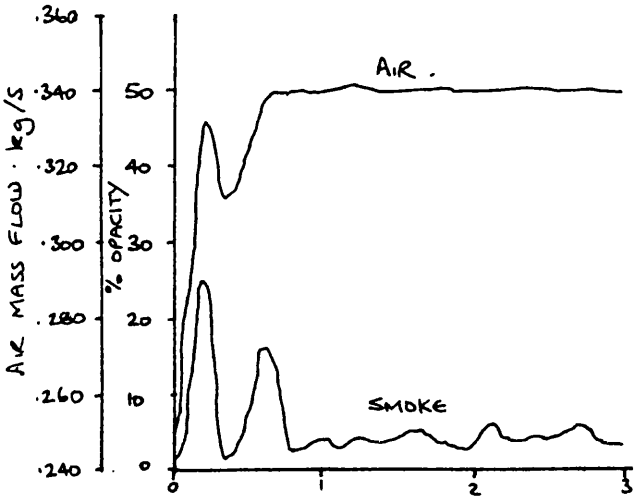

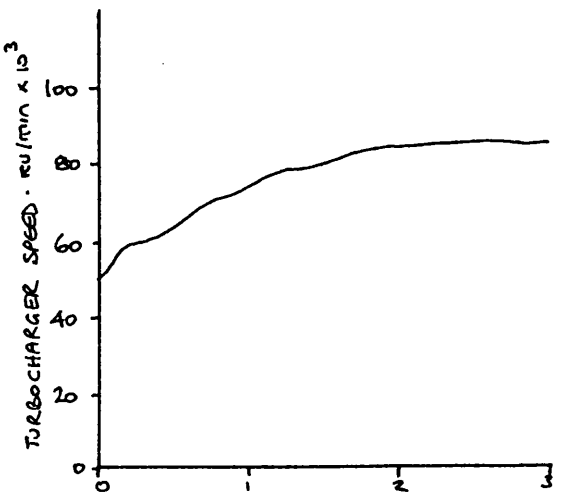

time ~ s

fig 5.16

Engine LEYLAND TL11 ENGINE—11.1L DISPLACEMENT Drawn By. E W ROBERTS

Title H2C 8640 : 270 : MK I TWINFLOW : FULLY OPEN : CONSTANT SPEED TRANSIENT :

Constant Speed Curve at 1400 rev/min

Holset / Leyland / Dowty / DoI Contract

Test No.	Timing	Amb'nt °C	Barometer Ins. Hg.
-	22	25	250·1

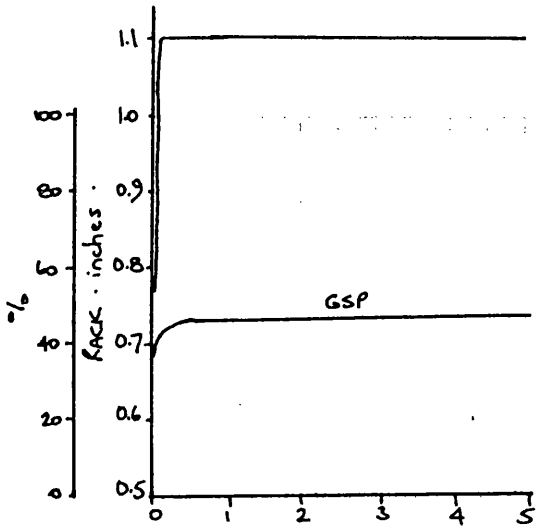

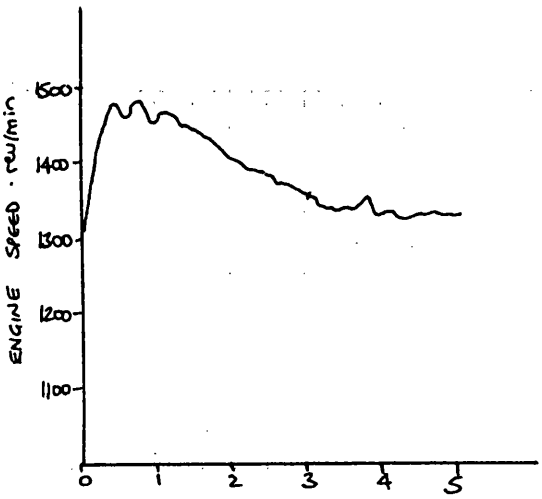

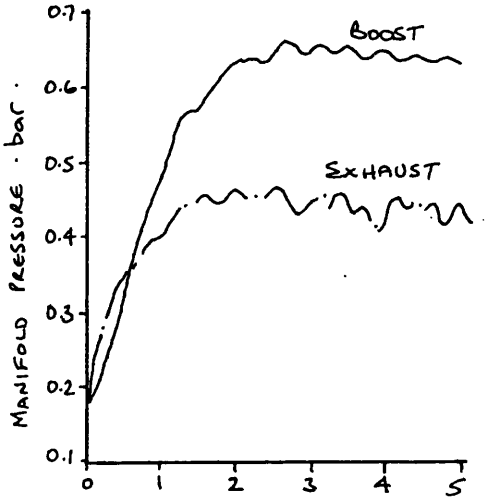

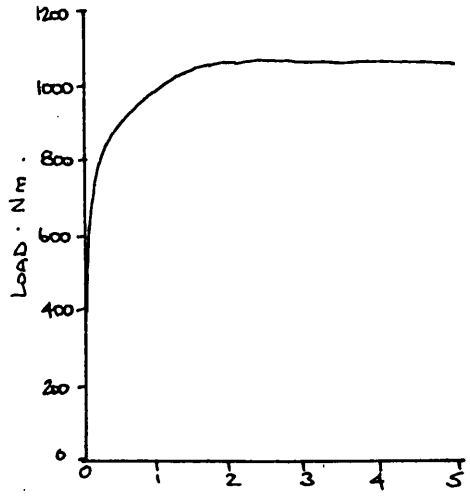

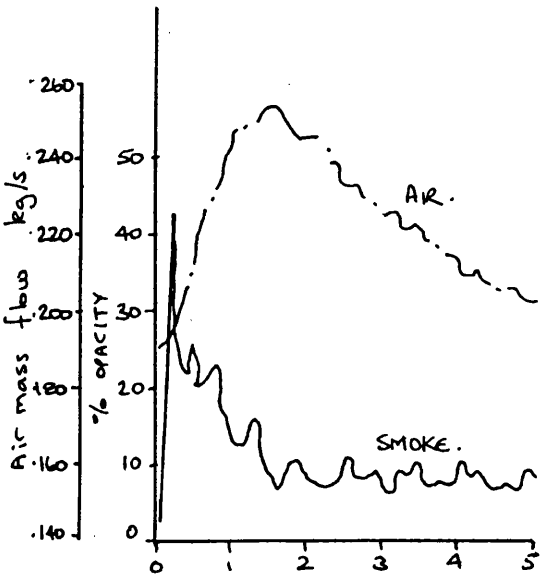

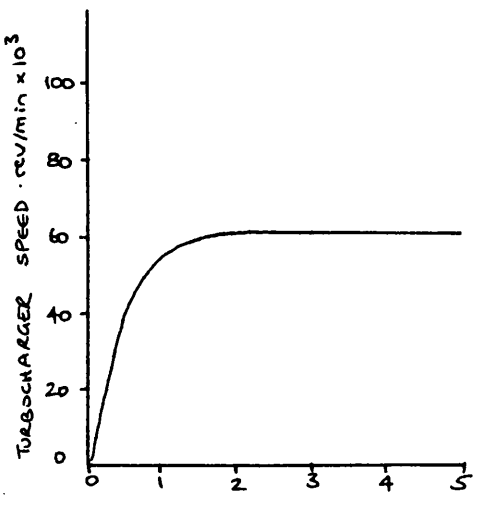

time ~ s

fig 5.17

Engine LEYLAND TL11 ENGINE—11.1L DISPLACEMENT Drawn By. E.W ROBERTS.

Title H2C 8640 .270 MK I TWINFLOW .FULLY RESTRICTED (50%) CONSTANT SPEED TRANSIENT.

Constant Speed Curve at 1400 rev/min

Holset / Leyland / Dowty / DoI Contract

Test No.	Timing	Amb'nt °C	Barometer Ins. Hg.
-	22	25	751

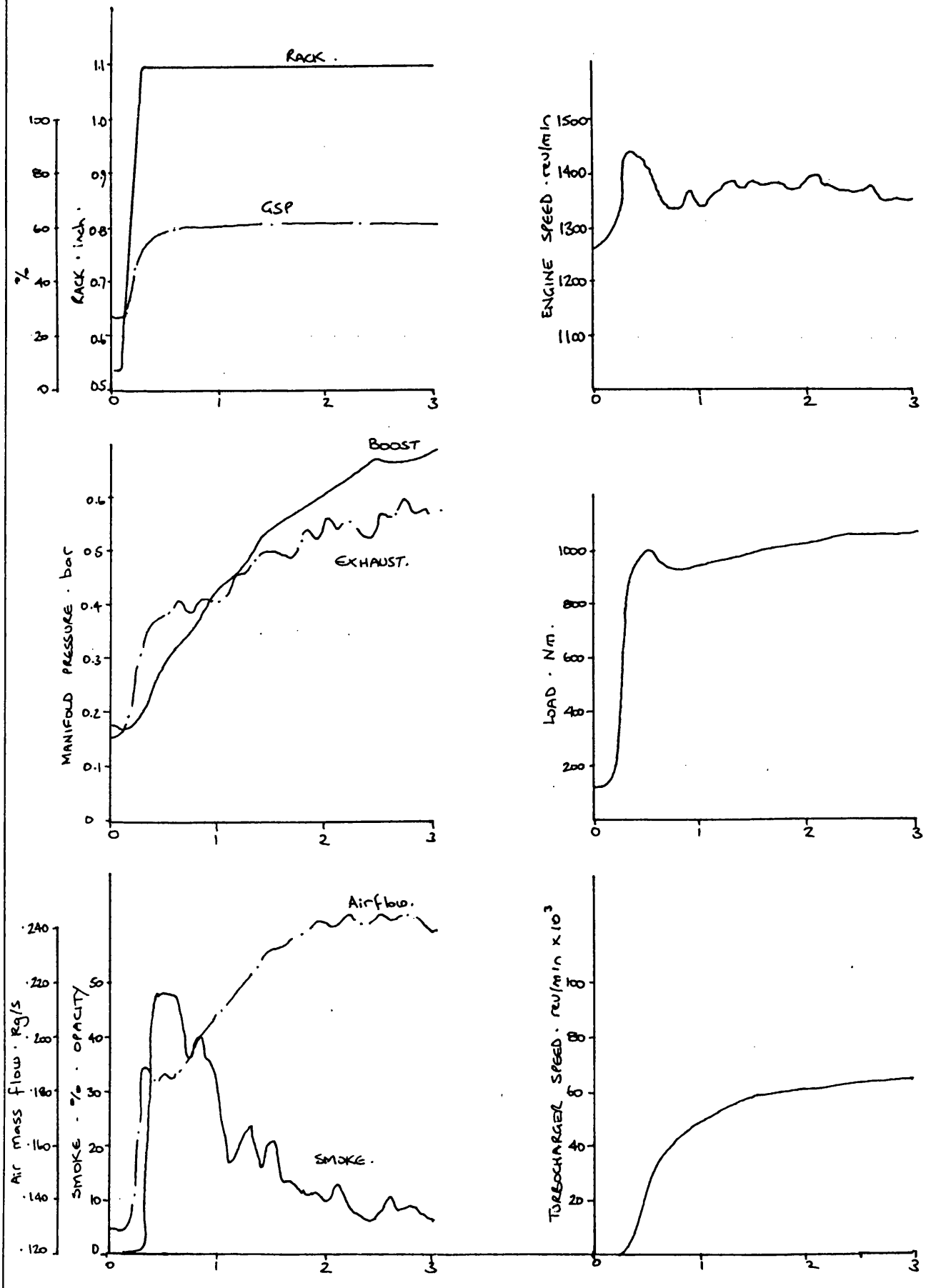

fig 5.18

Engine LEYLAND TL11 ENGINE—11.1L DISPLACEMENT Drawn By. EW ROBERTS

Title H2C 8640 · 270 · MKI · TWINFLOW · FULLY OPEN · CONSTANT SPEED TRANSIENT ·

Constant Speed Curve at 900 rev/min

Holset / Leyland / Dowty / DoI Contract

Test No.	Timing	Amb'nt °C	Barometer Ins. Hg.
–	22	25	750

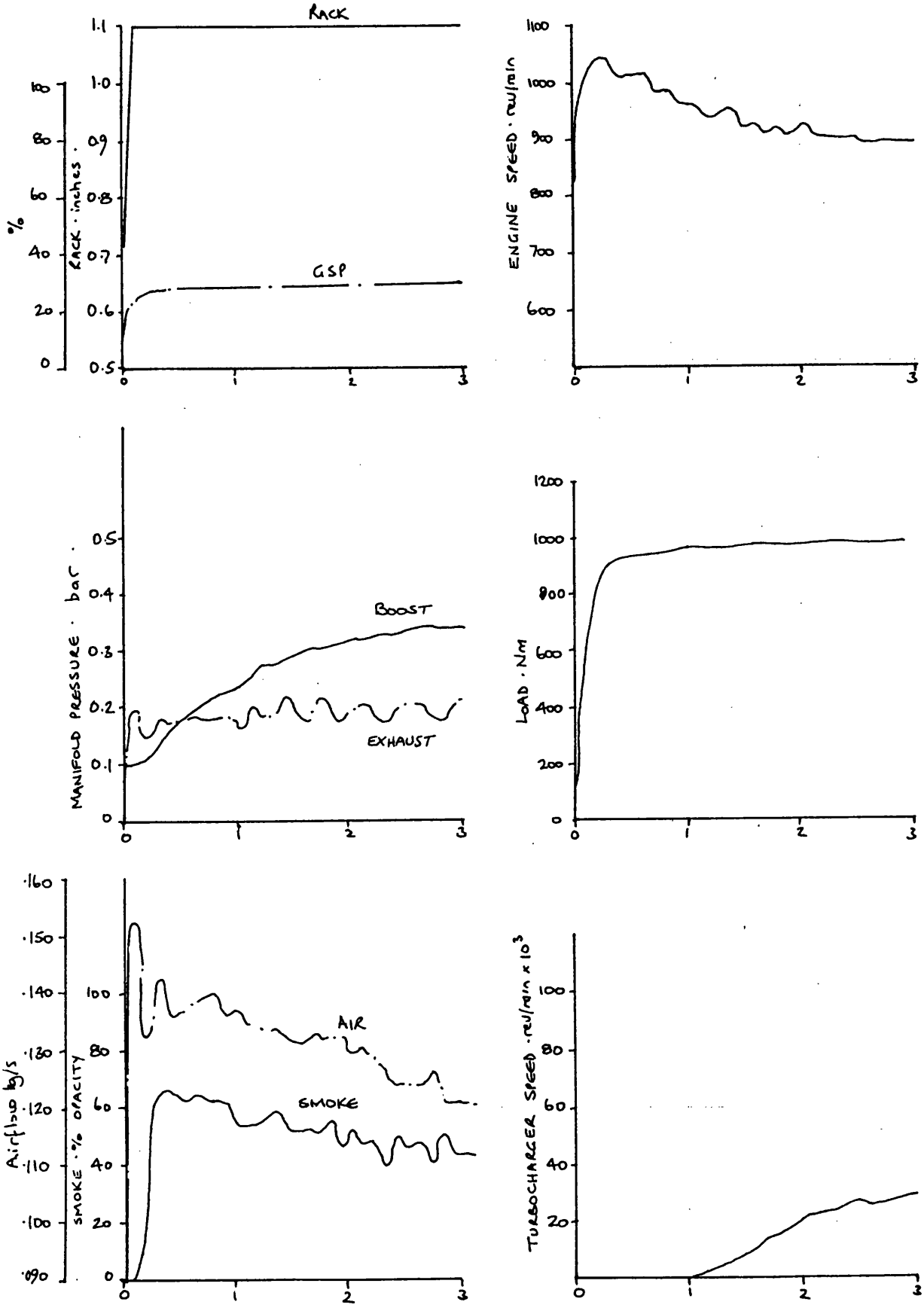

fig 5.19

Engine LEYLAND TL11 ENGINE—11.1L DISPLACEMENT Drawn By... E W ROBERTS

Title H2C 8640 .270. MKI. TWINFLOW : FULLY RESTRICTED (50%) CONSTANT SPEED TRANSIENT .

Constant Speed Curve at 900 rev/min

Holset / Leyland / Dowty / DoI Contract

Test No.	Timing	Amb'nt °C	Barometer Ins. Hg.
–	22	25	751

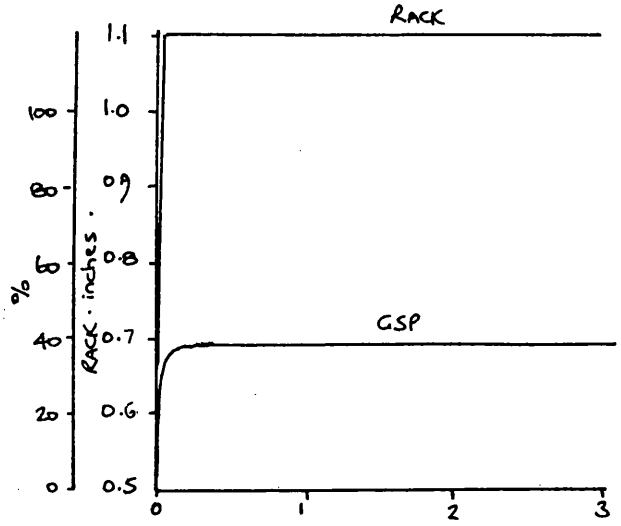

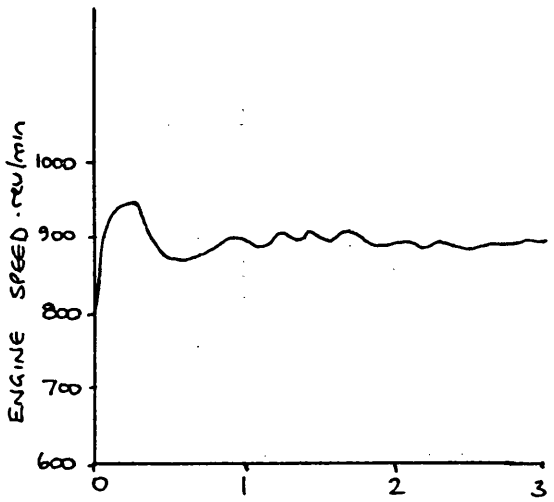

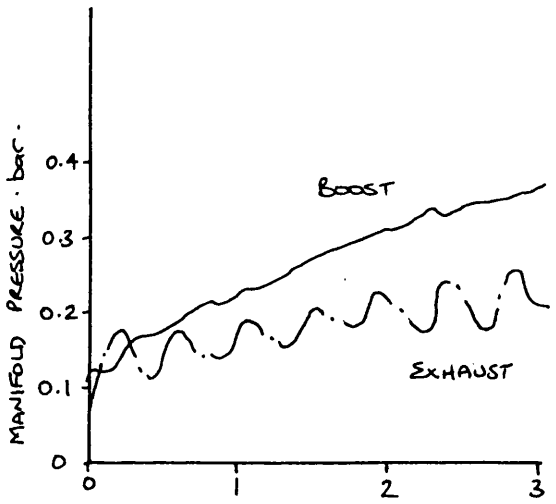

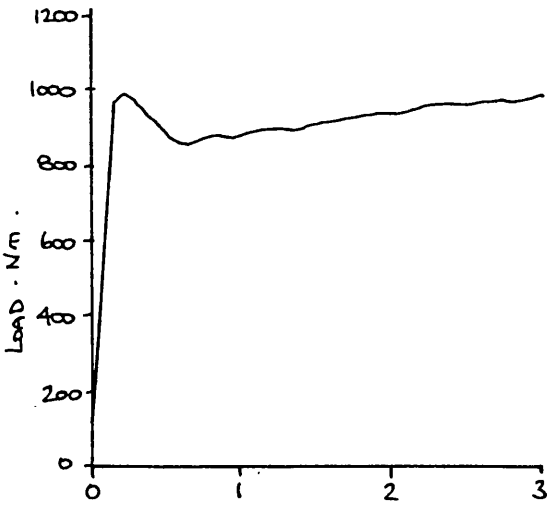

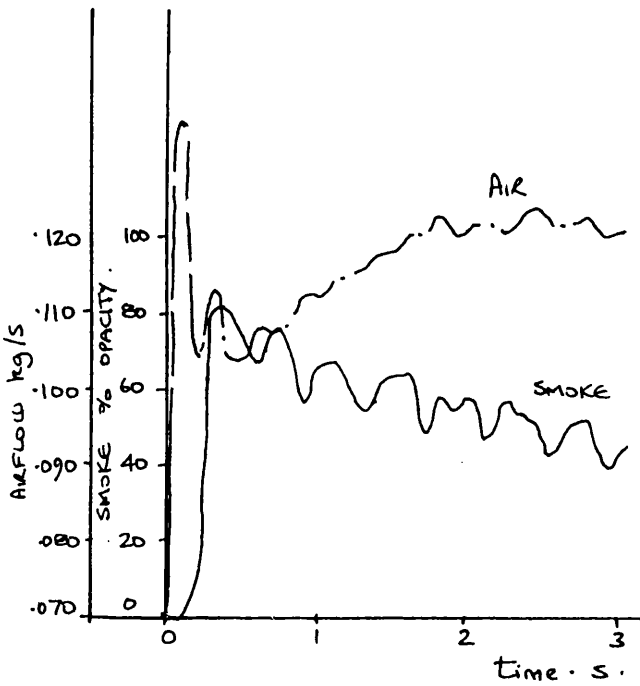

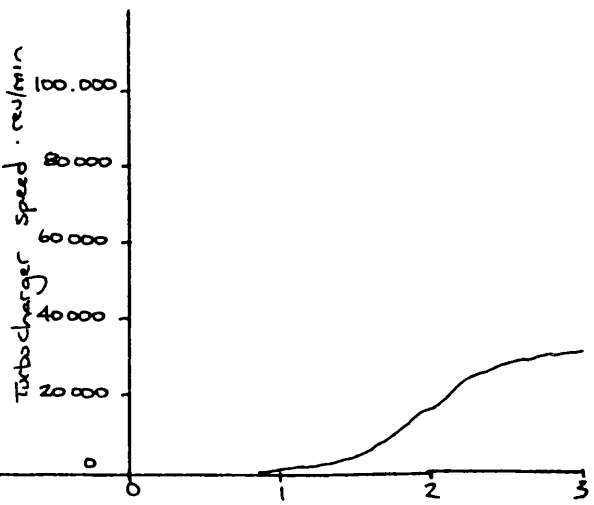

fig 5.20

Title TURBINE INLET RESTRICTION (SMOOTHED) - % AS A FUNCTION OF SPEED & LOAD

STEADY STATE OPTIMISATION.

Holset / Leyland / Dowty / DoI Contract

Test No.	Timing	Amb'nt °C	Barometer Ins. Hg.
–	VARIABLE	25	748

191 kW @ 2360 rev/min } 46% Torque - back-up @
1155 Nm @ 1350 rev/min } 59% of RATED SPEED.

LINES OF CONSTANT RESTRICTION

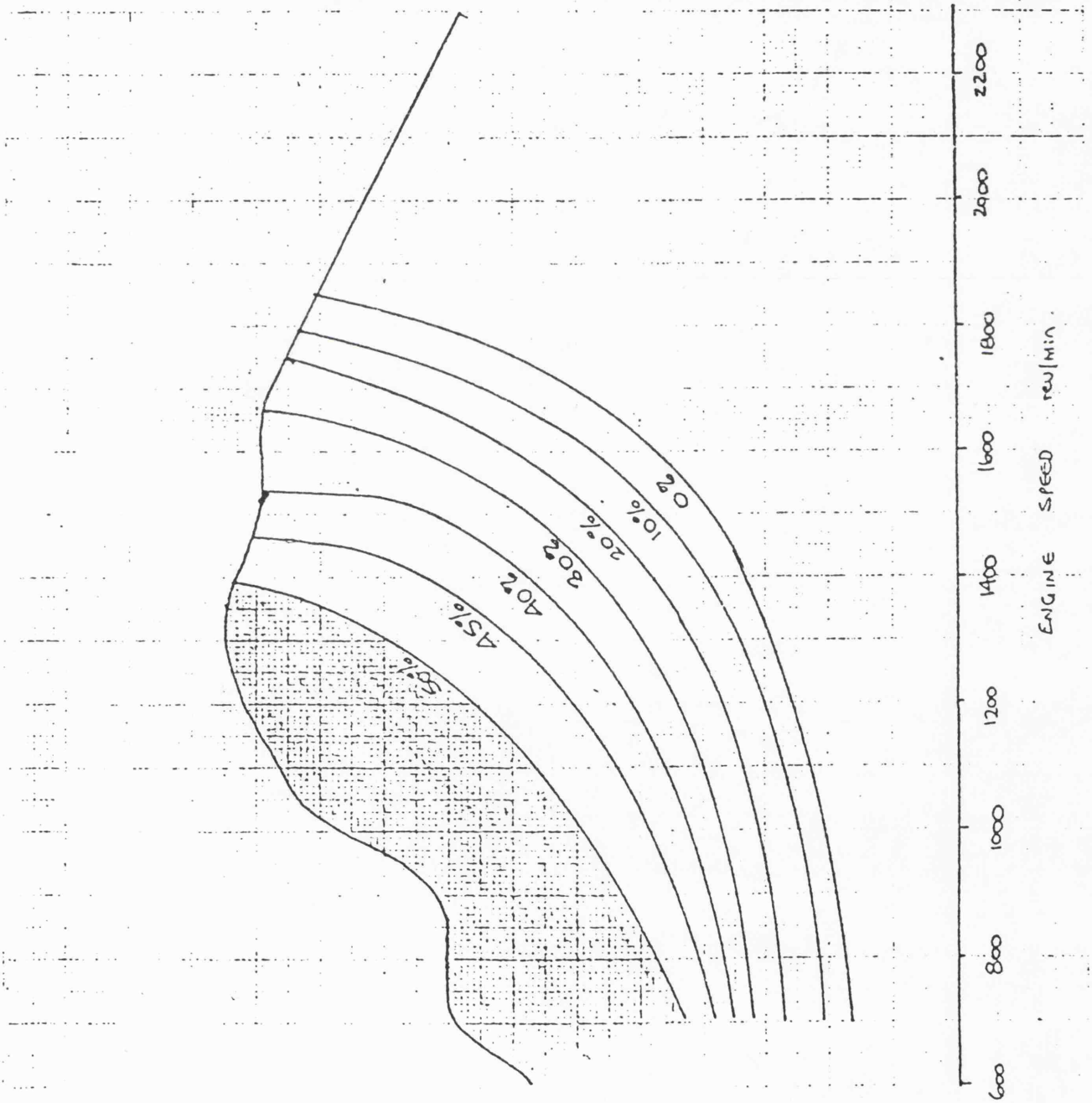

Drawn By. D. HOWARD

Title. BOOST PRESSURE (KN/m² above 1 BAR) AS A FUNCTION OF SPEED + LOAD

STEADY-STATE OPTIMISATION

Test No.	Timing	Amb'nt °C	Barometer Ins. Hg.
–	VARIABLE	22	748

Holset / Leyland / Dowty / DoI Contract

191 KW @ 2300rpm 1155 Nm @ 1360rpm

46% TORQUE BACK UP @ 59% OF RATED SPEED

LINES OF CONSTANT INLET MANIFOLD PRESSURE

KN/m² above 1 BAR

WITH LINES OF CONSTANT RESTRICTION SUPERIMPOSED.

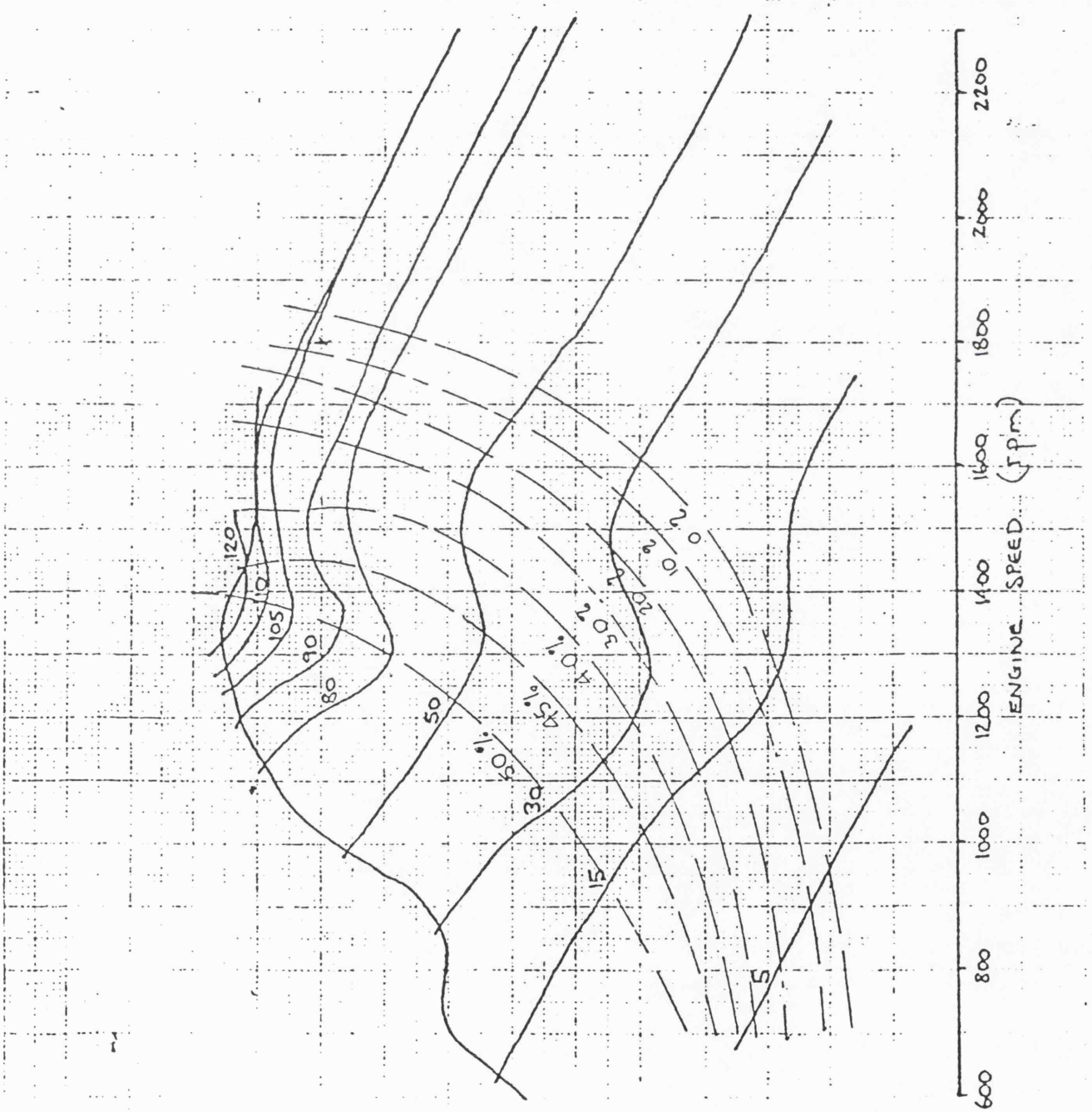

ENGINE TORQUE (Nm)

1200 1100 1000 900 800 700 600 500 400 300 200 100 0

fig 5.22

TURBINE CONTROL SCHEDULE	ENGINE SPEED - rev/min			
	800	1200	1600	1800
Fully open (0%)	0%	0%	0%	0%
Maximum Restriction for Load and Speed	50%	50%	34%	As above
Restriction Schedule	0 - 50%	0 - 50%	0 - 34%	As above
Boost Demand Schedule	As above	As above	1.08	0.8 bar

TRANSIENT TEST PROGRAMME FIG. 5.23

fig 5.23

ENGINE SPEED (rev/min)

	1800			1600				1200			800		
Test No.	400	403		300	301	302	303	200	201	202	100	101	102
Max. Boost Press. bar	.64	.80		.58	.90	1.01	1.08	.28	.56	.56	.10	.16	.16
Max. Pre-turbine Press.bar	.75	1.2		.64	1.09	1.28	1.40	.32	.68	.69	.16	.20	.20
Steady State ΔP - bar	.11	.10		.06	.19	.27	-	.04	.12	.13	.06	.04	.04
Area under Smoke Trace sq. units.	13.2	9.5		24.8	20.4	12.5	11.7	47.2	26.3	33.7	22.0	23.0	24.5
Time to achieve 80% of boost	1.25	.70		1.25	1.5	1.8	1.3	1.70	1.75	2.0	1.5	2.1	2.0
Max. Torque Nm	1000	1020		1050	1090	1100	1090	990	1080	1110	790	790	790
Torque after 1s	940	1000		1010	1020	1050	1040	830	1020	950	800	800	830

TABLE OF RESULTS

FIG. 5.24

fig 5.24

Engine LEYLAND TL11 ENGINE—11.1L DISPLACEMENT Drawn By... S.J. ROBERTS

Title... VG TURBOCHARGER FULLY OPEN

Constant Speed Curve at 1800 rev/min

Holset / Leyland / Dowty / DoI Contract

Test No.	DYNAMIC Timing	Amb'nt °C	Barometer Ins. Hg.
400	20	24	750

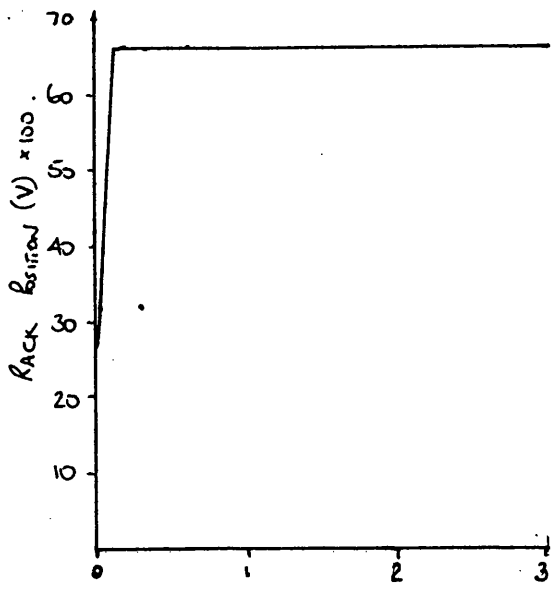

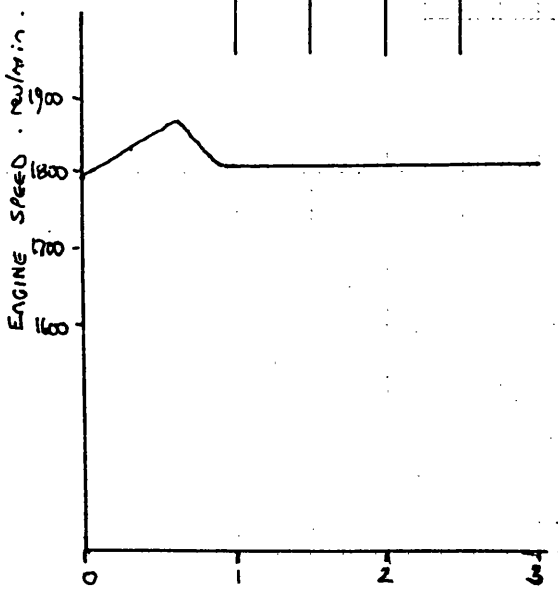

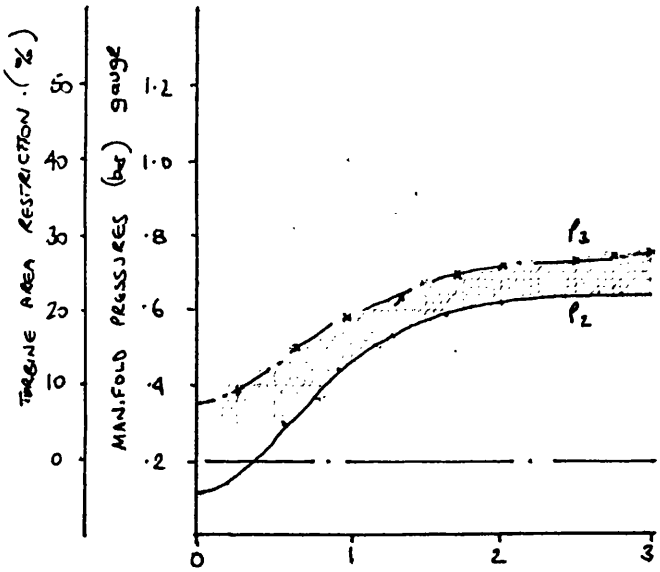

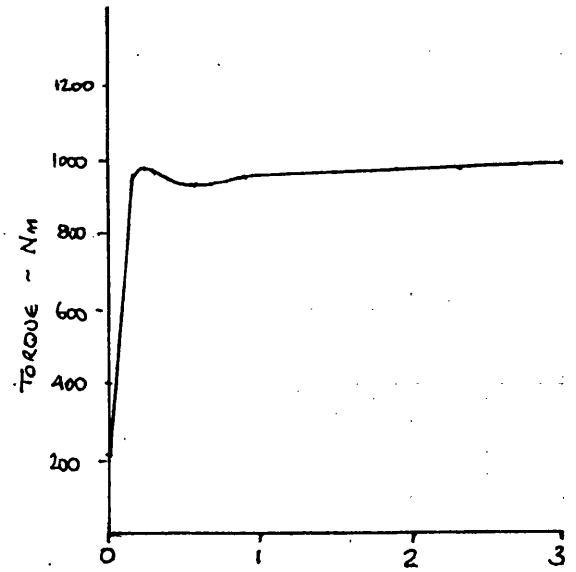

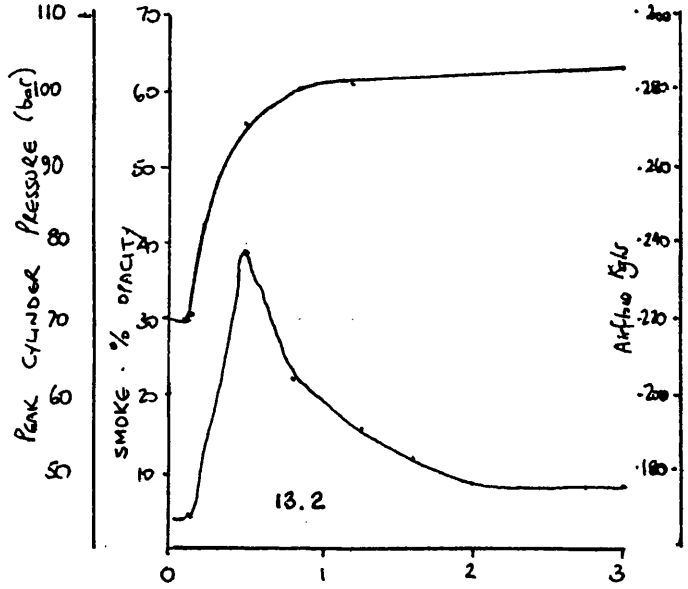

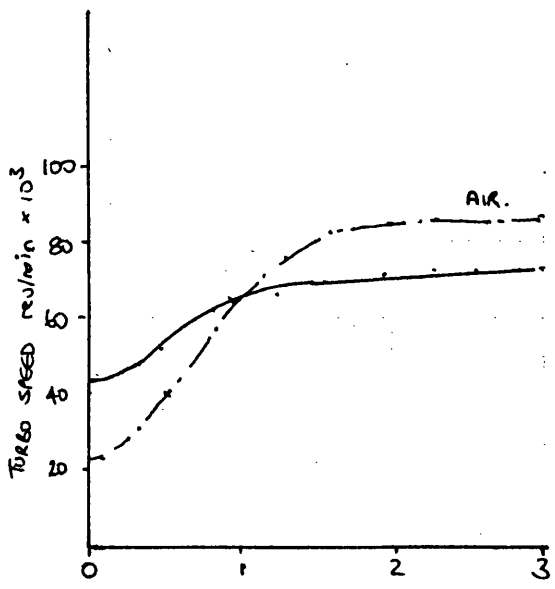

time ~ s

fig 5.25

Engine LEYLAND TL11 ENGINE—11.1L DISPLACEMENT Drawn By. E.W ROBERTS

Title V.G TURBOCHARGER UNDER CLOSED LOOP BOOST DEMAND

Constant Speed Curve at 1800 rev/min

Holset / Leyland / Dowty / DoI Contract

Test No.	Dynamic Timing	Amb'nt °C	Barometer Ins. Hg.
403	20	25	751

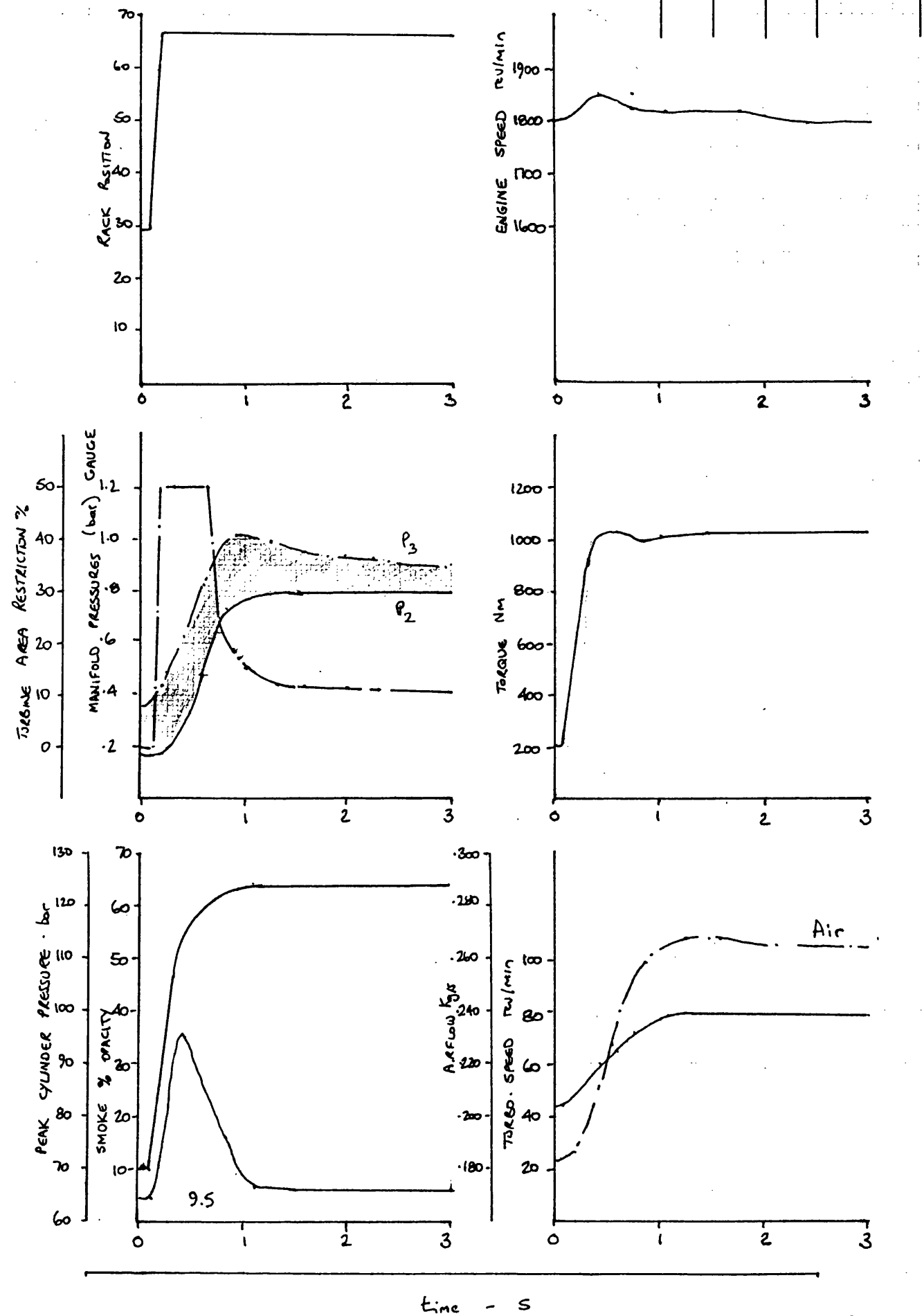

fig 5.26

Engine LEYLAND TL11 ENGINE—11.1L DISPLACEMENT Drawn By. E.W. ROBERTS

Title VG TURBOCHARGER FULLY OPEN

Constant Speed Curve at 1600 rev/min

Holset / Leyland / Dowty / DoI Contract

Test No.	DYNAMIC Timing	Amb'nt °C	Barometer Ins. Hg.
300	17.5	24	7.51

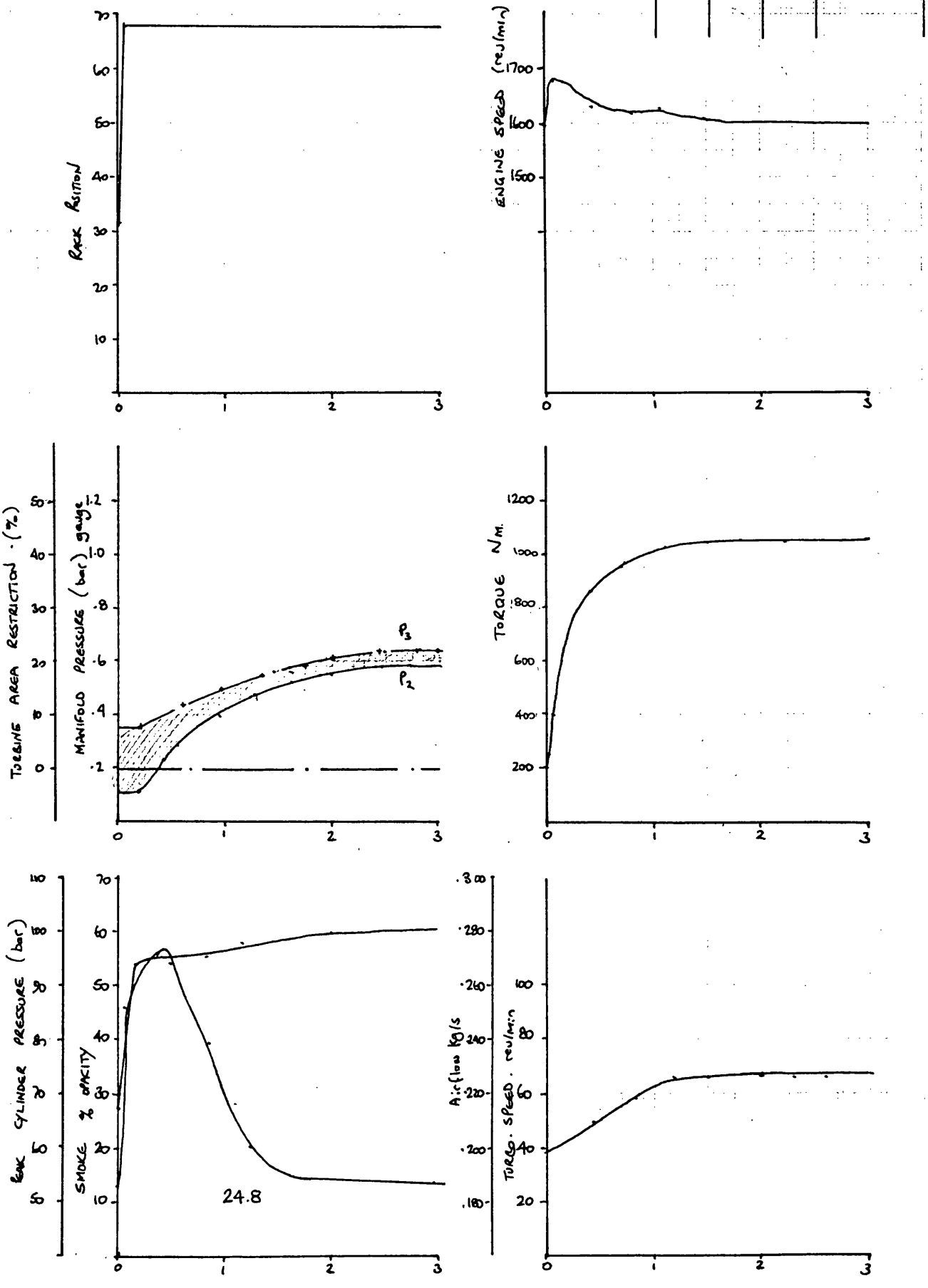

fig 5.27

Engine LEYLAND TL11 ENGINE—11.1L DISPLACEMENT Drawn By... E.N. ROBERTS

Title ... VG TURBOCHARGER 34% RESTRICTED

Constant Speed Curve at 1600 rev/min

Holset / Leyland / Dowty / DoI Contract

Test No.	DYNAMIC Timing	Amb'nt °C	Barometer Ins. Hg.
301	17.5	25	752

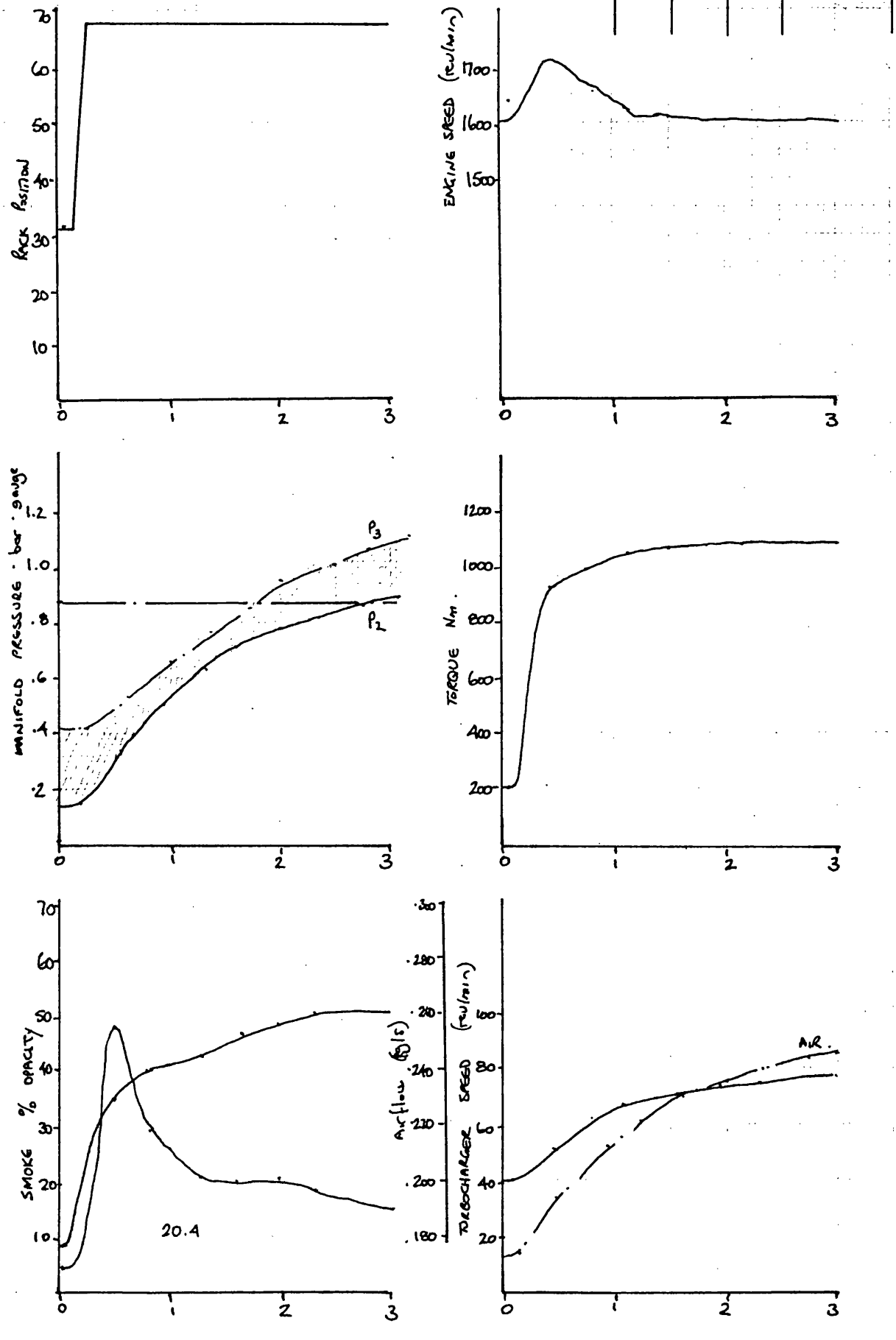

Fig 5.28

Engine LEYLAND TL11 ENGINE—11.1L DISPLACEMENT Drawn By... E.W ROBERTS

Title VG TURBOCHARGER FULLY OPEN TO 34% RESTRICTION

Constant Speed Curve at 1600 rev/min

Holset / Leyland / Dowty / DoI Contract

Test No.	DYNAMIC Timing	Amb'nt °C	Barometer Ins. Hg.
302	17.5	26	752

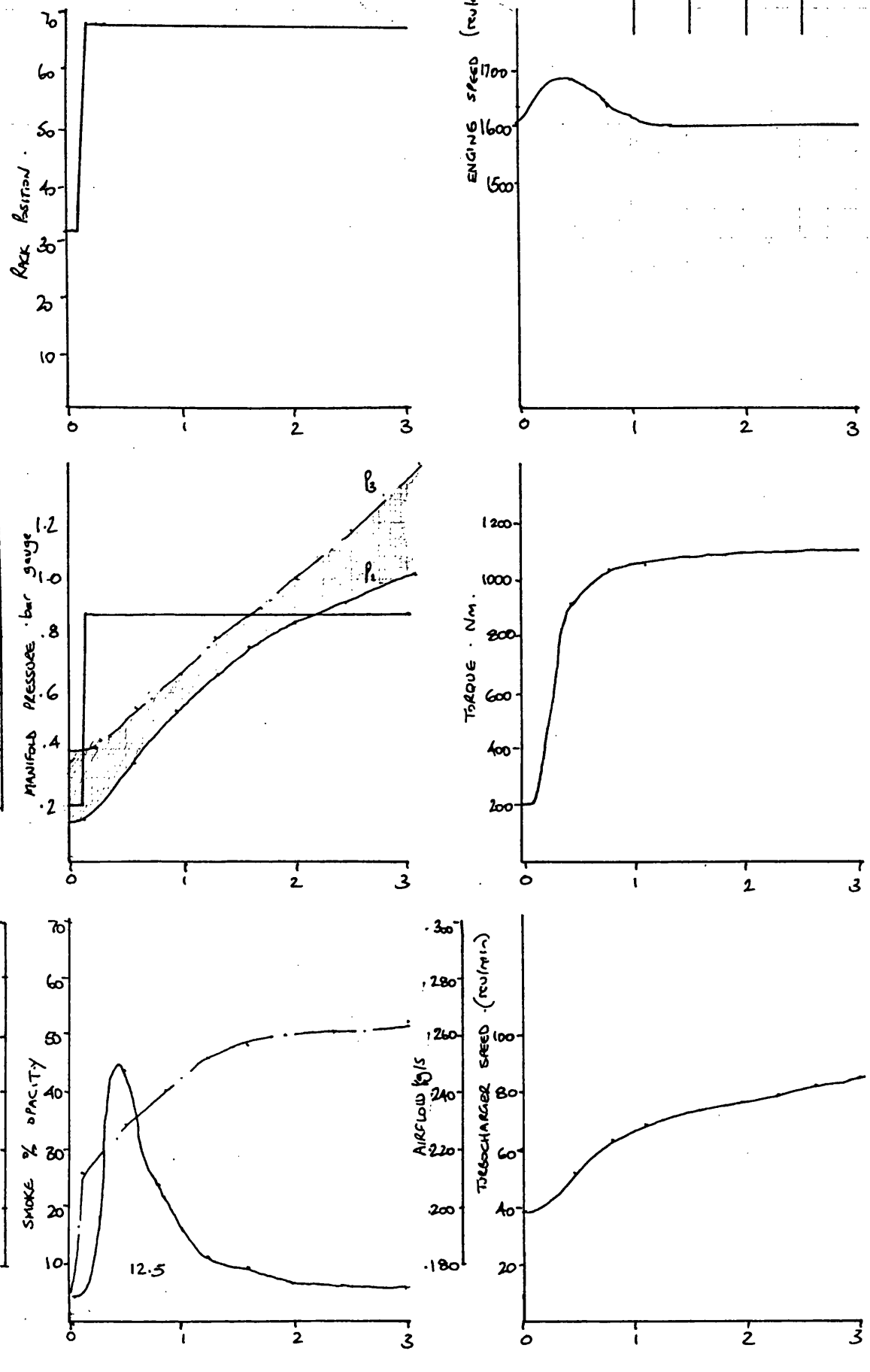

fig 5.29

Engine LEYLAND TL11 ENGINE—11.1L DISPLACEMENT Drawn By... E.W.ROBERTS.....

Title VG TURBOCHARGER UNDER CLOSED LOOP BOOST DEMAND

Constant Speed Curve at 1600 rev/min

Holset / Leyland / Dowty / DoI Contract

Test No.	Dynamic Timing	Amb'nt °C	Barometer Ins. Hg.
303	17.5	25	751

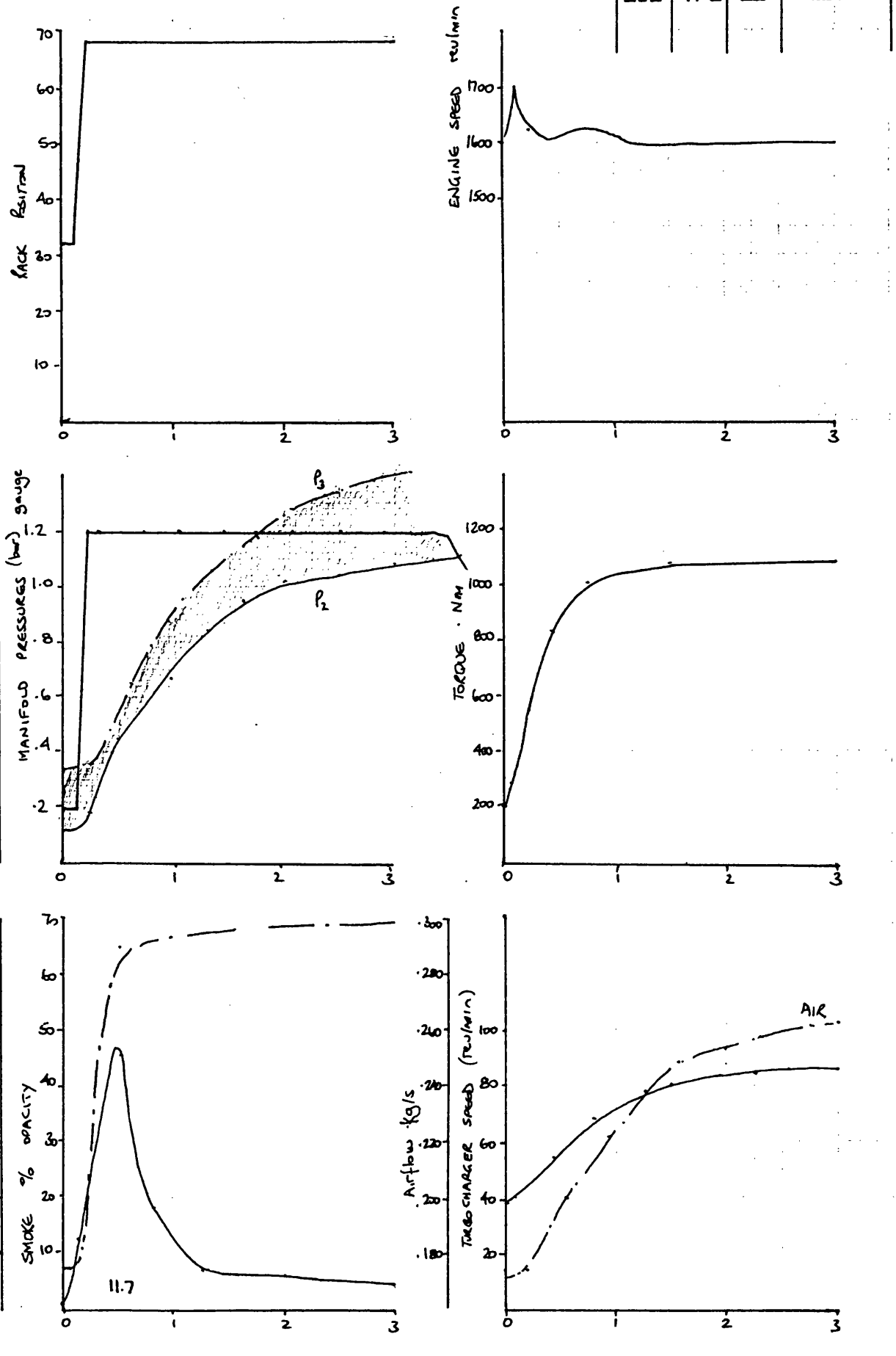

fig 5.30

Engine LEYLAND TL11 ENGINE—11.1L DISPLACEMENT Drawn By... E.W.ROBERTS

Title VG TURBOCHARGER FULLY OPEN

Constant Speed Curve at 1200 rev/min

Holset / Leyland / Dowty / DoI Contract

Test No.	DYNAMIC Timing	Amb'nt °C	Barometer Ins. Hg.
200	17	25	750

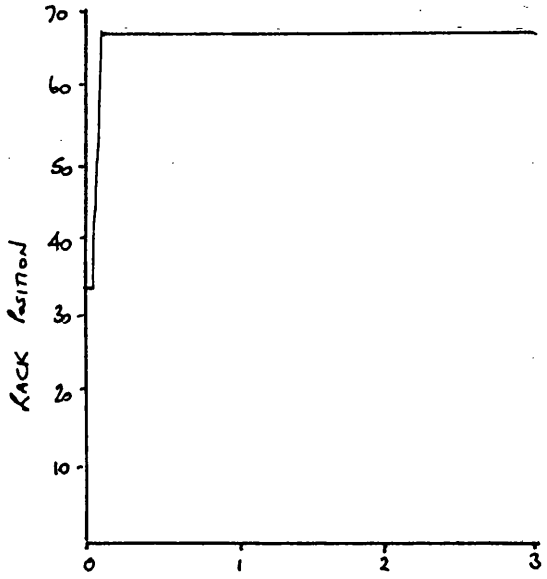

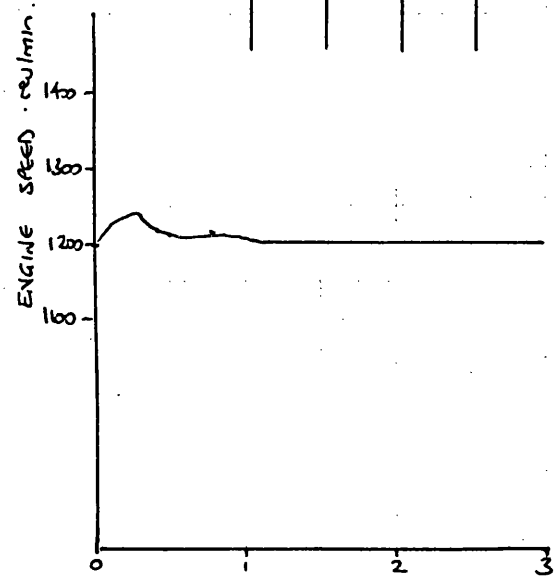

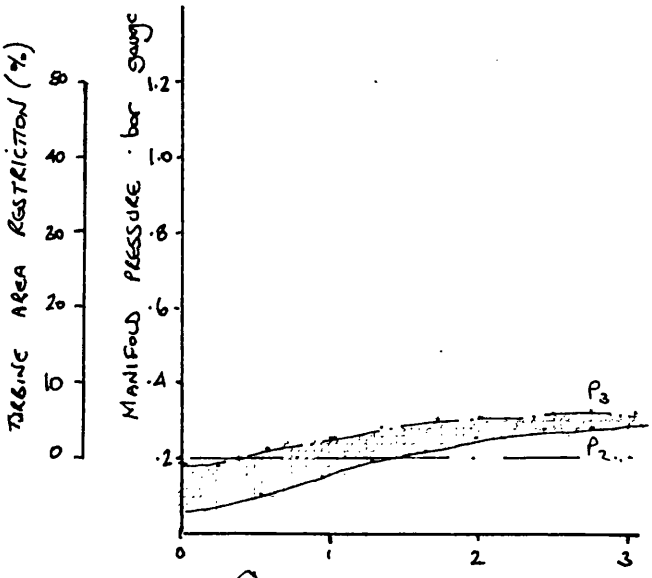

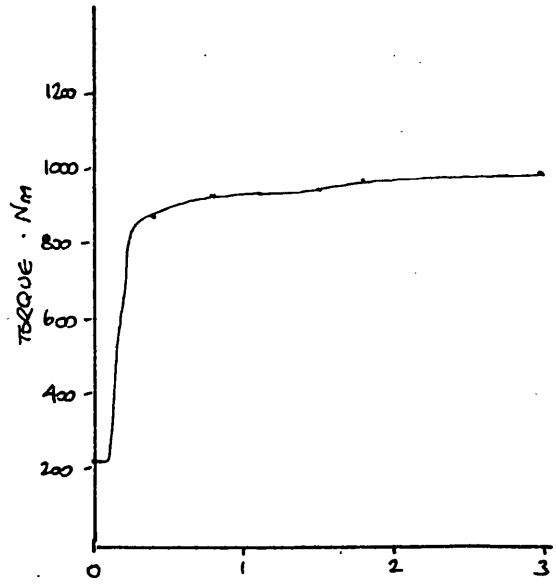

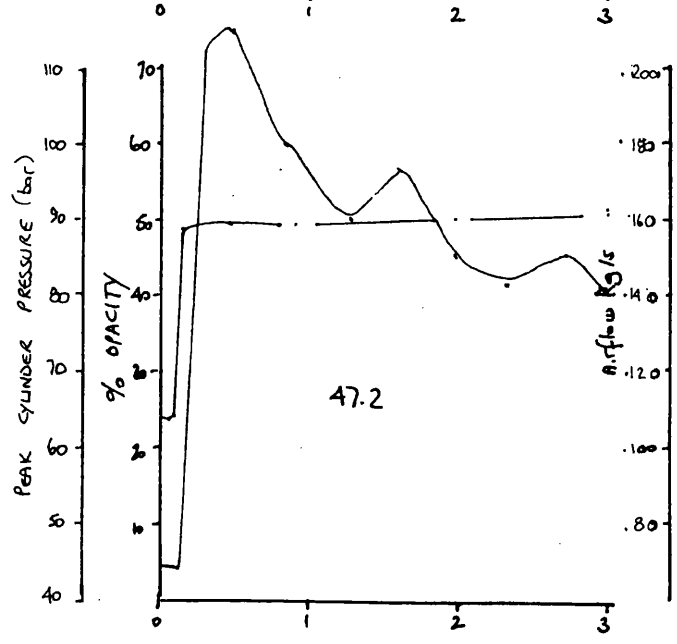

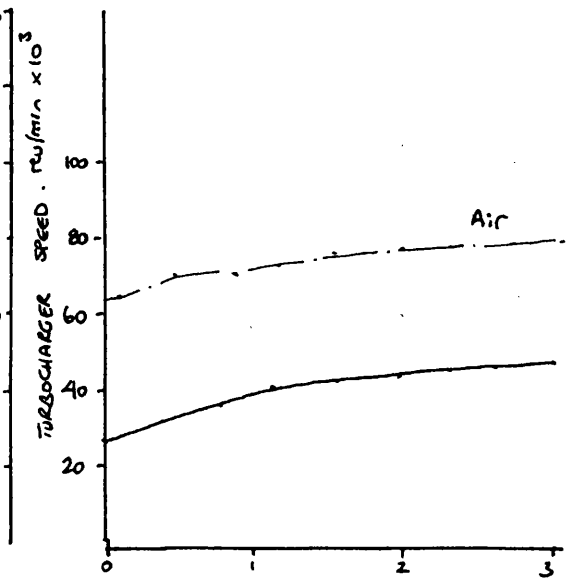

time - s

fig 5.31

Engine LEYLAND TL11 ENGINE—11.1L DISPLACEMENT Drawn By.... E.H. ROBERTS

Title.... VG TURBOCHARGER ..... 50% RESTRICTED

Constant Speed Curve at 1200 rev/min

Holset / Leyland / Dowty / DoI Contract

Test No.	Dynamic Timing	Amb'nt °C	Barometer Ins. Hg.
201	17	25	749

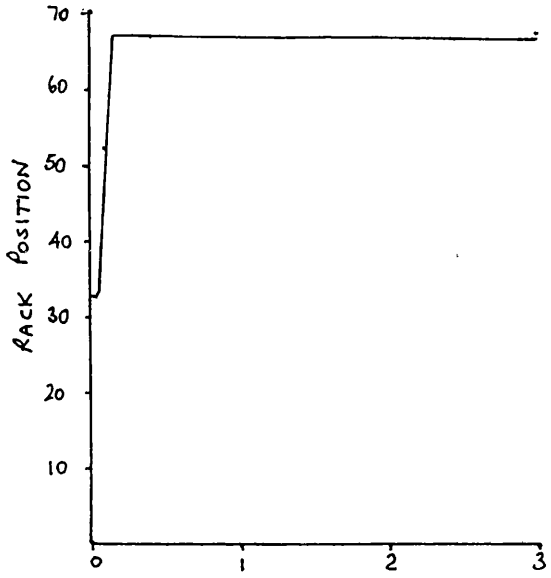

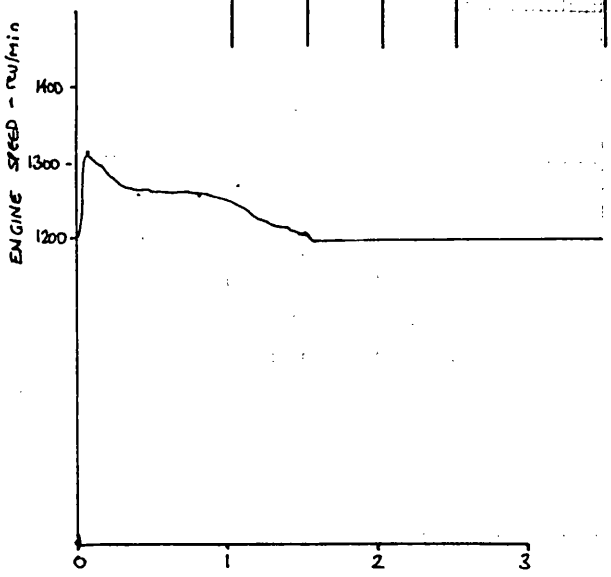

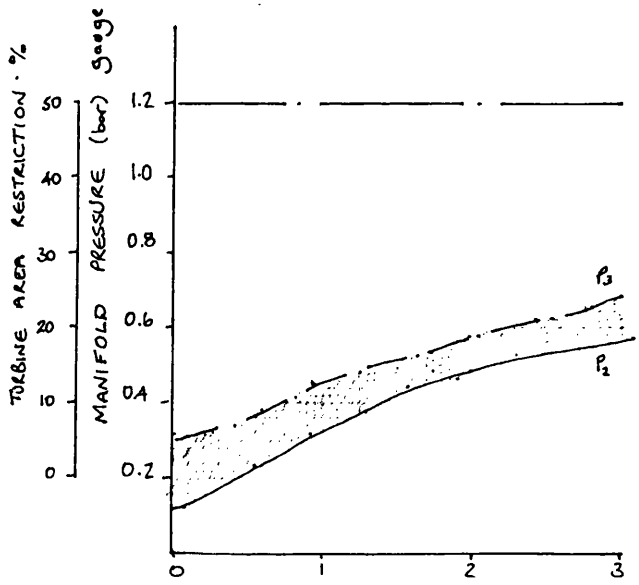

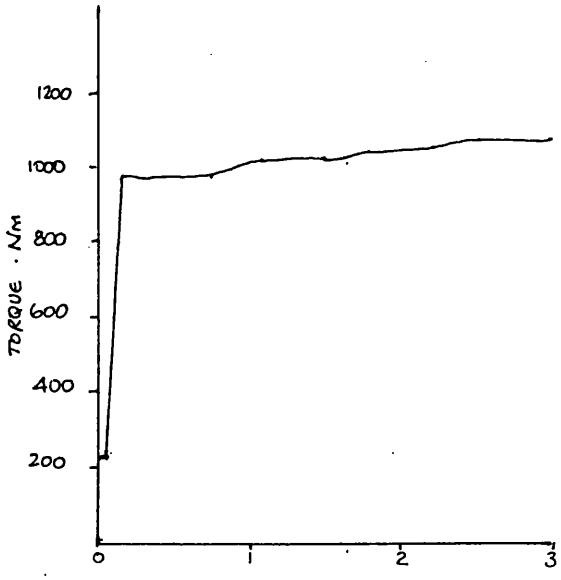

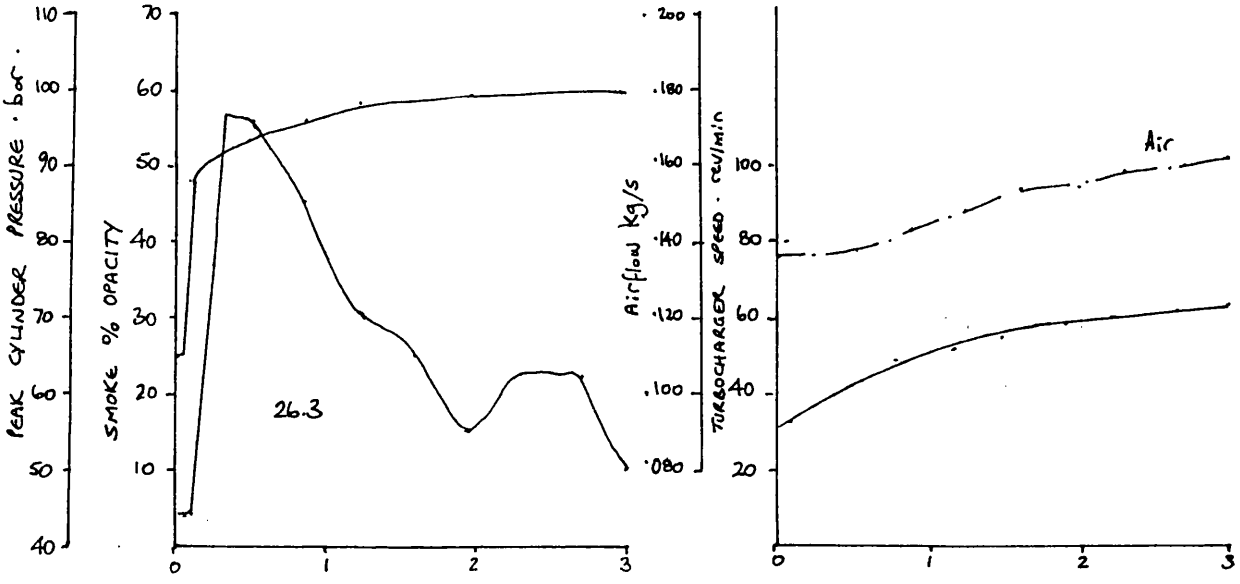

Time ~ s

fig 5.32

Engine LEYLAND TL11 ENGINE—11.1L DISPLACEMENT Drawn By... E.W.ROBERTS

Title... VG TURBOCHARGER FULLY OPEN TO 50% RESTRICTED

Constant Speed Curve at 1200 rev/min

Holset / Leyland / Dowty / DoI Contract

Test No.	Timing	Amb'nt °C	Barometer Ins. Hg.
202	17	25	7.51

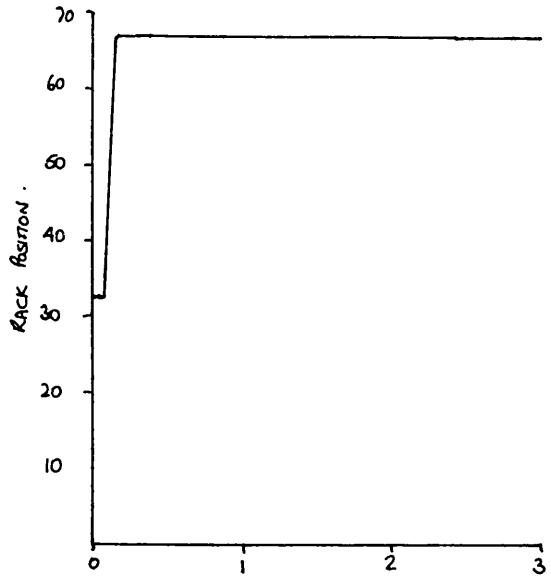

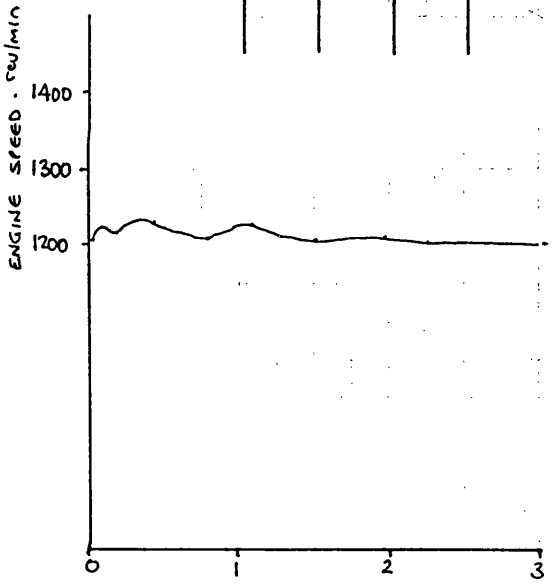

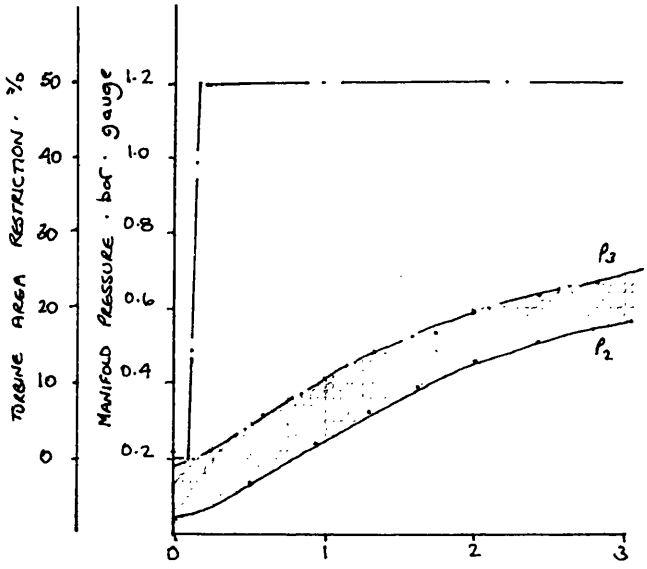

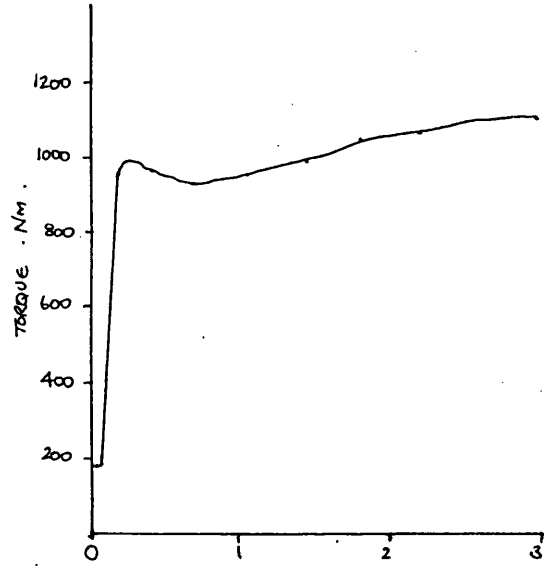

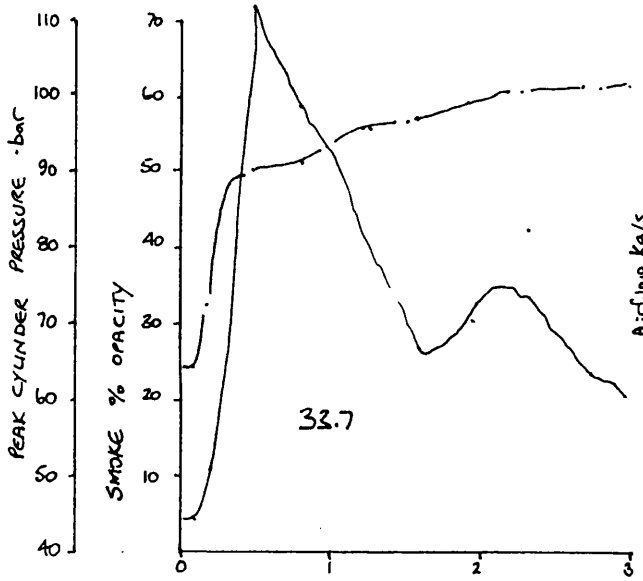

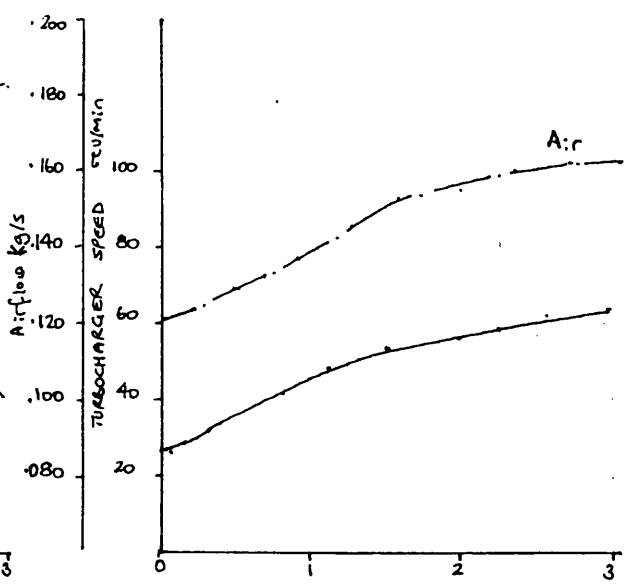

time ~ s

fig 5.33

Engine LEYLAND TL11 ENGINE—11.1L DISPLACEMENT Drawn By.... S.W. ROBERTS

Title VG TURBOCHARGER FULLY OPEN

Constant Speed Curve at 800 rev/min

Holset / Leyland / Dowty / DoI Contract

Test No.	DYNAMIC Timing	Amb'nt °C	Barometer Ins. Hg.
100	16.5	25	752

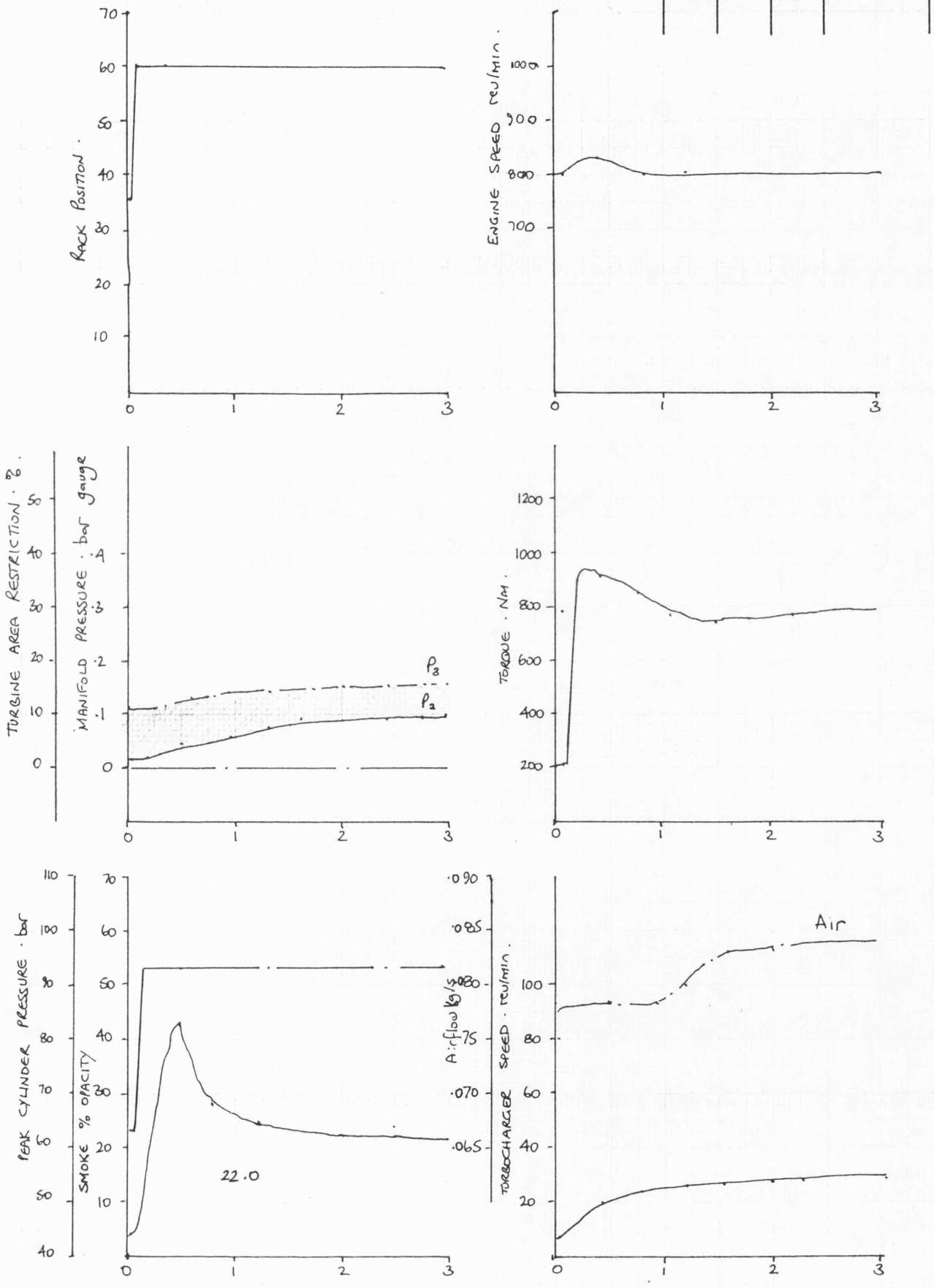

fig 5.34

Engine LEYLAND TL11 ENGINE—11.1L DISPLACEMENT Drawn By. S.W. ROBERTS

Title VG TURBOCHARGER FULLY RESTRICTED

Constant Speed Curve at 800 rev/min

Holset / Leyland / Dowty / DoI Contract

Test No.	Dynamic Timing	Amb'nt °C	Barometer Ins. Hg.
101	16.5	25	751

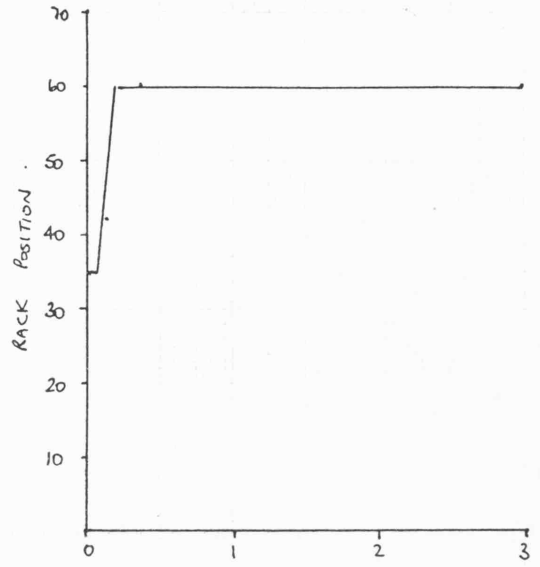

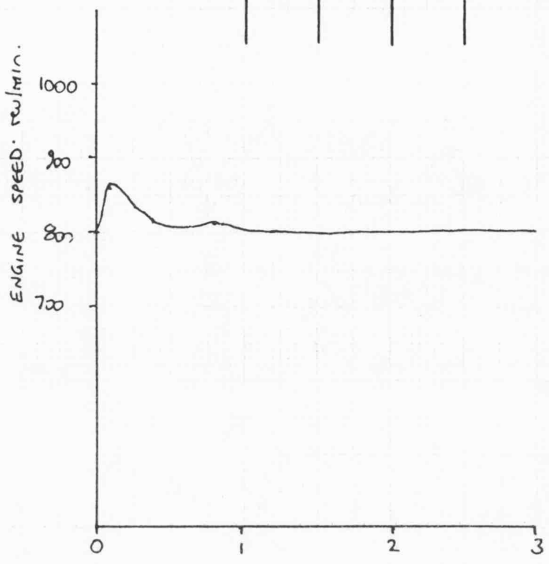

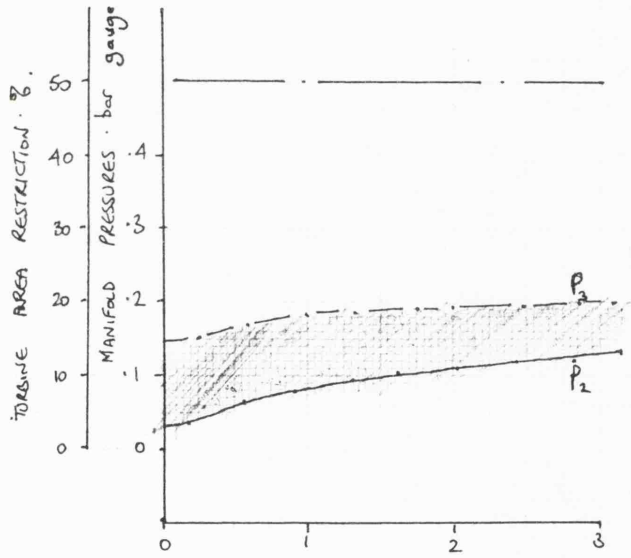

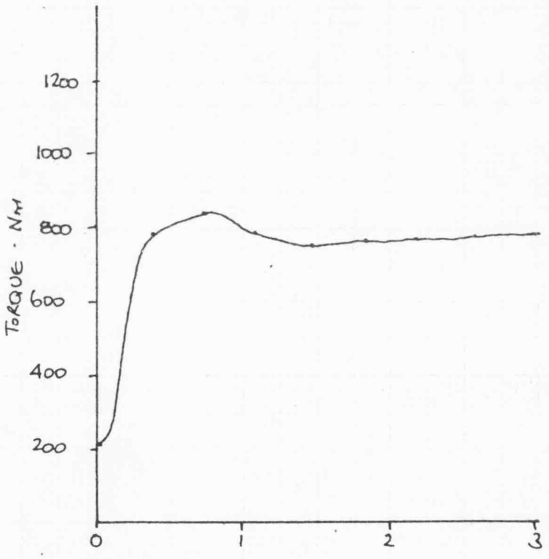

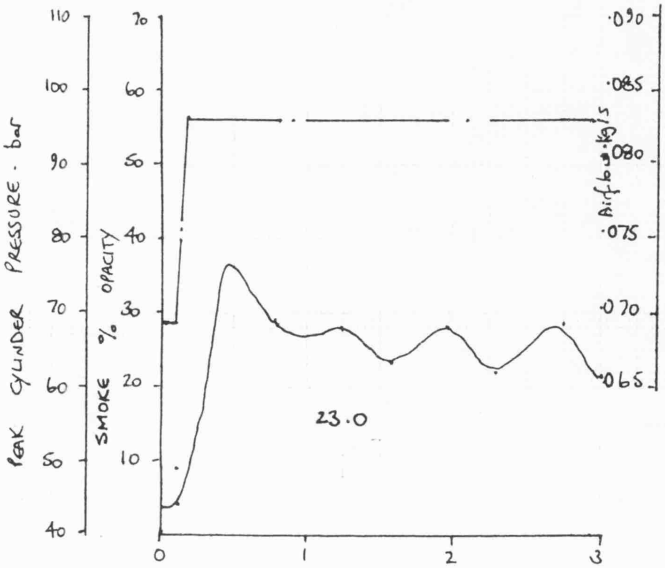

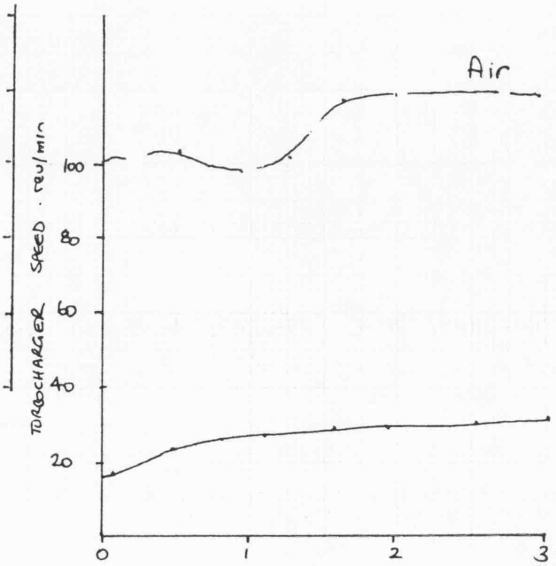

time · s

fig 5.35

Engine LEYLAND TL11 ENGINE—11.1L DISPLACEMENT Drawn By.. E.W.ROBERTS

Title.... VG TURBOCHARGER FULLY OPEN TO 50% RESTRICTED.

Constant Speed Curve at 800 rev/min

Holset / Leyland / Dowty / DoI Contract

Test No.	Timing	Amb'nt °C	Barometer Ins. Hg.
102	17	25	750

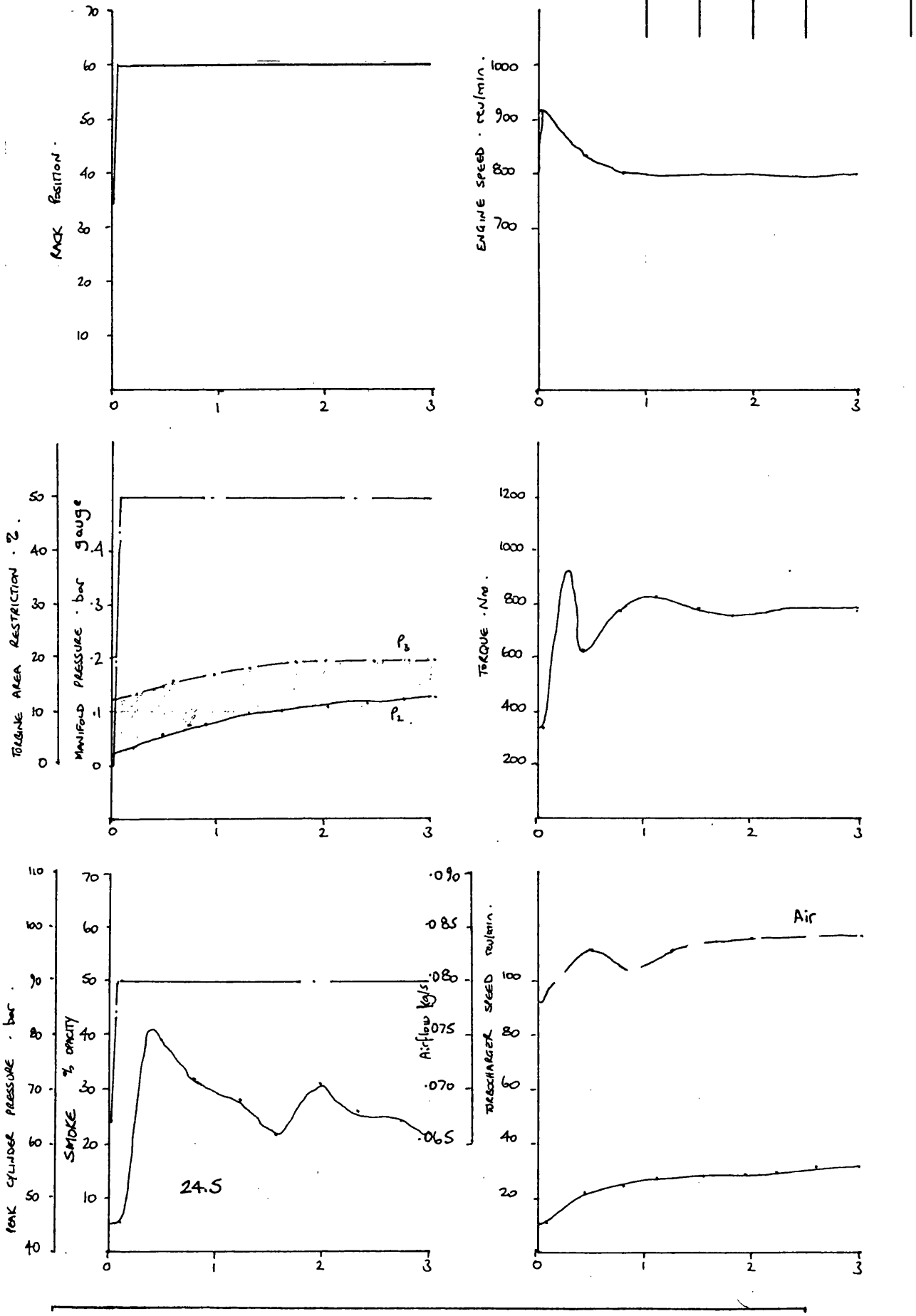

fig 5.36

NOMENCLATURE

Symbol	Description	Unit
m	mass	kg
p	pressure	kN/m^2
V	volume	m^3
T	temperature	K
U	internal energy	kJ/kg
Q	heat released	
W	piston work	
N	engine speed	rev/min
a	area	m^2
D	cylinder bore	m
V_m	mean piston speed	m/s
V_s	swept volume	m^3
$P_g - P_o$	cylinder pressure - compressor pressure	bar
P_{max}	maximum cylinder pressure	bar
V_p	mean piston velocity	m/s
A, B, C	empirical constants	-
AFBR	apparent fuel burning rate	-
β	premixed burning constant	-
C_p^1, C_p^2, C_p^3, C_p^4	Wiebe empirical burning constants	
τ	dimensionless time function, based on a total time allowed for combustion	
q	heat transfer rate	ψ/s
C_p	Specific heat at constant pressure	kJ/kg K

6. THEORETICAL INVESTIGATION

6.1. Introduction (66)

In Chapter 4 the limitations to the practical work carried out on the VG configured engine were found to be: 1) breathing, 2) cylinder pressure, 3) turbomachinery efficiency, 4) turbine non-dimensional turn down ratio. These constraints can be explored theoretically using mathematical modelling techniques, which allows the constraints to be investigated and quantified. The advent of fast digital computers made possible the solution of system models by complex numerical methods allowing realistic models to be solved.

6.2. Review of Engine Models (28, 29, 30)

Two separate and distinct models are available within the School for modelling the turbocharged engine during steady state operation and hence provide a general performance prediction. Both programs model certain component parts which when linked and assembled form the whole turbocharged engine. The programs are then run for a given set of input data and a solution found (if it exists) satisfying all the compatibility criteria. These being turbocharger power balance, heat work and mass transfer within the engine cylinder and manifolds and continuity of mass flow throughout the system.

One model (EMAT) uses a sequential iterative procedure which combines several 'nested loops' all of which have to be satisfied simultaneously to obtain equilibrium conditions (Fig. 6.0).

The second model uses a parallel integrative method and considers the engine as a series of thermodynamic control volumes linked by mass or energy transfer (filling and emptying) leading to a set of three differential equations; continuity, energy and equivalence ratio to be solved similtaneously at every crank angle degree within the 720^{o} degree cycle.

A general description of each program follows.

6.2.1. EMAT

The steady state iterative program EMAT models the engine by dividing the cycle into a relatively small number of discrete steps. It requires some engine data and engine results to estimate values for 'diagram efficiency' and heat rejection. It is made up as follows: In the open period the inlet and exhaust pressures allow for a calculated pressure difference across the valves assuming steady incompressible flow, the valves being fully open. The program also includes a simple scavenge model. The closed period follows a five point P-V cycle (Fig. 6.1). Heat release rate is represented by a simple diffusion burning model taking into account start and duration of injection as well as injection rate. An allowance is made for heat transfer. An exhaust pulse model is included to feed the turbine.

The program then links this engine model to the turbocharger model and allows an equilibrium turbocharger/engine operating point to be determined.

This program has been used very successfully at Bath for many years and has been modified to simulate two stage, variable geometry and compound engines. A full description is included in Ref. 10 and 30.

6.2.2. Bath cycle simulation program (Filling & Emptying - F & E)

In this model the engine is considered as a series of control volumes representing the inlet and exhaust manifolds and the cylinders which are linked to the turbocharger via variable orifices simulating valves and coupled by heat and/or mass transfer.

Calculations are performed over successive small crank angle i.e. time intervals, quasi-steady flow being assumed (i.e. momentarily steady flow) during the crank angle step, such that the rate of change of properties is constant during that step.

The main body of the program revolves around the theory of 'filling and emptying'. The varying conditions of gas with time in each control volume are governed by a simultaneous step-by-step charging and discharging of each control volume, controlled by boundary conditions, e.g. engine speed, piston and valve position, manifold pressures.

The equations of continuity, state, angular momentum and energy form a set of ordinary differential equations that are solved numerically (using the predictor corrector method) along equal increments of crank angle in terms of temperature, equivalence ratio and mass of gas in the volumes, and turbocharger speed.

The governing equations are as follows:-

$$\text{INITIAL CONDITIONS } M_{c_1} = \frac{P_{c_1} V_{c_1}}{R T_{c_1}} \qquad 1$$

$$\text{FINAL CONDITIONS } M_{c_2} = \frac{P_{c_2} V_{c_2}}{R T_{c_2}} \qquad 2$$

(PERFECT GAS LAW)

$$\text{ENERGY - } M_{c_2} U_{c_2} = M_{c_1} U_{c_1} + Q - W + m_i - h_{s_i} h_{s_o} \qquad 3$$

$$\text{CONTINUITY - } M_{c_2} = M_{c_1} + (m_i - m_o + m_f) \qquad 4$$

$$\text{CONSERVATION - } \frac{dM}{dt} = \sum_j \frac{dMj}{dt} \qquad 5$$

(where 'j' denotes different entries to, and exits from the control volume).

The following sub-models are called by the main program to complete the mathematical model:-

(a) Heat Transfer

Heat transfer to the cylinder walls is evaluated from wall surfaces

and instantaneous gas temperatures; wall temperatures are determined from a one dimensional heat conduction model. The model is based on the Woschni correlation (32)

$$q/a = a\, D^{-0\cdot2}\, p^{0\cdot8}\, T^{-0\cdot53} \left[6\, V_m + \frac{V_s\, T_r}{Cp_r\, V_r}(P - P_o)\right]^{0\cdot8} (Tg - Tw)$$

(b) Friction

Mechanical efficiency is estimated by an empirical formula derived from the results of Chen and Flynn (33) and is a function of engine speed and maximum cylinder pressure.

$$FMEP = A + B\, P_{max} + C\, V_p$$

(c) Combustion

The combustion model is based on the apparent fuel burning rate (AFBR) approach due to Wiebe (34).

Experimental burning rate curves are correlated to ignition delay, engine speed and equivalence ratio. Ignition delay is related to temperature and pressure of the cylinder charge, where:-

$$AFBR = \beta\, AFBR_p + (1 - \beta)\, AFBR_D$$

$$AFB\, R_p = Cp1\, Cp2,\, \tau^{cp-1} \left[1 - \tau^{cp1}\right]^{cp_2-1}$$

$$AFBR_D = Cp_3\, Cp_4 \times \tau^{cp_4-1}\, \ell \left[- Cp_3\, \tau^{cp_4}\right]$$

(d) Gas Exchange

Valves are treated by combining a curve of mean discharge coefficients obtained by averaging published data with the geometric formulation of KASTNER et al (31).

A flow chart of the program is included in Fig. 6.2 together with a schematic of a turbocharged engine (Fig. 6.3).

The estimation of the processes in the cylinder is based on the

following simplifying assumptions:

1. neglect of pressure wave interaction.
2. fluid properties change instantaneously and uniformly over the whole cylinder.
3. the flow is inviscid and wall friction is neglected.
4. ideal mixing.
5. the coefficients of heat transfer to the cylinder walls are spatially averaged.
6. fuel injection and combustion follow a simulated heat release pattern.

The filling and emptying treatment of the gas exchange process in the exhaust manifold is justified for compact and short exhausts manifolds. However, with long narrow and branched exhaust pipe systems the system described above fails to recognise the non-steady character of the flow in the pipe system.

The filling and emptying method considers the whole exhaust manifold as a volume and hence cannot take account of pressure wave superimposition caused by reflected waves from different branches, closed ends and the turbine. Pulse turbocharging inherently transfers energy in the form of pressure waves which was thus implicitly neglected.

6.2.3. Method of characteristics (35, 36)

The restriction of the filling and emptying method is that pressure wave action is neglected. The physical laws which primarily govern the process are those of mass momentum and energy conservation which when coupled with the relations describing the thermodynamic properties of the fluid lead to a set of three hyperbolic partial differential equations. The method of characteristics is a mathematical technique for solving these hyperbolic partial differential equations. These equations have distance (along the duct) and time as independent variables, the dependent variables being pressure, velocity and temperature grouped in combinations. Values are assigned to each dependent variable at all locations at a certain initial time, which together with information on conditions at the duct ends at all times and means of calculating the friction forces and heat fluxes at the duct walls, mean that values at all locations at any later time may be computed. In processes governed by hyperbolic equations disturbances to the fluid are transmitted only in discrete directions forming a network of lines known as characteristics, which cover the domain of integration.

Engine simulation programs based on the Methods of characteristics apply the technique to analyse pressure wave action in the intake and exhaust manifolds. Otherwise the programs are similar to quasi-steady filling and emptying models.

The most appropriate simulation for this work was considered to be the integrative program. The difficulty associated with the step by step method when compared with the iterative model is the large amount of computing time it requires. This is especially true at low speeds when a greater number of cycles or a smaller crank angle increment is necessary for the conditions of mass flows and turbocharger power to balance. This was overcome by calibrating the program over the whole speed range on the limiting torque curve but then concentrating the area of interest at only three speeds viz rated conditions (2100 rev/min) peak torque 1300 rev/min and 1100 rev/min. The object was to

move the peak torque speed to a value closer to 50% of rated speed.

6.2.4. Data input

The filling and emptying program requires a comprehensive data input. This was supplied by the engine manufacturer. It includes detail of (1) crank radius, (2) con rod length, (3) bore, (4) compression ratio, (5) valve and camshaft data, (6) manifold volumes and surface area, in addition to particulars on the combustion chamber and turbomachinery.

Manifold volumes were determined by measuring the amount of water required to fill them. Surface area was calculated from port diameters and volume. Fig. 6.4 shows the valve lift diagram. Fig. 6.5 and 6.6 show typical compressor and turbine maps. A 'data echo' is included in Fig. 6.7 which shows a LEYLAND engine file.

Initial estimates of pressures, temperatures and equivalence ratio in the control volumes are required in addition to a starting value for turbocharger speed. Six cycles with a 2^{o} step size were the running conditions normally specified. These were found to give acceptable results.

For each run, engine speed, fuelling, inlet and exhaust restriction, atmospheric temperature and pressure, static and dynamic timing were entered and could be altered as appropriate.

Matching program output to engine data is an interactive process whereby the different scale factors are altered in discrete steps as appropriate to effect a good match. Having established a datum performance the program can provide useful performance predictions when optimising turbocharger components, valve timing or uprating etc.

The Bath F and E program had not previously been used for detailed simulation work. Therefore confirmation runs were carried out for the base H2B LEYLAND configured engine, both to confirm the prediction

ability of the program and also to characterise the breathing, fmep and heat transfer coefficients.

Scale factors are available for the coefficient of discharge - C_D for both inlet and exhaust valves. Scale factors are also available on the compressor and turbine maps to control efficiencies and non-dimensional mass flow ($m \sqrt{T}/P$). It is unfortunate that the program did not include a friction scale factor. (These values have been adjusted manually).

6.3. Engine Calibrating Runs

6.3.1. Base H2B build (Fig. 6.8a/b, 6.19, 6.20, 6.21)

The program was run on a LTC fuel schedule with a H2B turbocharger in 200 rev/min steps between 900 and 2100 rev/min. The results used to effect a match were those derived from the base engine results (Fig. 4.56) which simulated a boost control schedule. Maximum power was 190 kW @ 2100 rev/min with a peak torque value of 990 Nm @ 1300 rev/min.

Great care was taken to match air fuel ratio, volumetric efficiency, boost pressure ratio and compressor efficiency in each case. Fig. 6.8 a/b shows the simulated base results and confirm that good correlation is possible though turbocharger speed is consistently 4000 rev/min below the base. Turbine inlet temperature (TIT) is within a band of $\pm 18^{o}$ which agrees closely, together with cylinder pressure which is within 5 bar (1%).

The lower cylinder pressure characteristic and higher turbine temperatures suggest that the Wiebe combustion constants require slight adjustment. There was no facility for altering these factors and no correlation to real burning rate curves was attempted. Dynamic timing was determined for the base engine and reproduced for the simulated run.

Fig. 6.19, 20 and 21 show the variation of cylinder, inlet and exhaust pressure during the open period for the base build at 2100, 1300 and 1100 rev/min respectively. The inlet and exhaust valve open periods are superimposed on the diagram.

The gas exchange period is that period during which the products of combustion are replenished by the fresh charge. It is a very useful guide for evaluating engine breathing and identifying potential problem areas.

6.3.1.1. Description of the gas exchange process (43, 44, 15)

This is made up as follows: the events begin when exhaust valve opens near the end of the expansion stroke (134° ATDC) see Fig. 6.19 in a process termed exhaust blowdown. The piston then travels towards top dead centre (TDC) displacing the products of combustion. Before the piston reaches the end of the exhaust stroke the air inlet valve opens (350° ATDC). For a short period both the air inlet and exhaust valves are open; this is called the overlap period. On the return stroke of the piston the exhaust valve closes (374° ATDC) and air fills the cylinder. The piston then returns towards TDC and the air valve closes (590° ATDC).

In many turbocharged engines the overlap period is extended taking advantage of the positive pressure differential across the cylinder which allows for scavenge air to displace the products of combustion from the clearance volume and reduce the exhaust gas temperature. It also allows the air valve to be opened earlier thereby enhancing cylinder filling since the valve takes a finite time to open and close.

The gas exchange diagrams for the base engine, Fig. 6.19, 6.20, 6.21 (2100, 1300 and 1100 rev/min) are included.
The following observations were made:

(a) 2100 rev/min - 190 kW: H2B (Figs. 6.8 and 6.19)

The exhaust blowdown period is difficult to model accurately due to the highly unsteady flow at exhaust valve opening (EVO). The cylinder pressure trace shows a rising characteristic at approximately 340° indicating that the piston is doing work on the gas to displace it through the exhaust valve. This implies an SFC penalty and that a larger exhaust valve EVO would be beneficial or alternatively advancing. The overlap is very short at 24° and suggests a naturally aspirated determined design. (The valve openings up to about 20° angle are very small). Due to the limitation of the exhaust valve the crossover period is marked by a negative process gradient implying high TIT for a comparatively low rating. The air valve closes at 590° ATDC suggest a 'high speed' camshaft > 2200 rev/min. A long open period assists in general cylinder filling. Cylinder

pressure is greater than boost pressure at 560° ATDC. The small effective valve open period thereafter probably has little effect; otherwise flow reversal occurs. Scavenge ratio i.e. $\frac{QAFR}{TAFR}$ is low at 1.005 reflecting the above statements. The inlet manifold pressure fluctuations are minimal suggesting that the manifold substantially damps out all pulsations.

(b) 1300 rev/min Peak Torque 990 Nm (Figs. 6.8 and 6.20)

Due to the reduced mass flow there is no pressure rise at approximately 330° in the cylinder trace leading to a good positive differential at valve overlap.

The cylinder pressure exceeds inlet manifold pressure at 540° ATDC with implied reverse flows thereafter until AVC. Scavenge ratio is 1.006. A much larger valve overlap e.g. 40° would prove beneficial at this speed by reducing TIT and possibly improving SFC.

(c) 1100 rev/min - 956 Nm (Figs. 6.8 and 6.21)

The same comments as above apply at 1100 rev/min excepting that the implied flow reversals before AVC will be worse. Scavenge ratio is 1.004. Volumetric efficiency decreases rapidly below 1300 rev/min.

In these calibrating tests the program has amply demonstrated its ability to reproduce all the important engine parameters accurately and allow close inspection of the gas exchange process.

An assessment was then made of the program's predictive ability against known data, that is for limited timing and boost swings at constant speed (1300 rev/min) on the LTC. These are discussed below.

6.3.2. Timing investigation (Fig. 6.9)

The results for this set of simulations are presented in Fig. 6.9.

The base engine was tested at constant speed (1300 rev/min) with LTC fuelling and timing varied over 15° related to the crank. For the simulations, the engine was matched at 15° BTDC and dynamic timing altered in 3° steps between 3 and 18° BTDC. Cylinder pressure gives good correlation albeit consistently 5 bar too optimistic. Turbocharger speed follows the same trend being within 2000 rev/min over the whole timing swing. The TIT characteristic was not as 'flat' as that determined during engine tests but was within 25° C for 12° timing swing. SFC was identical between 10° and 18° BTDC thereafter it continued to show improvement from .210 to .200 kg/kWh, whereas the base steadily deteriorated from .210 kg/kWh to .220 kg/kWh with increasing retard. This suggests the program views increasing retard too favourably. However, the implications of this variable on engine performance have been fully evaluated on the test bed.

6.3.3. Boost investigation (Fig. 6.10)

Fig. 6.10 shows the variation of turbine inlet area at constant speed (1300 rev/min) with limiting torque fuelling for the Mk IIb VG configured engine, that is the H2C turbocharger in which the turbine stage is of single entry construction. The simulation program was matched with turbine stage fully open i.e. 0% restriction. Variable geometry was simulated by altering the scale factors controlling non-dimensional mass flow ($m\sqrt{T}/P$) and efficiency respectively.

Good correlation was achieved with turbine inlet temperature being precisely the same as base at 0 and 50% restriction with only 20° C difference at 40% restriction.

Air flow, pressure ratio and turbocharger speed were all within acceptable limits. Predicted cylinder pressure followed the base results closely from 0 to 4% restriction but was 7 bar in excess of the measured value at 50% restriction (+ 6%). SFC in the 0 and 25% restriction case correlated very closely with measured results.

However, the program appeared to be insensitive to the enhanced boost available (implying higher combustion efficiency) with the higher restrictions. In addition frictional losses were over-estimated with the high cylinder pressure predicted for 50% restriction. The program predicted an almost constant value at .220 kg/kWh. However, this represented only a 3.3% error compared with measured results.

The datum performance of the base H2B engine has been reproduced with good accuracy on the filling and emptying program. Limited runs with known data have shown that the program provides useful performance predictions on the trends towards widely differing parameters. The results suggest that the program views retarded timing too favourably and exhibits an insensitivity to enhanced air fuel ratios on the LTC. Correlation with real burning rate curves should alleviate the above.

6.4. Theoretical Predictions - Parametric Studies

6.4.1. Optimised VG results (Figs. 6.11a/b/c)

The results from the full optimisation exercise (boost, timing and fuelling) were next simulated at 2100, 1300 and 1100 rev/min. Figs 6.11a, b and c present the results. These show that the simulation consistently over-estimates cylinder pressure by + 4, 6 and 10% respectively and under-estimates turbine inlet temperature by 5, 3 and 7% respectively for measured dynamic timing. This again would suggest that the Wiebe constants require adjustment. Higher cylinder pressures imply errors in the heat transfer and engine friction models. For the parametric study, only the differences each variable produces will be noted rather than the absolute value.

The engine with its three control parameters (boost, timing, fuelling) was very rigorously tested. However, the limitations imposed by hardware constraints included:-

1.	compressor efficiency	
2.	turbine efficiency	turbocharger
3.	turn down ratio	
4.	cylinder pressure limits	
5.	engine breathing	engine

Each constraint was individually studied and the implications for future designs assessed. For each test all parameters such as fuelling, ambient pressures, and temperature were kept constant.

6.4.2. Compressor efficiency (Fig. 6.12/13/14 Column 2)

In the range 1000 - 1600 rev/min the engine running lines at constant speed pass through the peak islands of efficiency on the compressor map (Fig. 4.40). This results in a higher turbine power requirement, higher temperatures throughout the cycle and an SFC penalty on the LTC. Fig. 6.12, 13 and 14 show the results of raising compressor

efficiency (column 2) on the engine performance when compared with the optimised H2C base (column 1) in each case.

(a) 2100 rev/min, Fig. 6.12

At this speed there is an SFC penalty of 1.2% to .2303 kg/kWh for an increase of 3.8% on compressor efficiency. This is attributed to a larger effective turbine back pressure and pumping work. The more efficient compressor stage increases turbocharger speed by 2500 rev/min to maintain the power balance with the turbine. This increases air mass flow by 3%, cylinder pressure by 2% and the mean heat transfer coefficient by 1.8%. Turbine inlet temperature (TIT) reduces by 17^{o} C due to the enhanced air fuel ratio + 0.82 to 25.45.

(b) 1300 rev/min, Fig. 6.13

The engine responds very favourably at 1300 rev/min to an enhanced compressor efficiency of + 4.6% to 72.5% by reducing SFC by 1% to .210 kg/kWh. Bmep rises by 1% to 12.58 bar. Air flow improved substantially (5%) to .202 kg/s enhancing air fuel ratio by 1.14 to 22.79. Cylinder pressure increased by 6 bar whilst TIT reduces by 24^{o} C. The lower SFC is associated with better combustion efficiency and a more favourable pressure drop across the cylinder.

(c) 1100 rev/min, Fig. 6.14

At 1100 rev/min the compressor efficiency is increased by 3.6% to 71.9%, SFC and bmep improve by 1.5%. Air flow increases by 3%, improving air fuel ratio by 0.7 to 21.13. Turbocharger speed rises by 3000 rev/min to 64313 rev/min. The lower SFC is again associated with better combustion and a higher pressure differential across the cylinder.

6.4.3. Enhanced turbine efficiencies (Fig. 6.12/13/14 Column 3)

One of the difficulties associated with a VG turbocharger is how to effect a good turn down ratio with the mimimum efficiency penalty. Therefore this set of simulations models the turbine stage as for the base but with enhanced efficiencies of approximately 2½%.

(a) 2100 rev/min (Fig. 6.12)

The general trends at 2100 rev/min are as for Case 1 above excepting that the effects are not as pronounced consistent with the lower gains in efficiency, SFC is 1.84% worse and is again due to a larger effective turbine back pressure. The turbine produces more power because it is more efficient and increases air mass flow 1.7% and cylinder pressure 1.5 bar. TIT is reduced by 8^{o} C. Turbocharger speed increases by 2000 rev/min to 87103 rev/min.

(b) 1300 rev/min (Fig. 6.13)

Fig. 6.13 shows that a 3% increase on turbine efficiency decreases SFC by 0.6% to .2113 kg/kWh. Turbocharger speed increases by 3000 rev/min enhancing air mass flow by 2.6%, and increasing cylinder pressure by 4 bar whilst TIT decreases by 9^{o} C. The higher turbine efficiency effects a more favourable pressure drop across the cylinder together with a higher overall AFR result in lower SFC.

(c) 1100 rev/min (Fig. 6.14)

The same trends are apparent at 1100 rev/min where SFC improves by 1.1% for +2.5% on turbine efficiency.

It is apparent that improving turbomachinery efficiency of either component has the same beneficial overall effect on engine performance except for the unexpected increase in SFC at 2100 rev/min. This parameter would allow significant up-fuelling to occur.

6.4.4. Greater turndown ratio (Fig.6.12/13/14 Column 4)

The design aim for the VG turbocharger was a 2.1 turn down ratio in non-dimensional mass flow whilst at the same time minimising the efficiency penalty. In practice a 1.6:1 ratio was achieved which limited the capability for low speed peak torque. In addition the theoretical and practical results indicate that at high speed the largest turbine housing possible should be fitted to minimise the pumping work. This is consistent with an AFR of 22.1.

(a) 2100 rev/min (Fig. 6.12)

For rated conditions at 2100 rev/min. The engine was simulated with a turbine housing giving a 3% increase in the non-dimensional swallowing capacity ($m\sqrt{T}/p$). The results show an improvement in SFC and BMEP of 1.5%. This is attributed to lower pumping work associated with the exhaust valve. The reduced turbine power decreases air flow by 2% to .290 kg/s and AFR by .5 to 24.18. Cylinder pressure is reduced by 2.5 bar and turbocharger speed by 3000 rev/min to 81700 rev/min whilst TIT rises by 7^{o} C.

(b) 1300 rev/min (Fig. 6.13)

At 1300 rev/min and 12.43 bar bmep a turn down ratio of 48% was simulated. This substantially alters the match; turbocharger speed rises by 17000 rev/min to 94000 rev/min and increases air availability by 11.3%. SFC deteriorates by nearly 5% due to excessive back pressure as the turbine becomes effectively choked and the engine is operating under an adverse pressure gradient. Peak cylinder pressure rises by 17 bar. The overall turbomachinery efficiency increases by only 1.5% making the comparison valid. The OAFR rises by 2.46 to 24.11. However TIT reduces by only 10^{o} C.

The simulation clearly shows that due to excessive back pressures (turbine choking) at this rating there is a large SFC penalty even when running at comparatively high air fuel ratios. This suggests that the greater turn down ratio available is most useful in reducing

peak torque speed.

(c) 1100 rev/min (Fig. 6.14)

A similar turn down ratio was applied at 1100 rev/min but at this speed the bmep is lower - 11.3 bar. The results were as follows SFC deteriorates by 0.7% due to higher back pressures. However air flow increases by 16% to give an AFR of 23.7. TIT reduces by 22^{o} C whilst cylinder pressure rises by 15 bar. Turbocharger speed increases by 18000 rev/min to 80000 rev/min to a pressure ratio of 2.05 suggesting that bmeps of 12.5 are obtainable. This would allow a 30% torque back-up at 50% of rated speed. To effect higher torque values cylinder pressure limits must be raised.

These results would confirm that a turbocharger with a 2.1 turn down ratio could move peak torque to 1100 rev/min and below on the Leyland TL11 engine whilst maintaining the mechanical and thermal limits. SFC however would remain substantially the same. To effect better SFC's the turbomachinery efficiencies should be significantly better than at present.

6.4.5. Low compression ratios (Fig. 6.12/13/14 Columns 5 & 6)

Another constraint imposed by mechanical considerations was that of cylinder pressure limits alluded to previously. This was alleviated to some extent by retarding injection timing on the engine. To effect higher power outputs with regard to cylinder pressure limits a lower compression ratio can be specified. The engine tested at the University was fitted with pistons giving a compression ratio (cr) of 15.75:1. The following tests simulated the engine fitted with 14.75 cr and 13.75 cr pistons.

Engine manufacturers specify the highest compression ratios consistent with cylinder pressure limits and cold starting. For direct injection engines this is normally between 14 and 17 to 1. Better thermal

efficiencies are associated with higher comrpession ratios due to the larger PV diagrams.

In addition low compression engines have cold start problems and also under adverse conditions emit a dense white smoke; a highly undesirable phenomenon associated with unburnt fuel vapour.

(a) 2100 rev/min (Fig. 6.12)

Inspection of Fig. 6.12 reveals that the model predicts SFC improvements of 1.3 and 1.8% respectively. Cylinder pressure reduces by 7 and 15 bar respectively with associated reductions in friction and heat transfer. TIT increases by 15^{o} and 25^{o} respectively enhancing turbine power and increasing turbocharger speed by 2000 and 3000 rev/min. Turbocharger efficiencies remaining sensibly constant. The pumping work increases which would imply a small SFC penalty. The better SFC's are associated with smaller exhaust pulses and lower friction losses. The heat transfer coefficient reduces by 2.6 and 5.7% respectively.

(b) 1300 rev/min (Fig. 6.13)

At 1300 rev/min there was a small SFC penalty of 0.5 and 0.7% respectively. Cylinder pressure was reduced by 8 and 16 bar respectively. Turbocharger speed increased by 1000 and 2000 rev/min with the exhaust temperature increase of + 9^{o} C and + 13^{o} C. The SFC deficit is attributed to the smaller work diagram.

(c) 1100 rev/min (Fig. 6.14)

Column 5 and 6 on Fig. 6.14 reveal a substantial improvement to SFC of 2.4 and 4.5% respectively which is in part due to better combustion and lower frictional losses. The pressure differential across the cylinder improves with the lower compression ratios reflecting directly in better SFC.

Cylinder pressures reduce by 5 and 10 bar respectively whilst exhaust temperatures increase by 16 and 33^{o} C respectively.

The results above clearly indicate that reducing compression ratio by an order of 1 and 2 respectively from 15.75 reduces peak cylinder pressure substantially; typically 8 and 16 bar. However this is at the expense of TIT which increases approximately by 25^{o} C. It follows that some injection advance is necessary to reduce TIT. Lowering compression ratio overall implies an SFC penalty over the greater part of the operating map.

6.4.6. Engine breathing (Fig. 6.12/13/14 Columns 7, 8 & 9)

A limiting factor in the testing sequence was the breathing or volumetric efficiency of the engine at speeds below 1300 rev/min. It is readily apparent that the easier it is to get the air in and out of the engine the greater the potential for increased power and better SFC (from the gas exchange). Results from engine tests revealed that volumetric efficiency reduces significantly below 1300 rev/min. In addition at rated conditions the gas exchange revealed that the exhaust valve appeared to limit gas throughput.

This set of simulations examines those parameters which primarily influence engine breathing that is (1) valves, (2) manifolding and porting, (3) valve timing.

6.4.6.1. Large valve head (Figs. 6.12/13/14 Column 7)

The first set of simulations models the engine with larger inlet and exhaust valves. An assessment of the head indicated that it was possible to fit valves of 59 mm diameter. The standard cylinder heads are fitted with valves of 55 and 46.5 mm diameter for inlet and exhaust respectively. This is based on naturally aspirated practice where the difficulty lies in getting the air into the cylinder in the short

time available. In the case of a pressure charged engine with large permissible valve open periods this is not a problem. Valves should be as large as possible to cope with the higher mass flows and be of equal size. For very high output engines four valve head configurations are more appropriate. Unfortunately the program had no facility to simulate a four valve head.

(a) 2100 rev/min (Fig. 6.12)

At 2100 rev/min the large valve head combination enhances SFC by + 2.3% whilst maintaining air flow (+ 1%) and cylinder pressure almost constant. This implies all the benefits accrue from the gas exchange process. These are associated with the larger flow capacity of the exhaust valves minimising pumping losses. TIT is reduced by 10^{o} C but scavenge ratio remains as before at 1.005.

(b) 1300 rev/min (Fig. 6.13)

Fig. 6.13 (Column 7) also shows an improvement in SFC of 1.3%. Air flow and cylinder pressure remains the same as base implying the benefit is wholly obtained during the gas exchange. TIT is reduced by 6^{o} C. The scavenge ratio is 1.006.

(c) 1100 rev/min (Fig. 6.14)

At 1100 rev/min a 1.2% improvement to SFC was noted, again due to the gas exchange process. TIT reduces by 6^{o} C. All other parameters remaining constant. Scavenge ratio is 1.0048.

6.4.6.2. Improved manifolding and porting (Figs. 6.12/13/14 Column 8)

An alternative approach to enlarging the valves is that of making the existing heads more gas flow efficient i.e. lower their resistance to flow. This can be achieved by careful attention to porting, manifold design and turbulence control.

(a) 2100 rev/min (Fig. 6.12)

The scale factor on the inlet valve coefficient of discharge (C_D) was adjusted such that volumetric efficiency was increased by 1% to 91.5%. This had the beneficial effect of reducing SFC by 1.6% to .2241 kg/kWh. Air flow increased by 0.7%. The improvement is attributed to the gas exchange process. Other trends are as for the large valve head excepting that the exhaust valve has not been altered therefore there remains an implied throttling process. TIT reduces by 3^{o} C. Scavenge ratio is 1.003.

(b) 1300 rev/min (Fig. 6.13)

Fig. 6.13 column 8 shows that the engine at 1300 rev/min responds favourably with an increase in volumetric efficiency of + 1.7%. The exhaust valve no longer presents an excessive restriction at the lower mass flows. SFC shows a 1.2% improvement to .209 7 kg/kWh. Air flow increases by 1.3%, improving air to fuel ratio by .3 to 21.94. The SFC benefit is associated with a better gas exchange process and a higher combustion efficiency. TIT reduces by 16^{o} C HTC, turbocharger speed, turbomachinery efficiency and cylinder pressure remain sensibly constant. Scavenge ratio is 1.005

(c) 1100 rev/min (Fig. 6.14)

At 1100 rev/min the same comments applying to the exhaust valve are true and the impressive gains in SFC of 4.3% to .207 kg/kWh occur for the same reasons. There is a gain of 2.3% in air mass flow purely due to the better breathing as turbocharger speed and efficiency remain constant. Scavenge ratio is 1.004.

6.4.63. Valve timing optimisation (134^{o} - 374^{o}) (350^{o} - 590^{o}) (ATDC) (Figs. 6.12/13/14 Column 9 & Figs. 6.22/23/24/25/26 (EVO-EVC) (AVO-AVC)

The camshaft fitted to the LEYLAND TL11 engine is of 'classic' high speed naturally aspirated design. It has a small overlap (24^{o}) and

air valve closing (avc) comparatively late at 590° ATDC to effect good cylinder filling at high speed. The reader is directed to reference 44 for a full discussion on valve timing.

Good volumetric efficiencies are accomplished by generous effective valve areas. However, the camshaft is designed for high speed operation and gives good results in the range 1300 to 2300 rev/min. Volumetric efficiency below 1300 rev/min deteriorates rapidly. This constraint made it very difficult to reduce peak torque speed. The program has clearly demonstrated that the engine would benefit from an increased air inlet and exhaust period. The design for the optimised camshaft is discussed in relation to the conflicting requirements of the different speeds.

(a) 2100 rev/min (Figs. 612 and 6.22)

At 2100 rev/min the gas exchange diagram Fig. 6.22 for the VG configured engine suggest that the exhaust valve is throttling the flow as the piston moves up towards TDC. Increasing exhaust valve opening duration would alleviate the above and assist scavenging at overlap.

The air valve opens very late at 350°, leading to loss of beneficial scavenge and early cylinder filling. The program suggests that the engine would respond favourably to these effects. Air valve closing at 590° is satisfactory. The scavenge ratio determined by the program for this speed is 1.004.

(b) 1300 rev/min (Figs. 6.13 and 6.23)

Fig. 6.23 suggests that the engine would react very favourably to a larger valve overlap. Advancing air valve opening (AVO) would also benefit early cylinder filling. The air valve closing period is late for this speed implying flow reversals i.e. flow out of the cylinder and into the inlet manifold before AVC. An earlier AVC would therefore be appropriate. Scavenge ratio for the VG base was

found to be 1.005.

(c) 1100 rev/min (Figs. 6.14 & 6.24)

Fig. 6.24 again suggests that a larger overlap would be beneficial at this speed. The highest TIT normally occurs at or around peak torque, a large overlap period would greatly assist in displacing the products of combustion in the clearance volume. The difficulties of flow reversal associated with late air valve closing become more acute with decreasing speed.

From consideration of the above the inlet and exhaust opening periods were alternately advanced and retarded and the duration varied until the 'best' results for each run were noted and then combined for the three speeds. The best camshaft selected on this basis was found to be; EVO 130°, EVC 380°, AVO 338° and AVC 568° ATDC. This gave an overlap period of 42°. It was found beneficial to advance AVC to 568° and reduce the open period by 10° to 230°. Exhaust valve closing was optimised at 380° and the duration lengthened to 250° giving an EVO of 130°. The exhaust blowdown period does not lend itself to simulation due to the highly unsteady nature of the flow.

An EVO of 130° is typical for this type of turbocharged engine. No attempt was made to alter the maximum lift due to consideration of stress, piston fouling and effectiveness.

The results from this optimisation exercise are presented on a speed basis. Fig. 6.12, 13 and 14, column 9, quantify these results and Fig. 6.25 and 26 are the respective gas exchange diagrams.

(d) 2100 rev/min (Figs. 6.12 & 6.25)

A 1.2% improvement to SFC was predicted at 2100 rev/min when compared with the base. The results are very similar to those for a high C_D factor reported previously. Retarding and shortening the AVO period has not adversely affected engine performance. Airflow has increased by 1½% while still maintaining the same cylinder pressures and exhaust temperatures.

Inspection of Fig. 6.25 i.e. the gas exchange diagram reveals that the rising cylinder pressure characteristic at 350^{o} ATDC has been alleviated. Unfortunately at the critical overlap period exhaust and inlet pressure are still in crossover for some 12^{o} C.A. adversely affecting scavenge ratio which is only 1.003. To minimise this effect a larger and more efficient turbine could be specified, thereby reducing mass flow or alternatively specifying a larger exhaust valve and port. AVC is well designed for the speed.

(e) 1300 rev/min (Figs. 6.13 & 6.26)

The peak torque speed shows an SFC improvement of 0.7% and increases air flow by 1.25% for a lower turbocharger speed. TIT reduces by 17^{o} C. Fig. 6.26, the gas exchange diagram, reveals a good differential throughout the overlap period and better early filling of the cylinder. Air valve closing is much better suited to this speed, and the scavenge ratio is 1.006.

The results from the parametric study have been collated on an SFC basis in Tables 6.15/16/17. The parameters are ranked according to their effectiveness for the three speeds in order of decreasing merit.

The parameters are then tabulated in Fig. 6.18 according to their effectiveness over the three speeds considered i.e. their overall effect is assessed by adding their ratings corresponding to the different speeds (1, 8). The lower the number the more effective the parameter, Tables 6.15/16 and 17 are considered first of all.

(a) 2100 rev/min (Fig. 6.15)

Fig. 6.15 shows that gains of up to + 2% are possible due to better breathing. The merits of better breathing during the gas exchange are that TIT reduces whilst power is increased, specifying a larger turbine was equally advantageous. Enhancing turbomachinery efficiency was not effective at rated conditions as pumping work increased disproportionately necessitating a rematch.

(b) 1300 rev/min (Fig. 6.16)

At this speed smaller SFC gains of 1.3% were predicted. These were due to better breathing and turbomachinery efficiency. A larger turn down ratio with comparable efficiencies resulted in a heavy SFC penalty of 5% due to turbine chocking suggesting that 12.5 bar bmep is approaching the limiting torque available with a single stage, nozzled, non-charge cooled turbocharger.

(c) 1100 rev/min (Fig. 6.17)

Fig. 6.17 indicates that almost all the variables within the parametric study had a beneficial effect on SFC, + 4.3% in the best case. This would confirm that reducing peak torque speed is difficult without attention to some if not all the parameters.

The final table, Fig. 6.18, emphasises that improved breathing and turbomachinery efficiency are the most significant factors for better SFC and torque rise. The calculations also demonstrate that the turbocharger affects the engine differently at different speeds. Engine tests will be required to verify the above but it does follow that the changes required by VG turbocharging would also benefit the production H2B base. Increasing the turn-down ratio was clearly advantageous in increasing the useful speed band and decreasing SFC at high speed. At the lower speeds however no SFC advantage can be expected with the present efficiencies.

LIST OF FIGURES

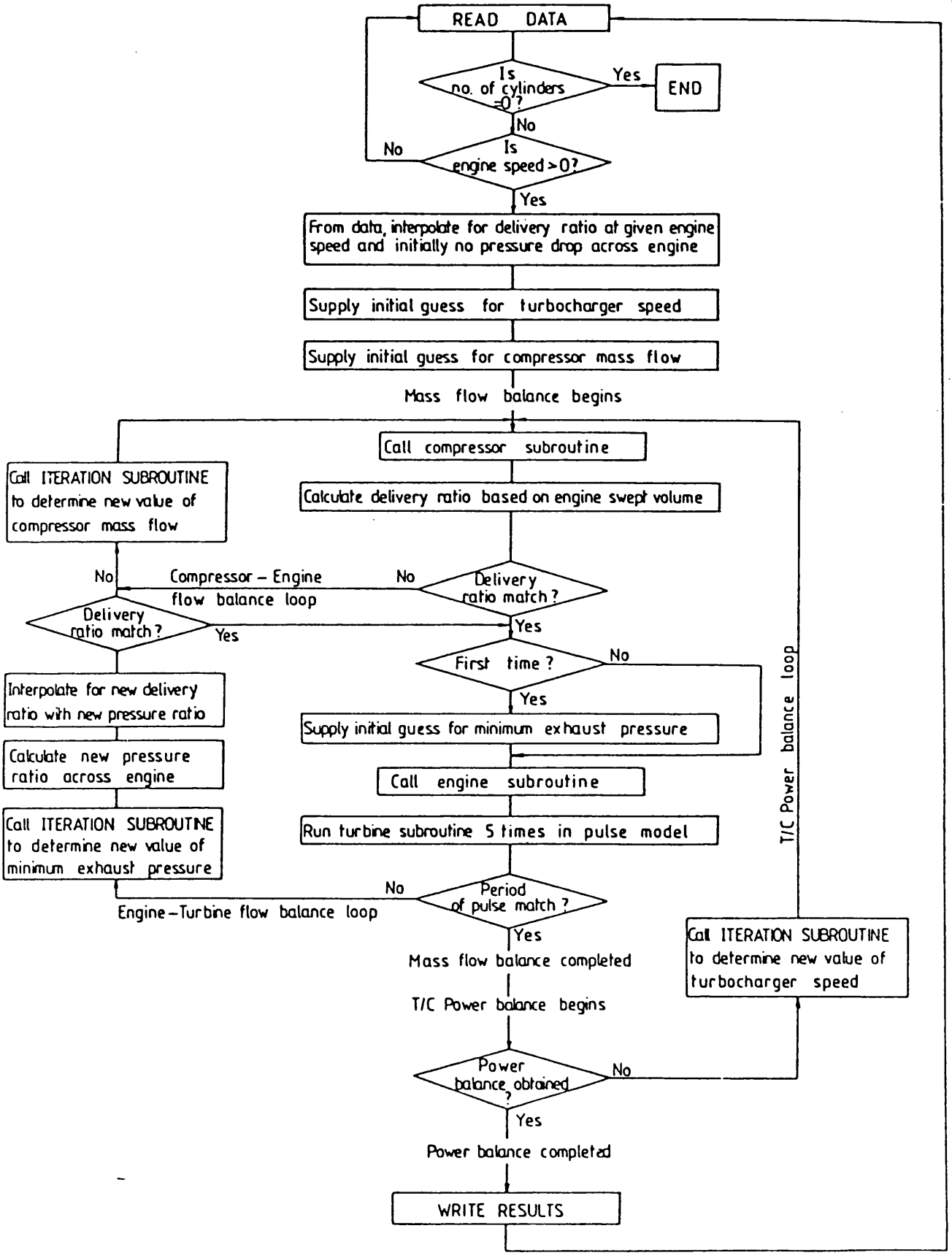

Fig. 6.0 Detailed Flow Diagram for Single Stage Turbocharged Diesel Engine Matching Program, EMAT.

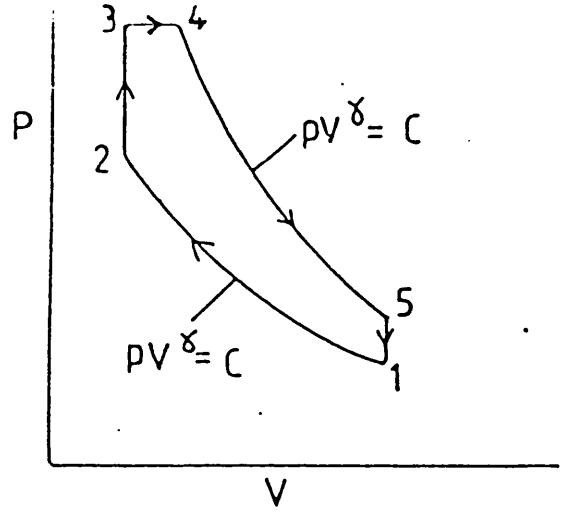

(a) AIR STANDARD CYCLE

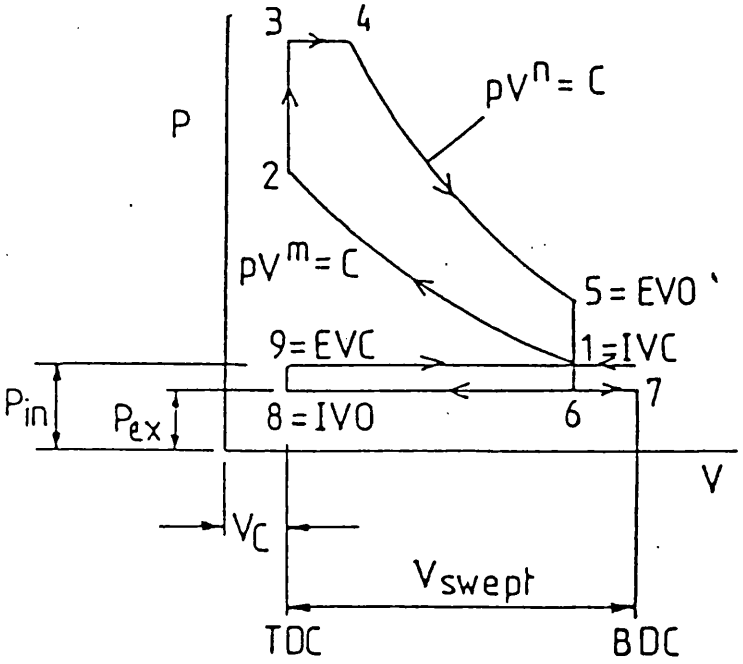

(b) MODIFIED AIR STANDARD CYCLE

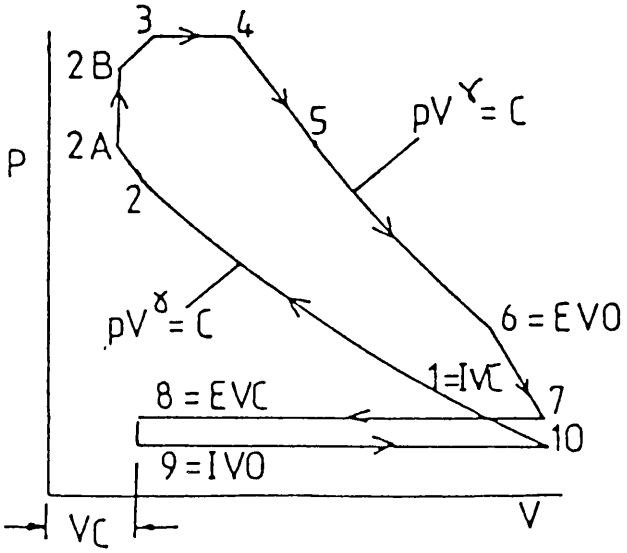

(c) FINAL FORM OF 'SIMPLE' CYCLE (five point)

Fig. 6.1 Variants of the Diesel Engine Cycle.

UNIVERSITY OF BATH DIESEL CYCLE SIMULATION PROGRAM (CSPTC)
FLOWCHART

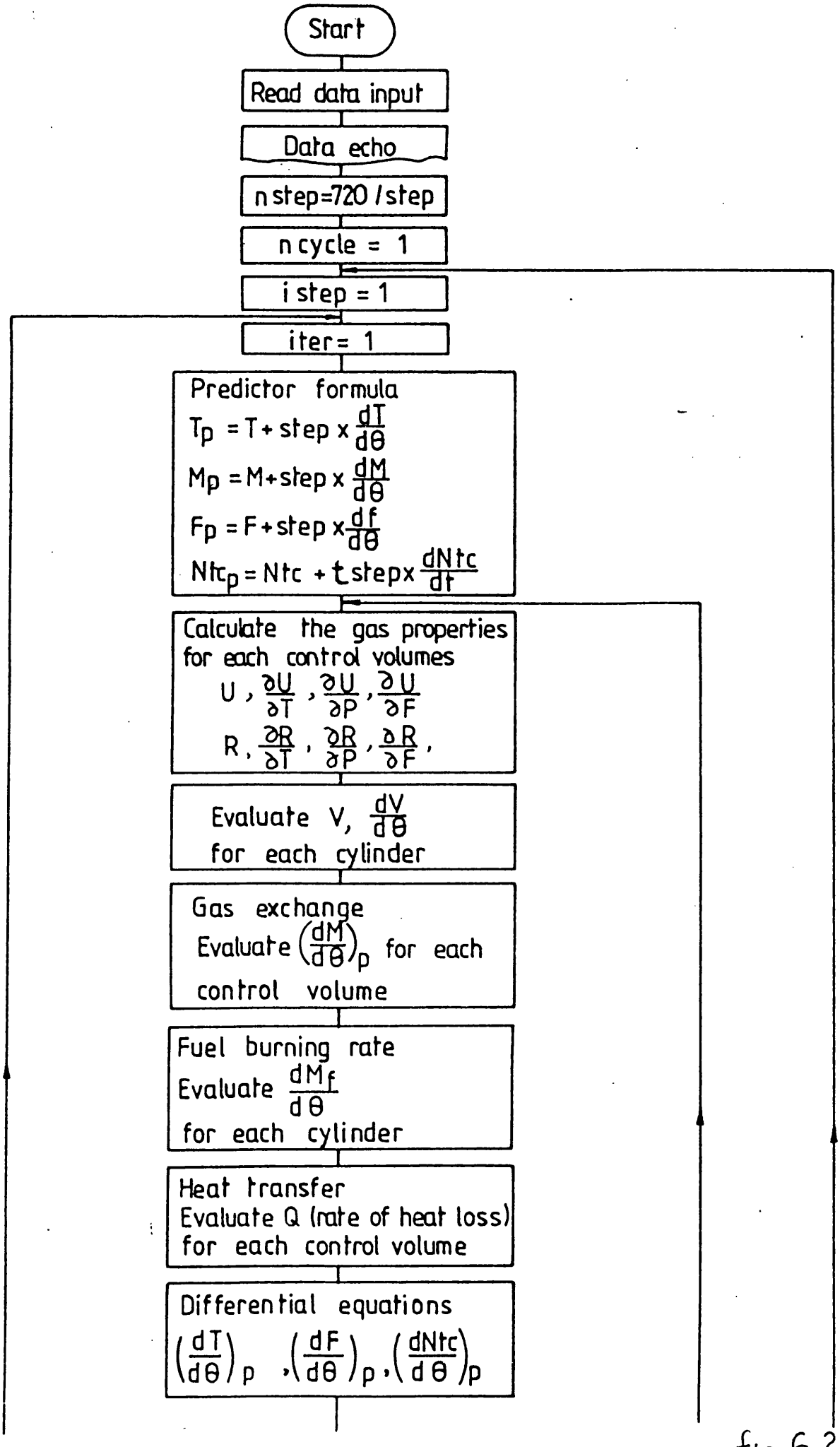

fig 6.2

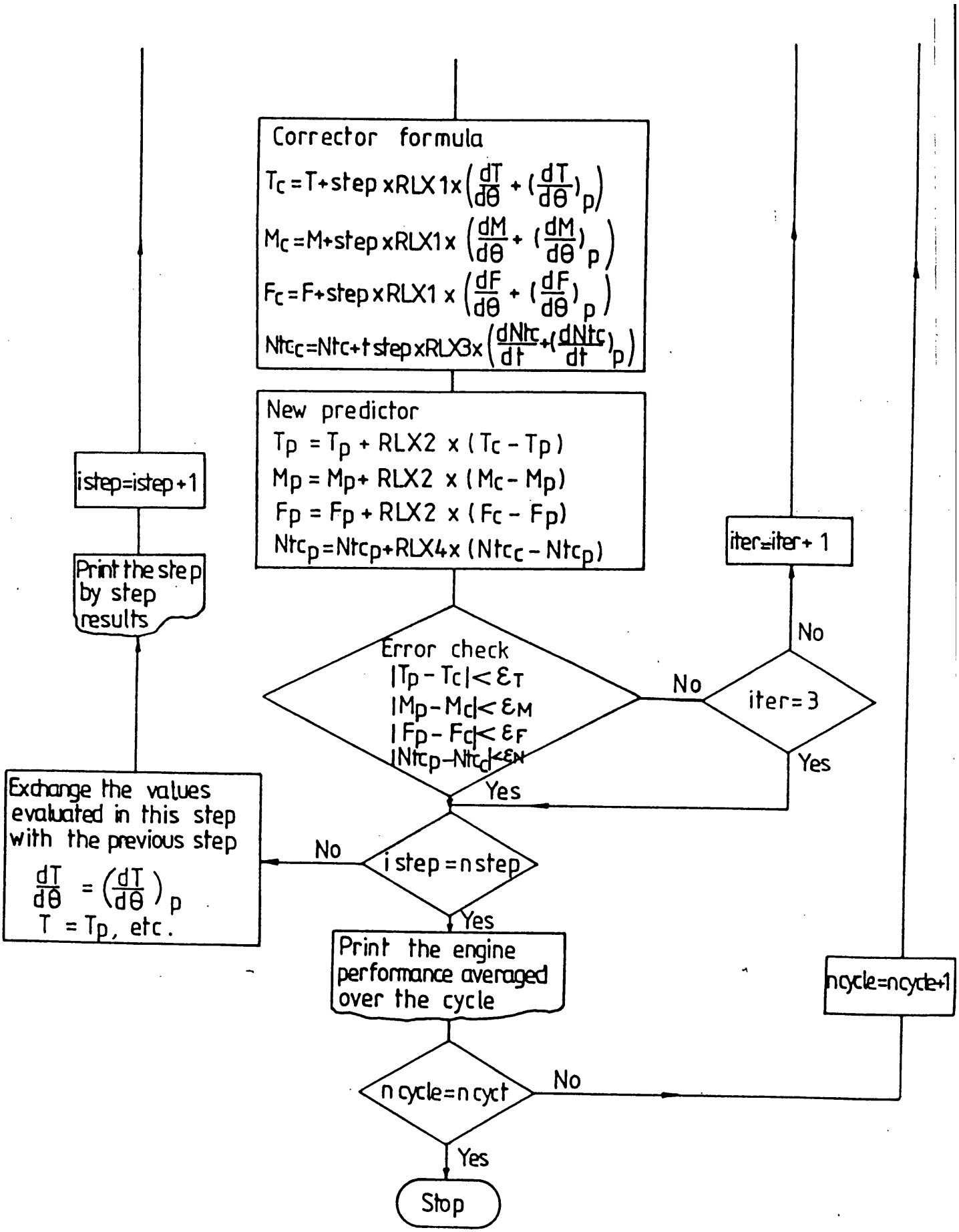
Corrector formula
$T_c = T + step \times RLX1 \times \left(\frac{dT}{d\theta} + \left(\frac{dT}{d\theta}\right)_p\right)$
$M_c = M + step \times RLX1 \times \left(\frac{dM}{d\theta} + \left(\frac{dM}{d\theta}\right)_p\right)$
$F_c = F + step \times RLX1 \times \left(\frac{dF}{d\theta} + \left(\frac{dF}{d\theta}\right)_p\right)$
$Ntc_c = Ntc + t\,step \times RLX3 \times \left(\frac{dNtc}{dt} + \left(\frac{dNtc}{dt}\right)_p\right)$
New predictor
$T_p = T_p + RLX2 \times (T_c - T_p)$
$M_p = M_p + RLX2 \times (M_c - M_p)$
$F_p = F_p + RLX2 \times (F_c - F_p)$
$Ntc_p = Ntc_p + RLX4 \times (Ntc_c - Ntc_p)$
istep=istep+1
Print the step by step results
iter=iter+1
No
Error check
$|T_p - T_c| < \varepsilon_T$
$|M_p - M_c| < \varepsilon_M$
$|F_p - F_c| < \varepsilon_F$
$|Ntc_p - Ntc_c| < \varepsilon_N$
No
iter=3
Yes
Yes
Exchange the values evaluated in this step with the previous step
$\frac{dT}{d\theta} = \left(\frac{dT}{d\theta}\right)_p$
$T = T_p$, etc.
No
i step = n step
Yes
Print the engine performance averaged over the cycle
ncycle=ncycle+1
n cycle=n cyct
No
Yes
Stop

fig 6.2 contd

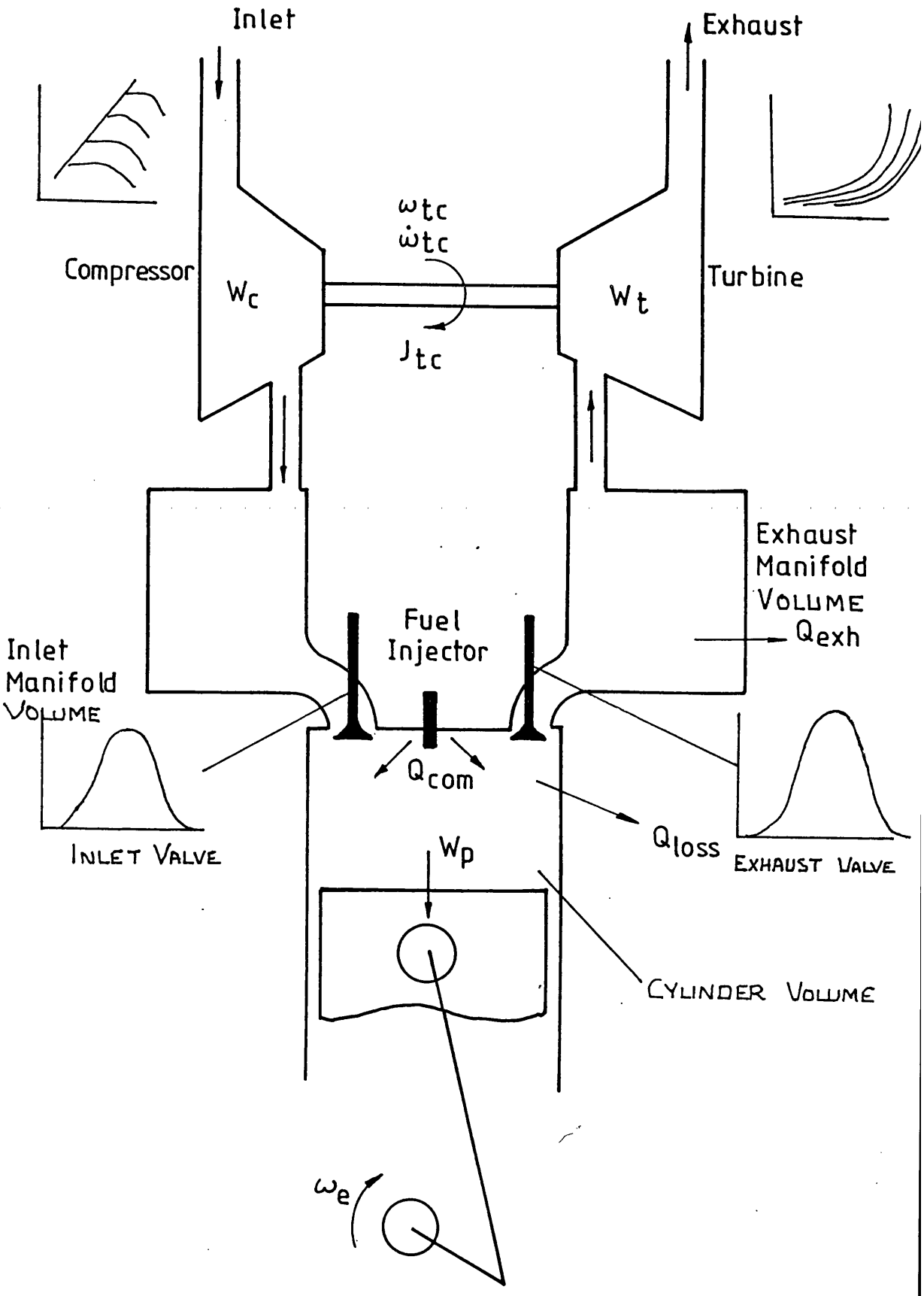

fig 6.3 SCHEMATIC OF A TURBOCHARGED ENGINE

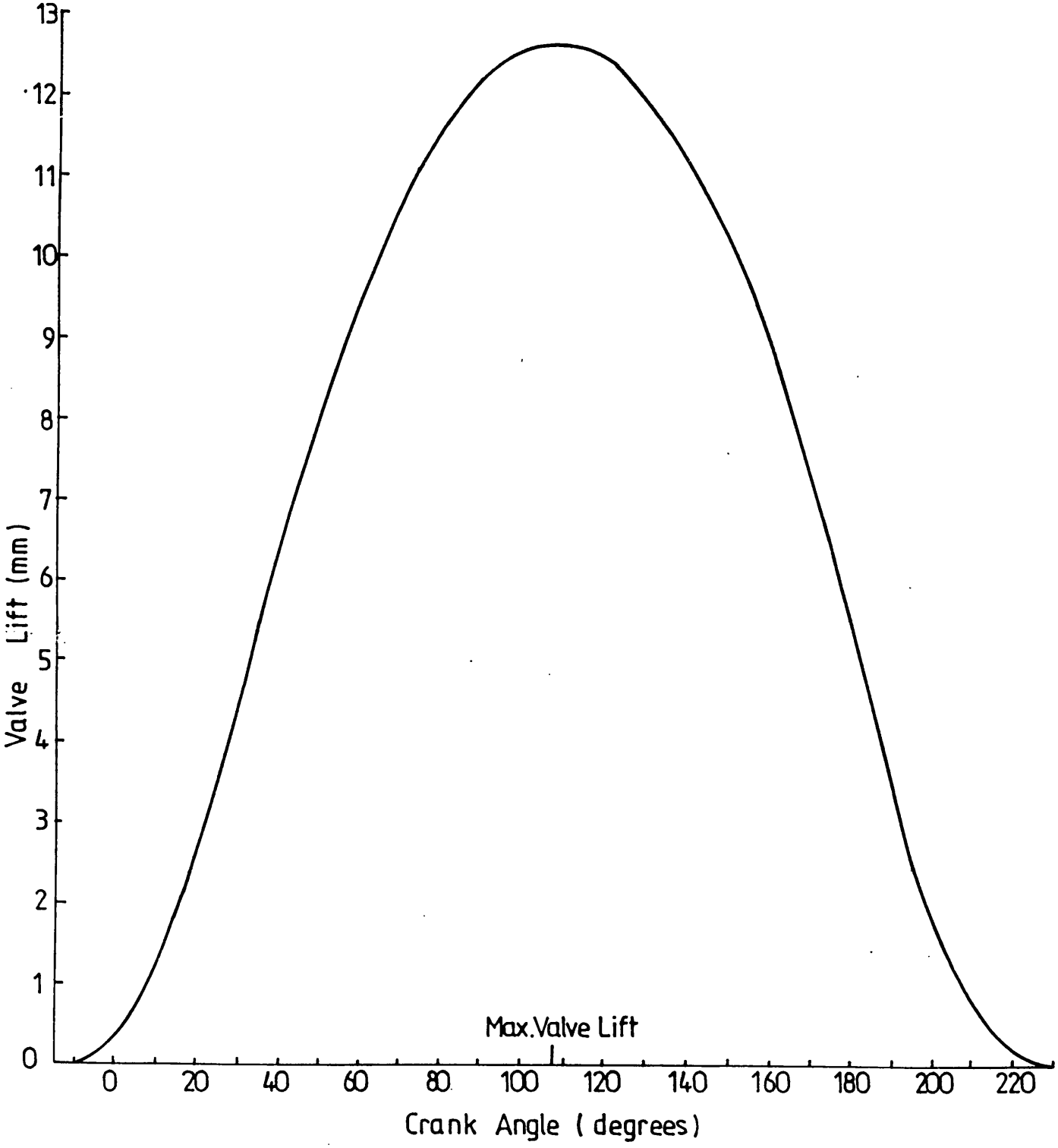

FIG 6.4 VALVE LIFT DIAGRAM FOR LEYLAND TL11V
(DRAWN FOR INLET VALVE)
EXHAUST VALVE LIFT IDENTICAL

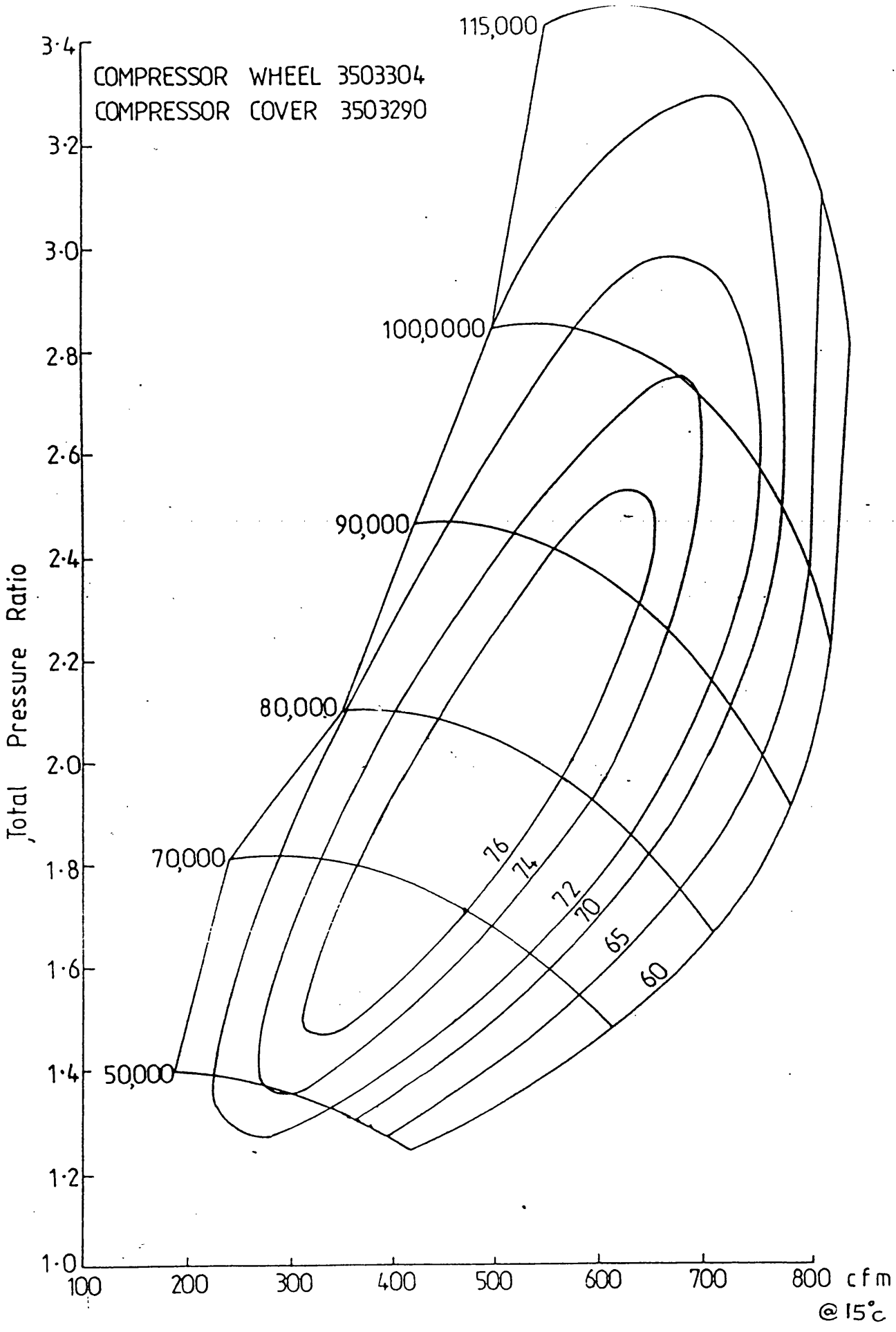

HOLSET 8640-H2C · COMPRESSOR MAP Fig 6.5

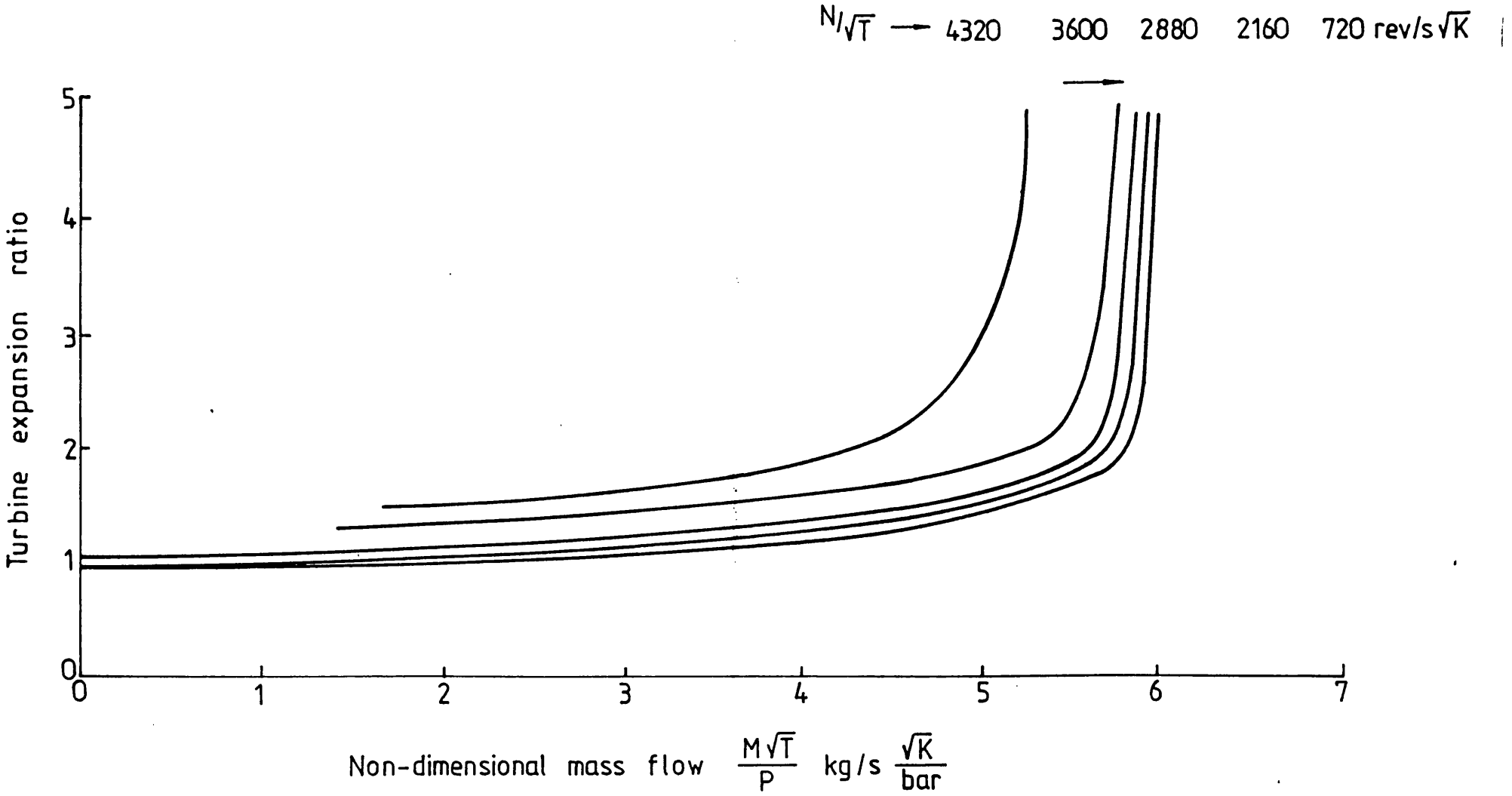

FIG 6.6 HOLSET H2B8081C L2543 TURBINE NON-DIMENSIONAL MASS FLOW CHARACTERISTIC

filling and emptying programme

****
leyland tl11 engine rated at 255bhp - 2100rev min.
****

data echo
**** ****

this is a 4-stroke 6 cylinder engine with single stage turbocharging

number of turbochargers 1
number of inlet manifolds 1
number of exhaust manifolds 2

cylinder	phase angle (advance cyl 1)	inlet manifold number	exhaust manifold number
1	0.0	1	1
2	240.0	1	1
3	480.0	1	1
4	120.0	1	2
5	600.0	1	2
6	360.0	1	2

h.p. turbo number	inlet manifold number	turbine entry number	exhaust manifold number
1	1	1	1
1	1	2	2

inlet manifold number	volume (lt)
1	4.885

exhaust manifold number	volume (lt)	surface area (cm2)
1	1.380	816.970
2	1.220	680.700

engine geometry
****** ********

friction scale factor 1.0

bore 127.08 mm.
stroke 146.05 mm.
con. rod length 266.70 mm.
compression ratio 15.75

engine speed 2100.0 rev/min

valve data
***** ****

exhaust valve

scale factor 1.0

dia 46.50 mm.
seat angle 30.0 deg.
seat width 2.80 mm
number of valves per cylinder 1

FILLING AND EMPTYING DATA ECHO fig 6.7

```
valve lift (mm)       0.00   0.35   1.25   2.50   4.30   6.40   8.00  10.50
crank angle (deg)  134.00 144.00 154.00 164.00 174.00 184.00 194.00 214.00

valve lift (mm)      11.60  12.25  12.60  12.70  12.65  12.45  12.00  11.25
crank angle (deg)  224.00 234.00 244.00 252.00 254.00 264.00 274.00 284.00

valve lift (mm)      10.25   8.80   3.50   1.80   0.75   0.25   0.00
crank angle (deg)  294.00 304.00 334.00 344.00 354.00 364.00 374.00

inlet valve                                          scale factor     0.90000

dia   55.00 mm.
seat angle  30.0 deg.
seat width  3.60 mm
number of valves per cylinder  1

valve lift (mm)       0.00   0.35   1.25   2.50   4.30   6.40   8.00  10.50
crank angle (deg)  350.00 360.00 370.00 380.00 390.00 400.00 410.00 430.00

valve lift (mm)      11.60  12.25  12.60  12.70  12.65  12.45  12.00  11.25
crank angle (deg)  440.00 450.00 460.00 468.00 470.00 480.00 490.00 500.00

valve lift (mm)      10.25   8.80   3.50   1.80   0.75   0.25   0.00
crank angle (deg)  510.00 520.00 550.00 560.00 570.00 580.00 590.00


calorific value of fuel:     42.800 kj/g
requested bmep       0.000 bar


heat release diagram:
  crank angle (tdc=0)
  712.00
  heat release (kj)
  4.9100
heat release model is imperial              scale factors   1.0000  1.0000


heat trans model is    woschni


  surface area   surface area   surface area   temperatue   temperature
   head (cm2)     piston (cm2)   liner (cm2)     head (k)      liner (k)
    97.9500        184.4440       107.0700       625.000       425.000

   h.t.c. exhaust
  manifold (w/m2/k)
      28.4000


atmospheric pressure 1.00000 bars
atmospheric temperature  296.20 k
turbine back pressure 0.09500 bars-gauge
compressor inlet pressure or depression -0.05800 bars-gauge

hp  turbo data
**  ***** ****                                          scale factor

*compressor map*
 holset h2b 8081c compressor map.                                1.0000
```

fig 6.7 CONTD

```
number of speed curves  7                                          1.00000
number of pressure ratios  6                                       1.00000
                                                                   0.98500
              nd speed (rev/min)/rootk
              pressure ratios
              nd mass flow (kg/s)*rootk/bar
              efficiencies

  2357.02
   1.160    1.200    1.210    1.225    1.225    1.225
   3.903    2.750    2.324    1.820    1.355    0.871
   0.591    0.690    0.739    0.739    0.690    0.650

  2946.28
   1.260    1.300    1.340    1.355    1.360    1.361
   4.880    3.834    3.525    2.943    2.169    1.219
   0.591    0.640    0.690    0.739    0.739    0.650

  3535.53
   1.400    1.480    1.540    1.541    1.550    1.551
   5.896    4.299    3.525    2.711    2.169    1.569
   0.591    0.690    0.739    0.739    0.709    0.670

  4124.79
   1.580    1.710    1.760    1.780    1.790    1.800
   6.740    4.958    4.377    3.447    2.866    2.056
   0.591    0.690    0.729    0.739    0.709    0.670

  4717.04
   1.810    1.900    2.000    2.060    2.080    2.090
   7.482    5.965    5.577    4.958    3.951    3.137
   0.591    0.640    0.690    0.729    0.729    0.699

  5303.30
   2.070    2.200    2.370    2.440    2.450    2.460
   8.017    6.429    5.887    5.074    4.725    3.625
   0.591    0.640    0.709    0.729    0.690    0.680

  5892.55
   2.450    2.600    2.670    2.750    2.760    2.770
   6.874    6.776    6.658    5.892    5.401    4.419
   0.591    0.640    0.690    0.719    0.690    0.621

*turbine map*
rotor inertia     300.00 kg.mm2
tip radius     90.000 mm.

                                                                   scale factors
 h2b 25cm2 p 3 turbine stage.                                        1.00000
number of speed curves  8                                          1.00000
number of expansion ratios  8                                      0.91000
                                                                   1.00000
number of turbine volutes  2.
                  nd speed (rev/min)/rootk
                  expansion ratios
                  nd mass flow (kg/s)*rootk/bar
                  efficiencies

   360.00
   1.010    1.100    1.200    1.400    1.600    2.000    2.200    5.000
   0.000    2.397    3.196    3.995    4.594    5.293    5.399    5.399
```

fig 6.7 contd

```
 0.000   0.360   0.260   0.220   0.200   0.180   0.150   0.100

 720.00
 1.020   1.100   1.200   1.400   1.600   2.000   2.200   5.000
 0.000   2.397   3.196   4.044   4.644   5.293   5.399   5.399
 0.000   0.560   0.460   0.380   0.340   0.290   0.180   0.150

1440.00
 1.030   1.100   1.200   1.400   1.600   2.000   2.200   5.000
 0.000   2.097   3.196   4.044   4.594   5.243   5.369   5.369
 0.000   0.640   0.680   0.640   0.590   0.520   0.440   0.400

2160.00
 1.040   1.150   1.200   1.400   1.600   2.000   2.200   5.000
 0.000   1.997   2.696   3.795   4.494   5.184   5.331   5.331
 0.000   0.560   0.660   0.700   0.700   0.660   0.550   0.500

2880.00
 1.050   1.300   1.400   1.500   1.600   2.000   2.200   5.000
 0.000   2.497   3.295   3.595   4.394   5.148   5.278   5.278
 0.000   0.360   0.540   0.640   0.680   0.700   0.700   0.650

3600.00
 1.060   1.400   1.500   1.600   1.800   2.000   2.200   5.000
 0.000   1.598   2.696   3.395   3.995   4.594   5.020   5.232
 0.000   0.220   0.322   0.440   0.500   0.570   0.600   0.550

4320.00
 1.070   1.600   1.700   1.800   1.900   2.000   2.200   5.000
 0.000   1.598   2.497   2.996   3.395   3.795   4.781   5.223
 0.000   0.160   0.210   0.260   0.320   0.360   0.440   0.400

5040.00
 1.080   1.700   1.800   1.900   2.000   2.100   2.200   5.000
 0.000   1.598   1.997   2.397   3.096   3.395   4.373   5.214
 0.000   0.050   0.080   0.120   0.140   0.220   0.400   0.350
```

fig 6.7 contd

Engine LEYLAND TL11—7962756 Project No. 2 W KOBERTS.

Title COMPARISON OF BASE WITH FILLING & EMPTYING RESULTS.

Power Curve

Test No.	Timing	Amb'nt °C	Barometer Ins. Hg.
83	22	25	730.5.

BASE H2B.

FILLING & EMPTYING THEORETICAL MATCHED RESULTS.

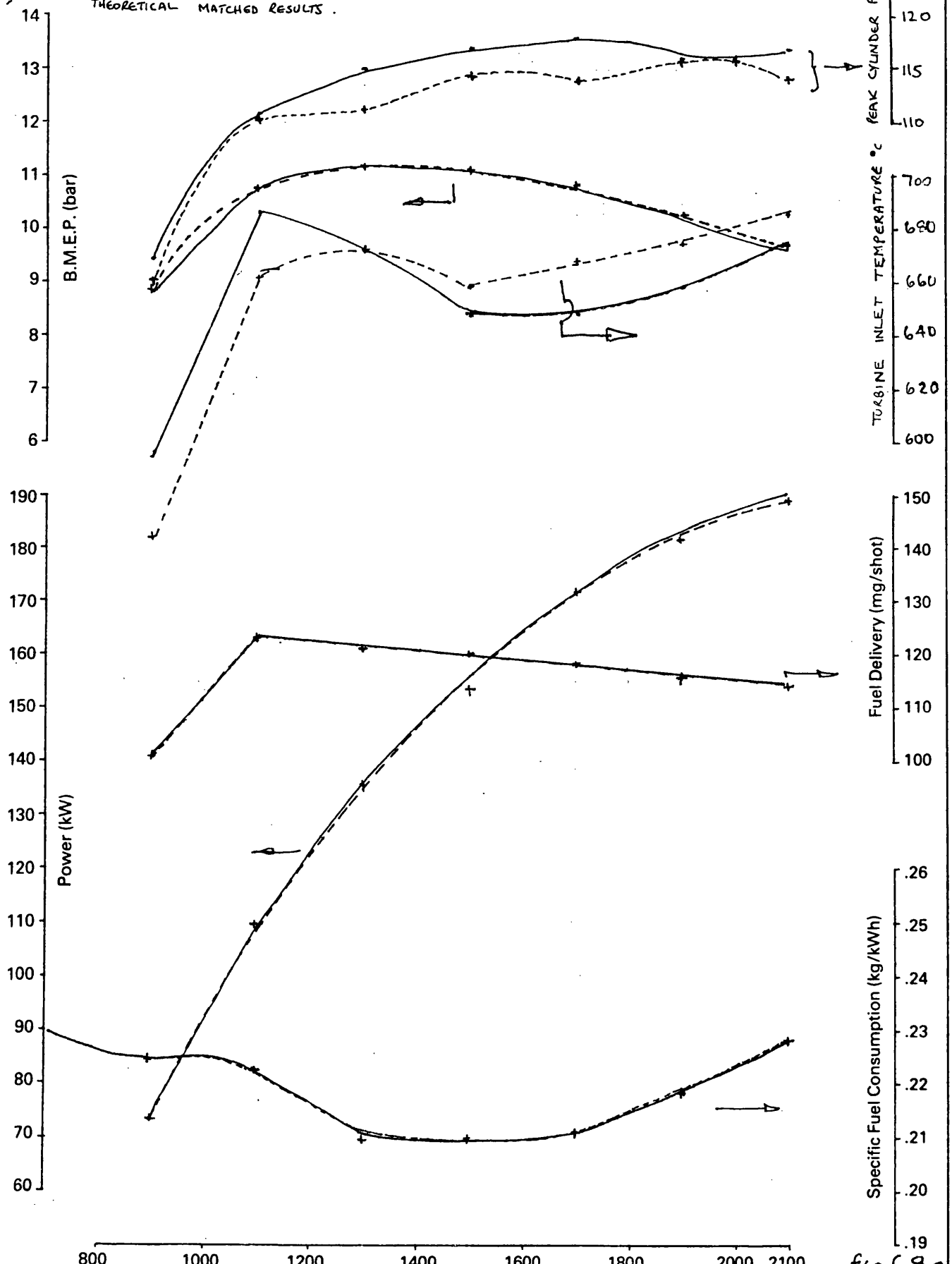

fig 6.8a

Engine LEYLAND TL11—7962756 Project No. E.W. ROBERTS

Title COMPARISON OF MATCHED BASE WITH FILLING & EMPTYING SIMULATION PROGRAMME

Power Curve

Test No.	Timing	Amb'nt °C	Barometer Ins. Hg.
83	22	25	730.5

BASE H2B.

FILLING & EMPTYING.

THEORETICAL MATCHED RESULTS:

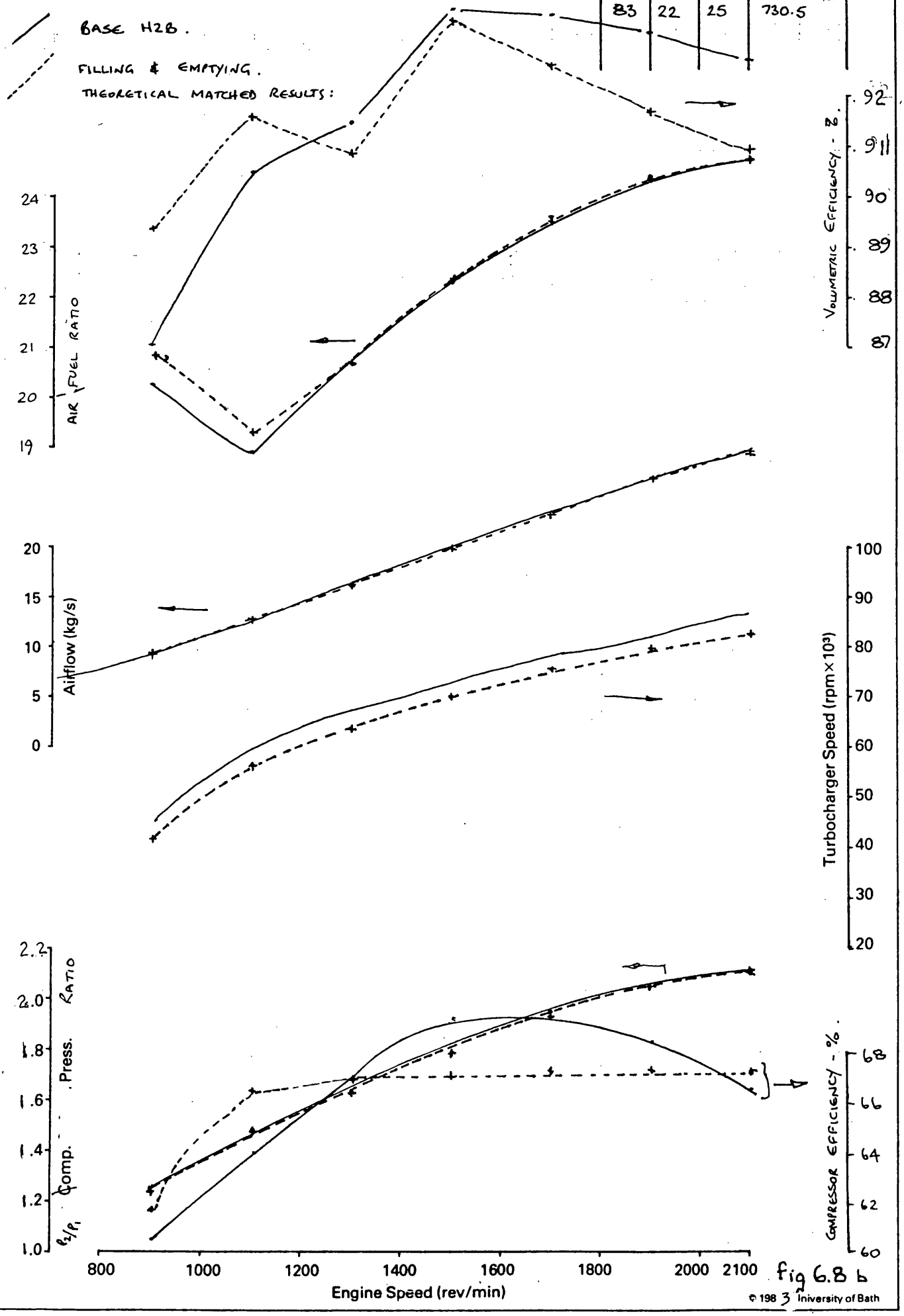

fig 6.8 b

Engine LEYLAND TL11 ENGINE—11.1 DISPLACEMENT

Drawn By C.W. Lovell

Title COMPARISON OF BASE WITH PREDICTED TIMING

Rating—190 kW at 2100 rev/min

RESULTS

Constant Speed Curve at 1300 rev/min

Holset / Leyland / Dowty / DoI Contract

Test No.	Timing	Amb'nt °C	Barometer Ins. Hg.
51	VARIABLE	25	74.1

H2B BASE.

FILLING & EMPTYING OUTPUT.
VARIABLE TIMING.

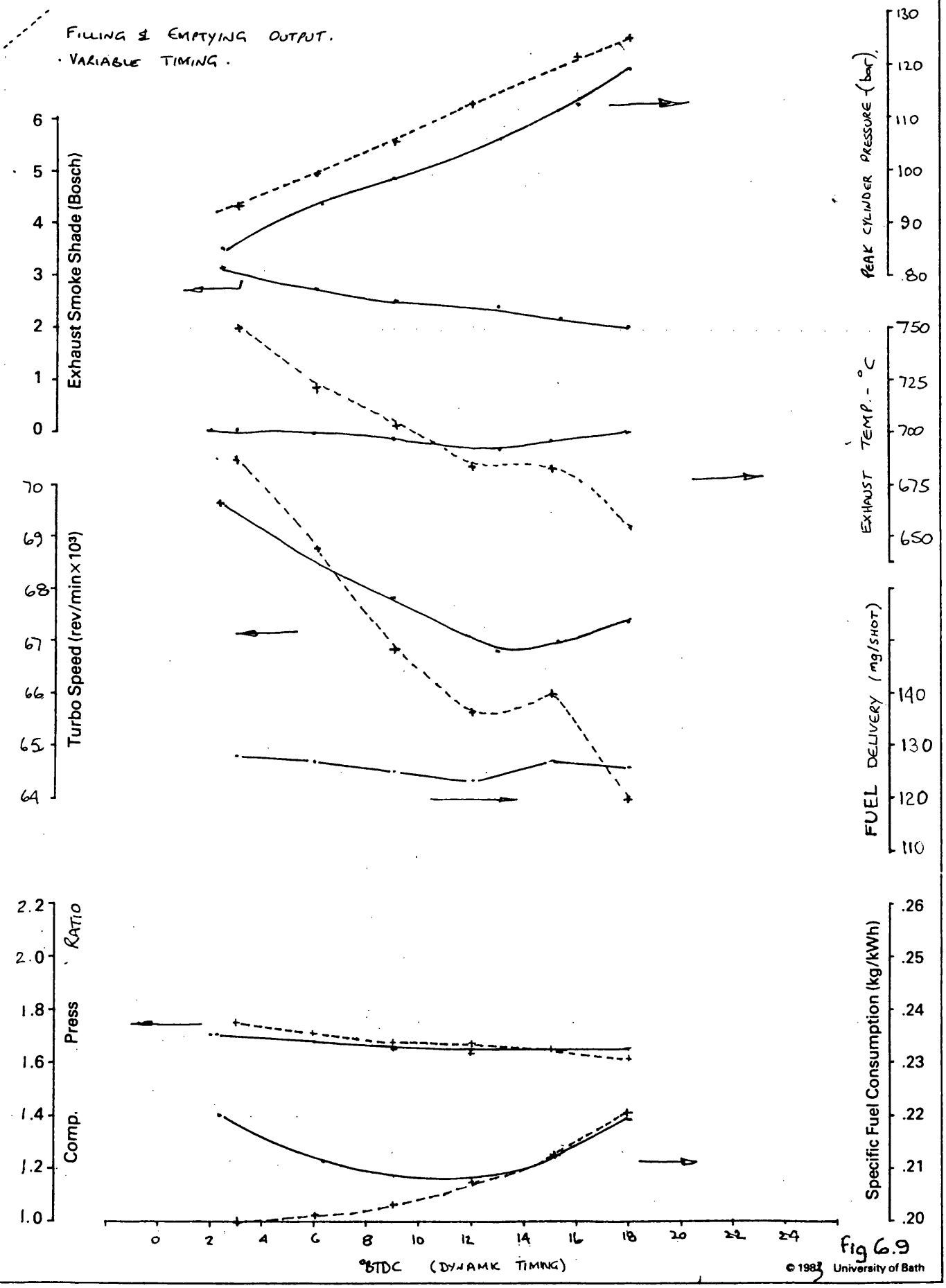

Fig 6.9

Engine LEYLAND TL11 ENGINE—11.1 DISPLACEMENT Drawn by .....

Title COMPARISON OF PREDICTED & ACTUAL VG RESULTS. Rating—190 kW at 2100 rev/min

Constant Speed Curve at 1300 rev/min

Holset / Leyland / Dowty / DoI Contract

Test No.	Timing	Amb'nt °C	Barometer Ins. Hg.
57	22.	25	
58			
59			
60			

VG WITH VARIOUS RESTRICTIONS.

SIMULATED VG WITH VARIOUS RESTRICTIONS.

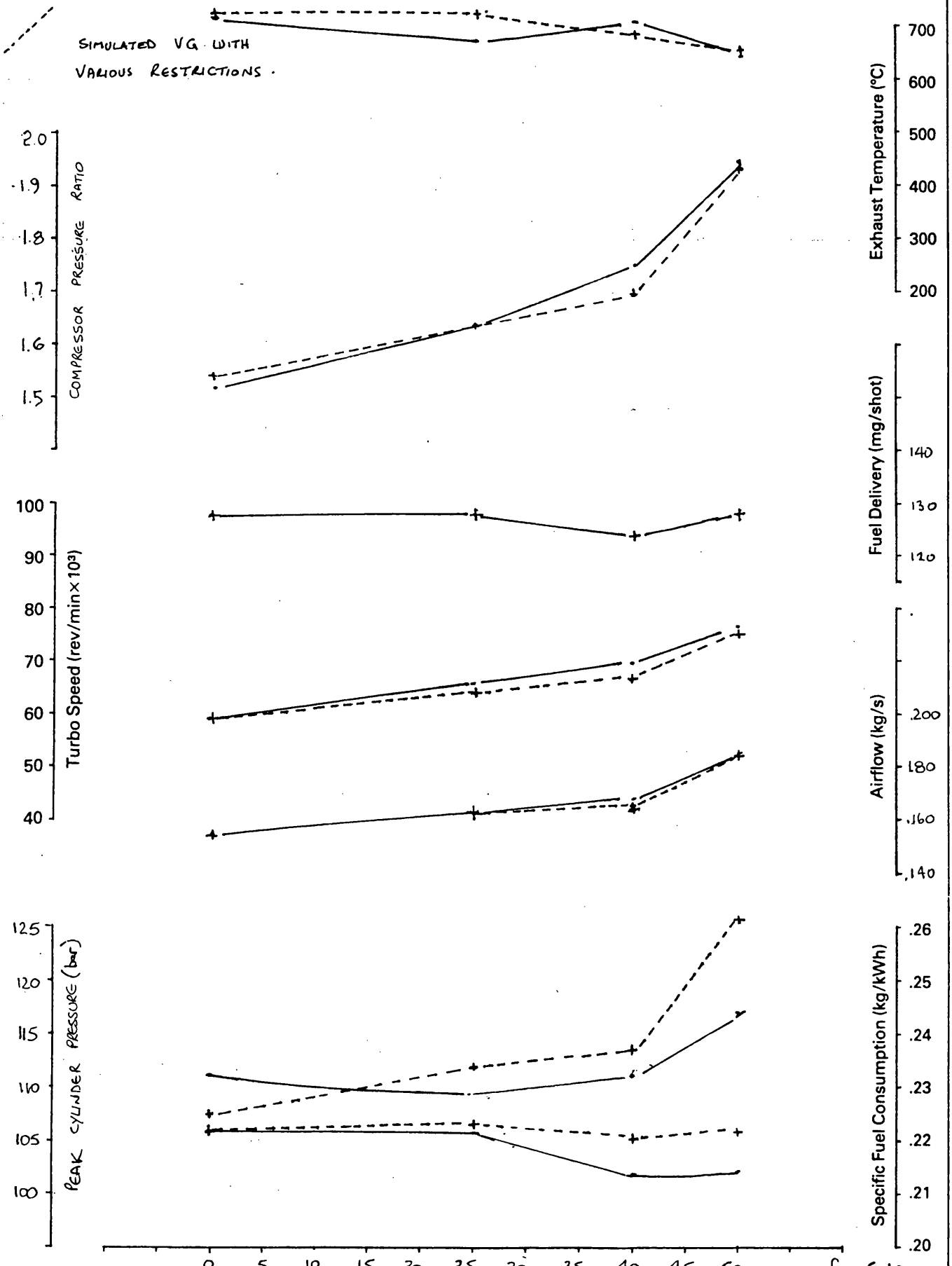

fig 6.10

2100 rev/min.	Optimised VG Configuration	Matched by filling and emptying program	% Difference
Power - kW	191.7	191.7	-
BMEP - bar	9.81	9.81	-
SFC - kg/kWh	.227	.227	-
Airflow - kg/s	.2993	.2961	-1.07
fuel delivery -mg/shot	.114	.114	-
Volumetric efficiency - %	90.9	90.53	-0.41
Turbocharger speed - rev/min	86213	94639	1.83
Compressor pressure ratio	2.01	2.01	-
Turbine expansion ratio	1.81	1.83	1.1
Compressor efficiency %	67.7	67.4	-0.44
Turbine Efficiency - %	62.0	61.2	-1.29
Turbine Inlet Temperature - K	956	903	-5.5
Peak Cylinder Pressure - bar	128	133	3.9

Dynamic Timing - 21° BTDC
Ambient Pressure - 97.4 kN/m²
Ambient Temperature - 298.4 K

Inlet Restriction - 3.70 kN/m²
Exhaust Restriction - 10.39 kN/m²

TABLE OF OPTIMISED RESULTS VERSUS SIMULATION - 2100 rev/min

Fig. 6.11(a)

1300 rev/min.	Optimised VG Configuration	Matched by filling and emptying program	% Difference
Power - kw	150.5	150.5	-
BMEP - bar	12.43	12.43	-
SFC - kg/kwh	.212	.212	-
Airflow - kg/s	.1923	.1936	0.68
fuel delivery -mg/shot	.136	.136	-
volumetric efficienty - %	92.3	92.3	-
Turbocharger speed - rev/min	77868	77044	-1.06
Compressor pressure ratio	1.98	1.98	-
Turbine expansion ratio	1.87	1.87	-
Compressor efficiency - %	67.9	68.0	0.15
Turbine efficiency - %	58	56.5	-2.59
Turbine inlet temperature - K	928	960	3.45
Peak cylinder pressure - bar	135	127	-5.93

Dynamic timing - 16° BTDC
Ambient Pressure - 100.4 kN/m^2
Ambient Temperature - 298.0
Inlet restriction - 1.49 kN/m^2
Exhaust restriction - 7.86 kN/m^2

Table of optimised results versus simulation - 1300 rev/min

fig. 6.11(b)

1100 rev/min	Optimised VG Configuration	Matched by Filling and Emptying program	% Difference
Power - kW	115.8	115.8	-
BMEP - bar	11.3	11.3	-
SFC - kg/kwh	.216	.216	-
Airflow - kg/s	.1437	.1413	-1.6
fuel delivery - mg/shot	.125	.125	-
Volumetric Efficiency - %	91.0	91.0	-
Turbocharger speed - rev/min	64839	62111	-4.2
Compressor pressure ratio	1.65	1.63	-1.21
Turbine Expansion Ratio	1.58	1.59	0.6
Compressor efficiency - %	68.4	68.3	-0.15
Turbine Efficiency - %	54.3	55.0	1.29
Turbine inlet temperature - K	947	876	-7.5
Peak Cylinder Pressure - bar	110	121.7	10.6

Dynamic Timing - 19.0° BTDC
Ambient Pressure - 98.9 kN/m²
Ambient Temperature - 298.0
Inlet Restriction - 0.82 kN/m²
Exhaust Restriction - 3.06 kN/m²

TABLE OF OPTIMISED RESULTS VERSUS SIMULATION - 1100 rev/min

Fig. 6.11(c)

2100 rev/min.	VG Optimised	+ 3.8% on Compressor	+ 2.4% on Turbine	+ 3% on $\dot{m}\sqrt{T}/p$	low C r 14.75	low C r 13.75	Large valves 59(56) 59(46.5)	High CD factor	Valve Timing
BMEP (bar)	9.81	9.69	9.72	9.97	9.86	9.92	10.04	9.96	9.93
SFC kg/kwh	.2276	.2303	.2295	.223	.2264	.2251	.2224	.224	.2248
Airflow kg/s	.2961	.306	.301	.2906	.300	.305	.299	.2984	.3003
AFR T	24.5	25.31	24.92	24.04	24.85	25.23	24.75	24.71	24.89
O	24.63	25.45	25.05	24.18	24.99	25.37	24.88	24.82	24.98
CYL.PRESS (bar)	133.42	136.17	134.92	130.9	126.1	118	133	134	133
Turbine inlet temperature (K)	900	883	892	907	915	925	890	897	900
Turbo speed rev/min	84639	87103	86466	81700	86186	87689	84514	84700	84310
η_{comp} %	67.4	71.2	67.2	68.5	67.2	67.3	67.2	67.2	67.2
η_{turb} %	61.2	60.5	63.6	60	61	61	61.5	61.2	62.0
$\eta_{overall}$ %	41.25	43.0	42.74	41.1	41.0	41.05	41.3	41.1	41.7
htc.kW/m^{2}K	.497	.501	.491	.481	.479	.464	.492	.497	.494

fig 6.12

1300 rev/min	VG optimised	+ 4.6% on compress	+ 3% on turbine	4 5% turndown on $m\sqrt{T}/p$	low c.r 14.75	low C.R. 13.75	Large Valves	High CD factor	Valve Timing
BMEP bar	12.43	12.58	12.52	11.99	12.40	12.37	12.60	12.62	12.52
SFC kg kwh	.2125	.2104	.2113	.220	.2135	.214	.210	.2097	.211
Air flow kg/s	.1923	.2024	.1973	.214	.1946	.1981	.1929	.1948	.1947
AFR T.	21.51	22.63	22.07	23.97	21.77	22.18	21.58	21.83	21.79
AFR O.	21.65	22.79	22.22	24.11	21.91	22.30	21.72	21.94	21.93
Cyl. press bar	135	141.3	139	152	127	119	135	135	136
Turbine inlet temperature (K)	927	903	918	917	936	940	921	911	910
Turbo speed rev/min	77868	81850	80730	94686	79016	80795	77395	77537	77317
η_{comp} %	67.9	72.5	67.8	65.4	67.9	67.8	68.0	68.1	68.1
η_{turb} %	58.	58	61	62.5	58.0	58.0	58.0	58.0	59.0
$\eta_{overall}$ %	39.38	42.05	41.36	40.88	39.38	39.32	39.44	39.50	40.18
η_{mean} HTC	.394	.406	.400	.422	.379	.365	.393	.397	.392

fig 6.13

1100 rev/min	VG optimised	+ 3.6% on Comp. Map.	+ 2.5% on turbine map	48% turn down on $M\sqrt{T}/\rho$	Low C.r. 14.75	Low C.r. 13.75	Large Valves	High CD factor
BMEP bar	11.30	11.45	11.43	11.33	11.55	11.81	11.41	11.76
SFC kg/kwh	0.2158	0.2125	0.213	0.217	.2106	.206	.2132	.2067
Air flow kg/s	.1413	.146	.1447	.1637	.1434	.146	.1421	.1446
AFR T	20.34	21.01	20.82	23.52	20.6	21.05	20.46	20.84
0	20.43	21.13	20.94	23.68	20.74	21.17	20.56	20.92
CYL. PRESS (bar)	122	126	126	143	116	111	122	124
Turbine inlet temperature (K)	876	866	873	854	892	909	870	861
Turbo speed rev/min	62111	64313	65261	80000	63840	66259	61853	61947
η_{comp} %	68.3	71.9	68.3	67.7	68.3	68.3	68.4	68.5
η_{turb} %	55.0	55.0	57.5	62.0	55.0	54.8	54.7	55.
$\eta_{overall}$ %	.376	.395	.392	.420	.376	.374	.374	.377
η_{mean} H.T.C. (kw/m^2 K)	0.339	0.348	0.348	0.377	.331	.321	.341	.349

fig 6.14

NOMINAL

2100 rev/min 190 kW

	PARAMETER	VG BASE	OPTIMISED	% DIFFERENCE
1	Large Valves	227.6	222.4	+ 2.3
2	Larger Turbine	227.6	223.1	+ 1.98
3	Optimised Valve Timing	227.6	224.8	+ 1.23
4	High CD Factor	227.6	224.1	+ 1.58
5	Low CR - 13.75	227.6	225.1	+ 1.1
6	Low CR - 14.75	227.6	226.5	+ 0.5
7	+ 3.8% on Comp.	227.6	230.4	- 1.23
8	+ 2.4% on Turb.	227.6	229.5	- 0.83

EFFECT OF VARIOUS PARAMETERS ON ENGINE SFC - 2100 rev/min.

fig 6.15

NOMINAL

1100 Nm 1300 rev/min

	PARAMETER	VG BASE	OPTIMISED	%
1	High CD factor	212.5	209.7	+ 1.3
2	Large Valves	212.5	210.0	+ 1.2
3	+ 4.6% on Comp.	212.5	210.4	+ 1.0
4	+ 3.0% on turb	212.5	211.3	+ 0.6
5	Optimised Valve Timing	212.5	211.5	+ 0.47
6	Low CR 14.75	212.5	213.5	- 0.47
7	Low CR 13.75	212.5	214.0	- 0.70
8	Tight Turbine (48%)	212.5	220.0	- 3.53

EFFECT OF VARIOUS PARAMETERS
ON ENGINE SFC - 1300 rev/min.

fig 6.16

NOMINAL

1000 Nm @ 1100 rev/min

	PARAMETER	VG BASE	OPTIMISED	% DIFFERENCE
1	High CD Factor	215.8	206.5	+ 4.3
2	Low CR 13.75	215.8	206.3	+ 4.4
3	Low CR 14.75	215.8	210.7	+ 2.4
4	+ 3.6% on Comp	215.8	212.6	+ 1.5
5	Large Valves	215.8	213.2	+ 1.2
6	+ 2.5% on Turbine	215.8	213.6	+ 1.0
7	Tight Turbine 48%	215.8	217.3	- 0.7

fig 6.17

EFFECT OF VARIOUS PARAMETERS ON ENGINE SFC - 1100 rev/min

	2100 rev/min	1300 rev/min	1100 rev/min	
High CD Factor	4	1	1	6
Large Valves	1	2	5	8
Valve Timing	3	5		
High Comp η	8	3	4	15
Low CR 13.75	5	7	2	14
Low CR 14.75	6	6	3	15
M $\sqrt{T}/p$	2	8	7	17
High Turb η	7	4	6	17

MORE EFFECTIVE

TABLE QUANTIFYING THE MOST EFFECTIVE PARAMETERS

fig 6.18

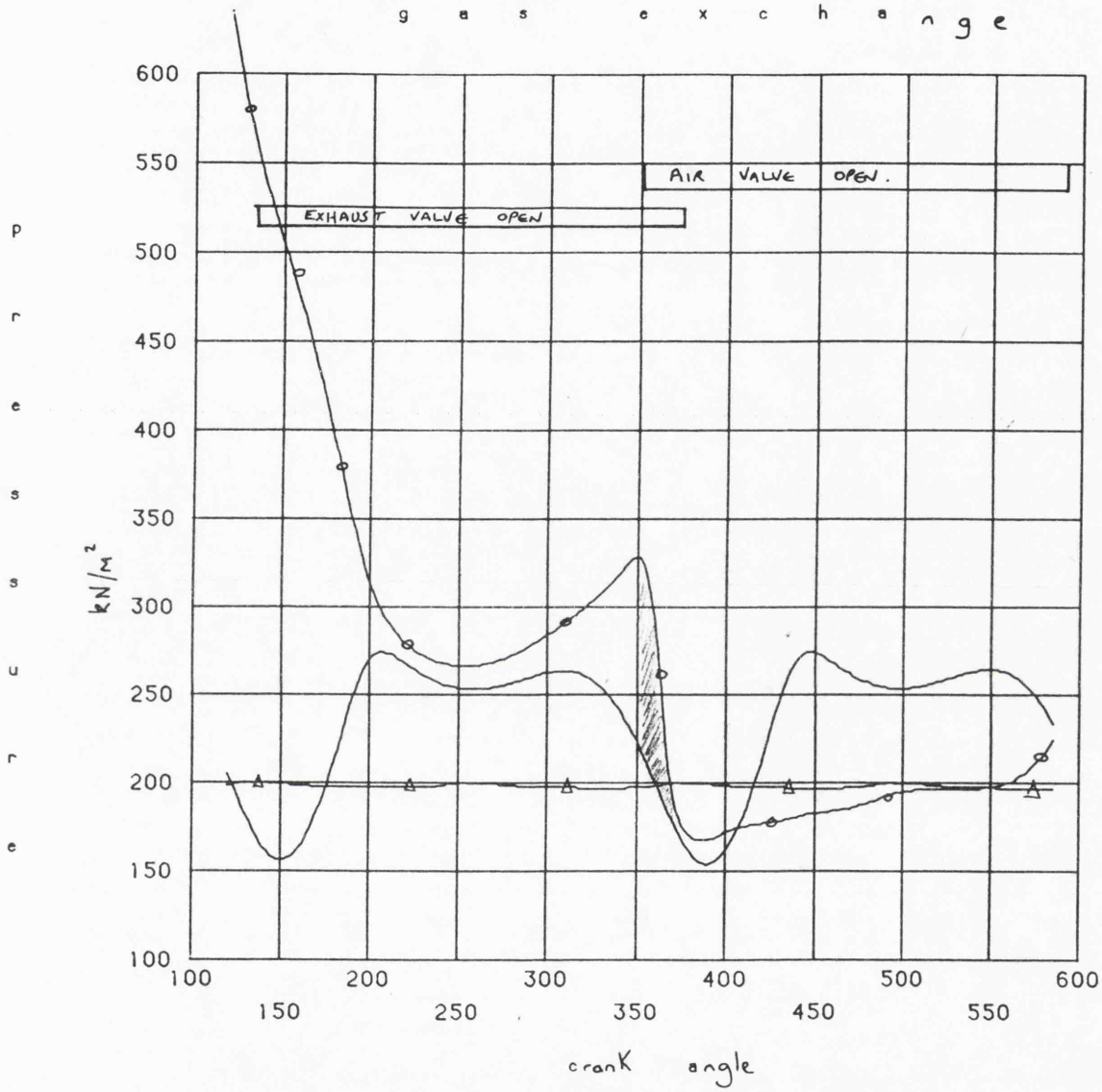

2100 rev/min 190 kW. BASE H2B.

fig 6.19

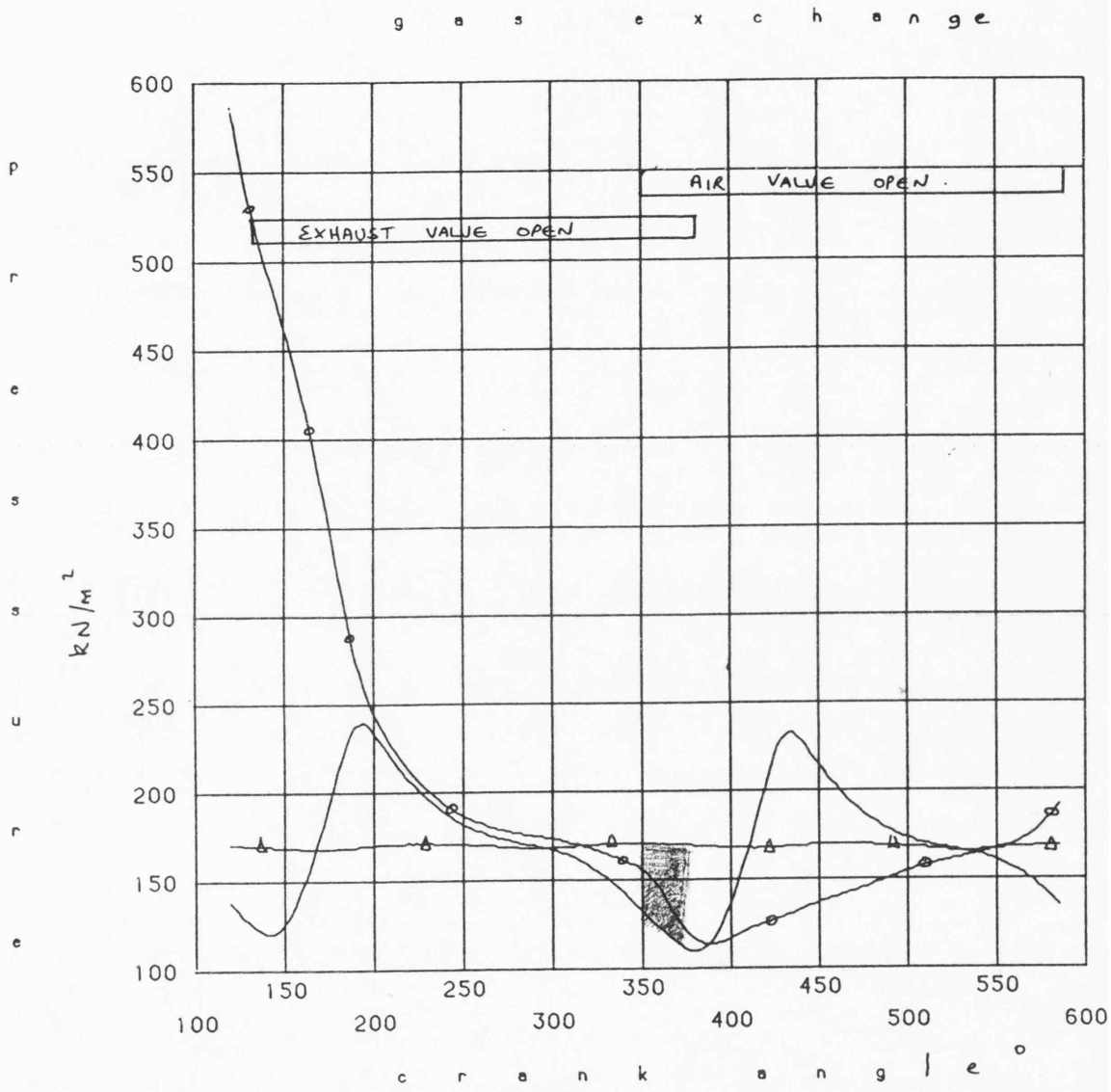

1300 rev/min 990 Nm (peak torque) BASE H2B

fig 6.20

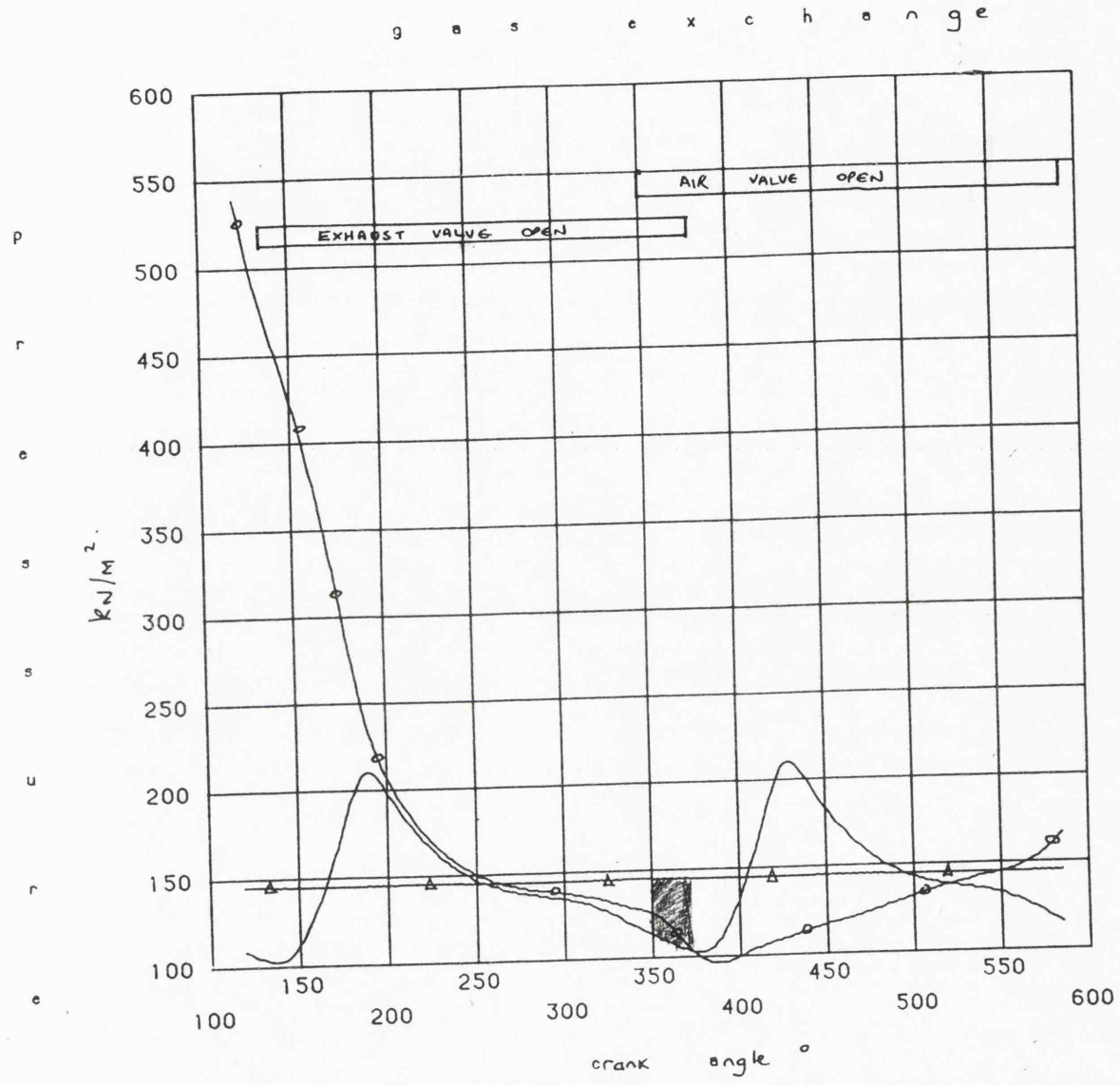

1100 rev/min 956 Nm. BASE H2B.

fig 6.21

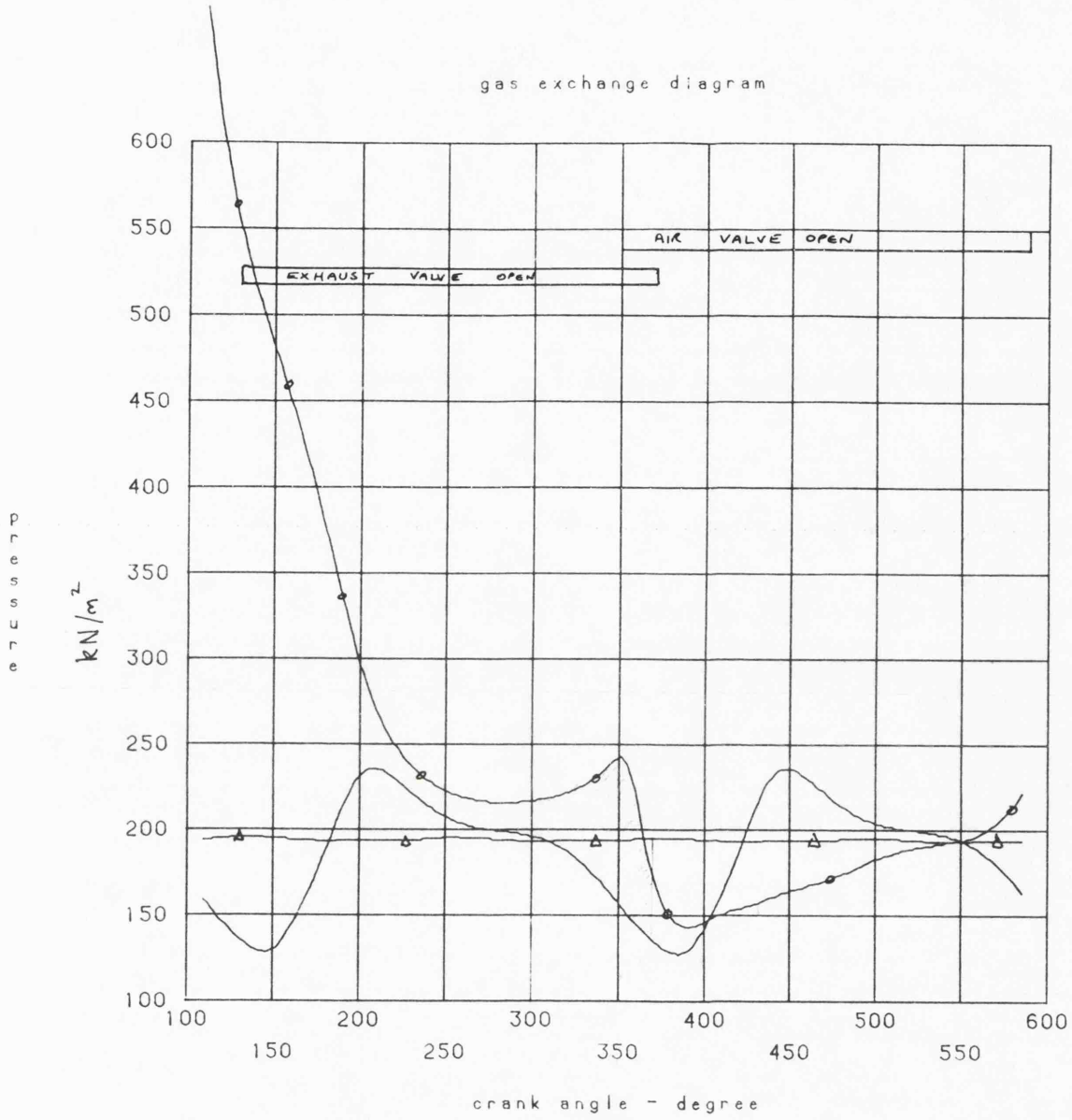

2100 rev/min 190 kW VG - OPTIMISED

fig 6.22

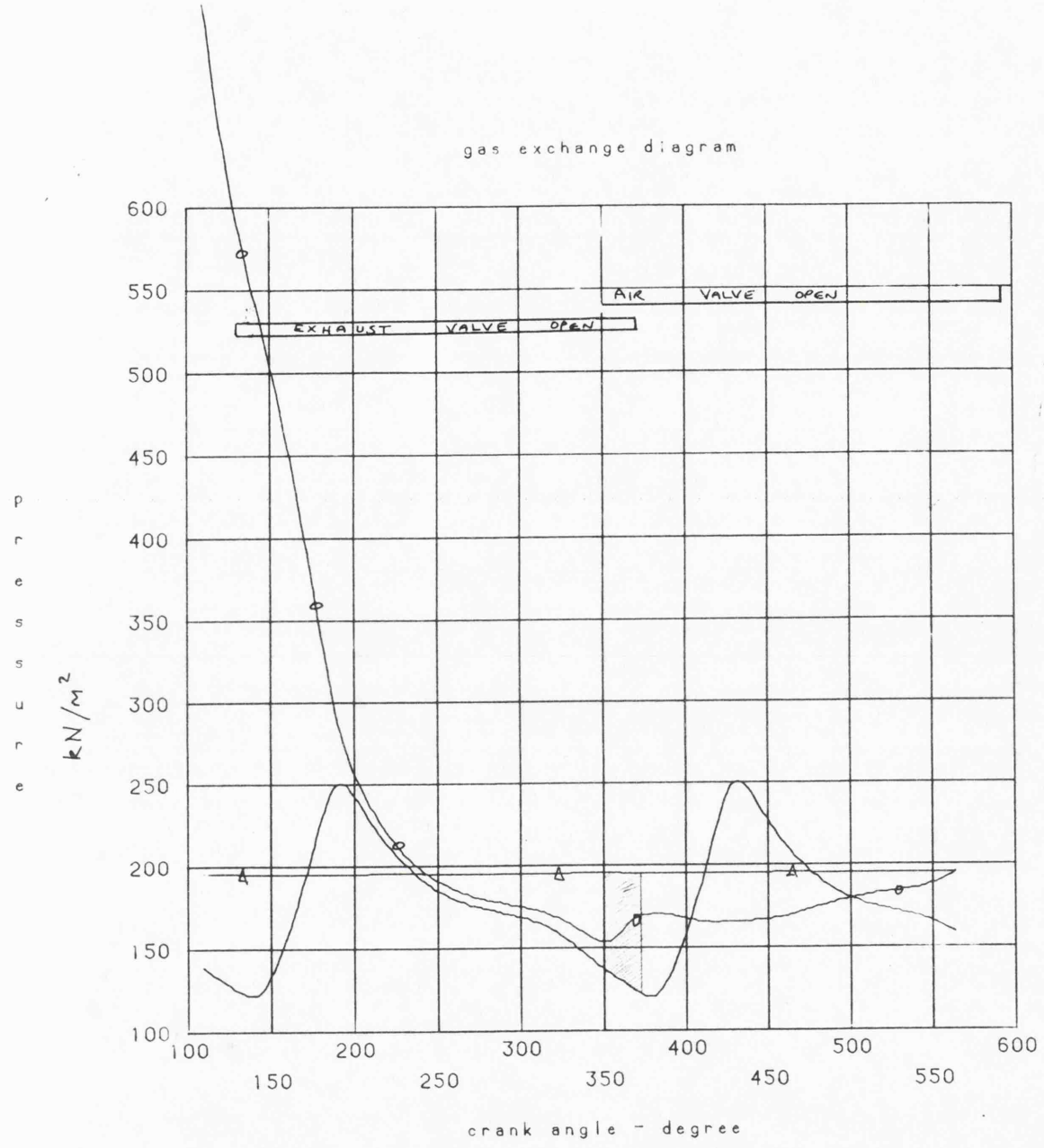

1300 rev/min ~ 1100Nm PEAK TORQUE · OPTIMISED VG

fig 6.23

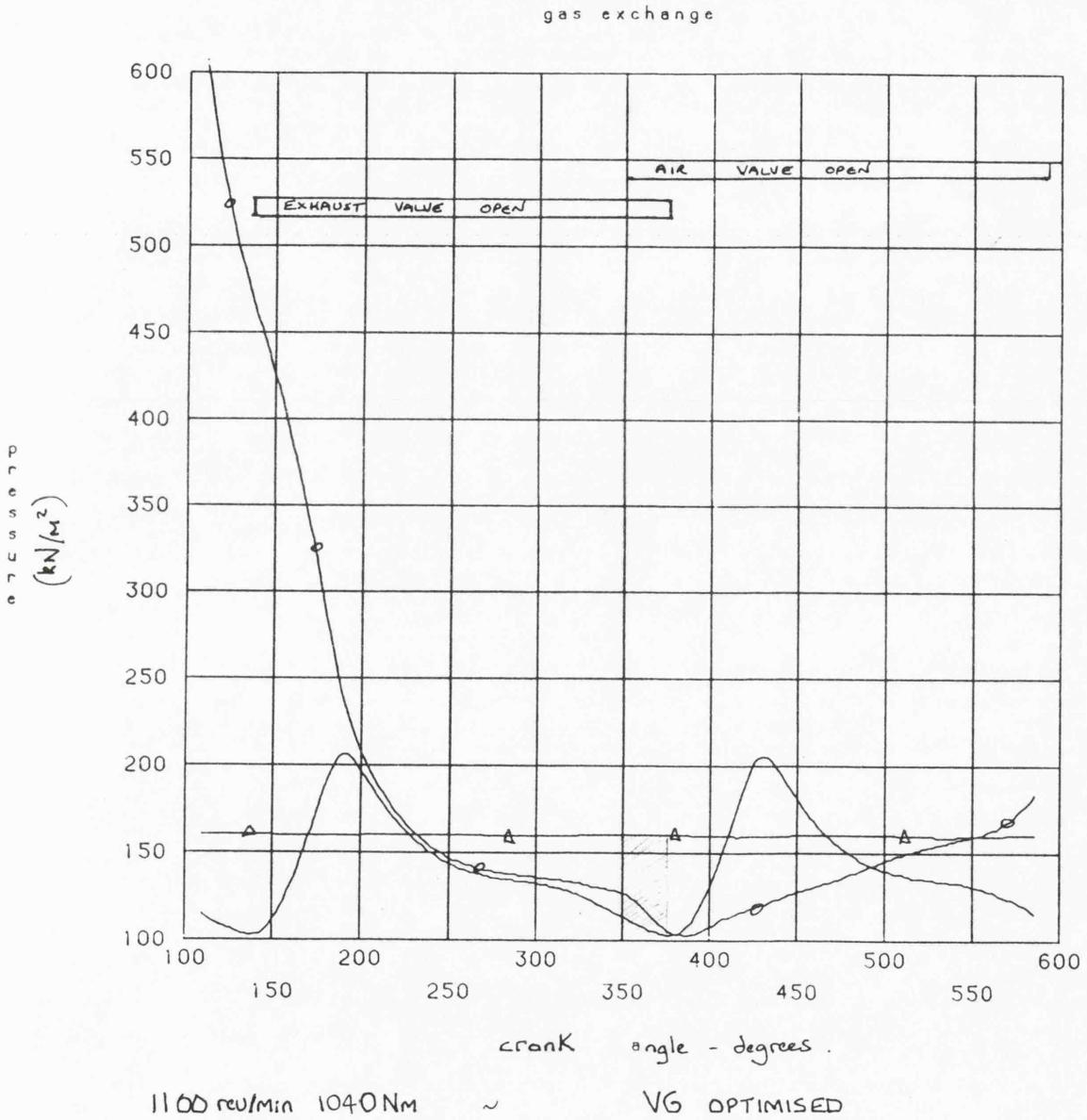

1100 rev/min 1040 Nm ~ VG OPTIMISED

fig 6.24

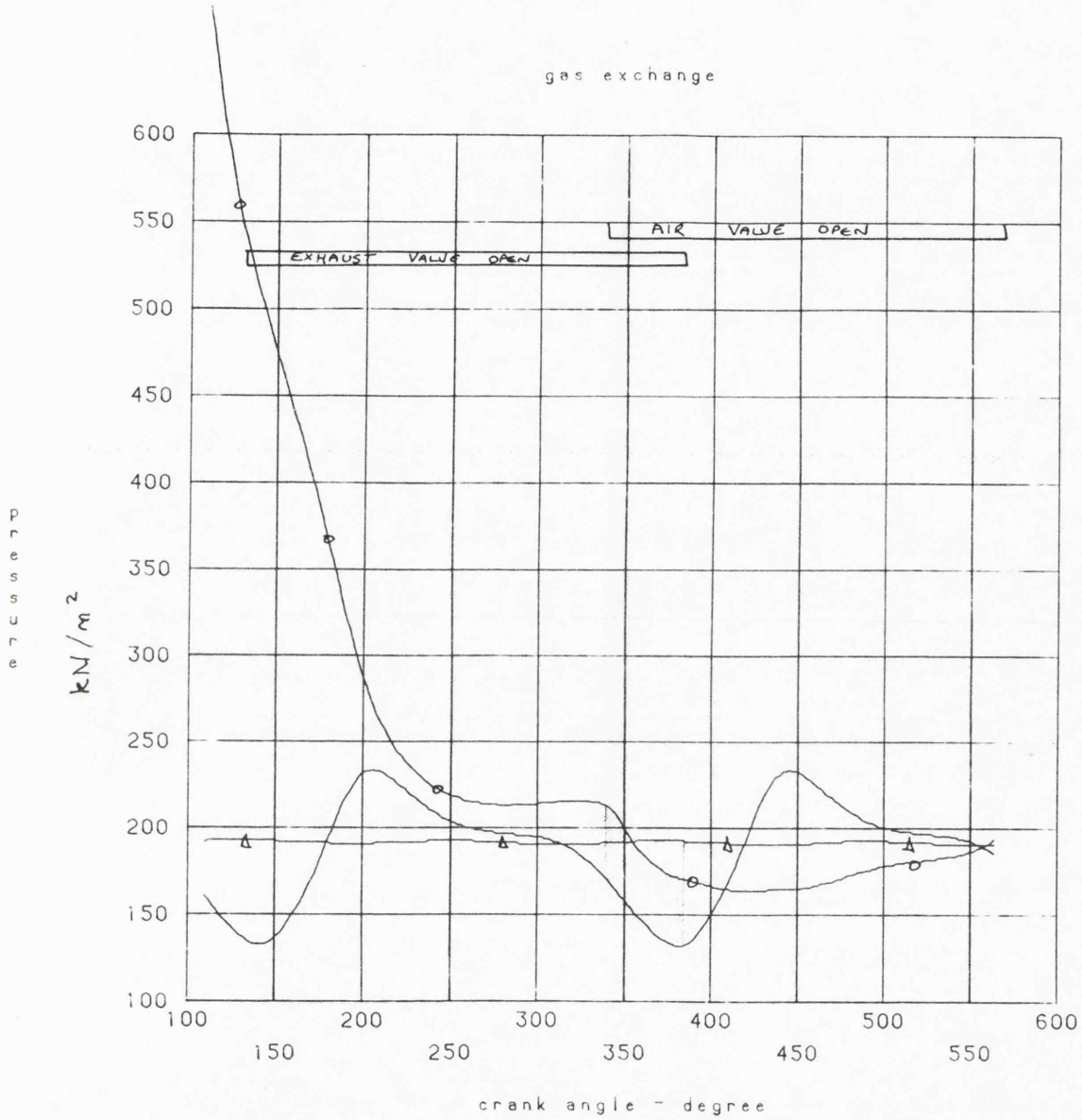

2100 rev/min 190kW - VG · OPTIMISED VALVE TIMING.

fig 6.25

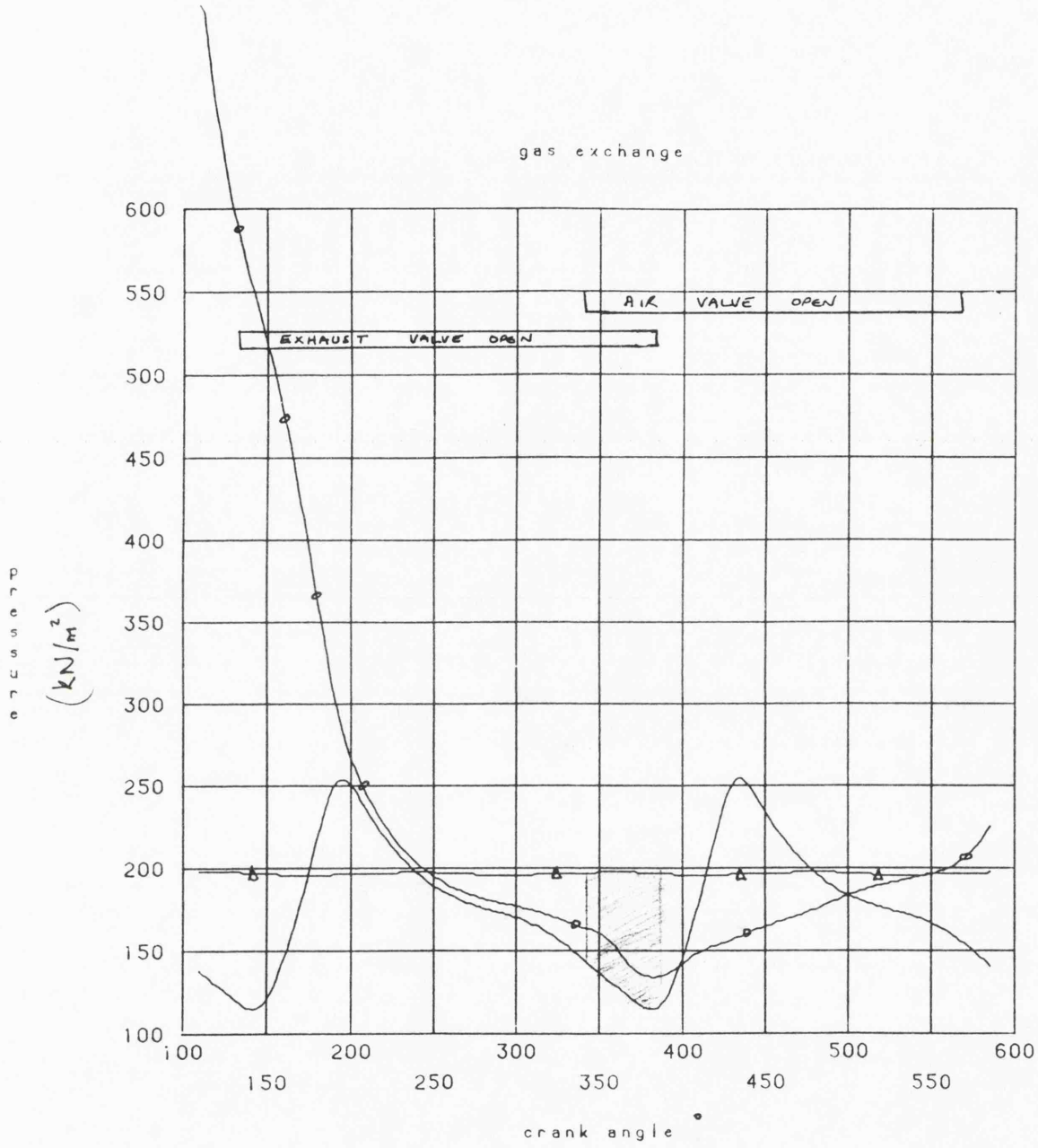

13.00 rw/min ~ 1106 Nm VG - OPTIMISED VALVE TIMING

fig 6.26

7. CONCLUSIONS AND SUGGESTIONS FOR FURTHER WORK

7.2 Introduction

This thesis investigated the complete testing and characterisation of a HOLSET turbocharger equipped with a variable area turbine stage applied to an automotive type LEYLAND TL11 engine. Control was effected by a programmable digital controller and was extended to include variable injection timing and electronic governing functions. This was to achieve an engine with good economy, acceleration and flexibility (torque back-up). An optimal type control strategy was implemented. That is, it was not self optimising. Actuation was achieved by electro-hydraulics, this was justified on the basis of cost, environment and standardisation. A new test bed was constructed to accurately and repeatedly determine the levels of engine performance. A new data acquisition system was also developed. Finally, a theoretical investigation explored those areas constrained by mechanical, and efficiency limits for the engine and turbocharger respectively.

This chapter reviews the control implementation and algorithms assessed for the VG configured engine both steady state and transiently. Appropriate conclusions together with suggestions for further work are drawn. The operation of the test facility is considered first of all.

7.2 Conclusions from the Experimental Work

7.2.1 Test Facility

The test facility proved very satisfactory in terms of repeatability and ease of testing. The built in redundancy allowed useful testing to continue even with several significant failures. The automatic regulation of engine functions aided testing by allowing the operator to concentrate on the test in progress. The coherent data reduction system and standardisation allowed efficient file handling and presentation.

7.2.2 Control Implementation

The design and development of the control parameters together with the

actuators and transducers proved adequate for the application. Three prototype VG turbochargers were tested (based on volute exit area and ring sleeve design) before satisfactory performance was obtained. All control parameters were fail safe, fail soft.

To implement the control system on the engine the following precautions were taken :

1) It was considered essential for this application to use a fire resisting working fluid.
2) The leads from the respective transducers were tied in a loop to avoid failure in the potting.
3) Great care was taken to minimise vibration through design and testing (stroboscope).

The reliability of the system was further improved by :

1) Mounting the servo-valves remotely (excepting for the integral unit on the fuel pump.
2) Locating all electronics remotely in the console.

With the features noted above the control implementation proved remarkably trouble free. The total number of hours run by each component were as follows :

i) Variable Timing Unit - 251 hours
ii) Electronic governor - 182 hours
iii) Variable Geometry Turbocharger - 160 hours
made up as follows (pneumatic actuation 98 hours)
(electro-hydraulic actuation 83 hours)

7.2.3 Control Algorithms

(i) Steady State

The engine in standard configuration was rigorously tested such as to establish a datum performance level. The engine was then configured with the control parameters and performance optimised dynamically. The results indicated that substantial improvements to LTC and part

load performance were possible. Unfortunately whilst peak torque was increased 9% to 1157 Nm peak torque speed could not be reduced to the design aim of 1050 rev/min. This was due to

1) falling volumetric efficiency with speed
2) falling turbomachinery efficiency with speed
3) limited turn down ratio
4) limiting cylinder pressure

The respective figures for torque back-up were 46% at 59% of rated speed compared with 21% at 62% rated speed for the standard case. Rated power was retained down to 1700 rev/min whilst SFC on the LTC compared favourably with base. Significant improvements to part load efficiency were achieved e.g. 225g/kwh island increased 25% though in the majority they were below peak torque.

An assessment with a route and simulated vehicle program (RSVP) revealed improvements of -0.48 mpg + 4.1% GEF for a fully laden vehicle on a 23 mile cross country run when compared with the base and improvements of +1% mpg and +3.2% GEF for an identical vehicle on a 90 mile motorway route. Significantly the program highlighted the disproportionate amount of time a laden vehicle operates in a narrow speed band on the LTC between peak torque and rated speed. To some extent therefore the results are disappointing, for in this region the base engine is well matched. It confirms however the correct choice of trim for turbine and compressor for the VG configured engine and indicates a larger turn down with better efficiencies is highly desirable.

To assess the likely SFC penalty of running a simplified control algorithm the engine was re-tested. Unfortunately a calibration error on the torque and cylinder pressure transducers makes comparison difficult but at part load SFC is not critically affected. The omission of retard at and around peak torque, however, implies an unacceptable torque deficit.

(ii) Transient Tests

The following conclusions can be drawn from the transient results. The base fitted with a twin entry unit exhibits good transient response in terms of smoke emission and load acceptance. This is achieved by an efficient turbine maintaining a positive differential through the transient.

The timing investigation clearly demonstrated that it is feasible to slew the injection timing control at the same rate as rack benefiting steady state SFC at light loads. Other benefits of modulating injection timing during engine acceleration were found to be reduced transient smoke and enhanced load acceptance though the effects of this parameter on noise emission were not investigated.

The performance of the VG MKI twin flow with the turbine stage unrestricted was found to be unsatisfactory. It was noted that peak smoke emission was reduced when compared to the twin entry base. The fully restricted performance was as expected disappointing due to the small turndown which manifested itself as a decreased turbine efficiency and lower manifold differential pressure. In some instances the restricted performance was worse.

An investigation was carried out with the MKII(b) unit and included boost and restriction algorithms. This unit clearly enhanced transient performance with increased restriction and demonstrated an ability to slew at the same rate as rack. This was effectively shown by a boost test at 1800 rev/min where the turbine initially becomes fully restricted; however, exhaust manifold pressures never become excessive. For the tests reported the unit always operated in crossover.

The speed determined schedule appeared to give the best results (restriction for speed); however, this implies a part load SFC penalty.

The boost schedule raises inlet manifold pressure significantly faster, differential, however rises disproportionally resulting in only small overall performance gains. The advantages of a boost schedule, however, in terms of parametric variations make it a very attractive solution. Peak smoke emission can be controlled by an electronic boost control. It is clear however that the VG unit has not been optimised for transient response.

7.3 Conclusions from the Theoretical Results

The object of this work was to achieve a 50% torque back-up at 50% of rated speed i.e. 1300 Nm @ 1050 rev/min. The theoretical predictions using a sophisticated engine simulation program based on the filling and emptying technique indicated that with appropriate modifications (primarily breathing and turn down), it was realistic to reduce peak torque speed to 1050 rev/min.

A peak torque of 1300 Nm however would appear very difficult without :

1) a higher cylinder pressure limit
2) a turbine with less sensitivity to choking (difficult with nozzled configuration)
3) charge cooling.

The engine as tested was limited to 1160 Nm, if peak torque speed were reduced to 1000 rev/min then the engine might be flexible enough producing for example 175 kW @ 2000 rev/min (rated conditions) thus achieving effectively 50% torque back-up with consequent benefits to noise, wear and SFC. This, together with a turn-down ratio of 4:1 would allow significant SFC improvement on the LTC.

7.4 Suggestions for Further Work

The merits of an electronically controlled VG configured engine have been clearly demonstrated in terms of flexibility and economy. The design aim of 50% torque back-up at 50% of rated speed were, however, not achieved. In order that the peak torque speed be reduced further work is required to both engine and turbocharger components.

The engine modifications desirable to effect the twin aims of high torque at low speed include :

1) increasing cylinder pressure limits reliably e.g. low compression ratio pistons of say 14.1 cr together with a peak cylinder pressure limit of 140 bars (2030 lb/in^2).
2) improve engine breathing especially below peak torque e.g. by fitting a camshaft with valve duration and timing arranged for better low speed breathing. Suitable figures are contained in the theoretical predictions.

The corresponding turbocharger modifications include :

1) improving turbomachinery efficiency
2) reducing the sensitivity of the nozzle ring to choking
3) effecting substantially more turn down i.e. 4:1

The turbocharger would benefit from a compressor with a 'flat' efficiency characteristic rather than the present 'onion ring'. Any efficiency advantage to the turbine would reflect directly in SFC and aid both acceleration and turn-down. The turbocharger match should be arranged to effect a 22:1 air fuel ratio at rated conditions; this together with variable timing would lead to a horizontal SFC characteristic of 200g/kWh or better dependant on overall turbocharger efficiency.

Thought should also be given to implementing a self-optimising control algorithm. Optimal calibration of an engine is subject to some systematic and some random deviations caused by manufacturing tolerances, deterioration with time and influence of different ambients. In a self-adaptive control algorithm, these deviations are avoided by self-adjusting control strategies.

REFERENCES

1. VON DER NUELL, W.T.
Turbocharging for Better Vehicle Engines.
The Garrett Corporation. Trans. SAE 1966.

2. GHADIRI-ZAREH, M.S.
'Variable Geometry Single Stage and Two Stage Turbocharging of High Output Transport Diesel Engines'.
Ph.D. thesis, University of Bath 1975.

3. SHEPHERD, D.G.
'Principles of Turbomachinery'.
Macmillan Co., London 1956.

4. WALLACE, F.J.
'Theoretical Assessment of the Performance Characteristics of Inward Radial Flow Machines'.
Proc. Institution of Mechanical Engineers, 172, pp 931-952, 1958.

5. BERENYI, S.G., RAFFA, C.J.
'Variable Area Turbocharger for High Output Diesel Engines',
SAE 790064 (SP-442), 1979.

6. CHAPPLE, P.M., FLYNN, P.F., MULLOY, J.M.
'Aerodynamic Design of Fixed and Variable Geometry Nozzless Turbine Casings'.
ASME Jl of Eng. for Power 1980.
Vol. 102, p.141, 79-GT-87.

7. CSER, G.
'Some Results of Combined Charging Applications'.
I.Mech.E. C64/78 1978.
Turbocharging and Turbochargers Conferences.

8. WALLACE, F.J.
'Matching of High Output Diesel Engines with Associated Turbomachinery'.
Proc. I.Mech.E. 48/1973, Vol. 187, p.548.

9. WALLACE, F.J., WAY, R.J.B., BAGHERY, A.
'Variable Geometry Turbocharging - the Realistic Way Forward'.
SAE 810336, Detroit, 1981.

10. BAGHERY, A.
'Variable Geometry Turbocharging of Transport Diesel Engines'.
Ph.D. thesis, Bath University 1975.

11. WATSON, N., JANOTA, M.S.
'High Output Turbocharging'.
Lecture notes from "Turbocharging the Internal Combustion Engine", 1977, Fluid Dynamics Institute, Dartmouth College, Hanover, N.H.

12. BALJE, O.E.
'Turbomachines. A Guide to Design, Selection and Theory', 1981.
John Wiley & Sons, New York.

13. WATSON, N., JANOTA, M.S.
'Turbocharging the Internal Combustion Engine'.
Macmillan Press, 1981.

14. BRANDS, M.C.
'Helmholtz Tuned Induction Systems for Turbocharged Diesel Engines'.
SAE 790069 - SP442.
Turbocharging and Turbocharged Engines, 1979.

15. POUNDER, C.C.
'Diesel Engines, Principles and Practice'.
Newnes, Second Edition 1962.

16. KIMBERLEY, J.A., VOSS, J.R.
'A Mid-Range Fuel Injection Pump and Electronics'.
SAE Paper 820448.

17. WOLLEN WEBER, W.E.
'The Turbocharger - A Vital Part of the Engine Intake and Exhaust Systems'.
SAE Paper 700534.

18. MYERS, P.S.
'The Diesel Engine for Truck Applications'.
SAE Paper 750128.

19. 'Turbine Design and Application'.
Volume Three NASA SP-290.

20. ZIARATI, M.R.
'Mathematical Modelling and Experimental Testing of Variable Geometry Inward Radial Flow Turbines'.
Ph.D. thesis, Bath University 1979.

21. FLAXINGTON, D., SZCZUPAK, D.T.
'Variable Area Radial - Inflow Turbines'.
Turbochargers and Turbocharging Conference 1982, C36/82,
The I.Mech.E. London.

22. WATSON, N.
'Resonant Intake and Variable Geometry Turbocharging System for a V8 Diesel Engine'.
Turbochargers and Turbocharging Conference 1982, C40/82.
The I.Mech.E. London.

23. MERRIT, E.
'Hydraulic Control Systems'.
John Wiley & Sons.

24. ALDIS, C.A.
'Comparison Between Turbocharging & Comprex Pressure Exchanger Supercharging of High Output Diesel Engines'.
Ph.D. thesis, Bath University 1982.

25. GREEN, G.L., WALLACE, D.
'Correlation Studies of an In-Line, Full Flow Opacimeter'.
SAE Paper 80 1373.

26. DIMMOCK, N.A.
'A Compressor Routine Test Code'.
Ministry of Aviation-Aeronautical Research Council.
Reports and Memoranda No. 3337.

27. BUCHI, A.J.
'Exhaust Turbocharging of Internal Combustion Engines, its Origins, Evolution, Present State of Development and Future Potentialities'.
Journal of the Franklin Institute, July 1953.

28. TARABAD, M., COLE, A.
'The Diesel Engine Cycle Simulation Program'.
Internal Report - February 1982.
Bath University, School of Engineering.

29. JANOTA, M.S., WATSON, N.
'Turbocharging - Post Experience Course'.
Lecture Notes, Imperial College, London, September 1979.

30. WALLACE, F.J., WAY, R.J.
'A Comprehensive Suite of Steady State and Transient Response Engine - Turbocharger Performance Prediction Programs'.
UNICEG 17/18 April 1980, King's College, London.

31. KASTNER, L.J., WILLIAMS, T.J. & WHITE, J.B.
'Poppet Valve Characteristics and their Influence on the Induction Process'.
Proc. I.Mech.E. Vol.178, 1964.

32. WOSCHNI, G.
'A Universally Applicable Equation for the Instantaneous Heat Transfer Co-efficients in the Internal Combustion Engine'.
SAE Paper 670931.

33. CHEN, S.K., FLYNN, P.F.
'Development of a Single, Cylinder C.I. Research Engine'.
SAE Paper 650733.

34. MARZOUK, M., WATSON, N. & PILLEY, A.D.
'A Combustion Correlation for Diesel Engine Simulation'.
SAE Paper 1980.

35. HARTREE, D.R.
'Some Practical Methods of Using Characteristics in the Calculation of Non-Steady Compressible Flow'.
US Atomic Energy Commission, ACCU-2713, 1953.

36. BENSON, R.S., GARG, WOLLATT, D.
'A Numerical Solution of Unsteady Flow Problems'.
Int. J. Mech. Sci. Vol. 6, 1964.

37. MEIER, E.
The Application of Pulse Convertors to 4-Stroke Diesel Engines with Exhaust Gas Turbocharging.
Brown Boveri Review, 1968, Vol. 55, No. 8.

38. BRANDS, M.C., WERNER, J.R., HOHNE, J.L. & KRAMER, S.
Vehicle Testing of Cummins Turbocompound Diesel Engine.
SAE 810073.

39. MELCHIOR, J., ANDRE-TALAMON, T.
Hyperbar System of High Supercharging.
SAE Paper 700723.

40. ANDRE-TALAMON, T.
New Aspects of Turbocharger Utilization with the Hyperbar Parallel Supercharging Turbocharging and Turbochargers Conference 1978.
C66/78, I.Mech.E. London.

41. EISELE, E., HIERETH, H. & POLZ, H.
Experience with Comprex Pressure Wave Supercharger on the High-Speed Passenger Car Diesel Engine.
Daimler-Benz A.G., SAE Paper 750334.

42. BENSON, R.S., SVENTNICKA, F.V.
Two Stage Turbocharging of Diesel Engines. A Matching Procedure and an Experimental Investigation.
SAE 740740.

43. BENSON, R.S., WHITEHOUSE, N.D.
Internal Combustion Engines. Volume II.
Pergamon Press, ISBN 008 0227201.

44. TAYLOR, C.F.
'The Internal Combustion Engine in Theory and Practice'.
Volume I. The M.I.T. Press, ISBN 0262700158.

45. BSAU 141a 1971. The Performance of Diesel Engines for Road Vehicles.

46. Engine Test Code SI and Diesel.
SAE J816B

47. Engine Rating Code - Diesel.
SAE J270.

48. Diesel Engine Smoke Measurement.
SAE J255.

49. Measurement of Intake Air or Exhaust Gas Flow of Diesel Engines.
SAE J244.

50. Engine Terminology and Nomenclature General.
SAE J604C.

51. Turbocharger Nomenclature and Terminology.
SAE J922AO.

52. Fuel Injection Nomenclature.
SAE J83OB.

53. Turbocharger Connections.
SAE J1135O.

54. REAMS, L. et al.
'Capabilities of Diesel Electronic Fuel Control'.
SAE Paper 820449.

55. WALZ, L.
'An Approach to the Application of Fuel Injection Equipment for Passenger Car Diesel Engines'.
SAE Paper 82045O.

56. TRENNE, M., IVES, A.
Closed Loop Design for Electronic Diesel Injection Systems.
SAE Paper 820447.

57. FLEMING, W.J.
'Engine Sensors - State of the Art'.
SAE Paper 820447.

58. FLEMING, W.J., WOOD, P.W.
Non-Contact Miniature Torque Sensor for Automotive Application.
SAE Paper 820206.

59. 'Two New Controls for Vehicular Diesels'.
Diesel and Gas Turbine - November 1981, p.61-65.

60. Hydraulic Handbook (5th Edition).
Trade & Technical Press Ltd.

61. Pneumatic Handbook (3rd Edition).
Trade & Technical Press Ltd.

62. SHINNERS, S.M.
Control System Design.
Wiley International Edition.

63. A Technical & Commercial Guide to Stepper Motors.
Electrical Research Association - Report 72-173.

64. POE, E.
Using the 6800 Microprocessor.

65. HUGGINS, E.
Microprocessors and Microcomputers.
Macmillan.

66. SCHWARZENBACH, J., GILL, K.F.
System Modelling and Control.
John Wiley & Sons, New York.

67. HEALEY, M.
Principles of Automatic Control
(Hodder & Stoughton).

68. TOELLE, A.D.
Microprocessor Control of the Automobile Engine.
SAE 770008

69. KENDALL, L.
Analogue to Digital Converters in Microprocessor Based
Automotive Systems.
SAE 770159.

APPENDIX 1

DATA REDUCTION PROGRAM LISTING

APPENDIX 2

SERVO PACK CALCULATIONS

The specification called for the following :

1) a small tank
2) an anti-rupture valve
3) a non-flammable working fluid
4) a dedicated pack
5) no external cooling
6) the oil bulk temperature not to exceed 40°C

Items 1) and 5) imply the use of an accumulator and the following configuration was adopted:

1) pump delivery = .25 mL/S
2) maximum pressure = 120 bar (gauge)
3) maximum demand is 0.0168L of oil over a period of 0.1S (intermittent)
4) minimum time intervals between demands is 10S
5) allowable differential pressure is 2.0 bar
6) isentropic process assumed

[Items 1), 2) and 3) below have slew rates of 0.1s)

The maximum demand is made up as follows : (flow rate L/S)

(1) VARIABLE GEOMETRY TURBOCHARGER :

$$Q = \frac{\pi \times 0.012^2 \times 0.006 \times 10}{4}$$

$$Q = 0.00678 \text{ L/S}$$

(2) ELECTRONIC GOVERNOR

$$Q = \frac{\pi \times 0.012^2 \times 0.015 \times 10}{4}$$

$$Q = 0.017 \text{ L/S}$$

cont'd...

APPENDIX 2 cont'd

(3) INJECTION TIMING

$$Q = \frac{\text{x } 0.022^2 \text{ x } 0.0381 \text{ x } 10}{4}$$

$$Q = 0.1448 \text{ L/S}$$

total flow requirements = 1 + 2 + 3

total flow = 0.0168L over 0.1s

now $P_1V_1 = P_2V_2 = P_3V_3$

hence $121\ V_2^{1.4} = 101\ V_3^{1.4}$

$$V_3 = \left(\frac{121}{101}\right)^{1/1.4} V_2$$

$$\underline{V_3 = 1.137\ V_2}$$

but $V_3 - V_2 = 0.0168$ L

hence $V_3 = 1.137\ (V_3 - 0.0168)$

$$\underline{V_3 = 0.1394 \text{ L}}$$

Assume pre-charge pressure = $0.9\ P_3$ i.e. 0.9 x 101

thus $91\ V_1 = 121\ V_2$

and $V_1 = \frac{121}{91}\ (0.1394 - 0.0168)$ assuming isothermal charging

$$\underline{V_1 = 0.163 \text{ L}}$$

initial oil flow to accumulator is $V_1 - V_2$

$= 0.163 - 0.1226$

$\doteq 0.0404$ L

and this would require :

$$\text{time} = \frac{0.0404}{0.025} \text{ S}$$

$$\underline{\text{time} = 1.6 \text{ S}} \text{ which is satisfactory.}$$

The nearest sized accumulator to V_1 was chosen,

i.e. 1 litre (with due allowance for leakage etc).

APPENDIX 3

REDUCED DATA SHEETS CORRESPONDING TO TESTS 10 - 98

AS PRESENTED IN FIG. 4.0

APPENDIX 4

PART LOAD RESULTS (CHAPTER 2)

SECTION	TYPE	TEST NO.*	NO. OF PAGES
(1)	H2B BASE	12 - 19	SHEET 1 to 16
(2)	MKI VG	21-24; 34-37	SHEET 1 to 4
(3)	MKII VG OPTIMISATION	73 - 81	SHEET 1 to 18
(4)	MKII VG SIMPLIFIED SCHEDULE	90 - 97	SHEET 1 to 8

* For full description of tests see fig. 4.0

SECTION	SHEET NO.	SPECIAL COMMENTS	TYPE	SPEED rev/min
1	1-6		BASE H2B LTC	2100
	1-6			2000
	2-6			1800
	2-6			1600
	3-6			1400
	3-6			1300
	4-6			1200
	4-6			1100
	5-6			1000
	5-6			900
	6-6			800
		% Restriction		
2	1-3	0	H2C MKII(b) BOOST INVESTIGATION-LTC	1800
	1-3	25		1800
	2-3	0		1300
	2-3	50		1300
	3-3	0		800
	3-3	50		800
		Dynamic Timing	-50% TORQUE	
3	1-10	9	H2B BASE-TIMING INVESTIGATION	1300
	1-10	7	"	1300
	2-10	4.5	"	1300
	2-10	17.5	"	1300
	3-10	17	"	1800
	3-10	8	"	1800
	4-10	4	"	1800
	4-10	21	"	800
	5-10	10	"	800
	5-10	7.5	"	800
	6-10	5	- LTC	1800
	6-10	10	- LTC	1800

cont'd...

APPENDIX 5

ELECTRONIC INSTRUMENTATION RESULTS

(supporting evidence)

The results are presented in four blocks :

1) BASE H2B RESULTS Sheets 1 - 6

2) BOOST INVESTIGATION (MKII) Sheets 1 - 3

3) TIMING INVESTIGATION (H2B) Sheets 1 - 10

4) MAPPING AND OPTIMISATION Sheets 1 - 5

A table of contents is given overleaf

SECTION	SHEET NO.	SPECIAL COMMENTS	TYPE	SPEED rev/min
3	7-10	17	H2B TIMING INVESTIGATION-LTC	1800
	7-10	18	" "	1300
	8-10	13	" "	1300
	8-10	2.5	" "	1300
	9-10	7.5	" "	800
	9-10	14.5	" "	800
	10-10	20.5	" "	800
4	1-5		OPTIMISED H2C - LTC	2300
	1-5		" "	2100
	2-5		" "	1900
	2-5		" "	1700
	3-5		" "	1500
	3-5		" "	1360
	4-5		" "	1100
	4-5		" "	900
	5-5		" "	700

APPENDIX 6

ROUTE AND SIMULATED VEHICLE PROGRAM (RSVP)

Supporting Data - Sheets 1 to 19 from Chapter 4

No.	TYPE	COMMENTS
1	W. Yorks Route	Bath TL11 Base 2100 rev/min 10 speed
2	Loops for above	" " " " " " "
3	Motorway Route	" " " " " " "
4	W. Yorks Route	Bath TL11 Base 2300 rev/min 5 speed
5	Loops for above	" " " " " " "
6	Motorway Route	" " " " " " "
7	Loops for above	" " " " " " "
8	W. Yorks Route	Bath TL11 VG 2100 rev/min 10 speed
9	Loops for above	" " " " " " "
10	Motorway Route	" " " " " " "
11	Loops for above	" " " " " " "
12	W. Yorks Route	Bath TL11 VG 2300 rev/min 5 speed
13	Loops for above	" " " " " " "
14	Motorway Route	" " " " " " "
15	Loops for above	" " " " " " "
16	W. Yorks Route	Leyland TL11 intercooled 2000 rev/min 10 speed
17	Loops for above	" " " " " " "
18	Motorway Route	" " " " " " "
19	Loops for above	" " " " " " "

APPENDIX 7

CSP OUTPUT (from Chapter 6)

No.	Speed	Type		Comments
1	2100	BASE H2B	*	Confirmation Runs
2	1900	BASE H2B		
3	1700	BASE H2B		
4	1500	BASE H2B		
5	1300	BASE H2B	*	
6	1100	BASE H2B	*	
7	900	BASE H2B		
8	1300	BASE H2B-21°BTDC		Timing Investigation
9	1300	BASE H2B-18 "		Predictive Capabilities
10	1300	BASE H2B-15 "		
11	1300	BASE H2B-12 "		
12	1300	BASE H2B- 9 "		
13	1300	BASE H2B- 6 "		
				Turn Down Investigation
14	1300	VG MKIIb H2C 0%		Predictive Capabilities
15	1300	VG " H2C 25%		
16	1300	VG " H2C 40%		
17	1300	VG " H2C 50%		
18	2100	VG (optimised) H2C 0%	*	Matched VG Base
19	1300	VG (optimised) H2C 50%	*	Matched VG Base
20	1100	VG (optimised) H2C 50%	*	Matched VG Base
				Predictive
21	2100	VG (optimised) + 3% on Comp. Efficiency		
22	1300	VG (optimised) + 3% on Comp. Efficiency		
23	1100	VG (optimised) + 3% on Comp. Efficiency		
24	2100	VG (optimised) + 3% on Turb Efficiency		
25	1300	VG (optimised) + 3% on Turb Efficiency		
26	1100	VG (optimised) + 3% on Turb Efficiency		
27	2100	VG (optimised) + 103% m $\sqrt{T/p}$		
28	1300	VG (optimised) + 45% m $\sqrt{T/p}$		
29	1100	VG (optimised) + 48% m $\sqrt{T/p}$		

APPENDIX 7 cont'd

No.	Speed	Type	Comments
30	2100	VG (optimised)	14.75 compression ratio
31	1300	VG (optimised)	14.75 compression ratio
32	1100	VG (optimised)	14.75 compression ratio
33	2100	VG (optimised)	13.75 compression ratio
34	1300	VG (optimised)	13.75 compression ratio
35	1100	VG (optimised)	13.75 compression ratio
36	2100	VG (optimised)	Larger valves
37	1300	VG (optimised)	Larger valves
38	1100	VG (optimised)	Larger valves
39	2100	VG (optimised)	Higher µvolumetric
40	1300	VG (optimised)	Higher µvolumetric
41	1100	VG (optimised)	Higher µvolumetric
42	2100	optimised valve timing *	
43	1300	optimised valve timing *	

* = 8 off gas exchange diagrams

APPENDIX 8

DRAWING REGISTER

Description	Drawing No.
ENGINE ADAPTOR PLATE - RL11 TO HYGATE COUPLING	7
3" AIR NOZZLE TO BS 1042	8
2¼" AIR NOZZLE TO BS 1042	9
3" REDUCING SECTION FOR USE WITH (8)	10
AIR INTAKE ADAPTOR (COMP END)	11
2¼" REDUCING SECTION - FOR USE WITH (9)	12
AIR BOX	13
AIR INTAKE ADAPTOR - H2C	14
ENGINE TEST SHEET	15
FUEL FLOW WEIGH GEAR	16
TDC TRIGGERING GEAR	17
DYNAMOMETER DRAWINGS	
SPINDLE	100(A)
OIL SEAL HALVES	101
END ADAPTOR AND PLATE	102
FRONT VIEW OF FABRICATION	103 (1/3)
SIDE VIEW OF FABRICATION	103 (2/3)
OUTLINE OF LUCAS HD2 - 3000	103 (3/3)
OUTLINE OF LUCAS HD2 - 3000	104
SUPPORTING BRACKETS	106
FIXING BOLT	107
TYCO LOAD CELL PLATE	108
TYCO LOAD CELL SCREW	109
BASE PLATE RESTRAINING DEVICE	110
LOAD CELL BOTTOM BRACKET	111
FUEL PUMP DRIVE LINE	
SPACING PLATE	1000
DRIVING SHAFT	1001
DRIVE TUBE	1002

cont'd...

APPENDIX 8 cont'd

Description	Drawing No.
LEYLAND SMOKEMETER STACK	501
STACK WITH BOSCH DETAIL	502
EXHAUST STACK FLANGE	503
ACTUATING LEVERS	504/505
RESTRICTORS (INLET/EXHAUST)	506
VARIABLE TIMING DEVICE	
BODY COMPLETE	6000
FRONT COVER	6001
SPLINED SHAFT	6002
REAR COVER	6003
SLIDING COLLAR	6004
GA - EXTERNAL VIEW	6005
REAR SHAFT	6006
GA - INTERNAL VIEW	6007
CYLINDER HEAD PRESSURE (6121) TRANS. MOD.	
TRANSDUCER SLEEVE	D8217
TRANSDUCER HOLDER	D8218
TRANSDUCER SLEEVE - HOUSING	D8220
TRANSDUCER SLEEVE EXT	D8221
ASSY OF PRESSURE TRANSDUCER	D8216
MACHINING OF CYL. HEAD	D8171
PLUG	D8223
'690' FUEL PUMP DRIVE LINE	
OIL SEAL HOUSING	304 779
DRIVING SHAFT (MODIFIED)	304 887
DISTANCE PIECE - INNER	304 889
DISTANCE PIECE	304 986
DISTANCE PIECE - OUTER	304 889
SUB-ASSEMBLY OF FUEL PUMP DRIVE	304 896

cont'd..

APPENDIX 8 cont'd

Description	Drawing No.
(690' FUEL PUMP DRIVE LINE cont'd	
COUPLING FLANGE	304 981
DRIVING CLAMP	NAJ 1298
DRIVE TUBE (MODIFIED)	NAJ 2186
DYNAMOMETER DRAWING	
INSTALLATION OF HD2 - 3000 PUMP	88 25 2037